CÁRMEN SOUSA

EVOLUTION OF THE IMMUNE SYSTEM IN ANTARCTIC NOTOTHENIOIDS

UNIVERSIDADE DO ALGARVE

Faculdade de Ciências e Tecnologia

Faro, 2021

CÁRMEN SOUSA

EVOLUTION OF THE IMMUNE SYSTEM IN ANTARCTIC NOTOTHENIOIDS

Doutoramento em Ciências Biológicas

Especialidade em Genética, Genómica e Evolução

Trabalho efetuado sob a orientação de:

Prof. Doutor Adelino V. M. Canário

Prof.ª Doutora Deborah M. Power

UNIVERSIDADE DO ALGARVE

Faculdade de Ciências e Tecnologia

Faro, 2021

CÁRMEN SOUSA

EVOLUTION OF THE IMMUNE SYSTEM IN ANTARCTIC NOTOTHENIOIDS

Doctoral Programme in Biological Sciences

Specialty in Genetic, Genomic and Evolution

Thesis carried out under the supervision of:

Prof. Adelino V. M. Canário

Prof. Deborah M. Power

UNIVERSIDADE DO ALGARVE

Faculdade de Ciências e Tecnologia

Faro, 2021

Título | Thesis title

Evolution of the immune system in Antarctic Notothenioids

Declaração de autoria de trabalho:

Declaro ser a autora deste trabalho que é original e inédito. Autores e trabalhos consultados estão devidamente citados no texto e constam da listagem de referências incluída.

Declaration of authorship:

This work has not previously been submitted for a degree in any university. To the best of my knowledge and belief, the thesis contains no material previously published or written by another person except where due reference is made in the thesis itself.

Cármen Sousa

Support

This study was funded by the Portuguese Foundation for Science and Technology (FCT) through a PhD grant (SFRH/BD/120040/20126) and project (FCT-NSFC/0002/2016).

Apoio

Este estudo foi suportado através de uma bolsa de Doutoramento concedida pela Fundação para a Ciência e Tecnologia (FCT): Bolsa de Doutoramento (SFRH/BD/120040/2016) e projeto (FCT-NSFC/0002/2016).

À minha avó

(que partiu durante esta minha jornada)

e aos meus pais

Acknowledgements

Esta jornada que durou 4 anos e, com toda a situação pandémica que vivemos desde 2019, foi recheada de muitos momentos, aprendizagens e colaborações.

Muitas pessoas ajudaram-me a melhorar tanto profissionalmente como pessoalmente, transmitiram-me conhecimentos, ajudaram-me a ultrapassar determinados desafios através da amizade, companheirismo e espírito de equipa. O meu doutoramento foi uma boa junção deste trabalho de equipa e colaborações tanto nacionais como internacionais.

Estou grata por todos aqueles que me deram "a mão" nesta fase tão exigente e tiveram palavras positivas e reconfortantes nos momentos em que as coisas pareciam não correr da forma prevista (panorama normal na Ciência e Investigação e nos doutoramentos).

Primeiramente, quero agradecer aos meus orientadores Prof Adelino Canário, Prof Deborah Power e Dr Pedro Guerreiro a oportunidade de trabalhar e estudar duas espécies de peixes antárticos e ter conseguido vivenciar duas experiências únicas e maravilhosas ao ir a um continente tão inóspito como a Antártida.

Quero agradecer aos meus colegas do CCMAR, que sempre me ajudaram no que puderam, especialmente à Soraia Santos, Alexandra Alves, Stefan Fernandes, Maoxiao Peng, Elsa Couto, Ana Patrícia Mateus e Vera Gomes. Um especial obrigada e uma enorme gratidão ao meu colega do grupo, Dr João Cardoso, uma pessoa bastante sem filtro, que me ajudou bastante a melhorar a minha escrita e a aumentar os meus conhecimentos em diversas áreas, com bastante paciência e dedicação.

À amiga algarvia de longa data, Soraia Santos, por seres quem és, sempre sincera e muito boa ouvinte e por estares sempre pronta para me "dar na cabeça" e para ajudar-me.

À amiga Alexandra Alves por todos os momentos partilhados no trabalho bem como fora do trabalho, todos os "azares" mas também muitos momentos de diversão que nos deram muitas aprendizagens.

Um agradecimento ao Propolar, por toda a ajuda na logística e preparação das campanhas Antárticas.

Um caloroso obrigada ao meu noivo, Rui Santos (aka Pgem), que apareceu na minha vida nos últimos 2 anos do meu doutoramento (fase mais exigente) e que teve toda a paciência, amizade, atenção, amor e companheirismo. Ah e por teres cozinhado mais e feito mais lides domésticas no último ano para eu me poder dedicar mais tempo à escrita.

E, por fim, aos meus pais por sempre estarem presentes, apoiarem e aconselharem apesar da distância física.

“Há apenas uma maneira de evitar críticas:

Não faça nada, não diga nada e, não seja nada.”

Aristóteles

Abstract

Notothenioids are the most abundant group of teleost fish found in the Southern Ocean. These fish evolved relatively recently from a single benthic ancestor and radiated and expanded in the extreme cold of Antarctica waters and their physiology was adapted accordingly. Surprisingly, little is known about their immune system and how immune defences were modulated during adaptation to the cold environment and to its water specific microbiome. The main objective of this thesis was to characterise the immune cellular and humoral responses to bacterial and viral-like challenges in immune tissues and plasma of two phylogenetically related notothenioids, *Notothenia coriiceps* and *Notothenia rossii*. The methodologies applied were based on DNA sequencing technologies and biochemical assays to measure functional plasma enzyme activity using a comparative approach. This study a) characterised and uncovered a role of iron-metabolism and of the pattern recognition receptors family toll-like receptors (TLRs) after a LPS immune challenge, b) characterised for the first time the transcriptomes of important immune tissues (head-kidney, skin, duodenum, liver and spleen) and their response to bacterial and viral challenges and in response to temperature, c) described the microbiome communities associated to important immune tissue barriers in recently caught and immune challenged notothenioids. The results contribute substantially to the understanding of the main immune and non-immune pathways in the defence against external agents in Antarctic notothenioids.

Keywords: notothenioids, immune system, transcriptome, microbiome, pathogens

Resumo

Os Nototenióides são o grupo de peixes teleósteos mais abundantes no Oceano Antártico. Estes peixes evoluíram recentemente de um ancestral bentónico comum e a sua fisiologia adaptou-se aquando da irradiação e expansão nas águas frias e extremas da Antártida. Surpreendentemente pouca informação é conhecida acerca do seu sistema imunológico e como as suas defesas imunológicas foram moduladas pela adaptação ao ambiente frio e ao microbioma único do oceano Antártico. O principal objetivo da tese foi caracterizar as respostas imunológicas ao nível celular e humoral contra patógenos agonistas bacterianos e virais em vários tecidos ligado ao sistema imune, bem como plasma sanguíneo em dois nototenióides. As metodologias aplicadas foram baseadas em tecnologias de sequenciação de ADN e em ensaios bioquímicos para quantificar a atividade de enzimas plasmáticas funcionais, através de uma abordagem comparativa. Neste estudo foram a) caracterizados e desvendados o papel de genes candidatos relacionados com o metabolismo do ferro e dos recetores de reconhecimento de padrões da família de recetores toll-like (TLRs) após exposição ao LPS, b) caracterizados pela primeira vez os transcriptomas de vários tecidos com função imunológica (rim, pele, duodeno, baço e fígado) e a sua resposta ao LPS, c) descritas as comunidades microbianas associadas aos principais tecidos imunológicos de barreira em recém capturados e após estimulação por agonistas bacterianos, virais e em resposta a aumento da temperatura. Estes resultados contribuem substancialmente para a compreensão dos principais componentes do sistema imune, bem como outras vias não imunes envolvidas na defesa contra agentes externos nos nototenióides antárticos.

Palavras-chave: Nototenióides, sistema imunitário, transcriptoma, microbioma, patógenos

Table of contents

List of Tables

List of Figures

Chapter 1

Chapter 2.1

Chapter 2.2

Chapter 5

List of Abbreviations

α-2M: alpha-2 macroglobulin

Aca: *Anolis carolinensis*

ACC: Antarctic circumpolar current

AFGP: antifreeze glycoprotein

APF: Antarctic polar front

APP: antimicrobial protein and peptide

Aliview: alignment viewer and editor software

ALR: melanoma (AIM)-like receptor

Ame: *Astyanax mexicanus*

AMP: antimicrobial peptide

ANOVA: analysis of variance

BALT: bronchus-associated lymphoid tissue

BI: Bayesian inference method

BLAST: basic local alignment search tool

bp: base pairs

BP: biological process

BSM: branch-site analysis

tBLASTn: translated basic local alignment search tool nucleotides

C: complement protein

CALT: conjunctiva-associated lymphoid tissue

CC: cellular component

Cd: cadmium

cDNA: complementary deoxyribonucleic acid

Cha: *Chionodracos hamatus*

Cgo: *Cottoperca gobio*

CLR: C-type lectin receptor

Cmi: *Callorhinchus milii*

CO_2: carbon dioxide

CRP: C-reactive protein

Cse: *Cynoglossus semilaevis*

Ct: threshold cycle

DALT: salivary duct-associated

DAMP: danger associated molecular pattern

DEPC: diethylpyrocarbonate water

DGE: differentially gene expression

Dla: *Dicentrarchus labrax*

Dma: *Dissostichus mawsoni*

Dre: *Danio rerio*

dsDNA: double stranded DNA

E: efficiency

E. coli: *Escherichia coli*

e.g.: for example

ENSEMBL: European bioinformatics institute annotated genomes portal

EST: expressed sequence tags

EU: European Union

ExPASy: expert protein analysis system

FC: fold-change

FDR: false discovery rate

Fe^{2+}: iron

FPKM: fragments per kilobase of transcript per million mapped reads

Gac: *Gasterosteus aculeatus*

GALT: gut-associated lymphoid tissue

Gga: *Gallus gallus*

GIALT: gill-associated lymphoid tissue

Gmo: *Gadus morhua*

GO: gene ontology

Gya: *Gymnodraco acuticeps*

HKEB: heat-killed bacteria

Hhi: *Hippoglossus hippoglossus*

Hsa: *Homo sapiens*

Hsp: heat shock protein

IFN: interferon

Ig: immunoglobulin

IL: interleukin

INFLR1: interferon receptor lambda 1

Ints10: integrator complex subunit 10

IP: intraperitoneal injection

KEGG: Kyoto encyclopedia of genes and genomes

KO: orthologs database

LALT: larynx-associated lymphoid tissue

Lch: *Latimeria chalumnae*

LDALT: lacrimal duct-associated lymphoid tissue

Loc: *Lepisosteus oculatus*

LnL: log likelihood

LOD: limit of detection

LOQ: limit of quantification

LPS: lipopolysaccharide

LRR: leucine-rich repeat

LRR-CT: LRR-carboxy terminal domain

LRR-NT: LRR- amino terminal domain

LRT: likelihood ratio test

M: molar or macrophage phenotype

MD: molecular dynamics

MALT: mucosa-associated lymphoid tissue

MAMP: microbe associated molecular pattern

MF: molecular function

MHC: major histocompatibility complex

MIF: migration inhibition factor

ML: maximum likelihood method

Mmu: *Mus musculus*

mRNA: messenger RNA

Muc: mucin

MUSCLE: multiple sequence alignment software

NALT: nasopharynx-associated lymphoid tissue

NC: *Notothenia coriiceps*

NCBI: national center for biotechnology information

Nco: *Notothenia coriiceps*

NGS: next-generation sequencing

NK: natural killer

NLR: nucleotide oligomerization domain-like receptor

NMR: nuclear magnetic resonance

NOD: nucleotide oligomerization domain

Nr: non-redundant

Ola: *Oryzias latipes*

Oni: *Oreochromis niloticus*

ORF: open reading frame

OTU: operational taxonomic unit

PAMP: pathogen-associated molecular pattern

PC: principal component

PCA: principal component analysis

PCR: polymerase chain reaction

PE: paired-end

Pfo: *Poecillia formosa*

Pge: *Pseudochaenichthys georgianus*

PHA: fish leucocytes

Pma: *Petromyzon marinus*

PO: peroxidase

Pol: *Paralichthys olivaceus*

Poly I:C: polyinosinic:polycytidylic acid

PRR: pattern recognition receptor

PSS: positive selection site

QC: quality control

qPCR: quantitative polymerase chain reaction

R^2: coefficient of determination

RIA: radioimmunoassay

RIG: retinoic-acid inducible

RLR: retinoic inducible-gene 1 (RIG1)-like receptor

RNA: ribonucleic acid

ROS: reactive oxygen species

rRNA: ribosomal ribonucleic acid

RT-qPCR: reverse transcriptase-quantitative polymerase chain reaction

Rty: *Rhincodon typus*

S: superfamily

SAA: serum amyloid protein A

SALT: skin-associated lymphoid tissue

SAP: Sub-Antarctic Polar front

Sau: *Sparus aurata*

SE: standard error

sIgR: secretory Ig receptor

SM: sites analysis

SMART: simple Modular Architecture Research Tool

Sp: species

SP: signal peptide

SQ: square

Ssa: *Salmo salar*

Sse: *Solea senegalensis*

ssRNA: single stranded RNA

Tbe: *Trematomus bernacchii*

TIR: toll/interleukin-1 receptor

TLR: toll-like receptor

TM: transmembrane

TMEM: transmembrane protein

TNF: tumour necrosis factor

Tni: *Tetraodon nigroviridis*

TRIF: TIR-domain-containing adaptor-inducing beta interferon

TRIM: tripartite motif

Tru: *Takifugu rubripes*

TSGD: teleost specific genome duplication

VT: variable time matrix

Xma: *Xiphophorus maculatus*

Xtr: *Xenopus tropicalis*

CHAPTER 1

General Introduction and main goals

1- General Introduction and main goals

The Southern Ocean surrounds the dry land mass of the Antarctic continent and constitutes an unique extreme cold aquatic environment (Beers and Jayasundara, 2015; O'Brien and Crockett, 2013). The Antarctic notothenioids are a suborder (Notothenioidei) of the order Perciformes, mostly endemic to Antarctica, that dominate the teleost fish fauna of Southern Ocean. The notothenioids are thought to have evolved from a single benthic ancestor through adaptive radiation since the cooling to the freezing point of the Southern Ocean 22.4 million years ago (Matschiner et al., 2015). Several peculiar physiological adaptations essential to inhabit and survive at low temperatures were discovered in the notothenioid clade, such as acquisition of antifreeze glycoproteins, which allow avoiding intracellular ice formation at temperatures near -1.9 ºC (Cheng and Chen, 1999; DeVries and Cheng, 2005; Hofmann et al., 2000). However, one of the areas least studied in Antarctic fishes is the immune system and whether and how it has been modified by evolution in the stable cold environment of Antarctica for the last 10 million years (Auvinet et al., 2020; O'Brien and Crockett, 2013).

The immune system has multiple components providing both own recognition and a line of defence against several pathogens. It is subdivided in innate (non-specific) and acquired (specific) immune system, and each possess humoral and cellular components (Kindt et al., 2007). The innate immunity is the most developed in fish and hence the most studied, although knowledge still lags behind of what is known about mammalian innate immunity (Akira et al., 2006; Berczi and Szentivanyi, 2003; Magnadóttir, 2006). The notothenioid immune system is suggested to have evolved in response to potential pathogens co-inhabiting the Antarctic ecosystem. The role of the microbiome in physiology has received much attention in the last decade and this is also the case for fishes (Butt and Volkoff, 2019; Perry et al., 2020). However, little information is available about the microbiome of Southern Ocean waters and more so of Antarctic fishes.

Therefore, the present thesis addresses a fundamental issue of scientific interest related to evolution of the immune system and its role on host-defence against potential pathogens in two notothenioid fishes, *Notothenia coriiceps* and *Notothenia rossii*.

1.1. The Antarctic environment

Antarctica is considered the highest, coldest, windiest, and driest continent and contains 95% of the world's ice. The Antarctic continent is surrounded by the Southern Ocean with three boundaries or polar fronts, the Sub-Antarctic Polar front (SAP), the Antarctic Polar Front (APF) and the Antarctic Circumpolar Current (ACC) front (Beers and Jayasundara, 2015). These act as physical barriers to preserve and maintain the unique physical, chemical, and biological characteristics of Antarctica (**Figure 1.1**). The ACC is located between 50º and 60º S, extending to a depth of 2,000 m, and transports more water than any other current in the world's oceans, and being responsible for the isolation of Antarctica from other continental shelves. The APF was formed gradually approximately 40 million years ago and circulates outside the ACC, blocking the intrusion of warmer waters in the Southern Ocean and the invasion of non-endemic marine organisms. The isolation created by the polar fronts results in a uniqueness of the Antarctic marine environment as the most thermal stable environment on the planet (Matschiner et al., 2015) with temperatures oscillating between +1.5 to -1.9 ºC at depths below 400 m throughout the year at high latitudes (Beers and Jayasundara, 2015; Wells and Eastman, 1994)(Cheng and Detrich, 2007).

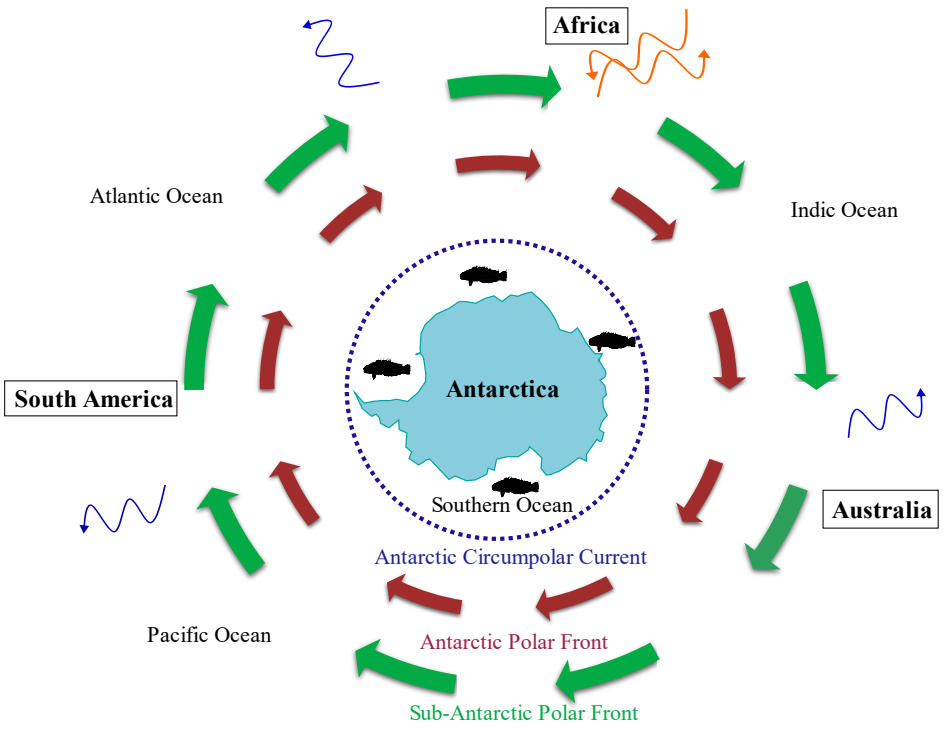

Figure 1.1. Schematic representation of the three main currents in the Southern Ocean. The green arrows represent the Sub-Antarctic Polar Front, the red arrows the Antarctic Polar Front with the direction of cold-water in blue and warm-water in orange. The dotted line around the Antarctic represents the Antarctic Circumpolar Current.

The Southern Ocean has a high heat capacity and affects the meridional overturning circulation, being important for redistribution of heat and freshwater in the global climate system (Giglio and Johnson, 2016). The aquatic environment is widely distributed in Antarctica and varies from fresh to hypersaline, mixed to stratified and from permanently ice covered to ice free (Wilkins et al., 2013).

Interannual variations of salinity in the Southern Ocean range between 33 and 34 in the practical salinity scale (Chaigneau and Morrow, 2002) and the pH is around 8 (Tynan et al., 2016). It occupies 10% of the world´s oceans and is rich in oxygen with levels (3.24-6.48 mg/L) almost 1.6-fold higher than in temperate waters (Robinson and Davison, 2008). This high oxygen content favours the formation of free radicals with the potential associated damage to marine organisms including fish (Chen et al., 2008; Song et al., 2016). Other water chemical properties can affect the marine organism's physiology, such as ion abundance and other metal compounds. Although the general ion content of the Southern Ocean is not well studied, there are reports on the abundance of magnesium (Mg^{2+}) and iron (Fe^{2+}) ions, as well as for heavy metals as mercury (Hg) and cadmium (Cd) (Bargagli, 2008; Seco et al., 2019; Thatje and Arntz, 2004). The high levels of Mg^{2+} have a relaxant effect on decapod crustaceans leading to a decrease of their metabolic rate (Thatje and Arntz, 2004). Since decapod crustaceans are only capable to regulate low levels of Mg^{2+}, it has been hypothesized that the high levels of Mg^{2+} together with the low seawater temperature are responsible for their lower diversity in the Antarctica region (Thatje and Arntz, 2004). Also, Fe^{2+} is important for primary production since this ion is required for the synthesis of chlorophyll and photosynthesis as well as for the reduction of several compounds namely carbon dioxide, sulphate and nitrate (Assmy et al., 2009; Brussaard et al., 2008; McBride et al., 2014) . Thus, Fe^{2+} is a key factor for phytoplankton growth resulting in an enhanced strength of the biological carbon pump, silica, and higher sequestration of atmospheric CO_2 in the deep ocean (Assmy et al., 2009; Brussaard et al., 2008; McBride et al., 2014). Natural Hg levels vary between 35 ± 0.39 pmol L^{-1} compared to other regions outside Antarctica (0.63 to 2.76 pmol L^{-1}) (Cossa et al., 2011). Marine organisms accumulate Hg with levels in Antarctic krill, *Euphasia superba*, 5 to 7 times higher in South Orkney islands than in South Georgia and the Antarctic Polar Front (Seco et al., 2019). Also, Cd is naturally elevated (approximately 0.7 nmol $^{-1}$) in Antarctic waters and several studies indicate the accumulation of this toxic metal in digestive organs of several marine organisms (Ahn et al., 1996; Choi et al., 2007). The vitellogenin gene was up-regulated in *Trematomus bernacchii*, possibly associated to elevated levels of Cd (Canapa et al., 2007).

1.2. The Antarctic microbiota

The marine microbiota is composed by a variety of microbes (e.g. bacteria, fungi, virus, and protists). In the Southern Ocean, bacterial microbiota dominate the biomass of different niches with functions ranging from primary production of energy (from CO_2) to colonization of the animals' mucosa where they participate in food digestion and immune defence (**Table 1.2**) (Sehnal et al., 2021; Wilkins et al., 2013). Most CO_2 is fixed by phytoplankton in the water column, transferred to higher trophic levels and exported to deep ocean (Henson et al., 2012). In some Antarctica regions, for instance in the Amundsen Sea, the organic carbon is recycled and mineralized in the water column via a microbial loop (Kim et al., 2019b).

There are evidences that 78% of bacterial operational taxonomic units (OTUs) are unique to the surface waters around Antarctica (Yau and Seth-Pasricha, 2019). The phyla most predominant in the surface seawater and at 200-400 m depth is Proteobacteria, mainly Gammaproteobacteria and Bacteroidetes, but at depth the diversity increases particularly in Actinobacteria, Deltaproteobacteria and Crenarchaeota (Kim et al., 2019b; Zhang et al., 2020a). The viruses are still largely unexplored in this polar region. It has been hypothesized they play a key role in the microbial loop through the lyses of the bacteria and consequently leading to changes in carbon and nutrient flow in the ecosystem (Säwström et al., 2007; Wilkins et al., 2013). Other study showed similar single stranded RNA (ssRNA) composition throughout the seasons with a predominance of several genera and families from Picornavirales order in Palmer station and Kaneohe bay and recently reported as responsible for viral infections in gentoo penguins (*Pygoscelis papua*) (De Souza et al., 2019; Miranda et al., 2016). In the Western Antarctica Peninsula, regional variation in lytic and lysogenic viral infections has been shown in prokaryotes, and it has been suggested that iron released by viral lysis is used for primary production (Evans and Brussaard, 2012). In Prydz bay, double stranded DNA (dsDNA) viruses are the most predominant, among them the Caudovirales (*Siphoviridae*, *Myoviridae*, and *Podoviridae*) are abundant in surface water and nucleocytoplasmic large DNA viruses (*Phycodnaviridae*, *Mimiviridae*, and *Pandoraviridae*) in bottom water (Gong et al., 2018).

1.3. The Antarctic fauna

The Antarctic fauna is known for having specific adaptations to the polar environment such as slow growth, gigantism, and higher longevity, especially in some invertebrates in deep waters, and the most well studied organisms will be highlighted. The slow growth (more than 20 years) can be found in most of the ectotherms such as the erect bryozoan *Cellarinella* nutti (Barnes et al., 2006). Abyssal gigantism is common among sea spiders (Pycnogonida), *Colossendeis* and *Ammothea*, and it has been hypothesized it is the result from a combination of low cold-driven metabolic rates and high oxygen availability (Shishido et al., 2019). Lastly, some organisms can achieve high longevity (> 100 years), such as the Antarctic bivalve *Cucullaea raea* (Buick and Ivany, 2004). In addition, there are examples of longevity combined to gigantism, for instance the polychaete *Aglaophamus trissophyllus*, the nemertine *Parborlasia corrugatus* and the bivalve *Adamussium colbecki* (Cronin et al., 2020; Davison and Franklin, 2002; Garraffoni et al., 2012).

1.3.1. Antarctic Notothenioids

The Antarctic fish fauna represents a small subset over than 33,000 teleost species thought to exist worldwide to date (FishBase; http://www.fishbase.org). It consists of 322 species of which 77% are grouped in 50 families from three Perciformes suborders i) the Notothenioidei, ii) the Cottioidei and iii) the Zoarcoidae (Eastman, 2005). The greatest number of species belong to the Notothenioidei and Cottioidei, which occupy the continental shelf (90%) and deep sea below 800 m and correspond to 90-95% of the fish biomass, respectively (Hu et al., 2016) (Eastman and Clarke, 1998; Stein, 2012). The Notothenioidei emerged after the Eocene, approximately 20-10 million years ago, radiated from a benthic ancestor and occupied different ecological niches (O'Brien and Crockett, 2013; Patarnello et al., 2011; Song et al., 2016). The Notothenioidei are divided in eight different families, Bovichtidae, Pseudaphritidae, Eleginopidae, Nototheniidae, Harpagiferidae, Artedidraconidae, Bathydraconidae and Channichthyidae (**Figure 1.2**). Four families (Nototheniidae, Harpagiferidae, Bovichtidae and e) also include non-Antarctic notothenioids that inhabit coastal waters of sub-Antarctic islands, South America, New Zealand, and Australia, such as *Notothenia angustata* (Nototheniidae), *Harpagifer bispinis* (Harpagiferidae) and *Champsocephalus esox* (Channichthyidae), with sister species in Antarctica (Matschiner et al., 2015).

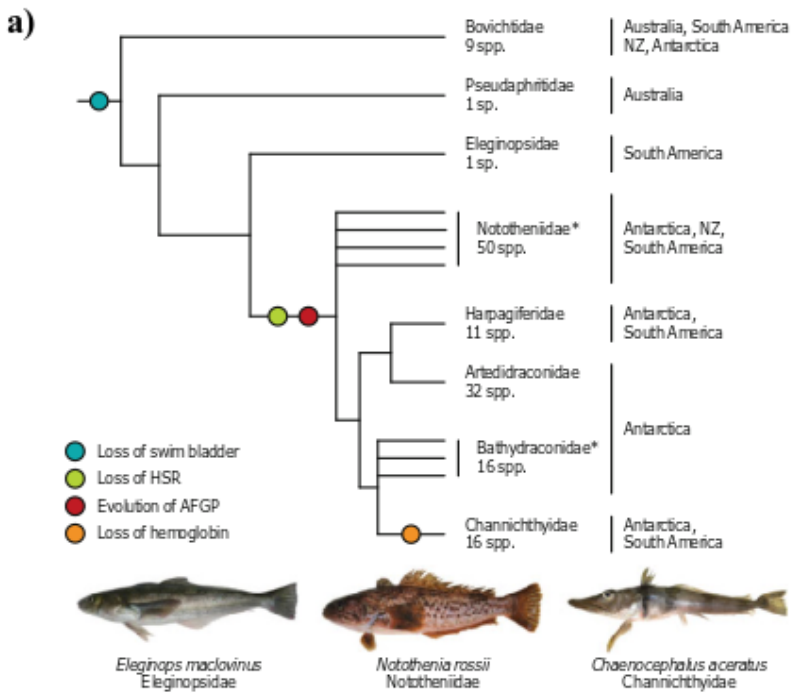

Figure 1.2. Simplified phylogenetic tree of Antarctic Notothenioid families and their distribution. The coloured circles highlight unique adaptations across families and family-specific adaptations [from (Matschiner et al., 2015)].

1

The biology of notothenioids was shaped by the cold-stable environment of Antarctica that drove physiological innovations allowing survival at sub-zero temperatures. Phenotypically, they vary in size, weight, body depth and skin colour. The Nototheniidae colonize a diversity of habitats, benthic, epibenthic, cryopelagic and pelagic and as a result also show a diverse diet, composed namely of euphausiids (krill), amphipods, salps and small fish, specially *Pleuragramma antarcticum* (La Mesa et al., 2004).

The single most important adaptation to the cold environment by notothenioids was the acquisition of antifreeze glycoproteins (AFGPs) which evolved from a pancreatic trypsinogen gene between 5 and 14 million years ago. The AFGPs decrease the freezing point of body fluids and avoid the rapid freezing of tissues and cells in contact with sea ice by inhibiting ice crystal formation and growth (**Figure 1.3**) (Matschiner et al., 2015). It has been hypothesized that is a case of convergent evolution, since AFGPs having evolved in at least seven species of the Gadidae family (from Arctic and temperate cold waters of the northern hemisphere) (Chen et al., 1997a). However, the origin of the gene in codfishes remains to be clarified but there are new evidences that different genomic processes lead to the genesis of AFGP in notothenioids and codfishes (Baalsrud et al., 2018) and the AFGP gene may be originated from non-coding

regions in codfish (Zhuang et al., 2019). Notothenioids also developed adaptations linked to buoyancy that allowed colonization and feeding over the whole water column. However, *Dissostichus mawsoni* and *Pleuragramma antarctica* are the only species neutrally buoyant (Fernández et al., 2012). Fish in this clade do not have a gas bladder, and buoyancy is achieved through reduced ossification (particularly evident in the scales) and increase of lipid deposits (subcutaneous and intermuscular) to decrease fish density and to generate static uplift (Wells and Eastman, 1994). Another adaptation is the lack of haemoglobin and erythrocytes which is unique in some species of the Channichthyidae (namely *Chionodraco hamatus* and *Chaenocephalus aceratus*) (Cocca et al., 1995; Ruud, 1954) and divided the notothenioids in two distinct groups: 1) the more abundant red-blooded notothens (such as *Notothenia coriiceps* and *Notothenia rossii*), , and 2) the white-blooded notothens which do not have red blood cells (Detrich and Amemiya, 2010). To compensate for the lack of red-blood cells, *Chionodraco hamatus* developed a larger heart (Hemmingsen et al., 1972) and a network of larger blood capillaries and vessels (Fitch et al., 1984). Other adaptations to extreme-cold are the absence of a heat-shock response, which is a cell stress response, despite several studies showing evidence for the presence of heat shock proteins (Hsp) and the constitutive expression of Hsp70 in two *Trematomus* spp. species under constant cold-stress (Place et al., 2004; Place and Hofmann, 2005b). Moreover, notothenioid fishes have specificities of microtubule assembly (Detrich et al., 2000), aerobic energy supply and higher mitochondrial density in muscle (Johnston et al., 1998; Pörtner, 2006).

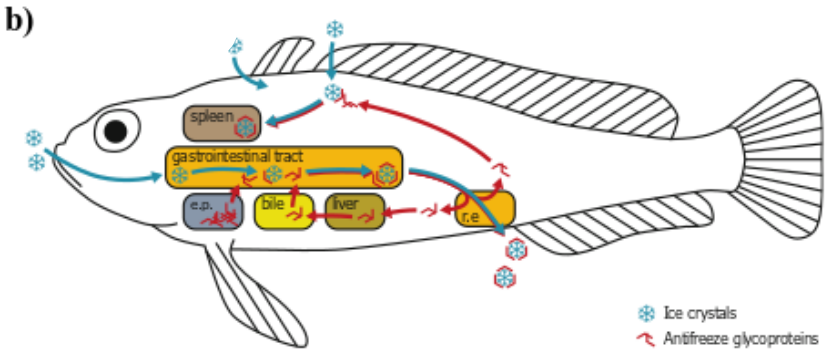

Figure 1.3. Schematic illustration of Antarctic notothenioid fish and the role of antifreeze glycoproteins (AFGP). The arrows elucidate the entry and transport of ice crystals in blue and AFGP pathways in red. The abbreviations indicate epithelium (e.p.) and rectum (r.e.).[from (Matschiner et al., 2015)].

The notothenioid fauna is now confronted with rapid environmental change due to climate change (IPCC, 2019) and this is most profound in the Antartica Peninsula, where the ice sheet is decreasing, and atmospheric temperatures have increased around 2ºC in the last 50 years (Cook et al., 2005). However, the evolution of notothenioids may have constrained their functional abilities to respond to thermal challenge as they are highly stenothermal (low tolerance to a wide range of temperatures (Bilyk et al., 2018).

1.3.1.1. *Notothenia coriiceps* and *Notothenia rossii*, Richardson 1844

N. rossii (also known as the marbled rockcod) is predominantly distributed at the northern and open areas of the Southern Ocean whereas *N. coriiceps* (also known as bullhead rockcod) is a coastal fish that can also be found at higher latitudes. Nonetheless these species are widely distributed, and their habitat overlaps in shallow coastal waters where *N. rossii* juveniles dwell before moving into open waters. These two species can be distinguished by the colour gradient of their skin which in *N. coriiceps* is yellow-black (**Figure 1.4**) with uniform colour or large dark patches on the dorso-lateral region while in *N. rossii* is grey-brown (**Figure 1.4**) with darker-lighter metallic-like spots. *N. coriiceps* is more sedentary (Casaux et al., 1990; Fanta and Meyer, 1998) and the growth rate is slower than *N. rossii* (Calì et al., 2017). *N. coriiceps* reaches a maximum length of 62 cm and estimated adult age between 2-16 years while *N. rossii* the estimated adult age and size is 6-18 and 92 cm (Calì et al., 2017; Merrett et al., 1992).

Figure 1.4. Photograph of *Notothenia coriiceps* captured off the Antarctica Peninsula, King George Island, Antarctica [photo Pedro M. Guerreiro].

Figure 1.5. Photograph of *Notothenia rossii* captured off Antarctica Peninsula, King George Island, Antarctica [photo Pedro M. Guerreiro].

Both in *N. coriiceps* and *N. rossii* the mature gonads (testis and ovary) can contribute to 40% of total body weight. They produce large eggs (4-5 mm in diameter) that possess positive buoyancy with an incubation time of three months. After hatching, they become pelagic for 6-8 months, then demersal in coastal waters until 6-9 years and mature *N. coriiceps* remain in these waters while *N. rossii* move offshore. Because of these characteristics, both *Notothenia* species are classified as semipelagic (Barrera-Oro et al., 2014; Eastman et al., 2011; Kock and Kellermann, 1991).

N. coriiceps feeds on a diversity of benthic organisms whereas *N. rossii*'s diet also include demersal preys such as krill, salp and fish, and are more active in periods with more luminosity (Donatti et al., 2008). *N. rossii* is an important fisheries and the increase in commercial fishing led to the depletion of native fish stocks in the 1970s, and consequently may have induced changes in population structure and life history traits (Calì et al., 2017). Today, fishing is prohibited under the Antarctic Treaty and Convention for the Conservation of Antarctic Living Resources (Calì et al., 2017; Donatti et al., 2008; Hureau J.C., 1970).

1.4. The immune system

The immune system is a set of processes that defend the organisms against foreign potential pathogens such as bacteria, virus, and fungi. This complex system is divided in non-specific (or innate) and specific (or acquired/adaptive) responses, and both immune defence mechanisms can be subdivided in humoral and cellular components that vary between innate and acquired immunities. A comparison between several humoral factors revealed that they have generally been conserved during vertebrate evolution, but species-specific evolutionary adaptations have also occurred (Huising et al., 2006).

1.4.1 The immune system of teleost fish

In last 300-450 million years, teleost fish diverged from the lineage giving rise to the mammals , hence significant differences of the immune system, at cellular and molecular levels are observed between fish and mammals (Volff, 2005). Teleost fish have developed an effective immune system, though less complex compared with mammals and without bone marrow or a lymphatic system. However, the teleost fish head-kidney is analogous to the mammalian adrenal gland as the principal hematopoietic organ, comprising immune cell production and endocrine cells that produce hormones linked to stress, catecholamines and steroids (mainly cortisol) (Geven and Klaren, 2017). It is generally assumed that the innate immune defence is more developed in fish and the acquired immunity is more developed in mammals. However, fish also possess B cells and immunoglobulins of adaptive immunity that are suggested to have appeared late and to be more developed in marine species than freshwater species (Chantanachookhin et al., 1991; Magnadottir et al., 2005).

The immune response is influenced by both intrinsic factors, such as immune cell repertoire, and extrinsic factors such as temperature, stress, food, pH, salinity, and oxygen availability. This makes the ecosystem a key factor in determining the immune response, and for ectotherms that do not regulate their body temperature, the environment may play a large role in the immune capacity and response. The high microbial load and pathogens (such as bacteria, fungi, viruses and parasites) that fish are exposed to is proposed to have shaped the evolution of their immune systems (Groff, 2001). For instance, 1 mL of seawater typically contains 10^6 bacteria and 10^8 viruses which can be even higher if the organic content is high (Tort et al., 2003; Uribe et al., 2011).

In several species of teleosts – e.g., rainbow trout (*Oncorhynchus mykiss*), catfish (*Ictalarus punctatus*), zebrafish (*Danio rerio*) and Argentine seabass (*Acanthistius brasilianus*) - the ontogeny of the immune system has been described for kidney, spleen and thymus and these tissues were proposed as primordial models of hematopoiesis, which is the process of formation and maturation of blood cells from the same precursor (Magnadottir, 2010; Magnadottir et al., 2006). However, the fish immune defence mechanisms are relatively poorly characterized compared to those of terrestrial vertebrates and even less in teleost fish of polar regions. Some studies suggest that low temperature habitats may increase the efficacy of non-

specific responses, namely in the respiratory burst of phagocytes (Ainsworth et al., 1991; Collazo et al., 1994), macrophages (Le Morvan et al., 1998) and activity of cytotoxic cells (Le Morvan-Rocher et al., 1995). However, other studies described that lower seawater temperatures may contribute to the slower innate immune response in cold-water fish compared to temperate fish species (Abram et al., 2017; MacKenzie et al., 2008; Magnoni et al., 2015; Tort et al., 2003).

1.4.2. Innate immunity

The innate immunity provides the basic immune defence of vertebrates and is the only type of immunity present in lower animals. It involves physical barriers, humoral and cellular components that responds immediately or within hours to stimulation by foreign pathogens. In teleost fish, the physical barriers include skin, intestine and gills which are protected by a body fluid called mucus and a microbial community. The humoral response is mediated by antimicrobial proteins and peptides (APPs), such as lysozyme, cytokines and anti-proteases, secreted by several bone marrow derived immune cells, such as neutrophils and mast cells, and pathogen recognition receptors (PRRs) who recognize antigens and pathogens-associated molecular patterns (PAMPs)(Gomez et al., 2013; Soulliere and Dixon, 2017). The PRRs survey the host/environment and include toll-like-receptors (TLRs), C-type lectin receptors, RIG-I-like receptors, and NOD-like receptors that are encoded in the germline of vertebrate host cells (Brubaker et al., 2015; Thaiss et al., 2016b) and the PAMPs typically involved in pathogenesis, include polysaccharides, lipopolysaccharides (LPS), peptidoglycan bacterial DNA, viral RNA (e.g. the synthetic analogue polyinosinic:polycytidylic acid, poly I:C) (Magor and Magor, 2001; Moresco et al., 2011; Uribe et al., 2011; Zhu et al., 2013). The cellular response is a cellular immunity mediated by different types of leucocytes, neutrophils, eosinophils, basophils, macrophages, dendritic cells, undifferentiated lymphocytes, natural killer (NK) cells and mast cells (Buchmann, 2014; Kindt et al., 2007; Magnadóttir, 2006) (**Figure 1.6**).

Several approaches have been applied to the study of innate immune in different fish species such as enzymatic assays (lysozyme, antitrypsin and anti-macroglobulin activities) and other immune parameters in blood plasma (ion content, haematocrit and blood cell counts) and immune tissues (such as ion content), cell culture and analysis of gene expression of immune tissues (RNA-seq and quantitative polymerase chain reaction).

1

2

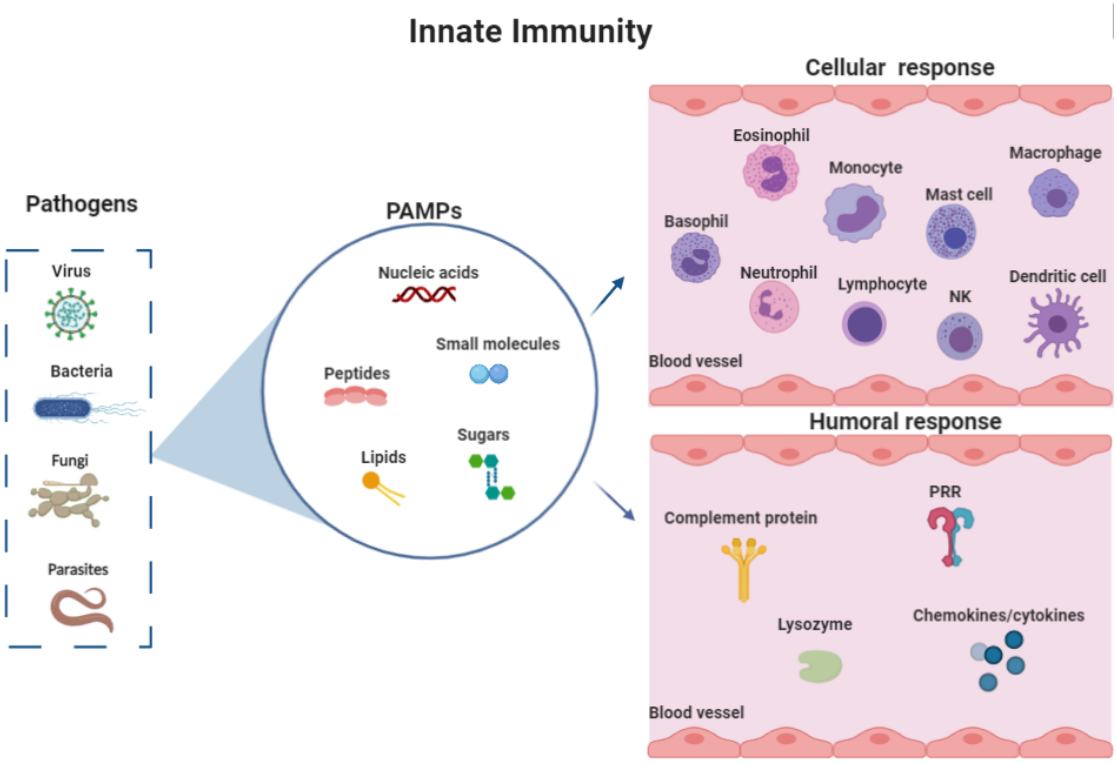

3

Figure 1.6. Illustration of the link between pathogen stimulus and the innate immune response of the host. The potential pathogens (virus, bacteria, fungi, parasites) possess pathogen-associated molecular patterns (PAMPs) such as nucleic acids, peptides, small molecules, lipids, and sugars. They induce the activation of innate immunity which is divided into the cellular response, resulting from leukocyte activation including eosinophil, neutrophil, basophil, macrophage, monocyte, mast cell, dendritic cells, lymphocytes, and natural killer (NK) cells) and humoral response such as complement protein, lysozyme, chemokines/cytokines and pathogen recognition patterns (PRR), namely toll-like receptors [BioRender software 2021 was used to prepare this illustration].

1.4.2.1. Physical Barriers

The fish epithelia are the first physical and chemical protection barriers against pathogens and are more important in innate immune defence in fishes than in terrestrial vertebrates because they are in permanent contact with an environment that has high microbial load (Verschuere et al., 2000). The innate immune system has various barrier components:

The mucosa-associated lymphoid tissues (MALT) are located along the surfaces of all mucosal tissues and possess approximately half of lymphocytes of the immune system. In mammals, the best well-known representatives are gut-associated lymphoid tissue (GALT), skin-associated lymphoid tissue (SALT), nasopharynx-associated lymphoid tissue (NALT) and bronchus-associated lymphoid tissue (BALT). The larynx-associated (LALT), salivary duct-

associated (DALT), conjunctiva-associated (CALT) and lacrimal duct-associated lymphoid tissue (LDALT) have also been described (Cesta, 2006; Kindt et al., 2007).

In mammals, the GALT possesses antigen transporting M cells and Peyer´s patches as well as several different immunoglobulin (Ig) isotypes in mucosal secretions, namely immunoglobulin A (IgA), immunoglobulin M (IgM) and immunoglobulin G (IgG). In teleost fish, the most representative MALT is SALT, NALT, GALT and gill-associated lymphoid tissue (GIALT) (Salinas, 2015) (**Figure 1.7**).

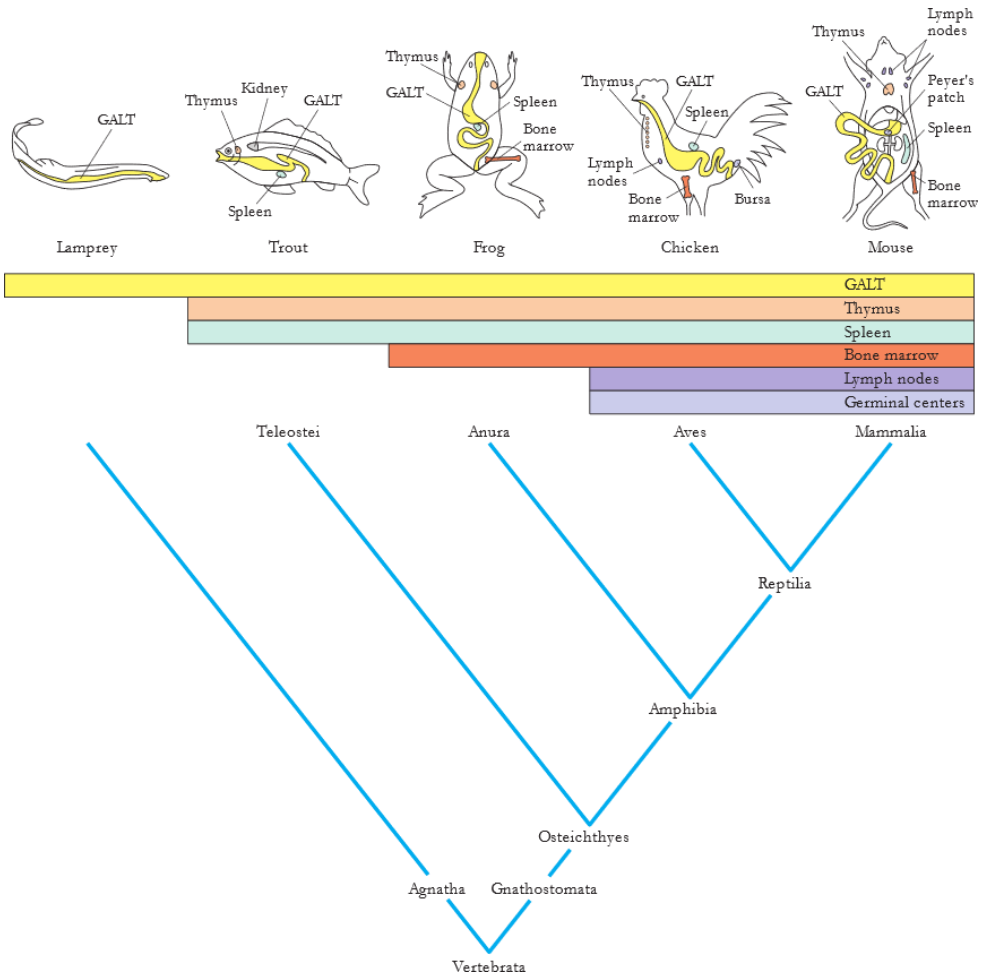

Figure 1.7. Schematic representation of the appearance of mucosa-associated lymphoid tissues and other immune tissues in vertebrates [from (Kindt et al., 2007)].

SALT is considered the most ancient in vertebrates and possess IgM and immunoglobulin T (IgT) or Z (IgZ), depending on the species, which are considered homologous of mammalian IgA (MacPherson et al., 2008), and a secretory Ig receptor (sIgR)

which is teleost fish specific (Rombout et al., 2014). The MALT of both mammals and teleost fish contain B cells (with Igs) and T cells (such as CD4 - helper and CD8 – cytotoxic and cells with TCRαβ and TCRγδ) and the abundance is similar in both (Gomez et al., 2013; Salinas et al., 2015; Toda et al., 2011).

The skin is the largest barrier organ and protects animals against external stressors. In all vertebrates the skin structure is similar and composed by the epidermis and dermis layers and have the same embryonic origin, respectively, in the ectoderm and in the mesoderm (Kanitakis et al., 2002). Nonetheless, histological difference exists depending on the specific vertebrate adaptation, either to a water-containing environment, such as the fish skin, or to a dry-land environment, such as mammalian skin. Teleost fish usually possess scales that have multiple functions, for example in the regulation of wave propagation, acting as an external tendon and with inherent hydrodynamic properties that are important to fish locomotion and swimming efficiency (Vernerey and Barthelat, 2014). Also, teleosts have a skin lacking keratinization and contain several immune cells (such as dendritic cells, macrophages, B cells and mast cells) and several humoral components (IgT, IgM and antimicrobial peptides) (Esteban and Cerezuela, 2015) (**Figure 1.8**).

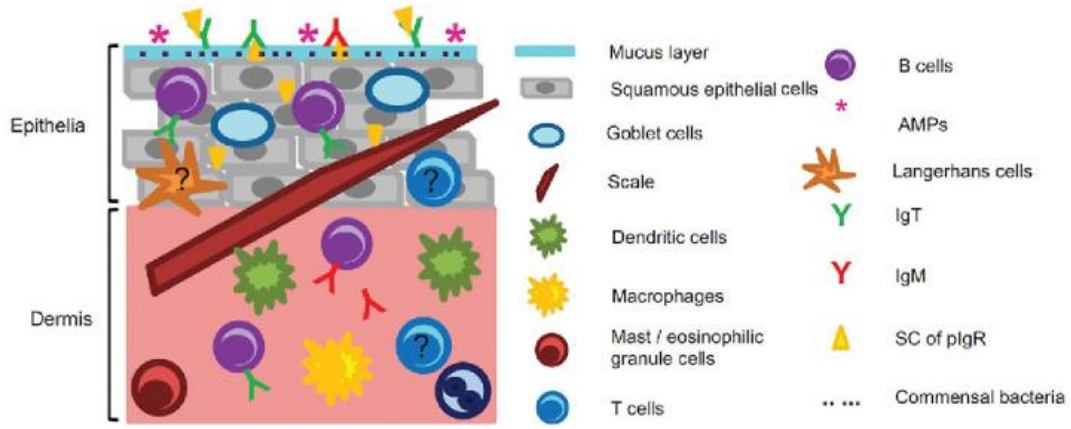

Figure 1.8. Schematic representation of teleost fish skin structure and its cellular and humoral components. AMPs indicates antimicrobial peptides, SC of pIgR indicates secretory polymeric immunoglobulin receptor and (?) indicates cells that are hypothesized to be present, however not proven until now [from (Esteban and Cerezuela, 2015)].

The intestine (or gut) is divided in three segments based on histology. The first segment or the anterior gut or foregut contains the absorptive cells or enterocytes. The second segment or the posterior gut contains large supranuclear vacuoles in the enterocytes, indicating high

pinocytotic activity, and an irregular microvilli zone. The third segment or hindgut has abundance of enterocytes with osmoregulatory capability (Rombout Jan et al., 2011). Generally, the teleost fish gut structure is composed of a mucus layer and columnar epithelial cells that contain goblet cells and may contain M-like cells. Also, the gut contains granulocytes, mast cells, T and B cells and antimicrobial peptides (Gomez et al., 2013). Detailed knowledge of the lymphocyte subsets distribution and the proportion of different secretory immunoglobulins is scarce in fish (Salinas et al., 2011, 2015), although there are studies that indicate a principal role of the second intestinal segment in the transport of antigens to the local and systemic lymphoid tissues. It has been suggested that the thymus and the intestine were the first organs to be populated with T cells in fish larval stages and only later the head-kidney and spleen (Rombout et al., 1985, 1989; Rombout Jan et al., 2011). In teleost fish the study of the bi-directional communication between brain and gut is more recent than in mammals and it has also been suggested in *Danio rerio* to be an important immune barrier. The two organs exchange reciprocal signals to coordinate function, namely immune mediators and mediators of environmental variables affecting fish behaviour and stress coping (Davis et al., 2016; Wang et al., 2016b) (**Figure 1.9**).

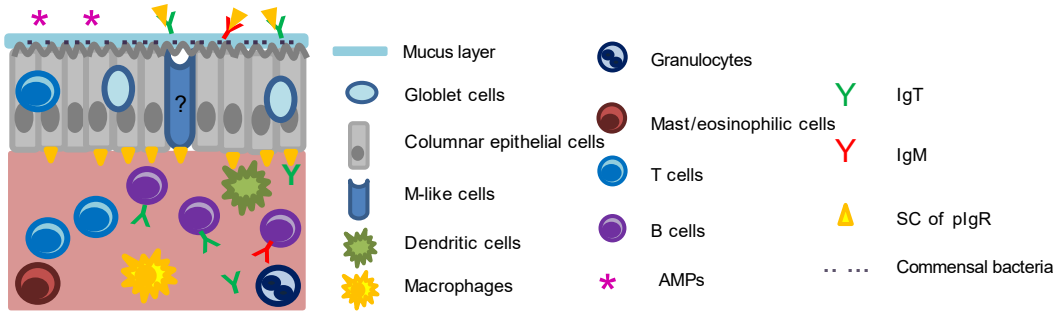

Figure 1.9. Schematic representation of teleost fish gut structure and its cellular and humoral components. AMPs indicates antimicrobial peptides, SC of pIgR indicates secretory polymeric immunoglobulin receptor and (?) indicates cells that is hypothesized to be present, however not proven until now [Adapted from (Gomez et al., 2013)].

The gills are an osmoregulatory organ but also contains some immune cells. This physical barrier is also a potential portal for the entrance of pathogens and a route for in vivo antigen uptake similar to skin and gut, since both organ barriers are in permanent contact with the aquatic environment. The histological structure is composed of a mucus layer and squamous epithelial cells with goblet cells and several immune cellular components (macrophages, dendritic cells, macrophages, granulocytes, agranulocytes, B and T cells) and humoral

components (antimicrobial peptides, IgT and IgM) according to the microbial community that inhabit the gills. However, the gills are not well studied as skin and gut and its importance in the immune defence need further studies (Gomez et al., 2013) (**Figure 1.10**).

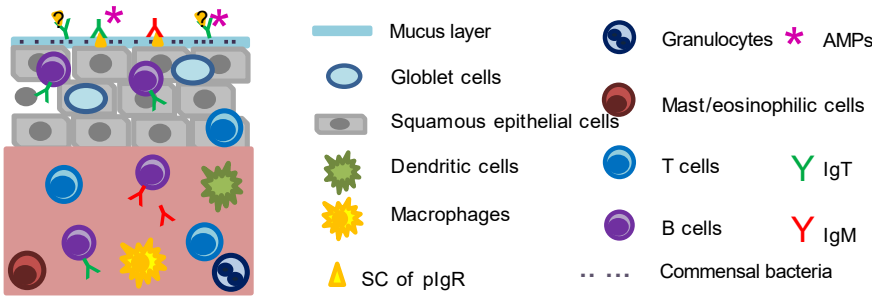

Figure 1.10. Schematic representation of teleost fish gill structure and its cellular and humoral components. AMPs indicates antimicrobial peptides, SC of pIgR indicates secretory polymeric immunoglobulin receptor and (?) indicates cells that are hypothesized to be present, albeit not proven until now [Adapted from (Gomez et al., 2013)].

The mucus present in mucosal barriers provides protection against pathogens and the predominant molecules are mucins. The mucins are glycoproteins produced by goblet cells with O-glycan attachment sites in skin and gut. Other immune relevant factors in mucous include the proteins lysozyme, lectins, calmodulin, immunoglobulins, complement, C-reactive proteins, proteolytic enzymes and antimicrobial peptides (Ángeles Esteban, 2012). The mucin composition differs between species in its protective ability, transport, viscoelasticity and adhesion (Johansson et al., 2011). The intestine of mammals and teleost fish possess similarities in their mucosal surfaces which is composed of two layers, an outer layer composed of the microbiota and the inner layer is the mucin rich mucous. In skin of higher vertebrates, 20 mucin genes have been characterized. However, the mucins remain poorly studied in teleost fish intestine. The studies that exist indicate large, secreted gel-forming mucin 2 (*muc2*) and mucin 5 subtype B (*muc5B*) in teleost fish mucosa. In *Cyprinus carpio*, *muc2* is more expressed in intestine and *muc5B* is more expressed in skin. Furthermore, in *Sparus aurata*, the membrane-bound mucin 18 (*muc18*) was identified in skin and gut mucous and suggested to respond to parasite infections by increasing the glycosylation levels and terminal glycosylation of mucous proteins to decrease the adherence of pathogens (Pérez-Sánchez et al., 2013; van der Marel et al., 2010). The large gel-forming glycoprotein mucin 5 subtype AC (*muc5AC*) and also *muc18* transcripts were reported in the *Salmo trutta m. trutta* transcriptome (Malachowicz et al., 2017). In *Hippoglossus hippoglossus* larvae skin transcriptome, the *muc18* and *muc24*, *muc5B*, *muc5AC* and intestinal mucin (*imuc*) genes were also identified (Alves et al., 2018).

The Microbiome represents the nucleic acid sequences of a collection of microscopic microorganisms such as bacteria and virus (Liu and Jiang, 2020). Microbiome studies in fish have increased significantly with the availability of high throughput sequencing and metagenomics using 16S rRNA and several bacterial genome regions (such as V3-V4 region) that allow the global bacterial microbiome to be covered (Bukin et al., 2019; Onywera and Meiring, 2020). The microbiome is diverse and varies between ecosystems oscillating according to intrinsic factors (such as genetic background, reproduction and age) and extrinsic factors (such as nutrients diets, season and water quality) (Butt and Volkoff, 2019; Campbell et al., 2011; Franchini et al., 2014; Vergara et al., 2007) (**Figure 1.11**). Teleost fish are good models to study vertebrate host-symbiont relationships owing to the ease of rearing and more limited bacterial diversity than mammals (Gallet et al., 2019). The fish microbiome that colonizes the epithelial barriers is crucial for homeostasis and immune defence against potential pathogens and the skin and gut are the best studied barriers (Butt and Volkoff, 2019; Callewaert et al., 2020).

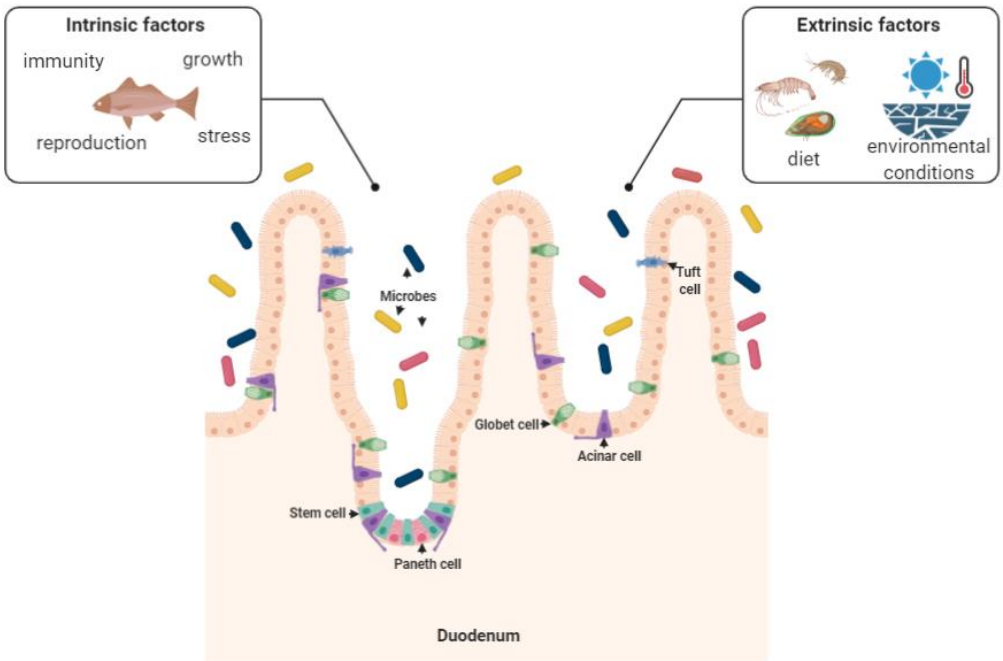

Figure 1.11. Schematic representation of an Antarctic fish gut microbiome. The duodenum epithelial barrier is represented as well as potential extrinsic and intrinsic factors that may affect the gut microbial diversity [BioRender software 2021 was used to prepare this illustration].

In the Southern Ocean, several studies have been performed on the skin microbiome, particularly in whales (Bierlich et al., 2018) and in teleost fish from the suborder Myctophiformes (Gallet et al., 2019). The dominant bacteria phyla in Antarctic fish skin belong to the Proteobacteria (class Gammaproteobacteria) and the Firmicutes (class Mollicute) (Gallet et al., 2019). This is similar to what was also described in teleosts from temperate waters such as *Dicentrarchus labrax* and *Sparus aurata* (Llewellyn et al., 2014; Rosado et al., 2019). Also, studies on the Notothenioidei found Actinobacteria (e.g. genus *Corynebacterium*), Proteobacteria (e.g. photobacterium genus), Firmicutes (e.g. clostridium genus), Thermi and Bacteroidetes (e.g. flavobacteriaceae genus) as the most abundant phyla in the gut of *Trematomus bernacchii*, *Chionodraco hamatus*, *Gymnodraco acuticeps* and *Pagothenia borchgrevinki* (Song et al., 2016; Ward et al., 2009). However, a comparison between the gut and skin microbiomes of the same individuals revealed significant differences, and the gut seems to have less bacterial diversity than the skin (Gallet et al., 2019). In addition, the microbiome differs between the four Antarctic species above suggesting a specific bacterial community linked to habitat, depth and diet (Silva et al., 2011; Song et al., 2016; Ye et al., 2014). However, there is also a common bacterial community (30%-40% of the total) between the four species that are related to the Antarctic environment. Also, the bacterial communities in gill, fin and gut of three Mycophida from the genera *Electrona*, *Protomyctophum* and *Gymnoscopelus* revealed low diversity and the dominant taxa present in the three tissues were Gammaproteobacteria and Mollicutes (Gallet et al., 2019). Another study targeting the gut of *N. coriiceps* and *C. aceratus* also indicated low diversity with a predominance of Gammaproteobacteria (Ward et al., 2009).

1.4.2.2. Humoral response

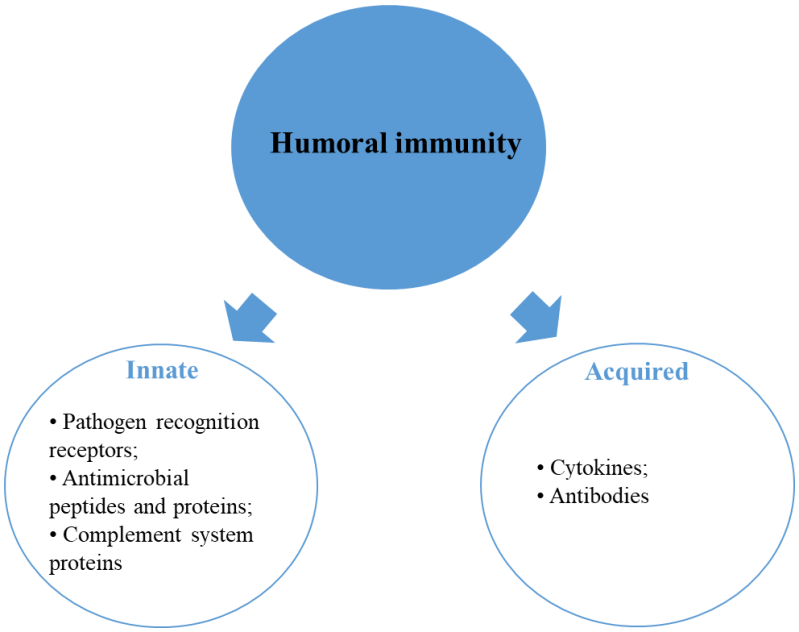

Figure 1.12. Schematic representation of the humoral components involved in innate and acquired immunity.

The humoral response is present in both innate and acquired immunity. The humoral immunity involves macromolecules present in extracellular fluids (such as mucous and blood), the innate immune defence includes antimicrobial peptides, complement proteins and other proteins and in acquired immune defence includes the cytokines and antibodies (**Figure 1.12**).

Transferrin is an iron-binding blood glycoprotein, which regulates the availability of free iron by chelating activity and iron transport. The level of this glycoprotein in the blood is considered a good indicator of the immune response to bacterial infection in teleost fish because bacteria have high capacity for iron absorption, iron that is required for their growth and multiplication (Ellis, 2001; Liu et al., 2012; Martínez et al., 2020; Stafford and Belosevic, 2003).

Hepcidin is a key regulator of iron entry and an antimicrobial peptide (AMP) with a role in the innate immune defence against pathogens (Krause et al., 2000; Park et al., 2001). This AMP was initially discovered in humans and subsequently in fish, birds and reptiles. The gene sequence and protein structure of hepcidin is conserved from fish to mammals (Wang et al., 2005). A gene family expansion in teleost fish resulted in seven hepcidin genes compared to two in mammals. The liver is the organ with the highest expression of hepcidin, although low levels are also detected in other tissues. Hepcidin blood levels are also considered to be a good indicator of immune response to bacterial exposure (Pigeon et al., 2001; Yang et al., 2007).

Lysozyme is an important enzyme of the innate immune response and protects against pathogen invasion through its lytic activity. It hydrolyses β-[1,4] linked glycoside bonds in the cell wall of Gram positive bacteria. It is considered one of the main anti-bacterial molecules in fish and its activity is induced rapidly by bacteria and conditions such as stress (Demers and Bayne, 1997; Douxfils et al., 2011; Saurabh and Sahoo, 2008; Wang et al., 2005). Lysozyme also lyses gram negative bacteria (Jollès and Jollès, 1984; Magnadóttir et al., 2002) and it is proposed to activate the complement system in fish blood (Bayne and Gerwick, 2001; Yada et al., 2008). This enzyme is synthetized mainly in the liver and extra-hepatic sites but it is also present in other tissues such as spleen and other components such as mucus and plasma (Saurabh and Sahoo, 2008). Cellular components of the immune system are also, responsible for the production of lysozyme, namely leucocytes, monocytes, macrophages and neutrophils. Recently, a variable number of human homologues of lysozyme C-type and G-type were identified in fish (Li et al., 2021b).

The cytokines are small proteins important for immune cell signalling that modulate the humoral and the cellular immune responses against pathogens and directly or indirectly mediate immune surveillance, growth, developmental and repair processes. The cytokine family includes chemokines, interferons (IFNs), interleukins (IL), tumour necrosis factor (TNF), peroxidases (PO) and lymphokines. The IFNs are important against viral infection, enhance MHC activation and regulation of the immune system. They are divided in three main types: type I such as IFN alpha (IFNα), type II such as IFN gamma (IFNγ) and type III such as interferon receptor lambda 1 (INFLR1). The chemokines are signalling molecules that induce chemotaxis in nearby cells and their major role is to guide the migration of cells, including monocytes/macrophages, mast cells, eosinophils, neutrophils and T-lymphocytes (Ono et al., 2003; Xie et al., 2003). Phytohemagglutinin (PHA), a mitogen from fish leucocytes is reported to increase the migration of leucocytes (Bridges and Manning, 1991; StG Howell, 1987), whereas migration inhibition factor (MIF) decreases their migration (Chang et al., 2008). The interleukins are involved in the development and differentiation of B and T cells, as well as other hematopoietic cells (Ben Menachem-Zidon et al., 2011; Brocker et al., 2010). Most types of cytokines are secreted by helper CD4 lymphocytes, monocytes/macrophages, and endothelial cells. This is the case of the interleukins that are a large gene family and encode proteins with different functions in the immune system. The first identified and best studied is interleukin-1 (IL-1) which is produced by macrophages after activation of host pattern recognition receptors (PRRs) by danger associated molecular patterns (DAMPs) or PAMPs.

Interleukins mediate the inflammatory response and are involved in cell proliferation, differentiation and apoptosis(Angosto et al., 2012; Chaves-Pozo et al., 2004; Pelegrín et al., 2004; Vojtech et al., 2012). IL-1β gene expression is induced by LPS, and it is one of the cytokine specific-responses in several fish species including *Dicentrarchus labrax* and *Sparus aurata* (Buonocore et al., 2006; Engelsma et al., 2001; Hong et al., 2001; Zou et al., 1999).

Protease inhibitors present in fish plasma include α-1-antitrypsin, α-2-antiplasmin and α-2-macroglobulin. Trypsin is a serine protease, highly specific for the hydrolysis of peptide bonds involving arginine and lysine residues, present in pancreatic tissue and acts in the digestive tract in vertebrates (Baird, 2013; Lemieux and Blier, 2007; Rackis, 1965). Trypsin has been characterized in marine fishes such as Japanese anchovy (*Engralius japonicus*), tropical sierra (*Scomberomorus concolor*) white leg shrimp (*Litopenaeus vannamei*) and Atlantic salmon (*Salmo salar*). It has a fast rate of autolysis, high catalytic efficiency at low temperatures, sensitivity to denaturation at high temperatures and lower optimal pH relative to mammalian form. The inhibitors α-1-Antitrypsin (the most stable) protects tissues from trypsin released from cells associated during inflammation and α-2 macroglobulin (α-2M, the most versatile) is the trypsin inhibitor best known in fish and both respond to bacterial challenges (Baird, 2013; Lemieux and Blier, 2007; Rackis, 1965). These two inhibitors are produced in the liver but also in cells from other tissues such as phagocytic cells (macrophages), fibroblasts and adrenocortical cells (Christybapita et al., 2007; Freedman, 1991; Hanif et al., 2005; Law et al., 2012).

Pentraxin-like proteins are a group of evolutionary conserved proteins which include C-reactive protein (CRP) and serum amyloid protein A (SAA), both of which are associated with the acute inflammatory response of the innate immune system. They are present in body fluids of vertebrates and invertebrates and in vertebrates they are predominantly synthetized in the liver in response to a tissue damage or injury (Armstrong, 2015; Roy et al., 2016). Several studies have reported the expression of CRP in teleost fish such as *Ictalarus punctatus* (Szalai et al., 1994), *Hoplias malabaricus* (Lund and Olafsen, 1998), *H. hippoglossus*, *Gadus morhua*, *Salmo salar* and *Oncorhynchus mykiss* (Hoover et al., 1998). Also, the pentraxins are suggested to play a role in the activation of the classical complement pathway (De Haas et al., 2000) and in the elimination of apoptotic cells (Nauta et al., 2003). CRP is constitutively expressed is most tissues, although some CRP/SAA are not transcribed in response to bacterial infections in some teleosts including the *S. salar* (Lund and Olafsen, 1998) and *Salvenilus alpinus* (Jensen et al., 1997). However, in *C. carpio* a CRP/SAAs response to *Aeromonas hydrophila* was observed

but not to *Escherichia coli* which is suggestive of species-specificity to bacteria (MacCarthy et al., 2008).

The complement system plays an important role in bacterial recognition and, consequently, in initiating the inflammation process through the lyses of bacterial cells (Ellis, 2001). The complement system is composed of three pathways: classical, alternative and lectin. The classical pathway starts by a complex antigen-antibody and then by the binding of IgG to the C1q component of C1 complex. The alternative pathway involves C3 activation through microbial surfaces (Boshra et al., 2006). The lectin pathway involves interactions with lectins and sugar moieties present on the surface of pathogens (Fujita et al., 2004). A recent study indicates that fish possess several active C3 isoforms: *Oryzias latipes* has 5 C3 isoforms, *S. salar* has 4, *S. aurata* has 9 isoforms, *Cynoglossus semilaevis* has 3 isoforms and *Latimeria chalumnae* has 2 isoforms (Najafpour et al., 2020). The alternative pathway seems to be more important in fish owing to the presence of more C3 isoforms compared to one isoform identified in *Homo sapiens*, and the presence of multiple isoforms is suggestive of enhanced capacity to activate the complement system against pathogenic microorganisms in fish (Najafpour et al., 2020; Sunyer and Tort, 1995; Tort et al., 2003).

1.4.2.3. Cellular response

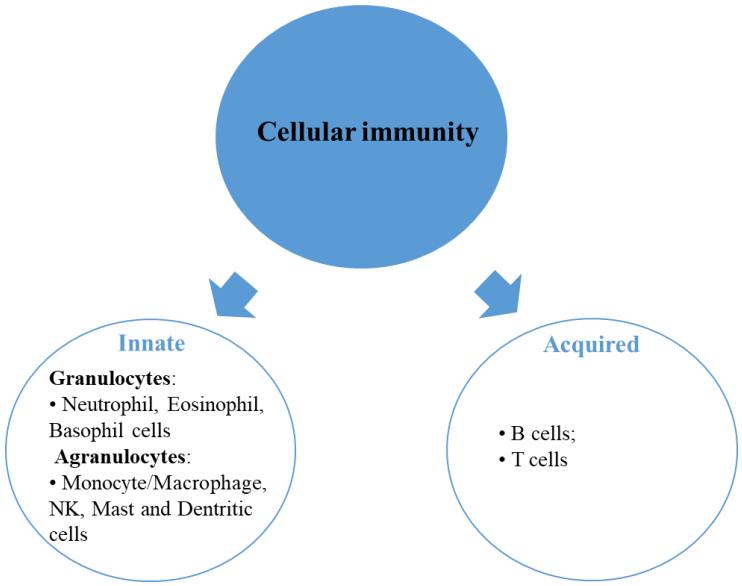

Figure 1.13. Schematic representation of the cellular components involved in innate and acquired immunity. NK indicates natural killer cells.

The most abundant immune cells are granulocytes, dendritic cells and natural killer cells in innate immunity and B and T cells in acquired immunity (**Figure 1.13**). The granulocytes include neutrophils, eosinophils, basophils and mast cells and in fish they are identified based on morphological, histochemical and ultrastructural similarities with mammalian cells (Hine and Thorne, 1997; Rowley et al., 1988) and the developing granulocytes are limited to hematopoietic organs. The nature, presence, and function of certain immune cells in teleost fish remain unclear and may be the cause of controversy as in the case of eosinophils, basophils, and mast cells (Reite and Evensen, 2006).

Neutrophils are the most abundant leukocytes in circulation in mammals (40%-70%) but they are less than 5% in teleost fish (Hamdani et al., 1998; Havixbeck and Barreda, 2015; Sasaki et al., 2002) and can vary in morphology according to species (Parish et al., 1986). These cells have multilobed nuclei, are short lived and highly motile to be capable to migrate into tissues with phagocytic activity. Also, they use pathways dependent and independent of oxygen to produce antimicrobial peptides and generate reactive oxygen and nitrogen species by increased respiratory burst activity compared to macrophages (Kindt et al., 2007).

Eosinophils have bilobed nucleus and phagocytic activity in teleost fish (Ellis, 1977). This type of granulocyte provides immune surveillance, contributes to T lymphocyte-mediated humoral immune responses and are associated to the response against parasites, particularly helminths, similarly to mammals (Balla et al., 2010; Huizinga and Nadakavukaren, 1997; Kindt et al., 2007).

Basophils are the largest type of granulocyte and possess numerous granules in the cytoplasm. These cells do not have phagocytic activity, are less abundant in circulation and are associated to certain allergic responses in mammals (Kindt et al., 2007). In most teleost species, basophils are rare and their function remains to be clarified (Ainsworth, 1992).

Mast cells have large numbers of granules in the cytoplasm and are related to allergic reactions in mammals. Although the products released from these cells are not well-known they are thought to be involved in the inflammatory response and react against several pathogens, similarly to mammals (Kindt et al., 2007; Reite and Evensen, 2006; Sfacteria et al., 2015).

Dendritic cells are characterized by long membrane extensions and antigen-presenting cells originated from a circulating monocyte precursor. They are present in several tissues and are especially abundant in mucosal surfaces. These cells express a wide range of PRR and are considered a messenger between innate and acquired immunities. They have the capability to

internalize antigens and present them to the major histocompatibility complex (MHC) I and II and thus to T cells (Bassity and Clark, 2012; Soleto et al., 2018).

Macrophages are also originated from circulating monocytes under inflammatory conditions and intermediates antimicrobial defence with phagocytic properties. There are several macrophage phenotypes (M1 and M2) and knowledge of their functions are derived from mammalian models. In teleost fishes, the best characterized phenotype is M1, which induces a diverse cytokine, chemokine and lipid mediators against foreign pathogens through phagocytosis and nutrient deprivation. However, the molecular mechanisms related to depolarization and function remains to be fully clarified (Grayfer et al., 2018; Hodgkinson et al., 2015).

NK cells are large granular lymphocytes with non-specific cytotoxic function by two mechanisms (granule exocytosis and FasL/Fas interaction) to target cell recognition and to lyse target cells in both fish and mammals. The NK cells have been extensively studied in teleost fish and their function is not restricted to MHC. They vary morphologically and functionally between species (Evans and Jaso-Friedmann, 1992; Fischer et al., 2013).

Natural antibodies (also known as natural IgM) are present at high levels in teleost fish. They are transferred from mother to embryo and their production is stimulated after to environmental antigens (Mor and Avtalion, 1990; Smith, 1940). Natural antibodies protect against several antigens, provide immediate defence against bacteria and viruses and they have a role in homeostasis maintenance (Boes, 2000; Whyte, 2007).

1.4.2.3.1. Cellular receptors

Based on their localization, PRRs are divided into membrane-bound PPRs, that includes the TLR and C-type lectin receptor (CLRs) groups, and cytoplasmatic PRRs, that include the nucleotide oligomerization domain (NOD)-like receptors (NLRs or NOD-like), retinoic inducible-gene 1 (RIG1)-like receptors (RLRs), and melanoma (AIM)-like receptors (ALRs) (absent in fish). Several immune cells possess these PRRs namely neutrophils, monocytes, macrophages and dendritic cells which recognize distinct pathogen components such as polysaccharides, lipopolysaccharides, peptidoglycan bacterial DNA and viral RNA.

TLRs are phylogenetically ancient and well conserved across vertebrates and respond to several PAMPs. TLRs are the best characterized innate immune receptors and may be subject to strong selective pressure under extreme conditions (Solbakken et al., 2016). The TLRs have a conserved structure and are composed of a type-I transmembrane protein containing extracellular leucine-reach repeat (LRR) domains, an intracellular toll-interleukin-1 receptor (TIR) domain, a LRR-carboxy domain (LRR-CT), a LRR- amino terminal domain (LRR-NT) and transmembrane regions (TM) (Botos et al., 2011; Jin and Lee, 2008; Palti, 2011). TLR4 was the first TLR discovered in mammals and found to mediate the activation of the immune system by LPS (Hoshino et al., 1999; Poltorak et al., 1998; Qureshi et al., 1999). However with the exception of *Danio rerio* it is mostly absent in teleost fish (Loes et al., 2019; Sepulcre et al., 2009). Some TLRs, such as TLR21, are fish-specific (Solbakken et al., 2016; Zhang et al., 2014).

CLRs are a large family of receptors that link carbohydrates in a calcium-dependent manner. CLR genes have been identified in fish, namely the mannose receptor gene in *Sparus aurata* and *Ctenopharyngodon idella*, however the role of these PRRs in fish remains to be clarified (Rodríguez et al., 2003; Wang et al., 2014; Yang et al., 2015).

NLRs are cytoplasmatic PRRs that possess leucine rich-repeat domains and they are divided into three subfamilies in fish, the NLR-A, resembling mammalian NODs, the NLR-B, resembling mammalian NLRP, and the fish-specific NLRC (Grayfer et al., 2018; Li et al., 2018). These PRRs subfamilies were identified in several teleosts but they were firstly identified in *Danio rerio*(Angosto and Mulero, 2014; Laing et al., 2008; Li et al., 2018, 2020a; Sahoo, 2020). These receptors are mostly linked to the recognition of whole or components of bacteria but they are also activated by synthetic double stranded RNA (dsRNA) and viral infections (Grayfer et al., 2018; Laing et al., 2008).

RLRs are the core cytosolic receptors that recognize viral RNAs and DNAs, and are stimulated by dsRNA through MDA5, LGP2 and RIG-I ligands in both mammals and fish (Biacchesi et al., 2009; Chen et al., 2017). Pathogenic bacteria or its components can also stimulate these receptors in teleost fish. As with mammalian RLRs, fish RLRs induce the production of several chemokine mediators but the specific ligands and signalling regulatory pathways are poorly understood (Chen et al., 2017; Grayfer et al., 2018).

1.4.2.4. Other immune tissues

The thymus, head-kidney, spleen and liver possess immunological functions and distinct roles in the defence against foreign pathogens.

The thymus is a lymphoid organ located close to the opercular cavity in teleost fish and produces T cells, antibodies by B cells and stimulates phagocytosis (Bowden et al., 2005; Chilmonczyk, 1992; Paiola et al., 2021). This organ is mostly linked to acquired immunity and it is only lightly touched in this thesis.

The head kidney or interrenal is the fish homolog of the adrenal gland and is a major hematopoietic organ, responsible for the production of both lymphoid (B and T cells) and myeloid (phagocytic cell) cells, and with key regulatory functions in immune-endocrine interactions and stress (Rauta et al., 2012). Two main corticosteroid hormones are produced by the adrenal gland: the glucocorticoid cortisol (corticosterone in rodents) and the mineralocorticoid aldosterone. However, fish do not produce aldosterone and cortisol, with both glucocorticoid and mineralocorticoid activity, is the main steroid produced by the head kidney. Cortisol regulates several immune functions such as leukocyte apoptosis and proliferation (Mommsen et al., 1999; Weyts et al., 1998b, 1998a), lysozyme activity (Wang et al., 2005), cytokine expression and antibody production (Castillo et al., 2009; Castro et al., 2011).

The spleen is a secondary and blood-filtering organ involved in innate and acquired immunity (antigen presentation, degradation, and antibody production) and plays a crucial role in haematopoiesis, specifically in red blood cell turnover and haemoglobin recycling (Ali et al., 2014; Rauta et al., 2012; Reyes-Cerpa et al., 2012). The spleen of both mammals and fishes contains abundant IgM^+ mature B cells (Bromage et al., 2004; Castro et al., 2019), T-cells $CD4^+$, $CD8^+$, cytokines and chemokines (Ashfaq et al., 2019; Lewis et al., 2019; Syahputra et al., 2019). Apart from cell and humoral components identification and measurement, spleen size can be used to identify inflammatory and infectious processes as it is usually enlarged in the presence of bacterial pathogens and parasites in both mammals and fish (Corbin et al., 2008; Zwollo, 2011).

The liver is an essential immune organ adjacent to GALT that activates hepatic stellate and Küpffer cells during the inflammatory process to induce the production of monocytes, NK, neutrophils, macrophages, dendritic cells and T-$CD8^+$ and T-$CD4^+$ cells in mammals. In *Oncorhynchus mykiss*, the liver has recently been recognized to contribute to immune

surveillance against high endotoxin and antigen levels through Küpffer cells and other intrahepatic immune cells (Möller et al., 2014). In *Danio rerio*, a negative regulator of Toll/IL-1R was also observed in liver under inflammatory process (Feng et al., 2016). Finally, it is important to highlight the bile in both mammals and fish that, although not considered an immune organ, supports the liver by containing a variety of antimicrobial products, antigens, lymphocytes, cytokines, chemokines and antibodies (Béland et al., 2012; Cheng et al., 2015; Heymann and Tacke, 2016; Sipka and Bruckner, 2014).

1.4.2.5. Innate immunity studies in Antarctic notothenioid fish

The information about the role of innate immunity among the Notothenioids remains fragmentary. There is evidence that *D. mawsoni* and *N. angustata* possess genes encoding hepcidin. Also, specificities in the type II hepcidin which is present exclusively in Antarctic species have been found (Xu et al., 2008). In *N. coriiceps* liver IFNγ was up-regulated in response to bacterial infection and MHC activation, something that is usually observed under viral pathogen infection in other teleosts.

Twelve TLRs have been identified in *N. coriiceps* (TLR1, TLR2, TLR3, TLR5, TLR5S, TLR7, TLR8, TLR9, TLR14, TLR21, TLR22, TLR23) of which three are fish-specific (TLR21-23). The kidney expressed the 12 TLR transcripts while other tissues (liver, stomach, and spleen) contained more specific TLRs transcripts (Ahn et al., 2014). *N. coriiceps* challenged with heat-killed bacteria (HKEB) and poly I:C showed tissue and pathogen-specific responses. In general, all 12 TLR were differentially expressed after HKEB and poly I:C exposure, although the tissue expression pattern was different between the liver, kidney and spleen and over time (6 h and 12 h). There is evidence that in *N. coriiceps* TLR21, TLR22 and TLR23 recognize and respond to HKEB and poly I:C infection agonists (Ahn et al., 2014).

1.4.3. Standard bacterial and viral immune stimulants in teleost fish

1.4.3.1. Lipopolysaccharides

LPS is a major component of the external layer of the cell wall of gram-negative bacteria (e.g. *Escherichia coli*) and an endotoxin and is the most studied immune challenger in fish and mammals. There are three principal regions in the LPS structure: a carbohydrate “O-antigen”,

an oligosaccharide core region and the lipid "A" portion, which is responsible for its endotoxic properties (Raetz and Whitfield, 2002; Swain et al., 2008). The lipid "A" structure is the most conserved across species. The "O-antigen" has remarkable structural diversity and functions depending on bacterial strains and the environmental characteristics of their habitats (Margesin, 2017; Whitfield et al., 2020). Generally, LPS triggers several inflammatory molecules such as tumour necrosis factor-2 (TNF2), interleukin (IL-1β) and cyclooxygenase-2 (COX2) (MACKENZIE, 2006). In mammals, several TLRs respond to LPS challenges, namely TLR4 (Iliev et al., 2005; MacKenzie et al., 2010; Swain et al., 2008), which is considered the principal LPS receptor by homodimerization of two TIR domains with the adaptor molecules and association to myeloid differentiation protein 2 (MD-2) to form the TLR4–MD-2 complex responsible for cell activation (TIRAP/MyD88 and TICAM1/2) (Vogel et al., 2003) and, consequently, type I IFN production, IL-1 and IL-18 cytokines production (**Figure 1.14**) (Huber et al., 2006; Jiang et al., 2005; Ko et al., 2017; Park and Lee, 2013; Tapping and Tobias, 1999; Wright et al., 1990; Zanoni et al., 2011).

In fish, LPS exposure induces type I IFN expression (Acerete et al., 2007; Haukenes and Barton, 2004; Holland et al., 2002), IL-1β up-regulation that provokes inflammatory responses by increasing leukocyte activity in the head-kidney (Hong et al., 2003; Jiang et al., 2008), lysozyme production (Köbsel and Ramadori, 1994), leucocytes migration and macrophage proliferation (Buonocore et al., 2006; Hong et al., 2001). Also, several studies have reported the interaction of LPS with the endocrine system, causing increases the release of corticotropin-releasing hormone, which stimulates adrenocorticotropic hormone, plasma cortisol and modulation of glucocorticoid receptor expression in different tissues (Acerete et al., 2007; Haukenes and Barton, 2004; Holland et al., 2002).

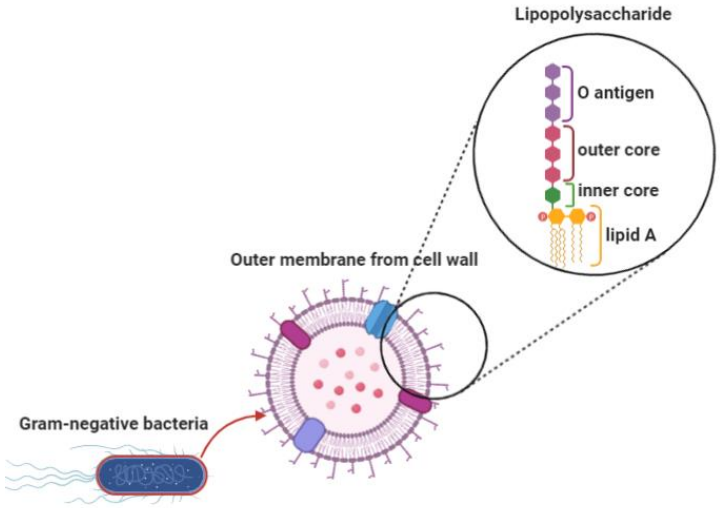

Figure 1.14. Structure of the lipopolysaccharide (LPS) molecule. The cell-wall of Gram-negative bacteria is composed by a lipopolysaccharide layer that stimulates the innate immune system of the host. The LPS molecule is composed by a carbohydrate O antigen, an outer and inner oligosaccharide core regions and a lipid A domain [BioRender software 2021 was used to prepare this illustration].

1.4.3.2. Poly I:C

Poly I:C is a synthetic analogue of double-stranded RNA composed of a polymer of inosinic acid in one strand and a polymer of cytidylic acid in the other strand, resembling a virus. TLR3 was reported to be specifically linked to the recognition of this viral agonist and to limit virus replication in the host cells in both immune (B cells, macrophages, dendritic cells) and non-immune cells (fibroblasts, endothelial cells, keratinocytes) (Matsumoto et al., 2011; Yu and Levine, 2011). Similarly to its effect on mammals, in teleosts poly I:C stimulates TLRs, in particular TLR3, for example, in *Danio rerio* (Phelan et al., 2005), *S. salar* (Svingerud et al., 2012), *O. mykiss* (Rodriguez et al., 2005) and *Paralychthys olivaceus* (Baoprasertkul et al., 2006; Zhou et al., 2014). Also, there is evidence the involvement of other PRR, such as retinoic-acid inducible (RIG) I-like (Jensen et al., 2002) and other humoral components such as IFN in *S. salar* (Jensen et al., 2002) and *O. mykiss* (Alkie et al., 2019; Zhu et al., 2016) as well as several cytokines in *O. mykiss* (Sakai et al., 2021).

1.5. Objectives of the thesis

The main aim of this PhD thesis is to establish to what extent the evolution of the immune system of Antarctic teleosts was shaped by the unique Antarctic environment. The teleost fish immune system is increasingly being investigated because of their simplicity among vertebrates and of their growing importance for aquaculture. However, the notothenioids are unique as they underwent speciation in isolation, in the freezing and oxygen rich waters of the Antarctic, relatively recently, approximately 20-10 million years ago. This makes it possible to gain insight into the influence of the Antarctic environment and the rates of immune system evolution by considering the repertoire of immune molecules and comparing them to the evolutionary proximate sister groups outside Antarctica. This aim is expected to be achieved by mapping the molecular elements using transcriptomic and metagenomic approaches and selecting skin and intestine as the representative targets of the mucosal-associated lymphoid tissues, and the head-kidney, spleen, and liver as immune tissues of two Antarctic notothenioids.

The two notothenioid species chosen for the study were *Notothenia coriiceps* and *Notothenia rossii* due to the available genome information for the former, their occupation of a similar environmental niches and the fact they are phylogenetically close, making it possible to explore general and specific evolutionary questions about of the immune repertoire. A further factor was their ease of capture and manipulation. Both species are relatively abundant throughout the Antarctic and are readily captured using a hook-and-line and can be maintained for a short duration under confined experimental conditions. These are important factors when working with wild species in an extreme environment and are often a limitation in polar research. This study is important to understand how the immune system of these cold-adapted species evolved, and it is hypothesized that its evolution has been shaped by the interplay between host response, microbiota, and cold-adaptive evolution. Furthermore, it is of utmost importance to understand how they respond to environmental change (such as pathogens and temperature rise) to establish their likely resilience under climate change. This PhD thesis was integrated in Noto-Immune, a collaborative project between Portugal and China.

For this study, the following specific objectives were proposed to achieve the global aim:

1) To test the hypothesis that innate immune system can induce iron deprivation as mechanism of defence against LPS exposure in in *Notothenia coriiceps* and *N. rossii*. For this purpose, several immune-related genes linked to iron metabolism were analysed and quantified after LPS exposure. The head-kidney and the liver were chosen because, respectively, it is the principal

hematopoietic tissue and it is the major tissue for iron storage. In addition, the iron ion levels on plasma were measured to evaluate the changes at a systemic level (Chapter 2.1).

2) To test the hypothesis that the evolution of the notothenioid TLR gene family was modulated by the low temperature conditions of Antarctica, TLRs from several notothenioids were compared to other vertebrates using bioinformatic methods. These included phylogenetic relationships among TLR, selective pressure analysis to identify amino acid changes of TLR family members across species, gene expression patterns of several TLR in the head-kidney and intestine. In addition, a LPS exposure experiment was performed and several biochemical parameters in plasma measured to assess if LPS caused gene expression and functional changes in *N. rossii* (Chapter 2.2).

3) To further test the hypothesis that Antarctic conditions shaped the evolution of immune genes and their function, global transcriptomes of three immune tissues (head-kidney, skin and intestine) from *N. coriiceps* were produced after 7 days of LPS stimulation. In parallel biochemical analysis of blood plasma was carried out to identify the systemic effect of LPS (Chapter 3).

4) To compare the differential immune response to bacterial and viral aggressions, transcriptomes of several immune tissues (skin, intestine, spleen, and liver) from *N. rossii* after exposure to bacterial LPS and viral Poly I:C were generated and analysed. In parallel functional parameters in blood plasma were measured to better understand the innate immune response in *N. rossii* (Chapter 4).

5) To better understand the interaction between environment, microbe, and host, the skin and intestine (gut) microbiome of *N. coriiceps* and *N. rossii*, maintained at the normal 2ºC and at a high temperature of 6ºC (global warming scenario), with and without LPS treatment were analysed (Chapter 5).

CHAPTER 2

Specific gene expression of Notothenoids to an immune challenge: lipopolysaccharide of bacterial origin

CHAPTER 2.1

LPS modulates the expression of iron-related immune genes in two Antarctic Notothenoids

LPS modulates the expression of iron-related immune genes in two Antarctic Notothenoids

Manuscript published in Frontiers in Physiology 11 (2020) 102

https://doi.org/10.3389/fphys.2020.00102

Acknowledgments

The authors would like to acknowledge Pedro Palma and Vera Gomes for help with iron measurements, Stefan Fernandes for help with RStudio software, and the 2017 crew of the Great Wall Chinese Antarctic Station for their hospitability and logistic support.

LPS modulates the expression of iron-related immune genes in two Antarctic notothenoids.

Martínez, D.[a,1,2], Sousa, C.[a,3], Oyarzún, R.[1,2,4], Pontigo, J.P.1, Canário, A.V.M.[3], Power, D.M.[3] Vargas-Chacoff, L.[1,2] and Guerreiro, P.M.[3]

a The authors contribute equally

1 Instituto de Ciencias Marinas y Limnológicas, Universidad Austral de Chile, Valdivia, Chile.

2 Centro Fondap de Investigación de Altas Latitudes (IDEAL), Universidad Austral de Chile, Valdivia, Chile.

3 Centro de Ciências do Mar (CCMAR), Universidade do Algarve, Campus de Gambelas, 8005-139 Faro, Portugal.

4 Escuela de Graduados, Programa de Doctorado en Ciencias de la Acuicultura, Universidad Austral de Chile, Puerto Montt, Chile.

2.1.1. Abstract

The non-specific immunity can induce iron deprivation as a defence mechanism against potential bacterial pathogens, but little information is available as to its role importance in Antarctic fish. In this study the response of iron metabolism related genes was evaluated in liver and head kidney of the Antarctic notothenioids *Notothenia coriiceps* and *N. rossii* 7 days after lipopolysaccharide (LPS) injection. Average plasma Fe^{2+} concentration was unaffected by treatment in either species. The gene expression response to LPS varied between tissues and species, being stronger in *Notothenia coriiceps* and more prominent in the head kidney than liver. The reaction to LPS was marked by increased individual variability in most genes analysed, even when the change in expression was not statistically significant, suggesting different individual sensitivity and coping responses in these wild fish. We found that iron related genes had an attenuated and homogenous response to LPS but there was no detectable relationship between plasma Fe^{2+} and gene expression. However, overall, in both tissues and

species LPS exposure set a multilevel response that concur to promote intracellular accumulation of iron, an indication that Antarctic Notothenoids use innate nutritional immunity as a resistance mechanism against pathogens.

Keywords*:* *Notothenia coriiceps*, *Notothenia rossii*, iron metabolism, Antarctic fish, nutritional immunity

2.1.2. Introduction

The vertebrates, including fishes, have developed innate and an adaptive immune systems composed both cellular and humoral components to respond to pathogens (Barandica and Tort, 2008). Both systems can be communicated through soluble mediators known as cytokines that regulate the magnitude of the immune response, controlling pathogen growth, promoting inflammation and triggering the adaptive immune response (Sompayrac, 2012). The main organs with immunological function in fish are the thymus, spleen, liver, head kidney and mucosa-associated lymphoid tissue (MALT). They can be grouped into primary and secondary immune organs according to their participation in the production, maturation, activation and proliferation of immune components (Soulliere and Dixon, 2017).

During inflammation, the innate immune system can induce several antimicrobial mechanisms, including the depletion of iron available to the pathogen at the systemic and cellular levels (Johnson and Wessling-Resnick, 2012). This defence mechanism, known as nutritional immunity, consists of the removal of iron from the circulation and its subsequent sequestration inside the cell (Collins, 2008). Proinflammatory cytokines such as IL-6 stimulate the transcription of hepcidin, triggering and potentiating the hypoferric response of inflammation (Nemeth et al., 2004a). Several bacterial pathogens obtain the iron they need for their survival and replication from an external source (Bethke et al., 2016, 2018; Calquín et al., 2018; Pulgar et al., 2015; Ratledge and Dover, 2000). For this reason, eukaryotic organisms must effectively control iron homeostasis, through the regulation of the proteins involved in its metabolism (Skaar, 2010).

In fish, iron is mainly taken up by the intestine (Bury and Grosell, 2003) where it can enter as heme iron, Fe^{2+} and Fe^{3+} (Bury and Grosell, 2003). Duodenal cytochrome B is

necessary to convert Fe^{3+} to Fe^{2+} (Bury and Grosell, 2003). The pool of Fe^{2+} interacts with the divalent metal transporter present on the apical side of the enterocytes (Andrews, 1999; Gunshin et al., 1997). Once inside the cell, the iron can be stored in the cytoplasmic ferritin (the portion of iron that is not for immediate use) (Torti and Torti, 2002), directed towards the mitochondria (for biosynthesis of the Fe-S cluster and heme group) or used in other routes of iron metabolism (Hentze et al., 2004).

The exit of iron from the enterocytes is regulated by ferroportin (Donovan et al., 2000). However, hepcidin can induce the degradation of ferroportin, controlling the release of iron from the basolateral membrane into the bloodstream (Nemeth et al., 2004b). The export of iron also depends on the presence of a copper-associated oxidase, hephaestin in intestinal cells or of ceruloplasmin in non-intestinal cells (Harris et al., 1999; Vulpe et al., 1999). The ferroxidase allows the iron to be loaded on to the cytoplasmic transferrin to be directed to other tissues that need it (Hentze et al., 2004). In which case, iron uptake can be mediated by transferrin receptor 1 (TfRC1) that is expressed in all tissues (Cheng et al., 2004) or by transferrin receptor 2 (TfRC2) that in mammals is found in hepatocytes, duodenal crypt cells and erythroid cells, suggesting a more specialized role of this receptor in iron metabolism (Kawabata et al., 1999). In fish, such as *Salmo salar* and *Eleginops maclovinus*, the expression of the main proteins involved in iron metabolism appears to be modulated by the presence of live bacterial pathogens (Martínez et al., 2017a; Pulgar et al., 2015)

Research on Antarctic fish immune responses has mainly addressed the effect of thermal stress on the metabolism of carbohydrates and antioxidant defence system (Klein et al., 2017b; Machado et al., 2014; Souza et al., 2018), or analysed the level of transcriptional response of immune genes after stimulation with Poly I:C and with heat-killed cells, *E. coli* (Ahn et al., 2016) and *Psychrobacter sp*. (Buonocore et al., 2016). Furthermore, cDNAs of iron metabolism proteins have been cloned, e.g., *ceruloplasmin* (*Cp*), *transferrin* (*Tf*), *ferritin heavy chain* (*Fth1*) and *divalent metal transporter 1* (*Dmt1*) (Scudiero et al., 2007, 2009), but no specific information is available on how they are regulated before an infectious process. Furthermore, there is no information on nutritional immunity associated with iron in Antarctic fish or if this type of immune response could be activated by the detection of pathogen-associated molecular patterns (PAMPs), which activate the immune system, but do not require iron. Therefore, the objective of the present study was to evaluate the transcriptional response of immune genes associated with iron in relation to stimulation with lipopolysaccharide (LPS) in the Antarctic Notothenoids *Notothenia coriiceps* and *Notothenia rossii*.

2.1.3. Material and Methods

2.1.3.1. Sample collection

Notothenia coriiceps (30 ± 2.4 cm of length and 384 ± 93 g of weight) and *N. rossii* (30 ± 4.2 cm of length and 312 ± 124.7 g of weight) were captured by hook-and-line from a boat, from 5-20 m deep in the waters near the Chinese Great Wall Station, at King George Island (GPS coordinates: 62°13′S, 58°58′W), in the Antarctic Peninsula, during late January 2017. Upon fishing fish were initially randomly placed in six 200 L flow-through plastic tanks for up to 3 days and then measured, weighed, tagged with opercular metal tags and allocated in groups with similar biomass and size distribution in the same flow-through system (two tanks per species; n=7-8 per tank). Fish were anesthetized in phenoxyethanol (0.02 ml/L) before all experimental manipulations and left undisturbed for 1 week before the experiments to acclimate. At day 0 fish were anesthetized as above and one group per species was injected intraperitoneally (IP) with saline (1.1% NaCl, 0.2 vol. % body weight) and acted as control, while the other group was IP-injected with LPS (1.5 mg/ml LPS *E. coli* O111:B4 in 1.1% NaCl, 0.2% vol body weight, to an effective dosage of 3 mg/kg). This procedure was repeated in day 2, when fish received a second injection of either saline (control) or LPS. At day 7 all fish were lethally anesthetized, blood was collected in heparinized syringes (ammonium salt heparin, 1000 U/ml, Sigma-Aldrich), and fish were sacrificed by cervical section to collect tissues. The head kidney and liver were dissected aseptically, immediately placed in RNAlater (Sigma-Aldrich), placed at 4°C for 24 hours and then stored at -20°C. The blood was centrifuged at 10,000 g for 5 min at 4°C, the plasma separated and stored at -80°C. Water parameters in tanks were monitored twice daily and were approximately constant throughout the experiment - temperature (2.1 ± 0.5°C), salinity (29 ± .5 ppt) and oxygen (10.5 ± 1.0 ppm). Two *N. coriiceps* died in the LPS group and no mortality was observed for *N. rossii*.

2.1.3.2. Blood plasma iron

For determination of iron, 1 ml of 5% nitric acid (Sigma-Aldrich) was added to the blood plasma (110 µl), followed by sonication for 10 min and centrifugation at 16,000 g for 5 min at room temperature. The supernatant was removed to a new 15 ml falcon tube and the Fe^{2+} fraction was measured at 259.940 nm in an Agilent Microwave Plasma Atomic Emission Spectroscope (4200 MP-AES, Agilent Technologies). Only Fe^{2+} was measured due to limitations of plasma volume and of the spectrometer which could not measure the Fe^{3+} emission wavelength. The Agilent MP-AES Expert software was used to calculate concentration based on a 14 points standard curve (range 4.47E-05 mM – 4.47E-08 mM) with automatic background subtraction provided by a blank (5% nitric acid), in accordance with the manufacturer's instructions. The limits of detection (LOD) and limit of quantification (LOQ) were calculated from three and ten times the standard deviation of 15 consecutive blank measurements, respectively (Li et al., 2013). The values obtained were 3.77E-05 mM to LOD and 1.26E-04 mM to LOQ. The presence of interference was analysed through spiking samples with 8.95E-04 mM (50 ppb) and 1.79E-03 mM (100 ppb) standards to the plasma samples and was found not to be significant. Recoveries were calculated from the same spiked plasma samples and estimated at 105%.

2.1.3.3. RNA processing and quantification

Total RNA was extracted from 50 mg of tissue using Trizol (Ambion), following the manufacturer's instructions. The RNA pellets were dissolved in diethylpyrocarbonate water (DEPC, Sigma-Aldrich) and stored at -80ºC. RNA was quantified spectrophotometrically at 260 nm (NanoDrop Technologies) and quality was checked using electrophoresis in 1% agarose gels. Total RNA (2 µg) was used as a template for reverse transcription reactions to synthesize cDNA using MMLV reverse transcriptase (Promega) and the oligo-dT primer (Invitrogen).

The cDNAs were diluted to 100 ng (2 µL) and used as a template for quantitative polymerase chain reaction (qPCR) of *ferritin heavy chain* (*Fth1*), *ferritin middle chain* (*Fm*), *ferroportin* (*Fp*), *transferrin* (*Tf*), general identification as *transferrin receptor* (*TfRC*) on NCBI database, however with higher similarity with *transferrin receptor type 1* (*TfRC1*) based in ENSEMBL and CCMAR Sea Genomics databases, general nomenclature as *hepcidin-like* (*Hamp*) identified on public NCBI database, however has more similarity to *hepcidin type 2 variant 4* (*Hamp2*) based on CCMAR Sea Genomics database, *ceruloplasmin* (*Cp*), *interleukin-*

6 receptor alpha chain (*IL-6Rα*), *IL-6 receptor beta chain* (*IL-6Rβ*), and *18s ribosomal RNA* (*18S*). The primers for interleukin-6 were not considered because they did not work very well. These primers were designed based on *Notothenia coriiceps* species because is the only genome partially published and available on public NCBI database (https://www.ncbi.nlm.nih.gov/) and further confirmed by blast against of several known genome of fish species that are phylogenetically similar such as *Danio rerio*, *Oryzias melastigma*, *Oreochromis niloticus*, *Gasterosteus aculeatus*, *Tetraodon nigroviridis*, *Xiphophorus maculatus* by public ENSEMBL database (https://www.ensembl.org/index.html) and *Dicentrarchus labrax* and *Sparus aurata* fish species by public CCMAR Sea Genomics database (http://146.193.226.37/). The qPCR reaction was performed according to a published protocol (Martínez et al., 2017b)A melting curve analysis confirmed that only one PCR product was amplified in all cases (the primer pairs used and their efficiencies are listed in **Table 2.1.1**). Expression levels were analyzed using the comparative Ct method ($2^{-\Delta\Delta CT}$) (Livak and Schmittgen, 2001). Data were expressed as the fold change in gene expression normalized to an endogenous reference gene (housekeeping 18s) and relative to the untreated control. PCR efficiencies were calculated according to the equation: $E=10^{[-1/slope]}$ (Rasmussen, 2001).

Table 2.1.1. qPCR primer pairs, product sizes and efficiency.

Primer	Nucleotide sequences (5′3′)	PCR product size	GenBank	*N. coriiceps*		*N. rossii*	
				Efficiency Liver (%)	Efficiency Head-kidney (%)	Efficiency Liver (%)	Efficiency Head-kidney (%)
Ferritin heavy chain (Fth1) Fw	AGTGGAGGCCCTTGAATGTGC	130pb	FM210467.1	97.4	109.4	95.8	94.2
Ferritin heavy chain (Fth1) Rv	GTCCAGGTAGTGAGTCTCGATGAA						
Ferritin middle chain (Fm) Fw	GGACACAGGATGCCGACATAA	121pb	XM_010792901.1	105	102.2	95.3	104.6
Ferritin middle chain (Fm) Rv	AACGCTACTCCACTTCCCCA						
Ferroportin (Fp) Fw	GCCATGGGTCACGTCATGTA	127pb	XM_010788639.1	97.4	107.2	96.6	92.7
Ferroportin (Fp) Rv	GTTAGACGGTGGTGGGAAGG						
Hepcidin type 2 (Hamp2) Fw	GAGCCGATGAGCGTTGAAAG	139pb	XM_010774309.1	105.9	105.9	94.9	99.9
Hepcidin type 2 (Hamp2) Rv	AGGACAATCCGCAGACACC						
Ceruloplasmin (Cp) Fw	GTTTCCAGCCACCTTTCAGACAGT	104pb	XM_010778042.1	109.6	98.7	100.9	101.3
Ceruloplasmin (Cp) Rv	TCGCCTCCATGCCACCTTTAAT						
Interleukin 6-receptor α chain (IL6Rα) Fw	TGGCAGCTTAAGCCAGAAGG	148pb	XM_010787044.1	109.7	97.6	106.3	96.7
Interleukin 6-receptor α chain (IL6Rα) Rv	GGCAATTGGAGCGTAGGTCT						
Interleukin 6-receptor β chain (IL6Rβ) Fw	GGACAATGAGATCGCCATGC	131pb	XM_010787241.1	100.7	98.3	101.5	100.8
Interleukin 6-receptor β chain (IL6Rβ) Rv	TGTCAACCCTTGATAAAGCCC						
Transferrin (Tf) Fw	CAGTGGTCAGGCGTTGAAGA	146pb	NM_001303296.1	107.3	105.9	99.1	95.8
Transferrin (Tf) Rv	TAGTAAGGCTCGGTGTGGGA						
Transferrin receptor type 1 (TfRC1) Fw	GTCCCCCAGAGAGAGTCCAT	127pb	XM_010774827.1	103.5	109.2	94.2	107.1
Transferrin receptor type 1 (TfRC1) Rv	TCGGAACAGGTTGAAGTCGG						
Housekeeping (18s) Fw	GTCCGGGAAACCAAAGTC	116pb	AF518193.1	107.9	101.6	108.6	99.7
Housekeeping (18s) Rv	TTGAGTCAAATTAAGCCGCA						

2.1.3.4. Statistical Analysis

Data is shown as mean ± standard error (SE) of the mean. Normality and homogeneity of the variances were verified using the Shapiro-Wilk test. The logarithmic transformation was used if data did not follow a normal distribution. The Student's t-test was used to compare the effect of LPS versus control for iron and gene expression data. The level of statistical significance was 5%. Because several comparisons did not achieve statistical significance and an increase in variability was observed in the LPS treated samples, a Principal Component Analysis (PCA) with rotation based on the Varimax equation with Kaiser Normalization was carried out order to determine the global sample distribution between control and LPS mean centered data in liver and head-kidney of the two species. A Principal Component Regression was applied to discriminate between control and LPS treatment groups. The software SPSS (IBM SPSS version 25) was used for the statistical analysis.

2.1.4. Results

2.1.4.1. Plasma iron and expression of iron-related immune genes

The concentration of plasma iron (Fe^{2+}) varied between $6.53x10^{-3}$ and $1.08x10^{-2}$ mM in *N. coriiceps* and $7.05x10^{-3}$ – $1.05x10^{-2}$ mM in *N. rossii*, with no statistical difference between control and LPS treatment (**Figure 2.1.1 a,b**).

The iron-related immune gene expression response to LPS varied with tissues and species. *N. coriiceps* was more responsive to LPS than *N. rossii*. In *N. coriiceps* of the nine genes analysed, 4 were significantly upregulated ($p<0.05$) in the liver and 7 in the head-kidney, 3 of which were common to both tissues - *Fth1*¸ *Tf* and *Hamp2* (**Figure 2a-i**). In contrast, in *N. rossii* only *Hamp2* was significantly upregulated in the liver and 3 genes were significantly upregulated in head kidney – *Fth1*, *Tf* and *Cp* (**Figure 2a-i**). *Fp* was significantly downregulated in *N. coriiceps* liver while *Cp* and *TfRC1* were significantly downregulated in *N. rossii* liver (**Figure 2.1.2 c,e,g**).

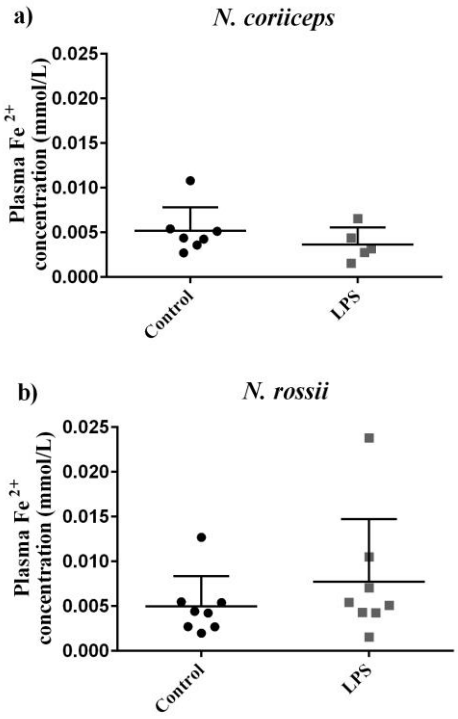

Figure 2.1.1. Iron concentration (Fe^{2+}) in plasma in fish receiving two injections (on day 0 and day 2) of saline (Control) or LPS. (a) *N. coriiceps (*n =7 and 5, respectively) (b) *N. rossii* (n=8). The final concentration was calculated considering the dilution factor (9x) and molar mass (55.847 g mol -1). No statistical differences are observed among different treatment groups (Student´s t-test, $P > 0.05$).

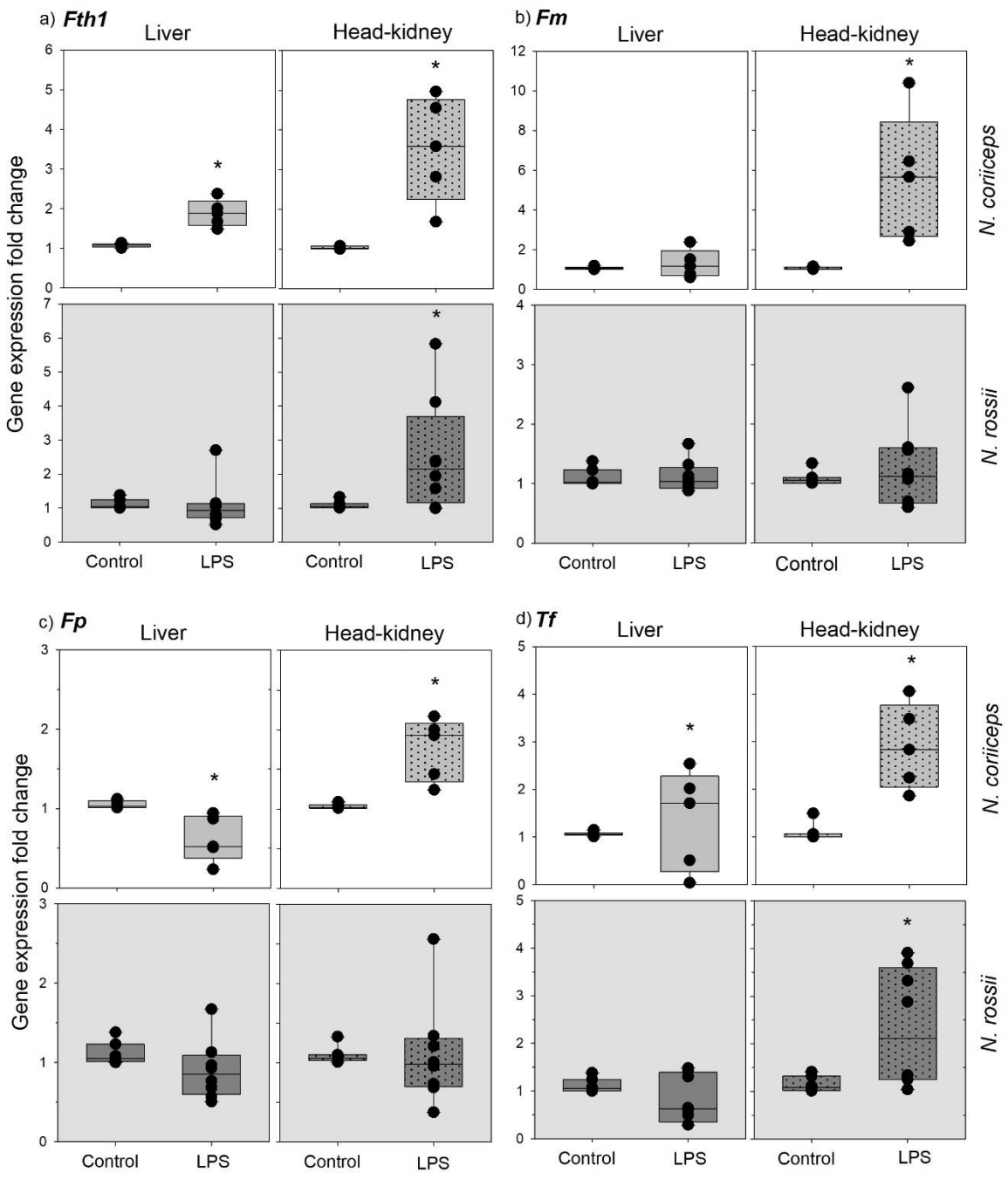
a) Fth1
Liver
Head-kidney
b) Fm
Liver
Head-kidney
c) Fp
Liver
Head-kidney
d) Tf
Liver
Head-kidney
Gene expression fold change
N. coriiceps
N. rossii
Control
LPS
Control
LPS
Control
LPS
Control
LPS

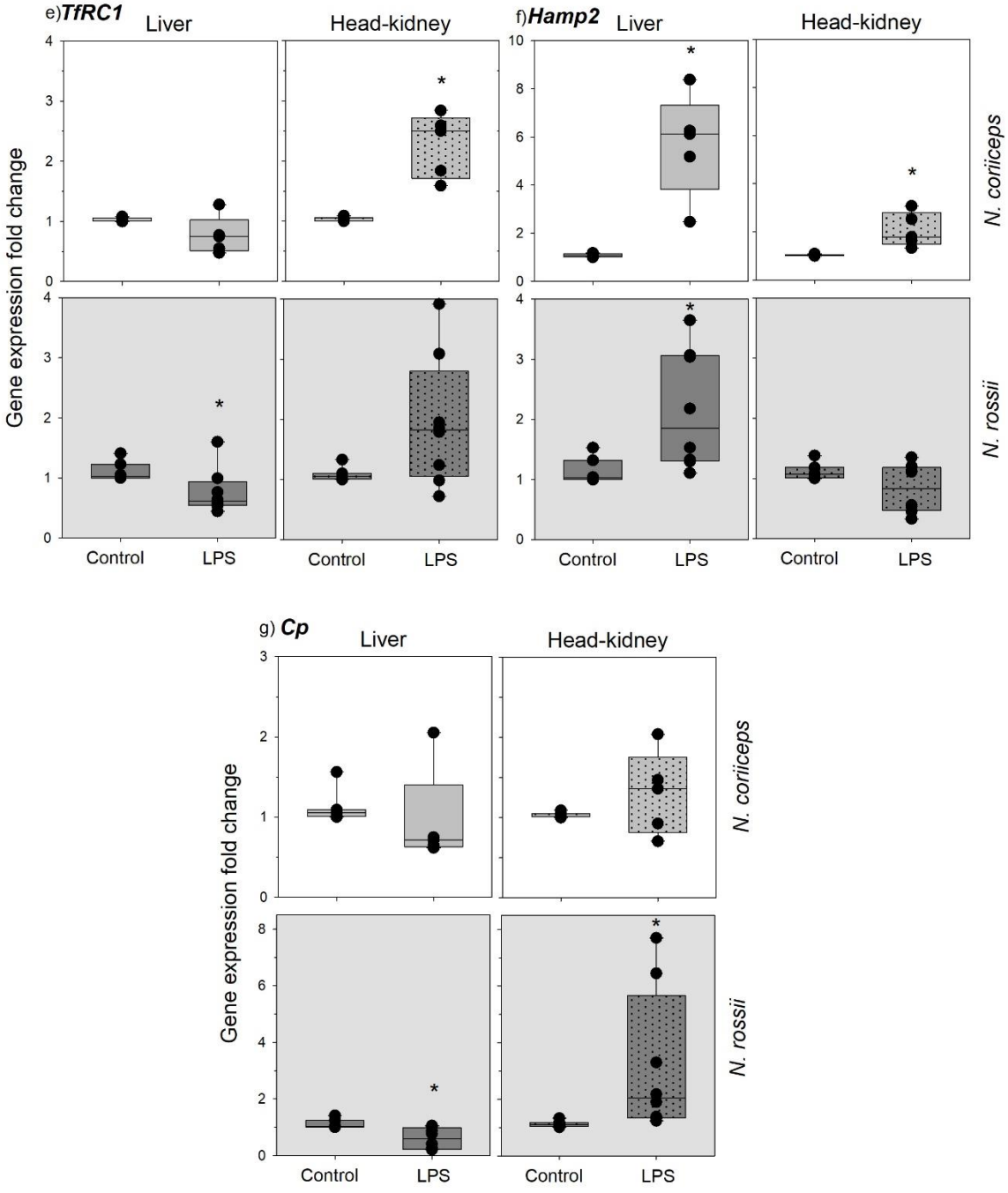
e)TfRC1
Liver
Head-kidney
f)Hamp2
Liver
Head-kidney
Gene expression fold change
N. coriiceps
N. rossii
Control
LPS
g) Cp
Liver
Head-kidney
Gene expression fold change
N. coriiceps
N. rossii
Control
LPS

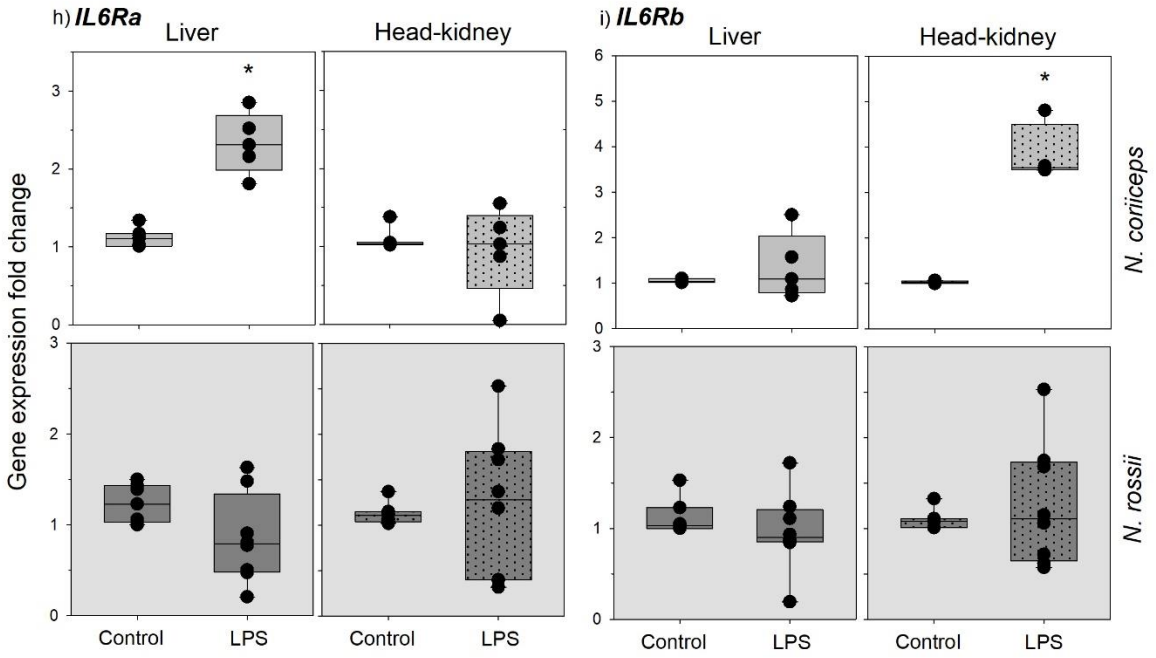

Figure 2.1.2. Gene expression of ferritin heavy chain (*Fth1*) (a), ferritin middle chain (*Fm*) (b), ferroportin (*Fp*) (c), transferrin (*Tf*) (d), transferrin receptor 1(*TfRC1*) (e), hepcidin 2 (*Hamp2*) (f), ceruloplasmin (*Cp*) (g), interleukin 6-receptor alpha chain (*IL6Ra*) (h), interleukin 6-receptor beta chain (*IL6Rb*), (i) in liver and head-kidney of *N. coriiceps* (NC) and *N. rossii* (NR) injected with serum saline (Control) or LPS. Relative expression was calculated by the 2_ΔΔCT method using the 18s ribosomal protein as the internal reference gene. Each grey bar value is the mean ± S.E.M and the black dot value correspond to each individual fish (n = 5-7 for *N. coriiceps* and n = 8 for *N. rossii*). Asterisks indicate statistical differences among different treatments for each tissue and species (Student´s t-test, $P < 0.05$).

2.1.4.2. Multivariate analysis

Since the response to LPS was relatively weak but an increase in gene expression variability was apparent, even when not statistically significant, we sought to determine if there was an association of the gene expression responses with the experimental groups using PCA for each tissue and species. In *N. coriiceps* liver, 78% of the gene expression variance was explained by the two first principal components (PC), 42% for PC1 and 36% for PC2. In head kidney, the two first PC explained 85% of the gene expression variance, 60.5% for PC1 and 25.2% for PC2. In *N. rossii* liver, 3 PC were required to explain almost 75% of the gene expression variance, 34.1% for PC1, 22.9% for PC2 and 18.3% for PC3. In head kidney, 3 PC explained 80% of the gene expression variance, 40.8% for PC1, 23% for PC2 and 15.7% for PC3. From the component coefficient matrix and the rotated component matrix (**Table 2.1.2**), the differentiation between genes and treatment groups occurred mainly along PC1 for both

tissues and species. A Principal Component Regression used the first 2 PC variables as regressors to determine the variance between the group clusters. For both immune tissues of *N. coriiceps* the clusters of control and LPS groups aggregated wide apart; the variance of control individuals was low and in contrast the LPS treatment had a higher variance (points less aggregated; **Figure 2.1.3 A,B**). By comparison, in *N. rossii* the clusters of the control and LPS groups were closer together. Furthermore, individuals of the control group clustered together, as in *N. coriiceps*, but individuals of LPS group appeared more dispersed, some of which close to the control group (**Figure 2.1.3 C,D**). Overall, all control individuals were correctly classified in the two species and 82% of *N. coriiceps* and 85% of *N. rossii* were correctly classified as belonging to the LPS group.

Table 2.1.2. Principal Component Analysis by rotation method (Varimax with Kaiser Normalization) applied in different iron-related genes in liver and head kidney of *N. coriiceps* and *N. rossii*.

Rotated component matrix										
Tissue - Species	**Liver – *N. coriiceps***		**Head kidney – *N. coriiceps***		**Liver – *N. rossii***			**Head kidney – *N. rossii***		
Genes	**Component**		**Component**		**Component**			**Component**		
	1	**2**	**1**	**2**	**1**	**2**	**3**	**1**	**2**	**3**
Ferritin heavy chain (*Fth1*)	0.924	−0.66	0.972	−0.002	−0.078	0.861	−0.371	0.639	0.089	0.673
Ferritin middle chain (*Fm*)	0.228	0.847	0.689	−0.676	0.906	−0.117	0.027	0.985	−0.001	0.069
Ferroportin (*Fp*)	−0.766	0.589	0.917	−0.281	0.922	0.177	−0.036	0.951	0.071	−0.094
Transferrin (*Tf*)	0.547	0.428	0.966	0.030	0.089	0.737	0.172	0.035	0.928	−0.009
Transferrin receptor type 1 (*TfRC1*)	−0.428	0.865	0.930	−0.023	0.559	0.764	0.012	0.301	0.550	0.571
Hepcidin type 2 (*Hamp2*)	0.962	0.221	0.917	0.226	−0.225	0.217	−0.808	−0.208	0.349	−0.686
Ceruloplasmin (*Cp*)	−0.47	0.901	0.603	0.692	0.022	0.643	−0.113	0.546	0.490	0.169
Interleukin 6-receptor α chain (*IL6Rα*)	0.968	−0.18	0.039	0.915	−0.023	0.619	0.674	−0.085	0.905	−0.069
Interleukin 6-receptor β chain (*IL6Rβ*)	0.424	0.847	0.875	−0.460	0.886	0.118	−0.062	0.972	−0.082	0.121
Cumulative Variance Explained (%)	*42.1*	*78.1*	*61.3*	*85.7*	*34.1*	*57.1*	*75.3*	*40.8*	*63.8*	*79.5*

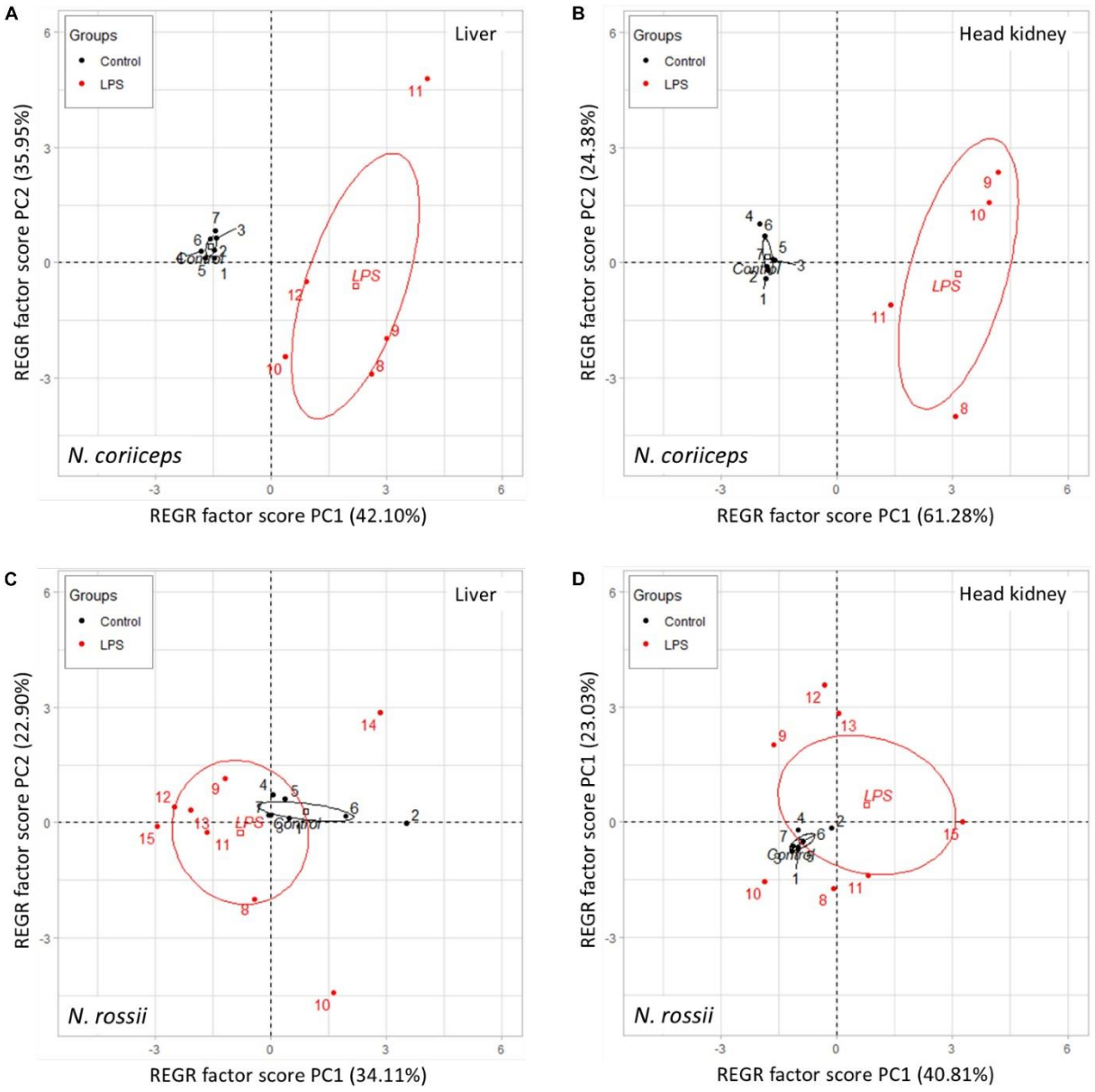

Figure 2.1.3. Scatterplot of principal component regression on two dimensions (PC1 and PC2) showing the confidence ellipses (95%) and respective centroids between control and LPS groups, in liver (A) and head-kidney (B) of *N. coriiceps* and in liver (C) and head-kidney (D) of *N. rossii*.

2.1.5. Discussion

This study found that stimulation with lipopolysaccharide, a gram-negative cell wall component, had no effect on circulating Fe^{2+} levels, of two closely Notothenioid species, *N. coriiceps* and *N. rossii*, but caused modifications in the expression of iron metabolism related immune genes, both in liver and in head kidney. This gene response showed important differences in magnitude between species, and the effects of LPS were more attenuated and variable in *N. rossii* when compared to *N. coriiceps*.

In the present study no significant changes were observed in plasma Fe^{2+} between the two *Notothenia* species and in response to LPS. Since Fe^{2+} concentrations were within the range of measurements made in other teleosts (Congleton and Wagner, 1991; Kopp et al., 2011, 2014), it suggests potentially similar requirements and homeostatic mechanisms between Antarctic and temperate fish. Although it has been shown in many vertebrate species that bacterial infection leads to a depletion of circulating iron reviewed by (Johnson and Wessling-Resnick, 2012; Skaar, 2010), most studies in fish showed either acute or week-lasting effects of LPS administration over the expression of iron-chelating or iron-transporting mechanisms but did not measure the ion itself (Liu et al., 2012; Martínez et al., 2017a; Prieto-Álamo et al., 2009) and thus the effectiveness and dynamics of LPS alone in lowering plasma iron is far from resolved. In rainbow trout, *Oncorhynchus mykiss*, LPS injection (1mg/kg) caused a significant decrease in plasma iron within 48-72 hours post-injection but circulating levels returned to normal by 96-120 hours (Congleton and Wagner, 1991) and similar kinetics were observed in Atlantic salmon, *Salmo salar*, injected an identical dosage (Langston et al., 2001). It is therefore also possible that an effect in Fe^{2+} plasma concentrations may have been missed in our time-frame and dosage, which followed previous studies on temperate fish (Chen et al., 2016; Guzman-Villanueva et al., 2013; Nayak et al., 2011; Seppola et al., 2015) but may less adequate in these Antarctic species. In the present study fish were injected twice, at 0 and 48 hours, and sampled at 72 hours after the last injection, a design chosen taken in consideration that low temperature habitats may contribute to a slower innate immune system response, as it has been described in cold-water fish when compared to temperate fish (Abram et al., 2017; Bonneaud et al., 2016; Chen et al., 2016; MacKenzie et al., 2008; Magnoni et al., 2015; Martínez et al., 2017a).

The overall gene expression response, albeit not as vigorous as in other vertebrates (Bethke et al., 2016; Collins, 2008; Johnson and Wessling-Resnick, 2012) , also suggests that an iron related immune response is active, much alike what it was seen in the sub-Antarctic Notothenioid *Eleginops maclovinus* (Martínez et al., 2017a), the Senegalese sole, *Solea senegalensis* (Prieto-Álamo et al., 2009) or the roughskin sculpin, *Trachidermus fasciatus* (Liu et al., 2012), among other fish species.

Several genes with important roles in iron metabolism responded in the liver and head kidney in one or both species. Interestingly, there were differences in responsiveness between the two species, with more genes responding and at a higher level in *N. coriiceps*. The reason for this is not immediately apparent but the two species, although captured in the same general

area, tend to segregate with *N. rossii* in open and deeper channels and *N. coriiceps* usually under rocks in shallower waters (Barrera-Oro et al., 2019; Jones et al., 2009; Kandalski et al., 2018), which could lead to different exposure to potential pathogens and different immune responsiveness. Some *N. coriiceps* specimens can be found near the surface in low tide, hiding in rock crevices surrounded by algal debris, thus possibly more exposed to microorganisms. Additionally, while *N. coriiceps* lives in these coastal shallow waters throughout its life, in the case of *N. rossii* only the juveniles appear to use these areas, with adults moving into deeper and open waters (Jones et al., 2009), and a life stage difference can thus account for some of the variance in the responses.

The liver is a major organ for iron storage and the site of synthesis for many proteins involved in iron metabolism. Although we have not determined iron levels in liver, the overall changes in gene expression in both species seem to favour iron accumulation in liver cells although this is more evident in *N. coriiceps*. In *N. coriiceps* liver upregulation of *Fth1* and *Tf* may promote binding of intracellular iron while upregulation of *Hamp2* and downregulation of *Fp* should inhibit its export (Neves et al., 2009; Torti and Torti, 2002; Zahringer et al., 1976). In *N. rossii* liver the export machinery seemed to be downregulated (increased *Hamp2* and *Cp* and reduced *TfRC1* transcription) but the net effect is expected to be in the same direction and would reduce iron availability for extracellular bacteria.

The fish head-kidney is involved in the immune response, but it is also the major haematopoietic organ, thus a likely responder to LPS and an important site for iron trafficking. In fact, expression of head-kidney hepcidin genes has been described as a crucial regulator of erythropoiesis during anaemia in fish (Neves et al., 2016). In our experiment, the tendency for intracellular accumulation of iron in the head kidney is apparent in *N. rossii* (by upregulation of *Tf*, *Fth1* and *Cp*) and also in *N. coriiceps* (upregulation of *Tf*, *Fth1*, *Fm*, and *Hamp2*) although in the later species iron turnover rate may be increased (by upregulation of *TfRC1* and *Cp*, possibly involved in extracellular transport). Overall this is consistent with previous reports which suggested an iron deficiency condition after LPS stimulation of the European sea bass, *Dicentrarchus labrax* (Neves et al., 2009) and the sub-Antarctic *Eleginops maclovinus* (Martínez et al., 2017a) and up-regulation of the same iron-related genes during experimentally induced anaemia in fish (Neves et al., 2016)

Interleukins are modulators of haematopoiesis, inflammation and immune responses. It has been further shown in fish that IL-6 is induced in macrophages during sepsis, and suggested

that this may concur to reduce iron availability by induction of hepcidin, as a means to limit the spread of infection (Costa et al., 2011). Interleukin 6 could not be analysed despite several attempts to isolate the IL-6 sequence in both species, based on the *N. coriiceps* genome (available in NCBI database, under ID: GCF_000735185.1) (Shin et al., 2014) and in our transcriptomic data on *N. rossii* (unpublished). However, the two interleukin 6 receptor genes were analysed, *IL-6Rα* was highly expressed in liver and *IL-6Rβ* was highly expressed in head kidney of *N. coriiceps*. Interestingly, no significant change in gene expression response occurred in *N. rossii*. The differential response of IL-6R genes between the two species is consistent with iron metabolism-related genes response which was higher in *N. coriiceps*. This may suggest that also in these species IL-6 cytokines are involved in the induction of the synthesis of the iron regulatory hepcidin during hypoferremia inflammation (Berczi and Szentivanyi, 2003; Nemeth et al., 2004a; Roy et al., 2016; Shi and Camus, 2006). As indicated above, either the timing or a lower general immune response may explain the observations of low or poor immune responses. Although unlikely because of their close phylogeny, it is also possible that the two species may employ alternative pathways in iron metabolism defense. Indeed, species differences in physiology seems to exist. *N. coriiceps* appear to have lower thermal tolerance than *N. rossii* based on endocrine, metabolic and antioxidant parameters (Kandalski et al., 2018). Also, the more active *N. rossii* seems to have higher antioxidant defense system (ROS scavenge) enzyme activity than *N. coriiceps*, which could be related to their habits and different metabolic rates (Klein et al., 2017b).

Regardless of the changes in the mean expression level of the genes tested, a striking effect of the LPS injection was the increase in the variability of the individual response, when compared to the fish injected with saline. This is observable when looking at the individual gene expression variation and becomes obvious when a PCA was performed. From the analysis it is obvious that some individuals clearly responded to LPS by mounting an immune/iron-related reaction, but not others. This lack of synchronicity in response to a seemingly stressful process has been observed in many species, especially when using wild-caught specimens, with likely variations in their life-history experiences (Robertson et al., 2016), nutrition state (Ahola et al., 2017), physiological conditions (Killen et al., 2017) or stress response norms (Balasch and Tort, 2019). In our case, fish were acclimated before the experiments and treated equally thereafter, but changes in size, age and possibly on social condition (Filby et al., 2010) still existed. Additionally, this variability was also observed on the nature of the genes that responded and not only on the magnitude of the response. This could reflect differences in

sensitivity or differences in baseline iron, resulting in an asynchronous response. As indicated above for plasma Fe^{2+} our initial assumption was that a slower metabolism at low temperature could delay the response to LPS compared to temperate teleosts, but this assumption may have been proven wrong. It is possible that an acute response to LPS may have been missed early in the relatively long timeframe of this experiment. Further studies, using several shorter time points, and including iron transport should help to understand innate nutritional immunity in Antarctic fish.

In summary, despite a less than robust immune response of Antarctic notothenoids marked by considerable individual variability we have shown that overall LPS promotes the mobilization of genes important for iron retention in liver and head-kidney which should contribute to lower iron levels in extracellular fluids and fight bacterial infection through iron starvation.

CHAPTER 2.2

Toll-like receptor evolution: does temperature matter?

Toll-like receptor evolution: does temperature matter?

Manuscript to submit to Molecular Biology and Evolution

Acknowledgments

The authors would like to acknowledge the 2017 and 2019 crews of the Great Wall Chinese Antarctic Station for their hospitability and logistical support, Bruno Louro for the *N. coriiceps* transcriptome assemblies and making them available in the sea genomics database (http://sea.ccmar.ualg.pt). This study was carried out with logistic and financial support of the Portuguese Polar Programme (FACC PROPOLAR 2016-2017) and funded by Portuguese Foundation for Science and Technology (FCT) through projects FCT-NSFC/0002/2016, PTDC/BIAANM/3484/2014 and CCMAR/Multi/04326/2019, and a PhD fellowship SFRH/BD/120040/2016 to CS.

Toll-like receptor evolution: does temperature matter?

Cármen Sousa[1], Stefan A. Fernandes[1], João C.R. Cardoso[1], Pedro M. Guerreiro[1], Liangbiao Chen[2], Adelino V.M. Canário[1,2], Deborah M. Power[1,2]

1Centro de Ciências do Mar (CCMAR), Universidade do Algarve, Campus de Gambelas, 8005-139 Faro, Portugal.

2College of Fisheries and Life Science, Shanghai Ocean University (SHOU), 201306 Shanghai, China.

2.2.1. Abstract

Toll-like receptors (TLRs), an ancient and well conserved group of pattern recognition receptors (PRRs) of innate immunity, recognize conserved pathogen associated molecular patterns (PAMPs). The unique fish fauna living at near-zero degrees temperature in Antarctic waters prompted the study of their TLR repertoire and evolution considering the microbiota they co-evolved with. Comparative analysis of Tlr in the teleost fish species rich lineage of Antarctic Nototheniidae, and the non-Antarctic sister lineage Bovichtidae, as well as teleosts from temperate regions and other vertebrates, revealed that the environment had little impact on gene number. Notable conservation of TLR family members occurred across vertebrates, including the Nototheniidae. the basal *D. mawsoni*, which along with Pleuronectiformes suffered notable gene loss. Selective pressure in the Tlr ectodomain and within the leucine-rich repeats involved in pathogen recognition of *tlr5*, *tlr8*, *tlr13*, *tlr21*, *tlr22* and *tlr23* in Nototheniidae may represent adaptation to a unique Antarctic microbiome. Lipopolysaccharide exposure in *N. rossii* significantly increased plasma lysozyme activity but *tlr5*, *tlr21* and *tlr22* gene expression in the head-kidney and anterior intestine was not affected 8 and 24 h post-challenge at +2ºC. A temperature increase from 2 to 6ºC significantly upregulated *tlr5* and *tlr22* expression in the head-kidney of control and LPS challenged fish and *tlr21* significantly decreased in the anterior intestine. Our data suggests that adaptation of Nototheniidae to the cold and stable Antarctic environment have not affected *tlr* gene number evolution, but species-specific changes occur that may affect PAMP recognition and function associated with co-evolving microbiota and their adaptation to specific niches.

Keywords: TLR, Antarctic fish, innate immunity, immune challenge, cold temperature, evolution

2.2.2. Introduction

The innate immune system is a defence mechanism present in all metazoans and provides a rapid and nonspecific cellular and humoral response against a wide range of viruses, bacteria, fungi, and parasites (Smith et al., 2019). The molecular elements of innate immunity include soluble mediators (such as, cytokines, chemokines, antimicrobial peptides, lytic enzymes, growth inhibitors) and innate immune cells such as granulocytes and phagocytes and cell receptors (Uribe et al., 2011). Tissues such as the thymus and head-kidney are the principal immune organs, while the spleen, liver and mucosa-associated lymphoid tissues , such as the skin and intestine, are secondary immune organs, but they all play a major role in innate immunity (Soulliere and Dixon, 2017). The antigen-specific acquired immune response involving B and T lymphocytes is poorly developed in fish while the innate immunity is the prevalent immune response (Katzenback, 2015; Uribe et al., 2011)

Innate immune host-cell receptors detect beneficial and pathogenic microorganisms through the recognition of microbe associated molecular patterns (MAMPs) and pathogen-associated molecular patterns (PAMPs, (Akira et al., 2006)). A broad repertoire of pattern recognition receptors (PRRs) is encoded in the germline of invertebrate and vertebrate host cells and include Toll-like-receptors (TLRs), C-type lectin receptors, RIG-I-like receptors, and NOD-like receptors that survey the host microbiome (Brubaker et al., 2015; Thaiss et al., 2016a). The TLR superfamily of PRRs are transmembrane (TM) type-I proteins best characterised for their interaction with PAMPs and modulation of host innate immunity through the NF-κB signalling pathway (Azam et al., 2019; Dorrington and Fraser, 2019; Liu et al., 2017).

A diverse range of pathogen derived macromolecules (proteins, lipids, carbohydrates, and nucleic acids) are recognized by the extracellular N-terminal leucine-rich repeat (LRR) motif of TLRs, which is under high selective pressure for pathogen recognition (Dhar et al., 2019; Wang et al., 2016a). TLRs are also characterized by a highly conserved Toll/interleukin-1 receptor (TIR) intracellular domain that after receptor interaction with PAMPs, trigger the

intracellular signalling cascade that leads to an inflammatory response (Ahn et al., 2014; Palti, 2011; Pietretti and Wiegertjes, 2014; Rosenstiel et al., 2009; Satake and Sasaki, 2010; Werling et al., 2009). The TIR domain recruits cytosolic adaptor proteins, such as myeloid differentiation factor (MyD88) and TIR-domain-containing adaptor-inducing beta interferon (TRIF)) that trigger immune signalling and induce the production of cytokines (Deguine and Barton, 2014; Moresco et al., 2011).

In humans and other mammals, 10 well-characterized TLRs (TLR1-TLR10) exist and in other vertebrates the gene number is variable. In teleost fishes, up to 16 Tlrs have been reported in temperate species but gene number varies across species (Barreiro et al., 2009; Ji et al., 2018; Liu et al., 2019). Exceptions are the cod (*Gadus morhua*) and the zebrafish (*Danio rerio*), which underwent isoform-specific gene family expansions to generate 42 and 24 *tlr* genes, respectively (Solbakken et al., 2016). The acquisition of extra *tlr* isoforms in cod has been correlated with the highly variable pathogen loads and community composition of the paleoclimatic Arctic conditions (Solbakken et al., 2016). In fact, the large number and diversity of bacteria and viruses found in aquatic environments is proposed to have strongly influenced innate immunity in teleosts (Groff, 2001). The vertebrate TLRs are classified into six superfamilies based on sequence similarity: TLR1 (TLR 1, 2, 14/18, 15, 25, 27), TLR3 (TLR3), TLR4 (TLR4), TLR5 (TLRs 5, 5S), TLR7 (TLR 7, 8, 9) and TLR11 (TLR 11, 13, 21, 22, 23) (Nie et al., 2018). In mammals, members of the TLR 1, 2, 4, 5 and 6 subfamilies are localized at the cell membrane and recognize mainly bacterial pathogens, while TLRs 3, 7, 8 and 9, are localized in the endosomes and respond more to viruses (Kawai and Akira, 2010; Liu et al., 2019). In teleosts, Tlr function in immunity is largely unexplored but protein homology indicates they probably recognise similar pathogens to mammals, and some recognize both bacterial and viral pathogen components (Liu et al., 2019; Palti, 2011).

Here we test the hypothesis that the Notothenioids, a group of fish adapted to the extreme cold of the Antarctic and exposed to a unique microbiome, possess a divergent Tlr repertoire relative to other teleosts. The Nototheniidae arose through adaptive radiation approximately 10 million years ago and is species rich relative to the non-Antarctic sister lineage. They acquired specific morphological and molecular modifications driven by habitat utilization and the extreme cold and stable sea water environment (range ca. -2ºC to +2ºC) (Near et al., 2015 Near et al., 2012). Comprehensive characterization and comparative sequence analysis was performed to define the *tlr* repertoire in the Antarctic Nototheniidae and the sister lineage represented by the sub-Antarctic *Cottoperca gobio* (family Bovichtidae) (Near et al., 2015) in relation to other teleost fishes and other vertebrates. Gene linkage analysis was

performed to map *tlr* gene evolution at the genome level and codon usage bias was used to establish if ancient adaptation events spanning speciation have occurred in *tlr* of Nototheniidae. The flatfish (Pleuronectiformes), which occupy a demersal niche, are cosmopolitan and undergo profound body remodelling during development and for which several genomes are available, were included to assess if these characteristics influenced *tlr* evolution. A lipopolysaccharide (LPS) challenge of *Notothenia rossii* was used to assess the transcriptional response of *tlr* under control and increased environmental water temperature.

2.2.3. Material and Methods

2.2.3.1. In silico databases searches

To characterize *tlr* gene members in Antarctic Notothenioidei , available molecular data for six species of Nototheniidae *Notothenia coriiceps* (Nco), *Chionodracos hamatus* (Cha), *Trematomus bernacchii* (Tbe), *Pseudochaenichthys georgianus* (Pge), *Gymnodraco acuticeps* (Gya), *Dissostichus mawsoni* (Dma) and *Cottoperca gobio* (Cgo) of the sub-Antarctic Bovichtidae were screened for homologues using the previously reported (Ahn et al., 2014) *N. coriiceps* sequences as the query using BLAST (Altschul et al., 1990). To increase the number of notothenids in the analysis an "in house" *de novo* multi-tissue transcriptome assembly of *N. rossii* was interrogated with *tlr* using the tBLASTn algorithm (**Supplementary table 2.2.1, Annex I**). The retrieved sequences were translated into predicted proteins with the ExPASy translation tool (Artimo et al., 2012) and their identity was confirmed by searching against the human sub dataset (human (taxid:9606)) Of non-redundant (nr) nucleotide database at the National Center for Biotechnology Information. The *tlr* gene complement in the genomes of seventeen other teleosts were also determined and included three other Perciformes (same order as Nototheniidae), and two other evolutionary proximate species within the Eupercaria clade the *Dicentrarchus labrax* (Dla, Moronidae family) and *Sparus aurata* (Sau, Sparidae family) (Hughes et al., 2018). Representatives of evolutionary related teleost taxonomic orders were also searched such as *Dicentrarchus labrax* (Dla) and *Sparus aurata* (Sau), Gasterosteiformes *Gasterosteus aculeatus* (Gac), one Beloniformes (*Oryzias latipes*, Ola), one Characiformes (*Astyanax mexicanus*, Ame), one Cichliformes (*Oreochromis niloticus*, Oni), two Cyprinodontiformes (*Poecillia formosa*, Pfo and *Xiphophorus maculatus*, Xma), one Cypriniformes (*Danio rerio*, Dre), one Gadiformes (*Gadus morhua*, Gmo), four

Pleuronectiformes (*Paralichthys olivaceus*, Pol, *Cyonoglossus semilaevis,* Cse, *Solea senegalensis* (Sse) and *Hippoglossus hippoglossus* (Hhi)), one Salmoniformes (*Salmo salar*, Ssa) and two Tetraodontiformes (*Takifugu rubripes*, Tru and *Tetraodon nigroviridis*, Tni). Putative *tlr* genes were retrieved based on their high sequence homologies (cut-off e ≤ -40) with the query sequences and database orthologue/paralogue genome annotations (**Supplementary table 2.2.1, Annex I**).

To better understand Tlr evolution in fish, the genomes of early diverging fish species such as the lobe-finned fish, *Latimeria chalumnae* (Lch), the ray-finned fish *Lepisosteus oculatus* (Loc), two cartilaginous fish, *Callorhinchus milii* (Cmi), *Rhincodon typus* (Rty) and the agnathan, *Petromyzon marinus* (Pma), were also interrogated for *tlr* genes. All searches were performed against the most recently annotated fish genome assemblies available from ENSEMBL or NCBI (Supplementary Table 1). The aminoacid *tlr* sequences from *T. bernacchii* and *N. coriiceps* were used to retrieve homologue genes from the genomes of 5 tetrapods in ENSEMBL (*Homo sapiens* (Hsa), *Mus musculus* (Mmu), *Gallus gallus* (Gga), *Anolis carolinensis* (Aca), *Xenopus tropicalis* (Xtr)), which were used for comparative analysis.

2.2.3.2. Sequence comparisons and phylogenetic analysis

The deduced Nototheniidae Tlr protein sequences were compared with the homologues from other species. Protein sequence were aligned with the MUSCLE algorithm available from the Aliview platform v1.22 (Laarson, 2014) and the percentage of amino acid sequence identity/similarity was calculated using GeneDoc v2.7 software. The localization of protein domains characteristic of TLRs such as the LRR (typical LRR conserved motif, LxxLxLxxNxL, where x represents any aa), TM and TIR motifs were predicted using ScanProsite (de Castro et al., 2006) and the Simple Modular Architecture Research Tool (SMART) (Letunic et al., 2021) and also by the identification of highly homologous sequence regions in the aligned sequences. The presence of a signal peptide was predicted using the SignalP 4.1 Server (Nielsen, 2017).

For the phylogenetic analysis, short incomplete sequences were removed from the multiple protein sequence alignment (Supplementary Table 1). Very similar sequences retrieved from the cod genome and that resulted from tandem gene duplications were also removed. The protein sequence alignment was manually edited to remove large gaps and misaligned sequences and the edited alignment containing the three main Tlr protein domains

(LRR, TM and TIR) were used for the construction of a phylogenetic tree using bayesian inference (BI) and maximum likelihood (ML) methods. The dataset used to construct both trees was based on an alignment of 431 sequences. Phylogenetic trees were constructed using the VT model that best fit the data given by model test-ng 0.1.5 in the CIPRES Science Gateway v3.3 (Miller et al., 2010). The BI tree was built using MrBayes (Ronquist et al., 2012) and 1.000.000 generation sampling and probability values to support tree branching. The ML tree was built using the RAxML v8.2.12 (Stamatakis, 2014) method with 1000 bootstrap replicates. Three cnidarian TLR-like sequences (obtained from Liu et al., 2019) were used to root the trees. Both the BI and ML trees were visualized in FigTree v1.4.3 (Rambaut and Drummond, 2010) and edited using Inkscape v0.92.3.

2.2.3.3. Neighbouring gene analysis

To better characterize the evolution of *tlr* genes in Notothenioidei and confirm if gene absence in Antarctic fish genomes was due to technical issues linked to genome assembly or a results of gene loss, the localization of five to seven genes in the neighbourhood of *tlr1*, *tlr2a* and *b*, *tlr5* and *5s*, *tlr8* and *tlr23* loci were characterized and compared across the four Nototheniidae representatives (*P. georgianus*, *N. coriiceps*, *T. bernacchii* and *D. mawsoni*) and the sub-Antarctic *C. gobio*, all of which Perciformes, and a Gasterosteiformes, *G. aculeatus*. Two Pleuronectiformes (*P. olivaceus* and *C. semilaevis*) were also included as the genomes of this teleost order possess a reduced *tlr* gene number in relation to other teleosts. The flanking genome regions of *tlr1*, *tlr2*, *tlr5*, *tlr5s* and *tlr8* characterised in *G. aculeatus* and in the *T. bernacchii* were used as the reference to identify homologue genome regions in other species. For *tlr23* the *P. georgianus* and *N. coriiceps* flanking genes were used. The criteria for species selection were a) the presence of the target genes and b) the quality of the genome assemblies. Neighbouring genes were identified using NCBI/ENSEMBL genome annotations or by sequence similarity searches against the genome assembly of each species.

2.2.3.4. Selective pressure analysis

Antarctic fish Tlr amino acid sequences were aligned with the remaining Perciformes and Pleuronectiformes orthologues using the Aliview platform v1.22 (Laarson, 2014) with the

default settings. To obtain multiple codon alignments PAL2NAL v14 (Suyama et al., 2006) was used with the gap removal option and Neighbour-Joining trees for each gene family were built in MEGA X v10.1.8 (Kumar et al., 2018) with 1000 bootstrap replicates. Tlr sequences that were incomplete were removed from the analysis. To identify potential sequence changes that might be associated with the adaptation to the Antarctic environment, a branch-site analysis (BSM) was performed for each Tlr on the ancestral branch of Antarctic fish. For the specific case of *tlr21* the branch-site analysis was performed on each *G. acuticeps* duplicates. A sites analysis (SM) was performed with the sequences of the Antarctic species if positive selection was identified on their ancestral branch.

The branch-site and sites analysis used to test for evolutionary pressure were based on the ML method of the Codeml (PAML v4.9 package (Yang, 2007)) in EasyCodeml (Gao et al., 2019) (**Additional data 1-15 in Annex I**). Codon substitution models were compared with likelihood ratio tests (LRT) calculated from the difference between their log likelihood (lnL) values.

2.2.3.5. Experimental immune challenge

Animal collection and experimentation were approved by the Portuguese Environment Agency, under the regulations set by the Treaty of Madrid for scientific investigation in Antarctica. The experiments performed complied with the EU and Portuguese regulations for animal experimentation.

The experiment was performed in January and February 2019, during the Antarctic summer. Adult *Notothenia rossii* (30.3 ± 0.35 cm total length and 312 ± 21.51 g weight, mean ± sem) were captured (at depths - 520 m) using hook-and-line in the bay of the Great Wall Station (′ 62° 12' 35.40" S; 58° 57' 26.39" W) located in King George Island in the Antarctic Peninsula region. Captured fish were transferred to the station and maintained at natural water conditions in a flow-through circuit with seawater pumped from the ocean. Fish were kept in 200L plastic tanks for at least 5 days before the immune challenge and fed daily with a mixture of limpets, amphipods and fish muscle. Water temperature (2.1 ± 0.5 ℃), salinity (29 ± 0.5 ppt) and oxygen levels (10.7 ± 0.4 mg/L) were monitored three times a day (7 am, 2 pm and 9 pm). No mortality was observed during acclimation or during the experiments.

For the immune challenge, fish were lightly anaesthetized in 2-phenoxyethanol (0.1 mL/L, Sigma-Aldrich) and the control fish (n = 6) were injected intraperitoneally (IP) with

saline buffer (0.2% (v/w) of 1.1% NaCl), the immune challenged group (n = 6) were injected with 1.5 mg/mL LPS in 0.2% (v/w) of 1.1% NaCl (LPS extracted from *Escherichia coli* O111:B4, L2630, Sigma-Aldrich, Portugal) (**Figure 2.2.1**). The dose of LPS amounted to 3 mg/kg and was selected based on (Seppola et al., 2015)(Chen et al., 2016; Guzmán-Villanueva et al., 2014; Nayak et al., 2011). To assess the impact of water temperature on the immune response of *N. rossii*, a similar immune challenge experiment was run in parallel in fish previously acclimated to and maintained at 6.0 ± 0.8 ºC in a semi-closed system. These fish were acclimated by increasing the seawater temperature by 1.0 ºC daily from 2 to 6ºC. In these tanks salinity and oxygen levels were equally monitored, with average values of 29 ± 0.5 ppt and 9.3 ± 0.9 mg/l respectively. (**Figure 2.2.1**). 0

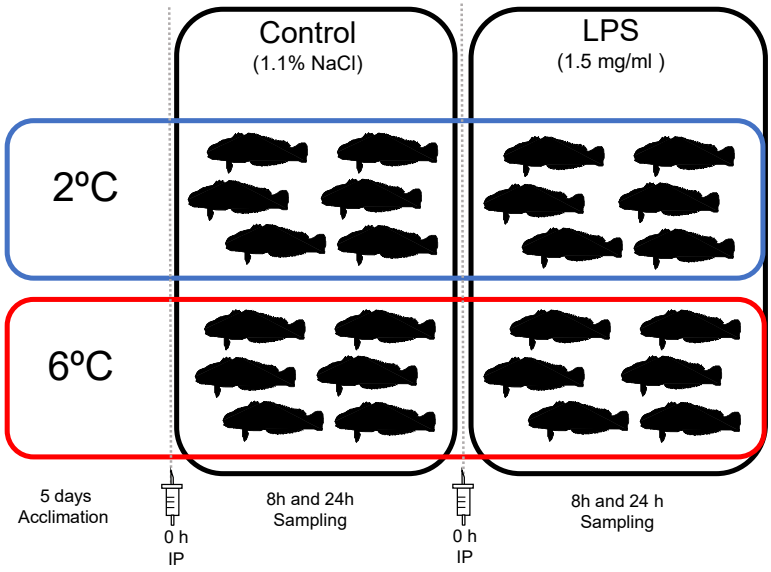

Figure 2.2.1. Schematic diagram of the experimental immune challenge. Adult *N. rossii* captured from the wild were acclimated to the experimental tanks at 2 ºC or at 6ºC before the immune challenge. Fish (n=6/ group) were IP-injected 0.2% (v/w) with bacterial lipopolysaccharide (LPS, 3 mg/kg in 1.1% NaCl) at 2 ºC and 6ºC. Control fish (sham) at both water temperatures were injected with saline vehicle. Tissue samples and plasma were collected at 8h and 24h post-injection.

Fish were sacrificed 8 h and 24 h post-IP injection with an overdose of 2-phenoxyethanol (1 mL/L, Sigma-Aldrich), weighed and blood was collected from the caudal vasculature using a heparinised 1-ml syringe fitted with a 21-gauge needle. Blood was centrifuged at 10,000 g, and 4 ºC for 4 minutes and the plasma collected and stored at -80ºC until analysis. For tissue sample collection the fish were decapitated and the central nervous system destroyed. The head-kidney (principal hematopoietic organ in teleosts) and anterior intestine (duodenum region) were dissected out and placed in RNA later (Sigma-Aldrich) at 4ºC for 24h before storage at -20ºC.

2.2.3.6. RNA extraction, cDNA synthesis and quantitative PCR analysis

Total RNA was extracted from *N. rossii* tissues (~25 mg) using an E.Z.N.A. Total RNA Kit I (Omega Bio-Tek, USA) and following the manufacturer's instructions. The DNase I digestion protocol was performed directly on the columns to eliminate contaminating genomic DNA with RNase-free DNase I (Omega Bio-Tek). The integrity of the extracted RNA was evaluated by 1% agarose gel electrophoresis and the quantity and quality of the RNA was assessed by absorbance using a NanoDrop One (Thermofisher, Spain). Approximately 500 ng of *N. rossii* DNase treated total RNA was used to synthesize cDNA in a final reaction volume of 20 µL with 200 ng of random hexamers (Jena Biosciences, Germany), 10 mM dNTPs (Promega, USA), 100 U RevertAid reverse transcriptase (RT, Promega) and 8 U of Ribolock RNase Inhibitor (ThermoFisher) for 10 min at 20 ℃, 50 min at 42 ℃ and 5 min at 72 ℃.

The expression of *tlr5*, *tlr21*, *tlr22* and *tlr25* in *N. rossii* was determined by real time quantitative PCR (RT-qPCR) using specific gene primers. The *tlr* gene transcripts selected were the only *tlr*s found in an "in house" immune-related multi-tissue (head-kidney, skin and intestine) transcriptomes of *N. coriiceps*, 7 days after LPS challenge. The reference genes selected for normalisation, beta-actin (*β-actin,* internal accession number TR9194|c3_g4_i8) and *18s* rRNA, did not vary in expression between any of the experimental groups. The cDNAs used for the RT-qPCR were diluted to a final concentration of 25 ng/µl for the candidate genes and to 10 ng/µl for *β-actin* and 0.01 ng/µl for *18s.* The qPCR reactions were performed in 96-well plates (Axygen, Germany) using a CFX96 Touch Real-Time PCR Detection System (Bio-Rad, USA). The final RT-qPCR reaction volume was 10 µl and it contained 2 µl of cDNA, 5 µl of SsoFast Evagreen Supermix (Bio-Rad) and 0.3 mM of each of the specific primers (forward and reverse, **Table 2.2.1**). The thermocycle used was: 95 ℃ for 30 sec, followed by 40 cycles of 95 ℃ for 5 sec and 10 sec at the annealing temperature. Melting curves 60 ℃ to 95 ℃ with an increment of 0.5 ℃ for each 10 s were performed to detect reaction specificity. To quantify transcript expression levels standard curves for each gene were performed during RT-qPCR reactions using serial dilutions (1:10) from 0.5 ηg/µl to 0.05 fg/µl of the quantified amplicon. All RT-qPCR analysis included a no template control and a -RT control. PCR efficiencies and the coefficient of determination (r^2) were calculated and were > 90 % for each target gene transcript analysed. Gene expression levels were normalized using the geometric

mean of the two reference genes (18S and *β*-actin) and the SQ mean of the target genes based on the standard curve method (Čikoš et al., 2007).

Table 2.2.1. qPCR primer pairs, product size, annealing temperatures, and efficiency.

	Sequences (5`→ 3`)	**bp**	**T (ºC)**	**Efficiency (%)**
tlr5 Fw	*TTTCGTCCAGAGGAGGGAGT*	168	55	90.4
tlr5 Rv	*TTGGTCCGATGTTCTCCAGC*			
tlr21 Fw	*TGGTGGAAATGTGAAGTATGATCC*	87	55	90.5
tlr21 Rv	*AGCACATCAATTAAATGACACCTCT*			
tlr22 Fw	*AGTTTCACCTGTGACTGCGA*	87	55	90.4
tlr22 Rv	*AAAGTTGGAGGCGTCAACCA*			
18S Fw	*TGACGGAAGGGCACCACCAG*	158	58	93.6
18S Rv	*AATCGCTCCACCAACTAAGAACGG*			
β-actin Fw	*AACCCAAACGACTGGCTCTG*	174	58	90
β-actin Rv	*TTCCACACATTCACACCGCA*			

2.2.3.7. Blood plasma total protein and enzyme activity

Total plasma protein was determined using a Quick Start ™ Bradford Protein Assay kit (Bio-Rad, Portugal) (Bradford, 1976) adapted for a 96-well plate and reactions were analysed at 590 nm at 25°C using a spectrophotometer (Agilent Technologies, USA).

The activity of lysozyme was measured using a turbidimetric assay (Ellis, 1990). Briefly, 130 µl of lyophilized *Micrococcus luteus* cells (0.6 mg/mL, Sigma-Aldrich) in 0.05 M sodium phosphate buffer, pH 6.2, was mixed with 20 µl of blood plasma in a flat bottomed 96 well-plate. For the standard curve, a concentration range from 50 U/ml to 500 U/ml of hen egg white lysozyme (Sigma-Aldrich) was used. All reactions were performed in duplicate and were incubated at 25°C for 10 minutes and then measured in a multiplate readers (Agilent Technologies) at 450 nm.

Antitrypsin activity was used to assess total antiprotease activity (Ellis, 2001). Trypsin from porcine pancreas (20 µl from a 5 mg/mL solution, Sigma-Aldrich) was mixed with *N. rossii* blood plasma (10 µL) for 10 minutes and then 200 µL of 0.1 M phosphate buffer pH 7.0 and 250 µL of 2% Azocasein (Sigma-Aldrich, Germany) was added. Reactions were performed in duplicate and were incubated for 1 hour at 4°C to simulate Antarctic water temperatures. Subsequently, 500 µL of 10% trichloroacetic acid (Sigma-Aldrich) was added to the reaction and it was incubated for a further 30 minutes at room temperature (21°C) and then the samples

were centrifuged at 10.000 rpm for 10 minutes. One hundred µL of the supernatant from each of the reactions was transferred to a 96-well plate and 100 µL sodium hydroxide (1N, NaOH, VWR, Spain) was added. Assays were measured in a multiplate reader (Agilent Technologies) at 450 nm.

2.2.3.8. Statistical analysis

Differences in gene expression and enzyme activity between the control and LPS-treated groups were assessed at 8h and 24h after exposure at different seawater temperatures (2ºC and 6ºC) using a three-way analysis of variance followed by Tukey´s test Normality was tested using the Shapiro-Wilk normality test. Graphs for the results of RT-qPCR were generated using SigmaPlot v12.5 and for enzymatic activity GraphPrism v6.01 was used. The statistical significance level was $p < 0.05$.

2.2.4. Results

2.2.4.1. Tlrs in fish and other vertebrates

Ten TLRs (*TLR1-TLR10*) genes exist in humans (*H. sapiens*) and based on aminoacid sequence similarity they cluster in six superfamilies containing various members: TLR1 (TLR1, 2, 6 and 10), TLR3 (TLR3), TLR4 (TLR4), TLR5 (TLR5 and 5S) and TLR7 (TLR7, TLR8 and TLR9). In other tetrapods, 12 TLR genes were found in *M. musculus*, 10 in *G. gallus*, 13 in *A. carolinensis* and 16 in *X. tropicalis* genomes (**Figure 2.2.2**). Sequence similarity searches identified fish homologues of the human genes and of the non-mammalian TLR11 (TLR 11, TLR13, TLR21, TLR22 and TLR23) superfamily (**Figure 2.2.2**). Homologues of the human TLR1 to TLR3, TLR5 and TLR7 to TLR9 were found in most fish genomes analysed but TLR6 was only retrieved from the genome of the lobe-finned fish (*L. chalumnae*) and the cartilaginous fish (*C. millii*). Homologues of human TLR4 were only identified in *D. rerio* and *L. oculatus* genomes. No homologues of human TLR10 were retrieved from any of the fish genomes analysed. Searches for Tlrs in the teleost genomes revealed that gene number was similar and varied from 11 to 16 except in *D. rerio* and *G. morhua* where 24 and 42 genes, respectively

were retrieved (**Figure 2.2.2**). The flatfish had less *tlr* genes than other teleosts and *S. senegalensis* and *C. semilaevis* had 6 and 7 genes, respectively.

Fish have an additional Tlr superfamily than human, with some members also identified in the amphibian, *Xenopus tropicalis* including, Tlr14/18, Tlr13, Tlr21 and Tlr22. Several Tlr, Tlr25, Tlr27, Tlr5s (a short isoform of Tlr5) and Trl23 were exclusive to the fish. In *L. oculatus*, a ray-finned fish which radiated before the teleosts 15 *tlr* genes were found that were homologues of the teleost *tlr1-5*, *tlr 7-9*, *tlr14/18*, *tlr22*, *tlr25* and *tlr27*. In the two cartilaginous fish *C. milii* and *Rhincodon typus* a smaller number of genes, 7 and 8, respectively, were identified that belonged to the superfamilies TLR1, TLR3 and TLR7. In *L. chalumnae* that has a more similar genome to tetrapods, 14 *tlr* genes were found and in agnathan, *Petromyzon marinus* a representative of the earliest divergent lineage of vertebrates, 11 *tlr* genes were retrieved (**Figure 2.2.2**).

In summary, *TLR* gene number has been mainly conserved across vertebrates although isoform maintenance was variable. Mammals lost the TLR11 superfamily and fishes apart from sharks retained the highest number of TLR11 superfamily members. A unique characteristic of the Perciformes and other members of the Eupercaria clade (*S. aurata* and *D. labrax*) relative to other teleosts was the retention of *tlr13*. The pleuronectiforms suffered extreme *tlr* gene loss and the cod (*tlr25*, *tlr8*, *tlr9* and *tlr22*) and zebrafish (*tlr4* and *tlr11*) underwent an extraordinary gene family expansion through tandem duplication of a few TLRs.

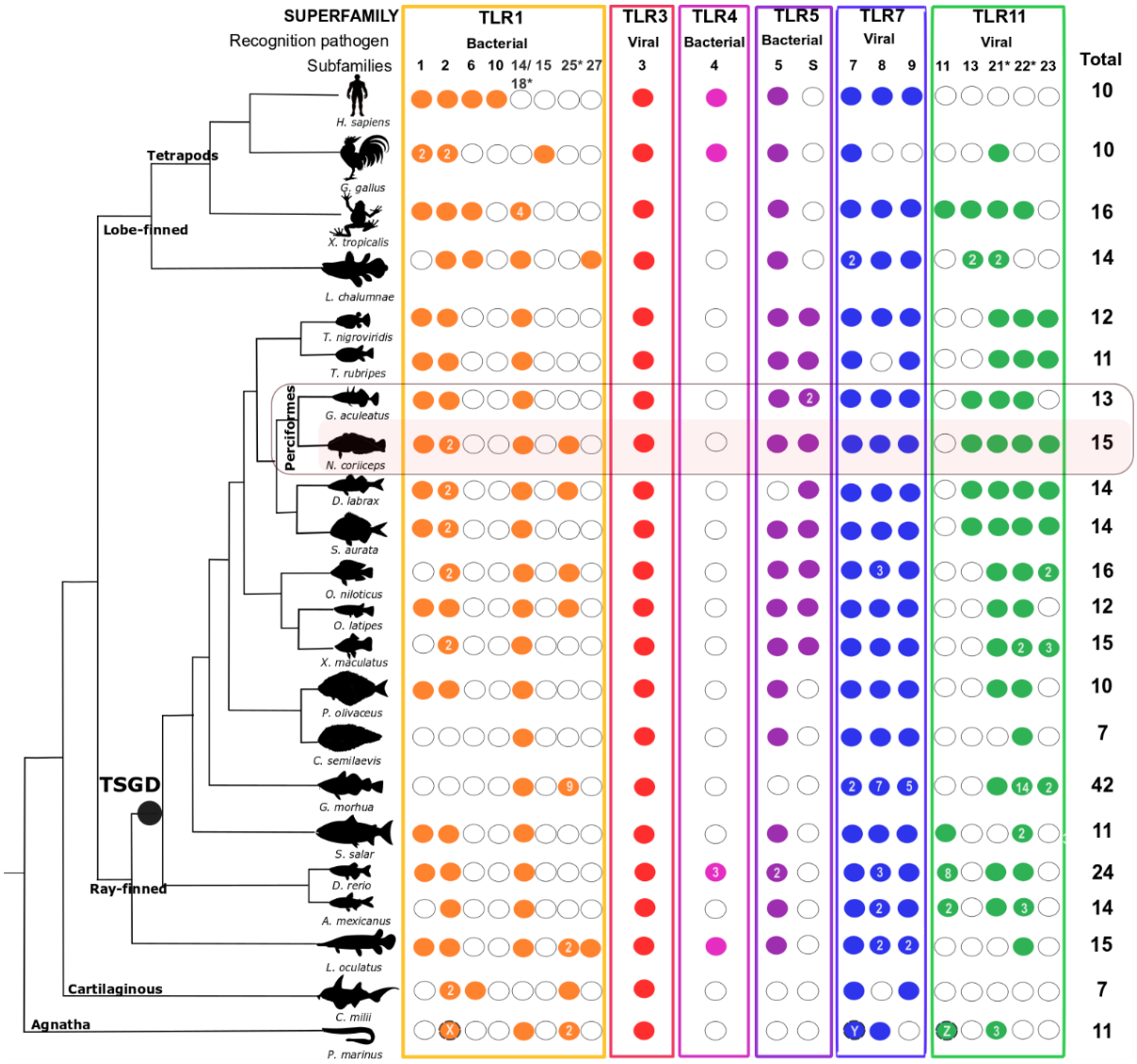

Figure 2.2.2. Dendrogram illustrating the representation of *TLRs* in vertebrate genomes. The *TLR* genes identified in different vertebrates, represented by coloured circles, belong to the six TLR superfamilies. When multiple genes for a given subfamily were identified gene number is indicated inside the circle. When a gene is absent this is indicated by a white circle. The profile of pathogen recognition for each TLR superfamily is indicated (Liu et al., 2019). The specific subfamily members that recognize a wider range of pathogens (viruses and bacteria) are indicated by "*" (Liu et al., 2019; Palti, 2011). *N. coriiceps* is included as a representative of the Notothenioidei. The Perciform branch to which the Notothenioidei belong is circled to highlight the Antarctic representatives with phylogenetically proximity to the teleosts and the Eupercaria clade (Hughes et al., 2018).Tlr superfamily members from human, chicken, reptile and *Xenopus* genomes are also represented. The total number of tlr genes found is indicated for each species. The figure was constructed taking into consideration the evolutionary relationship between the species represented using as the starting point the studies of (Ahn et al., 2016; Near et al., 2015). The teleost specific genome duplication (TSGD) event is indicated. Gene/transcript accession numbers of the tlrs identified and represented in the dendrogram are available in Supplementary Table 2.2.1.

2.2.4.2. Tlrs in Antarctic notothenioids and other teleosts

Sequence searches in six Antarctic Nototheniidae species revealed they have a distinct gene repertoire and *tlr* gene number was variable across the species (**Figure 2.2.3**). *D. mawsoni* (the toothfish), that produces anti-freeze proteins, had the lowest number of *tlr* genes (10) and *G. acuticeps*, a benthic sedentary species, had the highest number of *tlr* genes (16). The loss in *D. mawsoni* of *tlr1*, *tlr2*, *tlr5* and *tlr8* gene homologues explains the lower number of *tlr* genes in its genome. Although a genome is not available, analysis of a mixed tissue transcriptome of *N. rossii* revealed 12 *tlr* gene transcripts while in the genome of the evolutionary proximate species, *N. coriiceps*, 15 *tlr* genes were retrieved (**Figure 2.2.3**). In the *C. gobio* genome, a sub-Antarctic species 13 *tlrs* were identified and *tlr5S* and *tlr23* genes were absent. In all Notothenioidei (except *D. mawsoni*) in common with other teleosts two *tlr2* genes exist (**Figure 2.2.3**).

Comparison of *tlr* gene number in Antarctic and sub-Antarctic fish with other representatives of the Perciformes order, *G. aculeatus*, *S. aurata* and *D. labrax* (**Figure 2.2.2 and 2.2.3**) and Pleuronectiformes order, *P. olivaceus*, *H. hippoglossus*, *C. semilaevis* and *S. senegalensis* (**Supplementary figure 2.2.1**) revealed that gene number was variable with no clear pattern. In *G. aculeatus* (the closest Perciform representative to the Notothenioidei sub-order) 13 *tlr* genes were identified in common with what was found in *C. gobio*, although the pattern of gene retention and loss was different. For example, the *G. aculeatus* genome lacks *tlr25* and one *tlr2* duplicate, while *C. gobio* lost the duplicate *tlr5s* and retained duplicate *tlr2* genes (**Figure 2.2.3**).

In summary, there was no evidence of major gene family expansion or loss of TLR superfamilies in the Antarctic Nototheniidae. Retention of subfamily members was very similar in Nototheniidae except for *D. mawsoni* that specifically lost *tlr1* and *tlr7* superfamily members.

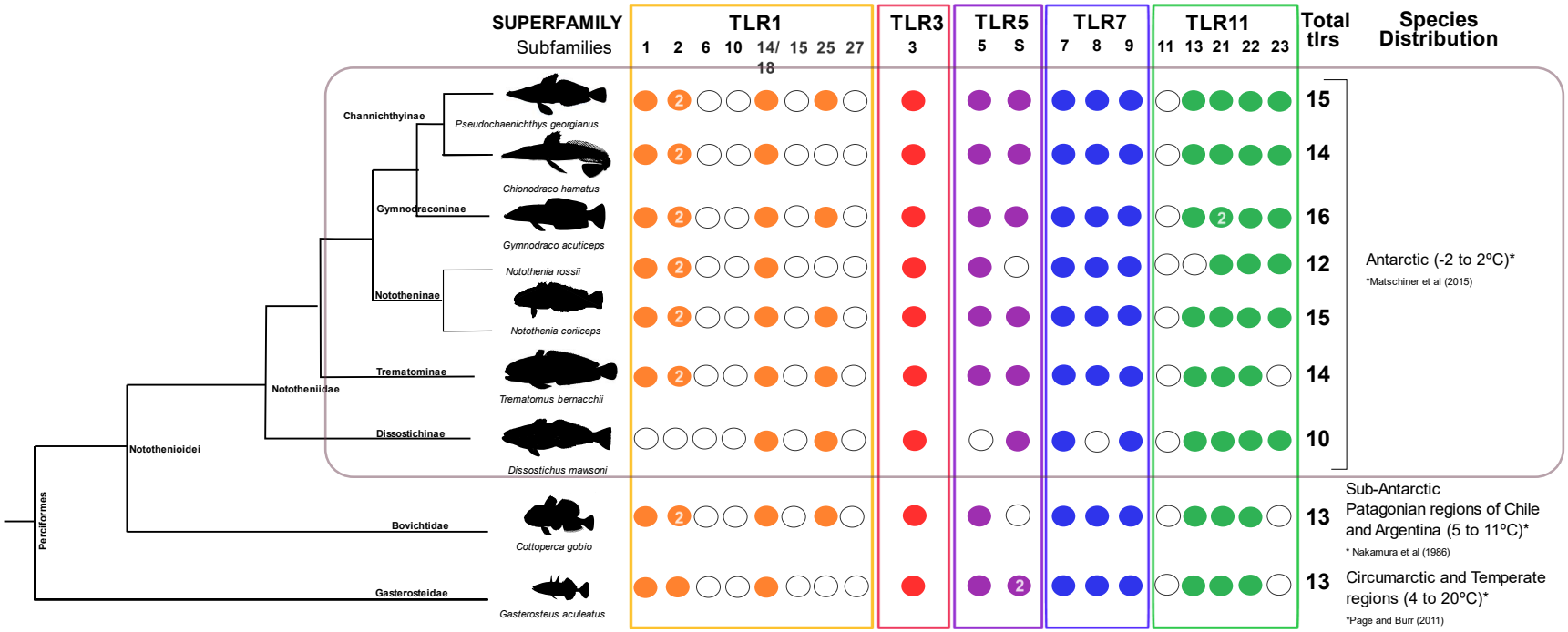

Figure 2.2.3. Detailed dendrogram of Tlr genes/transcripts identified in Nototheniidae. Tlr **g**enes/transcripts were distributed among the five TLR superfamilies as indicated by the coloured circles. When multiple genes were identified for a given Tlr isoform, gene number is indicated inside the coloured circles. Genes that were not identified are indicated with a white circle. *C. gobio* was used as a representative of the Nototheniidae sister-lineage and *G. aculeatus* was used as the representative of Perciformes outside the Notothenioidei. The figure was drawn considering the relative evolutionary relationship between the six Antarctic fish species and the sub-Antarctic fish using as starting point the studies of (Papetti et al., 2021). Gene/transcript accession numbers of the *tlrs* identified and represented in the dendrogram are available in Supplementary Table 2.2.1.

2.2.4.3. Phylogeny of Nototheniidae Tlrs with other vertebrates

Phylogenetic analysis of the deduced Tlr proteins of Nototheniidae with other vertebrates confirmed the existence of receptors that belong to the five TLR superfamilies (TLR1 (S1), TLR3 (S3), TLR5 (S5), TLR7 (S7) and TLR11 (S11)). The clustering of Nototheniidae sequences with other fish and tetrapod members confirmed the existence of subfamily members (**Figure 2.2.4 and in Annex I, Table 2.2.2**, **Supplementary figure 2.2.2-3**). The BI and ML trees of TLR share similar topologies and the Nototheniidae Tlrs cluster together and the Nototheniidae sequence branches are in most cases rooted with the genes retrieved from the representative of the sister-lineage, *C. gobio*. Moreover, the Tlrs from Antarctic and sub-Antarctic species tended to cluster with Tlr from other Perciformes and were more tightly clustered with the evolutionary proximate *G. aculeatus*. Both the BI and ML phylogenetic trees confirmed that all vertebrate TLRs shared common ancestry and that members of the TLR1 and TLR4 superfamilies were the first to radiate and TLR4 was the first to diverge clustering at the base of the other vertebrate superfamilies.

TLR1 and TLR4 superfamilies

Members of the TLR1 superfamily were the most diverse in Nototheniidae as well as in other teleost fish and tetrapods. In contrast, TLR4 members are absent from most other vertebrate genomes except for tetrapods, and a few fish orders, the Lepisosteiformes and the Cypriniformes where three gene copies that resulted from a species-specific duplication exist (**Figure 2.2.4 A**).

In vertebrates, the TLR1 superfamily is composed of 8 subfamilies, and the tree topology suggests that they group into two main clusters: one cluster contains Tlr1, Tlr2, Tlr6, Tlr10 and Tlr27 and the other Tlr14/18 and Tlr25 (**Figure 2.2.4 A**). The Tlr6 and Tlr10 cluster with tetrapod Tlr1. TLR10 and TRL6 were found in mammals, reptiles and amphibians, but not in fish. Members of the Tlr27 subfamily were only found in the early evolving fish genomes, the lobe-finned fish Coelacanthiformes (*L. chalumnae*), ray-finned fish Lepisosteiformes (*L. oculatus*) and the cartilaginous Orectolobiformes (*R. typus*). Sequence clustering also confirmed the absence of *tlr1* genes from representatives of teleosts (Cichliformes, *O. niloticus*; Cyprinodontiformes, *X. maculatus*; Gadiformes, *G. morhua*; Pleuronectiformes, *C. semilaevis*), the Coelacanthiformes and the cartilaginous Chimaeriformes (*C. milii*) (**Figure 2.2.4 A**).

Members of the Tlr2 subfamily exist in most of the vertebrate genomes analysed and they grouped with Tlr27, suggesting they shared a common evolutionary origin after the divergence from a common *tlr1* ancestral gene. Clustering of the two *tlr2* genes found in Notothenioidae and in other teleost fish suggests they arose during the teleost specific genome duplication and the paralogues were named *tlr2*a and *tlr2b*. In *P. marinus* (Petromyzontiformes representative) a single *tlr2-like* gene was found, and clustering suggested that it might have more sequence similarity with the vertebrate *tlr2*/*tlr27* gene precursor (**Figure 2.2.4 A**).

Members of the Tlr14/18 subfamily were confirmed in most teleost fish orders and a single gene was also found in Coelacanthiformes (*L. chalumnae*), Lepisosteiformes (*L. oculatus*) and in *P. marinus* but was absent from cartilaginous fishes (Chimaeriformes and Orectolobiformes). The Tlr25 subfamily members were only found in the Perciform *D. labrax* and in the representatives of Beloniformes, Cichliformes and species-specific gene duplications in Gadiformes generated 9 copies (**Supplementary table 2.2.1**). *Tlr25* species-specific gene duplicates were also found in the Lepisosteiformes and in *P. marinus* (**Figure 2.2.4 A**).

In the Notothenioidae, except for Dissostichus, the number of TLR1 superfamily members was similar to the sub-Antarctic sister clade (Bovichtidae) with a single gene for *tlr1*, *tlr14/18* and *tlr25* and duplicate *tlr2* genes (*tlr2a* and *tlr2b*) (**Figure 2.2.4 A**).

TLR3 and TLR11 superfamilies

A single *tlr3* gene was present in Notothenioidae, the sister clade, other Perciformes and in the other fish genomes analysed in common with all other vertebrates. The TLR11 superfamily includes genes for *tlr11*, *tlr13*, *tlr21*, *tlr22* and *tlr23* subfamilies and they were found in most fish including Notothenioidae (**Figure 2.2.4 B**). The tree typology revealed that TLR11 superfamily members grouped into two clusters: TLR11/TLR13/TLR21 and the TLR22/TLR23. The BI and ML trees confirmed the absence of a *tlr11* homologue in Notothenioidae and most other teleosts with the exception of the Salmoniformes (*S. salar*), Cypriniformes (*D. rerio*) and Characiformes (*A. mexicanus*) in which several gene copies exist (**Figure 2.2.4 B**). Members of the *tlr13* subfamily were only found in Perciformes including Notothenioidae and in the sister lineage suggesting that this gene only persisted in this order.

Tlr21 and *tlr22* genes were identified in fish and tetrapods but *tlr23* was exclusive to the fish. The phylogenetic trees confirmed the absence of *tlr21* from the Pleuronectiforme, *C. semilaevis* and the Salmoniforme *S. salar* but also in the two cartilaginous fish analysed. *Tlr22* was present in all teleost fish genomes analysed and gene duplicates were found in some teleosts

and 14 species-specific gene copies existed in the Gadiforme *G. morhua* (**Figure 2.2.4 B**, **Supplementary table 2.2.1**). *Tlr23* genes were duplicated in some teleosts but were absent in the Perciform *G. aculeatus* and in the representatives of the teleost orders Beloniformes, Pleuronectiformes, Salmoniformes, Characiformes and Cichliformes. In the early evolving fish genomes of *L. oculatus*, the two cartilaginous fishes and *P. marinus* the *tlr23* gene was also absent. Within the Nototheniidae clade, all species possessed a single *tlr21*, *tlr22* and *tlr23* gene except for *T. bernacchii*, and the sub-Antarctic *C. gobio* which lost *tlr23*. In the Nototheniidae Bathydraconidae *G. acuticeps* a species-specific gene duplication event generated two gene copies of *tlr21* (**Figure 2.2.4 B**).

TLR5 and TLR7 superfamilies

Members of the Tlr5 and Tlr7 superfamilies were the most recent TLR groups to emerge and shared a common ancestry. The TLR7 superfamily gene precursor duplicated to originate the Tlr7, Tlr8 and Tlr9 subfamilies (**Figure 2.2.4 C**) of fish and tetrapods. The Tlr5 ancestral gene duplicated during the teleost radiation and originated tlr5 and tl5S (**Figure 2.2.4 C**). Most of the Nototheniidae and teleosts retained the two *tlr5* genes. In *D. mawsoni* (Dissostichus) only *tlr5S* was retained and in the sub-Antarctic sister clade, Bovichtidae this gene was lost and *tlr5* persisted (**Figure 2.2.4 C**). The Pleuronectiformes and the Gadiforme *G. morhua* were an exception and generally lost both genes. The evolutionary trajectory of *tlr5* in the Cyprinidiformes *D. rerio* and in the Characiformes *A. mexicanus* differed from other teleosts (Euteleosteomorpha) and a single copy exists in *A. mexicanus* and species-specific duplicates exist in *D. rerio.* In other Perciformes (*S. aurata* and *D. labrax*) *tlr5* gene duplicates were also found (**Figure 2.2.4 C**, **Supplementary table 2.2.1**). No *tlr5* was found in the cartilaginous fishes or in *P. marinus*.

Within the Tlr7 superfamily, two main clusters existed one grouped the vertebrate Tlr9 members and the other the Tlr7 and Tlr8 subfamilies. Nototheniidae, the sister-lineage Bovichtidae and other vertebrates have a single copy of *tlr7*, *tlr8* and *tlr9* genes and exceptions are due to species-specific duplications such as the 2 copies of *tlr7*, 7 copies of *tlr8* and 5 copies of *tlr9* in *G. morhua* (**Figure 2.2.4 C**, **Supplementary table 2.2.1**). The phylogenetic tree revealed that *tlr7* was present in all fish species and *tlr8* genes were absent from Tetraodontiformes (*T. rubripes*) and *D. mawsoni* (Nototheniidae). The *tlr9* gene was absent from the Pleuronectiforme *S. senegalensis*. In the cartilaginous fish *C. milii tlr8* seemed to be

absent and in *P. marinus* the Pma_TlrY grouped outside the vertebrate TLR7 and TLR8 clusters (**Figure 2.2.4 C**).

Table 2.2.2. Tlrs identified in fish and other vertebrates. The table summarizes the outcome of the BI phylogenetic tree. Tlrs were classified according to sequence clustering. Lamprey sequences were not included.

Species		TLR1 SP								TLR3 SP	TLR4 SP	TLR5 SP		TLR7 SP				TLR11 SP					Total
Order	**Genus**	**1**	**2**	**6**	**10**	**14/18**	**25**	**27**	**2/27**	**3**	**4**	**5**	**5S**	**7**	**8**	**7/8**	**9**	**11**	**13**	**21**	**22**	**23**	**TLRs**
Primates	*Homo*	1	1	1	1	ni	ni	ni	ni	1	1	1	ni	1	1	ni	1	ni	ni	ni	ni	ni	**10**
Rodentia	*Mus*	1	1	1	1	ni	ni	ni	ni	1	1	1	ni	1	1	ni	1	2	1	ni	ni	ni	**13**
Galliformes	*Gallus*	2	2	ni	ni	ni	ni	ni	ni	1	1	1	ni	1	ni	ni	ni	ni	ni	1	ni	ni	**9**
Squamata	*Anolis*	1	2	1	ni	1	ni	ni	ni	1	1	1	ni	ni	ni	ni	ni	ni	1	1	1	ni	**10**
Anura	*Xenopus*	1	1	1	ni	4	ni	ni	ni	1	ni	1	ni	1	1	ni	1	1	1	1	1	ni	**16**
Coelacanthiformes	*Latimeria*	ni	1	1	ni	1	ni	1	ni	1	ni	1	ni	2	1	ni	1	ni	2	2	ni	ni	**14**
Lepisosteiformes	*Lepisosteus*	1	1	ni	ni	1	2	1	ni	1	1	1	ni	1	2	ni	2	ni	ni	ni	1	ni	**15**
Chimaeriformes	*Callorhinchus*	ni	2	1	ni	ni	1	ni	ni	1	ni	ni	ni	1	ni	ni	1	ni	ni	ni	ni	ni	**7**
Orectolobiformes	*Rhincodon*	1	1	ni	ni	ni	ni	1	ni	ni	ni	ni	ni	1	1	ni	1	ni	ni	ni	1	ni	**7**
Beloniformes	*Oryzias*	1	1	ni	ni	1	1	ni	ni	1	ni	1	1	1	1	ni	1	ni	ni	1	1	ni	**12**
Characiformes	*Astyanax*	ni	1	ni	ni	1	ni	ni	ni	1	ni	1	ni	1	2	ni	1	2	ni	1	3	ni	**14**
Cichliformes	*Oreochromis*	ni	2	ni	ni	1	1	ni	ni	1	ni	1	1	1	3	ni	1	ni	ni	1	1	2	**16**
Cyprinodontiformes	*Poecilia*	1	1	ni	ni	1	ni	ni	ni	1	ni	1	1	1	1	ni	1	ni	ni	1	2	2	**14**
	Xiphophorus	ni	2	ni	ni	1	ni	ni	ni	1	ni	1	1	1	1	ni	1	ni	ni	1	2	3	**15**
Cypriniformes	*Danio*	1	1	ni	ni	1	ni	ni	ni	1	3	2	ni	1	3	ni	1	8	ni	1	1	ni	**24**
Gadiformes	*Gadus*	ni	ni	ni	ni	1	9	ni	ni	1	ni	ni	ni	2	7	ni	5	ni	ni	1	14	2	**42**
Perciformes	*Gasterosteus*	1	1	ni	ni	1	ni	ni	ni	1	ni	1	2	1	1	ni	1	ni	1	1	1	ni	**13**
	Pseudochaenichthys	1	2	ni	ni	1	1	ni	ni	1	ni	1	1	1	1	ni	1	ni	1	1	1	1	**15**
	Gymnodraco	1	2	ni	ni	1	1	ni	ni	1	ni	1	1	1	1	ni	1	ni	1	2	1	1	**16**
	Notothenia	1	2	ni	ni	1	ni	ni	ni	1	ni	1	1	1	1	ni	1	ni	1	1	1	1	**14**
		1	2	ni	ni	1	ni	ni	ni	1	ni	1	ni	1	1	ni	1	ni	ni	1	1	1	**12**
	Trematomus	1	2	ni	ni	1	1	ni	ni	1	ni	1	1	1	1	ni	1	ni	1	1	1	ni	**14**
	Chionodraco	ni	1	ni	ni	ni	ni	ni	ni	ni	ni	ni	ni	ni	ni	ni	1	ni	ni	ni	ni	ni	**2**
	Dissostichus	ni	ni	ni	ni	1	1	ni	ni	1	ni	ni	1	1	ni	ni	1	ni	1	1	1	1	**10**
	Cottoperca	1	2	ni	ni	1	1	ni	ni	1	ni	1	ni	1	1	ni	1	ni	1	1	1	ni	**13**
Eupercaria incertae sedis	*Dicentrarchus*	1	2	ni	ni	1	1	ni	ni	1	ni	ni	1	1	1	ni	1	ni	1	1	1	1	**14**
Spariformes	*Sparus*	1	2	ni	ni	1	ni	ni	ni	1	ni	1	1	1	1	ni	1	ni	1	1	1	1	**14**
Pleuronectiformes	*Paralichthys*	1	1	ni	ni	1	ni	ni	ni	1	ni	1	ni	1	1	ni	1	ni	ni	1	1	ni	**10**
	Cynoglossus	ni	ni	ni	ni	1	ni	ni	ni	1	ni	1	ni	1	1	ni	1	ni	ni	ni	1	ni	**7**
	Solea	1	ni	ni	ni	ni	ni	ni	ni	1	ni	1	ni	1	1	ni	ni	ni	ni	ni	1	ni	**6**
	Hippoglossus	1	2	ni	ni	1	ni	ni	ni	1	ni	1	1	1	1	ni	1	ni	ni	1	1	ni	**12**
Salmoniformes	*Salmo*	1	1	ni	ni	1	ni	ni	ni	1	ni	1	ni	1	1	ni	1	ni	ni	ni	2	ni	**10**
Tetraodontiformes	*Tetraodon*	1	1	ni	ni	1	ni	ni	ni	1	ni	1	1	1	1	ni	1	ni	ni	1	1	1	**12**
	Takifugu	1	1	ni	ni	1	ni	ni	ni	1	ni	1	1	1	ni	ni	1	ni	ni	1	1	1	**11**

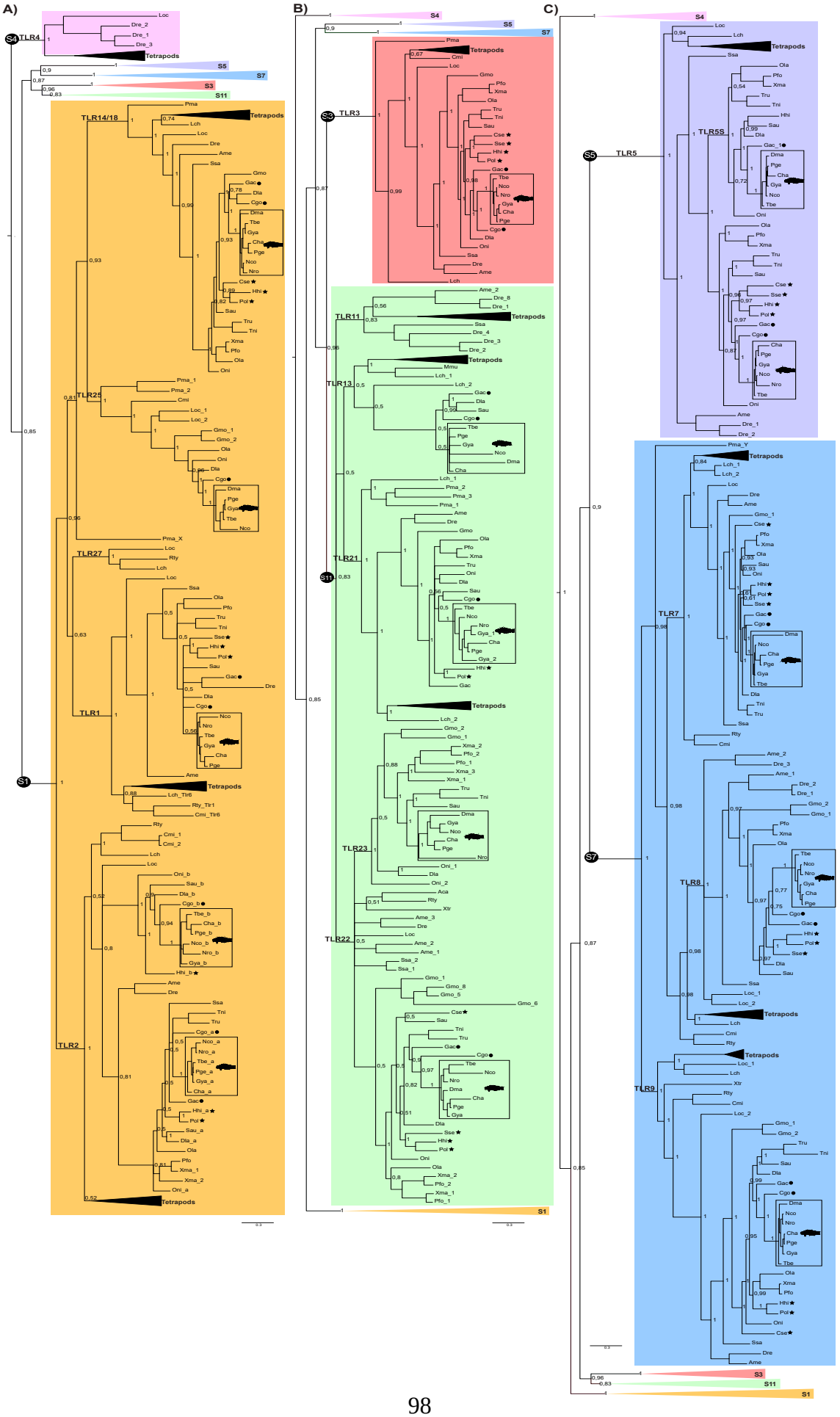
A)
B)
C)
TLR4
TLR14/18
TLR25
TLR27
TLR1
TLR2
TLR3
TLR11
TLR13
TLR21
TLR23
TLR22
TLR5
TLR5S
TLR7
TLR8
TLR9
Tetrapods
S1
S3
S4
S5
S7
S11

Figure 2.2.4. Simplified Tlr phylogenetic tree. The phylogenetic tree was constructed using the BI method and the full tree is available as Supplementary Figure 1. Branches corresponding to the six vertebrate TLR superfamilies are identified: S1 indicates the TLR1 superfamily (orange); S3 identifies the TLR3 superfamily (red); S4 identifies the TLR4 superfamily (pink); S5 identifies the TLR5 superfamily; S7 identifies the TLR7 superfamily (blue) and S11 identifies the TLR11 superfamily (green). Some branches of the phylogenetic tree are collapsed to facilitate interpretation and three subsections of the same phylogenetic tree show A) the TLR1 superfamily, B) the TLR11 and TLR3 superfamilies and, C) the TLR5, TLR7 and TLR4 superfamilies. The tetrapods branches were also collapsed. Accession numbers of the sequences used to construct the phylogenetic tree are available in Supplementary Table 1. The teleost *tlr2* duplicates were named, *tlr2a* and *tlr2b,* and TLR15 was not included in the phylogenetic tree since it was only found in chicken and lizard. Tree was rooted with the Cnidarian Tlr clade (Liu et al., 2019). The sea lamprey *tlrs* within the vertebrate TLR1 and TLR7 superfamilies are named *Pma_X* and *Pma_Y,* respectively since their assignment to the Tlr subfamilies was ambiguous. Only the posterior probability values for the main branches are indicated. A phylogenetic tree generated by the ML method is available as Supplementary Figure 2. The *tlrs* from Antarctic species are indicated with squares and with a *Notothenia* cartoon to facilitate their identification within the tree. The other Perciformes are indicated by a black dot and Pleuronectiformes by a black star.

2.2.4.4. Short-range gene linkage

To better understand Tlr gene loss in Nototheniidae, specifically *tlr1*, *tlr2*, *tlr5* and *tlr8* in *D. mawsoni*, *tlr23* in *T. bernacchii* and *tlr5s* and *tlr23* in *C. gobio* the neighbouring gene environment was characterized.

Tlr1 gene linkage

In the *G. aculeatus* genome *tlr1* maps in group IV and five neighbouring genes (*chrna9*, *ubec2ka*, *klb*, *ints10* and *slc25a51b*) were identified and homologue genome regions were found in other teleost genomes (**Figure 2.2.5 A**). In the *D. mawsoni* genome, a genome region containing *tlr1* neighbouring genes including *klb* and *ints10* was found in chromosome fragment JAAKFY010000022.1 but *tlr1* was absent. Chromosome 4 contains a homologue *TLR1* genome region in *H. sapiens* and three conserved neighbouring genes, *CHRNA9*, *UBEC2KA* and *KLB* map in close proximity to the *TLR1* gene. This suggests that this genome region was highly conserved during evolution and that gene loss in *D. mawsoni* was a consequence of a species-specific gene deletion event (**Figure 2.2.5 A**). A similar species-specific gene deletion occurred in the *C. semilaevis* genome.

Tlr2 gene linkage

The *TLR1* and *TLR2* genes are 38Mb apart on chromosome 4 in *H. sapiens*. In teleosts *tlr1* and *tlr2* genes mapped to different chromosomes and in the Nototheniidae and other teleosts *tlr2* gene duplicates mapped to different chromosomes or scaffolds (**Figure 2.2.5 B**). In the *T. bernacchii* genome the *tlr2a* gene mapped to NW_022987889.1 and *tlr2b* to NW_011369947.1. Flanking genes of *tlr2a* were *rnf175*, *fam11a*, *fgb* and *fga* and flanking genes of *tlr2b* were *pdia2*, *percc1*, *npy2r1*, *mnd1* and *fhdc1*. The gene *trim2*, was closely linked to *tlr2* and was also duplicated and *trim2b* shared the same genome region as *tlr2a* and *trim2a* with *tlr2b* (**Figure 2.2.5 B**). Both gene duplicates most likely arose during the teleost specific genome duplication event. In human, a single *TLR2* and *TRIM2* genes exist and were flanked by the neighbouring genes of *tlr2a and tlr2b* identified in *T. bernacchii* and other teleosts (**Figure 2.2.5 B**).

In the *G. aculeatus* genome a single *tlr2* gene maps to group VII and the flanking genes shared synteny with *tlr2a* and a homologue genome region to *tlr2b* was identified in group IX but *tlr2b* was absent indicating this gene was eliminated from the genome. In *D. mawsoni* no *tlr2* gene exists but a *tl2b* homologue genome region was found and the neighbouring genes of teleost *tlr2a* were dispersed in several genome fragments. In the case of *D. mawsoni* the incomplete genome assembly means it is unclear if the failure to identify *tlr2* is due to the assembly quality or a gene deletion event (**Figure 2.2.5 B**). In Pleuronectiformes, *tlr2a* maps to *P. olivaceus* NW_017863846.1 but this scaffold is very short and only encodes this gene. Homologue genes of the gene environment of *tlr2a* and *tlr2b* were found but mapped to diverse genome fragments. In *C. semilaevis* the *tlr2* gene duplicates were lost from chromosome 1 and chromosome 9 (**Figure 2.2.5 B**).

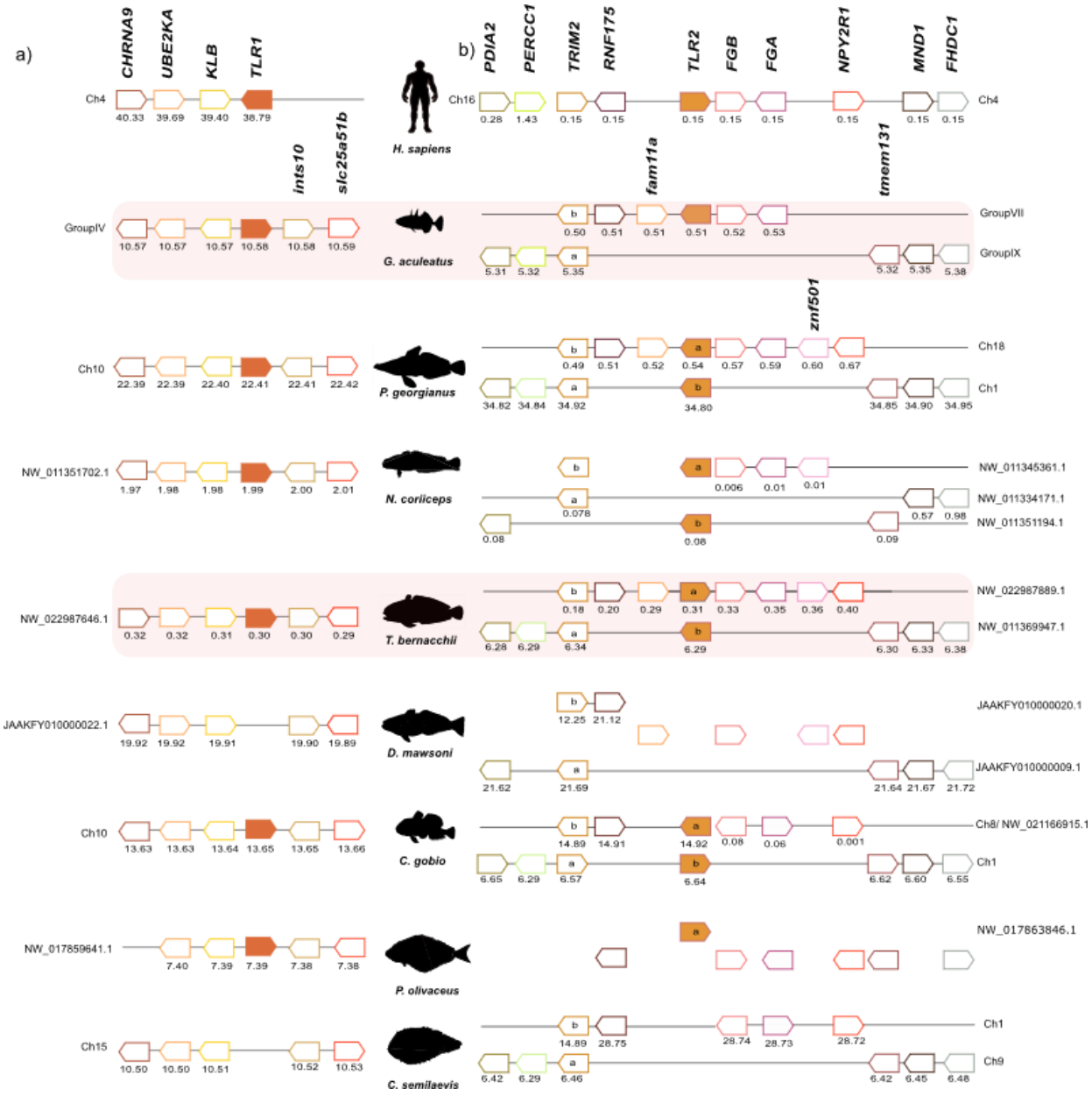

Figure 2.2.5. Synteny analysis of *tlr1* and *tlr2*. A) represents the *tlr1* and B) the *tlr2* neighbouring gene environments. Antarctic Nototheniidae species represented are *P. georgianus*, *N. coriiceps*, *T. bernacchii* and *D. mawsoni*. Other vertebrates include the *C. gobio* as the representative of the sister lineage, the *G. aculeatus* as another representative of the Perciformes order, two representatives of the Pleuronectiformes order (*P. olivaceus* and *C. semilaevis*) and *H. sapiens* as the tetrapod. The genome regions analysed are indicated by a line and predicted genes are represented by arrows and the arrowheads indicate gene orientation in the genome and the gene symbol is given. The *tlr* genes are represented by full-coloured arrows: *tlr1* in dark orange (A) and *tlr2* in light orange (B). Duplicate genes were named *a* and *b*. Neighbouring gene families are represented by arrows outlined in different colours and gene homologues were aligned. The gene positions in the genome assemblies analysed (Mega base pairs, Mbp) are indicated below. Only common genes are represented. The positions of the *tlr2a* neighbouring genes found in the *P. olivaceus* genome (NW_017863846.1) are not indicated because they were found in different genome regions. The gene environment of the *G. acuticeps* and *T. bernacchii* are assembled in chromosomes and were used as a reference. Neighbouring genes represented are: Cholinergic receptor nicotinic alpha 9 subunit (*chrn9a*), Ubiquitin conjugating enzyme E2 K (*ube2ka*), Klotho beta (*klb*), Integrator complex subunit 10 (*ints10*), Solute carrier family 25

member 51 (*slc25a51b*), Protein disulfide isomerase family A member 2 (*pdia2*), Proline and glutamate rich with coiled coil 1 (*percc1*), Tripartite motif containing 2 (*trim2*), Ring finger protein 175 (*rnf175*), Family with sequence similarity 11 member A (*fam11a*), Fibrinogen beta chain (*fgb*), Fibrinogen alpha chain (*fga*), Zinc finger protein 501 (*znf501*), Transmembrane protein 131 (*tmem131*), Meiotic nuclear division 1 (*mnd1*), FH2 domain containing 1 (*fhdc1*).

TRL5 gene linkage

Five neighbouring genes were identified in the genome environment of the teleosts *tlr5* (*adgrf3b*, *mep1a.1*, *brox*, *disp1* and *hmbox1*) and *tlr5S* (*dtnb*, *kif3c*, *rab10*, *lats1* and *nup43*). In *G. aculeatus* (group XVIII) and in the Nototheniidae, *P. georgianus* (chromosome 24) *tlr5* gene duplicates mapped to the same genome fragment (**Figure 2.2.6 A, B**). In *G. aculeatus* one of the *tlr5* genes was incomplete (lacks N-terminus) and may be a pseudogene. In the genome of the Nototheniidae, *N. coriiceps* and *T. bernacchii* conserved homologue genome regions were found for both *tlr5* and *tlr5S* but they mapped to different genome fragments. In *D. mawsoni* only *tlr5S* was identified and the flanking genes were conserved and mapped to JAAKFY010000011.1 along with the homologue genes flanking *tlr5*, which gene was missing (**Figure 2.2.6 A**). In *C. gobio* the *tlr5* gene and its conserved gene environment mapped to chromosome 24 but *tlr5S* was absent although the flanking genes were conserved in a genome region on scaffold NW_021167002.1. In the two Pleuronectiforms, *P. olivaceus* and *C. semilaevis tlr5* was mapped to conserved genome regions in scaffolds NW_017859659.1 and KI934270.1, respectively. The conserved genome region that flanks tlr5s was identified but the *tlr* gene was absent. In *H. sapiens*, *TLR5* maps to chromosome 1 and a homologue genome region to the teleost *tlr5s* was shared between chromosome 2 and 6 but *tlr5s* was absent and was presumably eliminated from the genome (**Figure 2.2.6 B**).

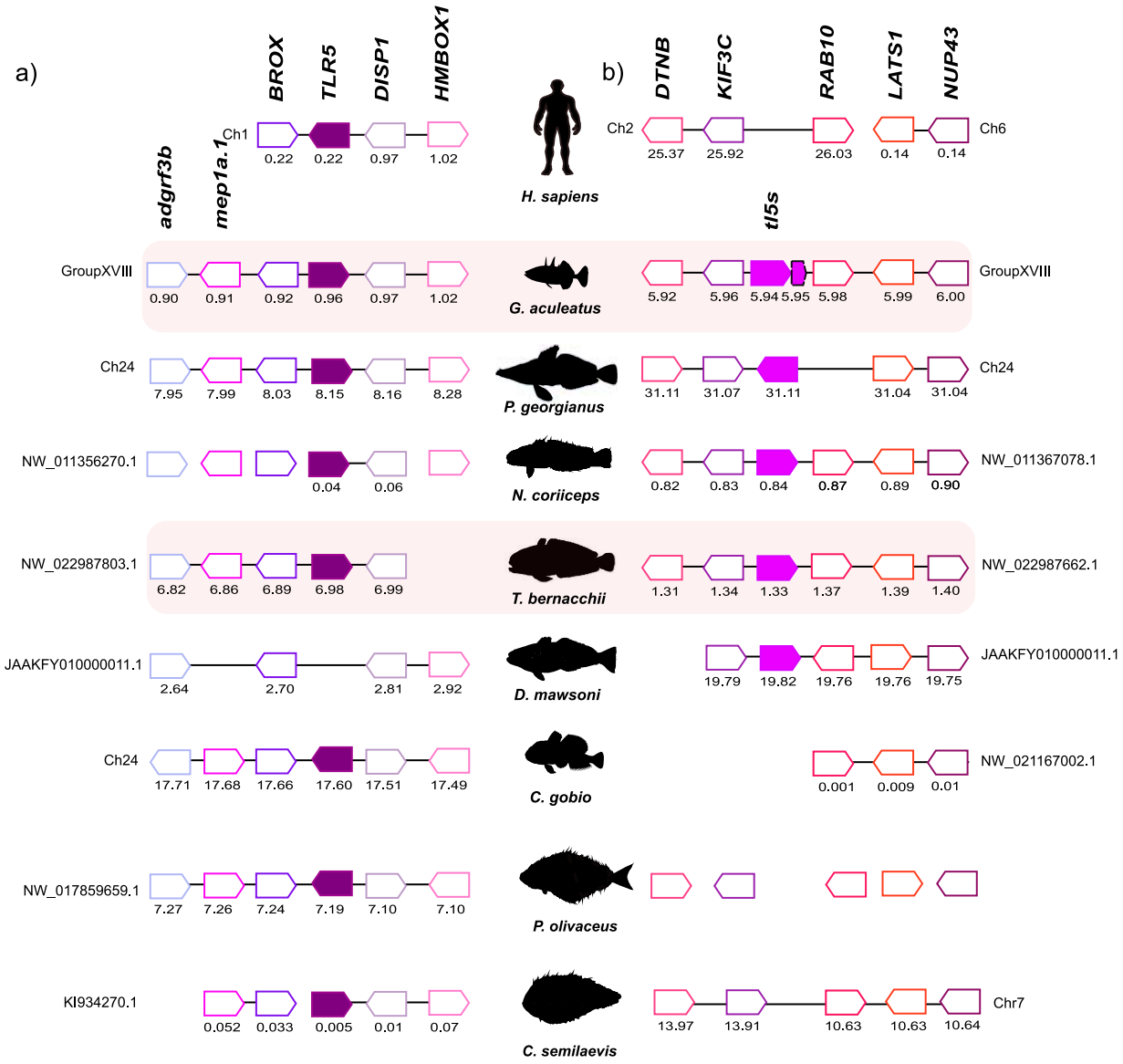

Figure 2.2.6. Synteny analysis of *tlr5* and *tlr5S*. A) represents the genome environment of *tlr5* and B) the neighbouring gene environments *of tlr5S*. In *G. aculeatus* (group XVII) and *P. georgianus* (chromosome 24) both genes map to the same genome regions. Antarctic Nototheniidae species represented are *P. georgianus*, *N. coriiceps*, *T. bernacchii* and *D. mawsoni*. Other vertebrates include the C. gobio as the representative of the sister lineage, the *G. aculeatus* as another representative of the Perciformes order, two representatives of the Pleuronectiformes order (*P. olivaceus* and *C. semilaevis*) and *H. sapiens* as the tetrapod. Genome regions analysed are indicated by a line and predicted genes are represented by arrows and the arrowhead indicates gene orientation and the gene symbol is given. *Tlr* genes are represented by coloured arrows: *tlr5* in dark purple (A) and *tlr5S* in light purple (B). Neighbouring gene families are represented by arrows outlined in different colours and gene homologues were aligned. Gene positions in the genome assemblies consulted (Mega base pairs, Mbp) are indicated below. Only common genes are represented. The positions of the *tlr5S* neighbouring gene homologues in the *P. olivaceus* genome (where *tlr5S* is absent) are not indicated because they were found in different genome regions. In the *G. aculeatus* genome two putative *tlr5S* genes were found that mapped in tandem. However, one copy is likely to be non-functional due to its smaller size and thus it is represented by a dashed outlined. The gene environment of *tlr* genes in *G. acuticeps* and *T. bernacchii* for which the genome is assembled in chromosomes were used as the reference. Neighbouring genes represented are: Adhesion G protein-coupled receptor F3b (*adgr3b*), Meprin A alpha (PABA peptide hydrolase) tandem duplicate 1 (*mep1a.1*), BRO1 domain and CAAX motif containing (*brox*),

Dispatched RND transporter family member 1 (*disp1*), Homeobox containing 1 (*hmbox1*), Kinesin family member 13B (*kif13b*), Dystrobrevin beta (*dtnb*), Kinesin family member 3C (*kif3c*), Ras-related protein Rab-10 (*rab10*), Large tumour suppressor kinase 1 (*lats1*), Nucleoporin 43 (*nup43*).

Tlr8 gene linkage

Tlr8 maps next to *tlr7* in group XVI of *G. aculeatus* genome (**Figure 2.2.7 A**). Four neighbouring genes (*gpm6bb*, *ofd1*, *rab9a*, *egfl6*) were identified and gene synteny was conserved in all representatives of the Nototheniidae and in the sister lineage, the Bovichtidae (*C. gobio*). The exception was *D. mawsoni* in which a genome region containing *tlr7*, *gpm6bb*, *ofd1* and *egfl6* genes was identified (JAAYFY010000018.1) but *tlr8* was absent (**Figure 2.2.7 A**). In *H. sapiens* TLR7 and TLR8 also map in proximity on chromosome X suggesting they probably arose through a tandem gene duplication prior to the teleost and tetrapod divergence.

TRL23 gene linkage

The *tlr23* gene mapped to chromosome 4 in *P. georgianus* and to NW_011369947.1 in the *N. coriiceps* genome and five neighbouring genes (*dmbx1*, *mknk1*, *mob3c*, *elovl1b* and *zfyve9b*) were characterized (**Figure 2.2.7 B**). In species where this gene is absent a conserved gene environment was identified in *D. mawsoni* (JAAKFY010000025.1), the *T. bernacchii* (NW_022987739.1), *C. gobio* (chromosome 4), *G. aculeatus* (group VIII), *P. olivaceus* (NW_017859646.1) and *C. semilaevis* (chromosome 2) genomes. This suggest that in teleosts retention of the *tlr23* gene was species-specific (**Figure 2.2.7 B**). In the *H. sapiens* genome, no *tlr23* homologue was found although a conserved genome region was found in chromosome 1.

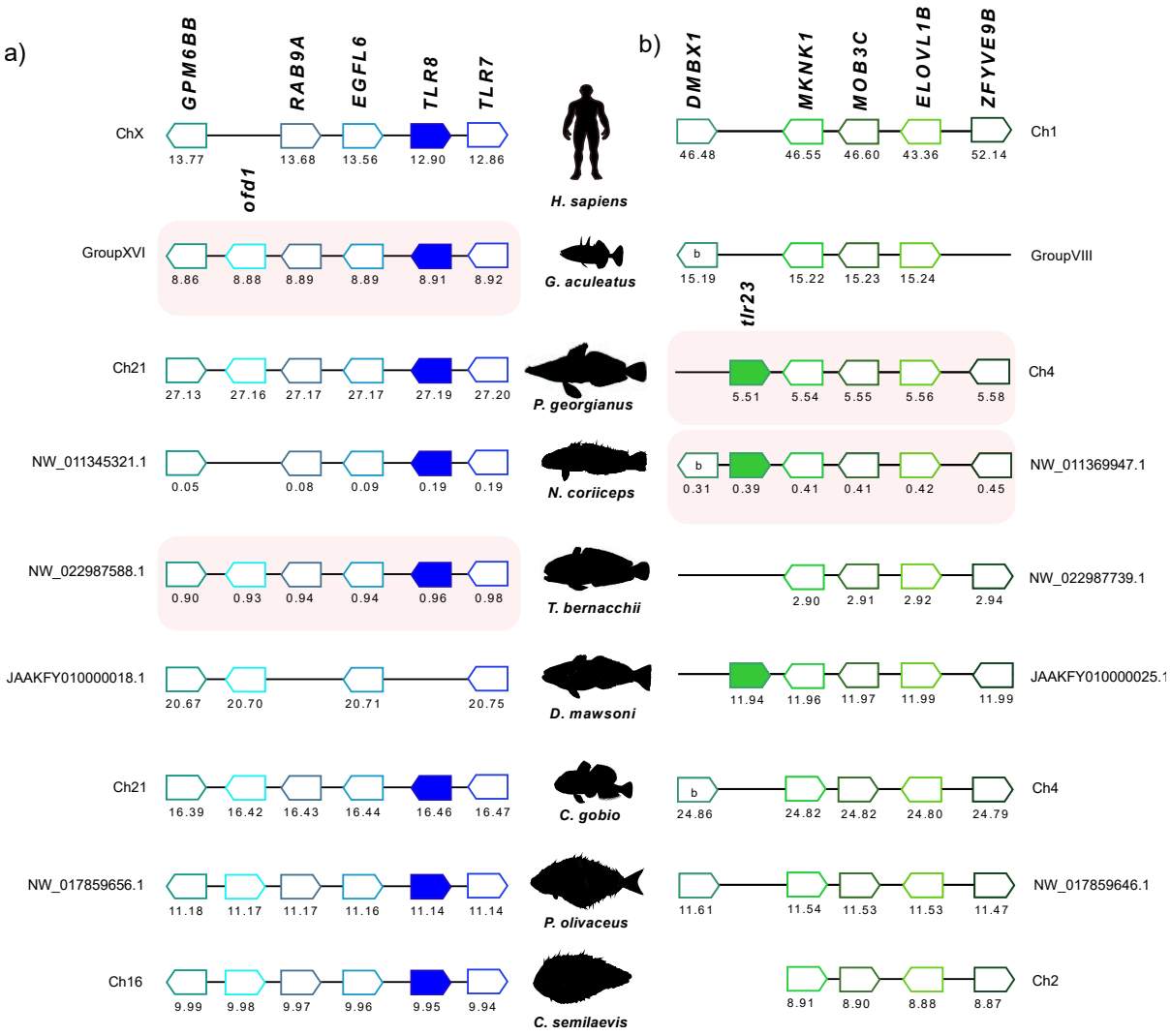

Figure 2.2.7. Synteny analysis of *tlr8* and *tlr23*. A) represents the genes flanking *tlr8* and B) the genes flanking *tlr23*. Antarctic Nototheniidae species represented are *P. georgianus*, *N. coriiceps*, *T. bernacchii* and *D. mawsoni*. Other vertebrates include the C. gobio as the representative of the sister lineage, the *G. aculeatus* as another representative of the Perciformes order, two representatives of the Pleuronectiformes order (*P. olivaceus* and *C. semilaevis*) and *H. sapiens* as the tetrapod. The genome regions analysed are indicated by a line and predicted genes are represented by arrows and the arrowhead indicates gene orientation in the genome and the gene symbol is given. *Tlr* genes are represented by fully-coloured arrows: *tlr8* is in blue (A) and *tlr23* is in green (B). Neighbouring gene families are represented by arrows outlined in colour and gene homologues were aligned. Only common genes are represented. For *tlr8* the gene environment in *G. aculeatus* and *T. bernacchii* that have the genome assembled in chromosomes were used as the reference for synteny maps. For *tlr23* the *P. georgianus* and *N. coriiceps* were used as the reference. Neighbouring genes represented are: Glycoprotein M6BB (*gpm6bb*), Oral-facial-digital syndrome 1 protein (*ofd1*), Ras-related protein Rab-9A (*rab9a*), Epidermal growth factor-like protein 6 (*egfl6*), Toll-like receptor 7 (*tlr7*), Diencephalon/mesencephalon homeobox 1 (*dmbx1*), MAP kinase-interacting serine/threonine-protein kinase 1 (*mknk1*), MOB kinase activator 3C (*mob3c*), Elongation of very long chain fatty acids protein 1 (*elovl1b*), Zinc finger FYVE-type containing 9B (*zfyve9b*).

2.2.4.5. Sequence comparisons and protein domain analysis

The protein structure of the 15 Nototheniidae Tlrs were compared across species and with the sub-Antarctic (*C. gobio*) and other Perciformes (**Supplementary table 2.2.2 and Figure 2.2.8**). Sequence comparisons of the deduced proteins revealed that they are relatively well conserved and share between 70-98% amino acid (aa) similarity and the Nototheniidae Tlr3, 5 and 23 are the most conserved (91-99% aa similarity). *C. gobio* Tlrs share 64-86% similarity with the Nototheniidae and with other Perciformes they are 48-86% similar. All deduced Nototheniidae and *C. gobio* sequences shared a conserved protein structure with the other teleosts and possessed several LRR motifs involved in pathogen recognition, and single TM and TIR domains. The exception was Tlr5S that lacked the TM and the TIR domain in all teleost fishes and may be a soluble receptor isoform. The main difference between Tlr isoforms was the number of LRRs within the ectodomain which were variable across the different subfamilies and Antarctic fish possessed a similar number of LRRs to other Perciformes. In addition, the presence and absence of a predicted signal peptide in the gene members of the same subfamily suggests that functional divergence may exist between the homologue genes as they may have different cellular localisations (**Figure 2.2.8, Supplementary figure 2.2.4-17**).

Members of the Tlr8, Tlr9 and Tlr21 possess the largest number of predicted LRR repeats at the ectodomain varying from 18 in most fishes to 19 in *C. gobio* and *T. bernacchii* in Tlr8, 16 in *G. aculeatus* to 20 in *C. hamatus* and *P. georgianus* for Tlr9 and 15 in *G. aculeat*us to 20 in *T. bernacchii* Tlr21. The duplicate *G. acuticeps* Tlr21 genes have a similar protein structure with 18 LRRs. The Tlr14/18 (LRRs 8-10) and Tlr25 (LRRs 7-8) possess the least number of LRR repeats. The Tlr subfamilies where conservation in LRR number exists were Tlr1 where all species possessed 9 LRR, Tlr 8 and TLr25. The Tlr subfamilies where most LRR variability was found was Tlr2a (8-12) and Tlr13 (10 to 15). Within the other superfamilies the number of LRRs varied only by 2 LRR units (eg: Tlr23 (13-15) and Tlr 3 (15-17).

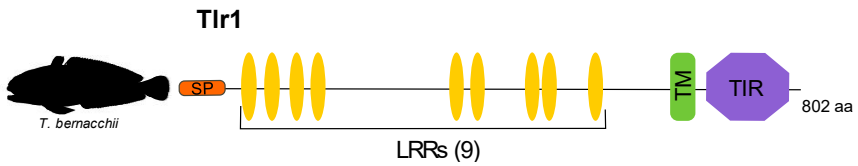

	SP	LRR	TM	TIR	Size (aa)
C. hamatus	P	9	1	1	800
P. georgianus	P	9	1	1	718

Nototheniidae	*G. acuticeps*	P	9	1	1	718
	N. coriiceps	P	8	1	1	687*
	N. rossii	P	9	1	1	718
	C. gobio	ni	9	1	1	717
	G. aculeatus	P	9	1	1	717

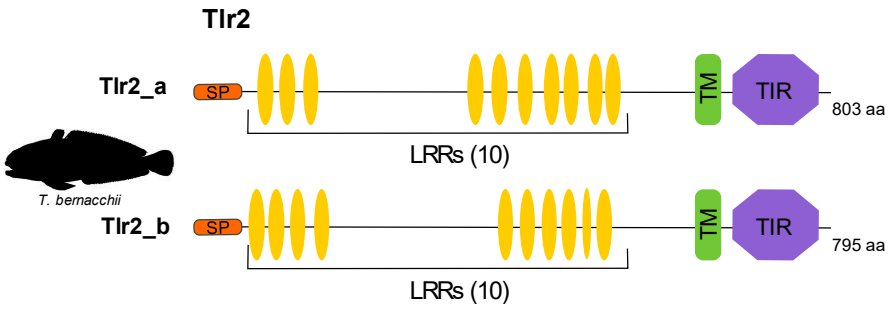

		SP	LRR	TM	TIR	Size (aa)
Nototheniidae	*C. hamatus*	P	11	1	1	802
		P	10	1	1	804
	P. georgianus	P	8	1	1	716
		P	10	1	1	708
	G. acuticeps	P	10	1	1	715
		P	11	1	1	634*
	N. coriiceps	ni	2	1	1	263*
		P	10	1	1	714
	N. rossii	ni	7	1	1	672*
		ni	ni	ni	ni	145*
	C. gobio	ni	12	1	1	778
		ni	9	1	1	708
	G. aculeatus	ni	8	1	1	718

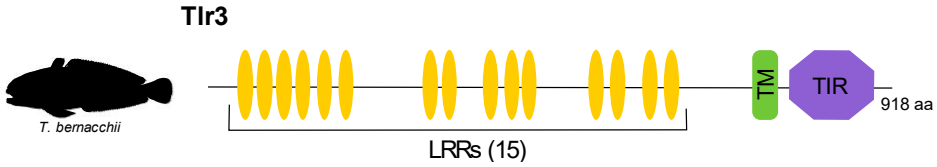

		SP	LRR	TM	TIR	Size (aa)
Nototheniidae	*C. hamatus*	P	17	1	1	842
	P. georgianus	ni	17	1	1	803
	G. acuticeps	ni	15	1	1	807
	N. coriiceps	ni	17	1	1	810
	N. rossii	ni	17	1	1	813
	D. mawsoni	ni	6	ni	ni	305*
	C. gobio	ni	17	1	1	813
	G. aculeatus		14	1	1	814

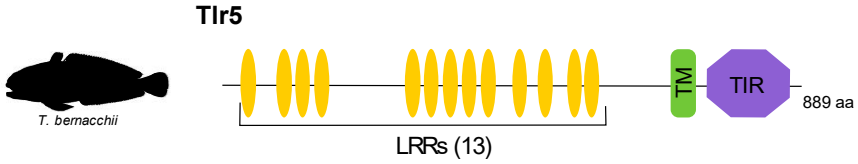

		SP	LRR	TM	TIR	Size (aa)
Nototheniidae	*C. hamatus*	ni	11	1	1	835
	P. georgianus	P	12	1	1	895
	G. acuticeps	P	12	1	1	889
	N. coriiceps	ni	10	1	1	889
	N. rossii	ni	8	1	1	587*
	C. gobio	P	10	1	1	889
	G. aculeatus	P	12	1	1	883

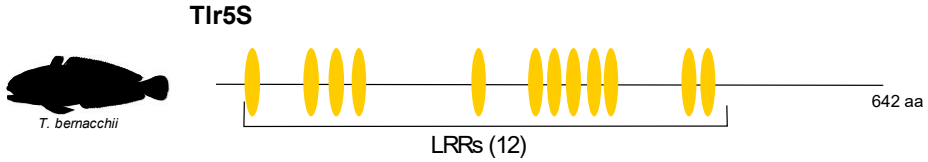

		SP	LRR	TM	TIR	Size (aa)
Nototheniidae	*C. hamatus*	ni	13	ni	ni	642
	P. georgianus	ni	13	ni	ni	642
	G. acuticeps	ni	12	ni	ni	642
	N. coriiceps	P	12	ni	ni	642

	D. mawsoni	ni	12	ni	ni	621
	G. aculeatus	P	11	ni	ni	647
		ni	6	ni	ni	265*

Tlr7

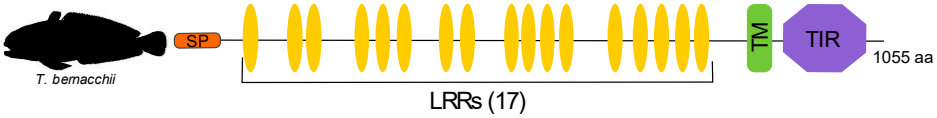

		SP	LRR	TM	TIR	Size (aa)
Nototheniidae	*C. hamatus*	ni	17	1	1	964
	P. georgianus	P	17	1	1	946
	G. acuticeps	P	17	1	1	946
	N. coriiceps	P	17	1	1	946
	N. rossii	ni	5	ni	ni	206*
	D. mawsoni	P	10	1	1	727*
	C. gobio	P	17	1	1	946
	G. aculeatus	P	19	1	1	927

Tlr8

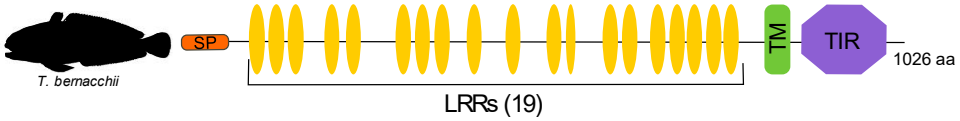

		SP	LRR	TM	TIR	Size (aa)
Nototheniidae	*C. hamatus*	P	18	1	1	1027
	P. georgianus	P	18	1	1	913
	G. acuticeps	P	18	1	1	913
	N. coriiceps	P	18	1	1	913
	N. rossii	P	18	1	1	913
	C. gobio	P	19	1	1	911
	G. aculeatus	ni	18	1	1	912

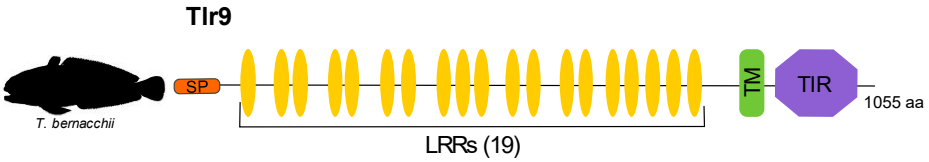

		SP	LRR	TM	TIR	Size (aa)
Nototheniidae	*C. hamatus*	P	20	1	1	939
	P. georgianus	P	20	1	1	939
	G. acuticeps	P	19	1	1	939
	N. coriiceps	P	19	1	1	941
	N. rossii	P	18	1	1	941
	D. mawsoni	P	19	1	ni	865*
	C. gobio	P	18	1	1	939
	G. aculeatus	P	16	1	1	939

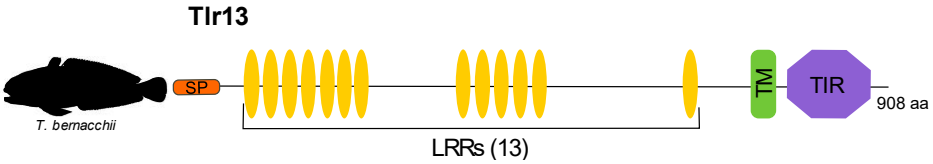

		SP	LRR	TM	TIR	Size (aa)
Nototheniidae	*C. hamatus*	ni	ni	1	1	150*
	P. georgianus	P	15	1	1	820
	G. acuticeps	P	15	1	1	820
	N. coriiceps	ni	11	1	1	996
	D. mawsoni	ni	10	1	1	698*
	C. gobio	P	11	1	1	827
	G. aculeatus	ni	10	1	1	816

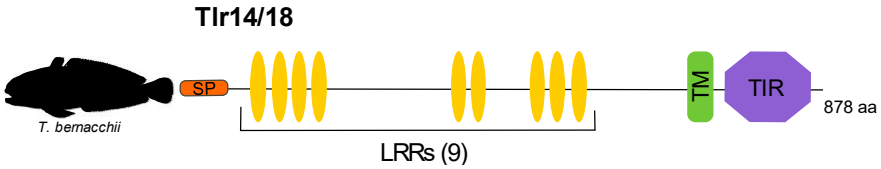

		SP	LRR	TM	TIR	Size (aa)

Nototheniidae	*C. hamatus*	P	9	1	1	878
	P. georgianus	P	9	1	1	722
	G. acuticeps	P	9	1	1	722
	N. coriiceps	P	9	1	1	722
	N. rossii	P	9	1	1	722
	D. mawsoni	ni	5	1	1	454*
	C. gobio	P	8	1	1	722
	G. aculeatus	ni	10	1	1	724

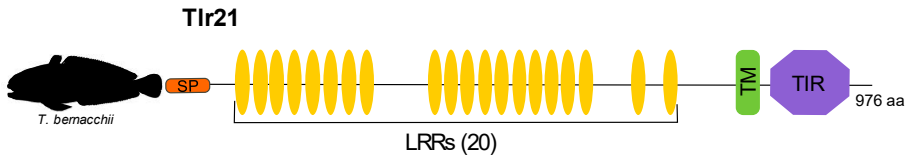

		SP	LRR	TM	TIR	Size (aa)
Nototheniidae	*C. hamatus*	P	18	1	1	978
	P. georgianus	P	18	1	1	978
	G. acuticeps	P	18	1	1	976
	N. coriiceps	P	19	1	1	973
	N. rossii	ni	17	1	1	996
	D. mawsoni	ni	ni	ni	1	197*
	C. gobio	P	17	1	1	974
	G. aculeatus	ni	15	1	1	928

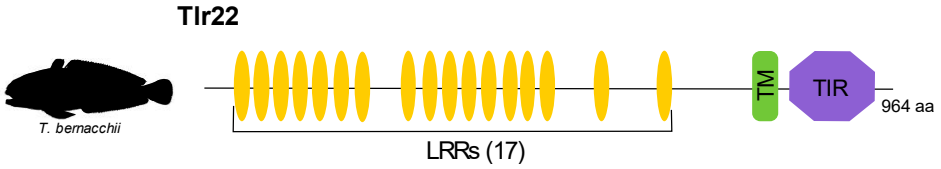

		SP	LRR	TM	TIR	Size (aa)
Nototheniidae	*C. hamatus*	ni	17	1	1	856
	P. georgianus	ni	17	1	1	962
	G. acuticeps	ni	17	1	1	962
	N. coriiceps	ni	17	1	1	819

	N. rossii	ni	16	1	1	1022
	D.mawsoni	P	18	1	1	960
	C. gobio	ni	17	1	1	942
	G. aculeatus	ni	18	1	1	961

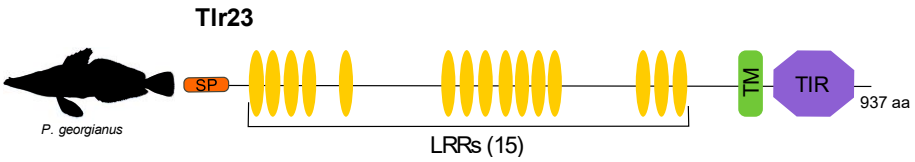

		SP	LRR	TM	TIR	Size (aa)
Nototheniidae	*C. hamatus*	P	15	1	1	948
	G. acuticeps	P	15	1	1	824
	N. coriiceps	P	13	1	1	799
	N. rossii	ni	9	1	1	625*
	D. mawsoni	P	14	1	1	798

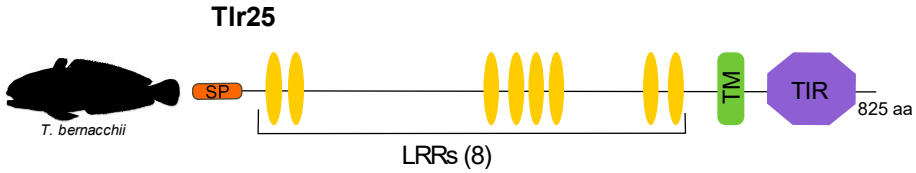

		SP	LRR	TM	TIR	Size (aa)
Nototheniidae	*P. georgianus*	P	7	1	1	778*
	G. acuticeps	ni	7	1	1	825
	D. mawsoni	P	8	1	1	739*
	C. gobio	P	8	1	1	826
	D. labrax	P	7	1	1	827

Figure 2.2.8. Tlr protein domain structure in Nototheniidae. The deduced structure of the Tlr proteins in the Antarctic teleost *T. bernacchii* are represented as an example of the structure across the Nototheniidae fish. For *tlr23*, which is missing from *T. bernacchii* the structure of the deduced protein in *P. georgianus* was used. The numbers of domains predicted in other Nototheniidae species as well as in the sub-Antarctic fish *C. gobio* and the evolutionary proximate perciform *G. aculeatus* are indicated in a table (except for *tlr25* where the *D. labrax* is represent). Domains represented are: LRR- Leucine rich motifs (yellow), TM- transmembrane domain (green), TIR, Toll/interleukin-1 receptor (purple). The presence of a signal peptide (SP) is also indicated (orange). LRR and TIR were predicted *in silico* using the ScanProsite (de Castro et al., 2006) and the SMART (Letunic et al., 2021) programmes. The signal peptide (SP) was predicted using the SignalP 4.1 Server (Nielsen, 2017) and TM domains were

predicted using the TMHMM Server v. 2.0 (http://www.cbs.dtu.dk/services/TMHMM/). The length (aa) of the predicted proteins is indicated. The complete sequence alignments mapping all the predicted domains is available in Supplementary Figure 2.2.4-8D. Tlr21 (197 aa) from *D. mawsoni* and Tlr25 (369 aa) from *N. coriiceps* are not represented as they are very incomplete. * Partial sequences, P- predicted.

3.4.6. Selective pressure analysis

Branch-site analysis for the ancestral Nototheniidae revealed that Tlr5 (BSM, $p = 0.0011$), Tlr8 (BSM, $p < 0.001$), Tlr13 (BSM, $p = 0.0018$), Tlr22 (BSM, $p < 0.001$) and Tlr23 (BSM, $p = 0.001$) were under positive selection (**Table 2.2.3**). Branch-site analysis was also performed for the duplicate *G. acuticeps* Tlr21_2 and revealed positive selection (BSM, $p < 0.001$) (**Table 2.2.3**). Site analysis was further performed for these receptors and identified several positive selection sites (PSS) within the ectodomain and inside the LRR motifs of Nototheniidae Tlr8, Tlr13, Tlr21, Tlr22 and Tlr23 (**Figure 2.2.9**) suggesting that this region was highly modified and resulted in most cases of species-specific modifications. PSS were also found within the TM and TIR domains of Tlr5 (**Supplementary figure 2.2.6**), Tlr8 (**Supplementary figure 2.2.7**), Tlr21 and Tlr22 (**Supplementary figure 2.2.8**). Tlr22, the teleost specific receptor was the most modified with 44 PSS identified (SM, $p < 0.001$) of which 41 were localized within the ectodomain and 27 were inside LRRs (**Figure 2.2.9, Table 2.2.3-4, Additional data 13 in Annex I**). The second most modified receptor in Nototheniidae was Tlr8 with 12 PSS (SM, $p < 0.001$) found within the ectodomain and 3 within LRRs (**Figure 2.2.9 A, Table 2.2.3-4, Additional data 8 in Annex I**). For *G. acuticeps* Tlr21 duplicates (Tlr21_2) 7 PSS were found in the ectodomain of which 3 mapped within LRR suggesting functional divergence after species-specific gene duplication (**Figure 2.2.9, Table 2.2.3-4, Additional data 12 in Annex I**). PSS were also found for Nototheniidae Tlr13 (1 site within LRRs, (SM, $p = 0.004$)) and Tlr23 (2 sites of which one is within LRRs, (SM, $p = 0.0004$)) (**Additional data 10 and 14, respectively in Annex I**). For Tlr5 and Tlr22 a single and two PSS were detected within the TM region, respectively PSS in the TIR domains were also detected for Tlr8 (1 PSS), Tlr21 (3 PSS) and Tlr22 (1 PSS).

Table 2.2.3. Selective pressure analysis for branch-site models. LRT Statistics (2ΔL) and *p*-values for the branch-site models on the ancestral Nototheniidae branch for Tlr5, Tlr8, Tlr13, Tlr22, Tlr23 and *G. acuticeps* Tlr21 duplicate (Tlr21_2).

Receptor	Model	np	Ln L	Estimates of parameters					Model compared	LRT P-value	Positive sites[a]
TLR5	Model A	28	-10165,09641	Site class	0	1	2a	2b			530 N 0.978*
				f	0,60473	0,33234	0,04061	0,02232			
				ω0	0,10087	1	0,10087	1			
				ω1	0,10087	1	9,07143	9,07143			
	Model A null	27	-10170,38592	1					Model A vs.Model A null	0,00114378	Not Allowed
TLR8	Model A	28	-16158.517734	Site class	0	1	2a	2b			823 A 0.965*
				f	0.57462	0.40766	0.01037	0.00735			
				ω0	0.07029	1.00000	0.07029	1.00000			
				ω1	0.07029	1.00000	998.99874	998.99874			
	Model A null	27	-16165.296401	1					Model A vs.Model A null	0.000231386	Not Allowed
TLR13	Model A	20	-7100.573648	Site class	0	1	2a	2b			
				f	0.64259	0.32938	0.01853	0.00950			
				ω0	0.06914	1.00000	0.06914	1.00000			
				ω1	0.06914	1.00000	14.37178	14.37178			
	Model A null	19	-7105.431583	1					Model A vs.Model A null	0.001826836	Not Allowed
TLR22	Model A	32	-17590.839397	Site class	0	1	2a	2b			344 S 0.962*,627 M 0.960*
				f	0.49499	0.44812	0.02986	0.02703			
				ω0	0.13232	1.00000	0.13232	1.00000			
				ω1	0.13232	1.00000	12.14526	12.14526			
	Model A null	31	-17602.159433	1					Model A vs.Model A null	0.000001954	Not Allowed
TLR23	Model A	16	-9143.957160	Site class	0	1	2a	2b			Not significant sites
				f	0.56141	0.41365	0.01436	0.01058			
				ω0	0.11399	1.00000	0.11399	1.00000			
				ω1	0.11399	1.00000	19.63740	19.63740			
	Model A null	15	-9147.279352	1					Model A vs.Model A null	0.009946886	Not Allowed
Gya_TLR21_2	Model A	28	-14048.172839	Site class	0	1	2a	2b			25 D 0.952*, 427 D 0.973*, 513 Q 0.956*, 552 R 0.998**, 577 D 0.973*
				f	0.55406	0.39020	0.03270	0.02303			615 M 0.976*,653 R 0.963*,770 D 0.975*,809 V 0.972*,815 S 0.974*
				ω0	0.06857	1.00000	0.06857	1.00000			
				ω1	0.06857	1.00000	53.35043	53.35043			
	Model A null	27	-14058.915882	1					Model A vs.Model A null	0.000003564	Not Allowed

[a]Only PSS with significant posterior probabilities are indicated. Asterisks indicate posterior probabilities P≥95%(*) and P>99%(**).

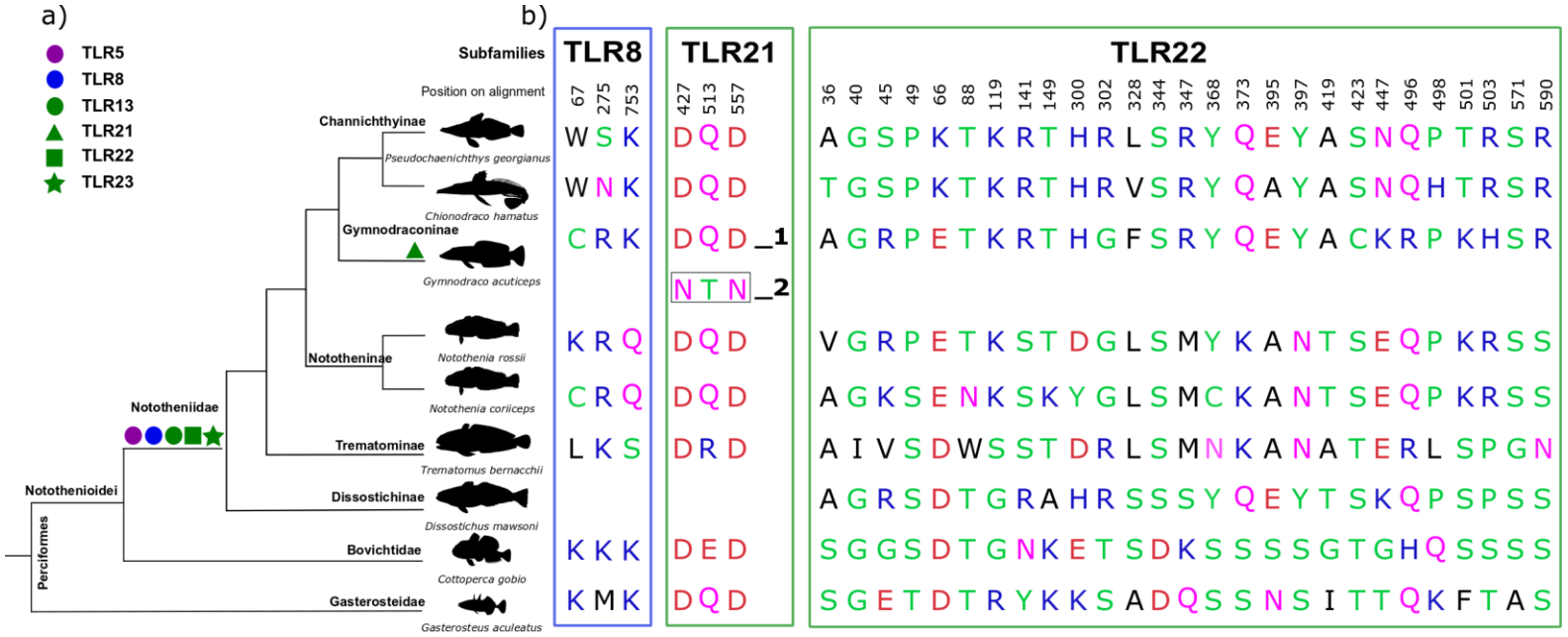

Figure 2.2.9. Evidence of positive selection in the LRR ectodomains of Nototheniidae Tlrs. Receptors represented are Tlr8 and Tlr21 and Tlr22. A) Positive selection identified with the Branch-site model are represented by coloured shapes on ancestral Nototheniidae branch and on Tlr21 duplicate in *G. acuticeps* (Tlr21_2) and PSS were only found for Tlr21_2 and are boxed. B) PSS as identified with the Branch-site and Sites models for Nototheniidae sequences. PSS are coloured according to their physicochemical properties: acidic in red, basic in blue, neutral in purple, polar in green, and hydrophobic in black using Weblogo vs3 annotation. Amino acid positions given refer to the edited multiple sequence alignment used for the selective pressure analysis (**Additional data 1-15 in Annex I**). The PSS represented were mapped in the sequences and are marked in red (**Supplementary figure 2.2.4-8**).

Table 2.2.4. Selective pressure analysis for site models. LRT Statistics (2ΔL) and *p*-values for the site models on the Nototheniidae sequences of Tlr5, Tlr8, Tlr13, Tlr22, Tlr23.

Receptor	Model	np	Ln L	Estimates of parameters				Model compared	LRT P-value	Positive sites[a]
TLR5	M2a	14	-2969,998729	p:	0.62742	0.36347	0.00911	M1a vs. M2a		
				ω:	0.10344	1.00000	4.70001			No significant sites found
	M1a	12	-2970,783667	p:	0.63311	0.36689				
				ω:	0.10281	1.00000			1	Not Allowed
	M8	14	-2969,998943	p0=0.94815	p=0.38730	q=0.78363		M7 vs.M8		
				(p1= 0.05185)	ω= 1.98531					
	M7	12	-2971,214751	p=0.27144		q=0.44370			0,296470369	Not Allowed
TLR8	M2a	14	-5382.496766	p:	0.29522	0.65107	0.05371	M1a vs. M2a		
				ω:	0.00000	1.00000	13.82641			No significant sites found
	M1a	12	-5417.313267	p:	0.42715	0.57285				
				ω:	0.00000	1.00000			0.000000000	Not Allowed
	M8	14	-5388.003906	p0=0.74956	p=0.00500	q=1.72148		M7 vs.M8		25 G 0.999**,27 K 0.987*,28 E 0.988*,48 W 1.000**,63 Q 0.988*,92 S 0.987*,275 V 0.995**,414 S 0.984*,501 K 0.985*,753 H 0.985*,761 K 0.987*
				(p1= 0.25044)	ω= 5.39259					
	M7	12	-5418.056161	p=0.02508		q=0.01283			0.000000000	Not Allowed
TLR13	M2a	12	-3257.897218	p:	0.73321	0.00000	0.26679	M1a vs. M2a		
				ω:	0.00000	1.00000	2.89533			No significant sites found
	M1a	10	-3262.616085	p:	0.46579	0.53421				
				ω:	0.00000	1.00000			0.008925285	Not Allowed
	M8	12	-3257.897218	p0=0.73321	p=0.00500	q=2.09224		M7 vs.M8		210 H 0.963*
				(p1= 0.26679)	ω= 2.89538					
	M7	10	-3263.427397	p=0.02050		q=0.00751			0.003965279	Not Allowed
TLR22	M2a	16	-5046.424216	p:	0.61339	0.15062	0.23598	M1a vs. M2a		
				ω:	0.00000	1.00000	5.25653			No significant sites found
	M1a	14	-5086.643355	p:	0.48532	0.51468				
				ω:	0.00000	1.00000			0.000000000	Not Allowed
	M8	16	-5046.642792	p0=0.69561	p=0.00500	q=1.39574		M7 vs.M8		24 T 0.963*,32 R 0.968*,36 A 0.957*,40 G 0.957*,45 S 0.999**,49 P 0.964*,66 K 0.951*,88 T 0.999**,119 K 0.994**,141 R 0.994**,149 T 0.951*,181 R 0.969*
				(p1= 0.30439)	ω= 4.52587					245 E 0.993**,254 S 0.969*,257 T 0.995**,273 Q 0.981*,300 H 0.992**,302 R 0.983*,328 L 0.996**,347 R 0.994**,368 Y 0.958*,373 Q 0.962*,
										395 E 0.995**,397 Y 0.954*,419 A 0.954*,423 S 0.964*,447 N 0.994**,477 V 0.995**,496 Q 0.957*,498 P 0.962*,501 T 0.998**,503 R 0.957*
										520 S 0.968*,544 N 0.991**,559 N 0.991**,571 S 0.972*,590 R 0.950*,642 E 0.954*,663 P 0.969*,707 T 0.977*,709 S 1.000**,760 T 0.960*,
	M7	14	-5090.346350	p=0.03100		q=0.01510			0.000000000	Not Allowed
TLR23	M2a	12	-4560.594806	p:	0.79957	0.00000	0.20043	M1a vs. M2a		
				ω:	0.17464	1.00000	3.91573			No significant sites found
	M1a	10	-4568.283926	p:	0.38807	0.61193				
				ω:	0.00000	1.00000			0.000457781	Not Allowed
	M8	12	-4560.595092	p0=0.79997	p=5.98663	q=27.59025		M7 vs.M8		333 T 0.976*, 515 S 0.974*
	M7	10	-4568.445931	p=0.02094		q=0.00655	0.00655		0.000389425	Not Allowed

[a]Only PSS with significant posterior probabilities are indicated. Asterisks indicate posterior probabilities P≥95%(*) and P>99%(**).

2.2.4.7. Experimental immune and temperature challenge

2.2.4.7.1. Tlr expression

Expression of *tlr5*, *tlr21* and *tlr22* was determined in the head-kidney and intestine of *N. rossii* (**Figure 2.2.10**). *tlr21* is the most abundant transcript in head-kidney and *tlr22* in the intestine. *Tlr* gene expression in the 2ºC LPS-challenged group at both 8 h and 24 h post-challenge was not significantly modified in the head-kidney and intestine in relation to the non-LPS challenged control (**Figure 2.2.10**). Similarly, in *N. rossii* maintained in 6ºC seawater no significant differences in *tlr5*, *tlr21* and *tlr22* gene expression were detected between the control and LPS-challenged groups. Comparison between animals maintained at 2ºC and at 6ºC revealed a significant increase ($n=6$, $p < 0.001$) in *Tlr5* gene expression in the head-kidney of control and LPS-challenged fish at 6ºC. In the head-kidney of control and LPS-challenged fish after 8 h, *tlr21* ($n=6$, $p < 0.001$) and *tlr22* ($n=6$, $p = 0.005$) transcripts were significantly increased in 6ºC compared to the 2 ºC group. In the intestine, *tlr21* was significantly down regulated ($n=6$, $p < 0.05$) after 24 h in both control and LPS-challenged groups at 6 ºC compared to the 2ºC group (**Figure 2.2.10**).

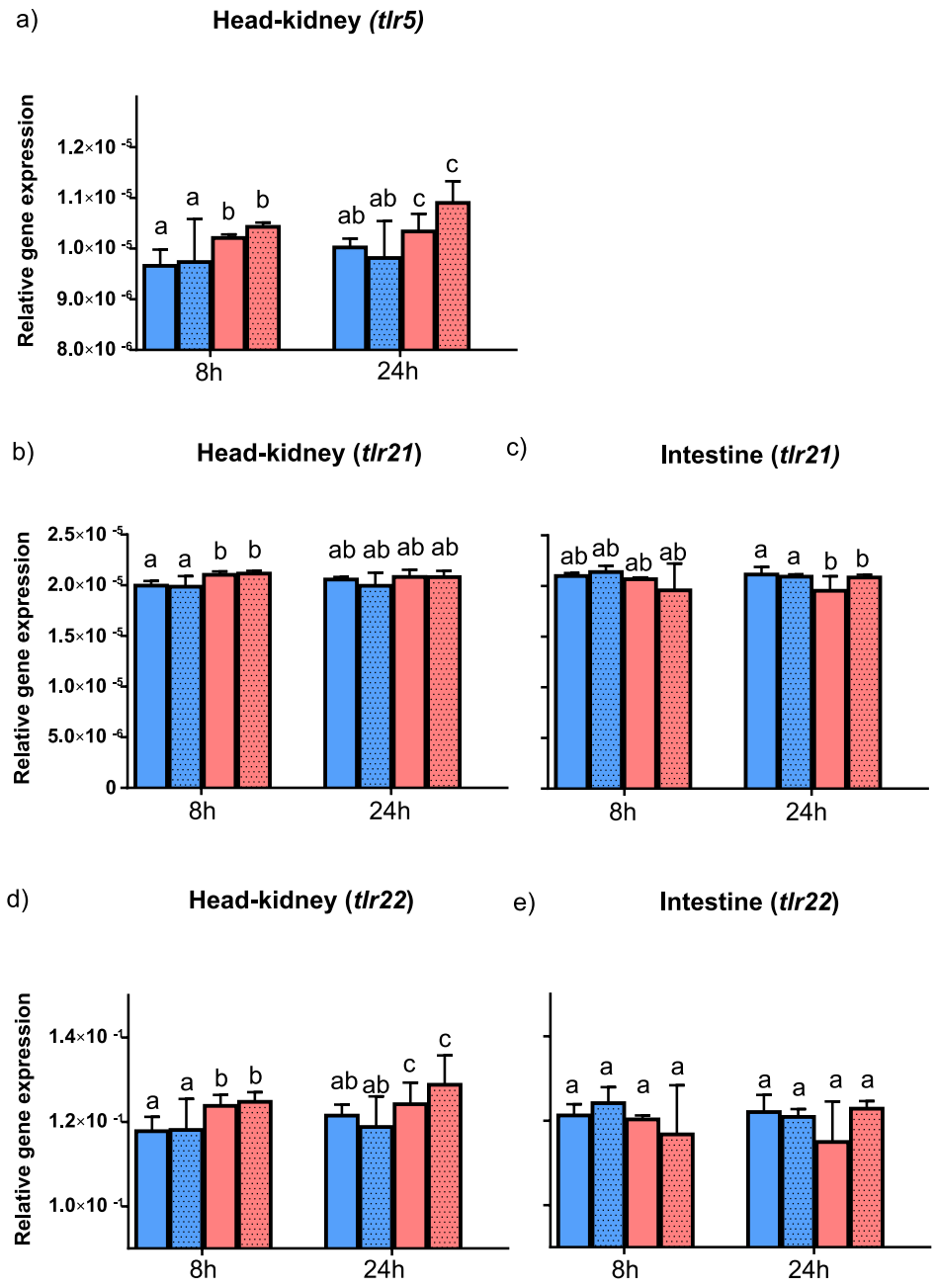

Figure 2.2.10. Quantitative PCR expression (ng/µl) of *N. rossii* transcripts for *tlr5*, *tlr21* and *tlr22* in LPS and temperature challenged fish. Gene transcript abundance was analysed in the head-kidney and intestine of control and experimental groups 8 h and 24 h post-injection. Expression of *tlr5* in the intestine is of very low abundance and was not quantifiable. The blue bars correspond to 2ºC and red bars to 6ºC seawater temperatures, smooth bars to the controls and dotted bars to the LPS groups. Data corresponds to the mean ± SEM of six different samples per group and gene expression levels were normalized using the geometric mean of two reference genes (*18s* and *β-actin*). SigmaPlot software v12.5 was used to assess the significance of differences between the experimental groups using three - way analysis of variance (ANOVA), post hoc Tukey´s test (Shapiro-Wilk normality test). Bars with asterisks are ($p < 0.05$) and double asterisks are ($p < 0.001$).

2.2.4.7.2. Blood plasma enzymatic activity

The concentration of total plasma proteins was similar in all experimental groups (data not shown). Lysozyme activity in *N. rossii* plasma was significantly higher (n = 6, p = 0.012) after 24 h of the LPS-challenged compared to the control group at 2ºC (**Figure 2.2.11 A**). No statistically significant differences in antitrypsin activity were detected between the control and LPS-challenged groups at both 2ºC and 6ºC. However, comparison of control and LPS-challenged groups at 2ºC and 6 ºC revealed that they are significantly different (control 2ºC versus control 6ºC and LPS 2ºC versus LPS 6ºC) at 8h and inhibition of enzyme activity significantly increased (n = 6, p = 0.032) in the 6 ºC groups compared to the 2ºC groups (**Figure 2.2.11 B**). Within the 2ºC experimental groups, a significant increase in antitrypsin activity was also detected in the control and LPS-injected groups at 24 h (n = 6, p = 0.007) when compared with the same groups at 8 h (**Figure 2.2.11 B**).

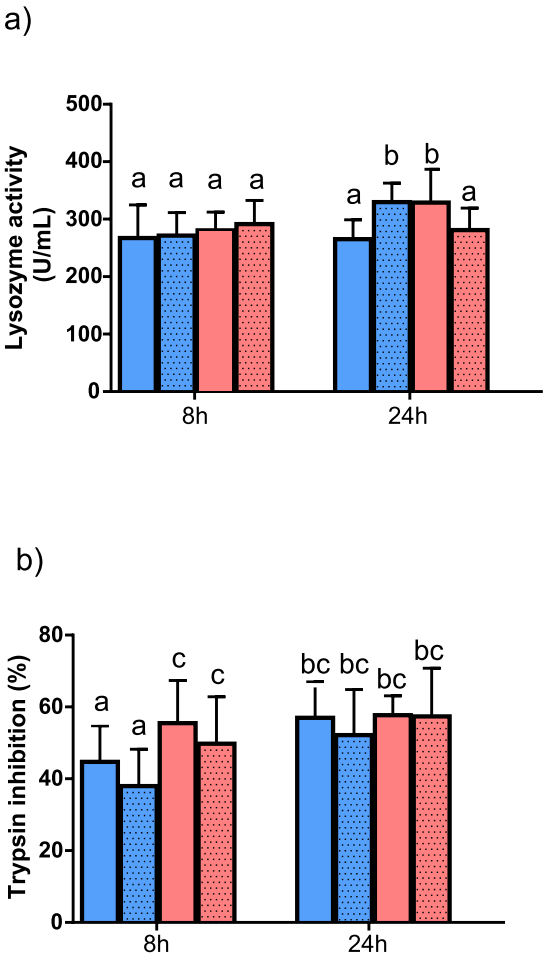

Figure 2.2.11. Plasma enzyme activity in LPS and temperature challenged *N. rossii*. (A) Lysozyme (U/ml) and **(B)** total protease inhibition (%) were measured in plasma from control and experimental groups. The blue bars correspond to 2ºC and red bars to 6ºC seawater temperatures, smooth bars to the controls and dotted bars to the LPS groups. Data corresponds to the mean ± SEM of six different samples per group. SigmaPlot software v12.5 was used to assess the significance of differences between the

experimental groups using three - way analysis of variance (ANOVA), post hoc Tukey´s test (Shapiro-Wilk normality test). Bars with asterisks and letters are ($p < 0.05$).

2.2.5. Discussion

The Nototheniidae are a stenothermal cold-adapted monophyletic teleost clade that evolved relatively recently in the cold-stable waters of Antarctica. Their diversification involved several rounds of species radiation that led to significant ecological, morphological, and genetic differentiation that contributed to their survival and environmental niche adoption. The impact of the Nototheniidae species radiation and environmental adaptation on immune system evolution, which is hypothesised to drive teleost speciation and success remains poorly described. Here we characterized the Tlr superfamily genes of the innate immune system in seven Antarctic teleost species and provide a comparative analysis with *tlr* genes in other teleosts.

The Nototheniidae possess a similar *tlr* gene number to other teleosts suggesting that speciation and adaptation to the Antarctic environment had little impact on receptor gene number. The only exception was *D. mawsoni* with only 10 Tlrs. Perciformes, which include Nototheniidae, unlike other teleost orders retain a homologue of the tetrapod *tlr13*. In addition, identification of a rapidly evolving species-specific Tlr21 duplicate (Tlr21_2) in *G. acuticeps* may be a unique adaptive character arising from neofunctionalization after gene duplication. Although the general protein structure and gene number of TLRs in Nototheniidae is well conserved, codon usage bias revealed significant modifications in the ectodomain and LRR motifs of Tlr5, Tlr8, Tlr13, Tlr22 and Tlr23. This suggests subtle modifications in ligand binding characteristics occurred presumably due to adaptation to the unique microbial community found in these frigid waters. Challenge with LPS failed to affect transcription of *tlr5*, *tlr21* and *tlr22* in immune-related tissues (head-kidney and intestine) in *N. rossii*. However, a 4ºC rise in sea water temperature from 2°C to 6°C significantly modified tissue expression levels of the three genes analysed.

2.2.5.1. Evolution of the Nototheniidae Tlrs

Comparative analysis of the genomes and transcriptome of Nototheniidae fishes relative to other fish and vertebrates revealed that the TLR gene repertoire is similar to other Perciformes suggesting that their recent radiation in the cold-stable Antarctica environment was not associated with significant modifications in Tlr gene repertoire or evolution as described for other gene families that contributed to their adaptation such as the expansion of antifreeze glycoproteins and zona pellucida proteins that confer protection from ice damage (Chen et al., 1997b, 2008; Kim et al., 2019a). The exception was *D. mawsoni* an early evolving lineage of the Nototheniidae where species-specific *tlr* gene deletions occurred.

Of the seven Nototheniidae genomes analysed *D. mawsoni* retained the lowest number of Tlr genes and linkage analysis revealed the homologues of *tlr1*, *tlr2* (*a* and *b*), *tlr5* and *tlr8* were deleted from its genome. The reason for *tlr* gene deletion in *D. mawsoni* is unclear but may be associated with its unique physiological adaptations. This species is considered the best model for studies of the evolutionary underpinning of secondary pelagicism (absence of a swim-bladder) in the Antarctic clade. The neutral buoyancy of *D. mawsoni* arose from significant genetic reprograming to favor fat deposition and modified bone development (Chen et al., 2019b). Morphological alterations in *D. mawsoni* to reduce body density and promote static lift include increased lipid deposits under skin and musculature and minimized bone mineralization (Eastman and DeVries, 1981) with an up regulation of genes involved in adipogenesis, triacylglycerol synthesis and fat storage in skeletal muscle and by favoring chondrogenesis over osteoblastogenesis (Chen et al., 2019b). In mammals Tlr non-immune functions are linked to bone development and increased osteoclast differentiation (Souza and Lerner, 2019), both of which are supressed in *D. mawsoni* (Eastman and DeVries, 1981), raising the possibility that in the Nototheniidae and teleosts in general *tlr* gene evolution may not only be influenced by their innate immune function.

An unanticipated result from our expanded comparative analysis of the *tlr* gene repertoire in fish was the reduced *tlr* gene number in the Pleuronectiform order (flatfish). The number of *tlr* gene members found in the four species analysed was variable and *S. senegalensis* and *C. semilaevis* had the most compact gene repertoire with 6 (*tlr1*, *tlr3*, *tlr5*, *tlr7*, *tlr8* and *tlr22*) and 7 (*tlr14/18*, *tlr3*, *tlr5*, *tlr7*, *tlr8*, *tlr9* and *tlr22*) *tlrs* genes, respectively. Like the Nototheniidae, extant flatfish of the Pleuronectiformes represent a monophyletic group (Shi et al., 2018). In the Nototheniidae and Pleuronectiform radiations chromosomal rearrangements and chromosomal fusions occurred independently in different species lineages (Auvinet et al., 2020)(García-Angulo et al., 2019). The compaction and reorganization of the genome in these two teleost lineages does not explain *tlr* gene deletions as the gene synteny was well conserved.

An intriguing observation is the common physiological characteristic of *D. mawsoni* and adult flatfishes as both lack a swim bladder and have a high content of polyunsaturated fatty acids in the organism (Cerdà and Manchado, 2013). In mammals changes in lipid metabolism and increased lipid storage affect innate immunity and cause modifications in Tlr signaling, endocytosis and cytokine secretion (Köberlin et al., 2016; Ruysschaert and Lonez, 2015). In fact, dyslipidemia and other metabolic diseases in mammals are closely connected to an altered immune response (Glass and Olefsky, 2012; Ka and Jin, 2021). Taking into consideration the interaction between lipid metabolism and Tlr activity these morphological/metabolic adaptations may explain the reduced Tlr repertoire in flatfish and *D. mawsoni*.

Identification of specific gene duplicates in Notothenoids fish compared to other teleosts (e.g. zona pellucida (ZP)-like proteins (Cao et al., 2016), mitochondrial proteins (Coppe et al., 2013) and antifreeze glycoprotein (Chen et al., 1997b; Near et al., 2012) have been associated with diversification of protein function as a consequence of their adaptation to the freezing environment (Chen et al., 2019b). However, conservation of species-specific duplicates of TLR subfamilies occurred in the case of the *tlr21* gene in the *G. acuticeps* genome and *tlr2* in all Nototheniidae and other teleosts and it was missing from *D mawsoni*. In our extended comparative analysis 3 further Tlr genes, homologues of the teleosts *tlr2b*, *tlr13* and *tlr25*, were identified in *N. coriiceps* compared to a previous study (Ahn et al., 2014). A similar gene repertoire was retrieved from the transcriptome of the congeneric species, *N. rossii*, further confirming conservation of Tlr gene members across Nototheniidae. Comparison of Antarctic Nototheniidae with the sub-Antarctic Bovichtidae representative, *C. gobio*, revealed loss of *tlr5s* and *tlr23* and in the closest Gasterosteriformes lineage, *G. aculeatus*, *tlr2b* and *tlr23* were lost indicating Tlr gene evolution was lineage and species-specific dependent. The TLR11 subfamily, is most conserved in aquatic vertebrates and was best conserved in Perciformes including the Nototheniidae. The TLR11 subfamily member *tlr13*, was up-regulated in the Perciform, *Miichthys miiuy*, from infection of *Vibrio anguillarum,* a bacteria that causes haemorrhagic septicaemia (Lages et al., 2019), and from viral simulation using Poly I:C (Signorino et al., 2014; Wang et al., 2016c). Studies of fish Tlr-ligand interactions will be essential to decipher the link between the TLR repertoire, infection, innate immune activation and disease resistance.

Overall, comparing Antarctic Nototheniidae and multiple teleost species, our analysis suggests that adaptation to the cold extreme Antarctica environment has not played a significant role in the Nototheniidae Tlr gene repertoire and the differences arose from species-specific events. In the Nototheniidae and the sister lineage Bovichtidae, Tlr gene number is similar to

other teleosts while the Gadiformes are peculiar as exuberant lineage-specific duplications and deletion events occurred. For example, in *G. morhua* 7 copies for *tlr8*, 14 copies *tlr22* and 9 copies for *tlr25* were found in the genome and *tlr5*/*tlr5*s, *tlr1* and *tlr2* genes were missing and this has been associated with the loss of *mhcII* and expansion of *mhcI* genes (Solbakken et al., 2016, 2017). This was correlated with the highly variable pathogen loads and community composition of the paleoclimatic Arctic conditions (Solbakken et al., 2016). However, we propose that the cod is an exception and its unique TLR repertoire and highly modified innate gene repertoire is a result of the rich number and frequency of repetitive tandem repeats within genes and gene promoter regions and significant genome rearrangement/recombination compared to other teleosts (Tørresen et al., 2017) (Sodeland et al., 2016).

2.2.5.2. Notothenioid Tlrs evolved under positive selection pressure

The accepted consensus is that TLRs are functionally conserved (Mikami et al., 2012). However, evidence from more refined analysis of the evolution of ligand recognition indicates positive selection of TLR3, 4, 5 and 15 in birds (Alcaide et al., 2008); TLR 4, 7 in wild rodents (Fornůsková et al., 2013); TLR1, 2, 6, 8 (Darfour-Oduro et al., 2015) and also for cetacean TLR (Xu et al., 2019) and Tlr5, 8, 13, 21, 22 and 23 in the present study of Antarctic Nototheniidae. Contrary to a previous study we failed to find the positive selection of Tlr2 in *T. bernacchii*, which was proposed to be associated with their radiation in an Antarctic environment (Varriale et al., 2012). Based on our in-depth analysis of TLR evolution we suggest that although the general protein framework of the protein has been conserved, the ligand interacting domain has changed presumably linked to their divergent pathogen recognition in different vertebrates. We propose a model that mirrors, although with less complexity, the highly conserved antibody structure in which changes to small protein segments (hypervariable regions) establishes the exquisitely refined antigen recognition (Jaton and Riesen, 1976). Our model explains the conundrum arising from the highly conserved TLR repertoire across most vertebrates despite their exposure to vastly different microbe loads, communities, and the surface or molecular characteristics of their pathogens.

Positive selection at the ectodomain, which recognize pathogen components, and within LRR motifs, was detected in Tlr5, Tlr8, Tlr13, Tlr22 and Tlr23 of all Antarctic Notothenioids. This was presumably driven by the unique microbiome bound by the circumpolar Antarctic currents. Of note is that selective pressure was common in members of the TLR11 superfamily,

which is rich in members in the teleosts. The members of this superfamily compared to other TLR families possess the largest number of LRRs and respond to viral infections (Chen et al., 2013; Matsuo et al., 2008; Pietretti and Wiegertjes, 2014). Protein modelling studies of Tlr22 LRRs in *D. rerio* revealed that changes in the LRR motif due to PSS, modified ectodomain structure towards a flattened horseshoe-shape conformation and caused a functional change towards sensing long-sized dsRNA (Sundaram et al., 2012b) (Sahoo et al., 2015). Positive selection in the *tlr22* duplicates of *G. morhua* and *Boleophthalmus pectinirostris* (Sundaram et al., 2012a, Solbakken et al., 2016; Qi et al., 2019; Qiu et al., 2019) were also associated with species-specific pathogen recognition. PSS of the duplicate *tlr21_2* TIR domain in *G. acuticeps* falls within the three conserved regions, box 1 (YDAFISY), box 2 (SSKLC-RD-PG) and box 3 (a conserved W surrounded by basic residues) that are involved in signal transduction (1 and 2) and receptor localization (3) (Slack et al., 2000). Previous studies in *Larimichthys polyactis* suggested that the TIR domain of *tlr21* mediates activation of the factor nuclear kappa B (Sun *et al*., 2016), suggesting divergent signalling may occur in the duplicate *Tlr2* in *G. acuticeps*. PSS were also detected in Tlr8 LRRs (known to be efficient against virus) and in the TM domain of Tlr5 (that mostly react to bacteria) and changes in the homologue receptor sequences in other teleosts were associated with adaptation to different environmental pathogens (Han et al., 2017). Functional data on amino acid mutations in the receptor TM domain is scarce but a TM mutation identified in Nototheniidae Tlr5 (PSS 530) is located near an important binding site for the plasma membrane auxiliary protein UNC93B1 which in mammals is responsible for the receptor trafficking and localization (Huh et al., 2014). The results of our extensive comparative analysis of TLR evolution in vertebrates and PSS analysis, indicate that the Tlr11 superfamily underwent a unique evolutionary process in the Antarctic Notothenioidei.

2.2.5.3. Notothenioid Tlr response is species-specific and changes with temperature increase

The distribution of the Tlr transcripts in head-kidney (*tlr5*, *tlr21* and *tlr22*) and intestine (*tlr21* and *tlr22*) of *N. rossii* confirmed their previously described tissue-specific distribution (Ahn et al., 2014; Qi et al., 2018). In LPS-stimulated *N. rossii* (8h and 24h later) no changes in *tlr* gene expression were detected, which conflicts with previous studies in other teleost fish where these genes were modified. For example, in *Larimichthys polyactis* head-kidney and spleen *tlr21* and *tlr22* were differentially expressed 6-12 h post LPS challenge (Qiu et al., 2019),

in *C. carpio tlr22* expression was increased in head-kidney (Li et al., 2017) and in Dabry´s sturgeon *tlr21* and *tlr22* expression was increased in the head-kidney leukocytes (Qi et al., 2018). Moreover, in the head-kidney of *N. coriiceps*, *tlr5* and *tlr22* were up-regulated 12 h post-challenge with heat-killed bacteria (*E.coli* O11:B4) but *tlr21* expression was unaltered (Ahn et al., 2014). In *D. rerio* and *O. mykiss* head-kidney *tlr5* expression was also found to be responsive to bacteria flagella (Hayashi et al., 2001; Meijer et al., 2004; Palti, 2011; Tsujita et al., 2004).

The reason for the difference between the response to LPS of *N. rossii* relative to *N. coriiceps* despite the similar treatment conditions, or to other teleosts was unclear. Particularly since the endotoxin LPS, a glycoprotein major component of the outer cell wall membrane of Gram-negative bacteria, is a common bacterial PAMP. Nonetheless, although bacterial LPS is considered identical (Ray et al., 1994) more recent studies reveal chemical divergence between different gram-negative species (Meredith et al., 2006; Nilsson et al., 2008) and within bacterial species with different phenotypes (Migale et al., 2015; Nilsson et al., 2008). This may contribute to explain the lack of response to LPS in our study, in fact cold adapted gram-negative bacteria have a modified cell wall including the structure of LPS within the O-antigen region (Ray et al., 1994). The stimulation of lysozyme activity 24h after LPS-challenge in *N. rossii* is similar to what has been previously described for *S. salar* (Nya and Austin, 2010; Paulsen et al., 2001). The lysozymes are a diverse and poorly conserved group of non-specific innate immune enzymes that hydrolyse the peptidoglycan layer of the bacterial cell wall and several genes were recently reported in Notothenioids (Li et al., 2021b). The functional requirement of peptidoglycan residues for lysozymes activity (Ragland and Criss, 2017) and lysozyme response to LPS in *N. rossii*, presumably highlights the pathogen specificity of the LRR region in TLRs particularly since the candidate Tlrs quantified may be more reactive to virus than bacteria.

Differences in the response to an LPS challenge of *N. rossii* and *N. coriiceps* was previously reported for iron metabolism genes (Martínez et al., 2020) with *N. coriiceps* being more responsive. The effect of water temperature was more profound than LPS on *tlr5, tlr21*and *tlr22* gene expression and the response was common to both control and immune-challenged *N. rossii*. Plasma antitrypsin activity was reduced by an increase in water temperature. The effect of water temperature on the regulation of *tlr* expression has previously been reported in *G. morhua* where an increase from 4 to 12°C increased expression of *tlr21* and *tlr22* in the head-kidney and spleen (Sundaram et al., 2012a). Although in *D. rerio*, temperature stress (from 23ºC to 31ºC) did not significantly modify *tlr21* and *tlr22* expression in the head-kidney and

spleen (Sundaram et al., 2012b). Heat stress is known to induce an innate immune response by activating the overexpression of various heat shock proteins. However, the function of these proteins was lost in notothenioids as part of their adaptation to the Antarctic environment (Hofmann et al., 2000).

2.2.6. Conclusion

Our study provides for the first time a comprehensive description of the TLR system in several Nototheniidae and suggests they possess a similar gene complement to other teleosts and that the TLR repertoire was highly conserved across vertebrates. Our analysis revealed that Nototheniidae Tlrs shared common origin with other vertebrate Tlrs and that members of TLR11 superfamily are conserved with other Perciformes. The only exception is *D. mawsoni* where a compact gene repertoire was found, and this resulted from species-specific gene deletions potentially a consequence of morphological and physiological adaptations associated with lipid and calcium metabolism. Our extended comparative analysis also revealed that gene deletions affected the evolution of *tlr*s in Pleuronectiformes a teleost extant where extreme morphological changes in lipid metabolism and skeletal rearrangement also occurred associated with adaptation to a benthic lifestyle. Tlr5, Tlr8, Tlr13, Tlr22 and Tlr23 suffered positive selection in the ancestral Nototheniidae clade potentially associated with their adaptation to the Antarctic environment and changes mostly affected the LRR motifs in a species-specific manner suggest that functional divergence to pathogen recognition may exist. *Tlr5*, *tlr21* and *tlr22* were not responsive to LPS challenge in the head-kidney and intestine at transcriptomic level but they were sensitive to temperature stress. Our study demonstrates that adaptation to freezing water temperatures have not played an important role in the evolution of Tlrs in Nototheniidae and potential changes in receptor function and pathogen recognition may be associated to the co-evolving microbiota environment and species-specific adaptation to their ecological niches.

2.2.7. Supplementary materials

Supplementary material 2.2.1. Methods

The detailed methods performed for the selective pressure analysis performed are described below. The amino acid positions given in the text refer to their positions in the edited alignment that was used for the analysis.

Supplementary material 2.2.2. Branch-Site analysis

The Branch-Site model aims to identify positive selection acting on a few sites of a predefined branch (foreground branch) by allowing ω to vary both across the branches and the sites of the phylogeny (Zhang *et al,* 2005). The alternative model A assumes four classes of sites where site class 0 presents $0 < \omega 0 < 1$ for both background and foreground branches, class 1 with $\omega 1 > 1$ for both background and foreground branches, class 2a with $0 < \omega 0 < 1$ for the background branches and $\omega 2 > 1$ for the foreground branches and class 2b where $\omega 1 = 1$ for the background branches and $\omega 2 > 1$ for the for foreground branches (Zhang et al., 2005). This model is then compared to an identical null model but where $\omega 2 = 1$ fixed (Zhang et al., 2005).

Supplementary material 2.2.3. Site analysis

Two pairs of models M1a (nearly neutral) vs M2a (positive selection) and M7 (beta) vs M8 (beta& ω) are useful for the identification of positively selected sites Wong *et al.,* (2004). Both consist in the comparison of a model where ω in all sites are limited to $0 < \omega \leq 1$ (M1a, M7) with a model which allows for $\omega > 1$ (M2a, M8). The models M1a and M2a allow for two classes of sites. M1a where $\omega 0$ is estimated from the data and may vary between $0 < \omega 0 < 1$ and $\omega 1 = 1$ which is fixed. M2a allows for one more sites class $\omega 2$, where $\omega 2 > 1$ (Wong *et al.,* 2004). The beta model (M7) fixes a ratio on a distribution $\omega \leq 1$ in all lineages and implements ten classes of sites against the beta-ω model (M8) which also implements a fixed ω for all lineages but attributes 11 classes of sites, 10 sites with $\omega \leq 1$, and one site with $\omega > 1$ to allow for positive selection (Wong *et al.,* 2004).

Supplementary material 2.2.4. Likelihood-Ratio test

The LRT analysis were conducted to compare a null model that does not allow for $\omega > 1$ in the distribution with an alternative model that does (Yang *et al.,* 2005). For each model pairs the LRT statistic $2\Delta l$, (twice the log likelihood difference) was compared with critical values retrieved from the χ^2 distribution (significance level of 5%). In specific cases of sites and

branch-site models where LRTs suggested positive selection, Bayes empirical Bayes (BEB) was used to calculate the posterior probabilities that each codon belongs to the site class of positive selection under their respective models (M2a, M8 for site models or alternative model A for branch-site model) (Yang, 2007). Sites were considered to be under positive selection if their posterior probability of $\omega > 1$ was equal or higher than 0.95 (Nozawa et al., 2009).

Supplementary material 2.2.5. Results

For the Branch-site analysis the ancestral branch of Notothenioidei as well as the ancestral branch of Pleuronectiformes were tested whenever possible. From the 12 tlrs for which the ancestral branch of Notothenioidei was tested only two identified positive selection, Tlr3 with a significant p-value of 0.000102623 and Tlr22 with a significant p-value of 0.013081816 and Tlr3 presented 2 PSS (422 and 591) with posterior probability > 0.95 (Supplementary File 1). From the 5 tlrs for which the ancestral branch of Pleuronectiformes was tested none presented evidence of positive selection.

Supplementary material 2.2.6. Additional Data 1-15

All the alignments, trees and Codeml control files from each Tlr are provided in the Annex I in digital format.

Supplementary table 2.2.1. List of species name, abbreviations, accession numbers and database source. The sequences that were not used for the phylogenetic tree are indicated. This table is provided in Annex I because is very extensive.

Supplementary table 2.2.2. Percent (%) of amino acid sequence identity between the Nototheniidae A) tlr1, B) tlr2, C) tlr3, D) tlr5, E) tlr5S, F) tlr7, G) tlr8, H) tlr9, I) tlr13, J) tlr14/18, K) tlr21, L) tlr22, M) tlr23 and N) tlr25 subfamilies and with other Perciformes fish.

a)

Tlr1	Gac	Dla	Sau	Pge	Gya	Nco	Nro	Tbe	Cha	Cgo	Pol	Sse	Hhi
Gac	100	75	71	75	75	75	75	75	75	76	70	66	71
Dla		100	75	76	77	77	77	77	76	79	74	71	74
Sau			100	73	73	72	72	72	72	75	74	71	75
Pge				100	97	96	95	95	98	80	72	69	73
Gya					100	95	95	95	96	80	73	69	73
Nco						100	98	95	96	81	72	69	73
Nro							100	94	95	81	72	69	73
Tbe								100	95	80	73	69	73
Cha									100	80	72	69	73
Cgo										100	74	71	75
Pol											100	73	87
Sse												100	73
Hhi													100

b)

Tlr2_a	Gac	Dla	Sau	Pge	Gya	Nco	Nro	Tbe	Cha	Cgo	Pol	Hhi
Gac	100	71	69	72	71	75	75	73	73	75	69	70
Dla		100	78	75	73	80	76	75	73	78	73	74
Sau			100	70	69	74	72	70	70	74	72	72
Pge				100	97	97	98	97	98	80	72	73
Gya					100	95	97	96	96	79	70	72
Nco						100	98	97	96	82	76	77
Nro							100	97	96	80	74	75
Tbe								100	96	80	72	72
Cha									100	79	72	73
Cgo										100	73	75
Pol											100	86
Hhi												100

Tlr2_b	Dla	Sau	Pge	Gya	Nco	Nro	Tbe	Cha	Cgo	Hhi
Dla	100	68	69	70	70	75	70	70	72	72
Sau		100	64	65	65	75	64	64	66	68
Pge			100	95	94	95	93	98	74	70
Gya				100	92	95	93	97	75	71
Nco					100	98	92	95	74	71
Nro						100	95	95	81	72
Tbe							100	94	74	70
Cha								100	74	70
Cgo									100	72
Hhi										100

c)

Tlr3	Gac	Dla	Sau	Pge	Gya	Nco	Nro	Tbe	Cha	Dma	Cgo	Pol	Cse	Sse	Hhi
Gac	100	76	72	70	71	72	72	71	71	75	76	70	67	69	70
Dla		100	77	72	72	74	74	72	72	74	78	75	69	72	74
Sau			100	67	68	69	69	69	69	72	74	72	66	71	72
Pge				100	97	93	93	92	98	95	76	68	65	66	68
Gya					100	93	93	93	97	96	76	68	65	67	68
Nco						100	98	93	94	94	77	69	66	67	68
Nro							100	93	94	95	77	69	66	67	69
Tbe								100	94	94	76	68	65	67	69
Cha									100	95	77	69	66	67	68
Dma										100	79	70	72	73	71
Cgo											100	74	68	71	73
Pol												100	71	76	87
Cse													100	73	70
Sse														100	75
Hhi															100

d)

Tlr5	Gac	Sau	Pge	Gya	Nco	Nro	Tbe	Cha	Cgo	Pol	Cse	Sse	Hhi
Gac	100	63	70	70	70	67	70	69	74	68	61	65	68
Sau		100	65	65	66	70	66	64	67	66	61	62	65
Pge			100	97	95	94	96	99	77	69	61	63	69
Gya				100	97	96	97	97	79	69	61	64	70
Nco					100	99	96	95	78	69	61	64	70
Nro						100	96	94	76	67	60	63	68
Tbe							100	96	78	69	62	64	70
Cha								100	78	68	61	63	68
Cgo									100	71	65	68	72
Pol										100	66	69	86
Cse											100	69	67
Sse												100	69
Hhi													100

e)

Tlr5S	Gac_1	Dla	Sau	Pge	Gya	Nco	Tbe	Cha	Dma	Hhi
Gac_1	100	77	70	80	76	77	77	77	77	69
Dla		100	77	72	80	80	80	80	76	74
Sau			100	70	72	72	73	72	68	68
Pge				100	97	97	98	92	76	70
Gya					100	97	96	98	93	70
Nco						100	97	98	93	70
Tbe							100	97	92	70
Cha								100	93	70
Dma									100	65
Hhi										100

f)

Tlr7	Gac	Dla	Sau	Pge	Gya	Nco	Nro	Tbe	Cha	Dma	Cgo	Pol	Cse	Sse	Hhi
Gac	100	86	80	84	84	84	81	84	83	66	86	81	77	80	81
Dla		100	82	85	82	85	79	85	85	66	87	79	75	79	78
Sau			100	80	85	80	76	79	80	61	81	83	78	84	83
Pge				100	98	98	97	97	99	76	87	82	78	81	81
Gya					100	98	98	98	98	76	87	82	78	81	82
Nco						100	99	98	98	76	87	82	78	81	81
Nro							100	97	98	91	83	81	70	79	79
Tbe								100	97	77	87	81	78	81	81
Cha									100	74	88	82	78	81	82
Dma										100	68	64	60	63	64
Cgo											100	83	78	82	83
Pol												100	79	83	91
Cse													100	80	77
Sse														100	83
Hhi															100

g)

Tlr8	Gac	Dla	Sau	Pge	Gya	Nco	Nro	Tbe	Cha	Cgo	Pol	Cse	Sse	Hhi
Gac	100	74	68	67	64	67	67	67	67	72	68	48	68	66
Dla		100	75	69	66	69	70	70	69	77	74	50	74	72
Sau			100	67	62	67	67	68	67	72	69	49	69	69
Pge				100	96	92	91	91	98	71	65	48	64	64
Gya					100	94	92	91	96	68	62	49	62	62
Nco						100	97	92	93	70	65	49	65	64
Nro							100	91	91	70	64	49	65	64
Tbe								100	91	71	66	48	65	66
Cha									100	71	65	48	65	64
Cgo										100	72	50	71	70
Pol											100	50	73	83
Cse												100	54	50
Sse													100	71
Hhi														100

h)

Tlr9	Gac	Dla	Sau	Pge	Gya	Nco	Nro	Tbe	Cha	Dma	Cgo	Pol	Cse	Hhi
Gac	100	73	65	71	71	71	71	72	71	65	72	66	61	67
Dla		100	69	72	72	72	72	72	72	66	74	69	66	70
Sau			100	65	64	64	65	65	64	64	66	63	59	64
Pge				100	97	95	95	94	99	89	76	66	62	67
Gya					100	95	95	95	97	89	76	66	62	66
Nco						100	98	94	95	89	76	66	62	67
Nro							100	95	95	90	76	66	62	67
Tbe								100	94	90	77	66	63	67
Cha									100	89	76	66	62	67
Dma										100	71	59	56	61
Cgo											100	68	65	68
Pol												100	63	82
Cse													100	63
Hhi														100

i)

Tlr13	Gac	Dla	Sau	Pge	Gya	Nco	Tbe	Cha	Dma	Cgo
Gac	100	73	71	66	67	58	66	74	64	71
Dla		100	78	70	71	62	70	81	65	76
Sau			100	70	71	61	69	81	65	75
Pge				100	97	84	93	98	86	73
Gya					100	84	93	97	87	73
Nco						100	82	98	73	64
Tbe							100	97	86	72
Cha								100	95	86
Dma									100	68
Cgo										100

j)

Tlr14/18	Gac	Dla	Sau	Pge	Gya	Nco	Nro	Tbe	Cha	Dma	Cgo	Pol	Cse	Hhi
Gac	100	82	82	78	78	78	78	78	78	69	81	78	77	77
Dla		100	86	80	80	80	80	81	80	80	83	79	76	78
Sau			100	80	81	81	82	81	81	80	83	79	78	79
Pge				100	97	94	95	95	98	94	82	76	73	73
Gya					100	95	96	96	97	94	83	75	73	73
Nco						100	98	94	95	93	82	75	73	73
Nro							100	95	96	94	82	75	73	73
Tbe								100	96	95	83	75	74	73
Cha									100	94	83	76	74	74
Dma										100	82	71	74	69
Cgo											100	79	76	78
Pol												100	78	76
Cse													100	88
Hhi														100

k)

Tlr21	Gac	Dla	Sau	Pge	Gya_1	Gya_2	Nco	Nro	Tbe	Cha	Dma	Cgo	Pol	Hhi
Gac	100	72	68	69	69	71	70	70	69	69	65	69	67	70
Dla		100	74	72	71	67	72	72	71	74	70	74	73	72
Sau			100	66	67	69	67	67	67	70	63	70	68	68
Pge				100	93	90	92	91	89	98	72	71	69	69
Gya_1					100	95	92	91	92	92	72	72	68	69
Gya_2						100	89	89	91	90	70	71	67	67
Nco							100	96	91	92	75	72	69	70
Nro								100	90	90	74	72	69	70
Tbe									100	89	73	72	70	69
Cha										100	73	71	68	69
Dma											100	67	67	67
Cgo												100	69	68
Pol													100	81
Hhi														100

l)

Tlr22	Gac	Dla	Sau	Pge	Gya	Nco	Nro	Tbe	Cha	Dma	Cgo	Pol	Cse	Sse	Hhi
Gac	100	59	59	60	60	59	60	59	57	60	62	58	52	56	59
Dla		100	66	63	63	62	62	62	60	64	68	67	55	63	68
Sau			100	60	60	59	60	60	57	61	64	61	54	60	62
Pge				100	95	90	91	88	96	91	69	59	53	60	60
Gya					100	90	92	88	93	91	68	60	53	60	60
Nco						100	96	87	90	90	67	59	53	59	59
Nro							100	89	89	91	69	60	54	61	60
Tbe								100	85	89	68	58	52	59	59
Cha									100	88	64	57	50	55	57
Dma										100	70	60	54	60	60
Cgo											100	64	54	61	65
Pol												100	58	66	81
Cse													100	56	57
Sse														100	66
Hhi															100

m)

Tlr23	Dla	Sau	Pge	Gya	Nco	Nro	Cha	Dma
Dla	100	48	49	48	48	53	48	49
Sau		100	62	62	61	63	62	63
Pge			100	97	92	93	98	92
Gya				100	93	95	96	94
Nco					100	96	91	91
Nro						100	94	92
Cha							100	93
Dma								100

n)

Tlr25	Dla	Pge	Gya	Nco	Tbe	Dma	Cgo
Dla	100	81	81	84	82	81	83
Pge		100	97	96	97	94	84
Gya			100	96	95	86	82
Nco				100	96	93	86
Tbe					100	95	84
Dma						100	83
Cgo							100

Supplementary figure 2.2.1. Detailed dendrogram of the Tlr members identified in Pleuronectiformes. The genes identified are represented within the six vertebrate TLR superfamily by coloured circles, when multiple genes were identified gene number is indicated inside the circles. Gene absence is indicated by a white circle. The *G. aculeatus* was included as a representative of the Perciforms for comparisons with the Pleuronectidae order and considering species distribution (Bai and Lee, 2010; Campos et al., 2013; Fang et al., 2010; Mayden et al., 1992; Neilson et al., 1989). Genes were obtained by searching their genome assemblies. Accession numbers are available as Supplementary Table 2.2.1.

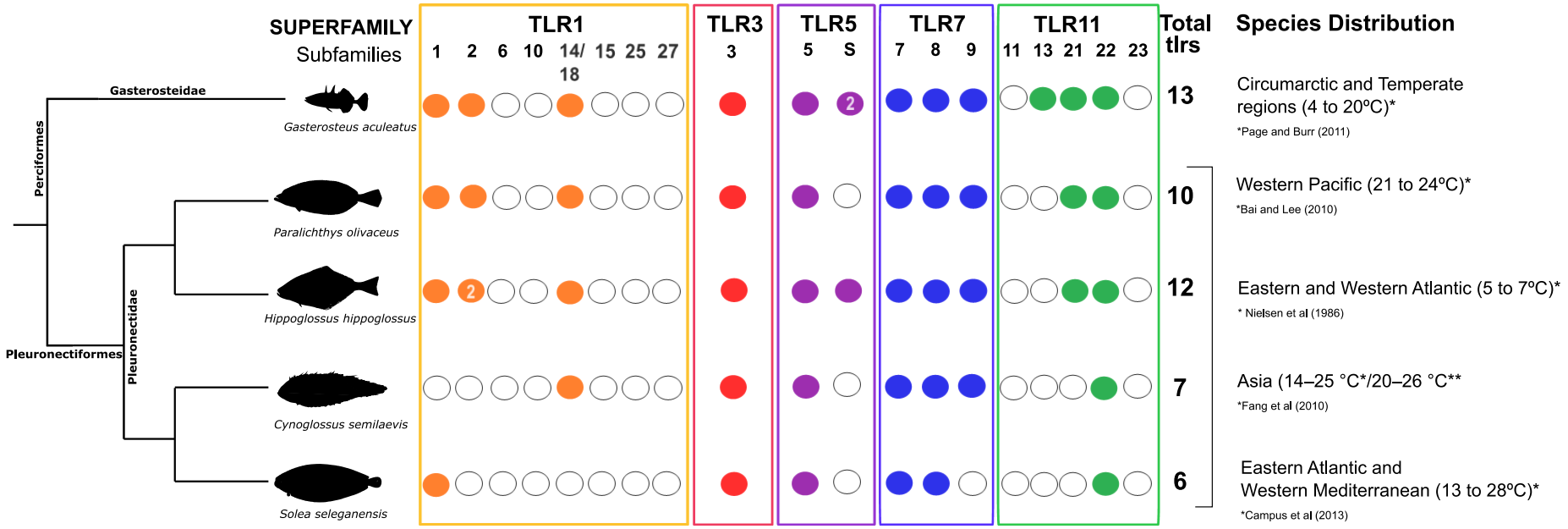

Supplementary figures 2.2.2. ML phylogenetic tree of Tlrs. Branches of the six vertebrate TLR superfamilies are identified by the corresponding numbers within black circles and with different colours: S1 indicates TLR1 superfamily (orange); S3 for TLR3 superfamily (red); S4 for TLR4 superfamily (pink); S5 for TLR5 superfamily; S7 for TLR7 superfamily (blue) and S11 for TLR11 superfamily (green). Within each superfamily cluster when multiple subfamilies exist, they were coloured with variations of the main representative colour and are also indicated. Accession numbers of the sequences used to construct the tree are available in Supplementary Table 1. The teleost *tlr2* duplicates were named as *tlr2a* and *tlr2b* and TLR15 were not used as they are only found in chicken and lizard. Tree was rooted with the Cnidarian Tlrs clade (Liu et al., 2019). The sea lamprey tlrs within the vertebrate TLR1, TLR7 and TLR11 superfamilies were named *tlrX*, *tlrY* and *tlrZ*, respectively since their identity assignment for the Tlr subfamilies was not clear. To facilitate their identification the *tlrs* from seven Antarctic species are highlighted in blue, other perciforms are indicated by a black dot and Pleuronectiforms by a black star.

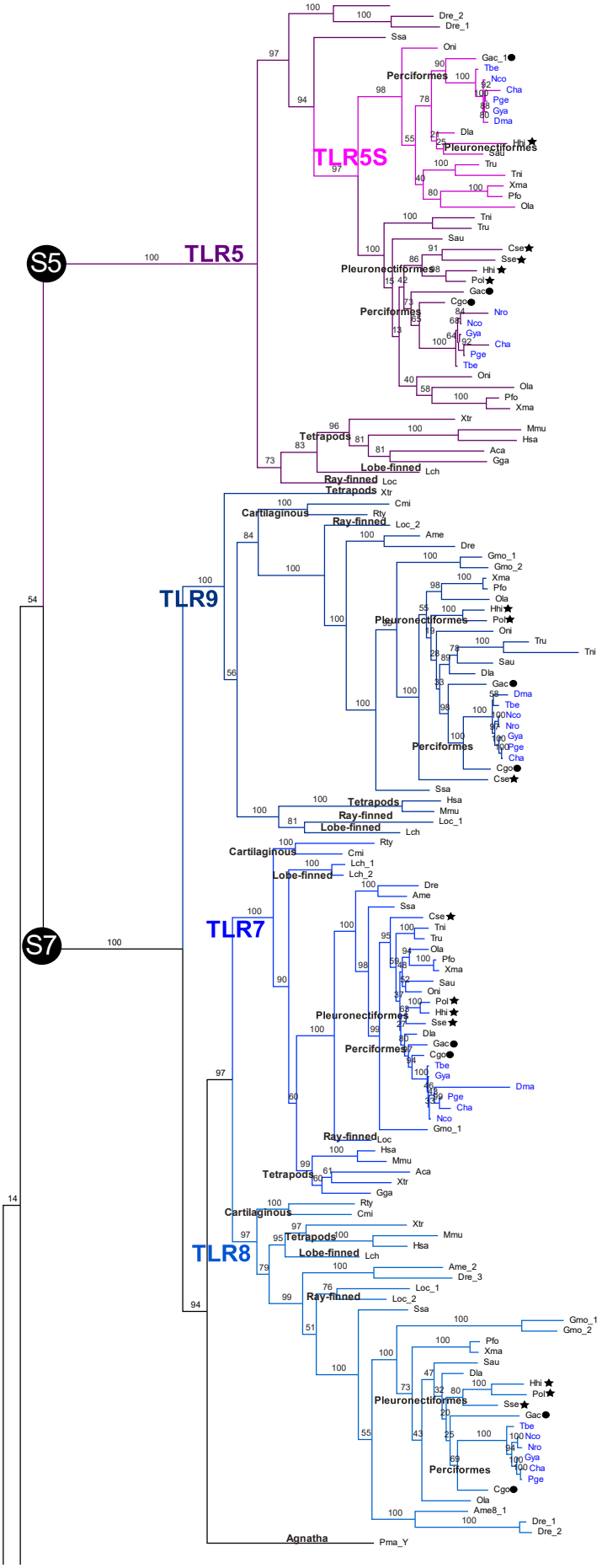
S5
S7
TLR5
TLR5S
TLR9
TLR7
TLR8
Perciformes
Pleuronectiformes
Tetrapods
Ray-finned
Lobe-finned
Cartilaginous
Agnatha
Dre_2
Dre_1
Ssa
Oni
Gac_1
Tbe
Nco
Cha
Pge
Gya
Dma
Dla
Hhi
Sau
Tru
Tni
Xma
Pfo
Ola
Cse
Sse
Pol
Gac
Cgo
Nro
Xtr
Mmu
Hsa
Aca
Gga
Lch
Loc
Cmi
Rty
Loc_2
Ame
Dre
Gmo_1
Gmo_2
Lch_1
Lch_2
Loc_1
Ame_2
Dre_3
Ame8_1
Pma_Y

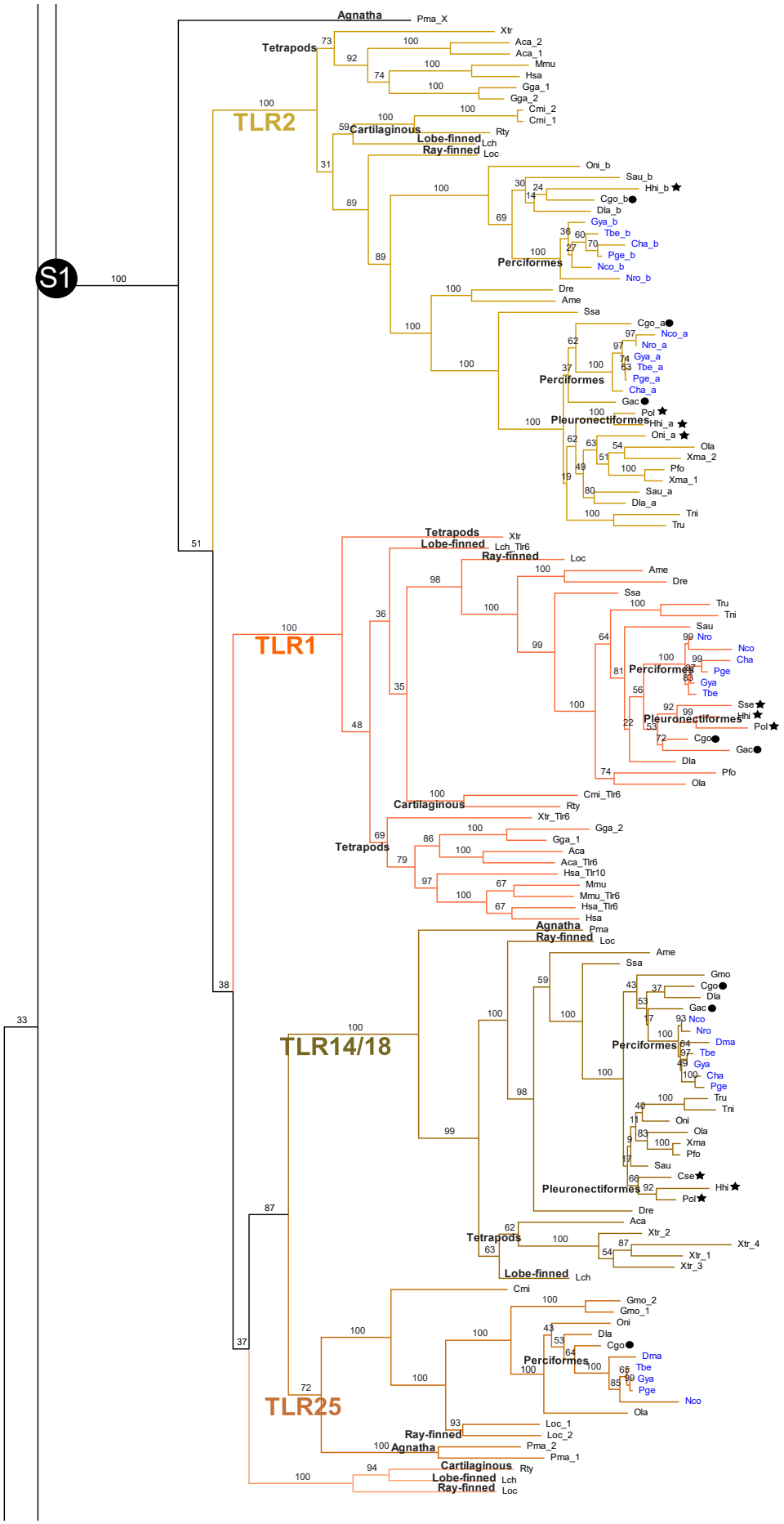
S1
TLR2
TLR1
TLR14/18
TLR25
Agnatha
Pma_X
Tetrapods
Xtr
Aca_2
Aca_1
Mmu
Hsa
Gga_1
Gga_2
Cmi_2
Cmi_1
Cartilaginous
Rty
Lobe-finned
Lch
Ray-finned
Loc
Oni_b
Sau_b
Hhi_b
Cgo_b
Dla_b
Gya_b
Tbe_b
Cha_b
Pge_b
Nco_b
Nro_b
Perciformes
Dre
Ame
Ssa
Cgo_a
Nco_a
Nro_a
Gya_a
Tbe_a
Pge_a
Cha_a
Gac
Pol
Pleuronectiformes
Hhi_a
Oni_a
Ola
Xma_2
Pfo
Xma_1
Sau_a
Dla_a
Tni
Tru
Lch_Tlr6
Cmi_Tlr6
Rty
Xtr_Tlr6
Gga_2
Gga_1
Aca
Aca_Tlr6
Hsa_Tlr10
Mmu
Mmu_Tlr6
Hsa_Tlr6
Hsa
Pma
Loc
Ame
Ssa
Gmo
Cgo
Dla
Gac
Nco
Nro
Dma
Tbe
Gya
Cha
Pge
Tru
Tni
Oni
Ola
Xma
Pfo
Sau
Cse
Hhi
Pol
Dre
Aca
Xtr_2
Xtr_4
Xtr_1
Xtr_3
Lch
Cmi
Gmo_2
Gmo_1
Oni
Dla
Cgo
Dma
Tbe
Gya
Pge
Nco
Ola
Loc_1
Loc_2
Pma_2
Pma_1
Cartilaginous
Rty
Lobe-finned
Lch
Ray-finned
Loc

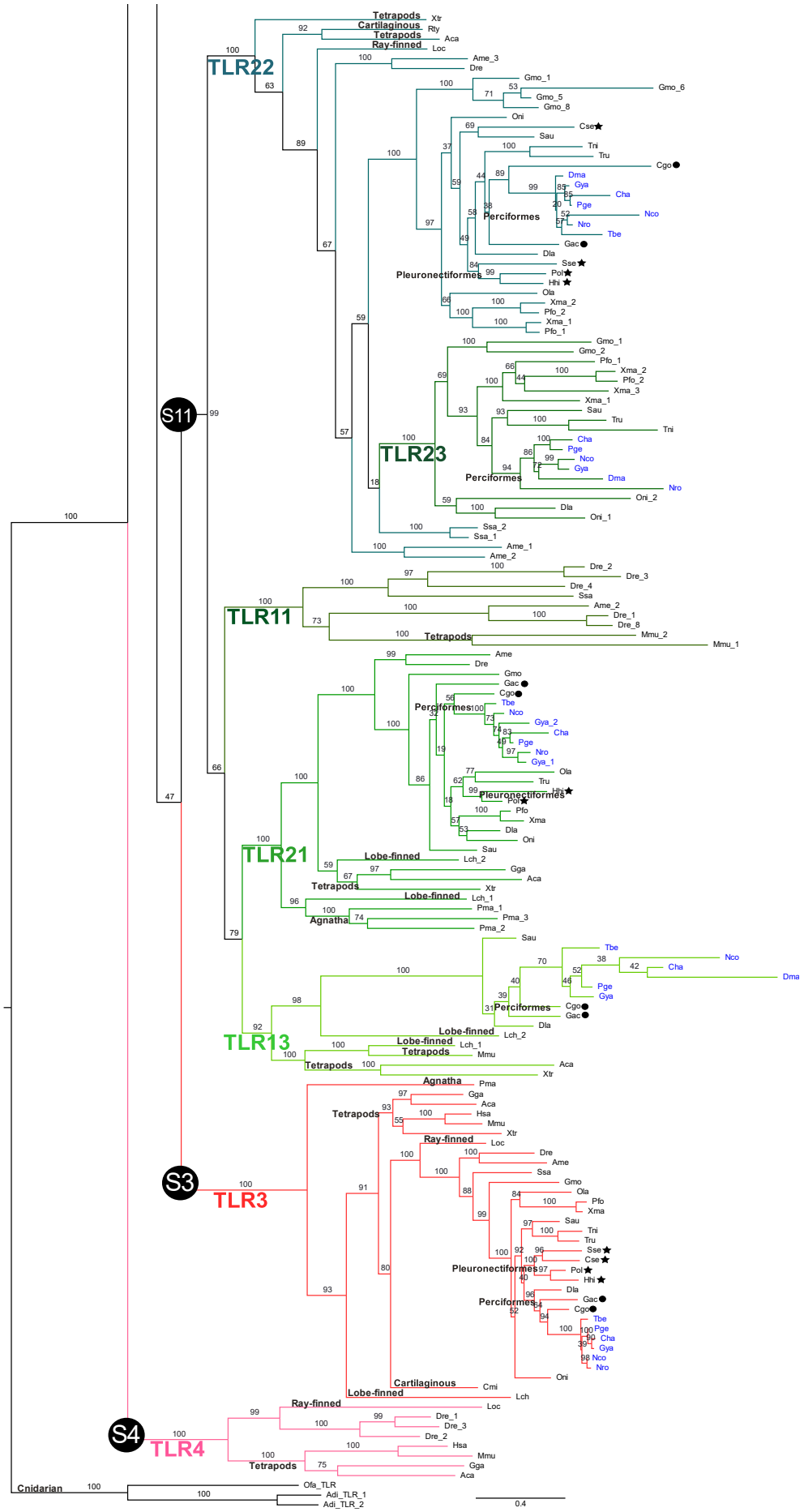
TLR22
TLR23
TLR11
TLR21
TLR13
TLR3
TLR4
S11
S3
S4
Tetrapods
Xtr
Cartilaginous
Rty
Tetrapods
Aca
Ray-finned
Loc
Ame_3
Dre
Gmo_1
Gmo_6
Gmo_5
Gmo_8
Oni
Cse
Sau
Tni
Tru
Cgo
Dma
Gya
Cha
Pge
Nco
Nro
Tbe
Perciformes
Gac
Dla
Sse
Pol
Hhi
Pleuronectiformes
Ola
Xma_2
Pfo_2
Xma_1
Pfo_1
Gmo_2
Xma_3
Oni_2
Oni_1
Ssa_2
Ssa_1
Ame_1
Ame_2
Dre_2
Dre_3
Dre_4
Ssa
Dre_1
Dre_8
Mmu_2
Mmu_1
Ame
Gmo
Gya_2
Gya_1
Lobe-finned
Lch_2
Gga
Lch_1
Pma_1
Pma_3
Pma_2
Agnatha
Mmu
Ray-finned
Loc
Cartilaginous
Cmi
Lch
Hsa
Ofa_TLR
Adi_TLR_1
Adi_TLR_2
Cnidarian
0.4

Supplementary figure 2.2.3. Complete BI phylogenetic tree of Tlrs. Branches of the six vertebrate TLR superfamilies are identified by the corresponding numbers within black circles and with different colours: S1 indicates TLR1 superfamily (orange); S3 for TLR3 superfamily (red); S4 for TLR4 superfamily (pink); S5 for TLR5 superfamily; S7 for TLR7 superfamily (blue) and S11 for TLR11 superfamily (green). Within each superfamily cluster when multiple subfamilies exist, they were coloured with variations of the main representative colour and are also indicated. Accession numbers of the sequences used to construct the tree are available in Supplementary Table 2.2.1. The teleost *tlr2* duplicates were named as *tlr2a* and *tlr2b* and TLR15 were not used as they are only found in chicken and lizard. Tree was rooted with the Cnidarian Tlrs clade (Liu et al., 2019). The sea lamprey tlrs within the vertebrate TLR1, TLR7 and TLR11 superfamilies were named *tlrX*, *tlrY* and *tlrZ*, respectively since their identity assignment for the Tlr subfamilies was not clear. To facilitate their identification the *tlrs* from seven Antarctic species are highlighted in blue, other perciforms are indicated by a black dot and Pleuronectiforms by a black star.

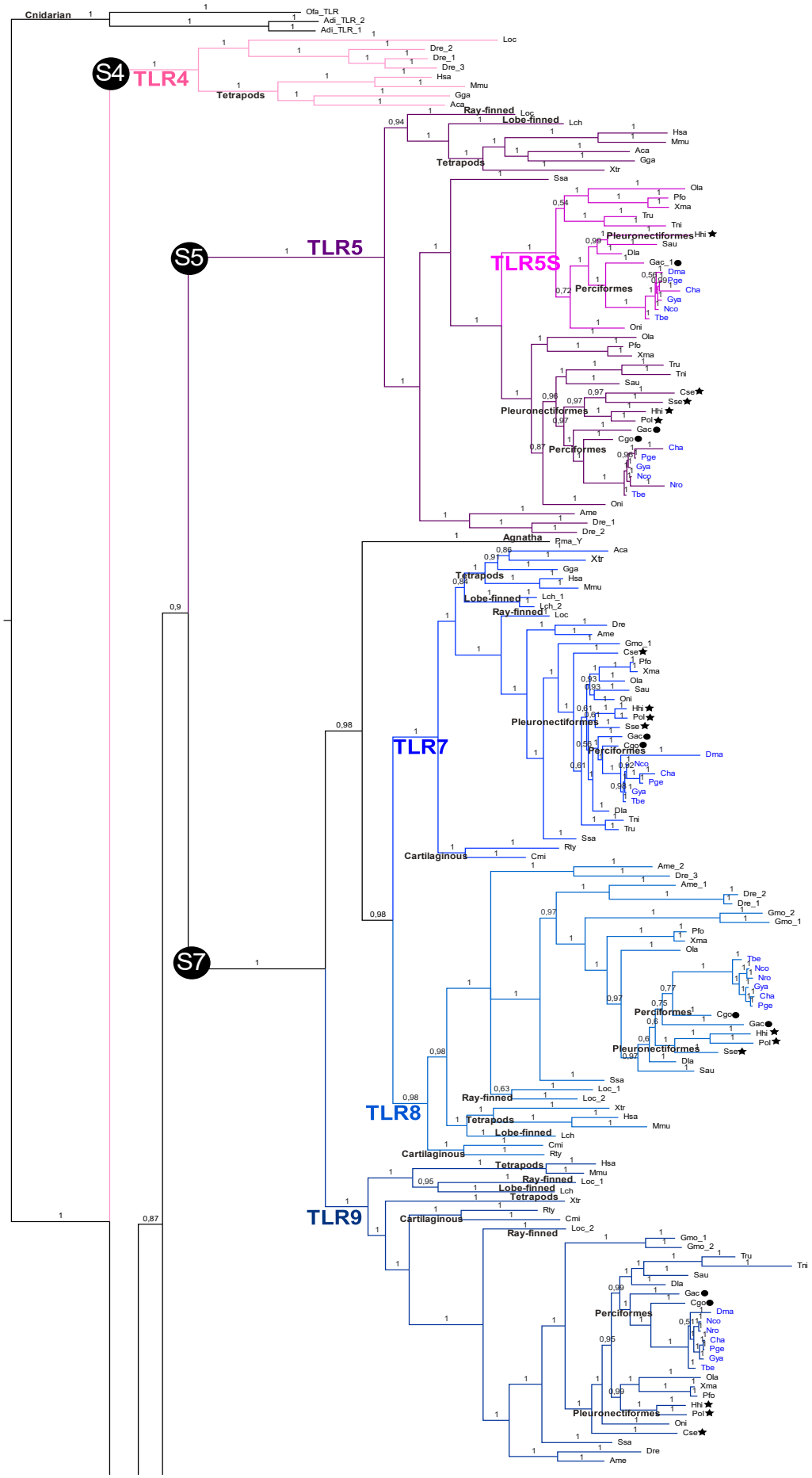
Cnidarian
Ofa_TLR
Adi_TLR_2
Adi_TLR_1
S4
TLR4
Tetrapods
Loc
Dre_2
Dre_1
Dre_3
Hsa
Mmu
Gga
Aca
Ray-finned
Lobe-finned
Lch
Xtr
Ssa
S5
TLR5
TLR5S
Perciformes
Pleuronectiformes
Ola
Pfo
Xma
Tru
Tni
Hhi
Sau
Dla
Gac_1
Dma
Pge
Cha
Gya
Nco
Tbe
Oni
Cse
Sse
Pol
Gac
Cgo
Nro
Ame
Dre_1
Dre_2
Agnatha
Rma_Y
Aca
Xtr
Gga
Hsa
Mmu
Lch_1
Lch_2
Loc
Dre
Ame
Gmo_1
Cse
Pfo
Xma
Ola
Sau
Oni
Hhi
Pol
Sse
Gac
Cgo
Dma
Nco
Cha
Pge
Gya
Tbe
Dla
Tni
Tru
Ssa
Rty
Cartilaginous
Cmi
S7
TLR7
TLR8
TLR9
Ame_2
Dre_3
Ame_1
Dre_2
Dre_1
Gmo_2
Gmo_1
Pfo
Xma
Ola
Tbe
Nco
Nro
Gya
Cha
Pge
Perciformes
Cgo
Gac
Hhi
Pol
Pleuronectiformes
Sse
Dla
Sau
Ssa
Loc_1
Loc_2
Ray-finned
Xtr
Hsa
Mmu
Tetrapods
Lobe-finned
Lch
Cmi
Rty
Cartilaginous
Hsa
Mmu
Ray-finned
Loc_1
Lobe-finned
Lch
Tetrapods
Xtr
Rty
Cmi
Cartilaginous
Loc_2
Ray-finned
Gmo_1
Gmo_2
Tru
Tni
Sau
Dla
Gac
Cgo
Perciformes
Dma
Nco
Nro
Cha
Pge
Gya
Tbe
Ola
Xma
Pfo
Hhi
Pol
Pleuronectiformes
Oni
Cse
Ssa
Dre
Ame

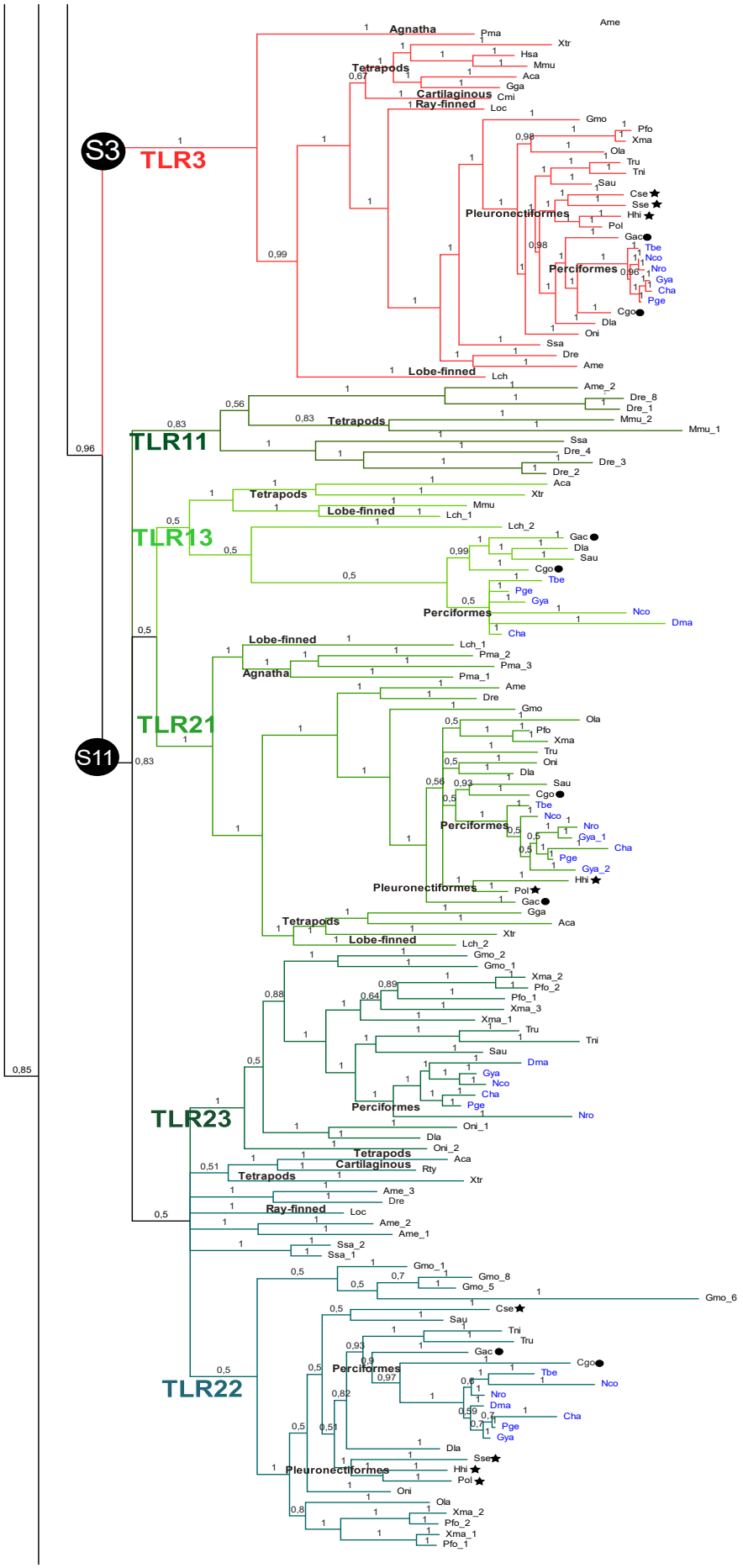
S3
TLR3
Agnatha
Tetrapods
Cartilaginous
Ray-finned
Pleuronectiformes
Perciformes
Lobe-finned
TLR11
TLR13
TLR21
S11
TLR23
TLR22

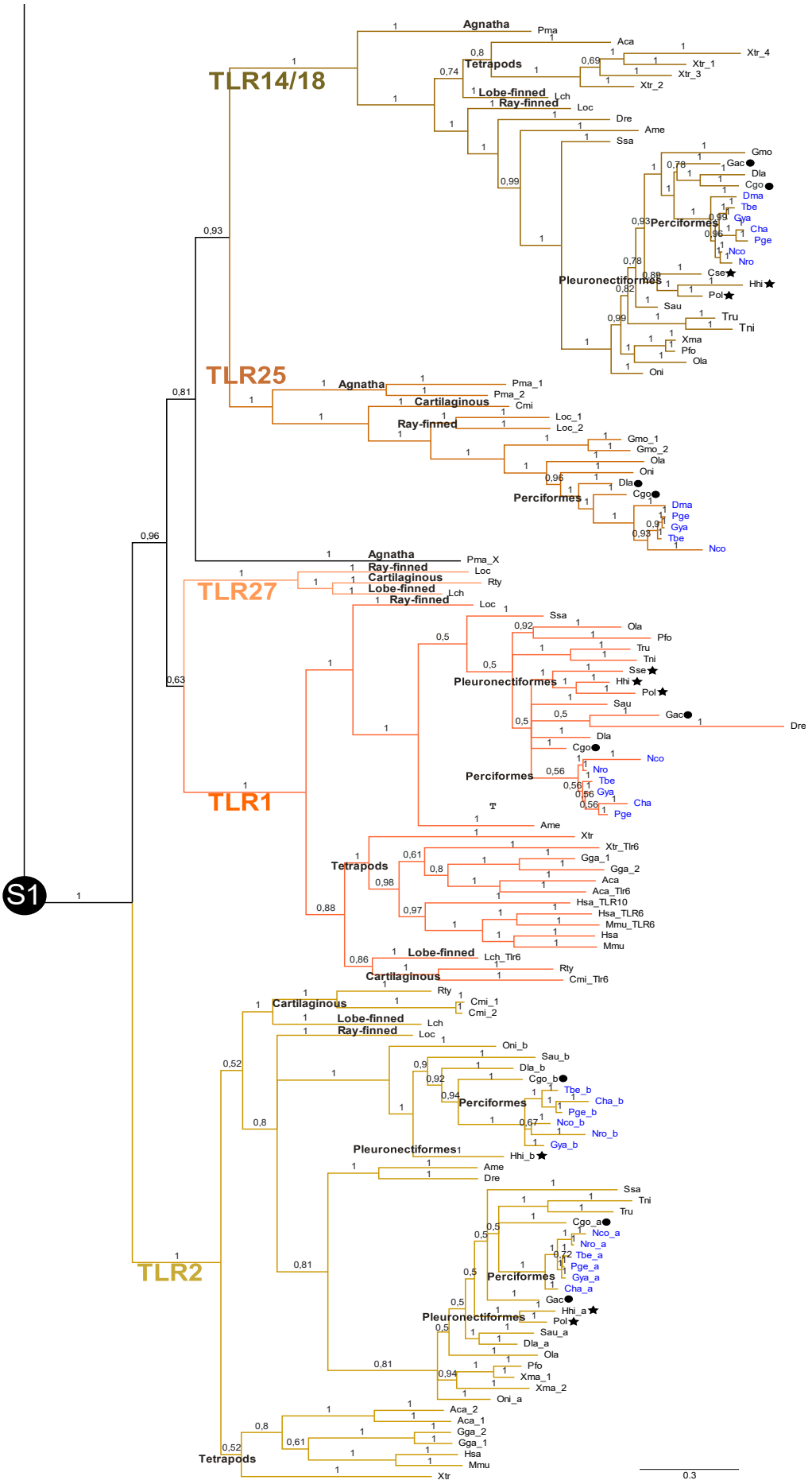
TLR14/18
Agnatha
Pma
Aca
Xtr_4
Tetrapods
Xtr_1
Xtr_3
Xtr_2
Lobe-finned
Lch
Ray-finned
Loc
Dre
Ame
Ssa
Gmo
Gac
Dla
Cgo
Dma
Tbe
Gya
Perciformes
Cha
Pge
Nco
Nro
Pleuronectiformes
Cse
Hhi
Pol
Sau
Tru
Tni
Xma
Pfo
Ola
Oni
TLR25
Agnatha
Pma_1
Pma_2
Cartilaginous
Cmi
Ray-finned
Loc_1
Loc_2
Gmo_1
Gmo_2
Ola
Oni
Dla
Perciformes
Cgo
Dma
Pge
Gya
Tbe
Nco
TLR27
Agnatha
Pma_X
Ray-finned
Loc
Cartilaginous
Rty
Lobe-finned
Lch
Ray-finned
Loc
Ssa
Ola
Pfo
Tru
Tni
Pleuronectiformes
Sse
Hhi
Pol
Sau
Gac
Dre
Dla
Cgo
Nco
Perciformes
Nro
Tbe
Gya
Cha
Pge
T
Ame
Xtr
Xtr_Tlr6
Gga_1
Gga_2
Aca
Aca_Tlr6
Hsa_TLR10
Hsa_TLR6
Mmu_TLR6
Hsa
Mmu
TLR1
Tetrapods
Lobe-finned
Lch_Tlr6
Rty
Cartilaginous
Cmi_Tlr6
S1
Rty
Cmi_1
Cmi_2
Cartilaginous
Lobe-finned
Lch
Ray-finned
Loc
Oni_b
Sau_b
Dla_b
Cgo_b
Tbe_b
Cha_b
Perciformes
Pge_b
Nco_b
Nro_b
Gya_b
Pleuronectiformes
Hhi_b
Ame
Dre
Ssa
Tni
Tru
Cgo_a
Nco_a
Nro_a
Tbe_a
Pge_a
Gya_a
Perciformes
Cha_a
Gac
Hhi_a
Pol
Pleuronectiformes
Sau_a
Dla_a
Ola
Pfo
Xma_1
Xma_2
Oni_a
TLR2
Aca_2
Aca_1
Gga_2
Gga_1
Hsa
Mmu
Tetrapods
Xtr
0.3

Supplementary figure 2.2.4. Multiple sequence alignments and sequence annotation of the Nototheniidae TLR1 superfamily members. A) Tlr1, B) Tlr2_a, C) Tlr2_b, D) Tlr14/18, E) Tlr25. Leucine-rich repeat (LRR) are highlighted in yellow and the consensus LRR motifs (LxxLxLxxNxL) is marked in bold; Transmembrane (TM) domain is highlighted in blue and Toll/IL-1 receptor (TIR) is marked in green. Protein domains were predicted using SMART, ScanProsite and TMHMM webservers and by sequence homology. The protein signal-peptide when predicted are highlighted in pink and amino acids coloured in red were found to be under positive selective pressure.

a)

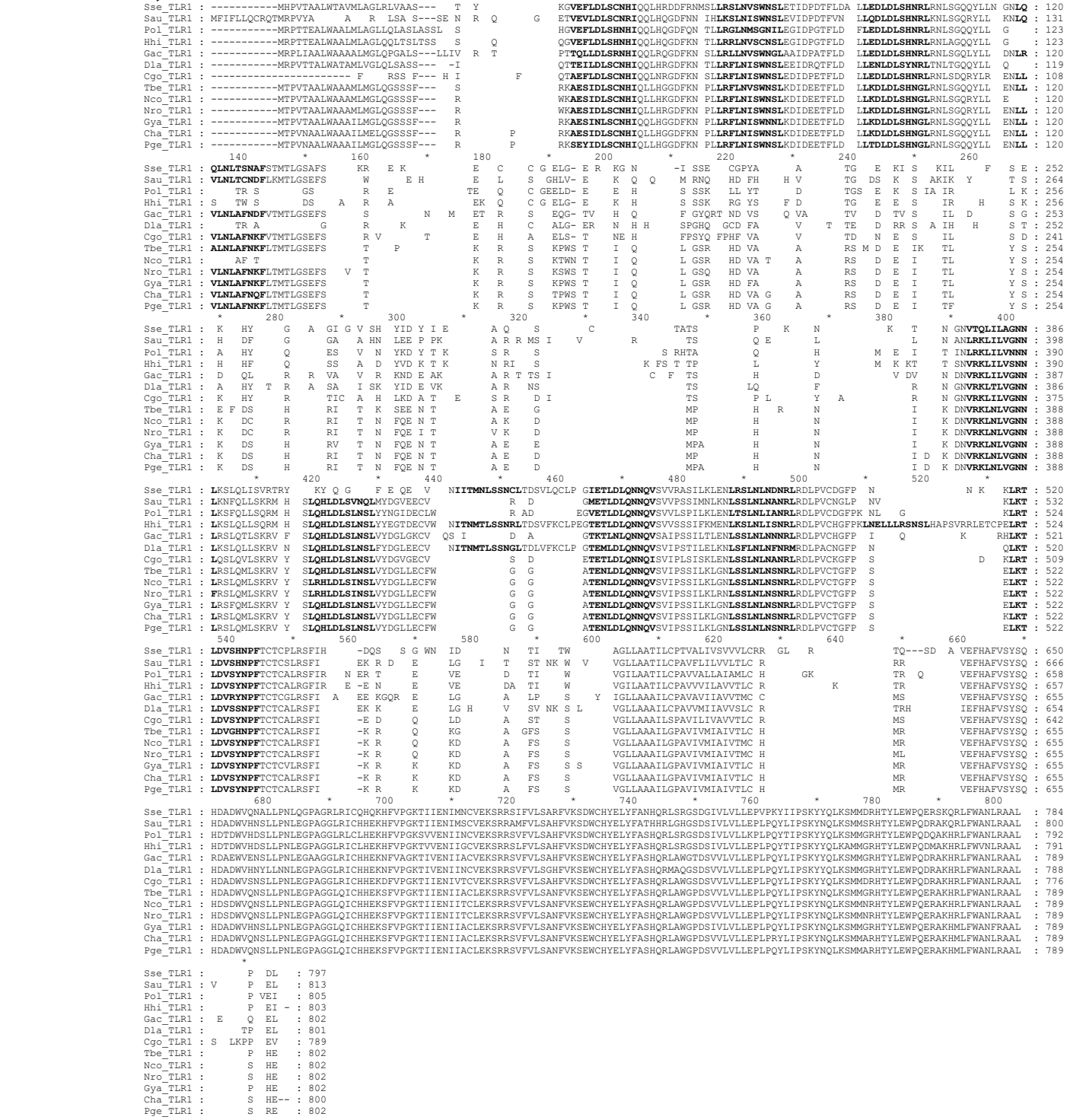

b)

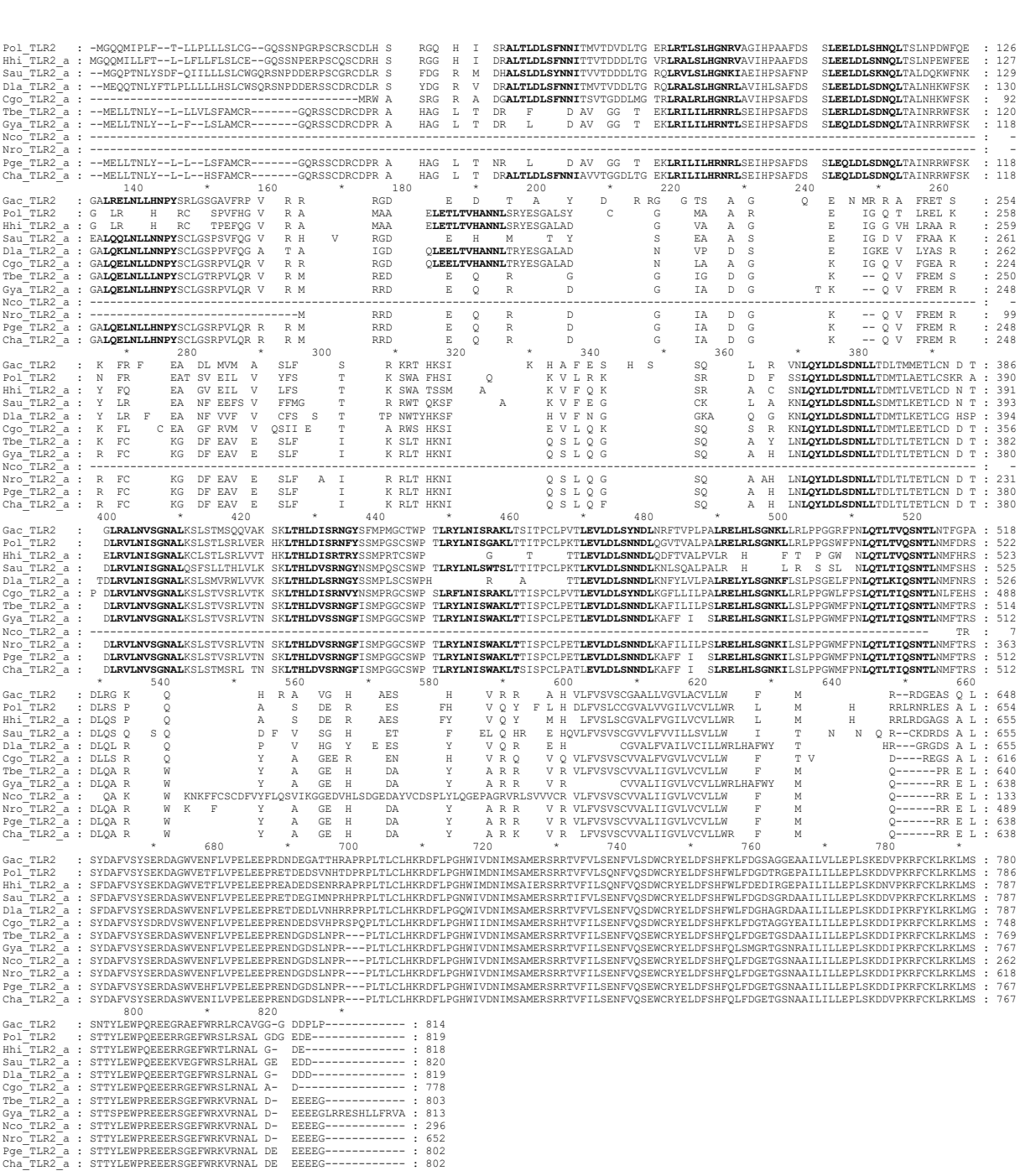

c)

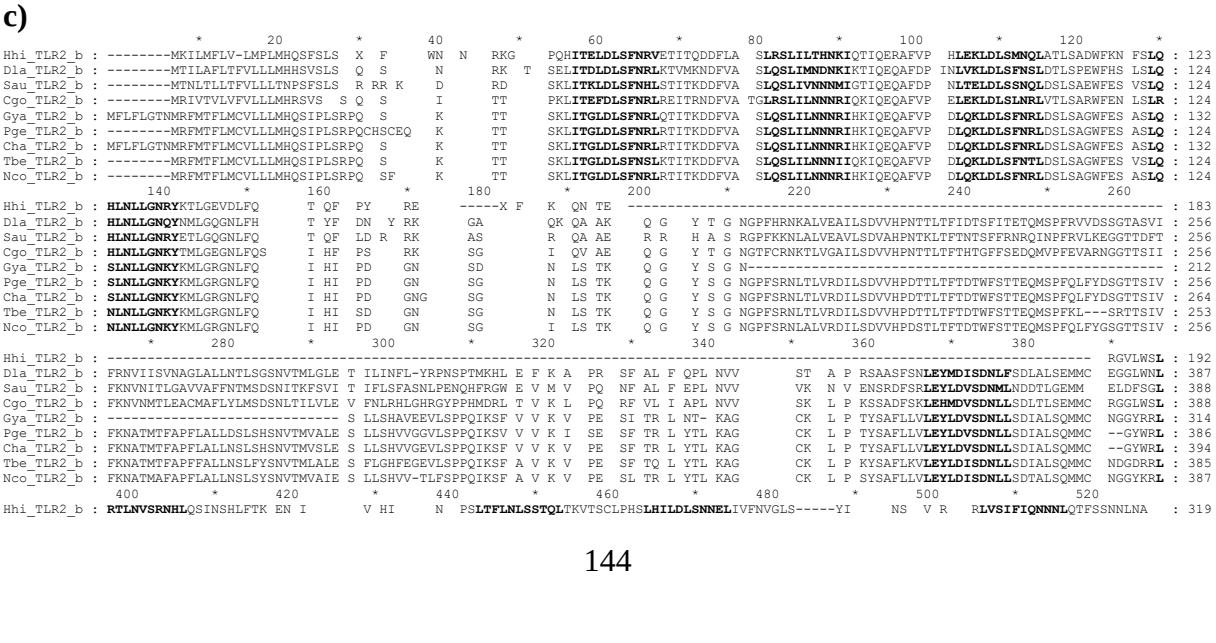

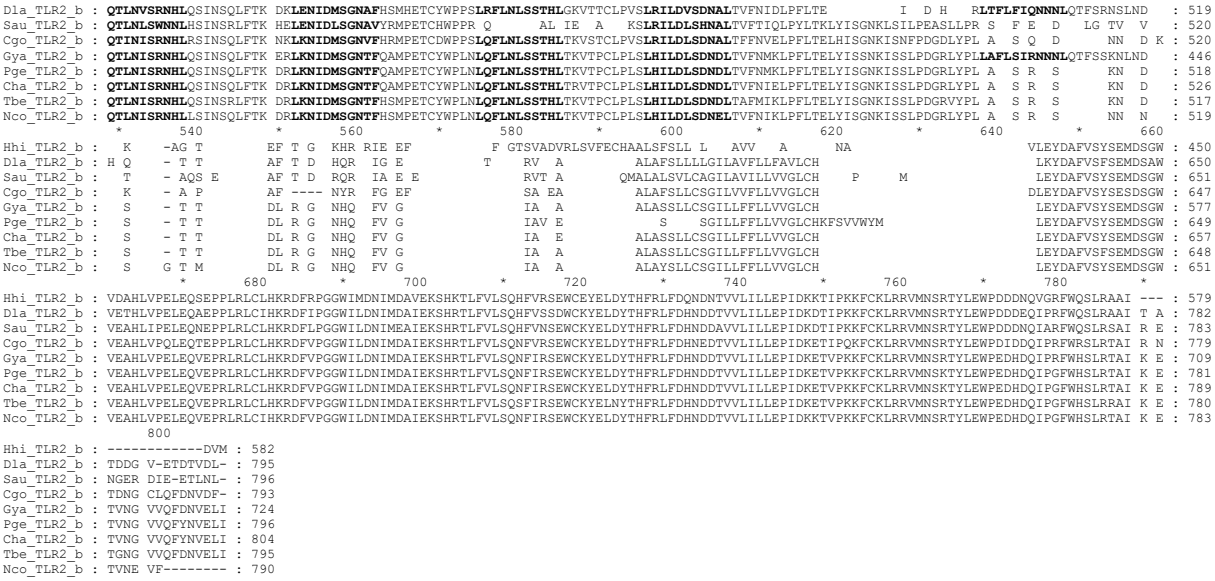

d)

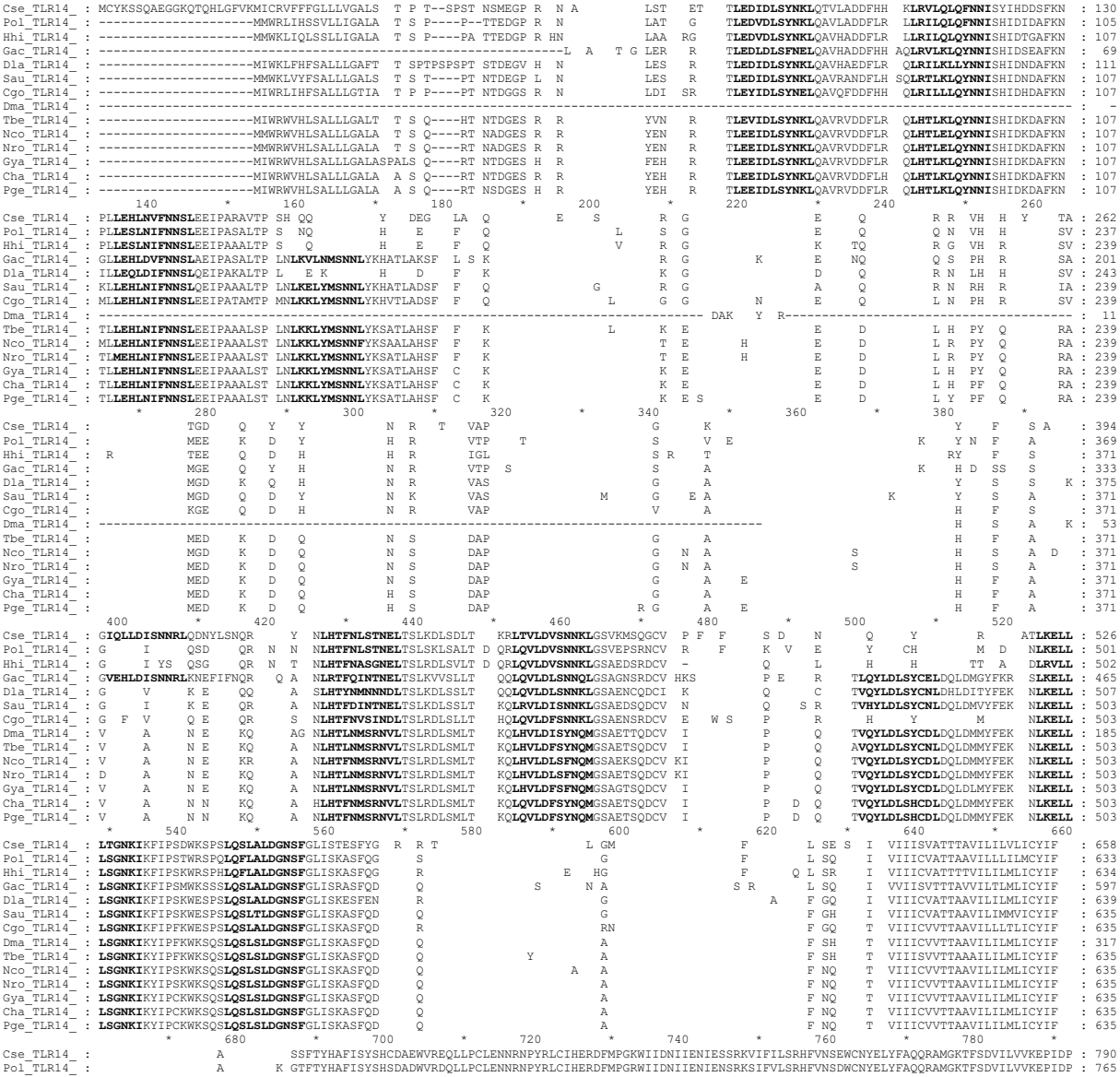

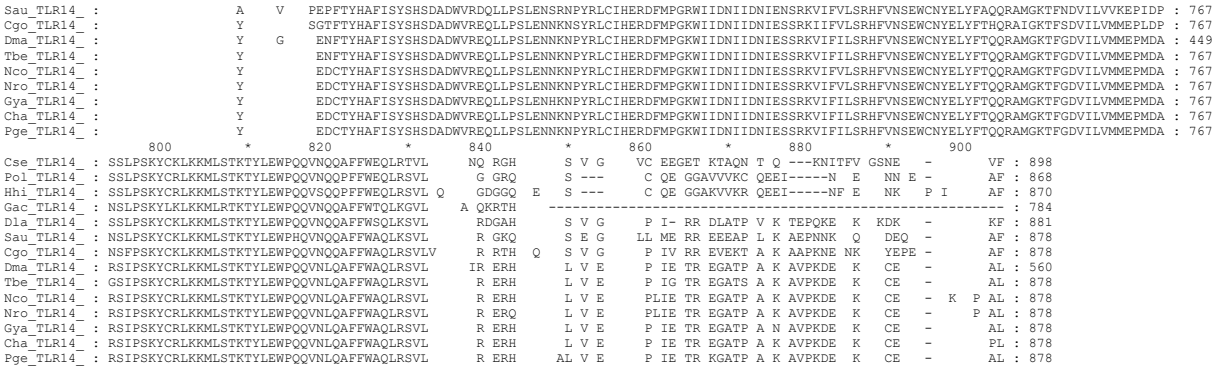

e)

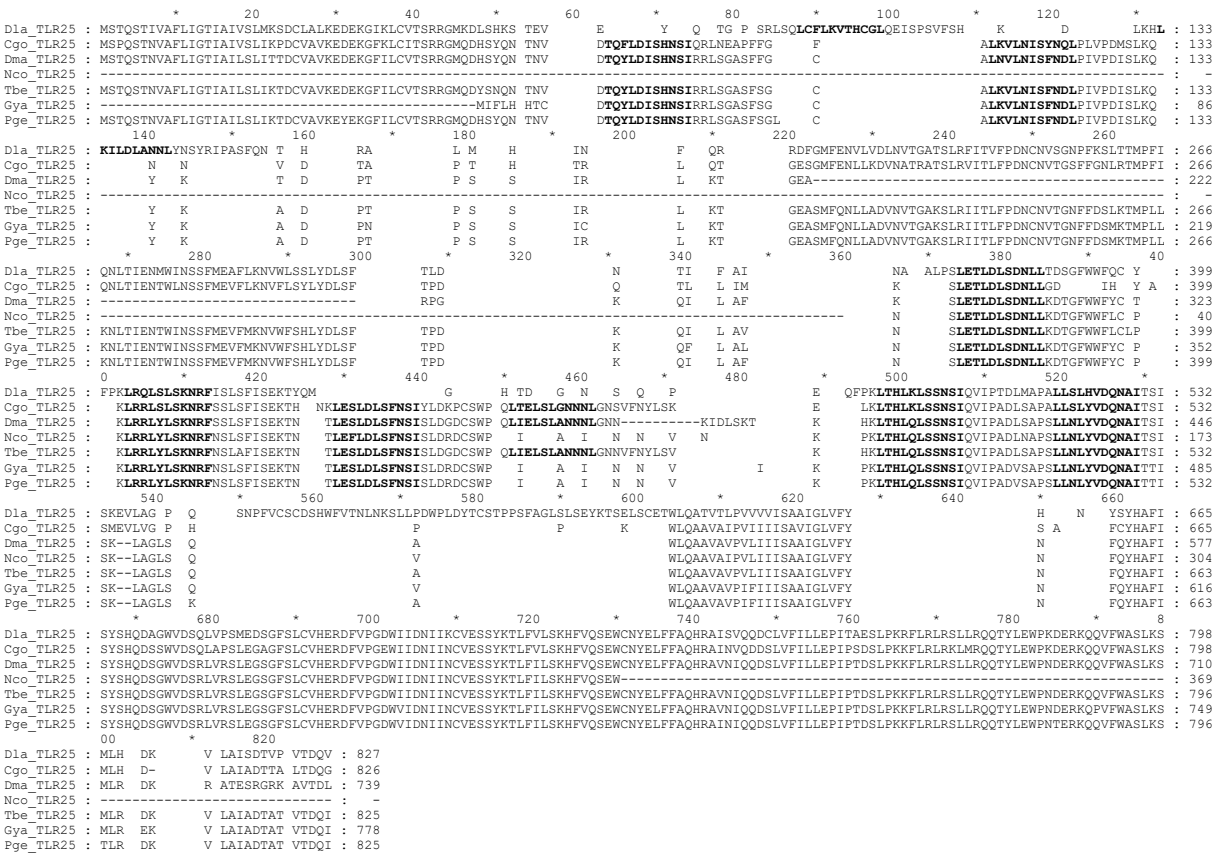

Supplementary figure 2.2.5. Multiple sequence alignments and sequence annotation of the Notothenioidae TLR3 superfamily members. Leucine-rich repeat (LRR) are highlighted in yellow and the consensus LRR motifs (LxxLxLxxNxL) is marked in bold; Transmembrane (TM) domain is highlighted in blue and Toll/IL-1 receptor (TIR) is marked in green. Protein domains were predicted using SMART, ScanProsite and TMHMM webservers. The protein signal-peptide when predicted are highlighted in pink. Amino acids coloured in red were found to be under positive selective pressure.

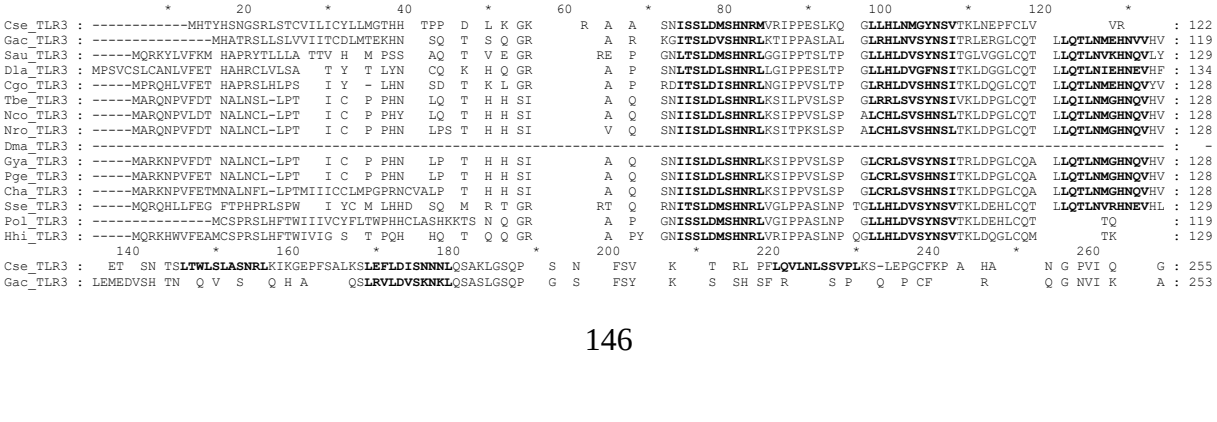

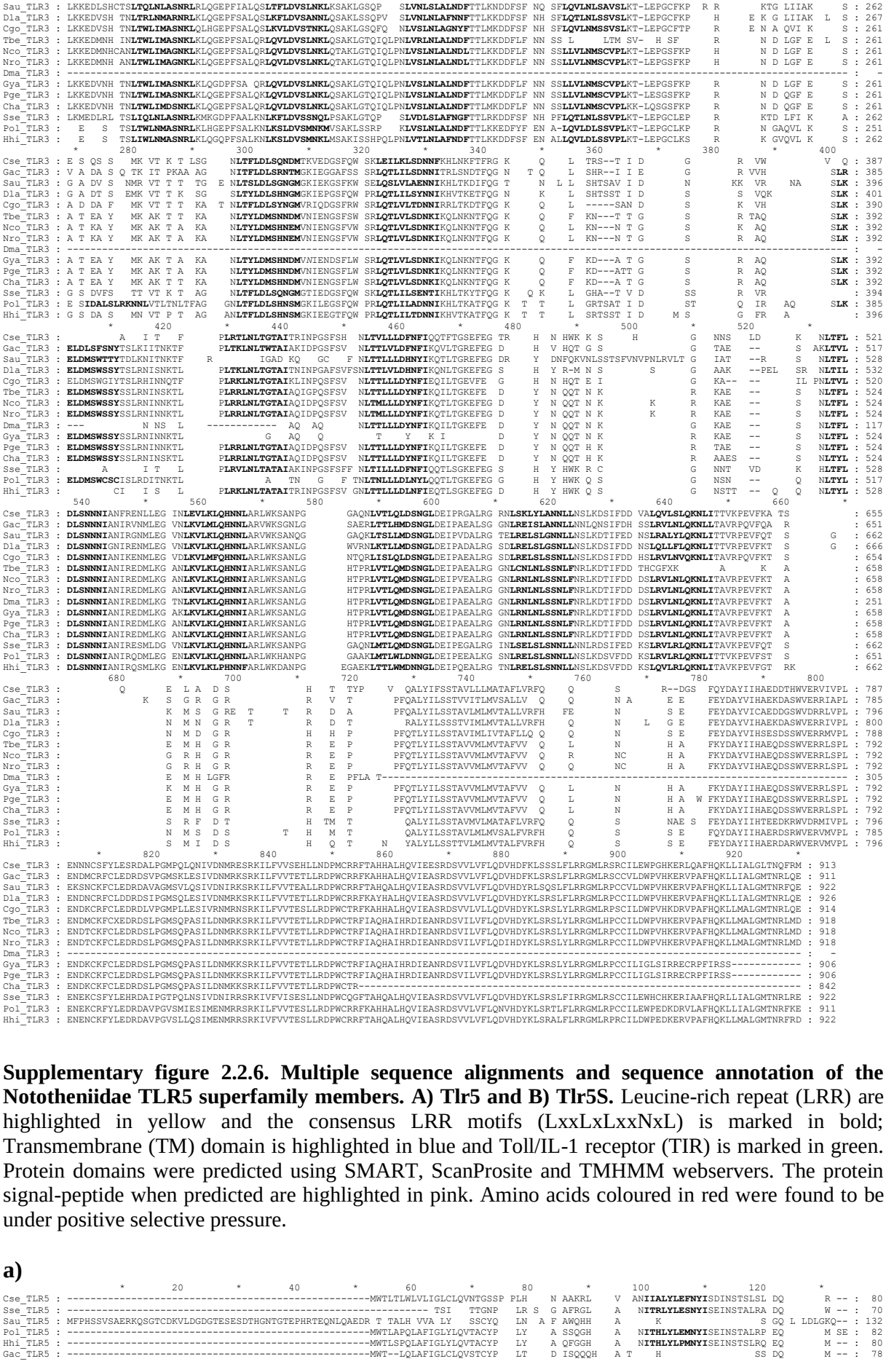

Supplementary figure 2.2.6. Multiple sequence alignments and sequence annotation of the Nototheniidae TLR5 superfamily members. A) Tlr5 and B) Tlr5S. Leucine-rich repeat (LRR) are highlighted in yellow and the consensus LRR motifs (LxxLxLxxNxL) is marked in bold; Transmembrane (TM) domain is highlighted in blue and Toll/IL-1 receptor (TIR) is marked in green. Protein domains were predicted using SMART, ScanProsite and TMHMM webservers. The protein signal-peptide when predicted are highlighted in pink. Amino acids coloured in red were found to be under positive selective pressure.

a)

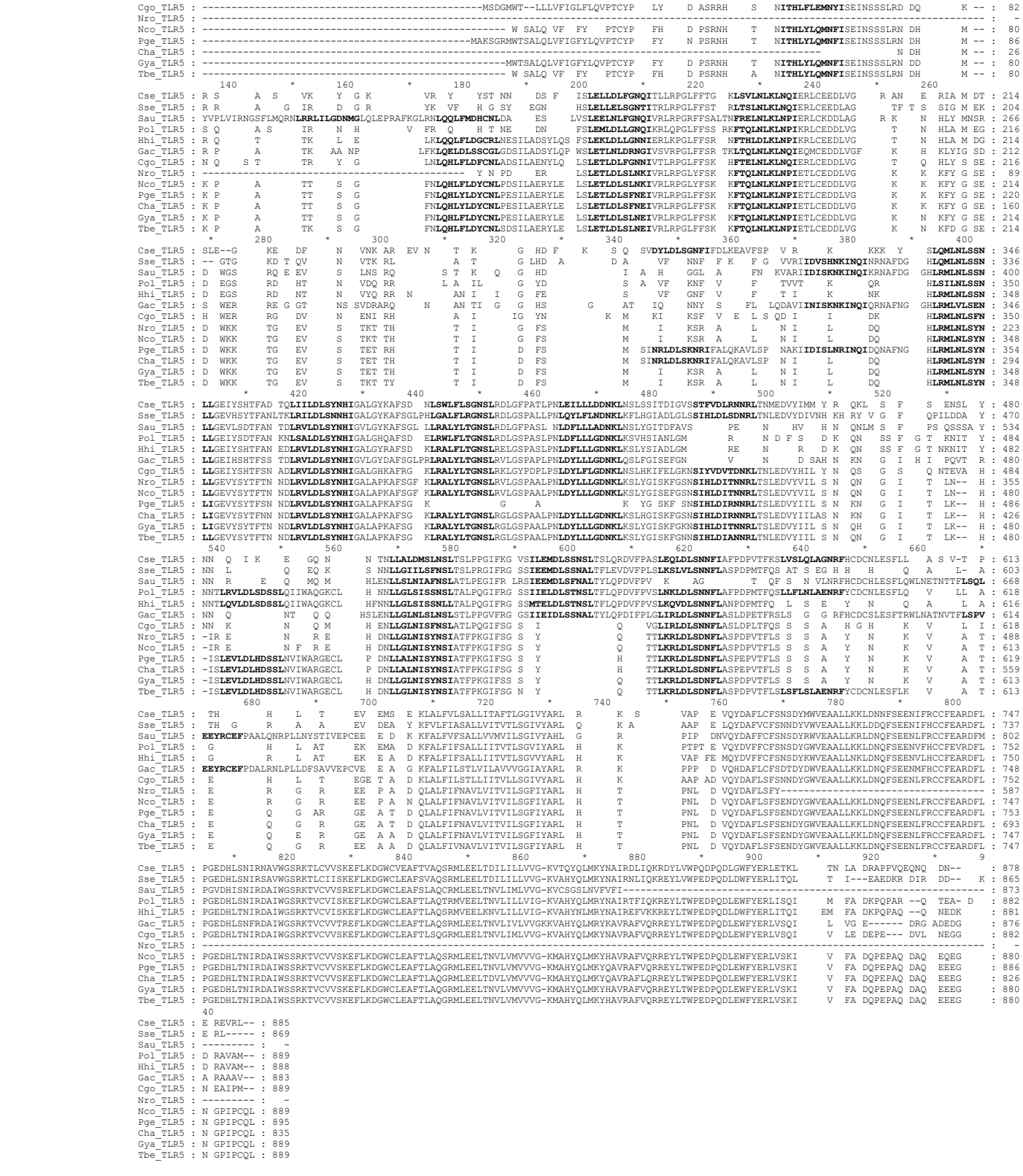

b)

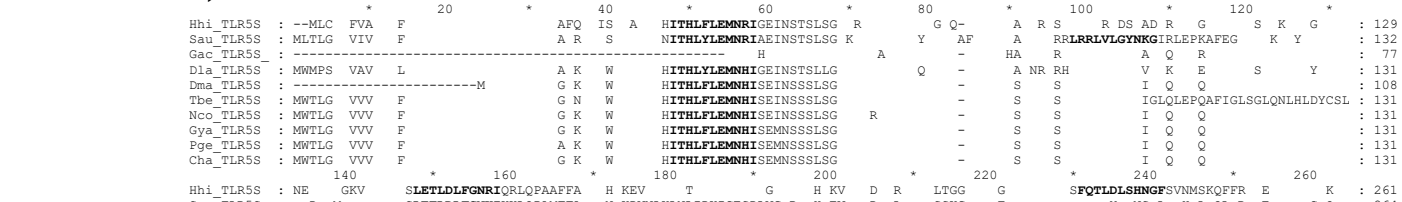

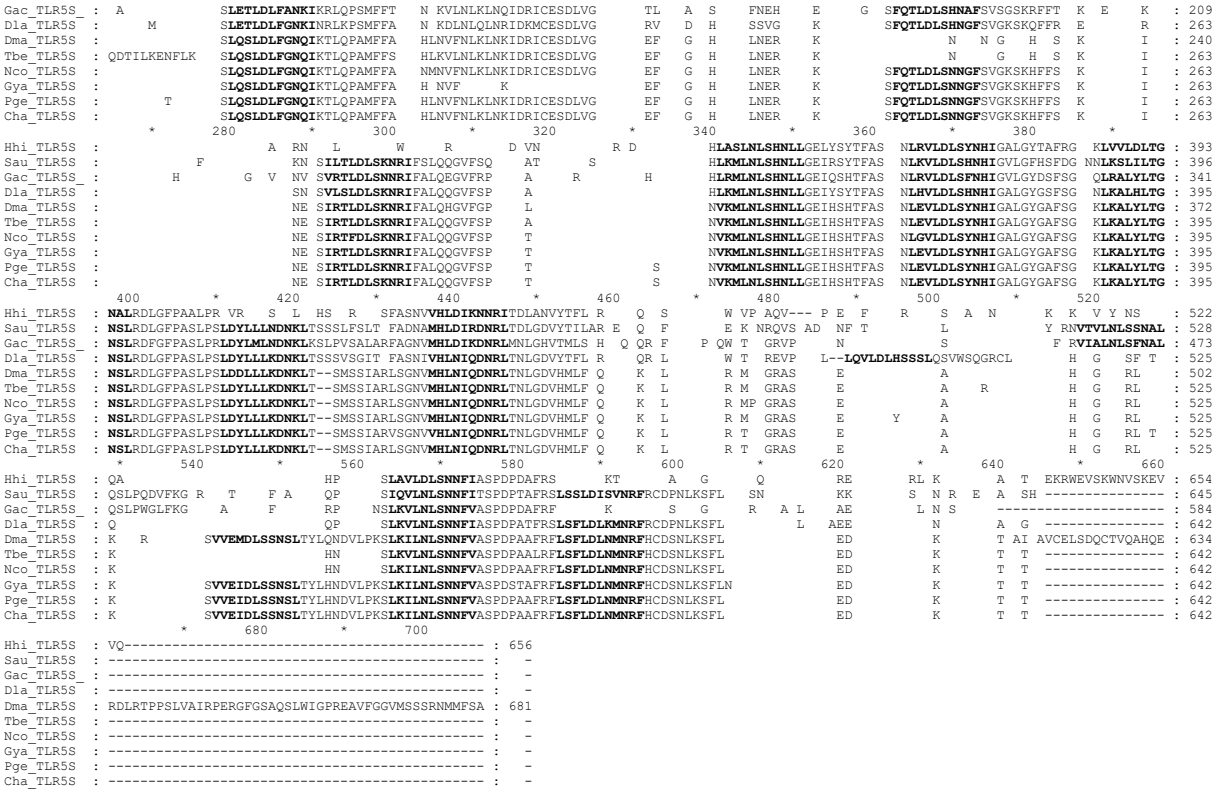

Supplementary figure 2.2.7. Multiple sequence alignments and sequence annotation of the Nototheniidae TLR7 superfamily members. A) Tlr7, B) Tlr8 and C) Tlr9. Leucine-rich repeat (LRR) are highlighted in yellow and the consensus LRR motifs (LxxLxLxxNxL) is marked in bold; Transmembrane (TM) domain is highlighted in blue and Toll/IL-1 receptor (TIR) is marked in green. Protein domains were predicted using SMART, ScanProsite and TMHMM webservers. The protein signal-peptide when predicted are highlighted in pink. Amino acids coloured in red were found to be under positive selective pressure.

a)

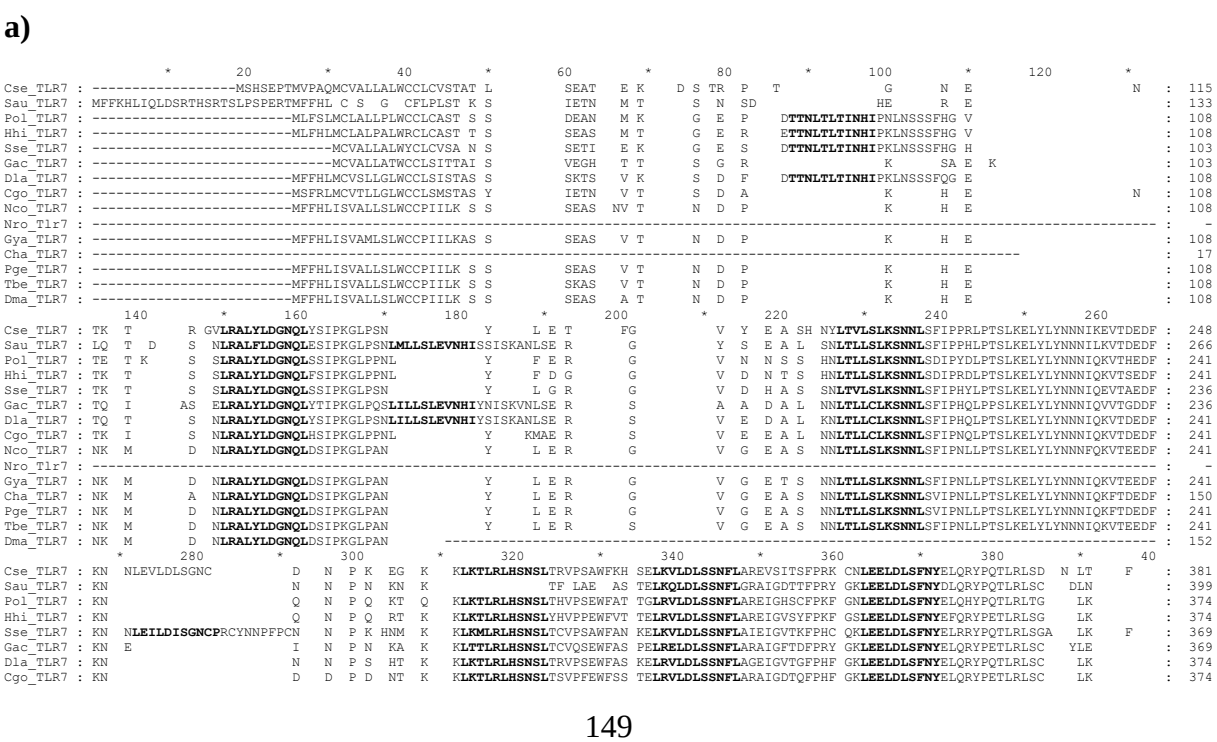

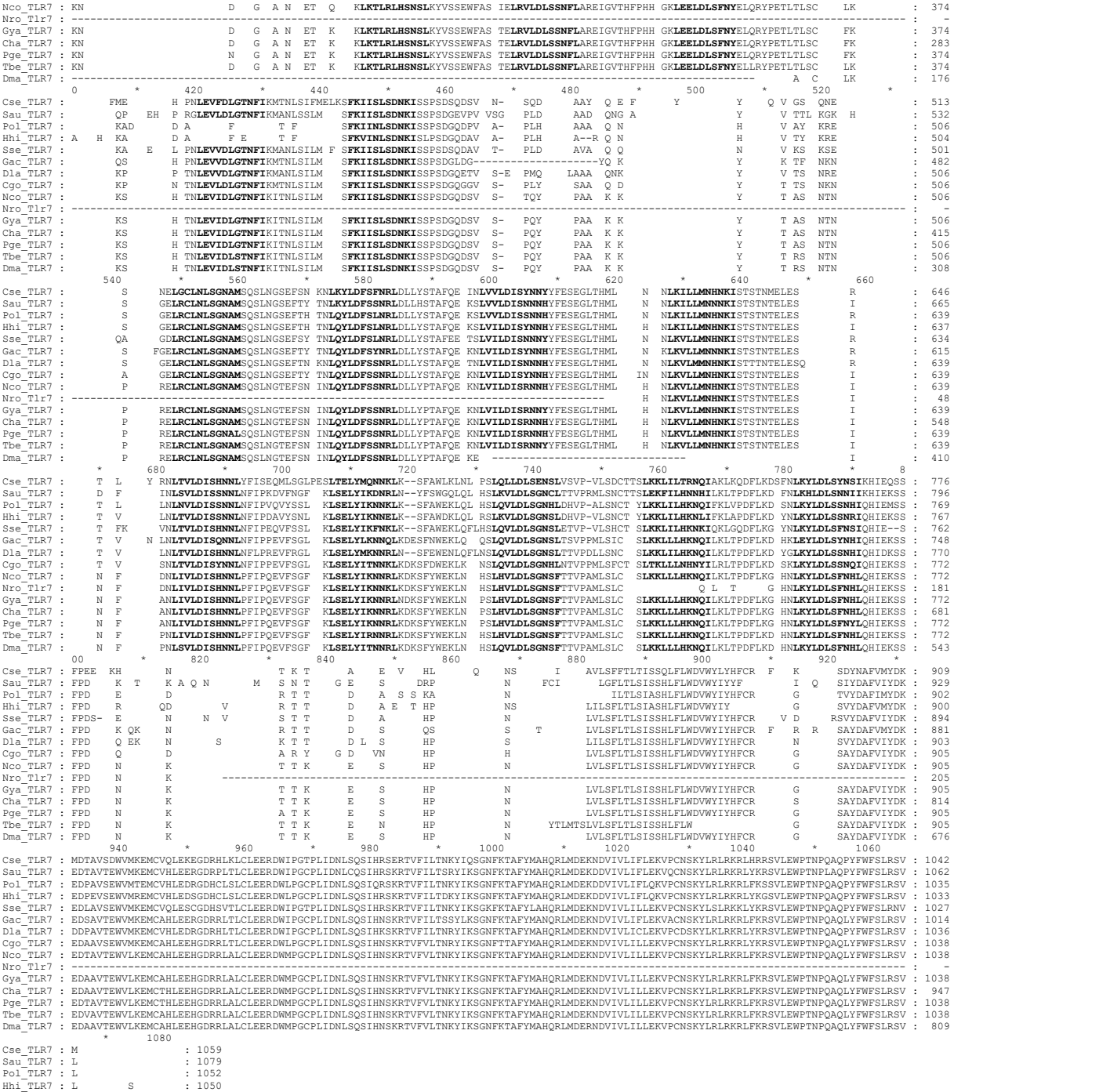

b)

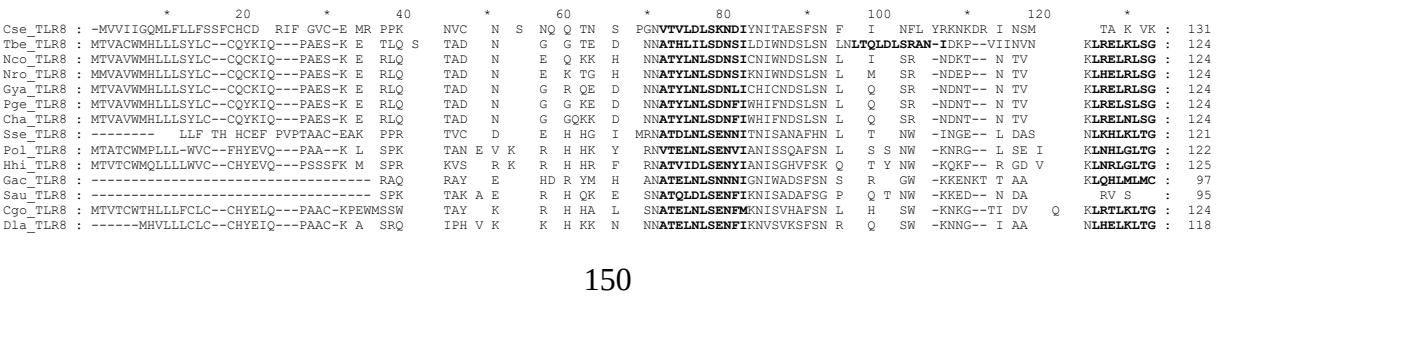

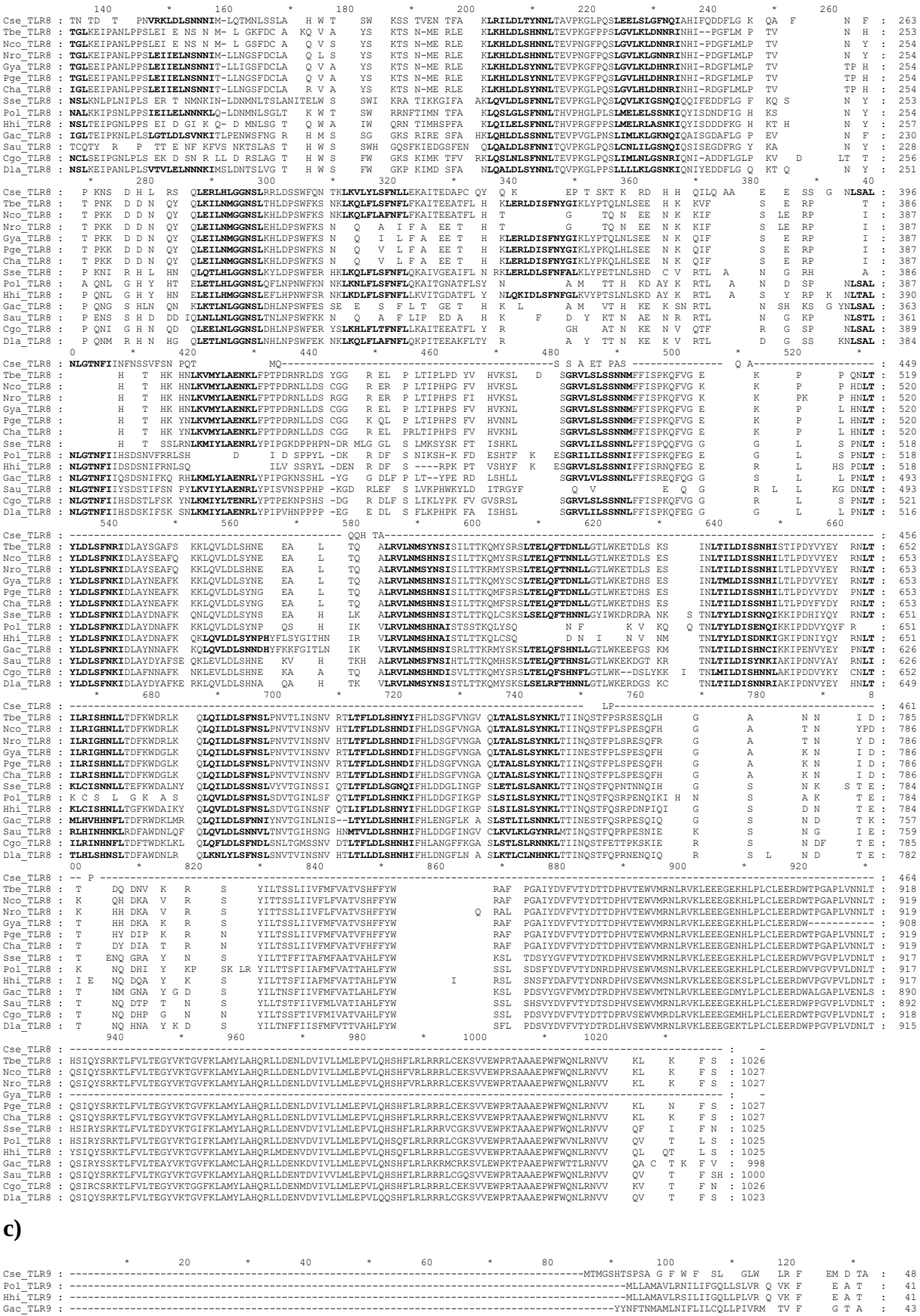

c)

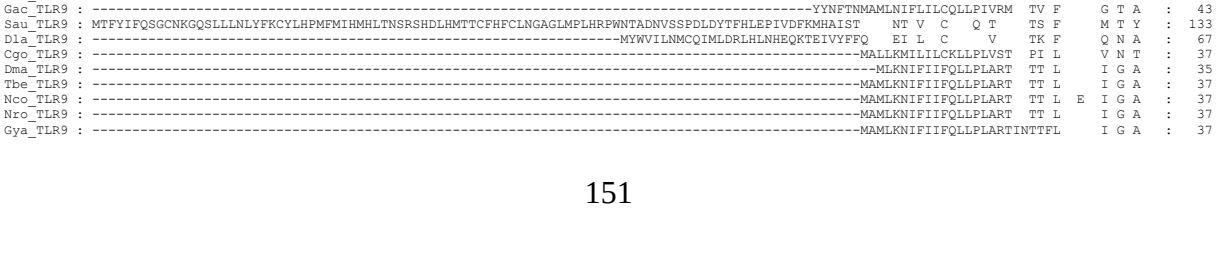

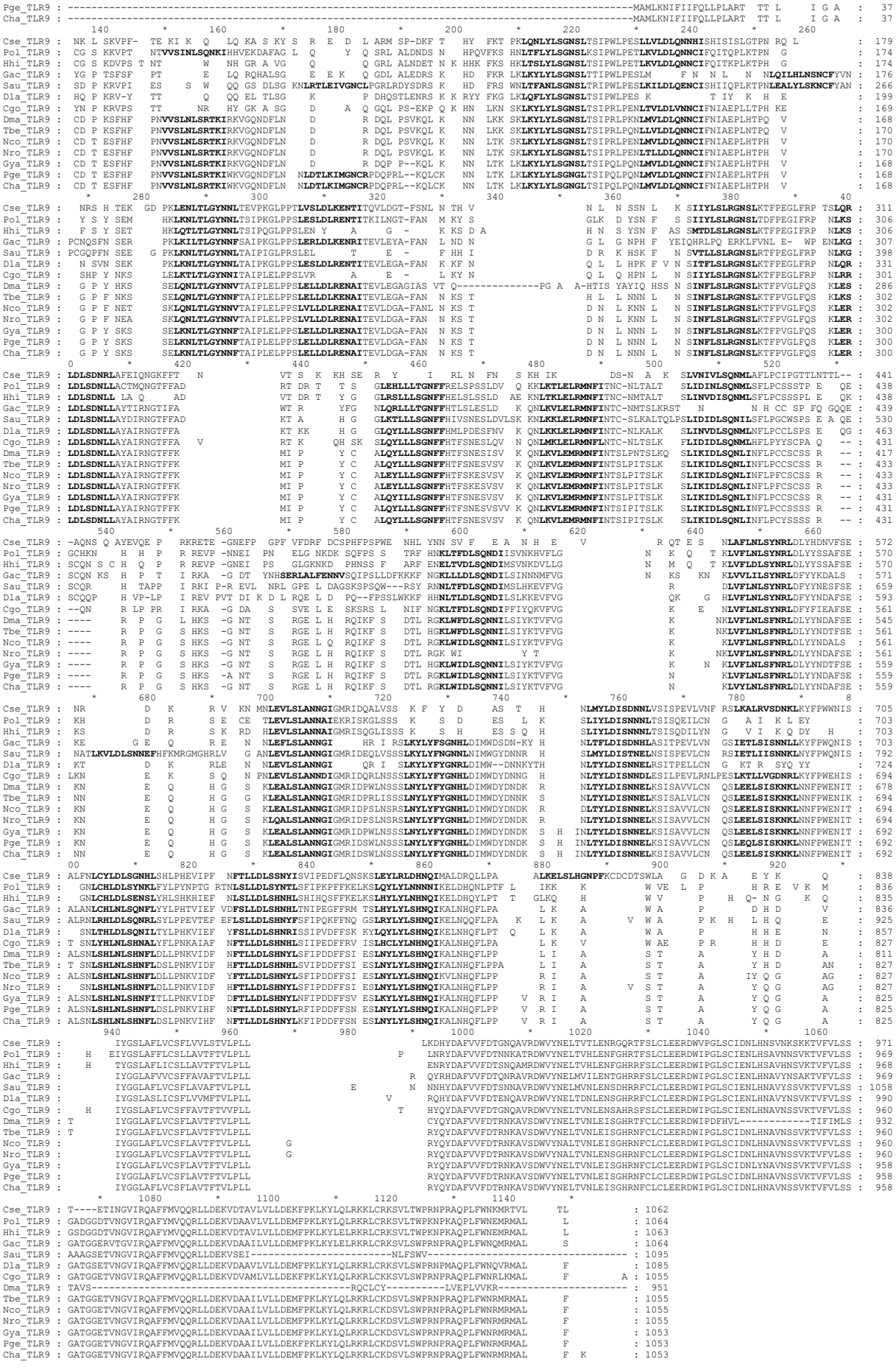

Supplementary figure 2.2.8. Multiple sequence alignments and sequence annotation of the Nototheniidae TLR11 superfamily members. A) Tlr13, B) Tlr21, C) Tlr22 and D) Tlr23. Leucine-rich repeat (LRR) are highlighted in yellow and the consensus LRR motifs (LxxLxLxxNxL) is marked in bold; Transmembrane (TM) domain is highlighted in blue and Toll/IL-1 receptor (TIR) is marked in green. Protein domains were predicted using SMART, ScanProsite and TMHMM webservers. The protein signal-peptide when predicted are highlighted in pink. Amino acids coloured in red were found to be under positive selective pressure.

a)

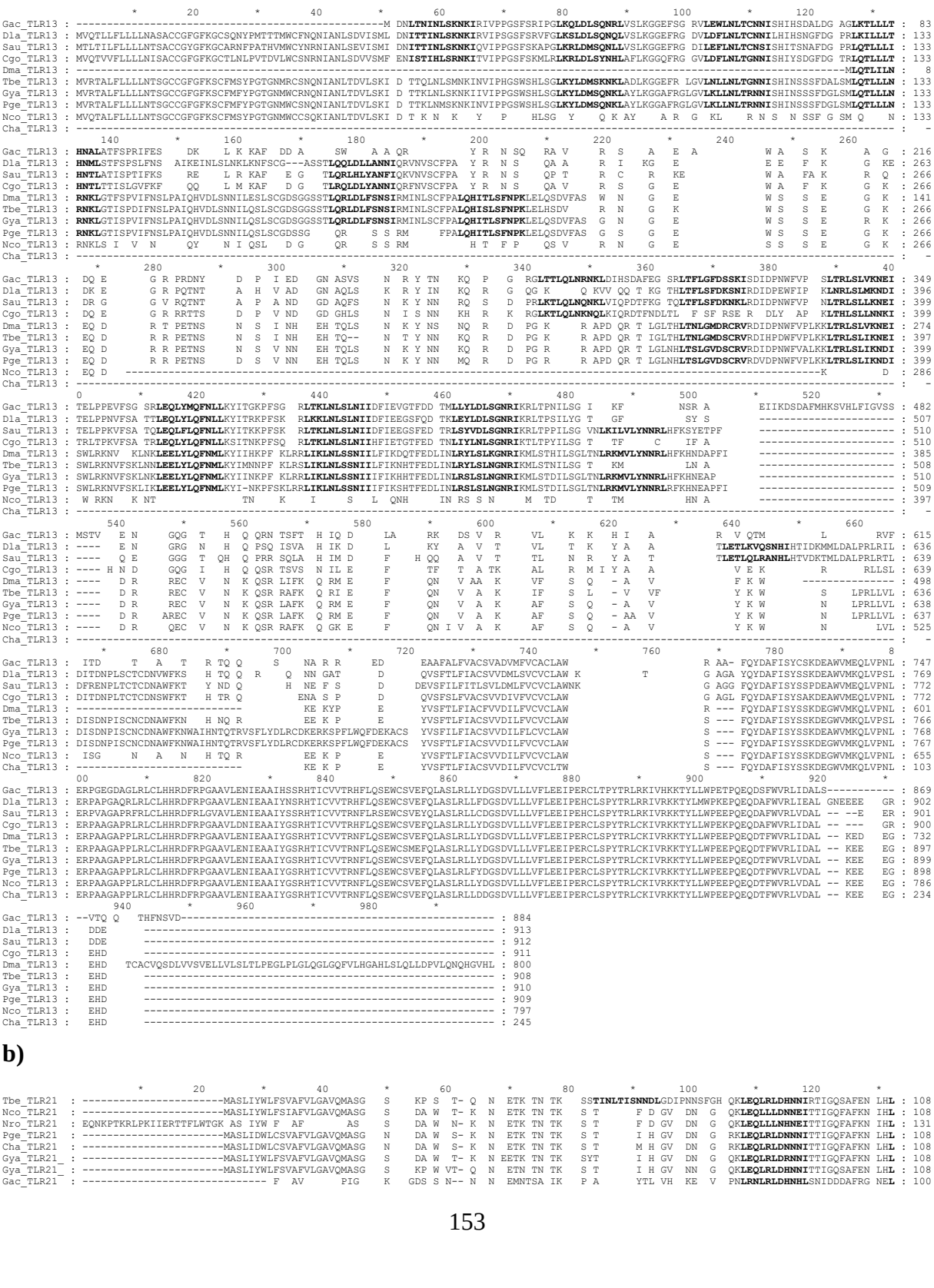

b)

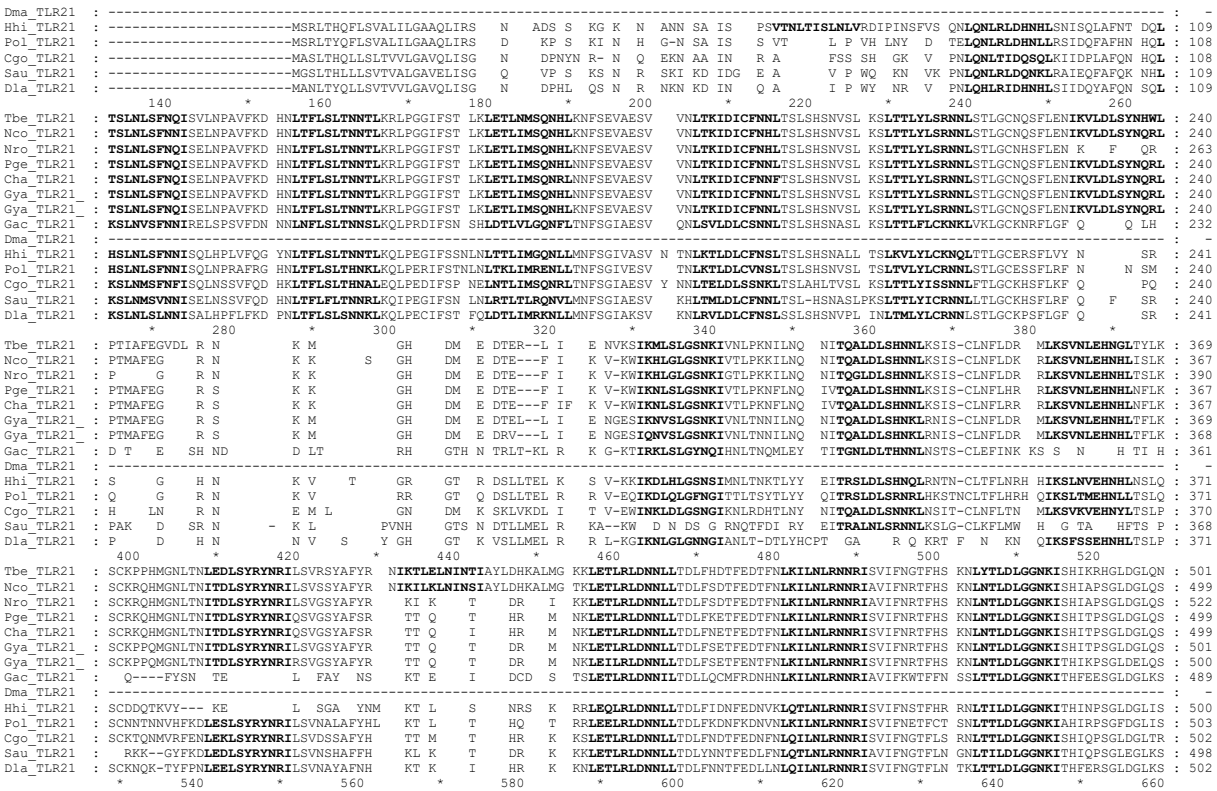

c)

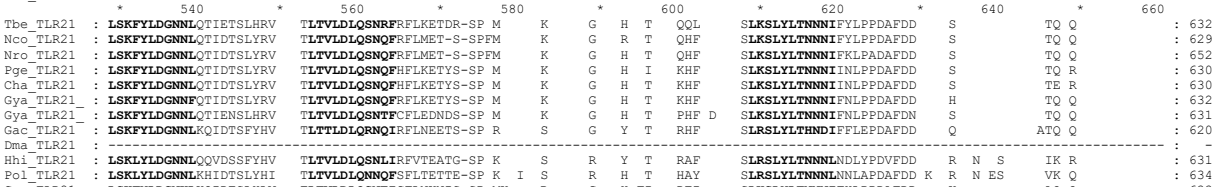

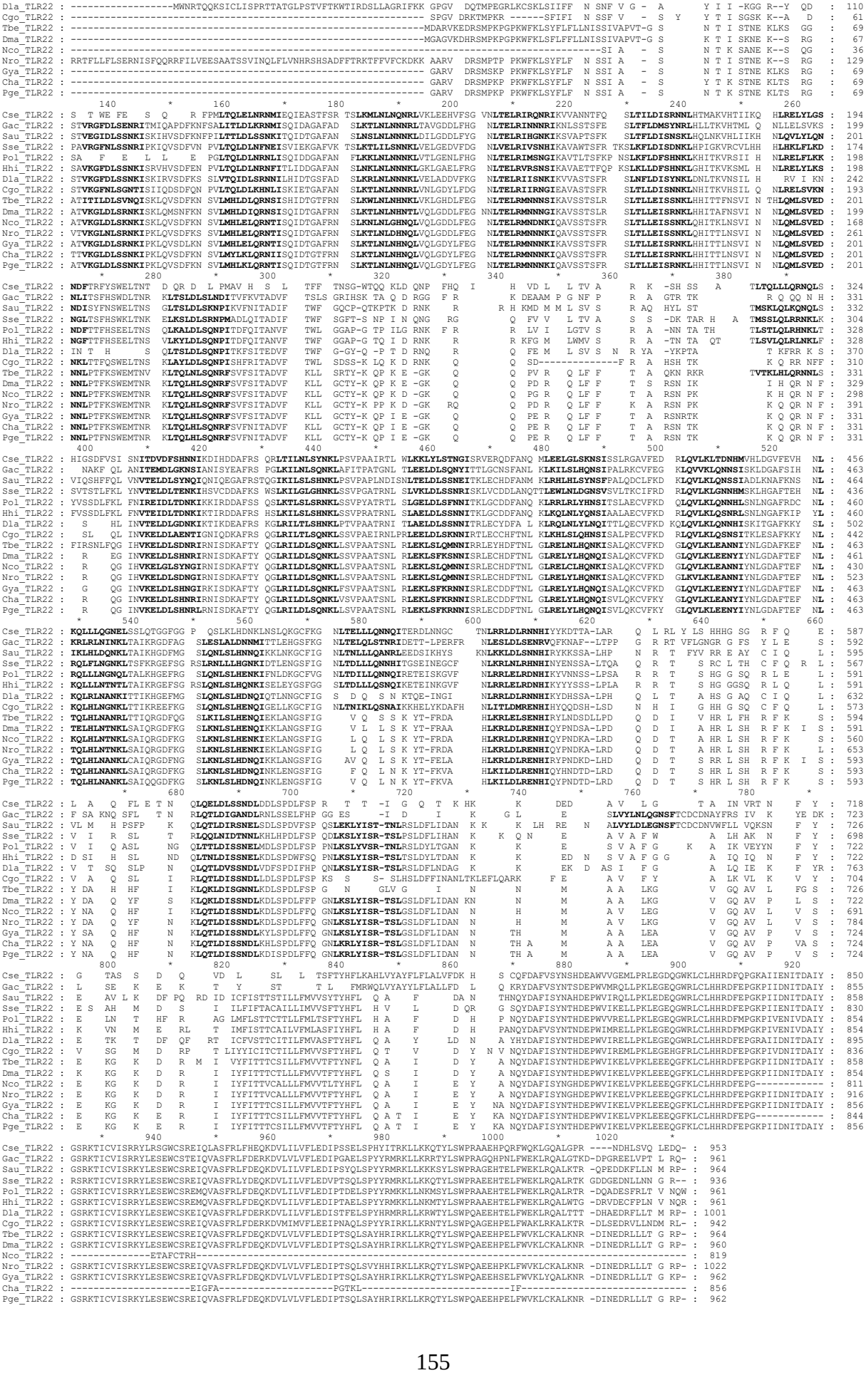

d)

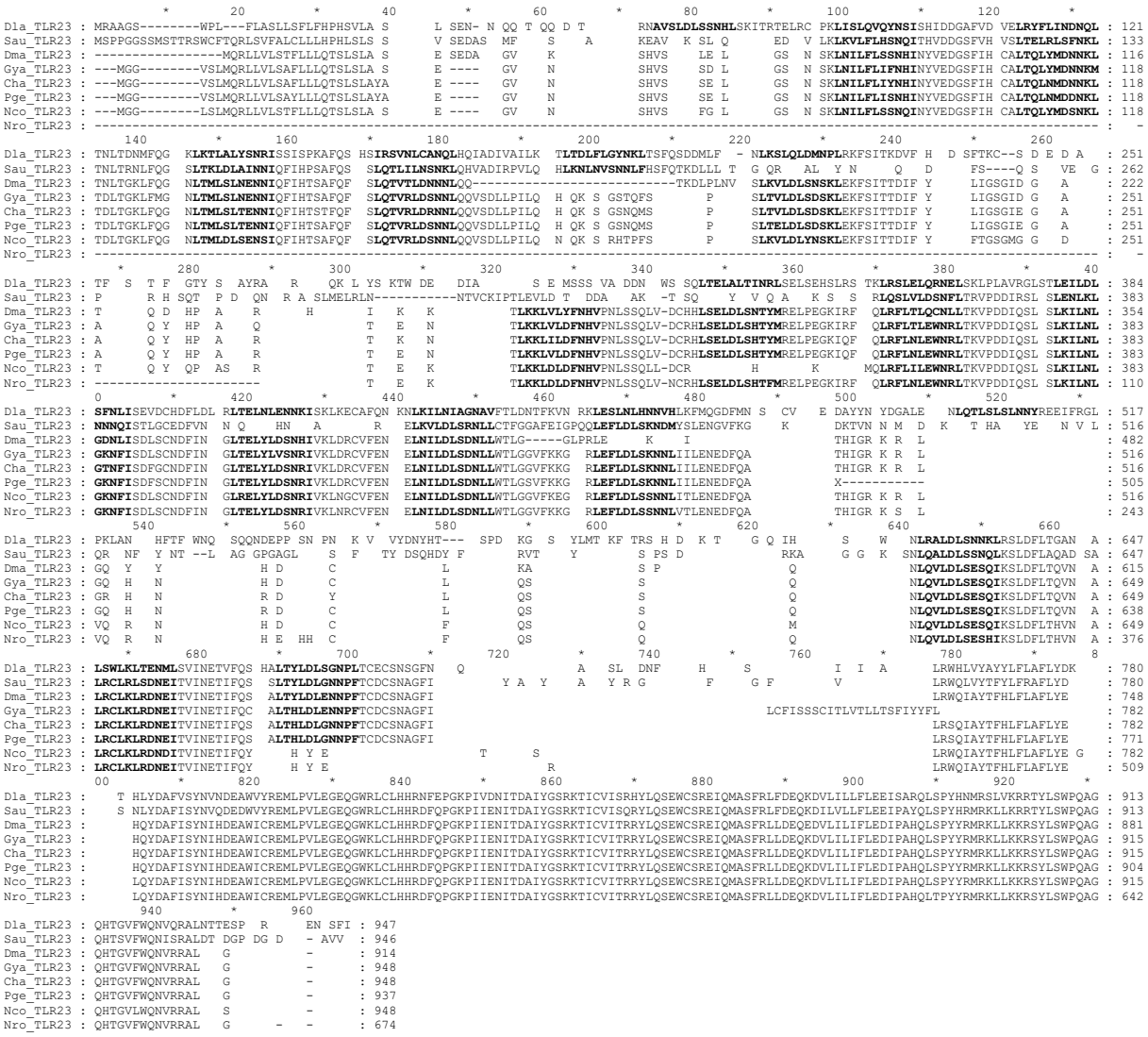

CHAPTER 3

Transcriptomic profiling of immune tissues in *Notothenia coriiceps* under a lipopolysaccharide challenge

Transcriptomic profiling of immune tissues in *Notothenia coriiceps* under a lipopolysaccharide challenge

Manuscript in preparation

Acknowledgements

The authors would like to acknowledge the year 2017 crew of the Great Wall Chinese Antarctic Station for their hospitability and logistic support and Elsa Couto for providing the cortisol data. This study was carried out with logistic and financial support of the Portuguese Polar Programme (FACC PROPOLAR 2016-2017) and funded by Portuguese Foundation for Science and Technology (FCT) through projects FCT-NSFC/0002/2016, PTDC/BIAANM/3484/2014 and CCMAR/Multi/04326/2019, and a PhD fellowship SFRH/BD/120040/2016 to CS.

Transcriptomic profiling of immune tissues in *Notothenia coriiceps* under lipopolysaccharide challenge

Cármen Sousa[1*], Deborah M Power[1,2], Pedro M Guerreiro[1], Bruno Louro[1], Liangbiao Chen[2,3,4] and Adelino V M Canário[1,2*]

[1]*CCMAR-CIMAR, Centre of Marine Sciences, University of Algarve, Campus de Gambelas, 8005-139 Faro, Portugal*

[2]*International Research Centre for Marine Biosciences, Ministry of Science and Technology, Shanghai Ocean University, Shanghai, China*

[3]*Key Laboratory of Exploration and Utilization of Aquatic Genetic Resources, Ministry of Education, Shanghai Ocean University, Shanghai, China*

[4]*National Demonstration Center for Experimental Fisheries Science Education, Shanghai Ocean University, Shanghai, China*

3.1. Abstract

The extreme conditions in the Antarctic have driven the evolution of a unique biodiversity at a macro- to microorganism scale. The Antarctic Notothenioids are a single lineage of teleosts that arose from a common benthic ancestor through adaptive radiation under a regime of paleoclimatic change. The evolutionary isolation of the Notothenioid and unique Antarctic conditions led to many physiological innovations, however little is known about immune adaptations. In the present study, the immune response to an endotoxin (lipopolysaccharide, LPS) challenge was evaluated 7 days later by characterizing plasma biochemical parameters and the transcriptional response of the head-kidney, skin, and the duodenum in the Antarctic bullhead *Notothenia coriiceps*. Results showed that plasma biochemical indicators were not significantly changed but 230 genes were differentially expressed across the 3 tissues in response to LPS challenge. Approximately 30% of the DEGs identified were related to immunity, and pathogen recognition receptors (such as NOD-like receptors) and humoral components (such as interferons) were well represented. The principal processes modified were tissue specific and associated with cellular energy metabolism and S-

nitrosylation in the head-kidney; mitochondrial depolarization in the duodenum; and protein ubiquitination in skin. The modest response to the LPS challenge in *N. coriiceps* compared to other species may be due to endotoxin source, administration route or the long interval between challenge and analysis.

Keywords: Antarctic fish; head-kidney; innate immunity; intestine; lipopolysaccharide; skin; transcriptomics

3.2. Introduction

The Antarctic teleost fish fauna belong mostly to the perciform suborder Notothenioidei which evolved from a benthic ancestor through adaptive radiation under a stable cold thermal environment (Clarke et al., 2007; Nowlin and Klinck, 1986; Rintoul, 2009). The Antarctic notothenioids have been the subject of evolutionary studies to establish timing and mode of lineage and character diversification (Matschiner et al., 2015; Near et al., 2012) under extreme cold conditions. Among the specific adaptations are the development of antifreeze glycoprotein (Cheng and Chen, 1999; DeVries and Cheng, 2005; DeVries and Wohlschlag, 1969)(Shin et al., 2014), buoyancy modifications as a result of reduced bone density and higher whole body lipid levels (Albertson et al., 2010), the absence of Malpighi glomerulus in the kidney (Eastman and Devries, 1986), high cellular mitochondrial densities (O'Brien and Sidell, 2000), cold-efficient cellular microtubule assembly (Detrich et al., 1989, 2000) and the absence of the heat shock response (Detrich et al., 2000; Hofmann et al., 2000; Place and Hofmann, 2005a). An additional unique characteristic of the *Channichthyidae* family of the notothenioids is the loss of haemoglobin and myoglobin (Kim et al., 2019a).

A physiological trait that has so far received limited attention in Antarctic notothenioids is the immune system. However, the isolation and rapid speciation of the notothenioids and the unique environmental conditions and microbial community of the Southern Ocean (Furbino et al., 2014; Kim et al., 2019a), offer an opportunity to gain insight into the influence of the environment on the immune repertoire. Teleost fishes, in common with other vertebrates, possess both innate and acquired immune responses (Magnadottir et al., 2006; Magor and Magor, 2001; Tort et al., 2003), although the former is proposed to have a more prominent role

(Sunyer, 2013; Zhu et al., 2013). The constant contact of fish epithelia or mucosal barriers (e.g. gills, skin and intestine) with a microorganism rich aquatic environment may explain why they have acquired such a formidable non-specific innate immune response, particularly at the level of mucosa´s (Gomez et al., 2013).

Studies on the relationship between water temperature and the immune response in teleost fish (Abram et al., 2017; Bonneaud et al., 2016; Chen et al., 2016; MacKenzie et al., 2008; Magnoni et al., 2015) indicate that immunity is generally delayed and suppressed by lower temperatures (Bly and Clem, 1992; Detrich et al., 1989; Le Morvan et al., 1998). *In vitro* studies of fish immune cells under reduced temperatures revealed cytotoxic activity (Le Morvan-Rocher et al., 1995), the macrophage response (Le Morvan et al., 1997) and the respiratory burst (Dexiang and Ainsworth, 1991) were enhanced. The few studies on immune system function in notothenioids indicate that low temperature does not inhibit phagocytosis (Silva et al., 2002) or the inflammatory response (O'Neill et al., 1988; Silva et al., 1998, 1999) and damage-repair of skin occurs but at a slow pace (Cunha Da Silva et al., 2005).

A recent small scale transcriptome in the Antarctic bullhead (*Notothenia coriiceps*) exposed to heat killed bacteria or polyinosinic:polycytidylic acid (poly I:C) revealed an inverse response in the main KEGG pathways identified in the liver, namely antigen processing and presentation and bacterial ligand exposure (Ahn et al., 2016). Other studies taking a candidate gene approach revealed that exposure of *N. coriiceps* and *N. rossii* to bacterial lipopolysaccharide (LPS), a typical pathogen associated molecular pattern (PAMP) from the outer layer of gram-negative bacteria (Bishop, 2005), modulated iron-related immune genes and the response was more prominent in the head-kidney than in the liver (Martinez et al., 2020).

The present study was designed to determine if the extreme cold environment and unique microbial community of the Southwestern Atlantic Ocean, a) drove evolutionary innovations at the level of the immune system in *N. coriiceps* and b) if this affected the tissue-specific immune response to a bacterial endotoxin (LPS) found in the cell-wall of gram-negative bacteria of the *Enterobacteriaceae* family, and abundant across the world including in the Antarctica continent (Araya et al., 2020). LPS stimulates host innate immunity in vertebrates (including fish) through toll-like receptor (TLRs) activation, cytokines and acute phase proteins (Swain et al., 2008). In the present study, the transcriptional response to LPS was analysed in the principal hematopoietic organ, the head-kidney, and two mucosal-associated lymphoid

tissues, the skin and intestine and the activity of serum enzymes associated with innate immunity were also analyzed.

3.3. Methods

3.3.1. Fish capture and maintenance

Fish collection and experimental protocols were approved by the Portuguese Environmental Agency, under the regulations set by the Treaty of Madrid for scientific investigation in Antarctica. The experiments performed complied with European Union and Portuguese regulations for animal experimentation.

Notothenia coriiceps, (30 ± 0.53 cm of total length and 384.4 ± 20.38g of weight) were captured by boat using a hook-and-line from a depth of 10 to 20 m in the waters near the Great Wall Station, King George Island in the Antarctic Peninsula (GPS coordinates: 62°13′S, 58°58′W) during the Antarctic summer (January and February) of 2017. Fish were kept on board in well oxygenated cold water and then transferred to the facilities on land where they were maintained in a flow-through seawater circuit in 200 L tanks for at least 3 days before the experiment. The water was continuously pumped from the ocean and tanks were monitored three times a day (7.00h, 14.00h and 21.00h) for water temperature (2.0 ± 0.8 ℃), salinity (28 ± 0.2 ppt) and oxygen (11 ± 2 mg/L).

Fish were fed daily with a mixture of limpets, amphipods and fish muscle.

3.3.2. Immune challenge experiments

Upon the acclimation period fish were lightly anesthetized in 2-phenoxyethanol (0.02 mL/L, Sigma-Aldrich, Spain) weighed and tagged with opercular marks. A small blood sample was removed from the caudal vasculature using a heparinised 1-ml Syringe fitted with a 23G needle. The control fish were returned to the tank while the sham (the saline injected control) fish received intraperitoneal (i.p.) injections of 0.2% v/w of 1.1% NaCl, and the LPS-injected treatment fish received 0.2% v/w of 1.5 mg/mL *E. coli* LPS 0111:B4 (L2630, Sigma-Aldrich)

in 1.1% NaCl. Fish were thus allocated in three experimental tanks (n=7 per tank) corresponding to, i) the non-injected control (n = 7), ii) the saline injected sham control (n = 7) and iii) the LPS-injected treatment at 3 mg/Kg (n = 7). A second injection was administered in the sham control and the LPS-treatment 48 hours later, following the process and amounts described above. The control group was not disturbed Five days after the second injection (day 7 of the experiment), fish were anaesthetized, and blood collected by caudal puncture before sacrificing the fish by cervical section and disruption of the CNS. The head-kidney, skin, and anterior intestine (duodenum region) were dissected out and stored in RNA later (Sigma-Aldrich). Two fish died in the LPS treated group and no mortality was observed in any of the other groups.

3.3.3. Biochemical parameters

Blood was centrifuged at 10,000 g for 5 minutes at 4°C immediately after collection and plasma was removed and frozen at -80°C until analysis. All the samples collected in each group were analysed (n = 5 for LPS, n = 7 for the sham controls and n = 7 non-injected control).

3.3.3.1. Total Plasma Protein

Total plasma protein was measured using a Quick Start™ Bradford Protein assay kit (Bio-Rad, Portugal) adapted for a 96-well plate (Bradford, 1976). Measurements were performed at 590 nm at a constant temperature (25°C) in a spectrophotometer (Microplate reader Benchmark, Bio-Rad, USA).

3.3.3.2. Lysozyme activity

The lysozyme activity in blood plasma was measured using a turbidimetric method (Ellis, 1990). In brief, 130 µl of lyophilized *Micrococcus luteus* cells (0.6 mg/mL in 0.05 M sodium phosphate buffer, pH 6.2, Sigma-Aldrich) were mixed with 20 µl of plasma in a flat

bottomed 96 well-plate. For the standard curve, hen egg white lysozyme (Sigma-Aldrich) was used, and the blank contained 150 µl of sodium phosphate buffer (Sigma-Aldrich). The reaction was incubated for 10 minutes at 25 ℃ and the absorbance was measured at 450 nm in a spectrophotometer (Microplate reader Benchmark, Bio-Rad).

3.3.3.3. Antitrypsin activity

The antitrypsin assay measures total antiprotease activity and is based on the method of Ellis (Ellis, 2001). The assay was performed in duplicate reactions at room temperature (21℃). In the optimized protocol 20 µl of trypsin from porcine pancreas (5 mg/mL water, Sigma-Aldrich) was mixed with 10 µL of *N. coriiceps* plasma for 10 minutes followed by the addition of 200 µL of 0.1 M phosphate buffer pH 7.0 and 250 µL of 2% Azocasein (A-2765, Sigma-Aldrich). The reaction was incubated for 1 hour at 21ºC and 500 µL of 10% trichloroacetic acid (Sigma-Aldrich) was added, followed by incubation for 30 minutes at room temperature (21℃) and centrifugation at 10,000 g for 10 minutes. The supernatant (100 µL) was added in duplicate to a 96-well plate followed by 100 µL sodium hydroxide (1N, NaOH, VWR, Spain). A blank reaction was prepared with NaOH (100 µl) and phosphate buffer (100 µl, VWR). Reaction products were measured at 450 nm in a spectrophotometer (Microplate reader Benchmark, Bio-Rad).

3.3.3.4. Plasma Cortisol

Plasma cortisol was measured using an in-house radioimmunoassay (RIA) as previously described (Guerreiro et al., 2006; Rotllant et al., 2005). Briefly, *N. coriiceps* plasma samples were diluted in phosphate buffer with 0.5g/L gelatine (VWR), pH 7.6 and heat denatured at 70℃ for 30 minutes, centrifuged (10.000 g for 10 minutes at 4ºC) and the supernatant used for the assays. The antisera used for the RIA was rabbit anti-cortisol-20 CR50 (Fitzgerald, USA). The diluted samples (1:20 in 500 µl gelatine buffer) in duplicate were incubated overnight with the cortisol antisera and [1,2,6,7-3H(N)] cortisol radiotracer (PerkinElmer, USA) in a final volume of 100 µl.

3.3.3.5. Statistical analysis

Data is expressed as mean ± sem. Differences in biochemical parameters between the control, sham and LPS-treated groups were analysed by one-way analysis of variance (ANOVA) followed by the Helm-Sidak post hoc test using SigmaPlot v12.5. Graphs were generated using GraphPrism v6.01. The threshold for significance was set at $p < 0.05$ (**Supplementary figure 3.1**).

3.3.4. RNA Extraction, construction of cDNA libraries and next-generation sequencing

Total RNA was extracted from ~25 mg of the head-kidney, skin and duodenum of 5 specimens of *N. coriiceps* per experimental group using an E.Z.N.A. Total RNA Kit I (Omega Bio-Tek, USA) and treated with RNase-free DNase I (Omega Bio-Tek) to remove any contaminating genomic DNA. The RNA integrity and quality were evaluated by electrophoresis on a 1% agarose gel and using spectrophotometers Nanodrop One (Thermofisher, Spain) and Qubit (Invitrogen, USA). Poly (A)+ messenger RNA (mRNA) was purified using a DynaBeads mRNA Purification Kit (Life Technologies, Carlsbad, CA) and prepared 45 paired-end complementary DNA (cDNA) libraries (with an insert size of 250 base pairs (bp) using a VAHTS stranded mRNA-*seq* Library Prep Kit from Illumina following the manufacturer´s protocol. Quality control analysis of the constructed library was performed using an Agilent Bioanalyzer DNA 1000 Kit (Agilent, #5067-1504). All libraries were sequenced using an Illumina Hiseq X Ten by Vazyme Biotech Co., Ltd, China.

Quality control and editing of raw reads to trim adapter sequences and low quality bases was performed using Trimgalore wrapper script v0.4.5 (Krueger, 2015) and output FastQC quality reports were obtained (Andrews, 2015). Mitochondrial and ribosomal reads were removed by aligning reads (BLASTn) against the *Notothenia coriiceps* mitochondrial genome (accession number NC_015653.1) and by identification of ribosomal gene products using Bowtie2 v2.3.4 (Langmead et al., 2009). *De novo* assembly of all reads was performed in Trinity v2.5.1 with the "-normalize reads" parameter defined (Haas et al., 2013), and the reference transcriptome obtained was used to map reads using the RSEM package v1.3.1 (Li et

al., 2009) followed by differential expression analysis using the EdgeR package v3.14.0 (Robinson et al., 2009) (**summary data in Supplementary table 3.1**).

3.3.5. Functional annotation of genes and pathways

Functional annotation was performed using the Trinotate v3.1.1 pipeline (Bryant et al., 2017) and integrated into an SQLite database v3.34.0 to allow fast efficient searching for terms with biological meaning. Annotations were based on the best deduced open reading frame (ORF) obtained with Transdecoder v1.03 (Smith-Unna et al., 2016). The UniProtKB/Swiss-Prot/EMBL Uniprot eggNOG databases (Bateman et al., 2017) were queried using BlastX and BlastP v2.7.1 for all contigs and ORF, respectively (e-value cut-off of 1e−5). The ORFs were also queried against PFAM using hmmscan in HMMER v3.1b2 (Finn et al., 2011).

Further functional annotations to identify signal peptides (signalP) (Emanuelsson et al., 2007), transmembrane regions (tmHMM) (Krogh et al., 2001) and for comparison to currently curated public annotation database (EMBL Uniprot eggnog/GO pathways) were implemented with a threshold FDR < 0.05. Gene Ontology (GO) analysis was obtained with the Trinotate pipeline procedures, initially with GO assignment of transcripts followed by enrichment analysis. GO terms were summarized by REVIGO (Supek et al., 2011), which removed redundant GO terms based on semantic similarity and graphical outputs were represented in Rstudio v1.0143 with a threshold set at FDR < 0.05. Additionally, a Fisher's exact test was applied to detect significantly only over/under-represented immune-related GO terms in the global transcriptome (FDR < 0.05). Pathway enrichment analysis of the differentially expressed genes was carried out using the Kyoto Encyclopedia of Genes and Genomes (KEGG) orthologs (KO) database to create KEGG pathways maps (Kanehisa et al., 2021) by KOBAS software that used the Fisher´s exact test as statistical method and FDR correction method of Benjamini and Hochberg (1995) (Bu et al., 2021).

3.3.6. Differential expression and Heatmap analyses

Differential gene expression (DGE) analysis was established using pairwise comparisons of the three treatment groups (non-injected control, sham and LPS) and the three

different tissues, head-kidney, duodenum, and skin. The cut-off threshold for significance was set at 0.05% FDR to obtain a strict selection of genes responding to handling during LPS injection and to endotoxin exposure. A total of 298 million paired-end (PE) raw transcriptome reads were generated from the RNA-seq analysis of the 45 libraries prepared from the head-kidney (Hk_1 to Hk_5), duodenum (Du_1 to Du_5) and skin (Sk_1 to Sk_5) from the non-injected control (C1-C5, n = 5 libraries/ tissue) sham control (S1-S5, n = 5 libraries/ tissues) and LPS-treatment (L1-L5, n = 5 libraries/tissue). Index and adapter sequences were trimmed using Trimmomatic (version 0.4.4 dev) and low quality bases were trimmed with cutadapt 1.15 in Python 2.7.11 (Bolger et al., 2014). TransRate software (version 1.0.3) was used for quality filtering and for optimization of the assembly in the absence of a reference genome (Smith-Unna et al., 2016).

A heatmap of DEGs was generated with the heatmap package from RStudio software v1.0.143 to facilitate visualization of the magnitude of the response of the head-kidney, duodenum and skin from *N. coriiceps* challenged with LPS. Analysis was performed between replicates of the same group and between treatment groups (control, sham and LPS) for each tissue 7-days post-challenge with LPS. The significance threshold was set at FDR < 0.05.

3.4. Results

3.4.1. Blood plasma biochemistry

Plasma protein, plasma total antiprotease activity, plasma lysozyme activity and plasma cortisol levels were not significantly different between any of the treatment groups after 7 days of experiment (**Supplementary figure 3.1**).

3.4.2. Characteristics of the head-kidney, duodenum, and skin reference transcriptomes

The 45 cDNA libraries generated 1,112 Mbp which assembled in 428,793 contigs with a N50 of 643 bp (**Supplementary table 3.1**). Tissue specific assemblies generated 51,506

contigs for the head-kidney, 58,916 for the duodenum and 66,329 for the skin, 18% of which were automatically annotated (**Table 3.1**). The contigs from the three immune tissues were annotated using UniProtKB/Swiss-Prot databases and resulted in 18% contig annotation. To increase the percentage of annotation the DEGs were manually annotated by interrogating the genomes of Notothenioidei (*N. coriiceps*, *Trematomus bernacchii*, *Pseudochaenichthys georgianus*, *Gymnodraco acuticeps*, *Dissostichus mawsoni* and *Cottoperca gobio*) available from the NCBI database (updated in 2020). After manual annotation, the overall annotation rate of DEGs was approximately 61% for the head-kidney, 57% for the duodenum and 66% for the skin (**Table 3.1**). One sample (L5) from the head-kidney of LPS challenge group had a lower number of reads and did not pass the FastQC parameters, hence and was excluded from the analysis.

Table 3.1. Transcriptome dataset annotation. Number of genes annotated in each immune tissue (head-kidney, duodenum, and skin) and the percentage (%) of annotation obtained using the different databases.

	Number		**~ %**	
Annotation to different databases:				
Genes with BlastX hit to SwissProt	77194		18	
Genes with BlastP hit to SwissProt	47577		11	
Genes with EGGNOG database	64582		15	
Genes with KEGG database	65496		15	
Annotated	49895		18	
Non-annotated	378898		88	
Treatment groups	**Control versus Sham**		**Sham versus LPS**	
	Number	**~ %**	**Number**	**~ %**
Total number of DE genes	329	0.08	401	0.1
Head-kidney	178	54	150	37
Duodenum	138	42	204	51
Skin	13	4	47	12
Summary of annotation of DE genes manually (NCBI):				
Annotation of DE genes				
Head-kidney	113	63	89	59
Duodenum	71	51	126	62
Skin	10	77	26	55
Annotation to known or predicted proteins				
Head-kidney	75	66	55	62
Duodenum	55	77	92	73
Skin	2	20	17	65
Annotation to hypothetical/uncharacterized proteins				
Head-kidney	23	20	18	20
Duodenum	13	18	23	18
Skin	1	10	5	19
Mapping to non-annotated genes				
Head-kidney	65	37	61	41
Duodenum	67	49	78	38
Skin	3	23	21	45

3.4.3. Immune related gene transcripts in head-kidney, duodenum, and skin transcriptomes

Of the GO terms within BP function, 360 genes were identified of which 46 (FDR < 0.05) were mostly related with the interleukin-6 response (**Figure 3.1 A**, **Supplementary table 3.2**). In MF, 43 genes were identified, and 29 enriched genes were linked to the interleukin-12 beta subunit binding (**Figure 3.1 B**, **Table 3.2**) and for the CC category, a total of 9 genes were identified of which 5 were related to the interleukin-6 receptor complex (**Figure 3.1 C**, **Supplementary table 3.2**). Other immune elements with an FDR > 0.05 were identified to have a better comprehension of the *N. coriiceps* immunome in the three tissue transcriptomes are listed in **Supplementary table 3.3**

Table 3.2. Differentially expressed genes (DEGs) in A-B) head-kidney, C-D) duodenum and E-F) skin transcriptomes between sham and LPS treated groups. Up- **(A, C, E)** and down- regulated **(B, D, F)** DEGs (FDR < 0.05). The DEGs involved in immune processes are indicated with a "x" symbol.

a) DEGs up-regulated in head-kidney (Sham versus LPS)

TRINITY sample	logFC	Pvalue	FDR	UniProtKB ID	Gene definition	Gene symbol	Organism	Immune system
TRINITY_DN134805_c3_g6	1,11E+14	6,82E-36	3,52E-31	Q9Y644	RFNG O-fucosylpeptide 3-beta-N-acetylglucosaminyltransferase	*rfng*	*Homo sapiens*	
TRINITY_DN158576_c1_g3	8,91E+14	5,18E-19	1,33E-14	N/A	Zinc-binding protein A33-like	*za33l*	*Gymonodraco acuticeps*	
TRINITY_DN159230_c9_g2	8,51E+14	4,07E-14	4,20E-10	Q9Y4D1	Dishevelled-associated activator of morphogenesis 1	*daam1*	*Homo sapiens*	
TRINITY_DN141612_c4_g1	1,00E+14	1,77E-10	7,02E-07	Q8WV35	Leucine rich repeat containing 29	*lrrc29*	*Homo sapiens*	
TRINITY_DN155301_c3_g7	7,86E+14	7,98E-10	2,74E-06	Q6ZSJ9	Protein shisa-6	*shisa6*	*Homo sapiens*	
TRINITY_DN151653_c3_g2	5,01E+14	1,13E-08	3,06E-05	P19474	E3 ubiquitin-protein ligase TRIM21	*trim21*	*Homo sapiens*	☒
TRINITY_DN157441_c2_g1	7,81E+14	6,20E-08	1,45E-04	Q14789	Golgin subfamily B member 1	*golgb1*	*Homo sapiens*	
TRINITY_DN116076_c0_g1	7,34E+14	1,21E-07	2,40E-04	P22897	Macrophage mannose receptor 1	*mrc1*	*Homo sapiens*	☒
TRINITY_DN142659_c1_g6	8,40E+14	3,08E-07	5,43E-04	A8MUP2	Methyltransferase-like protein 12, mitochondrial	*cskmt*	*Homo sapiens*	
TRINITY_DN143190_c3_g4	6,94E+14	1,54E-06	2,04E-03	Q8N3J9	Zinc finger protein 664	*znf664*	*Homo sapiens*	
TRINITY_DN151479_c4_g1	6,77E+14	3,46E-06	3,76E-03	Q86XP1	Diacylglycerol kinase eta	*dgkh*	*Homo sapiens*	
TRINITY_DN156831_c2_g1	4,46E+14	3,49E-06	3,76E-03	Q6PJ21	SPRY domain-containing SOCS box protein 3	*spsb3*	*Homo sapiens*	
TRINITY_DN158003_c1_g3	7,45E+14	5,92E-06	5,65E-03	N/A	Pyrin-like	mefv	*Notothenia coriiceps*	☒
TRINITY_DN163380_c1_g1	8,84E+14	7,84E-06	6,74E-03	Q8ND71	GTPase IMAP family member 8	*gimap8*	*Homo sapiens*	☒
TRINITY_DN159360_c4_g1	9,78E+14	1,14E-05	8,62E-03	F1RAW5	Shootin 3	*shtn3*	*Danio rerio*	
TRINITY_DN163488_c5_g4	6,75E+14	1,39E-05	9,95E-03	Q6UXP7	Family with sequence similarity 151 member B	*fam151b*	*Homo sapiens*	
TRINITY_DN141366_c1_g4	7,30E+14	1,66E-05	1,08E-02	Q14699	Raftlin	*rftn1*	*Homo sapiens*	☒
TRINITY_DN157950_c4_g1	4,03E+14	1,78E-05	1,13E-02	Q8WUY9	DEP domain containing 1B	*depdc1b*	*Homo sapiens*	
TRINITY_DN142629_c2_g4	6,75E+14	1,98E-05	1,20E-02	Q8NBP7	Proprotein convertase subtilisin/kexin type 9	*pcsk9*	*Homo sapiens*	
TRINITY_DN163764_c13_g2	7,25E+14	2,36E-05	1,36E-02	P50454	Serpin peptidase inhibitor, clade H (heat shock protein 47), member 1a	*serpinh1*	*Homo sapiens*	
TRINITY_DN155452_c2_g1	7,29E+14	2,62E-05	1,45E-02	Q99707	Methionine synthase	*mtr*	*Homo sapiens*	
TRINITY_DN156455_c6_g5	6,62E+14	3,14E-05	1,63E-02	Q7Z7L9	Zinc finger and SCAN domain-containing protein 2	*zscan2*	*Homo sapiens*	
TRINITY_DN141843_c3_g3	6,49E+14	3,41E-05	1,69E-02	Q9Y2G8	DnaJ (Hsp40) homolog, subfamily C, member 16	*dnajc16*	*Homo sapiens*	
TRINITY_DN137183_c4_g1	8,19E+14	5,60E-05	2,63E-02	Q8WWR8	Sialidase 4	*neu4*	*Homo sapiens*	
TRINITY_DN154786_c2_g2	6,58E+14	5,97E-05	2,75E-02	Q9BZV3	Interphotoreceptor matrix proteoglycan 2	*impg2*	*Homo sapiens*	
TRINITY_DN122607_c0_g1	7,94E+14	6,24E-05	2,85E-02	Q9NV96	Cell cycle control protein 50A-like	*tmem30a*	*Homo sapiens*	☒
TRINITY_DN142874_c0_g1	7,16E+14	7,32E-05	3,08E-02	Q9UPN3	Microtubule-actin cross-linking factor 1	*macf1*	*Homo sapiens*	
TRINITY_DN159422_c0_g3	6,95E+14	7,35E-05	3,08E-02	Q9BZP6	Acidic mammalian chitinase	*chia*	*Homo sapiens*	
TRINITY_DN163725_c2_g3	6,41E+14	7,48E-05	3,09E-02	Q9NS28	Regulator of G protein signaling 18	*rgs18*	*Homo sapiens*	
TRINITY_DN159639_c0_g1	8,38E+14	7,97E-05	3,19E-02	Q01130	Serine and arginine rich splicing factor 2a	*srsf2*	*Homo sapiens*	
TRINITY_DN141172_c4_g1	7,03E+14	8,57E-05	3,30E-02	P78325	ADAM metallopeptidase domain 8b	*adam8b*	*Homo sapiens*	☒
TRINITY_DN144517_c5_g2	8,25E+14	9,73E-05	3,66E-02	Q9Y3Z3	SAM domain and HD domain 1	*samhd1*	*Homo sapiens*	☒
TRINITY_DN151930_c0_g3	1,05E+14	1,20E-04	4,38E-02	P78310	Coxsackievirus and adenovirus receptor	*cxadr*	*Homo sapiens*	☒

b) DEGs down-regulated in head-kidney (Sham versus LPS)

TRINITY sample	logFC	Pvalue	FDR	UniProtKB ID	Gene definition	Gene symbol	Organism	Immune system
TRINITY_DN153367_c4_g1	-8,74E+14	1,86E-17	3,21E-13	A0A1S3L397	Nuclear factor 7, brain-like	*nf7bl*	*Salmo salar*	
TRINITY_DN151056_c2_g1	-5,57E+14	6,06E-13	4,47E-09	N/A	N-acetylmuramoyl-L-alanine amidase	*pglyrp2*	*Notothenia coriiceps*	☒
TRINITY_DN157841_c3_g1	-1,44E+14	2,69E-11	1,54E-07	Q7RTR2	NLR family CARD domain-containing protein 3	*nlrc3*	*Homo sapiens*	☒
TRINITY_DN156139_c0_g1	-1,07E+14	3,74E-10	1,38E-06	P17213	Bactericidal permeability-increasing protein	*bpi*	*Homo sapiens*	☒
TRINITY_DN163223_c0_g1	-6,82E+14	1,24E-09	3,99E-06	P04406	Glyceraldehyde-3-phosphate dehydrogenase	*gapdh*	*Homo sapiens*	
TRINITY_DN112255_c0_g1	-7,75E+14	1,67E-06	2,15E-03	P51649	Aldehyde dehydrogenase 5 family, member A1	*aldh5a1*	*Homo sapiens*	
TRINITY_DN142663_c1_g1	-3,86E+14	2,06E-06	2,56E-03	N/A	Peptidoglycan-recognition protein LB-like	*pgrp-lbl*	*Notothenia coriiceps*	☒
TRINITY_DN148291_c0_g2	-2,18E+14	2,09E-06	2,56E-03	P62241	40S ribosomal protein S8	*rps*	*Homo sapiens*	
TRINITY_DN145147_c0_g2	-8,53E+14	5,03E-06	5,08E-03	Q9UG22	GTPase IMAP family member 2	*gimap2*	*Homo sapiens*	
TRINITY_DN162708_c0_g2	-3,34E+14	7,47E-06	6,60E-03	O95398	Rap guanine nucleotide exchange factor (GEF) 3	*rapgef3*	*Homo sapiens*	
TRINITY_DN155536_c2_g1	-2,94E+14	1,23E-05	9,22E-03	Q53G44	Interferon-induced protein 44-like	*ifi44l*	*Homo sapiens*	☒
TRINITY_DN159517_c4_g4	-7,37E+14	1,46E-05	9,95E-03	Q9NQ25	SLAM family member 7	*slamf7*	*Homo sapiens*	☒
TRINITY_DN149357_c4_g1	-3,89E+14	1,48E-05	9,95E-03	N/A	Galactose-specific lectin nattectin-like	*lgals3l*	*Notothenia coriiceps*	
TRINITY_DN163005_c6_g2	-7,27E+14	1,74E-05	1,12E-02	Q16602	Calcitonin gene-related peptide type 1 receptor-like	*calcrl*	*Homo sapiens*	
TRINITY_DN140144_c4_g1	-4,14E+14	2,04E-05	1,22E-02	Q6IMW7	Parvalbumin 4	*pvalb4*	*Homo sapiens*	
TRINITY_DN157015_c0_g1	-7,99E+14	2,23E-05	1,31E-02	Q8NHV1	GTPase IMAP family member 7	*gimap7*	*Homo sapiens*	
TRINITY_DN112248_c0_g1	-8,11E+14	2,26E-05	1,31E-02	Q14156	EFR3 homolog A	*efr3a*	*Homo sapiens*	
TRINITY_DN162337_c2_g1	-7,18E+14	2,75E-05	1,51E-02	Q58EX7	Puratrophin-1	*plekhg4*	*Homo sapiens*	
TRINITY_DN143420_c2_g1	-2,43E+14	3,04E-05	1,60E-02	O60462	Neuropilin 2	*nrp2*	*Homo sapiens*	☒
TRINITY_DN175530_c0_g1	-3,21E+14	5,97E-05	2,75E-02	Q969X5	Endoplasmic reticulum-golgi intermediate compartment 1	*ergic1*	*Homo sapiens*	
TRINITY_DN143073_c3_g9	-6,93E+14	6,62E-05	2,96E-02	P34981	Thyrotropin-releasing hormone receptor a	*thrh*	*Homo sapiens*	
TRINITY_DN136770_c3_g1	-6,87E+14	1,32E-04	4,65E-02	P16035	Metalloproteinase inhibitor 2-like	*timp2*	*Homo sapiens*	

c) DEGs up-regulated in duodenum (Sham versus LPS)

TRINITY sample	logFC	Pvalue	FDR	UniProtKB ID	Gene definition	Gene symbol	Organism	Immune system
TRINITY_DN151616_c2_g1	1,08E+14	3,90E-10	4,97E-06	O60928	Potassium inwardly rectifying channel subfamily J member 1b	*kcnj13*	*Homo sapiens*	
TRINITY_DN148016_c1_g3	8,33E+14	5,58E-08	2,19E-04	Q53G44	Interferon-induced protein 44-like	*ifi44l*	*Homo sapiens*	☒
TRINITY_DN149976_c3_g1	3,36E+14	2,34E-07	7,24E-04	P68133	Actin, alpha skeletal muscle	*acta1*	*Homo sapiens*	
TRINITY_DN152124_c5_g2	9,15E+14	8,41E-07	1,71E-03	Q9BQ24	Zinc finger, FYVE domain containing 21	*zfyve21*	*Homo sapiens*	
TRINITY_DN122607_c0_g1	7,06E+14	1,18E-06	2,17E-03	Q9NV96	Cell cycle control protein 50A	*tmem30a*	*Homo sapiens*	☒
TRINITY_DN140296_c3_g2	9,13E+14	1,36E-06	2,43E-03	P08217	Chymotrypsin-like elastase family member 2A	*cela2a*	*Homo sapiens*	
TRINITY_DN162270_c2_g4	7,66E+14	1,78E-06	2,84E-03	Q9HCM9	Tripartite motif-containing protein 39	*trim39*	*Homo sapiens*	☒
TRINITY_DN142397_c4_g1	1,11E+14	3,18E-06	3,83E-03	P14222	Perforin-1	*prf1*	*Homo sapiens*	☒
TRINITY_DN138531_c1_g2	8,88E+14	4,78E-06	4,85E-03	Q7Z2Y8	Interferon-induced very large GTPase 1	*gvinp1*	*Homo sapiens*	
TRINITY_DN154075_c7_g7	8,73E+14	6,71E-06	5,99E-03	Q6UXB0	Protein FAM131A	*fam131a*	*Homo sapiens*	
TRINITY_DN137183_c4_g1	8,20E+14	8,39E-06	6,77E-03	Q8WWR8	Sialidase-4	*neu4*	*Homo sapiens*	
TRINITY_DN153528_c0_g2	9,89E+14	9,94E-06	7,91E-03	P07478	Trypsin-2	*prss2*	*Homo sapiens*	
TRINITY_DN153528_c0_g3	9,66E+14	1,21E-05	9,00E-03	P35030	Trypsin-3	*prss3*	*Homo sapiens*	☒
TRINITY_DN150459_c4_g3	7,22E+14	1,52E-05	1,01E-02	Q13368	MAGUK p55 subfamily member 3	*mpp3*	*Homo sapiens*	
TRINITY_DN130742_c0_g2	8,52E+14	1,58E-05	1,11E-02	P17538	Chymotrypsin A	*ctrb1*	*Homo sapiens*	
TRINITY_DN154899_c3_g1	8,19E+14	1,89E-05	1,22E-02	F1QTA4	FinTRIM family, member 16	*ftr16*	*Danio rerio*	
TRINITY_DN160991_c2_g2	9,70E+14	2,38E-05	1,40E-02	Q7TST0	Butyrophilin-like protein 1	*btnl1*	*Mus musculus*	☒
TRINITY_DN161643_c0_g1	7,82E+14	3,48E-05	1,83E-02	Q16760	Diacylglycerol kinase delta	*dgkd*	*Homo sapiens*	
TRINITY_DN153528_c0_g1	9,09E+14	4,11E-05	2,03E-02	P07477	Trypsin 1	*prss1*	*Homo sapiens*	
TRINITY_DN163678_c2_g1	6,90E+14	4,48E-05	2,15E-02	P19474	E3 ubiquitin-protein ligase TRIM21	*trim21*	*Homo sapiens*	☒
TRINITY_DN151930_c0_g3	9,36E+14	5,36E-05	2,45E-02	P01833	Polymeric immunoglobulin receptor	*pigr*	*Homo sapiens*	☒
TRINITY_DN151159_c1_g2	3,48E+14	6,02E-05	2,61E-02	P78310	Coxsackievirus and adenovirus receptor homolog	*cxadr*	*Homo sapiens*	☒
TRINITY_DN150181_c2_g1	7,00E+14	6,43E-05	2,67E-02	Q9Y572	Receptor-interacting serine-threonine kinase 3	*ripk3*	*Homo sapiens*	☒
TRINITY_DN122607_c1_g1	3,18E+14	7,34E-05	2,79E-02	A0ZSE6	Transmembrane protein 30C	*tmem30cp*	*Homo sapiens*	
TRINITY_DN143028_c5_g1	7,58E+14	7,91E-05	2,90E-02	O00115	Deoxyribonuclease-2-alpha	*dnase2*	*Homo sapiens*	
TRINITY_DN161264_c2_g2	6,77E+14	7,93E-05	2,90E-02	P15086	Carboxypeptidase B-like	*cpb1*	*Homo sapiens*	
TRINITY_DN135042_c1_g9	7,54E+14	8,06E-05	2,93E-02	Q9NPJ3	Acyl-CoA thioesterase 13	*acot13*	*Homo sapiens*	
TRINITY_DN154496_c1_g2	6,70E+14	8,57E-05	3,10E-02	Q4G0M1	Erythroferrone	*erfe*	*Homo sapiens*	☒
TRINITY_DN152678_c1_g1	2,79E+14	9,29E-05	3,30E-02	Q1LXJ7	Type I cytokeratin, enveloping layer, like	*cyt1l*	*Danio rerio*	
TRINITY_DN134620_c1_g2	9,39E+14	1,01E-04	3,47E-02	E7F0X0	High choriolytic enzyme 1-like	*hce2l2*	*Danio rerio*	
TRINITY_DN145863_c0_g1	8,09E+14	1,07E-04	3,58E-02	P19835	Carboxyl ester lipase, tandem duplicate 1	*cel.1*	*Homo sapiens*	
TRINITY_DN123020_c0_g1	9,47E+14	1,13E-04	3,68E-02	Q9UNI1	Chymotrypsin-like elastase family, member 1	*cela1*	*Homo sapiens*	
TRINITY_DN131342_c0_g1	6,88E+14	1,52E-04	4,50E-02	P21128	Endonuclease, polyU-specific	*endou*	*Homo sapiens*	
TRINITY_DN163340_c1_g1	8,25E+14	1,62E-04	4,71E-02	Q2QL34	Mpv17-like protein	*mpv17l*	*Homo sapiens*	

d) DEGs down-regulated in duodenum (Sham versus LPS)

TRINITY sample	logFC	Pvalue	FDR	UniProtKB ID	Gene definition	Gene symbol	Organism	Immune system
TRINITY_DN152521_c2_g4	-8,24E+14	6,27E-10	6,20E-06	Q9UGV2	Protein NDRG3	*ndrg3*	*Homo sapiens*	
TRINITY_DN149950_c2_g1	-8,13E+14	1,17E-09	9,90E-06	P19021	Peptidylglycine alpha-amidating monooxygenase	*pam*	*Homo sapiens*	
TRINITY_DN159842_c3_g5	-7,18E+14	3,79E-08	1,73E-04	P40189	Interleukin-6 receptor subunit beta	*il6st*	*Homo sapiens*	☒
TRINITY_DN163716_c15_g1	-4,16E+14	1,28E-07	4,72E-04	Q9Y6R4	Mitogen-activated protein kinase kinase kinase kinase 4	*map3k4*	*Homo sapiens*	
TRINITY_DN147164_c0_g1	-1,00E+14	1,61E-07	5,60E-04	Q5QJ38	Trichohyalin-like	*tchhl1*	*Homo sapiens*	
TRINITY_DN40234_c0_g1	-8,07E+14	2,82E-07	7,91E-04	P07585	Decorin	*dcn*	*Homo sapiens*	
TRINITY_DN156139_c0_g1	-9,11E+14	9,19E-07	1,81E-03	P17213	Bactericidal permeability-increasing protein	*bpi*	*Homo sapiens*	☒
TRINITY_DN160464_c1_g2	-1,10E+14	9,57E-07	1,82E-03	A0A1S3QYN5	Ladderlectin-like	n/a	*Salmo salar*	
TRINITY_DN157841_c3_g1	-7,61E+14	1,47E-06	2,52E-03	P02748	Complement component 9	*c9*	*Homo sapiens*	☒
TRINITY_DN115693_c0_g1	-1,04E+14	2,25E-06	3,08E-03	P55212	Caspase 6, apoptosis-related cysteine peptidase	*casp6*	*Homo sapiens*	
TRINITY_DN143935_c5_g2	-6,03E+14	3,12E-06	3,83E-03	Q7RTR2	NLR family CARD domain-containing protein 3	*nlrc3*	*Homo sapiens*	☒
TRINITY_DN146963_c5_g1	-7,74E+14	3,70E-06	4,19E-03	O43301	Heat shock protein 12A	*hspa12a*	*Homo sapiens*	
TRINITY_DN161763_c1_g3	-4,87E+14	3,89E-06	4,32E-03	P68032	Actin, alpha cardiac	*actc1*	*Homo sapiens*	
TRINITY_DN138887_c2_g6	-8,52E+14	4,23E-06	4,51E-03	P11511	Cytochrome P450, family 19, subfamily A, polypeptide 1b	*cyp19a1*	*Homo sapiens*	
TRINITY_DN150838_c5_g1	-7,37E+14	4,41E-06	4,56E-03	Q9BRQ3	Nudix (nucleoside diphosphate linked moiety X)-type motif 22	*nudt22*	*Homo sapiens*	
TRINITY_DN151358_c2_g8	-4,01E+14	5,86E-06	5,66E-03	O43736	Integral membrane protein 2A	*itm2a*	*Homo sapiens*	☒
TRINITY_DN125541_c0_g1	-7,50E+14	6,06E-06	5,71E-03	P35326	Small proline-rich protein 2A2	*sprr2a*	*Homo sapiens*	
TRINITY_DN161095_c1_g4	-4,64E+14	6,15E-06	5,71E-03	P63098	Calcineurin subunit B type 1	*ppp3r1*	*Homo sapiens*	
TRINITY_DN156110_c5_g4	-5,87E+14	6,22E-06	5,71E-03	Q6NXR0	Interferon-inducible GTPase 5	*irgc*	*Homo sapiens*	
TRINITY_DN151839_c2_g1	-7,29E+14	6,30E-06	5,71E-03	Q9NVS9	Pyridoxamine 5'-phosphate oxidase	*pnpo*	*Homo sapiens*	
TRINITY_DN145009_c4_g7	-4,47E+14	7,69E-06	6,38E-03	Q53EW6	STKc_SGK domain-containing protein	n/a	*Homo sapiens*	
TRINITY_DN136140_c0_g1	-4,36E+14	1,08E-05	8,37E-03	P08253	72 kDa type IV collagenase	*mmp2*	*Homo sapiens*	☒
TRINITY_DN156123_c1_g1	-6,80E+14	1,12E-05	8,46E-03	Q9BZW8	Natural killer cell receptor 2B4	*cd244*	*Homo sapiens*	☒
TRINITY_DN115615_c0_g1	-7,26E+14	1,39E-05	1,00E-02	Q15063	Periostin, osteoblast specific factor, transcript variant 1	*postn*	*Homo sapiens*	
TRINITY_DN157707_c2_g1	-7,41E+14	1,84E-05	1,21E-02	P05787	Keratin, type II cytoskeletal 8	*krt8*	*Homo sapiens*	
TRINITY_DN147340_c5_g1	-5,12E+14	1,90E-05	1,22E-02	Q9HBY8	Serum/glucocorticoid regulated kinase 2	*sgk2*	*Homo sapiens*	
TRINITY_DN125287_c0_g1	-4,50E+14	2,25E-05	1,36E-02	P02452	Collagen, type I, alpha 1a	*col1a1*	*Homo sapiens*	
TRINITY_DN162540_c4_g1	-2,68E+14	2,29E-05	1,38E-02	Q16653	Myelin-oligodendrocyte glycoprotein	*mog*	*Homo sapiens*	
TRINITY_DN138091_c1_g3	-8,13E+14	2,34E-05	1,39E-02	Q6PJ21	SPRY domain-containing SOCS box protein 3	*spsb3*	*Homo sapiens*	
TRINITY_DN147141_c2_g1	-7,89E+14	2,57E-05	1,48E-02	Q9HAQ2	Kinesin family member 9	*kif9*	*Homo sapiens*	
TRINITY_DN142695_c1_g4	-6,41E+14	2,71E-05	1,55E-02	Q86WX3	Protein S19 binding protein 1	*rps19bp1*	*Homo sapiens*	
TRINITY_DN161763_c1_g1	-5,71E+14	2,74E-05	1,55E-02	N/A	Actin, alpha skeletal muscle 3-like	*act3l*	*Notothenia coriiceps*	
TRINITY_DN147251_c0_g1	-5,81E+14	3,54E-05	1,84E-02	P02452	Collagen alpha-1(I) chain	*col1a1*	*Homo sapiens*	
TRINITY_DN151130_c2_g1	-4,10E+14	3,86E-05	1,98E-02	P60709	Actin beta	*actb*	*Homo sapiens*	
TRINITY_DN6238_c0_g1	-3,02E+14	4,07E-05	2,03E-02	P01344	Insulin-like growth factor 2	*igf2*	*Homo sapiens*	
TRINITY_DN141023_c4_g3	-5,14E+14	4,49E-05	2,15E-02	P51911	Calponin 1, basic, smooth muscle, b	*cnn1*	*Homo sapiens*	
TRINITY_DN143999_c4_g1	-7,53E+14	5,26E-05	2,43E-02	P11226	Lectin mannose-binding 2	*mbl2*	*Homo sapiens*	☒
TRINITY_DN128749_c0_g1	-5,95E+14	5,27E-05	2,43E-02	P12109	Collagen alpha-1(VI) chain	*col6a1*	*Homo sapiens*	
TRINITY_DN93353_c1_g1	-7,56E+14	5,27E-05	2,43E-02	P19113	Histidine decarboxylase	*hdc*	*Homo sapiens*	
TRINITY_DN92606_c0_g1	-2,94E+14	5,87E-05	2,61E-02	P09382	Beta-galactoside-binding lectin	*lgals1*	*Homo sapiens*	
TRINITY_DN153549_c4_g1	-9,78E+14	5,89E-05	2,61E-02	Q9NUS5	Adaptor related protein complex 5 subunit sigma 1	*ap5s1*	*Homo sapiens*	
TRINITY_DN139165_c1_g1	-3,37E+14	5,98E-05	2,61E-02	Q01995	Transgelin	*tagln*	*Homo sapiens*	
TRINITY_DN150906_c5_g2	-6,79E+14	6,27E-05	2,66E-02	Q99963	SH3-domain GRB2-like 3a	*sh3gl3a*	*Homo sapiens*	
TRINITY_DN153288_c0_g1	-4,17E+14	6,37E-05	2,67E-02	Q8WVV5	Butyrophilin subfamily 2 member A2	*btn2a2*	*Homo sapiens*	☒
TRINITY_DN153065_c2_g2	-2,97E+14	6,63E-05	2,71E-02	P18847	Activating transcription factor 3	*atf3*	*Homo sapiens*	
TRINITY_DN137049_c1_g1	-6,75E+14	7,03E-05	2,78E-02	Q9HCI6	E3 SUMO-protein ligase KIAA1586	*kiaa1586*	*Homo sapiens*	
TRINITY_DN157129_c2_g6	-8,68E+14	7,24E-05	2,79E-02	Q460N5	Protein mono-ADP-ribosyltransferase PARP14	*parp14*	*Homo sapiens*	
TRINITY_DN163390_c6_g1	-8,94E+14	7,30E-05	2,79E-02	Q7Z2H8	Proton-coupled amino acid transporter 1	*slc36a1*	*Homo sapiens*	
TRINITY_DN140611_c1_g2	-5,52E+14	8,72E-05	3,13E-02	Q15746	Myosin light chain kinase b	*mylk*	*Homo sapiens*	
TRINITY_DN138114_c0_g1	-6,66E+14	9,35E-05	3,30E-02	Q6ZSG1	Ring finger protein 165a	*rnf165a*	*Homo sapiens*	
TRINITY_DN135989_c1_g5	-3,07E+14	1,08E-04	3,58E-02	Q9NPI9	Inward rectifier potassium channel 16	*kcnj16*	*Homo sapiens*	
TRINITY_DN155812_c1_g1	-2,07E+14	1,09E-04	3,59E-02	Q7Z6B7	SLIT-ROBO Rho GTPase activating protein 1	*srgap1*	*Homo sapiens*	
TRINITY_DN148643_c5_g1	-7,26E+14	1,14E-04	3,71E-02	N/A	Claudin j	n/a	*Gymnodraco acuticeps*	
TRINITY_DN149321_c3_g4	-7,32E+14	1,18E-04	3,77E-02	Q5T7N3	KN motif and ankyrin repeat domain-containing protein 4	*kank4*	*Homo sapiens*	
TRINITY_DN112248_c0_g1	-7,44E+14	1,19E-04	3,78E-02	Q14156	EFR3 homolog A	*efr3a*	*Homo sapiens*	
TRINITY_DN136512_c10_g1	-3,59E+14	1,40E-04	4,29E-02	Q96IC2	RNA exonuclease 5	*rexo5*	*Homo sapiens*	
TRINITY_DN146256_c2_g3	-7,34E+14	1,43E-04	4,29E-02	O75791	GRB2 related adaptor protein a	*grap2*	*Homo sapiens*	☒
TRINITY_DN145763_c0_g1	-3,55E+14	1,53E-04	4,52E-02	P18065	Insulin-like growth factor-binding protein 2	*igfbp2*	*Homo sapiens*	☒

e) DEGs up-regulated in skin (Sham versus LPS)

TRINITY sample	logFC	Pvalue	FDR	UniProtKB ID	Gene definition	Gene symbol	Organism	Immune system
TRINITY_DN159639_c0_g1	8,87E+14	2,27E-12	1,51E-07	U3JA80	Serine and arginine rich splicing factor 2a	*srsf2a*	*Danio rerio*	
TRINITY_DN150109_c2_g2	8,44E+14	2,47E-06	9,09E-03	P07477	Cationic trypsin	*prss1*	*Homo sapiens*	
TRINITY_DN141237_c0_g7	7,65E+14	8,27E-06	2,19E-02	Q14863	POU domain, class 6, transcription factor 1-like	*pou6d1*	*Homo sapiens*	
TRINITY_DN137203_c7_g3	7,10E+14	8,91E-06	2,24E-02	A0A1S3L397	Nuclear factor 7, brain-like	*nf7bl*	*Salmo salar*	
TRINITY_DN162280_c2_g2	3,26E+14	1,43E-05	2,63E-02	Q96A28	SLAM family member 9	*slamf9*	*Homo sapiens*	☒
TRINITY_DN139257_c0_g1	4,05E+14	3,03E-05	4,51E-02	Q96C55	Zinc finger protein 524	*znf524*	*Homo sapiens*	
TRINITY_DN129892_c0_g1	3,15E+14	3,48E-05	4,92E-02	Q7Z2Y8	Interferon-induced very large GTPase 1	*gvinp1*	*Homo sapiens*	

f) DEGs down-regulated in skin (Sham versus LPS)

TRINITY sample	logFC	Pvalue	FDR	UniProtKB ID	Gene definition	Gene symbol	Organism	Immune system
TRINITY_DN151272_c3_g5	-7,81E+14	1,74E-08	2,88E-04	N/A	Cytochrome P450 2K1-like	*cy2k1l*	*Gymnodraco acuticeps*	
TRINITY_DN158576_c1_g3	-3,94E+14	3,95E-08	4,37E-04	N/A	Zinc-binding protein A33-like	*za33l*	*Gymnodraco acuticeps*	
TRINITY_DN143097_c2_g4	-7,44E+14	1,10E-06	5,11E-03	Q13216	Excision repair cross-complementation group 8	*ercc8*	*Homo sapiens*	
TRINITY_DN159712_c1_g3	-7,06E+14	4,19E-06	1,46E-02	Q96P20	NACHT, LRR and PYD domains-containing protein 3	*nlrp3*	*Homo sapiens*	☒
TRINITY_DN158530_c2_g1	-7,63E+14	6,29E-06	1,90E-02	Q6BDS2	UHRF1 binding protein 1	*uhrf1bp1*	*Homo sapiens*	
TRINITY_DN151209_c9_g1	-7,85E+14	9,13E-06	2,24E-02	Q7RTR2	NLR family CARD domain-containing protein 3	*nlrc3*	*Homo sapiens*	☒
TRINITY_DN156424_c1_g2	-8,13E+14	1,06E-05	2,34E-02	Q8NHV1	GTPase IMAP family member 7	*gimap7*	*Homo sapiens*	
TRINITY_DN149926_c4_g3	-7,68E+14	1,09E-05	2,34E-02	Q9PWM2	Homeobox B9a	*hxb9a*	*Danio rerio*	
TRINITY_DN137852_c4_g3	-8,71E+14	1,29E-05	2,60E-02	Q9UGT4	Sushi domain containing 2	*susd2*	*Homo sapiens*	
TRINITY_DN159613_c2_g1	-7,60E+14	2,64E-05	4,08E-02	Q14258	E3 ubiquitin/ISG15 ligase TRIM25	*trim25*	*Homo sapiens*	☒

a)

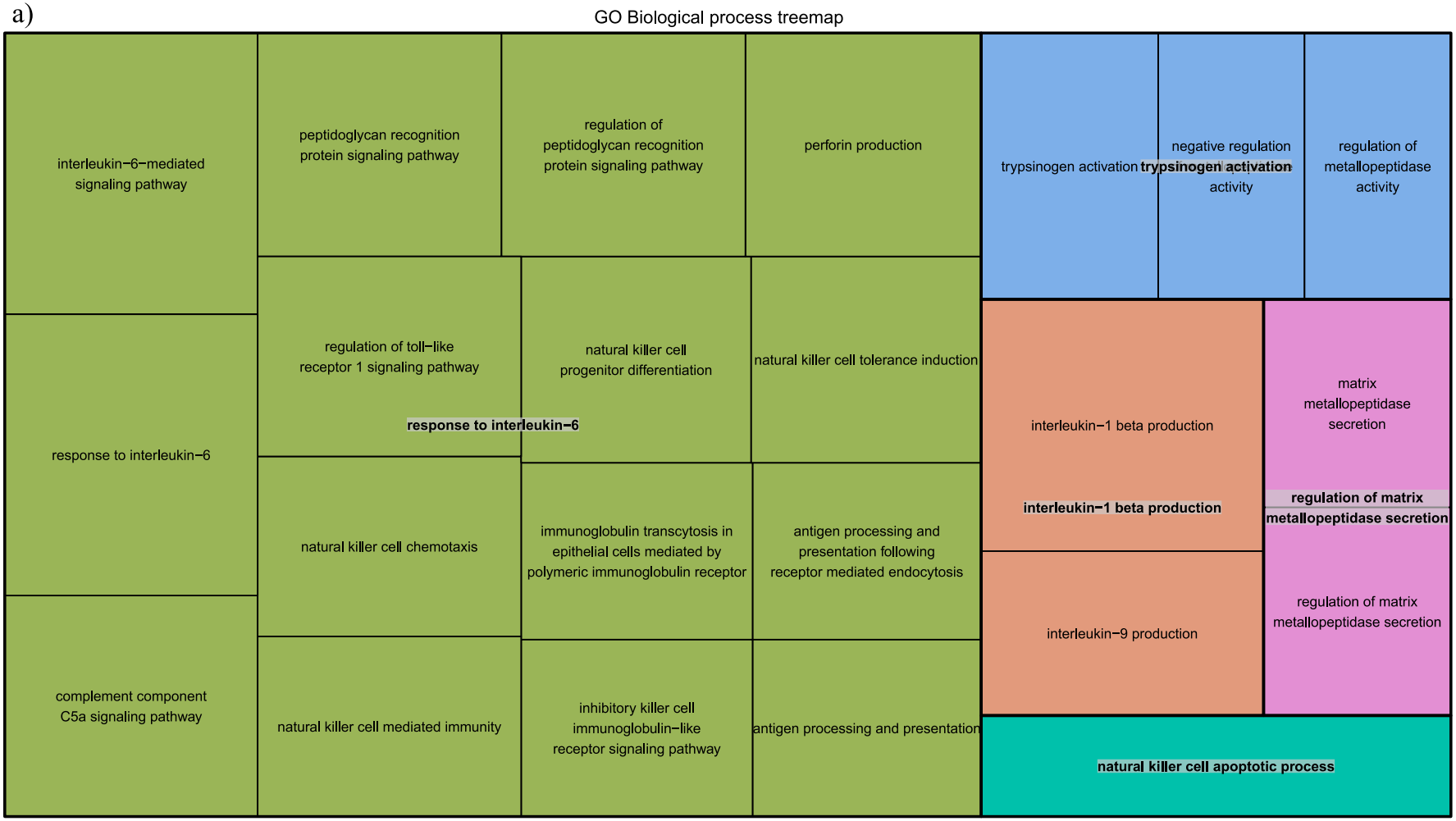
GO Biological process treemap
interleukin−6−mediated signaling pathway
peptidoglycan recognition protein signaling pathway
regulation of peptidoglycan recognition protein signaling pathway
perforin production
trypsinogen activation
negative regulation trypsinogen activation activity
regulation of metallopeptidase activity
response to interleukin−6
regulation of toll−like receptor 1 signaling pathway
natural killer cell progenitor differentiation
natural killer cell tolerance induction
response to interleukin−6
interleukin−1 beta production
interleukin−1 beta production
matrix metallopeptidase secretion
regulation of matrix metallopeptidase secretion
natural killer cell chemotaxis
immunoglobulin transcytosis in epithelial cells mediated by polymeric immunoglobulin receptor
antigen processing and presentation following receptor mediated endocytosis
interleukin−9 production
regulation of matrix metallopeptidase secretion
complement component C5a signaling pathway
natural killer cell mediated immunity
inhibitory killer cell immunoglobulin−like receptor signaling pathway
antigen processing and presentation
natural killer cell apoptotic process

b)

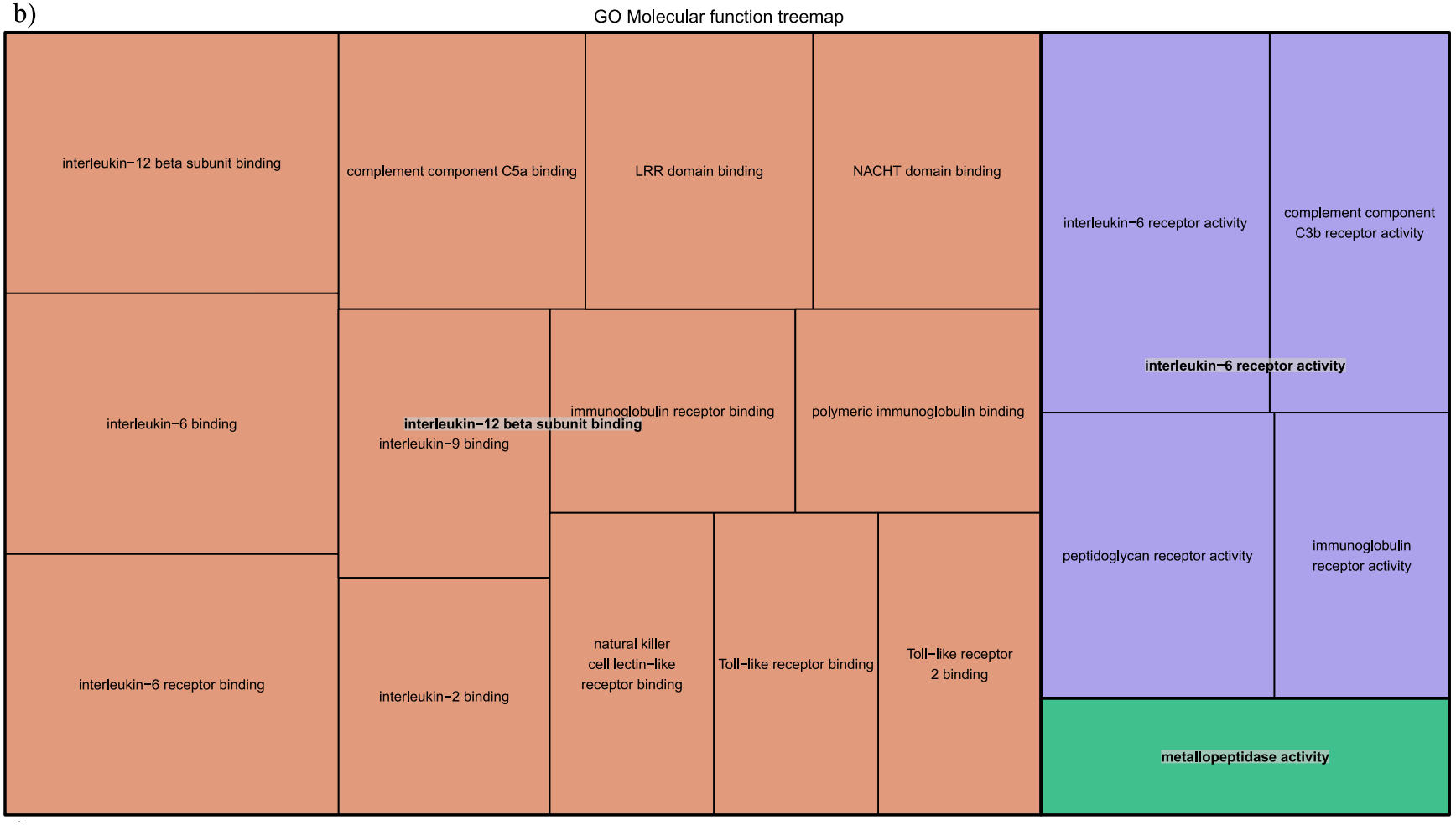
GO Molecular function treemap
interleukin−12 beta subunit binding
complement component C5a binding
LRR domain binding
NACHT domain binding
interleukin−6 receptor activity
complement component C3b receptor activity
interleukin−6 binding
interleukin−12 beta subunit binding
interleukin−9 binding
immunoglobulin receptor binding
polymeric immunoglobulin binding
interleukin−6 receptor activity
peptidoglycan receptor activity
immunoglobulin receptor activity
interleukin−6 receptor binding
interleukin−2 binding
natural killer cell lectin−like receptor binding
Toll−like receptor binding
Toll−like receptor 2 binding
metallopeptidase activity

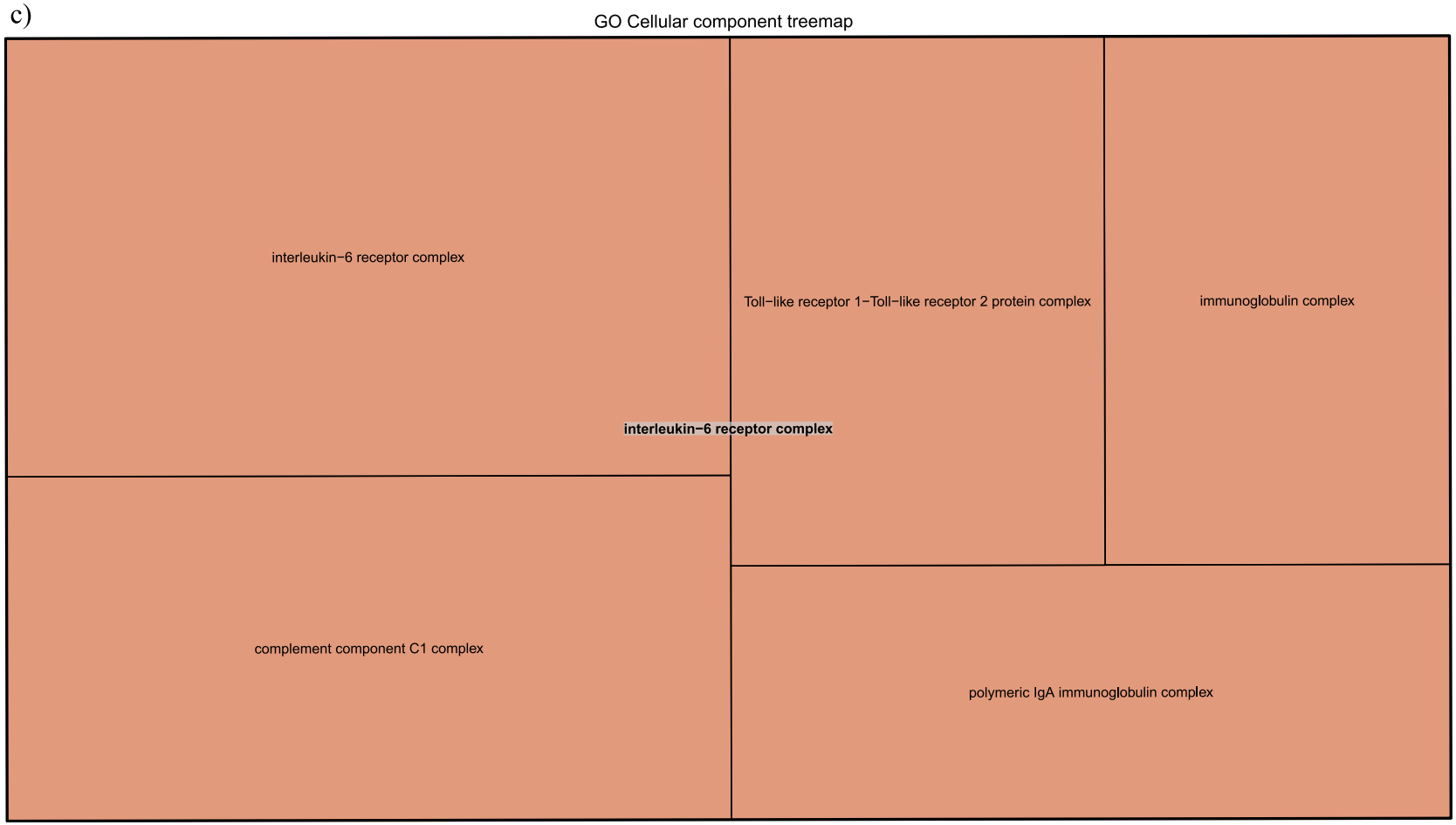

Figure 3.1. **Immune enriched GO using DEGs between the sham and LPS groups: A) molecular function B) and C) cellular component.** The tree map was generated with all the DEGs identified by the comparison of the head-kidney, duodenum and skin transcriptomes from, sham and LPS treated fished (FDR < 0.05). The size of the square plots represents the relative percentage of abundance (log10 p-value), and the colours represents the main processes involved.

3.4.4. Differentially expressed genes (DEGs) in the head-kidney, duodenum and skin

3.4.4.1. DEGs in control versus sham and sham versus LPS

Pairwise comparisons of the transcriptomes of the control versus sham (C versus S) injected fish were used to assess the potential impact on gene expression of handling stress. The comparison yielded approximately 330 differentially expressed gene transcripts (DEGs) linked to handling and injection. Of these 178 gene transcripts were from the head-kidney (130 up- and 48 down-regulated, 63% annotated); 139 gene transcripts were from the duodenum (77 up- and 61 down-regulated, 51% annotated) and 13 gene transcripts were from the skin (3 up- and 10 down-regulated, 77% annotated) (**Table 3.1**, **Supplementary table 3.4**).

Pairwise comparisons of the LPS and sham injected fish (S versus L) was used to assess the impact of endotoxin exposure on the head-kidney, duodenum and skin. The comparison yielded 401 DEGs, of which 150 were from the head-kidney (82 up- and 68 down-regulated, 59% annotated), 204 from the duodenum (73 up- and 131 down-regulated, 62% annotated) and 47 from the skin (17 up- and 30 down-regulated, 55% annotated) (**Table 3.1** and **3.2**).

3.4.5.2 Control versus sham DEGs

The most highly modified gene transcripts represented in the DEGs between the C and S groups were zinc finger protein 184 (*znf184*, up-regulated) and nuclear factor 7, brain-like (*nf7bl*, down-regulated) in the head-kidney, acyl-CoA dehydrogenase family, member 11 (*acad11*) and NLR family CARD domain containing 3 (*nlrc3*, both up-regulated) in the duodenum and GTPase IMAP family member 7 (*gimap7*, down-regulated) and GTPase IMAP family member 8-like (up-regulated) in the skin. Two DEGs were shared between the head-kidney and duodenum transcriptomes, *nlrc3* and *slc5a6*. A *gimap7* transcript was present in the DEGs of the three tissue transcriptomes (**Figure 3.2A**, **Supplementary table 3.4**).

a) Control vs Sham

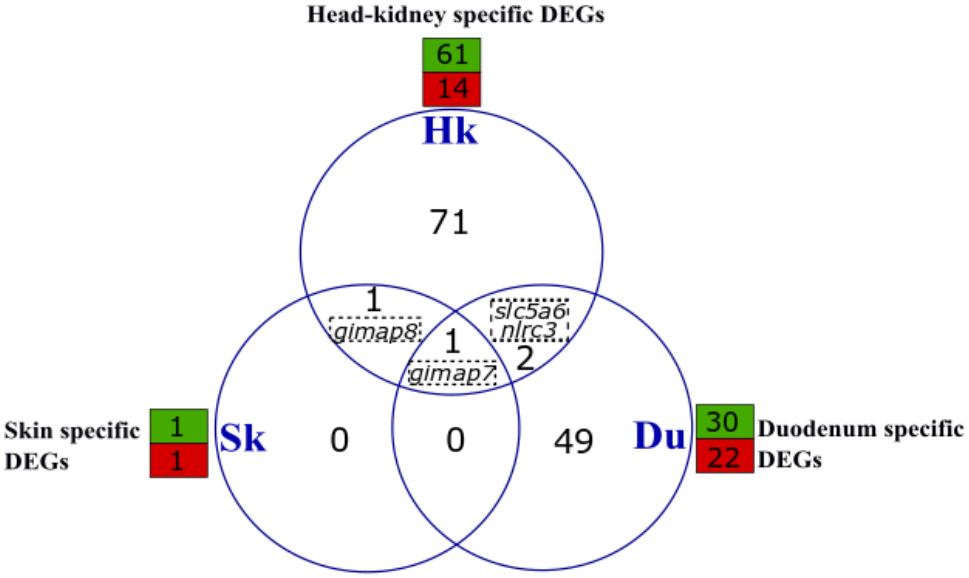

b) Sham vs LPS

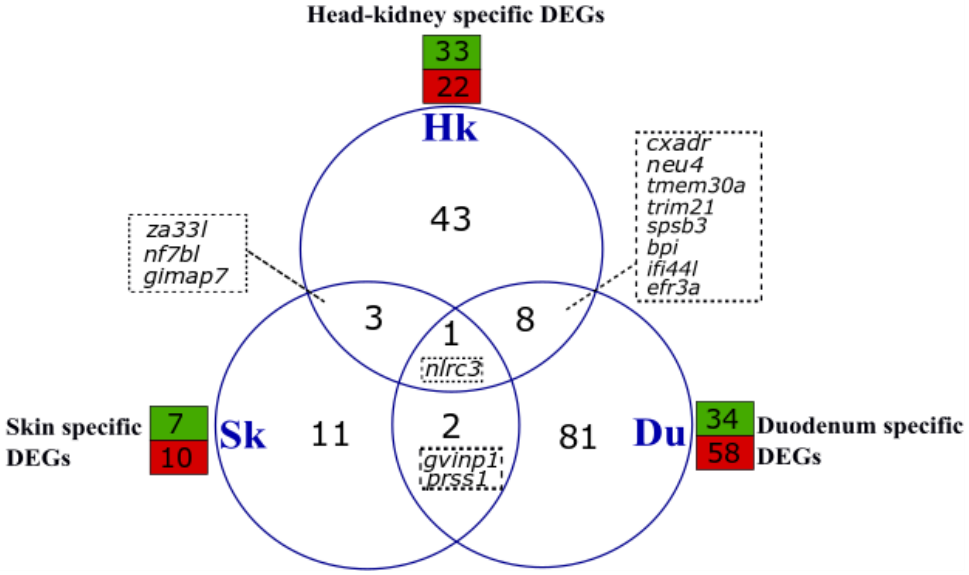

Figure 3.2. Venn diagram representing the number of DEGs in the three tissue transcriptomes of the a) Control versus Sham and b) Sham versus LPS. The Venn diagrams indicate the number of annotated DEGs that are specific to the head-kidney (Hk), duodenum (Du) and skin (Sk) or that are common between two or all tissues (FDR < 0.05). The green and red boxes represent the total number of up- or down-regulated genes. The dashed boxes contain the abbreviated name of some gene transcripts.

3.4.5.3. Sham versus LPS DEGs

In the comparison of the S and LPS-treated groups, the most highly modified gene transcripts were RFNG O-fucosylpeptide 3-beta-N-acetylglucosaminyltransferase (*rfng*) and zinc-binding protein A33-like (*za33l*) (both up-regulated) in the head-kidney, potassium inwardly rectifying channel subfamily J member 1b (up-regulated) and protein NDRG3-like (*ndrg3l*) (down-regulated) in the duodenum and serine and arginine rich splicing factor 2a (up-regulated) and cytochrome P450 2K1-like (*cyp2k1l*) (down-regulated) in the skin. The shared DEGs identified in the head-kidney and skin transcriptome of the LPS challenged group included zinc-binding protein A33-like (*za33l*), nuclear factor 7 brain-like, GTPase IMAP family member 7-like (**Figure 3.2 B**, **Table 3.2**). The shared DEGs represented in the transcriptomes of the head-kidney and duodenum of the LPS group were cell cycle control protein 50A-like (*tmem30a*), E3 ubiquitin-protein ligase TRIM21-like (*trim21*), SPRY domain-containing SOCS box protein 3-like (*spsb3*), bactericidal permeability-increasing protein-like (*bpi*), coxsackievirus and adenovirus receptor (*cxadr*), sialidase 4 (*neu4*), interferon-induced protein 44-like (*if44l*) and EFR3 homolog A (*efr3a*) (**Figure 3.2 B**, **Table 3.2**). The DEG, interferon-induced very large GTPase 1-like (*gvinp1*) and trypsin-1 (*prss1*) genes, were shared between the duodenum and skin transcriptomes and the NLR family CARD domain-containing protein 3-like gene was a common DEG to the three tissue transcriptomes (**Figure 3.2 B**, **Table 3.2**). Overall, the DEGs most modified were associated with S-nitrosylation, mitochondrial depolarization, protein ubiquitination and innate immune response (approximately 30% of DEGs) and included several chemokine mediators and immune cells (**Table 3.2**).

3.4.6. Heatmap of DEGs

A cluster analysis of DEGs was performed for each tissue (head-kidney, duodenum, and skin) and a heatmap (*log 2* expression) was generated. The heatmap revealed the magnitude of the effect on gene transcription of LPS compared to the sham. The samples from the control and sham treated groups were clustered together and formed treatment specific sub-clusters and the samples from the LPS treated group formed an independent cluster for each of the tissues analysed. In the LPS challenged-group the number of up-regulated genes was higher (64%) than down-regulated genes in the head-kidney (**Figure 3.3 A**), but in the duodenum (**Figure 3.3B**) and skin (**Figure 3.3 C**) there were more down-regulated genes (62% and 61%,

respectively) than up-regulated genes. This indicates that head-kidney responded more strongly to LPS compared to the other two tissues.

a)

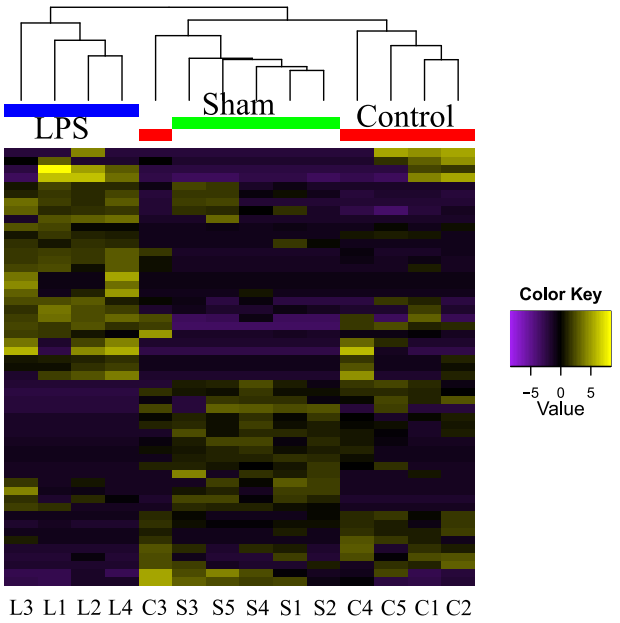

b)

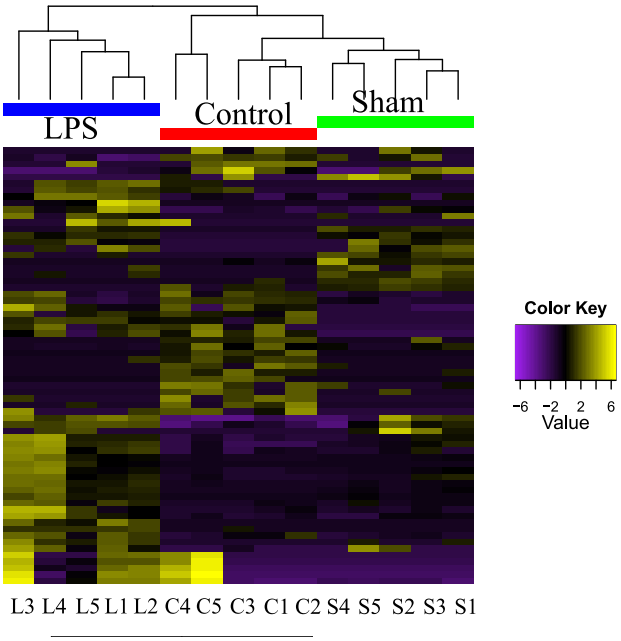

c)

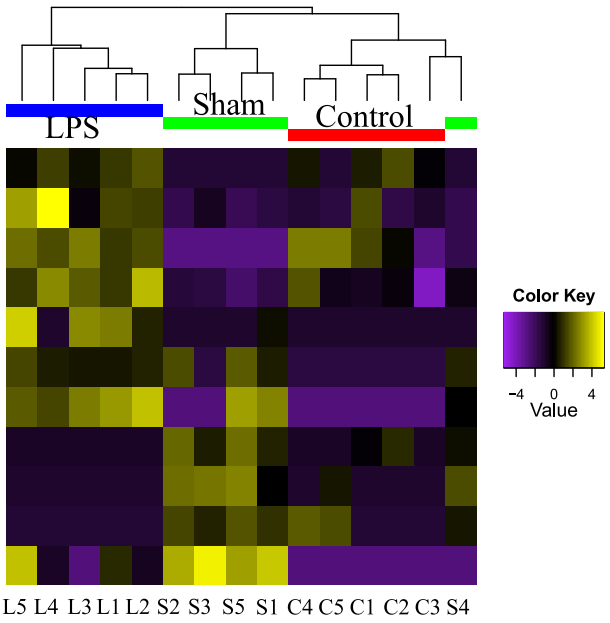

Figure 3.3. Heatmap generated from DEGs identified in the A) head-kidney, B) duodenum and C) skin transcriptomes of control, sham and LPS treated fish. The heatmap clustered DEGs (log2 expression) between control (C1-C5), sham (S1-S5) and LPS (L1-L4)- challenged fish in the three tissue transcriptomes (FDR < 0.05). The yellow colour in the gradient indicates up-regulation and the purple colour indicates down-regulation.

3.4.7. GO and KEGG orthology analysis of DEGs

DEGs were further analysed using GO and KEGG orthology analysis to gain insight into the main processes significantly modified in the head-kidney, duodenum, and skin transcriptomes between different treatments (FDR < 0.05, p < 0.05).

3.4.7.1. GO of control versus sham DEGs

Fisher's exact tests were applied to detect significantly over/under-represented immune-related GO terms in the tissue-specific transcriptomes (p < 0.05). Functional (GO) annotation of DEGs in C versus S treated transcriptomes identified 173 biological processes (BP), 198 cellular component (CC) and 130 molecular function (MF) categories in the head-kidney; 45 BP, 32 CC and 34 MF categories in the duodenum and 3 BP, 3 CC and 4 MF in skin (**Supplementary table 3.5**). The most enriched GO terms were related to translation and

transcription (BP, MF) in the head-kidney, metabolism (BP, MF) in the duodenum and DNA (BP, MF) in the skin (**Supplementary table 3.5**).

3.4.7.2. GO of sham versus LPS DEGs

Enriched GO terms in the DEGs of the transcriptomes of S versus LPS-challenged fish yielded 35 BP, 1 CC and 10 MF categories in the head-kidney (**Figure 3.4 A-C**, **Supplementary table 3.6**); 59 BP, 10 CC and 13 MF categories in the duodenum (**Figure 3.4 D-F**, **Supplementary table 3.6**) and 4 BP in the skin (**Figure 3.4 G**, **Supplementary table 3.5**). The most enriched GO terms in the head-kidney were related to protein modification and protein metabolism (BP) (**Figure 3.4 A**), NAD+ activity and NADP binding enzymes central to metabolism (MF) (**Figure 3.4 B**) and microtubule cytoskeleton (CC) (**Figure 3.4 C**). In the duodenum gene transcripts were related to interleukin-1 beta production, response to interleukin-6 and negative regulation of vascular permeability and formation of new blood vessels (BP) (**Figure 3.4 D**), extracellular molecule activity and binding (MF) (**Figure 3.4 E**) and structural and biochemical support to cells (CC) (**Figure 3.4 F**). The most enriched GO terms in skin were related to protein modification and progress of multicellular organisms (BP) (**Figure 3.4 G**).

a)

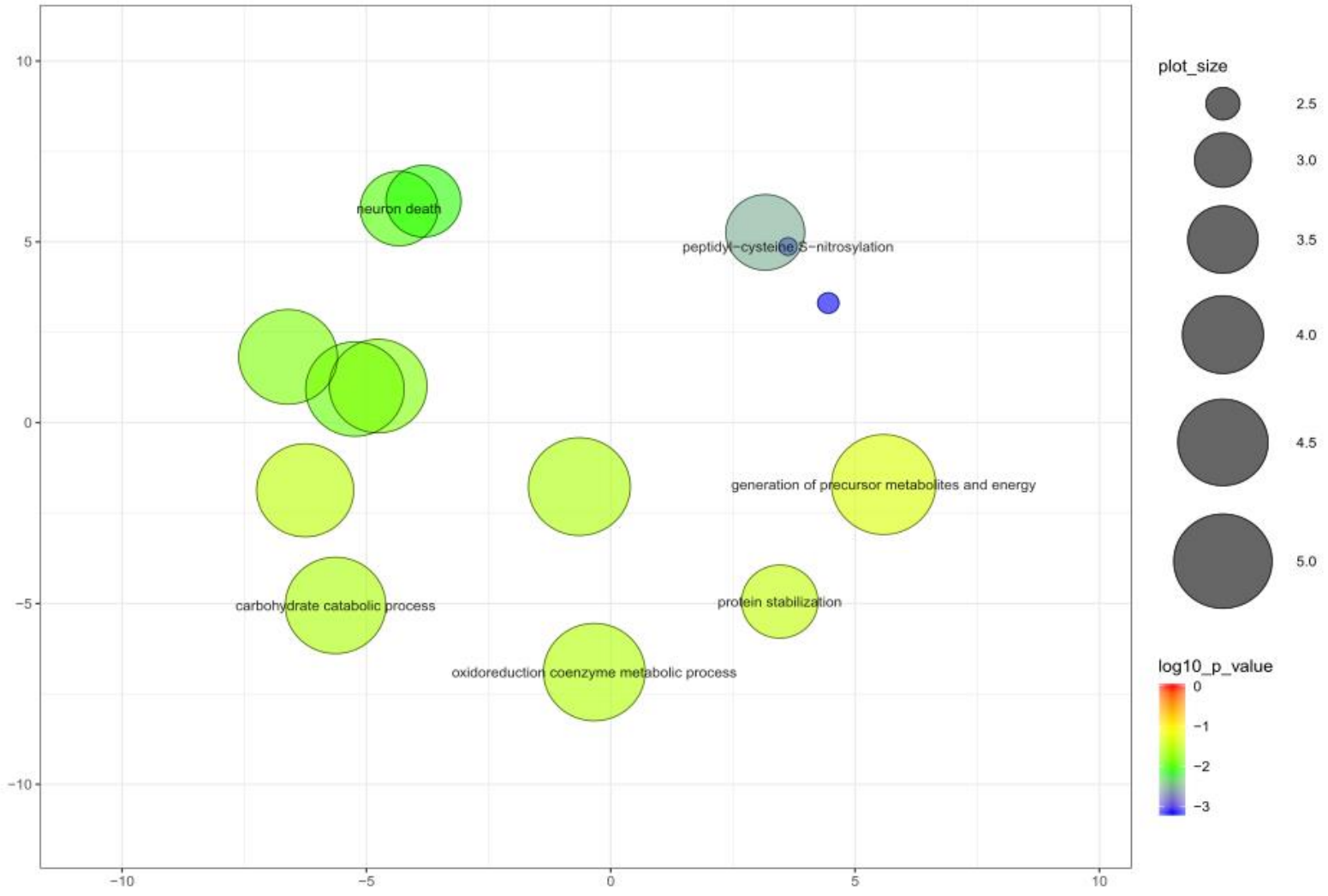
neuron death
peptidyl−cysteine S−nitrosylation
generation of precursor metabolites and energy
carbohydrate catabolic process
protein stabilization
oxidoreduction coenzyme metabolic process
10
5
0
−5
−10
−10
−5
0
5
10
plot_size
2.5
3.0
3.5
4.0
4.5
5.0
log10_p_value
0
−1
−2
−3

b)

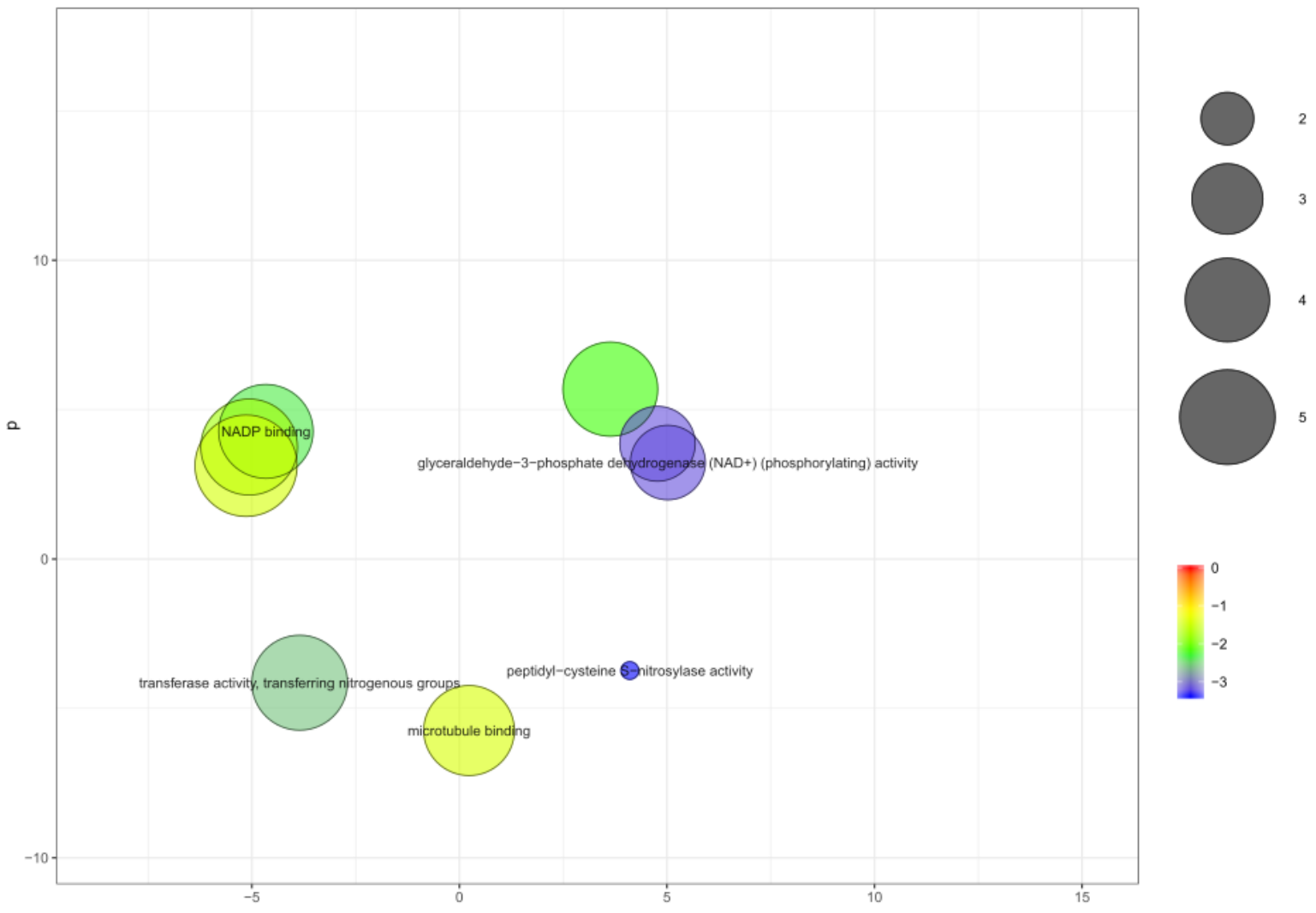
p
10
0
−10
−5
0
5
10
15
NADP binding
glyceraldehyde−3−phosphate dehydrogenase (NAD+) (phosphorylating) activity
transferase activity, transferring nitrogenous groups
peptidyl−cysteine S−nitrosylase activity
microtubule binding
2
3
4
5
0
−1
−2
−3

c)

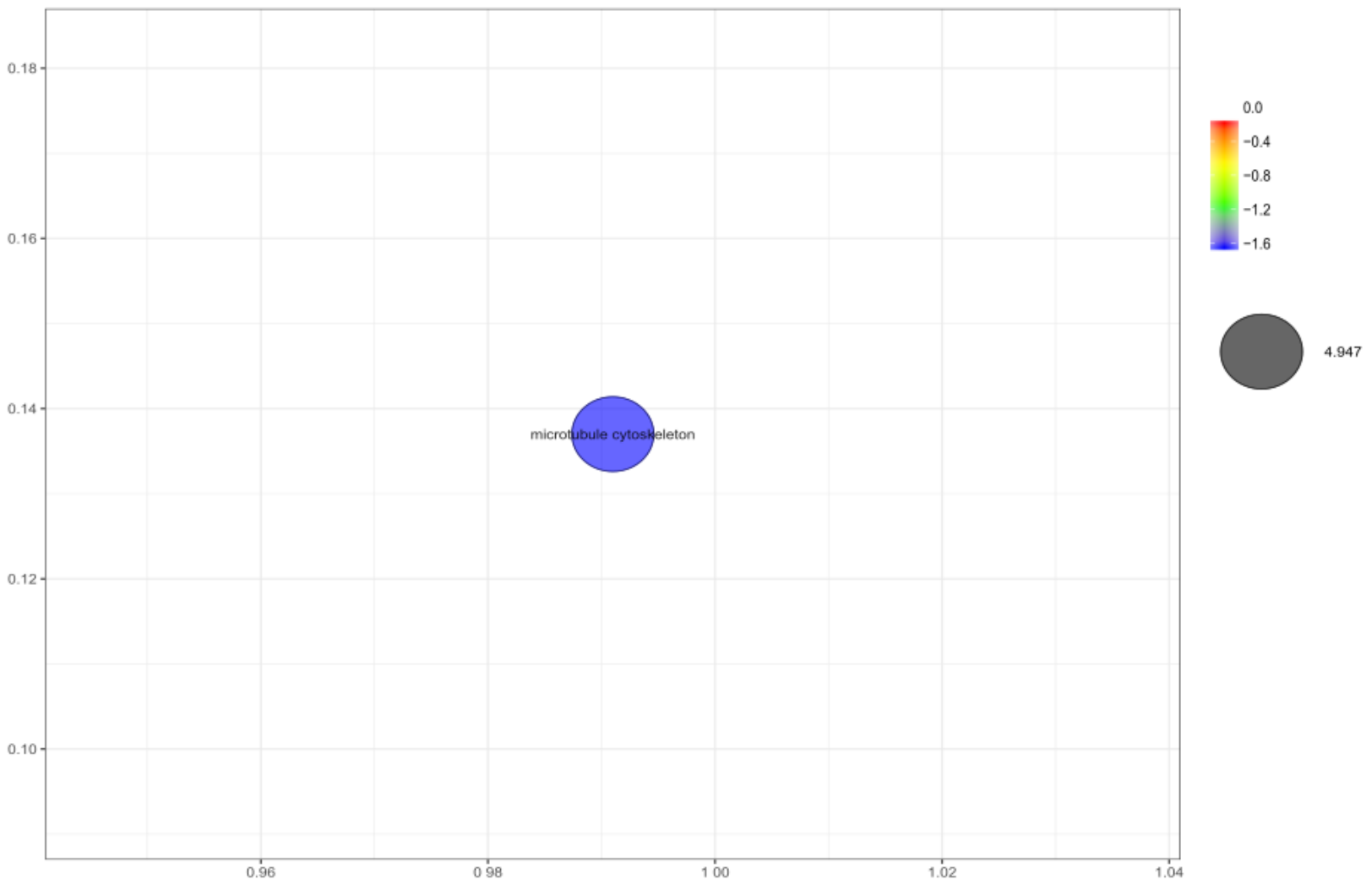
0.18
0.16
0.14
0.12
0.10
0.96
0 98
1 00
1.02
1.04
microtubule cytoskeleton
0.0
−0.4
−0.8
−1.2
−1.6
4.947

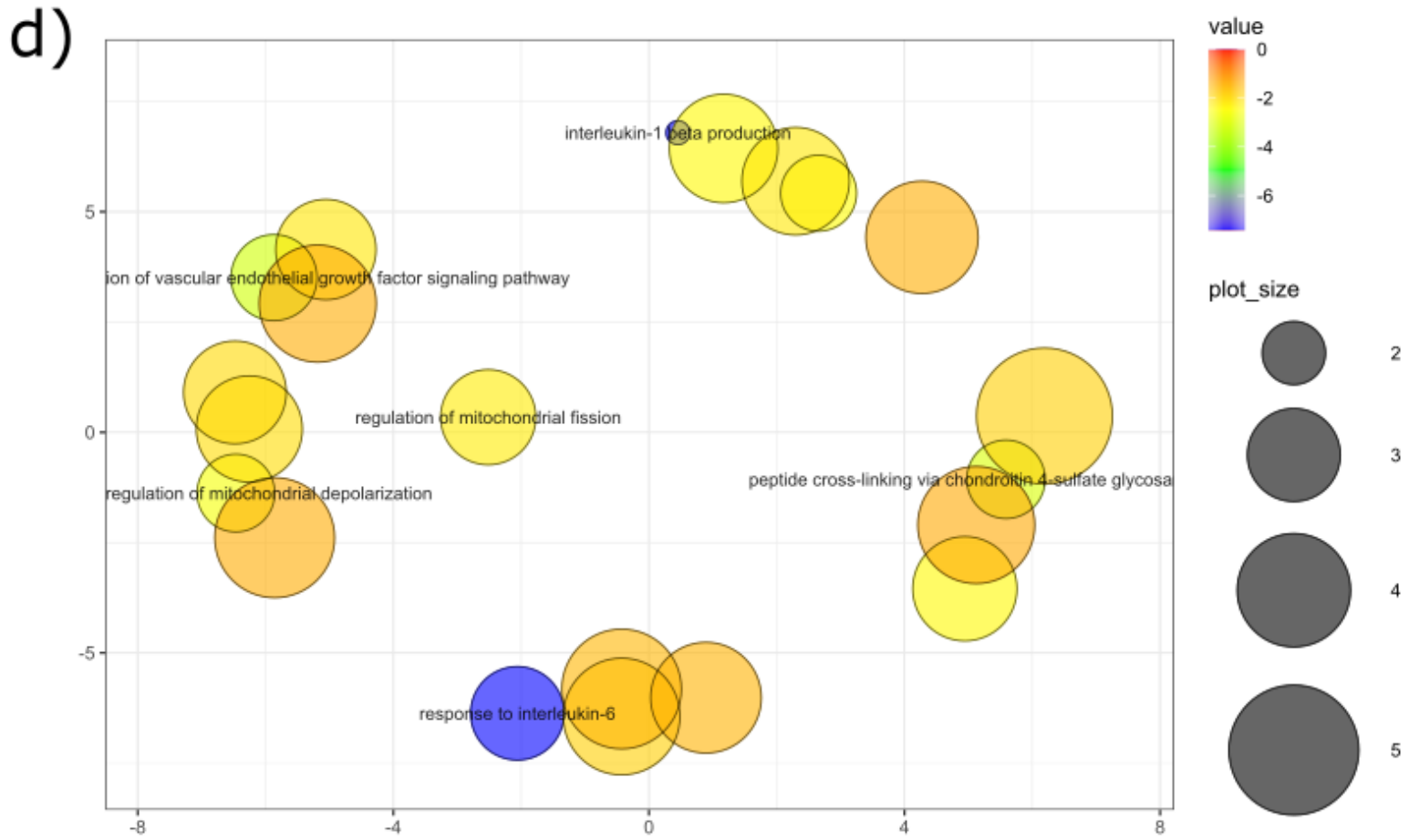
d)
interleukin-1 beta production
ion of vascular endothelial growth factor signaling pathway
regulation of mitochondrial fission
regulation of mitochondrial depolarization
peptide cross-linking via chondroitin 4-sulfate glycosa
response to interleukin-6
5
0
-5
-8
-4
0
4
8
value
0
-2
-4
-6
plot_size
2
3
4
5

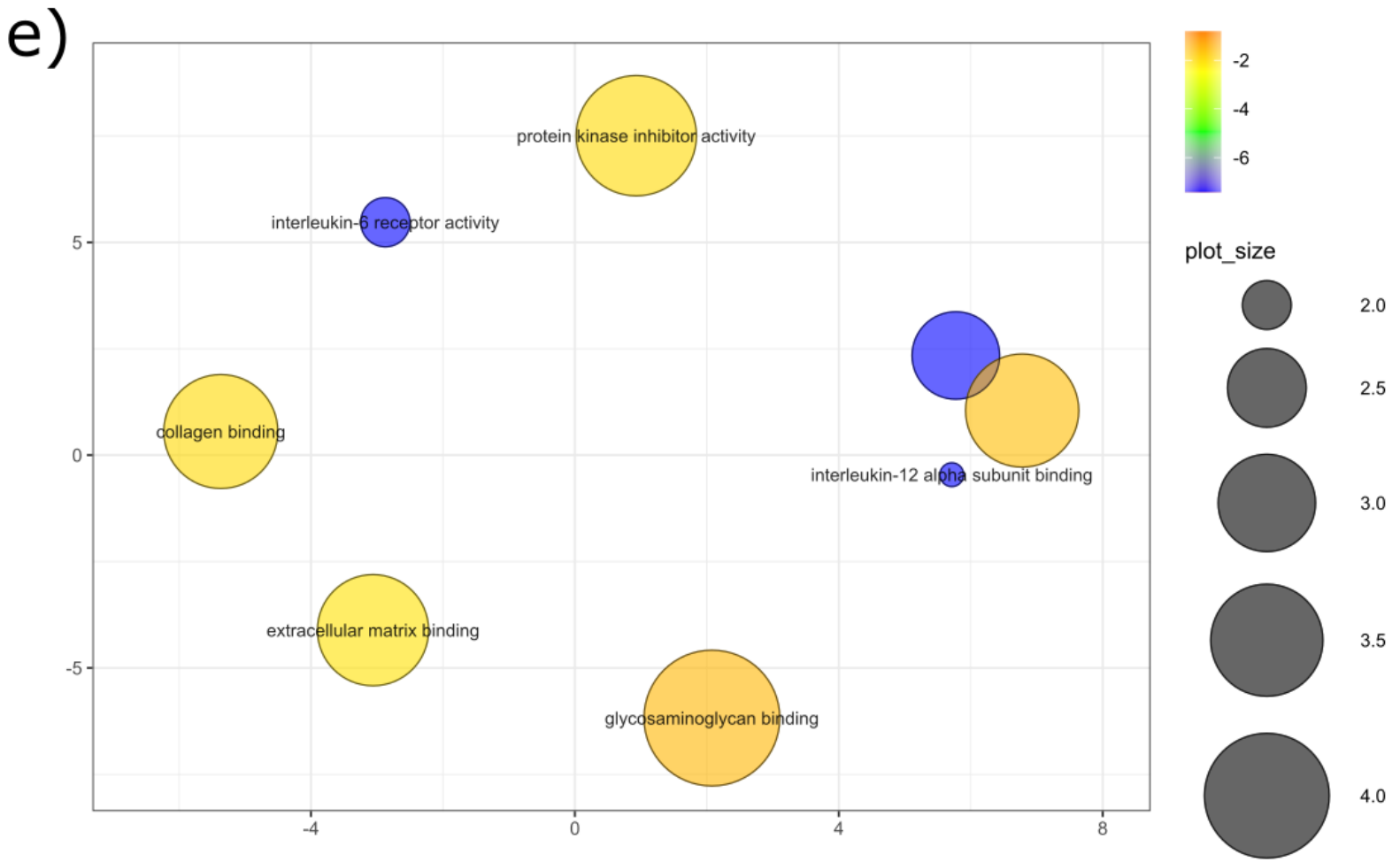
e)
protein kinase inhibitor activity
interleukin-6 receptor activity
collagen binding
interleukin-12 alpha subunit binding
extracellular matrix binding
glycosaminoglycan binding
5
0
-5
-4
0
4
8
-2
-4
-6
plot_size
2.0
2.5
3.0
3.5
4.0

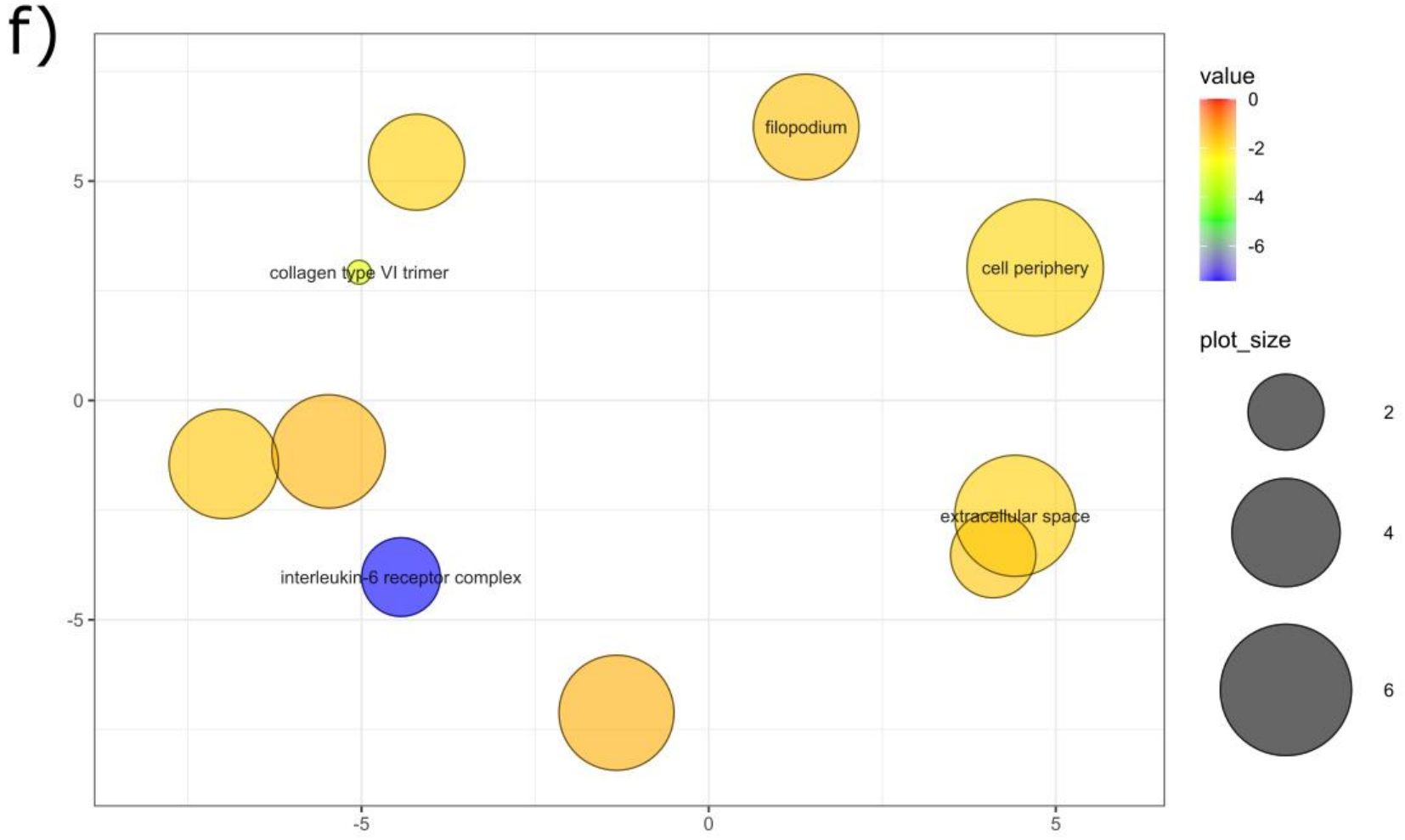
f)
filopodium
collagen type VI trimer
cell periphery
extracellular space
interleukin-6 receptor complex
5
0
-5
-5
0
5
value
0
-2
-4
-6
plot_size
2
4
6

g)

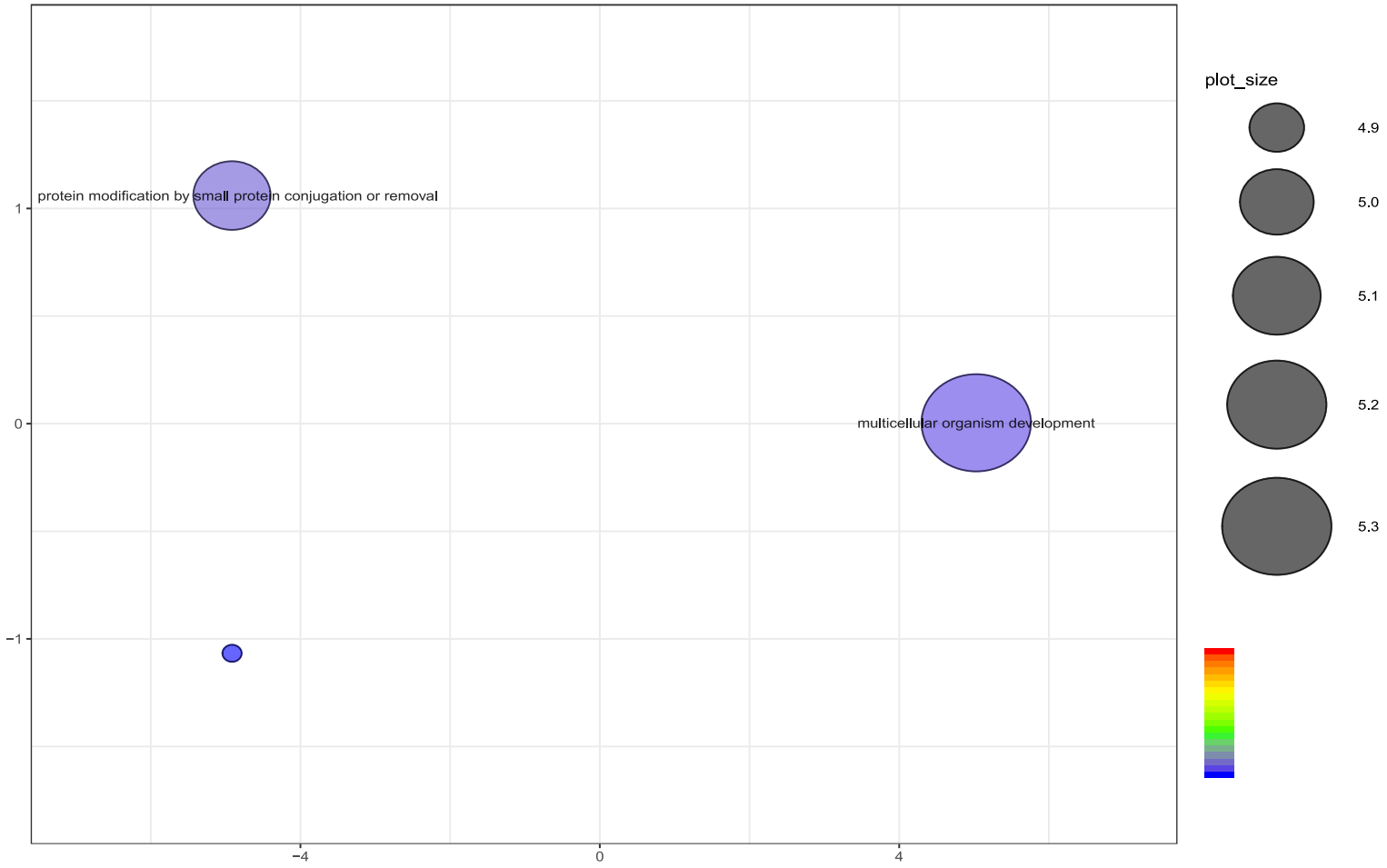
protein modification by small protein conjugation or removal
multicellular organism development
1
0
−1
−4
0
4
plot_size
4.9
5.0
5.1
5.2
5.3

Figure 3.4. Scatterplots generated using enriched GO terms of DEGs between the sham and LPS groups. Head-kidney: A) biological process (BP), B) molecular function (MF) and C) cellular component (CC). Duodenum: D) BP, E) MF and F) CC. Skin: G) BP. The scatterplots were generated using the DEGs (FDR < 0.05). The size of circles represents relative abundance (as a percentage of all DEGs in each category) and the colour gradient represents values of log10 (p-value). The vertical axis represents the semantic space y and the horizontal axis the semantic space x.

3.4.7.3. KEGG enrichment of control versus sham DEGs

KEGG enrichment analysis of DEGs in C versus S transcriptomes revealed that the five most enriched pathways represented in the head-kidney were: 1) ribosome, 2) adrenergic signalling in cardiomyocytes, 3) cardiac muscle contraction, 4) phagosome, and 5) B cell receptor signalling pathway (**Supplementary table 3.7 A**). For the duodenum the five most enriched KEGG pathways were: 1) protein digestion and absorption, 2) pancreatic secretion, 3) apoptosis, 4) IL-17 signalling and 5) cholinergic synapse (**Supplementary table 3.7 B**). In the skin, no enriched KEGG pathways were found (**Supplementary table 3.7 C**).

3.4.7.4. KEGG enrichment of sham versus LPS DEGs

For the DEGs identified from the comparison of S versus LPS-treatment four enriched KEGG pathways were identified in the head-kidney: 1) selenocompound metabolism, 2) biosynthesis of aminoacids, 3) other glycan degradation, and 4) other types of O-glycan biosynthesis (**Figure 3.5 A**, **Supplementary table 3.8 A**). For the duodenum the five most enriched KEGG pathways represented in the DEGs were: 1) protein digestion and absorption, 2) pancreatic secretion, 3) gastric acid secretion, 4) focal adhesion and 5) platelet activation (**Figure 3.5 B**, **Supplementary table 3.8 B-C**). For the skin, three enriched KEGG pathways were represented, 1) nucleotide excision repair, 2) RIG-I-like receptor signalling and 3) protein digestion and absorption (**Figure 3.5 C**, **Supplementary table 3.3 D**). It should be noted that some of represented pathways are linked to human diseases, as human was the model organism database reference. Although influenza A, viral myocarditis, and pertussis pathways are not directly relevant to fish they are still indicative of a response to pathogen. Furthermore, some of the genes involved are common to other pathways and therefore were not removed.

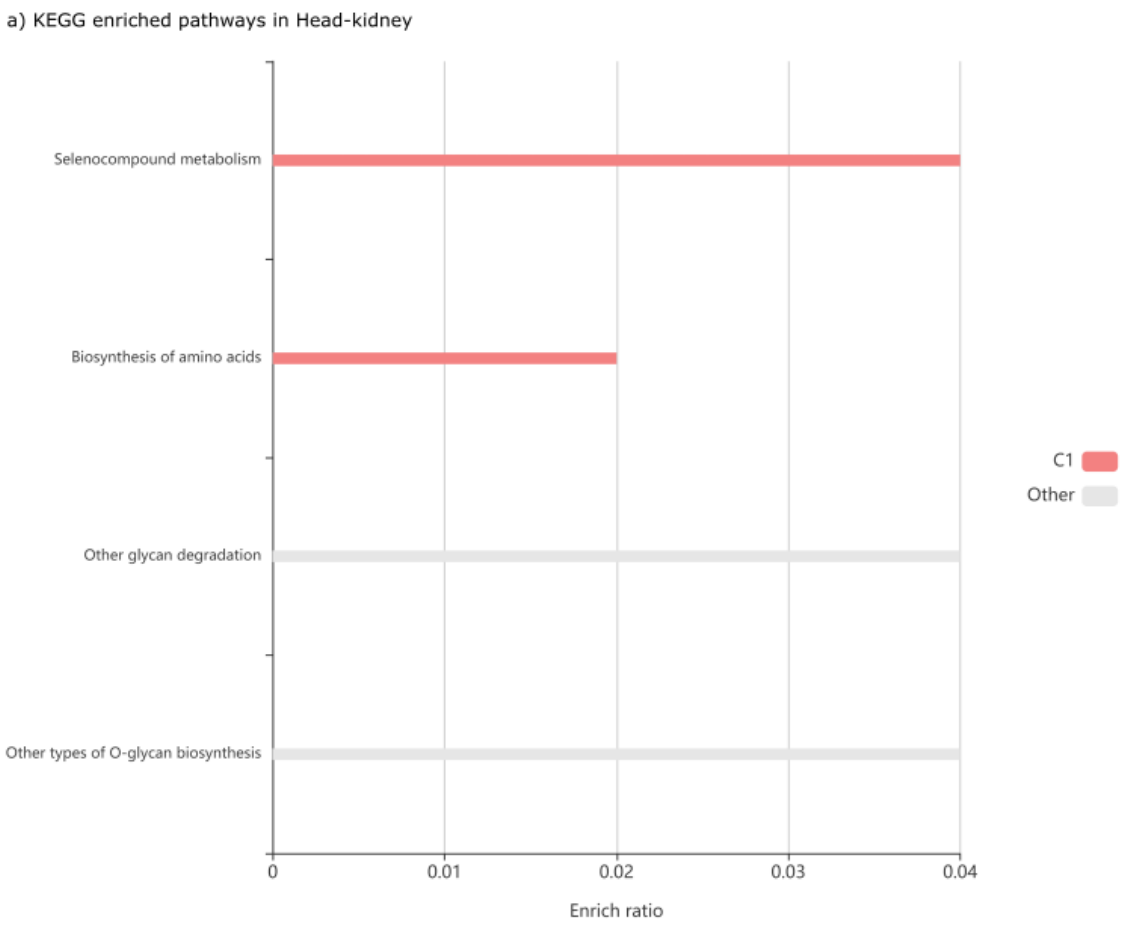
a) KEGG enriched pathways in Head-kidney
Selenocompound metabolism
Biosynthesis of amino acids
Other glycan degradation
Other types of O-glycan biosynthesis
0
0.01
0.02
0.03
0.04
Enrich ratio
C1
Other

b) KEGG enriched pathways in Duodenum

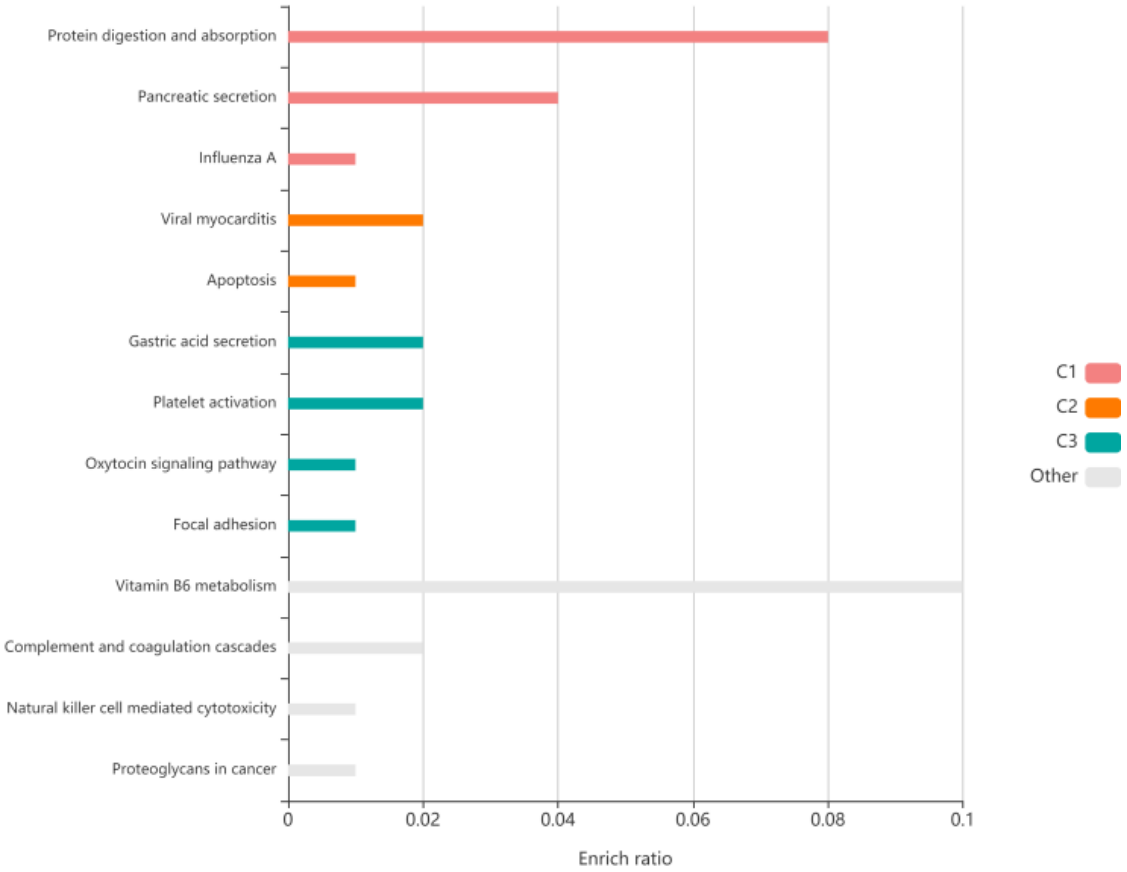

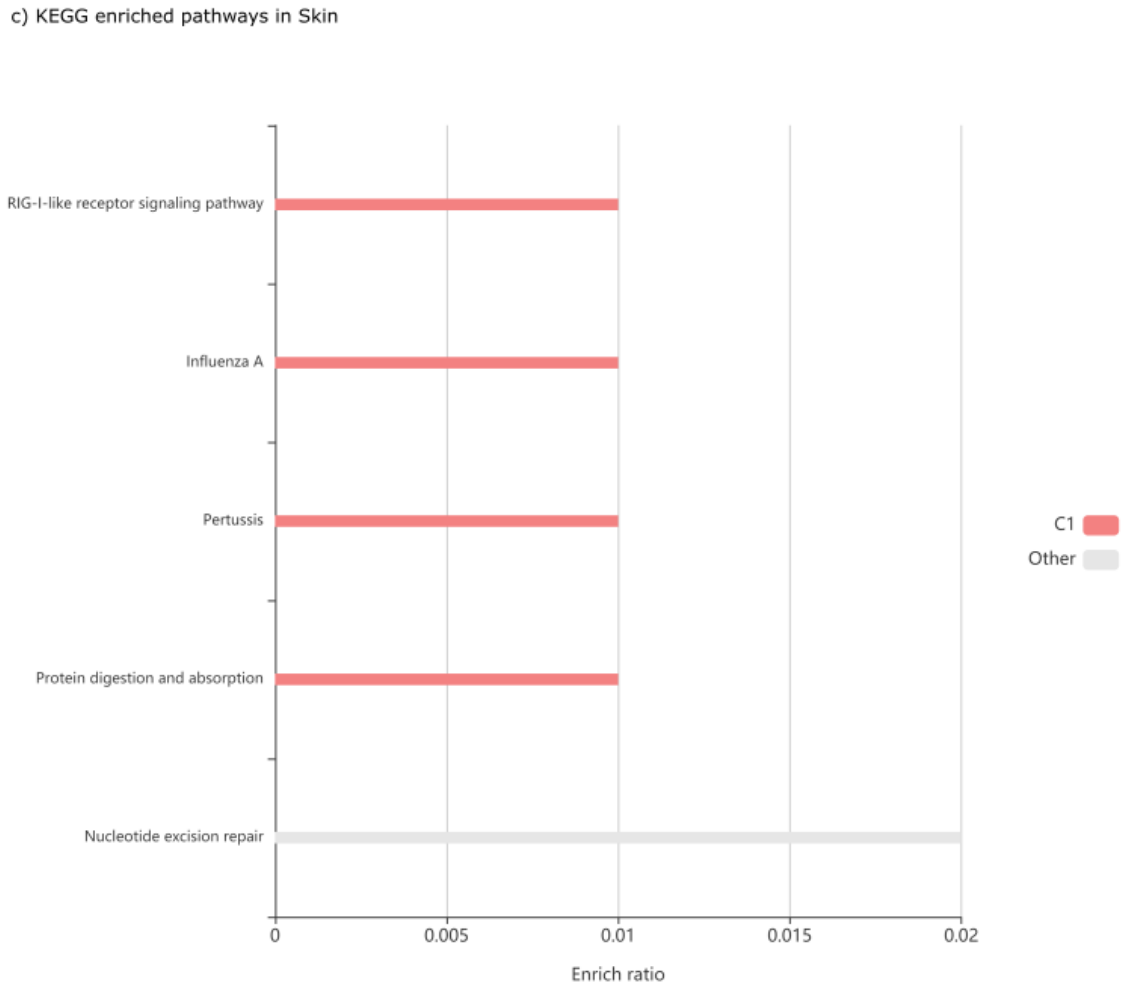

Figure 3.5. Bar plots of KEGG enriched pathways generated by DEGs between the sham and LPS groups. A) head-kidney, B) duodenum and C) skin. The bar plots were generated using the enrichment ratio (number of DEGs divided by the number of expected genes) of the KEGG pathways (FDR < 0.05). The colours represent the different pathways clusters (C1, C2, C3 and other).

3.5. Discussion

All the tissues, head-kidney, duodenum, and skin had modified tissue transcriptomes and in general the most modified processes were metabolism (up-regulated) and the immune system (down-regulated). The main transcriptional modifications in the immune process category were related to pathogen recognition via receptors like nucleotide-binding oligomerization domain-like (NOD) receptors and proteins of innate immunity against bacterial pathogens and interleukin 6. The modified transcriptional response was not mirrored by a modified systemic response as measured in the blood biochemical parameters. The common tissue specific DEG response elicited in samples from the 5 individuals further substantiated the notion that a conserved core response associated with *cis*- and *trans*- regulatory factors and metabolic energy production pathways occurred in *N. coriiceps*. Functional enrichment analysis of DEGs revealed that in the head-kidney nitric oxide signalling was most significantly modified, while in the duodenum, humoral innate compounds, respiration, and energy metabolism were enriched. The skin had a very low number of DEGs, and no immune parameters were represented, presumably due to the i.p. route of LPS exposure.

3.5.1. Biochemical indicators and LPS challenge

The similar levels of total plasma protein and cortisol in the control and LPS treated *N. coriiceps*, 7 days after treatment mirror observations in studies of Atlantic salmon (*Salmo salar*) exposed to LPS for 1 and 19 days (Langston et al., 2001). The high resistance and low response of fish to LPS has previously been assigned to the lack of the TLR4 recognition mechanism that in mammals mediates the down-stream immune activation, including TNF-α- and IL-1β-mediated inflammation (Berczi et al., 1966; Park and Lee, 2013; Swain et al., 2008). Based on previous studies of immunity in fish and shellfish in which an LPS challenge is administered we had anticipated a change in plasma lysozyme and antiprotease activity after i.p. LPS treatment in *N. coriiceps*. The lack of response to LPS detected in *N. coriiceps* has also been reported in gilthead sea bream (*Sparus aurata*) exposed to LPS for 24 hours when no change in antiprotease activity in blood sera was observed and in *Labeo rohita* exposed to LPS (20 EU kg^{-1}) for 7-15 days lysozyme activity was unchanged in blood sera from (Hanif et al., 2005;

Nayak et al., 2008). Taken together the results suggest that LPS is not always an effective stimulus of innate immunity in teleost fish.

A notable observation in control and LPS exposed *N. coriiceps* was the very low basal level of lysozyme activity in blood (50-90 $U.ml^{-1}$ at 22ºC) compared to other teleost species. For example, unstimulated lysozyme activity in plasma from European sea bass (*Dicentrarchus labrax*), included as a positive control in the present study was between 270 – 350 $U.ml^{-1}$, which was similar to previous studies assessing the effects of dietary manipulation on this enzyme (Obach et al., 1993; Yildiz and Altunay, 2011). In tilapia (*Oreochromis mossambicus*) plasma lysozyme varied between 770 - 1000 $U.ml^{-1}$ (at 22ºC) in fish fed different diets (Christybapita et al., 2007). The reason for the extremely low levels of plasma lysozyme detected in *N. coriiceps* was not established. Of note was the failure to detect gene transcripts for lysozyme in the tissue transcriptomes and this may be a consequence of low water temperatures. Support for this idea come from studies of the cold-water fish, *Brosme brosme* and *Gadus morhua*, in which lysozyme in the kidney was also very low, 40 and 150 U. ml^{-1}, respectively, (Lie et al., 1989). Other factors that may explain the low basal lysozyme activity in the wild captured *N. coriiceps* may be their overall physiological condition such as health status, diet and age (Simide et al., 2016).

The absence of a change in the plasma biochemical parameters in *N. coriiceps* exposed to LPS, may in part be due to the timeframe of the experiment (7 days post-i.p.), although the source of LPS may be a contributing factor. LPS is composed of an O-antigen polysaccharide, sugar and lipid A layers. The lipid A moiety varies with the species of gram-negative bacteria (Garate and Oostenbrink, 2013; Raetz, 1990) while O-antigen variations affect the virulence and infection process (Lerouge and Vanderleyden, 2002). Temperature has a substantial impact on the structure of LPS. This means the origin of the bacterial species, temperate or cold-waters, determines the thermal response of LPS (Kumar et al., 2002), as shown with bacterial LPS from the Siberian permafrost (Chattopadhyay, 2006) and confirmed with molecular dynamics (MD) simulations and nuclear magnetic resonance (NMR) spectroscopy (Wu et al., 2013). Since innate immune activation occurs through the recognition of microbe associated molecular patterns (MAMPs, (Akira et al., 2006) changes in LPS structure may interfere with host - bacteria recognition. We hypothesize that since the phenol isolated LPS used in the present study was from *E. coli* of temperate regions the relatively low biochemical and transcriptional response of *N. coriiceps* relative to other studies with temperate teleost fish species (Lulijwa et al., 2019; Watzke et al., 2007; Zoccola et al., 2017) might be linked to structural changes in

LPS caused by low temperature. This notion seems to be supported by the absence of response for serum lysozyme since modified interactions of LPS with immune related molecules also affect the efficacy of humoral mediator recognition (Ohno and Morrison, 1989). Interestingly, when *N. coriiceps* was exposed to fragmented, heat killed *E. coli 0111:B4* (HKEB, 1×10^7/mL; InvivoGen, San Diego, CA), a strong transcriptional response of toll-like receptors (TLR) occurred at 6 and 12 h post-challenge in the spleen but not in the liver or kidney (Ahn et al., 2014). Overall, a combination of the duration of the experiment, route of administration and source and form of LPS may explain the low response.

3.5.2. LPS as an immune challenge in teleost fish

The literature was surveyed to establish the LPS utilized in studies of the immune response in teleost fish and revealed a wide diversity of *E. coli* strains were the source of LPS and this may explain the sometimes-divergent results reported. For example, *E. coli O55:B5* (Bi et al., 2018; Bonneaud et al., 2016; Congleton and Wagner, 1991; Haukenes and Barton, 2004; Li et al., 2020b; Lu et al., 2018; Lulijwa et al., 2019; Nayak et al., 2008; Watzke et al., 2007), *E. coli B5:55* (Langston et al., 2001), *E. coli O111:B4* (Li et al., 2020c; Lu et al., 2018; Lulijwa et al., 2019; Martínez et al., 2020; Watzke et al., 2007; Zoccola et al., 2017), *E. coli O127:B8* (Jiang et al., 2020; Watzke et al., 2007), and *E. coli O26:B6* (Liu et al., 2016; MacKenzie et al., 2008; Xie et al., 2020) (Supplementary Table 9) have been used to assess immune activation in a diversity of teleost fish. In addition, some studies used heat-killed bacteria such as *E. coli O111:B4*, *Vibrio anguillarum O1*, *Vibrio harveyi*, *Aeromonas hydrophila*, and *Francisella noatunensis subsp. Orientalis* (fno) as a source of LPS (Ahn et al., 2014)(Cai et al., 2018; Christybapita et al., 2007; DALMO and SELJELID, 1995; Maekawa et al., 2021). Furthermore, in some studies the source of LPS or the *E. coli* serotype is not specified, making comparative analysis of the results in different fish species difficult (Abdel-Mageid et al., 2020; Hanif et al., 2005; Ko et al., 2017; Li et al., 2020c; Liu et al., 2018; MacKenzie et al., 2006; Palstra et al., 2018; Qin et al., 2020; Wang and Han, 2013).

The divergent response of fish to LPS has previously been assigned to the route of administration (i.p. or immersion), time of exposure (exposure time - hours to days), concentration (10 μg ml^{-1} to 6 mg kg^{-1}), the analytical approach (transcriptomic, serum assays or candidate genes), the fish species (temperate to cold adapted) and the developmental stage

(eggs to adults). A factor generally overlooked is the source and form of LPS and the possible consequence of temperature on its structure, and immune recognition (**Supplementary table 3.9**). Additional factors that limit comparisons of experiments with LPS in fish is the variety of analytical approaches and the candidate genes selected for analysis. For example, in *N. coriiceps* and *N. rossii* the LPS was administered i.p. and a candidate gene approach revealed the hypoferraemic response was modified (Martínez et al., 2020) (**Supplementary table 3.9**). Similarly, in *Ctenophcuyngodon idellus* exposure to LPS i.p. increased the expression of adiponectin receptors in the liver (Qin et al., 2020) and in *Trachinotus ovatus* a candidate gene approach revealed that i.p. exposure to LPS (O26:B6) provoked increased p65 (Xie et al., 2020). Of note is that some responses to LPS are strongly conserved irrespective of its origin, the species, or the analytical approach and this is the case for the hypoferraemic response in *N. coriiceps* and *N. rossii* (LPS from *E. coli O111:B4*), in *Oncorhynchus mykiss* (LPS from *E. coli* O55:B5) and in *Salmo salar* (LPS from *E. coli B5:55*) (Congleton and Wagner, 1991; Langston et al., 2001; Martínez et al., 2020).

3.5.3. The transcriptional response of teleosts to LPS

Recently several transcriptome studies have described the immune response to LPS in aquaculture fish species (*Lates calcarifer*, *Pelteobagrus fulvidraco*, *Salmo salar*, *Ictalurus punctatus*, *Schizothorax prenanti*) (Jiang et al., 2020; Li et al., 2020c; Liu et al., 2018; Palstra et al., 2018; Zoccola et al., 2017). However, transcriptome studies are far less frequent in wild fish like *N. coriiceps* and unlike the present study where the immune response of 3 tissues was analysed, previous studies have generally focused on a single immune tissue (MacKenzie et al., 2008; Palstra et al., 2018). Some transcriptome studies have analysed the immune repertoire without challenge, for example the Siamese fighting fish (*Betta splendens*) and identified immune-related genes and antimicrobial peptides (Amparyup et al., 2020). Overall, although the approach, the source of LPS and the species differed in transcriptome studies some common immune related responses occurred and this has contributed to understanding the immune response in advanced teleosts.

A large spectrum of protocols has been deployed to assess the immunostimulatory effects of LPS using whole tissue transcriptomes in teleost fish. In our study of *N. coriiceps* i.p. injection was selected as this was the most common procedure in other studies although the

experimental time course (7 days) differed from other studies where fish were killed 12 – 24 h after LPS exposure. Previous transcriptome studies using LPS were focused on different aquaculture species, *Lates calcarifer* (Zoccola et al., 2017), *Eptatretus burgeri* (Suzuki et al., 2004), *Ictalurus punctatus* (Liu and Jiang, 2020) and *Schizothorax prenanti* (Li et al., 2020c). Although studies of *Epinephelus fuscoguttatus* (Cai et al., 2018) and *Oreochromis niloticus* (Maekawa et al., 2021), used the pathogens *Vibrio harveyi* and *Francisella noatunensis* (*subsp. Orientalis*), respectively. The transcriptome results were highly variable between studies, but some common responses were found in relation to immunity that were also observed in *N. coriiceps*, although they tended to be tissue specific. Examples of this were modified iron metabolism, innate cellular responses (e.g. phagocytic activity), pathogen recognition receptors (Toll-like, C-type lectin) and innate humoral mediators like lysozyme, CXCL2-like chemokine and complement (Cai et al., 2018; Jiang et al., 2020; Li et al., 2020c; Liu et al., 2018; Maekawa et al., 2021; Palstra et al., 2018; Zoccola et al., 2017). Overall, the number and characteristics of DEGs of immune related gene transcripts varied substantially from study to study.

Transcriptome studies in Antarctic fish have mainly focussed on how their unique physiology evolved through gene and genome evolution. The earliest studies of Antarctic fish transcriptomes were based on expressed sequence tags (ESTs, (Chen et al., 2008)), but more recently NGS has extended the repertoire of tissues (liver, brain, gill), species (*N. coriiceps*, *Chaenocephalus aceratus* and *Pleuragramma antarcticum*) and the depth of the transcriptomes obtained (Shin et al., 2012, 2014). In a study of the head-kidney transcriptome of *T. bernacchii* gene ontology approaches were used to catalogue immune related gene contigs and the most highly represented processes were, the innate immune response (971), the inflammatory response (428), and the immune response (403) (Huth and Place, 2013). A comparative study of liver and brain between *C. aceratus, P. antarcticum* and *N. coriiceps* revealed that these fish possess more ubiquitin-conjugated proteins and this was linked to their importance in maintenance of proteins in their native conformation in an extremely cold-environment (Shin et al., 2012).

Studies of wild fish exposed to an immune challenge are infrequent due to the logistical difficulties linked to their capture and maintenance and the greater number of individuals required because of their genetic diversity and more variable response. Furthermore, when working in isolated regions such as the Antarctic there are experimental limitations dictated by conservation guidelines and the restricted infrastructures in field stations and transport logistics. This explains why few studies of the immune response exist in Notothenioidei. In the present

study the main response in the head kidney of *N. coriiceps* exposed for 7 days to LPS was modified cellular energy metabolism and energy production as well as S-nitrosylation (protein modification for signal transduction and functional regulation). These findings were coherent with previous results in an aquaculture species, the trout (*Oncorhynchus mykiss*), which also had a preponderance of modified gene transcripts linked to energy and metabolism 24-72 hours after i.p. LPS injection (MacKenzie et al., 2008). The increase in transcripts linked to energy metabolism, clearly reflects the energy demanding characteristics of the immune response and explains the poor growth of fish exposed to chronic stress or infections (Abdel-Tawwab et al., 2019; Bonneaud et al., 2016).

3.5.4. The transcriptional response to LPS in N. coriiceps

The immune response to LPS was tissue-specific, and much lower in the skin compared to the other tissues presumably due in part to the i.p. route of administration (**Figure 3.6 A-B**). Nevertheless, there was a conserved core response in the immune-related DEGs of the head kidney and duodenum, which encompassed pathogen-recognition receptors (PRRs) namely a NOD-like receptor (*nlrc3*), transmembrane protein 30A (*tmem30a*) that stimulates phagocytosis and humoral defence-related factors, bactericidal permeability-increasing protein-like (*bpi*) and type I interferon stimulated gene (*ifi44l*). Head kidney- enriched pathways were essentially related to aminoacids and selenocompound metabolism but the immune specific DEGs falling within the same general categories were mannose receptors (*mrc1*) and for the humoral response pyrin-like (*mefv*) and peptidoglycan recognition proteins (*pgrp-lbl*). The down-regulated DEGs were related to the inflammatory response and included the *IL-6 receptor* and PRRs (*nlr* and *mrc* receptors) particularly in the head-kidney and duodenum (**Figure 3.6 B**). Pathogen recognition (LPS) in *N. coriiceps* diverged from the more commonly described *tlr* in other teleost fish (Liu et al., 2016) and instead *nlr* and *mrc* receptor genes were more responsive and presumably play a more prominent role.

The *tmem30a* gene is poorly studied in fish, however several studies showed that LPS modify this gene expression in mammals (Hong et al., 2020; Yang et al., 2009). NOD-like (NLR) receptors are relatively well-studied intracellular sensors of PAMPs in mammals (Cell et al., 2017; Fritz and Girardin, 2005). In teleosts like *Scophthalmus maximus L.*(Hou et al., 2017) and *Larimichthys crocea* (Dong et al., 2016), exposure to bacteria was reported to modify

*nlr*3 and *mrc1,* respectively. While in the teleosts *Miichthys miiuy*, *Paralichthys olivaceus* and *Cirrhinus mrigala*, exposed to a pathogen, *nod1* was modified as part of the antibacterial defence response (Chu et al., 2021; Li et al., 2015; Park et al., 2012; Swain et al., 2013). Changes in the humoral response due to bacterial pathogen exposure was reported in *Ictalurus punctatus* (Xu et al., 2005) and *Megalobrama amblycephala* (Tang et al., 2015) where in common with what was observed in *N. coriiceps bpi* was modified. Similarly, peptidoglycan recognition proteins (e.g. *pgrp-lbl*), that bind multiple components of bacteria are a well characterized part of the innate humoral response in *Danio rerio* (Li et al., 2007) and *Cyprinus carpio L.* (Zhang et al., 2019). *Ifi44l*, is more typically associated with a viral challenge in *Danio rerio* (Briolat et al., 2014) and its presence in both head kidney and duodenum suggests it also responds a bacterial stimulus (LPS). Overall, although the transcriptional response of *N. coriiceps* to i.p. LPS was not identical to that of other teleosts exposed to bacterial pathogens, the recruitment of PRRs for pathogen identification and humoral factors for pathogen neutralization is a well-conserved response.

The DEGs identified in the mucosal-associated lymphoid tissues, the duodenum and skin, had little in common except for the enriched pathway related to protein digestion and absorption and the *nlrc3* gene, which was upregulated by LPS in all three tissues suggesting it is important for bacterial recognition (**Figure 3.6 B**). Despite *nlrc3* being poorly studied, *nlrc3* expression has been shown to change after LPS stimulation,namely in head kidney cells of *Paralichthys olivaceus* and *Lates calcarifer* (Li et al., 2016; Paria et al., 2016). The duodenum had the highest number of DEGs of all the tissue analysed probably due to direct and continuous exposure to LPS. Most DEGs belonged to highly enriched pathways linked to the immune system particularly to the platelet activation, complement and coagulation cascades. The most notably modified process in *N. coriiceps* duodenum was mitochondrial depolarization linked to the protein digestion and absorption pathway, which has not previously been reported in fish under LPS exposure. It is possible that this reflects the higher cellular mitochondrial density in the Antarctic fish (O'Brien and Sidell, 2000), but it may also be related to the upregulation in the duodenum of inflammasome immune related genes, such as *nlrp3*, which have been associated with mitochondrial depolarization and mitophagy in mammals (Gurung et al., 2015). In *Danio rerio*, *nlrp3* is involved in cytokine processing and secretion (Li et al., 2020a), and a similar relationship probably exists in *N. coriiceps* as an elevated number of DEGs for cytokines occurred in the LPS exposed duodenum, as well as a gene for signal transduction (*il6st*) that respond to a bacterial challenge (Reyes-Cerpa et al., 2012). Also, metabolic pathways linked to

pancreatic secretion and vitamin B6 were highly enriched. Vitamin B6 was previously reported in mice as inhibitor of macrophage activation in order to prevent LPS-induced infection (Shan et al., 2020). Curiously, in the skin some DEGs were linked to mitochondrial function and more specifically the generation of reactive oxygen species (ROS), a process linked with the inflammatory response in fish were modified (Ko et al., 2017; Lulijwa et al., 2019). In line with this increased ROS generation occurred in *Lobeo rohita*, after 7 and 15 days exposure to LPS (Nayak et al., 2008). A characteristic transcriptional response to bacterial exposure in a variety of teleost fish is upregulation of complement (**Supplementary table 3.9**) and this was evident in DEGs of the duodenum but not the other tissue of *N. coriiceps* (**Figure 3.6 B**).

The results of the present study contrasted with those of (Ahn et al., 2014) on the same species, and where several Tlr genes were found to be up-regulated in liver, spleen and kidney after *N. coriiceps* were immersed in heat killed *E. coli* (HKEB) for 6-12h (Ahn et al., 2014). Although the two studies are not directly comparable due to mode and duration of the challenge, that the different source and corresponding difference in structure of LPS may explain the lack of *tlr* response of our study. The same authors also assessed the transcriptional changes in pooled livers from *N. coriiceps* immersed in HKEB for 12h. They identified 567 DEGs in liver and the most enriched immune related processes were the antigen processing and presentation pathway and TLRs related pathways, TNF pathway, T cell receptors, B cells, interleukins and chemokines (Ahn et al., 2016). Although, there was little overlap in DEGs between the previous and the present study some common processes were identified: antigen processing and presentation in skin, chemokines in the head-kidney and interleukins in both skin and duodenum. The results from the present and the previous transcriptome studies revealed that despite inhabiting freezing waters *N. coriiceps* responded rapidly to an immune challenge and that overall, there was a conserved response with other teleosts. Furthermore, a tissue-specific response to LPS occurred and a strong metabolic component was detected in common with a microarray study of trout (MacKenzie et al., 2008). A unique facet of the response to LPS in *N. coriiceps* was up-regulation of genes linked to mitochondria possibly linked to their importance in the adaptation to life in sub-zero conditions.

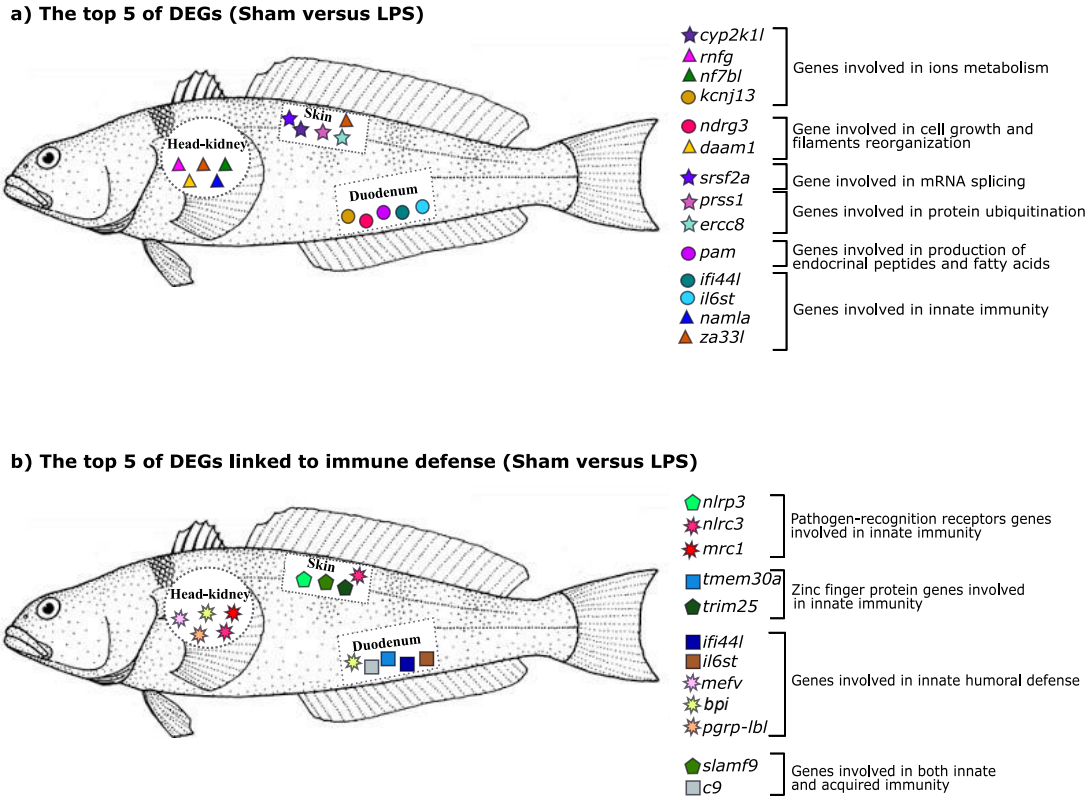

Figure 3.6. Comparison of A) overall DEGs and B) DEGs linked to immune defence in three tissue transcriptomes between Sham and LPS groups. The coloured symbols represent the top 5 genes for each tissue involved in A) several processes (listed on right) and B) immune processes (listed on right). The genes with significantly higher expression are labelled on the corresponding tissues. Cytochrome P450 2K1-like (*cyp2K1l*), RFNG O-fucosylpeptide 3-beta-N-acetylglucosaminyltransferase (*rfng*), nuclear factor 7-brain like (*nf7bl*), potassium inwardly rectifying channel subfamily J member 1b (*kcnj13*), Protein NDRG3 (*ndrg3*), disheveled-associated activator of morphogenesis 1-like (*daam1*), serine and arginine rich splicing factor 2a (*srsf2a*), trypsin-1 (*prss1*), excision repair cross-complementation group 8 (*ercc8*), peptidylglycine alpha-amidating monooxygenase (*pam*), interferon-induced protein 44-like (*ifi44l*), interleukin-6 receptor subunit beta (*il6st*), pyrin-like (*mefv*), zinc-binding protein A33-like (*za33l*), NACHT, LRR and PYD domains-containing protein 3 (*nlrp3*), NLR family CARD domain-containing protein 3 (*nlr3c*), macrophage mannose receptor 1 (*mrc1*), tripartite motif-containing protein 39 (*trim39*), cell cycle control protein 50A (*tmem30a*), bactericidal permeability-increasing protein (*bpi*), peptidoglycan-recognition protein LB-like (*pgrp-lb*), SLAM family member 9 (*slamf9*) and complement 9 (*c9*) [*Notothenia coriiceps* image credit: Tony Ayling from FishTEDB database].

3.6. Conclusion

This study demonstrated that LPS (*E. coli* O111:B4) exposure did not provoke a systemic immune response in the Antarctic *N. coriiceps*. However non-immune processes linked to energy metabolism, mitochondrial polarization and protein ubiquitination were mostly

up-regulated in skin, head-kidney, and duodenum transcriptomes after 7 days of i.p. injection which suggests tissue-specificity.

Pathogen detection was not stronger that explains the lower number of immune genes changed possibly linked to the LPS structure used (originated from a temperate region) which may suggest an adaptation of *N. coriiceps* immune defence to the LPS structure from cold bacteria specific of this extreme environment. The immune components identified were mostly down-regulated highlighting the NOD-like receptors (NLRs) and mannose receptors (MRCs) which are poorly studied in teleosts. This finding is interesting because the Toll-like receptors are the principal pathogen recognition receptors usually reported as very responsive to this bacterial endotoxin defence in teleosts. Our findings suggest that NLRs and MRCs may have an important role in LPS recognition in *N. coriiceps* and lead us to hypothesize that both may had adapted to the cold and unique Antarctica environment.

I propose two models that summarizes the up-regulated (**Figure 3.7**) and down-regulated (**Figure 3.8**) processes and components according to our DEGs, KEGG and GO enrichment analysis in response to LPS. In the up-regulated model the three tissues (skin, head-kidney and duodenum) are respond through and increase in proteins digestion, where aminoacid metabolism, leads to the antigen presentation that in turn signal cells to activate immune cells. The mitochondria have multiple roles linked to energy production but also as signalling organelles contributing to cell proliferation, cell death, cell differentiation and to establish immune cells phenotypes and their functions (**Figure 3.7**). In the down-regulated model, all tissues are involved in immune defence through several humoral components and transcription factors (**Figure 3.8**). The two models are linked and suggest that *N. coriiceps* are still responding to LPS, however the production of humoral components are inhibited which indicate a homeostasis balance to return to normal (unstimulated) condition.

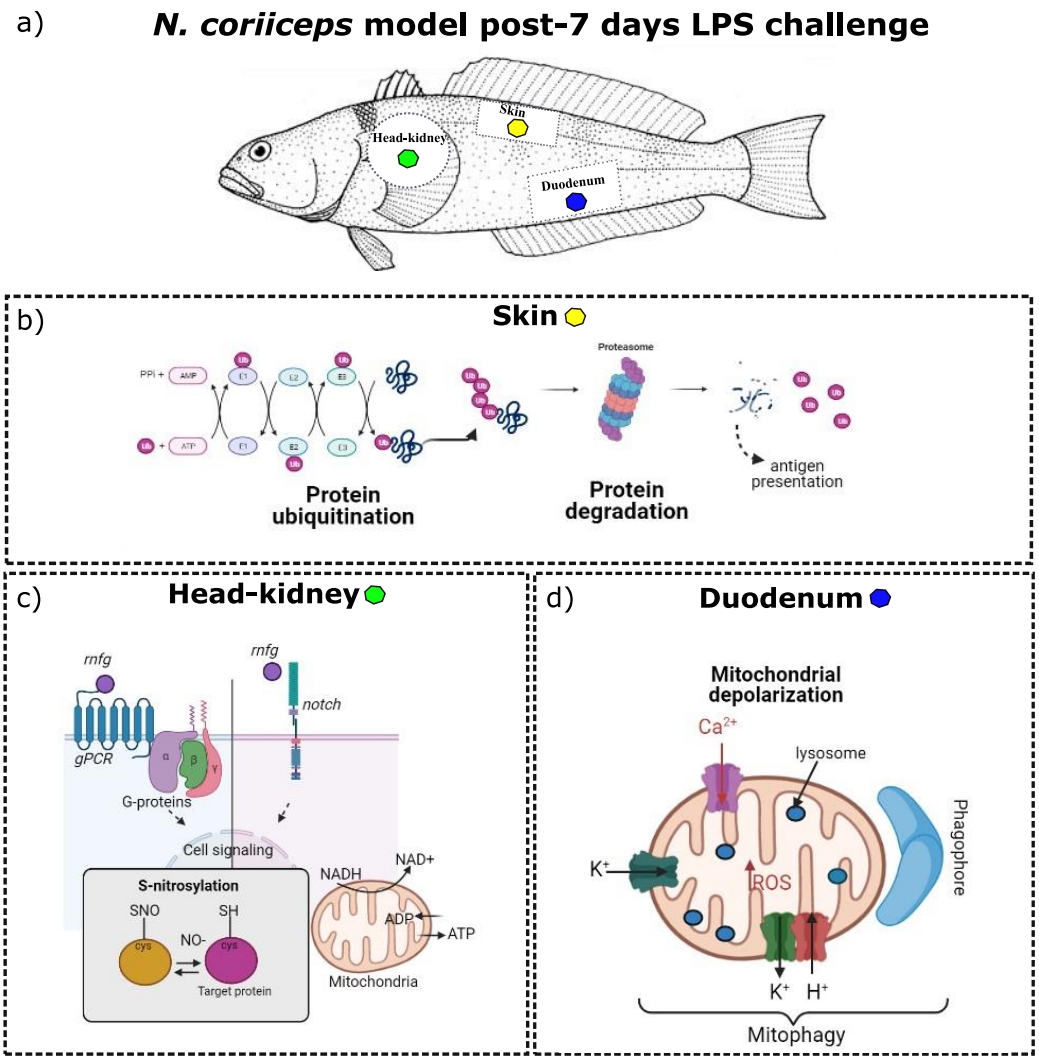

Figure 3.7. A) ***N. coriiceps*** **model of up-regulated DEGs functions in B) skin, C) head-kidney and D) duodenum after LPS treatment.** The coloured symbols represent the different tissues, yellow – skin, green – head-kidney and blue – duodenum. Protein-protein interactions (PPi), ubiquitin (ub), enzymes ubiquitin thioester (E1-E3), RFNG O-fucosylpeptide 3-beta-N-acetylglucosaminyltransferase (*rfng*), G-protein coupled receptors (*gpcr*), S-nitrosylation (SNO), no reaction with cysteine thiol group (SH), nitric oxide (NO), cysteine (cys), calcium ion (Ca^{2+}), potassium ion (K^{+}), hydrogen ion (H^{+}), adenosine diphosphate (ADP), adenosine triphosphate (ATP), nicotinamide adenine dinucleotide oxidized form (NAD^{+}) and nicotinamide adenine dinucleotide reduced form (NADH).

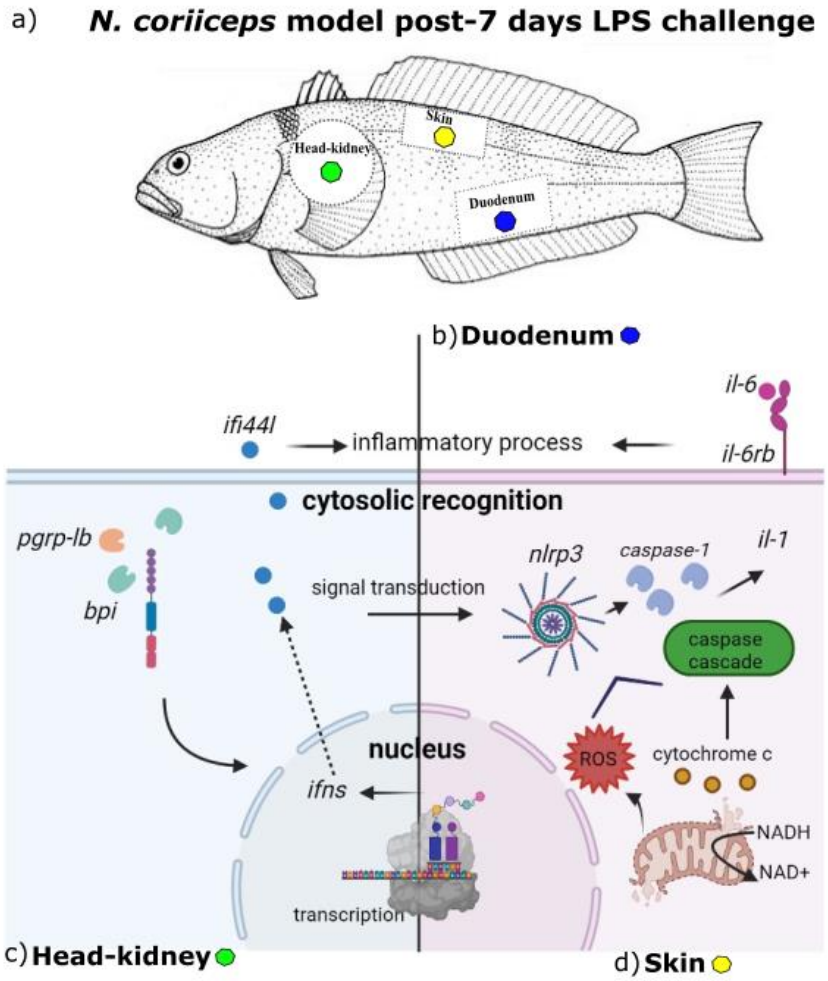

Figure 3.8. A) *N. coriiceps* model between down-regulated DEGs functions in B) duodenum, C) head-kidney and D) skin tissues transcriptomes between Sham and LPS groups. The discontinuous box is representative of duodenum which inserts in the same functions altered in skin transcriptome. The coloured symbols represent the different tissues, yellow – skin, green – head-kidney and blue – duodenum. The genes highlighted and interferon-induced protein 44-like (*ifi44l*), peptidoglycan-recognition protein LB-like (*pgrp-lb*), lipopolysaccharide (LPS), bactericidal permeability-increasing protein(bpi), NLR family CARD domain-containing protein 3 (*nlrc3*), interferons (*ifns*), interleukin-6 (*il-6*), interleukin-6 receptor beta (*il-6rb*), NACHT, LRR and PYD domains-containing protein 3 (*nlrp3*), interleukin-1 (*il-1*), reactive oxygen species (ROS), nicotinamide adenine dinucleotide oxidized form (NAD^+) and nicotinamide adenine dinucleotide reduced form (NADH).

3.7. Supplementary materials

3.7.1 Supplementary tables

Supplementary Table 3.1. **Assemblies input and output of samples from A) head-kidney, B) duodenum and C) skin.** The samples, raw reads, post QC reads, bases, post QC bases (assembly input)

and total sequences, length, percentage (%) GC, N50, median contig length, average contig, total assembled bases, total trinity genes and total trinity transcripts (assembly output) were evaluated for sequencing quality and representativity.

a) Assemblies input and output of samples in head-kidney

Head-kidney														
Group	Assemblies input					Assemblies output								
	Samples		Raw reads	Bases	Post QC bases	Total Sequences	Length	%GC	N50 (bp)	Median contig length (bp)	Average contig (bp)	Total assembled bases	Total Trinity genes	Total Trinity Transcripts
Control	C1	Fw	8,309,941	1,205,753,494	1,204,695,040	8307313	30-149	48	643	388	548	235185	378554	428791
		Rv		1,136,308,390	1,135,052,792									
	C2	Fw	5,497,430	796,954,141	796,058,669	5493697			643	388	548	235185	378554	428791
		Rv		752,431,064	751,446,498									
	C3	Fw	9,150,282	1,329,637,987	1,328,495,181	9148166		49	643	388	548	235185	378554	428791
		Rv		1,251,853,827	1,250,537,086									
	C4	Fw	8,288,899	1,201,343,968	1,200,262,691	8286593		48	643	388	548	235185	378554	428791
		Rv		1,132,802,898	1,131,509,952									
	C5	Fw	7,833,433	1,136,608,949	1,135,599,124	7831598			643	388	548	235185	378554	428791
		Rv		1,070,791,712	1,069,587,164									
Sham	S1	Fw	7,572,753	1,098,249,944	1,097,264,679	7570833		49	643	388	548	235185	378554	428791
		Rv		1,034,163,420	1,032,982,984									
	S2	Fw	9,681,149	1,405,094,440	1,403,773,175	9677463			643	388	548	235185	378554	428791
		Rv		1,320,069,716	1,318,458,215									
	S3	Fw	9,327,103	1,353,068,449	1,351,940,783	9325582		48	643	388	548	235185	378554	428791
		Rv		1,268,181,973	1,266,816,586									
	S4	Fw	8,145,891	1,180,351,384	1,179,220,350	8142830		49	643	388	548	235185	378554	428791
		Rv		1,110,621,579	1,109,298,293									
	S5	Fw	7,461,417	1,079,975,683	1,078,456,749	7452728			643	388	548	235185	378554	428791
		Rv		1,017,038,722	1,015,400,181									
LPS	L1	Fw	7,287,011	1,057,442,742	1,056,440,280	7284383		48	643	388	548	235185	378554	428791
		Rv		992,811,685	991,664,610									
	L2	Fw	6,894,296	999,202,554	998,205,462	6891589		50	643	388	548	235185	378554	428791
		Rv		945,424,626	944,281,482									
	L3	Fw	9,226,262	1,338,205,669	1,337,027,142	9224753		47	643	388	548	235185	378554	428791
		Rv		1,268,598,521	1,267,249,406									
	L4	Fw	7,736,934	1,123,653,946	1,122,758,901	7735652		49	643	388	548	235185	378554	428791
		Rv		1,059,136,644	1,058,025,159									

b) Assemblies input and output of samples in duodenum

Duodenum														
Group	Assemblies input					Assemblies output								
	Samples		Raw reads	Bases	Post QC bases	Total Sequences	Length	%GC	N50 (bp)	Median contig length (bp)	Average contig (bp)	Total assembled bases	Total Trinity genes	Total Trinity Transcripts
Control	C1	Fw	7307396	1,06E+09	1,06E+09	7303843	30-149	47	643	388	548	235185	378554	428791
		Rv		9,93E+08	9,92E+08									
	C2	Fw	8723615	1,27E+09	1,26E+09	8718963		48	643	388	548	235185	378554	428791
		Rv		1,18E+09	1,18E+09									
	C3	Fw	10857979	1,58E+09	1,57E+09	10856302			643	388	548	235185	378554	428791
		Rv		1,49E+09	1,49E+09									
	C4	Fw	9291413	1,35E+09	1,35E+09	9289922			643	388	548	235185	378554	428791
		Rv		1,27E+09	1,27E+09									
	C5	Fw	8700745	1,26E+09	1,26E+09	8698605			643	388	548	235185	378554	428791
		Rv		1,19E+09	1,19E+09									
Sham	S1	Fw	8115735	1,18E+09	1,18E+09	8113926			643	388	548	235185	378554	428791
		Rv		1,11E+09	1,11E+09									
	S2	Fw	9196394	1,33E+09	1,33E+09	9193856			643	388	548	235185	378554	428791
		Rv		1,26E+09	1,26E+09									
	S3	Fw	5283505	7,67E+08	7,66E+08	5280633			643	388	548	235185	378554	428791
		Rv		7,16E+08	7,16E+08									
	S4	Fw	9413336	1,36E+09	1,36E+09	9409863			643	388	548	235185	378554	428791
		Rv		1,29E+09	1,29E+09									
	S5	Fw	8169104	1,19E+09	1,18E+09	8165142			643	388	548	235185	378554	428791
		Rv		1,08E+09	1,07E+09									
LPS	L1	Fw	9390679	1,36E+09	1,36E+09	9388638			643	388	548	235185	378554	428791
		Rv		1,28E+09	1,28E+09									
	L2	Fw	9539967	1,38E+09	1,38E+09	9535715			643	388	548	235185	378554	428791
		Rv		1,3E+09	1,3E+09									
	L3	Fw	5772806	8,37E+08	8,36E+08	5771371		47	643	388	548	235185	378554	428791
		Rv		7,83E+08	7,82E+08									
	L4	Fw	5610880	8,13E+08	8,12E+08	5609301		48	643	388	548	235185	378554	428791
		Rv		7,61E+08	7,6E+08									
	L5	Fw	9813092	1,42E+09	1,42E+09	9809249		47	643	388	548	235185	378554	428791
		Rv		1,34E+09	1,34E+09									

c) Assemblies input and output of samples in skin

Skin															
Group	Assemblies input					Assemblies output									
	Samples		Raw reads	Bases	Post QC bases	Total Sequences	Length	% GC	N50 (bp)	Median contig length (bp)	Average contig (bp)	Total assembled bases	Total Trinity genes	Total Trinity Transcripts
Control	C1	Fw	7577102	1,1E+09	1,1E+09	7575379	30-149	48	643	388	548	235185	378554	428791
		Rv		1,04E+09	1,03E+09									
	C2	Fw	7846633	1,14E+09	1,14E+09	7843365	30-149	47	643	388	548	235185	378554	428791
		Rv		1,07E+09	1,07E+09									
	C3	Fw	7983929	1,16E+09	1,16E+09	7980996	30-149	48	643	388	548	235185	378554	428791
		Rv		1,09E+09	1,09E+09									
	C4	Fw	4691712	6,83E+08	6,82E+08	4690435	30-149	48	643	388	548	235185	378554	428791
		Rv		6,45E+08	6,45E+08									
	C5	Fw	6612845	9,58E+08	9,57E+08	6608895	30-149	48	643	388	548	235185	378554	428791
		Rv		9,07E+08	9,06E+08									
Sham	S1	Fw	2619865	3,8E+08	3,79E+08	2617431	30-149	47	643	388	548	235185	378554	428791
		Rv		3,57E+08	3,57E+08									
	S2	Fw	7412426	1,08E+09	1,08E+09	7410028	30-149	47	643	388	548	235185	378554	428791
		Rv		1,02E+09	1,01E+09									
	S3	Fw	6790660	9,79E+08	9,78E+08	6789093	30-149	47	643	388	548	235185	378554	428791
		Rv		9,12E+08	9,11E+08									
	S4	Fw	9071580	1,32E+09	1,32E+09	9067476	30-149	47	643	388	548	235185	378554	428791
		Rv		1,24E+09	1,24E+09									
	S5	Fw	5433180	7,9E+08	7,89E+08	5431611	30-149	47	643	388	548	235185	378554	428791
		Rv		7,43E+08	7,42E+08									
LPS	L1	Fw	1685546	2,45E+08	2,45E+08	1685093	30-149	47	643	388	548	235185	378554	428791
		Rv		2,3E+08	2,3E+08									
	L2	Fw	8645912	1,25E+09	1,25E+09	8643838	30-149	47	643	388	548	235185	378554	428791
		Rv		1,18E+09	1,18E+09									
	L3	Fw	5991988	8,7E+08	8,69E+08	5990645	30-149	48	643	388	548	235185	378554	428791
		Rv		8,22E+08	8,21E+08									
	L4	Fw	4750450	6,9E+08	6,9E+08	4748912	30-149	47	643	388	548	235185	378554	428791
		Rv		6,44E+08	6,44E+08									
	L5	Fw	7050650	1,02E+09	1,02E+09	7048497	30-149	48	643	388	548	235185	378554	428791
		Rv		9,55E+08	9,54E+08									

Supplementary Table 3.2. The pooled immunome GO terms of skin, head kidney and duodenum: A) biological process (BP), B) molecular function (MF) and C) cellular component (CC). The GO terms involved in immune response and immune defence mechanisms in *N. coriiceps* ($p < 0.05$ to > 0.05) between sham and LPS challenged groups.

a)

GO Function	GO	Term	P-value
BP			
	GO:0032635	interleukin-6 production	3,79E-08
	GO:0070741	response to interleukin-6	3,79E-08
	GO:0032611	interleukin-1 beta production	3,79E-08
	GO:0032675	regulation of interleukin-6 production	3,79E-08
	GO:0070102	interleukin-6-mediated signaling pathway	3,79E-08
	GO:0071354	cellular response to interleukin-6	3,79E-08
	GO:0034130	toll-like receptor 1 signaling pathway	1,21E-07
	GO:0034131	regulation of toll-like receptor 1 signaling pathway	1,21E-07
	GO:0038178	complement component C5a signaling pathway	1,47E-06
	GO:0061057	peptidoglycan recognition protein signaling pathway	2,06E-06
	GO:0061058	regulation of peptidoglycan recognition protein signaling pathway	2,06E-06
	GO:0061059	positive regulation of peptidoglycan recognition protein signaling pathway	2,06E-06
	GO:0061060	negative regulation of peptidoglycan recognition protein signaling pathway	2,06E-06
	GO:0006910	phagocytosis, recognition	2,06E-06
	GO:0035944	perforin production	3,18E-06
	GO:0034130	toll-like receptor 1 signaling pathway	3,18E-06
	GO:0034131	regulation of toll-like receptor 1 signaling pathway	3,18E-06
	GO:0034133	positive regulation of toll-like receptor 1 signaling pathway	3,18E-06
	GO:0034132	negative regulation of toll-like receptor 1 signaling pathway	3,18E-06
	GO:0034158	toll-like receptor 8 signaling pathway	7,84E-06
	GO:0030101	natural killer cell activation	1,12E-05
	GO:0043320	natural killer cell degranulation	1,12E-05
	GO:0001787	natural killer cell proliferation	1,12E-05
	GO:0001779	natural killer cell differentiation	1,12E-05
	GO:0035747	natural killer cell chemotaxis	1,12E-05
	GO:0042267	natural killer cell mediated cytotoxicity	1,12E-05
	GO:0002519	natural killer cell tolerance induction	1,12E-05
	GO:0002228	natural killer cell mediated immunity	1,12E-05
	GO:0002370	natural killer cell cytokine production	1,12E-05
	GO:0070246	natural killer cell apoptotic process	1,12E-05
	GO:0035782	mature natural killer cell chemotaxis	1,12E-05
	GO:0002321	natural killer cell progenitor differentiation	1,12E-05
	GO:0002771	inhibitory killer cell immunoglobulin-like receptor signaling pathway	1,12E-05
	GO:0002222	stimulatory killer cell immunoglobulin-like receptor signaling pathway	1,12E-05
	GO:0034138	toll-like receptor 3 signaling pathway	1,21E-05
	GO:0032023	trypsinogen activation	1,21E-05
	GO:0034139	regulation of toll-like receptor 3 signaling pathway	1,21E-05
	GO:0034141	positive regulation of toll-like receptor 3 signaling pathway	1,21E-05
	GO:0034140	negative regulation of toll-like receptor 3 signaling pathway	1,21E-05
	GO:0034162	toll-like receptor 9 signaling pathway	1,43E-05
	GO:0034163	regulation of toll-like receptor 9 signaling pathway	1,43E-05
	GO:0034165	positive regulation of toll-like receptor 9 signaling pathway	1,43E-05
	GO:0034164	negative regulation of toll-like receptor 9 signaling pathway	1,43E-05
	GO:0032638	interleukin-9 production	1,43E-05
	GO:0034154	toll-like receptor 7 signaling pathway	1,46E-05
	GO:0034155	regulation of toll-like receptor 7 signaling pathway	1,46E-05
	GO:0034157	positive regulation of toll-like receptor 7 signaling pathway	1,46E-05
	GO:0034156	negative regulation of toll-like receptor 7 signaling pathway	1,46E-05
	GO:0034130	toll-like receptor 1 signaling pathway	2,38E-05
	GO:0002415	immunoglobulin transcytosis in epithelial cells mediated by polymeric immunoglobulin receptor	5,36E-05
	GO:0002771	inhibitory killer cell immunoglobulin-like receptor signaling pathway	5,36E-05
	GO:0002222	stimulatory killer cell immunoglobulin-like receptor signaling pathway	5,36E-05
	GO:0002377	immunoglobulin production	5,36E-05
	GO:0002224	toll-like receptor signaling pathway	5,36E-05
	GO:0002751	antigen processing and presentation following receptor mediated endocytosis	6,02E-05
	GO:0002745	antigen processing and presentation initiated by receptor mediated uptake of antigen	6,02E-05
	GO:0019882	antigen processing and presentation	6,02E-05
	GO:0034134	toll-like receptor 2 signaling pathway	6,37E-05
	GO:0035661	MyD88-dependent toll-like receptor 2 signaling pathway	6,37E-05

GO:0034135	regulation of toll-like receptor 2 signaling pathway	6,37E-05
GO:1990773	matrix metallopeptidase secretion	8,57E-05
GO:1905048	regulation of metallopeptidase activity	8,57E-05
GO:1905049	negative regulation of metallopeptidase activity	8,57E-05
GO:1905050	positive regulation of metallopeptidase activity	8,57E-05
GO:1904464	regulation of matrix metallopeptidase secretion	8,57E-05
GO:0002224	toll-like receptor signaling pathway	1,20E-04
GO:0002749	antigen processing and presentation initiated by toll-like receptor mediated phagocytosis of antigen	1,20E-04
GO:0002376	immune system process	1,00E+00
GO:0001819	positive regulation of cytokine production	1,00E+00
GO:0009617	response to bacterium	1,00E+00
GO:0002376	immune system process	1,00E+00
GO:0002377	immunoglobulin production	1,00E+00
GO:0030889	negative regulation of B cell proliferation	1,00E+00
GO:0002331	pre-B cell allelic exclusion	1,00E+00
GO:0002376	immune system process	1,00E+00
GO:0002377	immunoglobulin production	1,00E+00
GO:0030889	negative regulation of B cell proliferation	1,00E+00
GO:0002331	pre-B cell allelic exclusion	1,00E+00
GO:0098586	cellular response to virus	1,00E+00
GO:0006935	chemotaxis	1,00E+00
GO:0002376	immune system process	1,00E+00
GO:2000562	negative regulation of CD4-positive, alpha-beta T cell proliferation	1,00E+00
GO:0050728	negative regulation of inflammatory response	1,00E+00
GO:0032689	negative regulation of interferon-gamma production	1,00E+00
GO:1902714	negative regulation of interferon-gamma secretion	1,00E+00
GO:0032815	negative regulation of natural killer cell activation	1,00E+00
GO:0043322	negative regulation of natural killer cell degranulation	1,00E+00
GO:0032722	positive regulation of chemokine production	1,00E+00
GO:0001819	positive regulation of cytokine production	1,00E+00
GO:1900426	positive regulation of defense response to bacterium	1,00E+00
GO:0045089	positive regulation of innate immune response	1,00E+00
GO:0032732	positive regulation of interleukin-1 production	1,00E+00
GO:2001181	positive regulation of interleukin-10 secretion	1,00E+00
GO:2000778	positive regulation of interleukin-6 secretion	1,00E+00
GO:0043032	positive regulation of macrophage activation	1,00E+00
GO:0045591	positive regulation of regulatory T cell differentiation	1,00E+00
GO:2000406	positive regulation of T cell migration	1,00E+00
GO:0032760	positive regulation of tumor necrosis factor production	1,00E+00
GO:0032823	regulation of natural killer cell differentiation	1,00E+00
GO:0032496	response to lipopolysaccharide	1,00E+00
GO:0002376	immune system process	1,00E+00
GO:0090024	negative regulation of neutrophil chemotaxis	1,00E+00
GO:0002376	immune system process	1,00E+00
GO:0002376	immune system process	1,00E+00
GO:0002376	immune system process	1,00E+00
GO:0002377	immunoglobulin production	1,00E+00
GO:0030889	negative regulation of B cell proliferation	1,00E+00
GO:0002331	pre-B cell allelic exclusion	1,00E+00
GO:0002376	immune system process	1,00E+00
GO:0002377	immunoglobulin production	1,00E+00
GO:0030889	negative regulation of B cell proliferation	1,00E+00
GO:0002331	pre-B cell allelic exclusion	1,00E+00
GO:0002376	immune system process	1,00E+00
GO:0002376	immune system process	1,00E+00
GO:0090197	positive regulation of chemokine secretion	1,00E+00
GO:0002532	production of molecular mediator involved in inflammatory response	1,00E+00
GO:0002376	immune system process	1,00E+00
GO:0002862	negative regulation of inflammatory response to antigenic stimulus	1,00E+00
GO:0002376	immune system process	1,00E+00
GO:0002376	immune system process	1,00E+00
GO:0002376	immune system process	1,00E+00
GO:0002862	negative regulation of inflammatory response to antigenic stimulus	1,00E+00
GO:0002376	immune system process	1,00E+00
GO:0002376	immune system process	1,00E+00
GO:0002376	immune system process	1,00E+00
GO:0002376	immune system process	1,00E+00

GO:0002376	immune system process	1,00E+00
GO:0090024	negative regulation of neutrophil chemotaxis	1,00E+00
GO:0002376	immune system process	1,00E+00
GO:0090197	positive regulation of chemokine secretion	1,00E+00
GO:0002532	production of molecular mediator involved in inflammatory response	1,00E+00
GO:0002376	immune system process	1,00E+00
GO:0002376	immune system process	1,00E+00
GO:0071220	cellular response to bacterial lipoprotein	1,00E+00
GO:0002376	immune system process	1,00E+00
GO:0002376	immune system process	1,00E+00
GO:0006954	inflammatory response	1,00E+00
GO:0032740	positive regulation of interleukin-17 production	1,00E+00
GO:0045086	positive regulation of interleukin-2 biosynthetic process	1,00E+00
GO:0032753	positive regulation of interleukin-4 production	1,00E+00
GO:0050870	positive regulation of T cell activation	1,00E+00
GO:0042102	positive regulation of T cell proliferation	1,00E+00
GO:2000318	positive regulation of T-helper 17 type immune response	1,00E+00
GO:2000570	positive regulation of T-helper 2 cell activation	1,00E+00
GO:0002376	immune system process	1,00E+00
GO:0002862	negative regulation of inflammatory response to antigenic stimulus	1,00E+00
GO:0002376	immune system process	1,00E+00
GO:0002376	immune system process	1,00E+00
GO:0032695	negative regulation of interleukin-12 production	1,00E+00
GO:0032815	negative regulation of natural killer cell activation	1,00E+00
GO:0032733	positive regulation of interleukin-10 production	1,00E+00
GO:0002376	immune system process	1,00E+00
GO:0090197	positive regulation of chemokine secretion	1,00E+00
GO:0002532	production of molecular mediator involved in inflammatory response	1,00E+00
GO:0002376	immune system process	1,00E+00
GO:0002376	immune system process	1,00E+00
GO:0002376	immune system process	1,00E+00
GO:0090197	positive regulation of chemokine secretion	1,00E+00
GO:0002532	production of molecular mediator involved in inflammatory response	1,00E+00
GO:0002376	immune system process	1,00E+00
GO:0002376	immune system process	1,00E+00
GO:0002376	immune system process	1,00E+00
GO:0002862	negative regulation of inflammatory response to antigenic stimulus	1,00E+00
GO:0002376	immune system process	1,00E+00
GO:0090197	positive regulation of chemokine secretion	1,00E+00
GO:0002532	production of molecular mediator involved in inflammatory response	1,00E+00
GO:0002376	immune system process	1,00E+00
GO:000695	inflammatory response	1,00E+00
GO:0001782	B cell homeostasis	1,00E+00
GO:0002376	immune system process	1,00E+00
GO:0030888	regulation of B cell proliferation	1,00E+00
GO:0002376	immune system process	1,00E+00
GO:0001819	positive regulation of cytokine production	1,00E+00
GO:0009617	response to bacterium	1,00E+00
GO:0002376	immune system process	1,00E+00
GO:005077	regulation of immune response	1,00E+00
GO:0002414	immunoglobulin transcytosis in epithelial cells	1,00E+00
GO:0002376	immune system process	1,00E+00
GO:0050862	positive regulation of T cell receptor signaling pathway	1,00E+00
GO:0002376	immune system process	1,00E+00
GO:0002376	immune system process	1,00E+00
GO:0001819	positive regulation of cytokine production	1,00E+00
GO:0009617	response to bacterium	1,00E+00
GO:0002376	immune system process	1,00E+00
GO:0001819	positive regulation of cytokine production	1,00E+00
GO:0009617	response to bacterium	1,00E+00
GO:0002376	immune system process	1,00E+00
GO:0070229	negative regulation of lymphocyte apoptotic process	1,00E+00
GO:0002376	immune system process	1,00E+00
GO:0070229	negative regulation of lymphocyte apoptotic process	1,00E+00
GO:0002376	immune system process	1,00E+00
GO:0034165	positive regulation of toll-like receptor 9 signaling pathway	1,00E+00
GO:0002376	immune system process	1,00E+00

GO:0002376	immune system process	1,00E+00
GO:0002376	immune system process	1,00E+00
GO:0002376	immune system process	1,00E+00
GO:0002376	immune system process	1,00E+00
GO:0002376	immune system process	1,00E+00
GO:0002376	immune system process	1,00E+00
GO:0002862	negative regulation of inflammatory response to antigenic stimulus	1,00E+00
GO:0002376	immune system process	1,00E+00
GO:0006954	inflammatory response	1,00E+00
GO:0006968	cellular defense response	1,00E+00
GO:0002376	immune system process	1,00E+00
GO:0050776	regulation of immune response	1,00E+00
GO:0002376	immune system process	1,00E+00
GO:0002376	immune system process	1,00E+00
GO:0032695	negative regulation of interleukin-12 production	1,00E+00
GO:0032815	negative regulation of natural killer cell activation	1,00E+00
GO:0032733	positive regulation of interleukin-10 production	1,00E+00
GO:0002376	immune system process	1,00E+00
GO:0006954	inflammatory response	1,00E+00
GO:0070233	negative regulation of T cell apoptotic process	1,00E+00
GO:0032740	positive regulation of interleukin-17 production	1,00E+00
GO:0045086	positive regulation of interleukin-2 biosynthetic process	1,00E+00
GO:0032753	sitive regulation of interleukin-4 production	1,00E+00
GO:0050870	positive regulation of T cell activation	1,00E+00
GO:0042102	positive regulation of T cell proliferation	1,00E+00
GO:2000318	positive regulation of T-helper 17 type immune response	1,00E+00
GO:2000570	positive regulation of T-helper 2 cell activation	1,00E+00
GO:0002376	immune system process	1,00E+00
GO:0002376	immune system process	1,00E+00
GO:0002376	immune system process	1,00E+00
GO:0002377	immunoglobulin production	1,00E+00
GO:0030889	negative regulation of B cell proliferation	1,00E+00
GO:0002376	immune system process	1,00E+00
GO:0002376	immune system process	1,00E+00
GO:0002376	immune system process	1,00E+00
GO:0002376	immune system process	1,00E+00
GO:0006968	cellular defense response	1,00E+00
GO:0002376	immune system process	1,00E+00
GO:0006954	inflammatory response	1,00E+00
GO:0002376	immune system process	1,00E+00
GO:0002376	immune system process	1,00E+00
GO:0002376	immune system process	1,00E+00
GO:0090024	negative regulation of neutrophil chemotaxis	1,00E+00
GO:0002376	immune system process	1,00E+00
GO:0090024	negative regulation of neutrophil chemotaxis	1,00E+00
GO:0002376	immune system process	1,00E+00
GO:0090024	negative regulation of neutrophil chemotaxis	1,00E+00
GO:0002376	immune system process	1,00E+00
GO:0002376	immune system process	1,00E+00
GO:0002376	immune system process	1,00E+00
GO:0002590	negative regulation of antigen processing and presentation of peptide antigen via MHC class I	1,00E+00
GO:0002376	immune system process	1,00E+00
GO:0006968	cellular defense response	1,00E+00
GO:0002376	immune system process	1,00E+00
GO:0050776	regulation of immune response	1,00E+00
GO:0002376	immune system process	1,00E+00
GO:0002376	immune system process	1,00E+00
GO:0006954	inflammatory response	1,00E+00
GO:0002376	immune system process	1,00E+00
GO:0002376	immune system process	1,00E+00
GO:0090024	negative regulation of neutrophil chemotaxis	1,00E+00
GO:0002376	immune system process	1,00E+00
GO:0006968	cellular defense response	1,00E+00
GO:0002376	immune system process	1,00E+00
GO:0002376	immune system process	1,00E+00
GO:0002376	immune system process	1,00E+00
GO:0032675	regulation of interleukin-6 production	1,00E+00

GO:0032680	regulation of tumor necrosis factor production	1,00E+00
GO:0042742	defense response to bacterium	1,00E+00
GO:0002376	immune system process	1,00E+00
GO:0002376	immune system process	1,00E+00
GO:0002590	negative regulation of antigen processing and presentation of peptide antigen via MHC class I	1,00E+00
GO:0002376	immune system process	1,00E+00
GO:0090197	positive regulation of chemokine secretion	1,00E+00
GO:0002532	production of molecular mediator involved in inflammatory response	1,00E+00
GO:0006968	cellular defense response	1,00E+00
GO:0002376	immune system process	1,00E+00
GO:0006954	inflammatory response	1,00E+00
GO:0002376	immune system process	1,00E+00
GO:0002376	immune system process	1,00E+00
GO:0090024	negative regulation of neutrophil chemotaxis	1,00E+00
GO:0006968	cellular defense response	1,00E+00
GO:0002376	immune system process	1,00E+00
GO:0006954	inflammatory response	1,00E+00
GO:0002376	immune system process	1,00E+00
GO:0050776	regulation of immune response	1,00E+00
GO:0002376	immune system process	1,00E+00
GO:0050776	regulation of immune response	1,00E+00
GO:0002376	immune system process	1,00E+00
GO:0050776	regulation of immune response	1,00E+00
GO:0034165	positive regulation of toll-like receptor 9 signaling pathway	1,00E+00
GO:0002414	immunoglobulin transcytosis in epithelial cells	1,00E+00
GO:0002376	immune system process	1,00E+00
GO:0071220	cellular response to bacterial lipoprotein	1,00E+00
GO:0002376	immune system process	1,00E+00
GO:0002376	immune system process	1,00E+00
GO:0032675	regulation of interleukin-6 production	1,00E+00
GO:0032680	regulation of tumor necrosis factor production	1,00E+00
GO:0002376	immune system process	1,00E+00
GO:0006909	phagocytosis	1,00E+00
GO:0002225	positive regulation of antimicrobial peptide production	1,00E+00
GO:0045089	positive regulation of innate immune response	1,00E+00
GO:0030889	negative regulation of B cell proliferation	1,00E+00
GO:0002331	pre-B cell allelic exclusion	1,00E+00
GO:0002377	immunoglobulin production	1,00E+00
GO:0002376	immune system process	1,00E+00
GO:0002376	immune system process	1,00E+00
GO:0032695	negative regulation of interleukin-12 production	1,00E+00
GO:0032815	negative regulation of natural killer cell activation	1,00E+00
GO:0032733	positive regulation of interleukin-10 production	1,00E+00
GO:0002376	immune system process	1,00E+00
GO:0002376	immune system process	1,00E+00
GO:0006909	phagocytosis	1,00E+00
GO:0002225	positive regulation of antimicrobial peptide production	1,00E+00
GO:0045089	positive regulation of innate immune response	1,00E+00
GO:0002376	immune system process	1,00E+00
GO:0032695	negative regulation of interleukin-12 production	1,00E+00
GO:0032815	negative regulation of natural killer cell activation	1,00E+00
GO:0032733	positive regulation of interleukin-10 production	1,00E+00
GO:0002376	immune system process	1,00E+00
GO:0002376	immune system process	1,00E+00
GO:0002377	immunoglobulin production	1,00E+00
GO:0030889	negative regulation of B cell proliferation	1,00E+00
GO:0002331	pre-B cell allelic exclusion	1,00E+00
GO:0050728	negative regulation of inflammatory response	1,00E+00
GO:0002376	immune system process	1,00E+00
GO:0050729	positive regulation of inflammatory response	1,00E+00
GO:1904996	positive regulation of leukocyte adhesion to vascular endothelial cell	1,00E+00
GO:0070555	response to interleukin-1	1,00E+00
GO:0002376	immune system process	1,00E+00
GO:0002376	immune system process	1,00E+00
GO:0002590	negative regulation of antigen processing and presentation of peptide antigen via MHC class I	1,00E+00
GO:0050715	positive regulation of cytokine secretion	1,00E+00
GO:0002376	immune system process	1,00E+00

GO:0045954	positive regulation of natural killer cell mediated cytotoxicity	1,00E+00
GO:0042271	susceptibility to natural killer cell mediated cytotoxicity	1,00E+00
GO:0002376	immune system process	1,00E+00
GO:0002376	immune system process	1,00E+00
GO:0002377	immunoglobulin production	1,00E+00
GO:0030889	negative regulation of B cell proliferation	1,00E+00
GO:0002376	immune system process	1,00E+00
GO:0002376	immune system process	1,00E+00
GO:0002377	immunoglobulin production	1,00E+00
GO:0030889	negative regulation of B cell proliferation	1,00E+00
GO:0002331	pre-B cell allelic exclusion	1,00E+00
GO:0002376	immune system process	1,00E+00
GO:0002376	immune system process	1,00E+00
GO:0002376	immune system process	1,00E+00
GO:0071356	cellular response to tumor necrosis factor	1,00E+00
GO:1990869	cellular response to chemokine	1,00E+00
GO:0071347	cellular response to interleukin-1	1,00E+00
GO:0071222	cellular response to lipopolysaccharide	1,00E+00
GO:0098586	cellular response to virus	1,00E+00
GO:0006954	inflammatory response	1,00E+00
GO:0044828	negative regulation by host of viral genome replication	1,00E+00
GO:1900016	negative regulation of cytokine production involved in inflammatory response	1,00E+00
GO:1902714	negative regulation of interferon-gamma secretion	1,00E+00
GO:0050713	negative regulation of interleukin-1 beta secretion	1,00E+00
GO:0032715	negative regulation of interleukin-6 production	1,00E+00
GO:1900165	negative regulation of interleukin-6 secretion	1,00E+00
GO:0032720	negative regulation of tumor necrosis factor production	1,00E+00
GO:0000294	negative regulation of tumor necrosis factor secretion	1,00E+00
GO:0002230	positive regulation of defense response to virus by host	1,00E+00
GO:0002376	immune system process	1,00E+00
GO:0002377	immunoglobulin production	1,00E+00
GO:0030889	negative regulation of B cell proliferation	1,00E+00
GO:0002331	pre-B cell allelic exclusion	1,00E+00

b)

GO Function	GO	Term	P-value
MF			
	GO:0042163	interleukin-12 beta subunit binding	3,79E-08
	GO:0005138	interleukin-6 receptor binding	3,79E-08
	GO:0004915	interleukin-6 receptor activity	3,79E-08
	GO:0019981	interleukin-6 binding	3,79E-08
	GO:0042164	interleukin-12 alpha subunit binding	3,79E-08
	GO:0004475	mannose-1-phosphate guanylyltransferase activity	1,21E-07
	GO:0019983	interleukin-9 binding	1,43E-05
	GO:0001850	complement component C3a binding	1,47E-06
	GO:0001851	complement component C3b binding	1,47E-06
	GO:0001855	complement component C4b binding	1,47E-06
	GO:0001856	complement component C5a binding	1,47E-06
	GO:0004876	complement component C3a receptor activity	1,47E-06
	GO:0004878	complement component C5a receptor activity	1,47E-06
	GO:0004877	complement component C3b receptor activity	1,47E-06
	GO:0001861	complement component C4b receptor activity	1,47E-06
	GO:0001849	complement component C1q complex binding	1,47E-06
	GO:0016019	peptidoglycan immune receptor activity	2,06E-06
	GO:0032089	NACHT domain binding	4,19E-06
	GO:0030275	LRR domain binding	4,19E-06
	GO:0035325	Toll-like receptor binding	5,92E-06
	GO:0042164	interleukin-12 alpha subunit binding	6,02E-06
	GO:0042163	interleukin-12 beta subunit binding	8,96E-06
	GO:0046703	natural killer cell lectin-like receptor binding	1,21E-05
	GO:0035325	Toll-like receptor binding	1,21E-05
	GO:0019976	interleukin-2 binding	5,26E-05
	GO:0046703	natural killer cell lectin-like receptor binding	5,26E-05
	GO:0005134	interleukin-2 receptor binding	5,26E-05
	GO:0001792	polymeric immunoglobulin receptor activity	5,36E-05
	GO:0001790	polymeric immunoglobulin binding	5,36E-05
	GO:0019763	immunoglobulin receptor activity	5,36E-05
	GO:0034987	immunoglobulin receptor binding	5,36E-05
	GO:0035325	Toll-like receptor binding	5,36E-05
	GO:0019865	immunoglobulin binding	5,36E-05
	GO:0046703	natural killer cell lectin-like receptor binding	5,87E-05
	GO:0035325	Toll-like receptor binding	5,87E-05
	GO:0035663	Toll-like receptor 2 binding	6,37E-05
	GO:0008237	metallopeptidase activity	8,57E-05
	GO:0035325	Toll-like receptor binding	1,20E-04
	GO:0001791	IgM binding	1,00E+00
	GO:0005136	interleukin-4 receptor binding	1,00E+00
	GO:0001791	IgM binding	1,00E+00
	GO:0005136	interleukin-4 receptor binding	1,00E+00
	GO:0005136	interleukin-4 receptor binding	1,00E+00

c)

GO Function	GO	Term	P-value
CC			
	GO:0005896	interleukin-6 receptor complex	3,79E-08
	GO:0005893	interleukin-2 receptor complex	3,79E-08
	GO:0005602	complement component C1 complex	1,47E-06
	GO:0062167	complement component C1q complex	1,47E-06
	GO:0035354	Toll-like receptor 1-Toll-like receptor 2 protein complex	3,18E-06
	GO:0035354	Toll-like receptor 1-Toll-like receptor 2 protein complex	2,38E-05
	GO:0071749	polymeric IgA immunoglobulin complex	5,36E-05
	GO:0019814	immunoglobulin complex	5,36E-05
	GO:0001772	immunological synapse	1,00E+00

Supplementary table 3.3. GO terms of skin, head kidney and duodenum associated to innate and acquired immunity found in *N. coriiceps* (FDR > 0.05) between sham and LPS challenged groups.

Gene name	Gene symbol	Transcript ID	Immune tissues					
			Duodenum		Head-kidney		Skin	
			logFC	Pvalue	logFC	Pvalue	logFC	Pvalue
Pathogen recognition receptors								
toll-like receptor 5S	tlr5s	TRINITY_DN155586_c1_g2	-0,921209	0,102023	0,330787	0,54712	-0,27219	0,623573
toll-like receptor 21	tlr21	TRINITY_DN153455_c0_g3	0,041238	1	ND	ND	-0,02612	1
toll-like receptor 22	tlr22	TRINITY_DN161134_c0_g1	1,935205	0,009347	1,05445	0,105591	0,575312	0,56466
toll-like receptor 25	tlr25	TRINITY_DN143923_c0_g2	0	1	0	1	0	1
MYD88 innate immune signal transduction adaptor	myd88	TRINITY_DN149255_c2_g2	-0,828629	0,067129	-0,32751	0,66259	-0,94411	0,195214
Iron metabolism pathway								
iron-sulfur cluster assembly 1	isca1	TRINITY_DN158336_c3_g1	-0,394755	0,512673	-0,32437	0,472076	-0,07678	0,898168
ferritin middle chain	fm	TRINITY_DN151529_c0_g1	0,134133	0,808032	0,307049	0,481659	0,145723	0,770575
ferritin, heavy polypeptide 1a	fth1a	TRINITY_DN163552_c3_g2	-0,256971	0,584936	-0,48893	0,259852	-0,35393	0,535704
ferritin, heavy polypeptide 1b	fth1b	TRINITY_DN153313_c0_g1	-0,148505	0,78265	-0,64758	0,101363	1,223508	0,265248
ferritin, heavy polypeptide-like 31	fthl31	TRINITY_DN152920_c0_g1	ND	ND	ND	ND	5,952003	0,043577
hepcidin type 2	hamp2	TRINITY_DN158150_c3_g3	-0,556771	0,24786	-0,35037	0,372918	-1,17671	0,0559
ferredoxin 1	fdx1	TRINITY_DN142521_c1_g4	0,514339	0,256418	0,117602	0,831745	0,092343	0,863963
transferrin receptor type 1	tfrc1	TRINITY_DN151097_c1_g1	0,057121	0,922543	-0,08724	0,837004	-0,21054	0,688664
iron-responsive element binding protein 2	ireb2	TRINITY_DN162110_c3_g1	-0,473882	0,385284	-0,19371	0,682837	-0,28817	0,656629
ceruloplasmin	Cp	TRINITY_DN122801_c0_g1	0	1	0	1	0	1
Innate humoral immunity								
interferon induced with helicase C domain 1	ifih1	TRINITY_DN138343_c0_g1	0,406723	0,361268	0,511285	0,269002	-0,19137	0,701312
interferon regulatory factor 5	irf5	TRINITY_DN140377_c2_g1	0,157294	0,881042	0,336152	0,620345	-0,38334	0,596872
interferon regulatory factor 10	irf10	TRINITY_DN149366_c0_g1	0,371971	0,614432	0,303799	0,554693	-0,47284	0,449056
tumor necrosis factor receptor-associated factor 3 interacting protein 1	traf3ip1	TRINITY_DN150198_c2_g2	-0,220895	0,807002	-0,05845	0,981345	-0,0872	0,909854
tumor necrosis factor receptor-associated factor 6	traf6	TRINITY_DN162995_c0_g2	0,238693	0,835808	0,584792	0,525421	-0,55164	0,510472
tumor necrosis factor receptor superfamily, member 21	tnfrsf21	TRINITY_DN152787_c3_g1	0,776172	0,343941	-0,40825	0,532705	-0,18864	0,814765
tumor necrosis factor, alpha-induced protein 3	tnfaip3	TRINITY_DN154799_c0_g2	-1,221941	0,036557	-0,43027	0,424876	-0,62961	0,318418
tumor necrosis factor, alpha-induced protein 6	tnfaip6	TRINITY_DN145499_c2_g1	0,372122	0,568572	ND	ND	-1,3517	0,088631
transforming growth factor beta activated kinase 1 (MAP3K7) binding protein 1	tab1	TRINITY_DN156646_c3_g3	0,259585	0,750138	-0,62056	0,375101	0,567401	0,358831
transforming growth factor beta activated kinase 1 (MAP3K7) binding protein 2	tab2	TRINITY_DN136443_c4_g2	-0,014284	1	0,031452	0,979088	-0,34148	0,49329
lysozyme g isoform 1	lyzg	TRINITY_DN151142_c2_g4	1,931808	0,062058	-0,3493	0,658963	ND	ND
lysozyme g isoform 2	lyzg	TRINITY_DN151142_c2_g3	0,100961	0,854555	-0,05092	0,897885	-0,13517	0,850774
lysozyme g isoform 3	lyzg	TRINITY_DN154321_c0_g5	-0,205882	0,822741	0,233602	0,692126	0,187225	0,801773
lysozyme g isoform 4	lyzg	TRINITY_DN150037_c1_g1	2,553233	0,006412	0,360384	0,476218	0,642694	0,269097
lysozyme c	lyzc	TRINITY_DN161115_c3_g1	-1,399815	0,360628	-2,04015	0,412837	-0,312	0,849137
receptor for activated C kinase 1	rack1	TRINITY_DN159637_c3_g1	1,024645	0,193108	-0,44955	0,256431	6,507515	0,014516
protein tyrosine phosphatase receptor type C	ptprc	TRINITY_DN163497_c7_g1	0,307429	0,476509	0,314978	0,449494	-0,25293	0,607356
protein kinase C, beta a	prkcba	TRINITY_DN152910_c2_g2	0,075813	1	-0,39778	0,69541	0,429052	0,509176
protein kinase C, delta a	prkcda	TRINITY_DN159920_c0_g1	0,086553	0,9227	0,228617	0,625015	-0,56885	0,349413
protein kinase C, epsilon a	prkcea	TRINITY_DN145869_c0_g1	0,345045	0,729892	0,510313	0,60051	-0,76241	0,719393
protein kinase C, theta	prkcq	TRINITY_DN142604_c0_g2	0,487615	0,569645	0,387641	0,494732	-1,08815	0,157213
protein kinase C, zeta	prkcz	TRINITY_DN145076_c7_g2	-0,504757	0,249322	0,163872	0,697733	0,49345	0,382156
cytokine receptor-like factor 1a	crlf1a	TRINITY_DN148504_c0_g1	-0,014305	1	ND	ND	-0,40862	0,523251
cytokine receptor-like factor 3	crlf3	TRINITY_DN139907_c1_g1	0,198124	0,775735	0,267884	0,543557	0,048972	0,934619
suppressor of cytokine signaling 3b	socs3b	TRINITY_DN142002_c5_g1	-0,79686	0,223668	-0,63402	0,285788	-1,31228	0,076794
suppressor of cytokine signaling 5b	socs5b	TRINITY_DN133006_c0_g1	-0,115085	0,9268	-0,02188	0,977436	-0,04194	0,963993
suppressor of cytokine signaling 6a	socs6a	TRINITY_DN147051_c0_g1	-0,183207	0,748923	-0,11629	0,88133	-0,24498	0,70867
interleukin 2 inducible T cell kinase	itk	TRINITY_DN159827_c0_g1	-0,251545	0,755485	0,355856	0,392791	0,525379	0,442868
interleukin enhancer binding factor 2	ilf2	TRINITY_DN125857_c0_g1	0,177559	0,93579	-0,24133	0,518383	-0,00153	1
nuclear factor, interleukin 3 regulated, member 6	nfil3-6	TRINITY_DN158193_c2_g2	-0,213666	0,641308	-0,18786	0,733517	-0,19254	0,805374
chemokine (C-X-C motif) receptor 3, tandem duplicate 1	cxcr3.1	TRINITY_DN160517_c3_g1	0,212889	0,744989	-0,04557	0,90406	0,340643	0,582858
chemokine-like receptor 1	cmklr1	TRINITY_DN149705_c1_g1	0,450215	0,411141	-0,15373	0,759019	0,099392	0,890614
chemokine (C-C motif) receptor 9a	ccr9a	TRINITY_DN156338_c0_g2	-0,996694	0,204541	-6,65E-01	0,19171	-0,24502	0,722539
chemokine (C-C motif) ligand 44	ccl44	TRINITY_DN141586_c1_g1	ND	ND	-0,75695	0,445686	0,219449	0,674694
C5a anaphylatoxin chemotactic receptor	c5ar1	TRINITY_DN155897_c2_g2	-0,256072	0,848336	-0,46635	0,295207	-0,60445	0,3832
Innate cellular immunity								
neutrophil cytosolic factor 4	ncf4	TRINITY_DN147584_c0_g2	-0,053334	0,966499	-0,43868	0,33919	-0,66645	0,26188
monocyte to macrophage differentiation-associated	mmd	TRINITY_DN107919_c0_g1	-3,842059	0,04093	-0,21194	0,646668	-0,0981	0,835973
natural killer cell triggering receptor	nktr	TRINITY_DN147748_c4_g1	-0,188562	0,91689	1,413542	0,095852	-0,14808	0,854342
macrophage migration inhibitory factor	mif	TRINITY_DN141413_c1_g2	0,209222	0,699555	-0,20461	0,673857	0,953104	0,063896
macrophage expressed 1, tandem duplicate 1	mpeg1.1	TRINITY_DN162026_c8_g4	0,253398	0,646737	-1,05E-01	0,811881	-0,01789	1
macrophage stimulating 1 receptor b	mst1rb	TRINITY_DN153524_c5_g4	-0,096678	0,854222	-0,35389	0,722034	0,703187	0,420132
lymphocyte specific protein 1 a	lsp1a	TRINITY_DN161162_c0_g2	-0,27294	0,546542	0,445796	0,302541	-0,26515	0,687717
activated leukocyte cell adhesion molecule a	alcama	TRINITY_DN136619_c0_g1	0,269439	0,541712	1,954051	0,041737	0,270822	0,708752
Acquired immunity								
mucolipin 1b	mcoln1b	TRINITY_DN141936_c6_g2	ND	ND	0,565836	0,550306	ND	ND
immunoresponsive gene 1, like	irg1l	TRINITY_DN143559_c0_g1	ND	ND	ND	ND	0,357545	0,652964
novel immune-type receptor 1b	nitr1b	TRINITY_DN163619_c5_g2	0,595238	0,513705	0,444261	0,519139	0,889768	0,212703
tyrosine kinase with immunoglobulin-like and EGF-like domains 1	tie1	TRINITY_DN148567_c2_g1	0,254431	0,7183	0,117339	0,860006	0,267484	0,655799
B cell linker	blnk	TRINITY_DN144994_c2_g2	0,75596	0,388007	0,13048	0,758481	-0,65108	0,38801
switching B cell complex subunit SWAP70b	swap70b	TRINITY_DN154031_c0_g1	1,419408	0,00558	1,31403	0,021359	0,117077	0,828792
immunoglobulin-like domain containing receptor 2	ildr2	TRINITY_DN146770_c0_g5	-0,394474	0,709384	ND	ND	-0,17875	0,95864
immunoglobulin superfamily, member 3	igsf3	TRINITY_DN147293_c0_g2	-0,187588	0,892743	ND	ND	-0,60716	0,490959
immunoglobulin light 3 variable 2	igl3v2	TRINITY_DN158498_c1_g1	2,38788	0,040212	-0,19435	0,764896	0,693863	0,541608
immunoglobulin light 4 variable 8	igl4v8	TRINITY_DN163393_c1_g1	-0,165263	0,724127	-0,16359	0,738761	1,038122	0,092135
immunoglobulin light 4 variable 8	iglv4-8	TRINITY_DN163393_c1_g1	-0,165263	0,724127	-0,16359	0,738761	1,038122	0,092135
immunoglobulin light iota constant 1, s1	igiC1S1	TRINITY_DN147828_c1_g1	0,540042	0,2762	0,146725	0,750526	0,265725	0,679898
immunoglobulin superfamily, member 9Ba	igsf9ba	TRINITY_DN140788_c0_g1	ND	ND	0,210231	0,839578	ND	ND
immunoglobulin heavy variable 1-1	ighv1-1	TRINITY_DN161000_c1_g1	0,668551	0,315552	0,541258	0,193273	-0,17355	0,777509
immunoglobulin heavy variable 1-2	ighv1-2	TRINITY_DN154442_c1_g1	-1,087589	0,328865	0,294554	0,572503	-1,22175	0,187801
immunoglobulin heavy variable 3-2	ighv3-2	TRINITY_DN152031_c2_g2	1,375957	0,437751	2,735322	0,026069	ND	ND
immunoglobulin heavy variable 4-1	ighv4-1	TRINITY_DN147640_c0_g1	ND	ND	-0,04864	0,943632	1,258756	0,580633
immunoglobulin heavy variable 6-2	ighv6-2	TRINITY_DN159159_c0_g1	-0,547853	0,45988	-0,68433	0,255577	-2,06169	0,031041
immunoglobulin heavy variable 10-1	ighv10-1	TRINITY_DN162448_c4_g1	1,222214	0,351663	-0,86393	0,303731	2,173265	0,373185
CD74 molecule, major histocompatibility complex, class II invariant chain a	cd74a	TRINITY_DN156515_c0_g1	0,121325	0,762744	0,087142	0,833234	0,109924	0,827057
CD81 molecule b	cd81b	TRINITY_DN142381_c1_g1	0,453624	0,394074	-0,24621	0,560316	0,446992	0,441945
CD99 molecule-like 2	cd99l2	TRINITY_DN143409_c2_g1	0,306477	0,775569	0,312292	0,527875	-0,07631	0,969655
CD151 antigen, like	cd151l	TRINITY_DN160686_c1_g1	-0,13779	0,755713	0,483575	0,299186	0,087994	0,86755
CD164 molecule, sialomucin	cd164	TRINITY_DN158014_c1_g1	-0,251782	0,611894	0,249832	0,575618	-0,55477	0,25967
CD276 molecule	cd276	TRINITY_DN135065_c0_g1	0,07589	0,932536	0,125992	0,826692	0,369959	0,467171

a)

TRINITY sample	logFC	Pvalue	FDR	Gene ID	Acronym	UniProtKB Accession no.	Organism	Immune system	Stress
TRINITY_DN134805_c3_g6	1,08E+14	2,14E-33	1,19E-28	Zinc finger protein 184	znf184	Q99676	Homo sapiens		
TRINITY_DN161228_c0_g1	9,94E+14	2,98E-09	5,53E-05	Macrophage mannose receptor 1	mrc1	P22897	Homo sapiens	x	
TRINITY_DN154336_c1_g7	7,89E+14	1,31E-07	8,08E-04	A-kinase anchor protein 13	akap13	Q12802	Homo sapiens		
TRINITY_DN154232_c1_g1	7,16E+14	8,19E-07	2,54E-03	Deoxyribonuclease-1-like	dnase1l1	P49184	Homo sapiens	x	
TRINITY_DN157242_c0_g1	9,28E+14	1,34E-06	3,57E-03	NLR family, CARD domain containing 3	nlrc3	Q7RTR2	Homo sapiens	x	
TRINITY_DN136433_c1_g1	7,98E+14	1,75E-06	4,06E-03	Parvalbumin 3	pvalb3	Q7ZT36	Homo sapiens		
TRINITY_DN163223_c0_g1	8,20E+14	2,00E-06	4,13E-03	Glyceraldehyde-3-phosphate dehydrogenase	gapdh	P04406	Homo sapiens	x	
TRINITY_DN160440_c3_g3	7,44E+14	5,84E-06	1,05E-02	Discoidin domain receptor tyrosine kinase 1	ddr1	Q08345	Homo sapiens		
TRINITY_DN157315_c0_g5	7,37E+14	6,02E-06	1,05E-02	Creatine kinase, muscle a	ckma	Q90X19	Danio rerio		
TRINITY_DN156139_c0_g1	8,89E+14	6,45E-06	1,06E-02	Bactericidal permeability-increasing protein-like	bpi	P17213	Homo sapiens	x	
TRINITY_DN145717_c0_g1	5,73E+14	9,30E-06	1,36E-02	Troponin T3b, skeletal, fast	tnnt3	P45378	Homo sapiens		
TRINITY_DN140144_c4_g1	6,47E+14	1,01E-05	1,36E-02	Parvalbumin beta-like	n/a	A0A1S3S2P0	Salmo salar		
TRINITY_DN153686_c4_g1	9,89E+14	1,07E-05	1,38E-02	creatine kinase, muscle a	ttpa	P49638	Homo sapiens		
TRINITY_DN149521_c2_g1	5,62E+14	1,18E-05	1,40E-02	B-cell receptor CD22	cd22	P20273	Homo sapiens	x	
TRINITY_DN153853_c2_g2	2,54E+14	1,29E-05	1,47E-02	Mononecidin	n/a	Q8UUG0	Morone saxatilis	x	
TRINITY_DN151130_c2_g6	6,07E+14	1,77E-05	1,76E-02	Actin, alpha 1b, skeletal muscle	acta1	P68133	Homo sapiens		
TRINITY_DN142517_c4_g7	9,15E+14	2,02E-05	1,83E-02	Kinesin family binding protein	kifbp	Q96EK5	Homo sapiens		
TRINITY_DN143456_c1_g2	7,74E+14	2,10E-05	1,83E-02	Tubulin beta chain	tbb	P07437	Homo sapiens	x	
TRINITY_DN136703_c3_g1	5,21E+14	2,11E-05	1,83E-02	Elongation factor 1-alpha 1	eef1a1	P68104	Homo sapiens	x	
TRINITY_DN163330_c5_g3	6,97E+14	2,19E-05	1,83E-02	High affinity choline transporter 1	slc5a7	Q9GZV3	Homo sapiens		
TRINITY_DN162987_c4_g1	6,98E+14	2,19E-05	1,83E-02	Nemo-like kinase, type 2	nlk	Q9UBE8	Homo sapiens		
TRINITY_DN148345_c1_g5	5,47E+14	2,22E-05	1,83E-02	Signal peptidase complex subunit 2	spcs2	Q15005	Homo sapiens		
TRINITY_DN91259_c0_g1	5,60E+14	2,56E-05	2,01E-02	60S ribosomal protein L23a	rpl23a	P62750	Homo sapiens		
TRINITY_DN148284_c3_g2	9,31E+14	2,60E-05	2,01E-02	GTPase IMAP family member 7	gimap7	Q8NHV1	Homo sapiens		
TRINITY_DN131881_c1_g2	5,68E+14	2,71E-05	2,07E-02	40S ribosomal protein S12	rps12	P25398	Homo sapiens		
TRINITY_DN144112_c2_g1	5,76E+14	2,96E-05	2,18E-02	Prothymosin alpha	ptma	P06454	Homo sapiens		
TRINITY_DN148902_c3_g5	7,95E+14	3,27E-05	2,25E-02	Voltage-dependent T-type calcium channel subunit alpha-1I-like	cacna1i	Q9P0X4	Homo sapiens		
TRINITY_DN140935_c1_g4	5,69E+14	3,31E-05	2,25E-02	40S ribosomal protein S15	rps15	P62841	Homo sapiens		
TRINITY_DN123605_c0_g1	5,98E+14	3,31E-05	2,25E-02	60S ribosomal protein L34	rpl34	P49207	Homo sapiens		
TRINITY_DN230036_c0_g1	5,44E+14	4,08E-05	2,50E-02	60S ribosomal protein L8	rpl8	P62917	Homo sapiens		
TRINITY_DN148890_c5_g4	7,51E+14	4,16E-05	2,50E-02	Guanine nucleotide-binding protein G(o) subunit alpha	gnai1	P63096	Homo sapiens		
TRINITY_DN141871_c1_g1	4,29E+14	4,17E-05	2,50E-02	Myosin, heavy polypeptide 1.1, skeletal muscle	myhz1.1	B8A568	Danio rerio		
TRINITY_DN163651_c8_g1	5,15E+14	4,25E-05	2,52E-02	Myelin-oligodendrocyte glycoprotein	mog	Q16653	Homo sapiens	x	
TRINITY_DN143360_c2_g2	8,59E+14	4,56E-05	2,63E-02	Butyrophilin-like protein 8	btnl8	D6RIR7	Homo sapiens	x	
TRINITY_DN161904_c6_g3	4,46E+14	5,32E-05	2,90E-02	Myosin light chain, phosphorylatable, fast skeletal muscle a	mylpf	Q96A32	Homo sapiens	x	
TRINITY_DN141540_c5_g1	6,32E+14	5,54E-05	2,94E-02	Zinc finger protein 79	znf79	Q15937	Homo sapiens		
TRINITY_DN138242_c1_g1	6,05E+14	5,81E-05	2,99E-02	60S ribosomal protein L10a	rpl10a	P62906	Homo sapiens		
TRINITY_DN136727_c2_g2	5,29E+14	5,91E-05	2,99E-02	40S ribosomal protein SA	rpsa	P08865	Homo sapiens		
TRINITY_DN151618_c0_g4	6,77E+14	6,38E-05	3,12E-02	Golgin subfamily B member 1	golgb1	Q14789	Homo sapiens		
TRINITY_DN140225_c0_g2	6,07E+14	6,66E-05	3,13E-02	40S ribosomal protein S7	rps7a	P62081	Homo sapiens		
TRINITY_DN163297_c2_g1	4,74E+14	6,80E-05	3,16E-02	NACHT, LRR and PYD domains-containing protein 12	nlrp12	P59046	Homo sapiens	x	
TRINITY_DN113574_c0_g1	5,91E+14	6,99E-05	3,20E-02	60S ribosomal protein L30	rpl30	P62888	Homo sapiens	x	
TRINITY_DN145989_c1_g1	7,54E+14	7,17E-05	3,25E-02	Voltage-dependent R-type calcium channel subunit alpha-1E	cacna1e	Q15878	Homo sapiens		
TRINITY_DN160959_c3_g3	5,46E+14	7,42E-05	3,25E-02	40S ribosomal protein S3a	rps3a	P61247	Homo sapiens		
TRINITY_DN126929_c0_g1	5,52E+14	7,61E-05	3,31E-02	60S ribosomal protein L7a	rpl7a	P62424	Homo sapiens		
TRINITY_DN160872_c0_g4	6,29E+14	7,91E-05	3,38E-02	Sarcoplasmic/endoplasmic reticulum calcium ATPase 1	atp2a1	O14983	Homo sapiens		x
TRINITY_DN131562_c2_g1	5,82E+14	7,95E-05	3,38E-02	60S ribosomal protein L23	rpl23	P62829	Homo sapiens		
TRINITY_DN152274_c3_g1	4,69E+14	8,01E-05	3,38E-02	Myosin, heavy chain 4	myhc4	A2BGX6	Danio rerio		
TRINITY_DN150843_c0_g1	4,34E+14	8,37E-05	3,43E-02	Alpha-tropomyosin	tpm1	P09493	Homo sapiens		x
TRINITY_DN120312_c0_g1	5,53E+14	9,35E-05	3,59E-02	40S ribosomal protein S24	rps24	P62847	Homo sapiens		
TRINITY_DN103756_c0_g1	5,30E+14	1,08E-04	4,04E-02	60S ribosomal protein L36a	rpl36a	P83881	Homo sapiens		
TRINITY_DN135901_c1_g2	5,03E+14	1,14E-04	4,17E-02	Receptor of activated protein C kinase 1	rack1	P63244	Homo sapiens	x	
TRINITY_DN139327_c4_g7	8,09E+14	1,25E-04	4,41E-02	Sodium-dependent multivitamin transporter	slc5a6	Q9Y289	Homo sapiens		
TRINITY_DN119827_c0_g1	4,60E+14	1,26E-04	4,42E-02	Ferritin light chain 1	ftl	P02792	Homo sapiens	x	
TRINITY_DN96990_c0_g1	5,24E+14	1,27E-04	4,42E-02	40S ribosomal protein S17	rps17	P08708	Homo sapiens		
TRINITY_DN137865_c1_g1	4,15E+14	1,35E-04	4,56E-02	Actin, alpha, cardiac muscle 1b	actc1	P68032	Homo sapiens		
TRINITY_DN148282_c3_g2	4,07E+14	1,42E-04	4,69E-02	40S ribosomal protein S2	rps2	P15880	Homo sapiens		
TRINITY_DN160717_c2_g3	6,65E+14	1,44E-04	4,71E-02	GTPase IMAP family member 2	gimap2	Q9UG22	Homo sapiens		
TRINITY_DN107767_c0_g1	5,58E+14	1,45E-04	4,71E-02	60S ribosomal protein L18	rpl18	Q07020	Homo sapiens		
TRINITY_DN156496_c2_g1	2,96E+14	1,46E-04	4,71E-02	A kinase (PRKA) anchor protein 17A	akap17a	Q02040	Homo sapiens	x	
TRINITY_DN135377_c8_g1	4,48E+14	1,51E-04	4,80E-02	60S ribosomal protein L38	rpl38	P63173	Homo sapiens		

b)

TRINITY sample	logFC	Pvalue	FDR	UniProtKB ID	Gene definition	Gene symbol	Organism	Immune system	Stress
TRINITY_DN155904_c0_g2	-8,75E+14	7,43E-15	2,07E-10	A0A1S3L397	Nuclear factor 7, brain-like	*nf7bl*	*Salmo salar*		
TRINITY_DN159360_c4_g1	-9,83E+14	7,36E-07	2,41E-03	F1RAW5	Shootin 3	*shtn3*	*Danio rerio*		
TRINITY_DN157121_c6_g3	-7,21E+14	3,99E-06	7,66E-03	Q9Y644	RFNG O-fucosylpeptide 3-beta-N-acetylglucosaminyltransferase	*rnfg*	*Homo sapiens*		
TRINITY_DN159274_c3_g5	-6,81E+14	5,86E-06	1,05E-02	A0A087Y6W0	DELTA-sagatoxin-Srs1a-like	n/a	*Amazon molly*	☒	
TRINITY_DN143041_c0_g4	-4,86E+14	7,36E-06	1,14E-02	Q91994	Homeobox protein OTX1 B-like	*otx1b*	*Danio rerio*		
TRINITY_DN156633_c4_g1	-4,26E+14	2,39E-05	1,91E-02	Q8ND71	GTPase IMAP family member 8	*gimap8*	*Homo sapiens*	☒	
TRINITY_DN160901_c3_g2	-7,84E+14	3,12E-05	2,25E-02	Q96PJ5	Fc receptor-like protein 4	*fcrl4*	*Homo sapiens*	☒	
TRINITY_DN154717_c1_g7	-9,61E+14	7,37E-05	3,25E-02	P31994	Low affinity immunoglobulin gamma Fc region receptor II	*fcgr2b*	*Homo sapiens*	☒	
TRINITY_DN155504_c5_g1	-7,47E+14	8,35E-05	3,43E-02	Q14155	Rho guanine nucleotide exchange factor (GEF) 7b	*arhgef7*	*Homo sapiens*		
TRINITY_DN162997_c0_g1	-3,34E+14	9,17E-05	3,59E-02	Q9UPC5	Probable G-protein coupled receptor 34	*gpr34*	*Homo sapiens*		
TRINITY_DN162324_c2_g1	-8,94E+14	9,52E-05	3,63E-02	Q9NQ25	SLAM family member 7	*slamf7*	*Homo sapiens*	☒	
TRINITY_DN27609_c0_g1	-6,53E+14	1,52E-04	4,80E-02	O14718	Visual pigment-like receptor peropsin	*rrh*	*Homo sapiens*		
TRINITY_DN149803_c2_g2	-7,31E+14	1,53E-04	4,80E-02	Pseudogene	Putative zinc finger protein 840	*znf840p*	*Notothenia coriiceps*		
TRINITY_DN151809_c2_g1	-8,18E+14	1,53E-04	4,80E-02	Q7Z7H3	Ciliogenesis associated TTC17 interacting protein	*catip*	*Homo sapiens*		

Supplementary table 3.4. **DEGs in A-B) head-kidney, C-D) duodenum and E-F) skin transcriptomes between Control and Sham treated groups.** Only unique DEGs are listed that showed up (A) and down- regulation (B) in head-kidney, up (C) and down-regulation (D) in duodenum and up (E) and down-regulation (F) in skin (F) (FDR < 0.05). The DEGs involved in immune and stress processes were identified with "x".

c)

TRINITY sample	logFC	Pvalue	FDR	Gene ID	Acronym	UniProtKB Acession no.	Organism	Immune system	Stress
TRINITY_DN136418_c0_g1	9,39E+14	1,21E-10	1,76E-06	Acyl-CoA dehydrogenase family, member 11	acad11	Q709F0	Homo sapiens		
TRINITY_DN163898_c3_g1	9,22E+14	9,56E-09	7,94E-05	NLR family CARD domain containing 3	nlrc3	Q7RTR2	Homo sapiens	x	
TRINITY_DN158327_c0_g5	8,57E+14	2,90E-08	1,69E-04	Cathepsin Z	ctsz	Q9UBR2	Homo sapiens	x	
TRINITY_DN158456_c2_g5	7,25E+14	1,05E-07	4,07E-04	STE20-like serine/threonine-protein kinase	slk	Q9H2G2	Homo sapiens		
TRINITY_DN156920_c0_g2	2,37E+14	1,86E-07	6,76E-04	D-aspartate oxidase	ddo	Q99489	Homo sapiens		
TRINITY_DN140177_c3_g2	7,71E+14	1,94E-06	3,76E-03	Protein kinase C and casein kinase substrate in neurons 1b	pacsin1	Q9BY11	Homo sapiens		
TRINITY_DN160464_c1_g2	8,59E+14	5,17E-06	7,00E-03	Ladderlectin-like	n/a	A0A1S3M3S9	Salmo salar	x	
TRINITY_DN149873_c1_g8	6,60E+14	8,60E-06	9,80E-03	Cytochrome P450 2K1-like	n/a	A0A1S3S117	Salmo salar		
TRINITY_DN138641_c6_g1	7,51E+14	1,23E-05	1,25E-02	Lysosomal alpha-glucosidase	gaa	P10253	Homo sapiens	x	
TRINITY_DN139327_c4_g7	8,11E+14	1,45E-05	1,38E-02	Sodium-dependent multivitamin transporter	slc5a6	Q9Y289	Homo sapiens		
TRINITY_DN151726_c0_g1	1,16E+14	1,64E-05	1,49E-02	Septin-7-like	septin7p9	Pseudogene	Notothenia coriiceps		
TRINITY_DN142695_c1_g4	7,06E+14	1,81E-05	1,54E-02	Ribosomal protein S19 binding protein 1	rps19bp1	Q86WX3	Homo sapiens		
TRINITY_DN151542_c4_g9	1,06E+14	1,89E-05	1,55E-02	MET proto-oncogene, receptor tyrosine kinase	met	P08581	Homo sapiens	x	
TRINITY_DN147862_c3_g7	3,64E+14	2,27E-05	1,79E-02	Cholinergic receptor nicotinic alpha 7 subunit	chrna7	P36544	Homo sapiens		
TRINITY_DN160537_c3_g2	7,04E+14	2,87E-05	2,17E-02	Methionine synthase	mtr	Q99707	Homo sapiens		
TRINITY_DN159904_c0_g7	7,80E+14	4,00E-05	2,78E-02	Caspase-1-A	casp1	P29466	Homo sapiens	x	
TRINITY_DN147024_c4_g1	3,82E+14	4,63E-05	2,98E-02	Nucleotide binding protein 1	nubp1	P53384	Homo sapiens	x	
TRINITY_DN137926_c0_g1	3,17E+14	4,73E-05	2,99E-02	Proto-Oncogene C-Fos	fos	P01100	Homo sapiens	x	x
TRINITY_DN149950_c2_g1	8,14E+14	4,82E-05	3,01E-02	Peptidylglycine alpha-amidating monooxygenase	pam	P19021	Homo sapiens		
TRINITY_DN138887_c2_g6	7,76E+14	8,33E-05	4,53E-02	Cytochrome P450, family 19, subfamily A, polypeptide 1b	cyp19a1	P11511	Homo sapiens		
TRINITY_DN159288_c3_g3	6,75E+14	8,44E-05	4,53E-02	Phosphatidate cytidylyltransferase 2	cds2	O95674	Homo sapiens		
TRINITY_DN161919_c1_g2	3,63E+14	8,77E-05	4,53E-02	Karyopherin alpha 5 (importin alpha 6)	kpna5	O15131	Homo sapiens	x	
TRINITY_DN156301_c0_g1	2,19E+14	8,79E-05	4,53E-02	Coiled-coil domain containing 82	ccdc82	Q8N4S0	Homo sapiens		
TRINITY_DN162382_c9_g2	6,75E+14	8,86E-05	4,53E-02	BTB/POZ domain-containing protein 3	btbd3	Q9Y2F9	Homo sapiens		
TRINITY_DN153065_c2_g2	2,96E+14	9,93E-05	4,65E-02	Growth regulation by estrogen in breast cancer	greb1	Q4ZG55	Homo sapiens		
TRINITY_DN148412_c8_g1	8,79E+14	1,07E-04	4,74E-02	Electron transfer flavoprotein dehydrogenase	etfdh	Q16134	Homo sapiens		x
TRINITY_DN163559_c7_g4	8,77E+14	1,09E-04	4,74E-02	Trichohyalin-like	tchhl1	Q5QJ38	Homo sapiens		
TRINITY_DN157752_c0_g2	2,26E+14	1,10E-04	4,74E-02	Transmembrane protein 176B	tmem176b	Q3YBM2	Homo sapiens		
TRINITY_DN146617_c8_g1	6,72E+14	1,11E-04	4,74E-02	Proteolipid protein 2	plp2	Q04941	Homo sapiens	x	
TRINITY_DN155225_c0_g1	4,00E+14	1,12E-04	4,75E-02	Ciliogenesis and planar polarity effector 2	cplane2	Q9BU20	Homo sapiens		

d) DEGs down-regulated in the duodenum of Control versus Sham

TRINITY sample	logFC	Pvalue	FDR	Gene ID	Acronym	UniProtKB Acession no.	Organism	Immune system	Stress
TRINITY_DN157234_c0_g2	-1,03E+14	2,67E-08	1,69E-04	GTP cyclohydrolase 1	gch1	P30793	Homo sapiens	x	
TRINITY_DN159360_c4_g1	-8,68E+14	3,92E-08	2,07E-04	Zinc finger protein 37	zfp37	Q9Y6Q3	Homo sapiens		
TRINITY_DN162782_c0_g1	-8,26E+14	5,34E-08	2,39E-04	MAGUK p55 subfamily member 3	mpp3b	Q13368	Homo sapiens		
TRINITY_DN158150_c3_g4	-8,02E+14	4,58E-07	1,21E-03	Hepcidin	hamp	P81172	Homo sapiens	x	
TRINITY_DN161270_c0_g1	-6,89E+14	1,33E-03	1,33E-03	Trypsin-7-like	n/a	N/A	Notothenia coriiceps		
TRINITY_DN113150_c0_g1	-6,93E+14	1,14E-06	2,65E-03	Haptoglobin	hp	P00738	Homo sapiens	x	
TRINITY_DN152946_c2_g1	-9,00E+14	1,43E-06	3,08E-03	GTPase IMAP family member 7	gimap7	Q8NHV1	Homo sapiens		
TRINITY_DN137467_c7_g3	-8,54E+14	3,12E-06	5,49E-03	C2 calcium-dependent domain containing 2	c2cd2	Q9Y426	Homo sapiens		
TRINITY_DN140296_c3_g2	-8,56E+14	4,70E-06	6,98E-03	Elastase 2-like	ela2l	P08217	Homo sapiens		
TRINITY_DN127262_c0_g1	-8,12E+14	6,04E-06	7,80E-03	Endonuclease domain-containing 1 protein	endod1	O94919	Homo sapiens		
TRINITY_DN161264_c2_g2	-8,07E+14	7,47E-06	9,05E-03	Carboxypeptidase B1	cpb1	P15086	Homo sapiens		
TRINITY_DN138963_c6_g1	-5,60E+14	1,29E-05	1,25E-02	Membrane palmitoylated protein 7	mpp7	Q5T2T1	Homo sapiens		
TRINITY_DN141444_c11_g4	-7,28E+14	1,29E-05	1,25E-02	Trypsin-like	prss1	P07477	Homo sapiens		
TRINITY_DN148016_c1_g3	-4,91E+14	3,05E-05	2,27E-02	Interferon-induced protein 44-like	ifi44l	Q53G44	Homo sapiens	x	
TRINITY_DN145806_c0_g1	-3,28E+14	3,59E-05	2,41E-02	Stonustoxin subunit alpha-like	n/a	Q98989	Synanceia horrida	x	
TRINITY_DN136221_c1_g1	-5,53E+14	3,88E-05	2,75E-02	Peptidase inhibitor R3HDML	r3hdml	Q9H3Y0	Homo sapiens		
TRINITY_DN142397_c4_g1	-8,15E+14	4,26E-05	2,88E-02	Perforin-1	prf1	P14222	Homo sapiens	x	
TRINITY_DN144299_c0_g1	-5,49E+14	5,32E-05	3,21E-02	Mucin-5AC-like	muc5ac	P98088	Homo sapiens	x	
TRINITY_DN138253_c2_g4	-5,57E+14	6,48E-05	3,69E-02	Desumoylating isopeptidase 2	desi2	Q9BSY9	Homo sapiens		
TRINITY_DN130742_c0_g2	-8,13E+14	9,92E-05	4,65E-02	Chymotrypsinogen B1	ctrb1	P17538	Homo sapiens		
TRINITY_DN145863_c0_g1	-8,12E+14	1,07E-04	4,74E-02	Carboxyl ester lipase	cel	P19835	Homo sapiens		
TRINITY_DN134508_c0_g3	-8,67E+14	1,12E-04	4,75E-02	Interferon-induced very large GTPase 1	gvinp1	Q7Z2Y8	Homo sapiens		

e)

TRINITY sample	logFC	Pvalue	FDR	Gene ID	Acronym	UniProtKB Acession no.	Organism	Immune system	Stress
TRINITY_DN159459_c0_g2	7,25E+14	7,27E-07	2,82E-02	GTPase IMAP family member 8	gimap8	Q8ND71	Homo sapiens	x	

f) DEGs down-regulated in the skin of Control versus Sham

TRINITY sample	logFC	Pvalue	FDR	Gene ID	Gene symbol	Pathway or Function		Immune system	Stress
TRINITY_DN152946_c2_g1	-1,23E+14	5,53E-10	4,30E-05	GTPase IMAP family member 7	gimap7	Q8NHV1	Homo sapiens		

Supplementary table 3.5. Enriched GO terms in A) head-kidney, B) duodenum and C) skin in DEGs between Control and Sham groups. The enriched GO terms are identified as biological process (BP), molecular function (MF) and cellular component (CC) (FDR < 0.05).

a)

Tissue	GO	Term	P-value	Ontology
Head-kidney				
	GO:0005783	endoplasmic reticulum	8,19E-07	CC
	GO:0070062	extracellular exosome	8,19E-07	CC
	GO:0005634	nucleus	8,19E-07	CC
	GO:0004536	deoxyribonuclease activity	8,19E-07	MF
	GO:0004519	endonuclease activity	8,19E-07	MF
	GO:0006308	DNA catabolic process	8,19E-07	BP
	GO:0005576	extracellular region	1,98E-06	CC
	GO:0090729	toxin activity	1,98E-06	MF
	GO:0044179	hemolysis in other organism	1,98E-06	BP
	GO:0005737	cytoplasm	2,00E-06	CC
	GO:0005829	cytosol	2,00E-06	CC
	GO:0015630	microtubule cytoskeleton	2,00E-06	CC
	GO:0005634	nucleus	2,00E-06	CC
	GO:0004365	glyceraldehyde-3-phosphate dehydrogenase (NAD+) (phosphorylating) activity	2,00E-06	MF
	GO:0008017	microtubule binding	2,00E-06	MF
	GO:0051287	NAD binding	2,00E-06	MF
	GO:0050661	NADP binding	2,00E-06	MF
	GO:0035605	peptidyl-cysteine S-nitrosylase activity	2,00E-06	MF
	GO:0006006	glucose metabolic process	2,00E-06	BP
	GO:0006096	glycolytic process	2,00E-06	BP
	GO:0000226	microtubule cytoskeleton organization	2,00E-06	BP
	GO:0051402	neuron apoptotic process	2,00E-06	BP
	GO:0035606	peptidyl-cysteine S-trans-nitrosylation	2,00E-06	BP
	GO:0050821	protein stabilization	2,00E-06	BP
	GO:0005576	extracellular region	5,86E-06	CC
	GO:0042151	nematocyst	5,86E-06	CC
	GO:0044218	other organism cell membrane	5,86E-06	CC
	GO:0046930	pore complex	5,86E-06	CC
	GO:0015267	channel activity	5,86E-06	MF
	GO:0090729	toxin activity	5,86E-06	MF
	GO:0006812	cation transport	5,86E-06	BP
	GO:0052331	hemolysis in other organism involved in symbiotic interaction	5,86E-06	BP
	GO:0046931	pore complex assembly	5,86E-06	BP
	GO:0005737	cytoplasm	6,83E-06	CC
	GO:0005856	cytoskeleton	6,83E-06	CC
	GO:0031514	motile cilium	6,83E-06	CC
	GO:0005524	ATP binding	6,83E-06	MF
	GO:0004111	creatine kinase activity	6,83E-06	MF
	GO:0030030	cell projection organization	6,83E-06	BP
	GO:0005737	cytoplasm	1,02E-05	CC
	GO:0070062	extracellular exosome	1,18E-05	CC
	GO:0016021	integral component of membrane	1,18E-05	CC
	GO:0005886	plasma membrane	1,18E-05	CC
	GO:0030246	carbohydrate binding	1,18E-05	MF
	GO:0007155	cell adhesion	1,18E-05	BP
	GO:0044297	cell body	1,76E-05	CC
	GO:0005737	cytoplasm	1,76E-05	CC
	GO:0005856	cytoskeleton	1,76E-05	CC
	GO:0030175	filopodium	1,76E-05	CC
	GO:0030027	lamellipodium	1,76E-05	CC
	GO:0005524	ATP binding	1,76E-05	MF
	GO:0090131	mesenchyme migration	1,76E-05	BP
	GO:0010628	positive regulation of gene expression	1,76E-05	BP
	GO:0005737	cytoplasm	1,77E-05	CC
	GO:0005615	extracellular space	1,77E-05	CC
	GO:0005524	ATP binding	1,77E-05	MF
	GO:0004111	creatine kinase activity	1,77E-05	MF
	GO:0009408	response to heat	1,77E-05	BP
	GO:0016301	kinase activity	1,77E-05	MF
	GO:0016772	transferase activity, transferring phosphorus-containing groups	1,77E-05	MF
	GO:0005737	cytoplasm	2,10E-05	CC
	GO:0005874	microtubule	2,10E-05	CC
	GO:0005525	GTP binding	2,10E-05	MF
	GO:0003924	GTPase activity	2,10E-05	MF
	GO:0005200	structural constituent of cytoskeleton	2,10E-05	MF
	GO:0007017	microtubule-based process	2,10E-05	BP
	GO:0030864	cortical actin cytoskeleton	2,11E-05	CC
	GO:0005737	cytoplasm	2,11E-05	CC
	GO:0005829	cytosol	2,11E-05	CC
	GO:0070062	extracellular exosome	2,11E-05	CC
	GO:0005615	extracellular space	2,11E-05	CC
	GO:0016020	membrane	2,11E-05	CC
	GO:0043209	myelin sheath	2,11E-05	CC
	GO:0005730	nucleolus	2,11E-05	CC
	GO:0005886	plasma membrane	2,11E-05	CC
	GO:0032587	ruffle membrane	2,11E-05	CC
	GO:0008144	drug binding	2,11E-05	MF
	GO:0005525	GTP binding	2,11E-05	MF
	GO:0003924	GTPase activity	2,11E-05	MF
	GO:0003729	mRNA binding	2,11E-05	MF
	GO:0019901	protein kinase activity	2,11E-05	MF
	GO:0003723	RNA binding	2,11E-05	MF
	GO:0003746	translation elongation factor activity	2,11E-05	MF
	GO:0000049	tRNA binding	2,11E-05	MF
	GO:0007568	aging	2,11E-05	BP
	GO:0035690	cellular response to drug	2,11E-05	BP
	GO:0071364	cellular response to epidermal growth factor stimulus	2,11E-05	BP
	GO:1990090	cellular response to nerve growth factor stimulus	2,11E-05	BP
	GO:1903427	negative regulation of reactive oxygen species biosynthetic process	2,11E-05	BP
	GO:0010942	positive regulation of cell death	2,11E-05	BP
	GO:0010976	positive regulation of neuron projection development	2,11E-05	BP
	GO:0051260	protein homooligomerization	2,11E-05	BP
	GO:0016021	integral component of membrane	2,39E-05	CC
	GO:0005764	lysosome	2,39E-05	CC
	GO:0005741	mitochondrial outer membrane	2,39E-05	CC

GO:0005525	GTP binding	2,39E-05	MF
GO:0005737	cytoplasm	2,56E-05	CC
GO:0022625	cytosolic large ribosomal subunit	2,56E-05	CC
GO:0070062	extracellular exosome	2,56E-05	CC
GO:0005730	nucleolus	2,56E-05	CC
GO:0005634	nucleus	2,56E-05	CC
GO:0045296	cadherin binding	2,56E-05	MF
GO:0070180	large ribosomal subunit rRNA binding	2,56E-05	MF
GO:0003723	RNA binding	2,56E-05	MF
GO:0003735	structural constituent of ribosome	2,56E-05	MF
GO:0008283	cell proliferation	2,56E-05	BP
GO:0000027	ribosomal large subunit assembly	2,56E-05	BP
GO:0006412	translation	2,56E-05	BP
GO:0070062	extracellular exosome	2,96E-05	CC
GO:0005634	nucleus	2,96E-05	CC
GO:0033613	activating transcription factor binding	2,96E-05	MF
GO:0042393	histone binding	2,96E-05	MF
GO:0030154	cell differentiation	2,96E-05	BP
GO:0008283	cell proliferation	2,96E-05	BP
GO:0043486	histone exchange	2,96E-05	BP
GO:0043066	negative regulation of apoptotic process	2,96E-05	BP
GO:0043154	negative regulation of cysteine-type endopeptidase activity involved in apoptotic process	2,96E-05	BP
GO:0051092	positive regulation of NF-kappaB transcription factor activity	2,96E-05	BP
GO:0045944	positive regulation of transcription by RNA polymerase II	2,96E-05	BP
GO:0022627	cytosolic small ribosomal subunit	3,31E-05	CC
GO:0005925	focal adhesion	3,31E-05	CC
GO:0016020	membrane	3,31E-05	CC
GO:0005654	nucleoplasm	3,31E-05	CC
GO:0003723	RNA binding	3,31E-05	MF
GO:0003735	structural constituent of ribosome	3,31E-05	MF
GO:0097421	liver regeneration	3,31E-05	BP
GO:0001649	osteoblast differentiation	3,31E-05	BP
GO:0000028	ribosomal small subunit assembly	3,31E-05	BP
GO:0042274	ribosomal small subunit biogenesis	3,31E-05	BP
GO:0000056	ribosomal small subunit export from nucleus	3,31E-05	BP
GO:0006364	rRNA processing	3,31E-05	BP
GO:0006412	translation	3,31E-05	BP
GO:0003735	structural constituent of ribosome	3,31E-05	MF
GO:0005840	ribosome	3,31E-05	BP
GO:0022625	cytosolic large ribosomal subunit	3,31E-05	CC
GO:0070062	extracellular exosome	3,31E-05	CC
GO:0005739	mitochondrion	3,31E-05	CC
GO:0045296	cadherin binding	3,31E-05	MF
GO:0003723	RNA binding	3,31E-05	MF
GO:0003735	structural constituent of ribosome	3,31E-05	MF
GO:0042254	ribosome biogenesis	3,31E-05	BP
GO:0006412	translation	3,31E-05	BP
GO:0022625	cytosolic large ribosomal subunit	4,08E-05	CC
GO:0005925	focal adhesion	4,08E-05	CC
GO:0016020	membrane	4,08E-05	CC
GO:1990932	5.8S rRNA binding	4,08E-05	MF
GO:0003723	RNA binding	4,08E-05	MF
GO:0003735	structural constituent of ribosome	4,08E-05	MF
GO:1990090	cellular response to nerve growth factor stimulus	4,08E-05	BP
GO:0002181	cytoplasmic translation	4,08E-05	BP
GO:0006412	translation	4,08E-05	BP
GO:0005622	intracellular	4,08E-05	BP
GO:0005840	ribosome	4,08E-05	BP
GO:0030016	myofibril	4,17E-05	CC
GO:0016459	myosin complex	4,17E-05	CC
GO:0032982	myosin filament	4,17E-05	CC
GO:0001725	stress fiber	4,17E-05	CC
GO:0030018	Z disc	4,17E-05	CC
GO:0051015	actin filament binding	4,17E-05	MF
GO:0030898	actin-dependent ATPase activity	4,17E-05	MF
GO:0005524	ATP binding	4,17E-05	MF
GO:0016887	ATPase activity	4,17E-05	MF
GO:0005516	calmodulin binding	4,17E-05	MF
GO:0000146	microfilament motor activity	4,17E-05	MF
GO:0019901	protein kinase activity	4,17E-05	MF
GO:0030048	actin filament-based movement	4,17E-05	BP
GO:0007512	adult heart development	4,17E-05	BP
GO:0046034	ATP metabolic process	4,17E-05	BP
GO:0055009	atrial cardiac muscle tissue morphogenesis	4,17E-05	BP
GO:0048739	BMP signaling pathway	4,17E-05	BP
GO:0060070	canonical Wnt signaling pathway	4,17E-05	BP
GO:0060048	cardiac muscle contraction	4,17E-05	BP
GO:0048739	cardiac muscle fiber development	4,17E-05	BP
GO:0014898	cardiac muscle hypertrophy in response to stress	4,17E-05	BP
GO:0001701	in utero embryonic development	4,17E-05	BP
GO:0006936	muscle contraction	4,17E-05	BP
GO:0030049	muscle filament sliding	4,17E-05	BP
GO:0030239	myofibril assembly	4,17E-05	BP
GO:0043462	regulation of ATPase activity	4,17E-05	BP
GO:0008217	regulation of blood pressure	4,17E-05	BP
GO:0008016	regulation of heart contraction	4,17E-05	BP
GO:0060420	regulation of heart growth	4,17E-05	BP
GO:0002027	regulation of heart rate	4,17E-05	BP
GO:0002026	regulation of the force of heart contraction	4,17E-05	BP
GO:0045214	sarcomere organization	4,17E-05	BP
GO:0006941	striated muscle contraction	4,17E-05	BP
GO:0055010	ventricular cardiac muscle tissue morphogenesis	4,17E-05	BP
GO:0007522	visceral muscle development	4,17E-05	BP
GO:0030016	myofibril	4,58E-05	CC
GO:0032982	myosin filament	4,58E-05	CC
GO:0051015	actin filament binding	4,58E-05	MF
GO:0005524	ATP binding	4,58E-05	MF
GO:0005516	calmodulin binding	4,58E-05	MF

GO:0003774	motor activity	4,58E-05	MF
GO:0016459	myosin complex	4,58E-05	CC
GO:0030686	90S preribosome	5,91E-05	CC
GO:0005604	basement membrane	5,91E-05	CC
GO:0005737	cytoplasm	5,91E-05	CC
GO:0005829	cytosol	5,91E-05	CC
GO:0022627	cytosolic small ribosomal subunit	5,91E-05	CC
GO:0070062	extracellular exosome	5,91E-05	CC
GO:0031012	extracellular matrix	5,91E-05	CC
GO:0016020	membrane	5,91E-05	CC
GO:0043025	neuronal cell body	5,91E-05	CC
GO:0005634	nucleus	5,91E-05	CC
GO:0005886	plasma membrane	5,91E-05	CC
GO:0015935	small ribosomal subunit	5,91E-05	CC
GO:0043236	laminin binding	5,91E-05	MF
GO:0005055	laminin receptor activity	5,91E-05	MF
GO:0043022	ribosome binding	5,91E-05	MF
GO:0003723	RNA binding	5,91E-05	MF
GO:0003735	structural constituent of ribosome	5,91E-05	MF
GO:0098609	cell-cell adhesion	5,91E-05	BP
GO:0000447	endonucleolytic cleavage in ITS1 to separate SSU-rRNA from 5.8S rRNA and LSU-rRNA from tricistronic rRNA transcript (SSU-rRNA, 5.8S rRNA, LSU-rR	5,91E-05	BP
GO:0000461	endonucleolytic cleavage to generate mature 3'-end of SSU-rRNA from (SSU-rRNA, 5.8S rRNA, LSU-rRNA)	5,91E-05	BP
GO:0030855	epithelial cell differentiation	5,91E-05	BP
GO:0000028	ribosomal small subunit assembly	5,91E-05	BP
GO:0006407	rRNA export from nucleus	5,91E-05	BP
GO:0006412	translation	5,91E-05	BP
GO:0030686	90S preribosome	6,66E-05	CC
GO:0022627	cytosolic small ribosomal subunit	6,66E-05	CC
GO:0070062	extracellular exosome	6,66E-05	CC
GO:0031012	extracellular matrix	6,66E-05	CC
GO:0005925	focal adhesion	6,66E-05	CC
GO:0030529	intracellular ribonucleoprotein complex	6,66E-05	CC
GO:0016020	membrane	6,66E-05	CC
GO:0005815	microtubule organizing center	6,66E-05	CC
GO:0005730	nucleolus	6,66E-05	CC
GO:0005634	nucleus	6,66E-05	CC
GO:0043234	protein complex	6,66E-05	CC
GO:0005840	ribosome	6,66E-05	CC
GO:0032040	small-subunit processome	6,66E-05	CC
GO:0003730	mRNA 3'-UTR binding	6,66E-05	MF
GO:0048027	mRNA 5'-UTR binding	6,66E-05	MF
GO:0008266	poly(U) RNA binding	6,66E-05	MF
GO:0019901	protein kinase binding	6,66E-05	MF
GO:0003723	RNA binding	6,66E-05	MF
GO:0003735	structural constituent of ribosome	6,66E-05	MF
GO:1990948	ubiquitin ligase inhibitor activity	6,66E-05	MF
GO:0030154	cell differentiation	6,66E-05	BP
GO:0002181	cytoplasmic translation	6,66E-05	BP
GO:2000059	negative regulation of protein ubiquitination involved in ubiquitin-dependent protein catabolic process	6,66E-05	BP
GO:1904667	negative regulation of ubiquitin protein ligase activity	6,66E-05	BP
GO:0001843	neural tube closure	6,66E-05	BP
GO:0010628	positive regulation of gene expression	6,66E-05	BP
GO:1902255	positive regulation of intrinsic apoptotic signaling pathway by p53 class mediator	6,66E-05	BP
GO:0050821	protein stabilization	6,66E-05	BP
GO:0042274	ribosomal small subunit biogenesis	6,66E-05	BP
GO:0006364	rRNA processing	6,66E-05	BP
GO:0016021	integral component of membrane	7,37E-05	CC
GO:0005886	plasma membrane	7,37E-05	CC
GO:0005829	cytosol	7,42E-05	CC
GO:0022627	cytosolic small ribosomal subunit	7,42E-05	CC
GO:0005783	endoplasmic reticulum	7,42E-05	CC
GO:0070062	extracellular exosome	7,42E-05	CC
GO:0031012	extracellular matrix	7,42E-05	CC
GO:0005925	focal adhesion	7,42E-05	CC
GO:0030529	intracellular ribonucleoprotein complex	7,42E-05	CC
GO:0005730	nucleolus	7,42E-05	CC
GO:0005634	nucleus	7,42E-05	CC
GO:0048027	mRNA 5'-UTR binding	7,42E-05	MF
GO:0003735	structural constituent of ribosome	7,42E-05	MF
GO:0030154	cell differentiation	7,42E-05	BP
GO:0002181	cytoplasmic translation	7,42E-05	BP
GO:0043066	negative regulation of apoptotic process	7,42E-05	BP
GO:0006412	translation	7,42E-05	BP
GO:0003735	structural constituent of ribosome	7,42E-05	MF
GO:0005840	ribosome	7,42E-05	BP
GO:0005737	cytoplasm	7,61E-05	CC
GO:0022625	cytosolic large ribosomal subunit	7,61E-05	CC
GO:0070062	extracellular exosome	7,61E-05	CC
GO:0005925	focal adhesion	7,61E-05	CC
GO:0016020	membrane	7,61E-05	CC
GO:0005730	nucleolus	7,61E-05	CC
GO:0005634	nucleus	7,61E-05	CC
GO:0042788	polysomal ribosome	7,61E-05	CC
GO:0045296	cadherin binding	7,61E-05	MF
GO:0003723	RNA binding	7,61E-05	MF
GO:0000470	maturation of LSU-rRNA	7,61E-05	BP
GO:0006412	translation	7,61E-05	BP
GO:0005783	endoplasmic reticulum	7,91E-05	CC
GO:0005789	endoplasmic reticulum membrane	7,91E-05	CC
GO:0005793	endoplasmic reticulum-Golgi intermediate compartment	7,91E-05	CC
GO:0031673	H zone	7,91E-05	CC
GO:0031674	I band	7,91E-05	CC
GO:0016021	integral component of membrane	7,91E-05	CC
GO:0016020	membrane	7,91E-05	CC
GO:0048471	perinuclear region of cytoplasm	7,91E-05	CC
GO:0016529	sarcoplasmic reticulum	7,91E-05	CC
GO:0033017	sarcoplasmic reticulum membrane	7,91E-05	CC
GO:0005524	ATP binding	7,91E-05	MF

GO:0016887	ATPase activity	7,91E-05	MF
GO:0005509	calcium ion binding	7,91E-05	MF
GO:0005388	calcium-transporting ATPase activity	7,91E-05	MF
GO:0006816	calcium ion transport	7,91E-05	BF
GO:0045988	negative regulation of striated muscle contraction	7,91E-05	BF
GO:0031448	positive regulation of fast-twitch skeletal muscle fiber contraction	7,91E-05	BF
GO:0006942	regulation of striated muscle contraction	7,91E-05	BF
GO:0031672	A band	8,01E-05	CC
GO:0036464	cytoplasmic ribonucleoprotein granule	8,01E-05	CC
GO:0014704	intercalated disc	8,01E-05	CC
GO:0005859	muscle myosin complex	8,01E-05	CC
GO:0032982	myosin filament	8,01E-05	CC
GO:0051015	actin filament binding	8,01E-05	MF
GO:0005524	ATP binding	8,01E-05	MF
GO:0005516	calmodulin binding	8,01E-05	MF
GO:0003774	motor activity	8,01E-05	MF
GO:0006936	muscle contraction	8,01E-05	BF
GO:0022627	cytosolic small ribosomal subunit	9,35E-05	CC
GO:0016020	membrane	9,35E-05	CC
GO:0005634	nucleus	9,35E-05	CC
GO:0005840	ribosome	9,35E-05	CC
GO:0015935	small ribosomal subunit	9,35E-05	CC
GO:0032403	protein complex binding	9,35E-05	MF
GO:0003723	RNA binding	9,35E-05	MF
GO:0003735	structural constituent of ribosome	9,35E-05	MF
GO:0031369	translation initiation factor binding	9,35E-05	MF
GO:0034101	erythrocyte homeostasis	9,35E-05	BF
GO:0097421	liver regeneration	9,35E-05	BF
GO:0000462	maturation of SSU-rRNA from tricistronic rRNA transcript (SSU-rRNA, 5.8S rRNA, LSU-rRNA)	9,35E-05	BF
GO:0042274	ribosomal small subunit biogenesis	9,35E-05	BF
GO:0006364	rRNA processing	9,35E-05	BF
GO:0006413	translational initiation	9,35E-05	BF
GO:0006412	translation	9,35E-05	BF
GO:0005622	intracellular	9,35E-05	CC
GO:0022625	cytosolic large ribosomal subunit	1,08E-04	CC
GO:0005634	nucleus	1,08E-04	CC
GO:0003735	structural constituent of ribosome	1,08E-04	MF
GO:0010033	response to organic substance	1,08E-04	BF
GO:0032526	response to retinoic acid	1,08E-04	BF
GO:0006412	translation	1,08E-04	BF
GO:0003735	structural constituent of ribosome	1,08E-04	MF
GO:0005622	intracellular	1,08E-04	CC
GO:0005840	ribosome	1,08E-04	CC
GO:0044297	cell body	1,14E-04	CC
GO:0005737	cytoplasm	1,14E-04	CC
GO:0005829	cytosol	1,14E-04	CC
GO:0030425	dendrite	1,14E-04	CC
GO:0070062	extracellular exosome	1,14E-04	CC
GO:1990630	IRE1-RACK1-PP2A complex	1,14E-04	CC
GO:0016020	membrane	1,14E-04	CC
GO:0030496	midbody	1,14E-04	CC
GO:0005739	mitochondrion	1,14E-04	CC
GO:0043005	neuron projection	1,14E-04	CC
GO:0043025	neuronal cell body	1,14E-04	CC
GO:0005634	nucleus	1,14E-04	CC
GO:0043204	perikaryon	1,14E-04	CC
GO:0048471	perinuclear region of cytoplasm	1,14E-04	CC
GO:0001891	phagocytic cup	1,14E-04	CC
GO:0015935	small ribosomal subunit	1,14E-04	CC
GO:0045296	cadherin binding	1,14E-04	MF
GO:0030332	cyclin binding	1,14E-04	MF
GO:0008656	cysteine-type endopeptidase activator activity involved in apoptotic process	1,14E-04	MF
GO:0019899	enzyme binding	1,14E-04	MF
GO:0008200	ion channel inhibitor activity	1,14E-04	MF
GO:0042803	protein homodimerization activity	1,14E-04	MF
GO:0005080	protein kinase C binding	1,14E-04	MF
GO:0019903	protein phosphatase binding	1,14E-04	MF
GO:0030292	protein tyrosine kinase inhibitor activity	1,14E-04	MF
GO:0030971	receptor tyrosine kinase binding	1,14E-04	MF
GO:0043022	ribosome binding	1,14E-04	MF
GO:0003723	RNA binding	1,14E-04	MF
GO:0042169	SH2 domain binding	1,14E-04	MF
GO:0035591	signal adaptor activity	1,14E-04	MF
GO:0006919	activation of cysteine-type endopeptidase activity involved in apoptotic process	1,14E-04	BF
GO:0007049	cell cycle	1,14E-04	BF
GO:0071333	cellular response to glucose stimulus	1,14E-04	BF
GO:0071363	cellular response to growth factor stimulus	1,14E-04	BF
GO:0007369	gastrulation	1,14E-04	BF
GO:0030308	negative regulation of cell growth	1,14E-04	BF
GO:0010629	negative regulation of gene expression	1,14E-04	BF
GO:1903208	negative regulation of hydrogen peroxide-induced neuron death	1,14E-04	BF
GO:0033137	negative regulation of peptidyl-serine phosphorylation	1,14E-04	BF
GO:0050765	negative regulation of phagocytosis	1,14E-04	BF
GO:0051898	negative regulation of protein kinase B signaling	1,14E-04	BF
GO:0017148	negative regulation of translation	1,14E-04	BF
GO:0030178	negative regulation of Wnt signaling pathway	1,14E-04	BF
GO:0001649	osteoblast differentiation	1,14E-04	BF
GO:0043473	pigmentation	1,14E-04	BF
GO:0043065	positive regulation of apoptotic process	1,14E-04	BF
GO:0030822	positive regulation of cAMP catabolic process	1,14E-04	BF
GO:0030335	positive regulation of cell migration	1,14E-04	BF
GO:0051343	positive regulation of cyclic-nucleotide phosphodiesterase activity	1,14E-04	BF
GO:2000543	positive regulation of gastrulation	1,14E-04	BF
GO:0042998	positive regulation of Golgi to plasma membrane protein transport	1,14E-04	BF
GO:0043547	positive regulation of GTPase activity	1,14E-04	BF
GO:2001244	positive regulation of intrinsic apoptotic signaling pathway	1,14E-04	BF
GO:0051901	positive regulation of mitochondrial depolarization	1,14E-04	BF
GO:0032436	positive regulation of proteasomal ubiquitin-dependent protein catabolic process	1,14E-04	BF

GO:0006351	biological_process^transcription, DNA-templated	1,46E-04	BF
GO:0022625	cytosolic large ribosomal subunit	1,51E-04	CC
GO:0033291	eukaryotic 80S initiation complex	1,51E-04	CC
GO:0005925	focal adhesion	1,51E-04	CC
GO:0003723	RNA binding	1,51E-04	MF
GO:0003735	structural constituent of ribosome	1,51E-04	MF
GO:0034463	90S preribosome assembly	1,51E-04	BF
GO:0048318	axial mesoderm development	1,51E-04	BF
GO:0042474	middle ear morphogenesis	1,51E-04	BF
GO:0001503	ossification	1,51E-04	BF
GO:0006417	regulation of translation	1,51E-04	BF
GO:0007605	sensory perception of sound	1,51E-04	BF
GO:0001501	skeletal system development	1,51E-04	BF
GO:0006412	translation	1.51E-04	BF

b)

Tissue	GO	Term	P-value	Ontology
Duodenum				
	GO:0005615	extracellular space	4,70E-06	CC
	GO:0036457	keratohyalin granule	4,70E-06	CC
	GO:0017171	serine hydrolase activity	4,70E-06	MF
	GO:0061436	establishment of skin barrier	4,70E-06	BP
	GO:0006508	proteolysis	4,70E-06	BP
	GO:0003676	nucleic acid binding	6,04E-06	MF
	GO:0016787	hydrolase activity	6,04E-06	MF
	GO:0046872	metal ion binding	6,04E-06	MF
	GO:0005615	extracellular space	7,47E-06	CC
	GO:0004180	carboxypeptidase activity	7,47E-06	MF
	GO:0004181	metallocarboxypeptidase activity	7,47E-06	MF
	GO:0008270	zinc ion binding	7,47E-06	MF
	GO:0006508	proteolysis	7,47E-06	BP
	GO:0005737	cytoplasm	1,29E-05	CC
	GO:0005874	microtubule	1,29E-05	CC
	GO:0005525	GTP binding	1,29E-05	MF
	GO:0003924	GTPase activity	1,29E-05	MF
	GO:0005200	structural constituent of cytoskeleton	1,29E-05	MF
	GO:0007017	microtubule-based process	1,29E-05	BP
	GO:0005615	extracellular space	1,29E-05	CC
	GO:0004252	serine-type endopeptidase activity	1,29E-05	MF
	GO:0006508	proteolysis	1,29E-05	BP
	GO:0072562	blood microparticle	1,86E-05	CC
	GO:0070062	extracellular exosome	1,86E-05	CC
	GO:0005615	extracellular space	1,86E-05	CC
	GO:0046872	metal ion binding	1,86E-05	MF
	GO:0004252	serine-type endopeptidase activity	1,86E-05	MF
	GO:0007586	digestion	1,86E-05	BP
	GO:0006508	proteolysis	1,86E-05	BP
	GO:0031000	response to caffeine	1,86E-05	BP
	GO:0035094	response to nicotine	1,86E-05	BP
	GO:0007584	response to nutrient	1,86E-05	BP
	GO:0010033	response to organic substance	1,86E-05	BP
	GO:0005615	extracellular space	2,45E-05	CC
	GO:0046872	metal ion binding	2,45E-05	MF
	GO:0004252	serine-type endopeptidase activity	2,45E-05	MF
	GO:0007586	digestion	2,45E-05	BP
	GO:0005737	cytoplasm	3,16E-05	CC
	GO:0030529	intracellular ribonucleoprotein complex	3,36E-05	CC
	GO:0003727	single-stranded RNA binding	3,36E-05	MF
	GO:0032197	transposition, RNA-mediated	3,36E-05	BP
	GO:0044194	cytolytic granule	4,26E-05	CC
	GO:0005829	cytosol	4,26E-05	CC
	GO:0031904	endosome lumen	4,26E-05	CC
	GO:0005576	extracellular region	4,26E-05	CC
	GO:0016021	integral component of membrane	4,26E-05	CC
	GO:0016020	membrane	4,26E-05	CC
	GO:0005886	plasma membrane	4,26E-05	CC
	GO:0005509	calcium ion binding	4,26E-05	MF
	GO:0042802	identical protein binding	4,26E-05	MF
	GO:0022829	wide pore channel activity	4,26E-05	MF
	GO:0006915	apoptotic process	4,26E-05	BP
	GO:0006968	cellular defense response	4,26E-05	BP
	GO:0019835	cytolysis	4,26E-05	BP
	GO:0002357	defense response to tumor cell	4,26E-05	BP
	GO:0051607	defense response to virus	4,26E-05	BP
	GO:0002418	immune response to tumor cell	4,26E-05	BP
	GO:0001771	immunological synapse formation	4,26E-05	BP
	GO:0051712	positive regulation of killing of cells of other organism	4,26E-05	BP
	GO:0051260	protein homooligomerization	4,26E-05	BP
	GO:0005737	cytoplasm	4,58E-05	CC
	GO:0005795	Golgi stack	4,58E-05	CC
	GO:0005634	nucleus	4,58E-05	CC
	GO:0005819	spindle	4,58E-05	CC
	GO:0005524	ATP binding	4,58E-05	MF
	GO:0004674	protein serine/threonine kinase activity	4,58E-05	MF
	GO:0007049	cell cycle	4,58E-05	BP
	GO:0051301	cell division	4,58E-05	BP
	GO:0090166	Golgi disassembly	4,58E-05	BP
	GO:0018105	peptidyl-serine phosphorylation	4,58E-05	BP
	GO:0046777	protein autophosphorylation	4,58E-05	BP
	GO:0006468	protein phosphorylation	4,58E-05	BP

GO:0008360	regulation of cell shape	4,58E-05	BP
GO:0005615	extracellular space	7,18E-05	CC
GO:0004252	serine-type endopeptidase activity	7,18E-05	MF
GO:0006508	proteolysis	7,18E-05	BP
GO:0005737	cytoplasm	8,77E-05	CC
GO:0005634	nucleus	8,77E-05	CC
GO:0008565	protein transporter activity	8,77E-05	MF
GO:0006606	protein import into nucleus	8,77E-05	BP
GO:0005615	extracellular space	9,35E-05	CC
GO:0046872	metal ion binding	9,35E-05	MF
GO:0004252	serine-type endopeptidase activity	9,35E-05	MF
GO:0007586	digestion	9,35E-05	BP
GO:0006508	proteolysis	9,35E-05	BP
GO:0005615	extracellular space	9,92E-05	CC
GO:0004252	serine-type endopeptidase activity	9,92E-05	MF
GO:0007586	digestion	9,92E-05	BP
GO:0006508	proteolysis	9,92E-05	BP
GO:1990622	CHOP-ATF3 complex	9,93E-05	CC
GO:0005730	nucleolus	9,93E-05	CC
GO:0046982	protein heterodimerization activity	9,93E-05	MF
GO:0042803	protein homodimerization activity	9,93E-05	MF
GO:0000978	RNA polymerase II proximal promoter sequence-specific DNA binding	9,93E-05	MF
GO:0001078	transcriptional repressor activity, RNA polymerase II proximal promoter sequence-specific DNA binding	9,93E-05	MF
GO:0034198	cellular response to amino acid starvation	9,93E-05	BP
GO:0030968	endoplasmic reticulum unfolded protein response	9,93E-05	BP
GO:0006094	gluconeogenesis	9,93E-05	BP
GO:0070373	negative regulation of ERK1 and ERK2 cascade	9,93E-05	BP
GO:1903984	positive regulation of TRAIL-activated apoptotic signaling pathway	9,93E-05	BP
GO:1990440	positive regulation of transcription from RNA polymerase II promoter in response to endoplasmic reticulum stre	9,93E-05	BP
GO:0035914	skeletal muscle cell differentiation	9,93E-05	BP
GO:0006351	transcription, DNA-templated	9,93E-05	BP
GO:0005737	cytoplasm	1,08E-04	CC
GO:0005576	extracellular region	1,08E-04	CC
GO:0052689	carboxylic ester hydrolase activity	1,08E-04	MF
GO:0004771	sterol esterase activity	1,08E-04	MF
GO:0004806	triglyceride lipase activity	1,08E-04	MF
GO:0016042	lipid catabolic process	1,08E-04	BP
GO:0016787	hydrolase activity	1,08E-04	MF
GO:0008152	metabolic process	1,08E-04	BP

c)

Tissue	GO	Term	P-value	Ontology
Skin				
	GO:0005783	endoplasmic reticulum	6,88E-05	CC
	GO:0005576	extracellular region	6,88E-05	CC
	GO:0005634	nucleus	6,88E-05	CC
	GO:0005509	calcium ion binding	6,88E-05	MF
	GO:0004536	deoxyribonuclease activity	6,88E-05	MF
	GO:0003677	DNA binding	6,88E-05	MF
	GO:0004520	endodeoxyribonuclease activity	6,88E-05	MF
	GO:0006309	apoptotic DNA fragmentation	6,88E-05	BP
	GO:0006259	DNA metabolic process	6,88E-05	BP
	GO:0010623	programmed cell death involved in cell development	6,88E-05	BP

Supplementary table 3.6. E**nriched GO terms of DEGs between Sham and LPS groups in A) head-kidney, B) duodenum and C) skin.** The enriched GO terms are identified as biological process (BP), molecular function (MF) and cellular component (CC) in *N. coriiceps* (FDR < 0.05).

a)

Tissue	GO	Term	P-value	Ontology
Head-kidney				
	GO:0035605	peptidyl-cysteine S-nitrosylase activity	4,13E-04	MF
	GO:0035606	peptidyl-cysteine S-trans-nitrosylation	4,13E-04	BP
	GO:0017014	protein nitrosylation	6,81E-04	BP
	GO:0018119	peptidyl-cysteine S-nitrosylation	6,81E-04	BP
	GO:0004365	glyceraldehyde-3-phosphate dehydrogenase (NAD+) (phosphorylating) activity	6,99E-04	MF
	GO:0043891	glyceraldehyde-3-phosphate dehydrogenase (NAD(P)+) (phosphorylating) activity	6,99E-04	MF
	GO:0016769	transferase activity, transferring nitrogenous groups	2,62E-03	MF
	GO:0018198	peptidyl-cysteine modification	3,02E-03	BP
	GO:0050661	NADP binding	4,35E-03	MF
	GO:0016620	oxidoreductase activity, acting on the aldehyde or oxo group of donors, NAD or NADP as acceptor	5,79E-03	MF
	GO:0016903	oxidoreductase activity, acting on the aldehyde or oxo group of donors	6,48E-03	MF
	GO:0051402	neuron apoptotic process	8,42E-03	BP
	GO:0070997	neuron death	1,03E-02	BP
	GO:0006096	glycolytic process	1,17E-02	BP
	GO:0006757	ATP generation from ADP	1,17E-02	BP
	GO:0006165	nucleoside diphosphate phosphorylation	1,19E-02	BP
	GO:0046939	nucleotide phosphorylation	1,19E-02	BP
	GO:0046031	ADP metabolic process	1,29E-02	BP
	GO:0009135	purine nucleoside diphosphate metabolic process	1,32E-02	BP
	GO:0009179	purine ribonucleoside diphosphate metabolic process	1,32E-02	BP
	GO:0009185	ribonucleoside diphosphate metabolic process	1,38E-02	BP
	GO:0006090	pyruvate metabolic process	1,47E-02	BP
	GO:0009132	nucleoside diphosphate metabolic process	1,53E-02	BP
	GO:0051287	NAD binding	1,68E-02	MF
	GO:0044724	single-organism carbohydrate catabolic process	2,16E-02	BP
	GO:0015630	microtubule cytoskeleton	2,18E-02	CC
	GO:0006006	glucose metabolic process	2,19E-02	BP
	GO:0019362	pyridine nucleotide metabolic process	2,40E-02	BP
	GO:0046496	nicotinamide nucleotide metabolic process	2,40E-02	BP
	GO:0016052	carbohydrate catabolic process	2,50E-02	BP
	GO:0072524	pyridine-containing compound metabolic process	2,51E-02	BP
	GO:0046034	ATP metabolic process	2,63E-02	BP
	GO:0006733	oxidoreduction coenzyme metabolic process	2,72E-02	BP
	GO:0019318	hexose metabolic process	3,12E-02	BP
	GO:0009167	purine ribonucleoside monophosphate metabolic process	3,38E-02	BP
	GO:0050821	protein stabilization	3,39E-02	BP
	GO:0009126	purine nucleoside monophosphate metabolic process	3,42E-02	BP
	GO:0005996	monosaccharide metabolic process	3,54E-02	BP
	GO:0009161	ribonucleoside monophosphate metabolic process	3,63E-02	BP
	GO:0050662	coenzyme binding	3,64E-02	MF
	GO:0008017	microtubule binding	3,79E-02	MF
	GO:0009123	nucleoside monophosphate metabolic process	3,82E-02	BP
	GO:0009205	purine ribonucleoside triphosphate metabolic process	3,85E-02	BP
	GO:0009199	ribonucleoside triphosphate metabolic process	4,08E-02	BP
	GO:0009144	purine nucleoside triphosphate metabolic process	4,64E-02	BP
	GO:0006091	generation of precursor metabolites and energy	4,80E-02	BP
	GO:0006732	coenzyme metabolic process	4,97E-02	BP

b)

Tissue	GO	Term	P-value	Ontology
Duodenum				
	GO:0032635	interleukin-6 production	3,79E-08	BP
	GO:0070741	response to interleukin-6	3,79E-08	BP
	GO:0032611	interleukin-1 beta production	3,79E-08	BP
	GO:0032675	regulation of interleukin-6 production	3,79E-08	BP
	GO:0070102	interleukin-6-mediated signaling pathway	3,79E-08	BP
	GO:0071354	cellular response to interleukin-6	3,79E-08	BP
	GO:0042163	interleukin-12 beta subunit binding	3,79E-08	MF
	GO:0005138	interleukin-6 receptor binding	3,79E-08	MF
	GO:0004915	interleukin-6 receptor activity	3,79E-08	MF
	GO:0019981	interleukin-6 binding	3,79E-08	MF
	GO:0042164	interleukin-12 alpha subunit binding	3,79E-08	MF
	GO:0005896	interleukin-6 receptor complex	3,79E-08	CC
	GO:0005893	interleukin-2 receptor complex	3,79E-08	CC
	GO:1900747	negative regulation of vascular endothelial growth factor signaling pathway	5,82E-04	BP
	GO:1902548	negative regulation of cellular response to vascular endothelial growth factor stimulus	5,82E-04	BP
	GO:0019800	peptide cross-linking via chondroitin 4-sulfate glycosaminoglycan	8,35E-04	BP
	GO:0005589	collagen type VI trimer	1,41E-03	CC
	GO:1900746	regulation of vascular endothelial growth factor signaling pathway	2,16E-03	BP
	GO:1902547	regulation of cellular response to vascular endothelial growth factor stimulus	2,16E-03	BP
	GO:0051901	positive regulation of mitochondrial depolarization	2,28E-03	BP
	GO:1904181	positive regulation of membrane depolarization	3,04E-03	BP
	GO:0051900	regulation of mitochondrial depolarization	3,05E-03	BP
	GO:0090131	mesenchyme migration	3,49E-03	BP
	GO:0030204	chondroitin sulfate metabolic process	3,65E-03	BP
	GO:0090141	positive regulation of mitochondrial fission	3,73E-03	BP
	GO:0090130	tissue migration	4,00E-03	BP
	GO:0018149	peptide cross-linking	4,21E-03	BP
	GO:0003254	regulation of membrane depolarization	5,64E-03	BP
	GO:0090140	regulation of mitochondrial fission	5,94E-03	BP
	GO:0001890	placenta development	6,63E-03	BP
	GO:0010596	negative regulation of endothelial cell migration	7,33E-03	BP
	GO:1903510	mucopolysaccharide metabolic process	7,95E-03	BP
	GO:0050840	extracellular matrix binding	8,64E-03	MF
	GO:0046426	negative regulation of JAK-STAT cascade	9,41E-03	BP
	GO:0016239	positive regulation of macroautophagy	1,00E-02	BP
	GO:0010633	negative regulation of epithelial cell migration	1,05E-02	BP
	GO:0014068	positive regulation of phosphatidylinositol 3-kinase signaling	1,05E-02	BP
	GO:0005518	collagen binding	1,06E-02	MF
	GO:0004860	protein kinase inhibitor activity	1,09E-02	MF
	GO:0019210	kinase inhibitor activity	1,16E-02	MF
	GO:0051881	regulation of mitochondrial membrane potential	1,17E-02	BP
	GO:0030203	glycosaminoglycan metabolic process	1,23E-02	BP
	GO:0071944	cell periphery	1,25E-02	CC
	GO:0007519	skeletal muscle tissue development	1,26E-02	BP
	GO:0005615	extracellular space	1,40E-02	CC
	GO:0042060	wound healing	1,43E-02	BP
	GO:0006022	aminoglycan metabolic process	1,46E-02	BP
	GO:0032982	myosin filament	1,50E-02	CC
	GO:0016525	negative regulation of angiogenesis	1,54E-02	BP
	GO:2000181	negative regulation of blood vessel morphogenesis	1,54E-02	BP
	GO:1901343	negative regulation of vasculature development	1,66E-02	BP
	GO:0046425	regulation of JAK-STAT cascade	1,70E-02	BP
	GO:0072562	blood microparticle	1,96E-02	CC
	GO:0014706	striated muscle tissue development	2,01E-02	BP
	GO:0005581	collagen trimer	2,03E-02	CC
	GO:0016241	regulation of macroautophagy	2,15E-02	BP
	GO:0090288	negative regulation of cellular response to growth factor stimulus	2,26E-02	BP
	GO:0030175	filopodium	2,28E-02	CC
	GO:0060537	muscle tissue development	2,31E-02	BP
	GO:0010594	regulation of endothelial cell migration	2,46E-02	BP
	GO:0010822	positive regulation of mitochondrion organization	2,53E-02	BP
	GO:0047485	protein N-terminus binding	2,60E-02	MF

GO:0001822	kidney development	2,71E-02	BP
GO:2000021	regulation of ion homeostasis	2,75E-02	BP
GO:0014066	regulation of phosphatidylinositol 3-kinase signaling	2,96E-02	BP
GO:0010508	positive regulation of autophagy	3,11E-02	BP
GO:0005539	glycosaminoglycan binding	3,12E-02	MF
GO:0019887	protein kinase regulator activity	3,19E-02	MF
GO:0009611	response to wounding	3,23E-02	BP
GO:0009612	response to mechanical stimulus	3,27E-02	BP
GO:0016459	myosin complex	3,37E-02	CC
GO:0019207	kinase regulator activity	3,79E-02	MF
GO:0010821	regulation of mitochondrion organization	3,88E-02	BP
GO:0010632	regulation of epithelial cell migration	3,95E-02	BP
GO:0010628	positive regulation of gene expression	3,99E-02	BP
GO:0048608	reproductive structure development	3,99E-02	BP
GO:0007568	aging	4,07E-02	BP
GO:0030336	negative regulation of cell migration	4,13E-02	BP
GO:0006469	negative regulation of protein kinase activity	4,15E-02	BP
GO:2000146	negative regulation of cell motility	4,28E-02	BP
GO:0005578	proteinaceous extracellular matrix	4,36E-02	CC
GO:0090287	regulation of cellular response to growth factor stimulus	4,40E-02	BP
GO:0042391	regulation of membrane potential	4,43E-02	BP
GO:0033673	negative regulation of kinase activity	4,44E-02	BP
GO:0018209	peptidyl-serine modification	4,51E-02	BP
GO:0051271	negative regulation of cellular component movement	4,63E-02	BP

c)

Tissue	GO	Term	P-value	Ontology
Skin				
	GO:0016567	protein ubiquitination	3,08E-02	BP
	GO:0032446	protein modification by small protein conjugation	3,44E-02	BP
	GO:0007275	multicellular organismal development	3,71E-02	BP
	GO:0070647	protein modification by small protein conjugation or removal	4,08E-02	BP

Supplementary table 3.7. Enriched KEGG pathways of DEGs from A) head-kidney and B) duodenum comparing Control and Sham groups in *N. coriiceps*.

a) KEGG enriched pathways represented in head-kidney transcriptome of the sham group

KEGG enrichment pathway analysis					Experimental groups	
ID	Term	Nr genes involved	PValue	FDR	Control	Sham
hsa03010	Ribosome	18	7.23e-24	6.29e-22		☒
hsa04261	Adrenergic signaling in cardiomyocytes	4	2.63e-3	9.13e-2		☒
hsa04260	Cardiac muscle contraction	3	3.15e-3	9.13e-2		☒
hsa04145	Phagosome	3	2.86e-2	3.94e-1		☒
hsa04662	B cell receptor signaling pathway	2	3.51e-2	3.94e-1		☒
hsa04020	Calcium signaling pathway	3	3.63e-2	3.94e-1		☒
hsa04540	Gap junction	2	4.28e-2	4.14e-1		☒

b) KEGG enriched pathways represented in the duodenum transcriptome of the sham group

KEGG enrichment pathway analysis					Experimental groups	
ID	Term	Nr genes involved	PValue	FDR	Control	Sham
hsa04974	Protein digestion and absorption	4	7.94e-5	6.60e-3		☒
hsa04972	Pancreatic secretion	4	1.40e-4	6.60e-3		☒
hsa04210	Apoptosis	3	5.46e-3	1.71e-1		☒
hsa04657	IL-17 signaling pathway	2	1.97e-2	3.42e-1		☒
hsa04725	Cholinergic synapse	2	3.90e-2	3.91e-1		☒
hsa00450	Selenocompound metabolism	1	4.06e-2	3.91e-1		☒
hsa04142	Lysosome	2	4.31e-2	3.91e-1		☒

Supplementary table 3.8. Enriched KEGG pathways of A) head-kidney, B) duodenum and C) skin DEGs between Sham and LPS groups in *N. coriiceps*.

a) KEGG enriched pathways in the head-kidney transcriptome of the LPS group

KEGG enrichment pathway analysis					Experimental groups	
ID	Term	Nr genes involved	PValue	FDR	Sham	LPS
hsa01230	Biosynthesis of amino acids	2	2.07e-2	4.39e-1		☒
hsa00450	Selenocompound metabolism	1	4.24e-2	4.39e-1		☒
hsa00511	Other glycan degradation	1	4.58e-2	4.39e-1		☒
hsa00514	Other types of O-glycan biosynthesis	1	4.75e-2	4.39e-1		☒

b) KEGG enriched pathways in the duodenum transcriptome of the LPS group

KEGG enrichment pathway analysis					Experimental groups	
ID	Term	Nr genes involved	PValue	FDR	Sham	LPS
hsa04974	Protein digestion and absorption	10	1.46e-11	1.62e-9		☒
hsa04972	Pancreatic secretion	6	8.27e-6	4.59e-4		☒
hsa04971	Gastric acid secretion	3	6.72e-3	2.26e-1		☒
hsa05416	Viral myocarditis	3	8.98e-3	2.26e-1		☒
hsa05164	Influenza A	4	1.02e-2	2.26e-1		☒
hsa04510	Focal adhesion	4	1.81e-2	2.75e-1		☒
hsa05205	Proteoglycans in cancer	4	1.81e-2	2.75e-1		☒
hsa04611	Platelet activation	3	1.98e-2	2.75e-1		☒
hsa04650	Natural killer cell mediated cytotoxicity	3	2.48e-2	2.86e-1		☒
hsa04210	Apoptosis	3	2.58e-2	2.86e-1		☒
hsa00750	Vitamin B6 metabolism	1	3.32e-2	3.35e-1		☒
hsa04921	Oxytocin signaling pathway	3	3.91e-2	3.62e-1		☒
hsa04610	Complement and coagulation cascades	2	4.63e-2	3.96e-1		☒

c) KEGG enriched pathways in the skin transcriptome of the LPS group

KEGG enrichment pathway analysis					Experimental groups	
ID	Term	Nr genes involved	PValue	FDR	Sham	LPS
hsa05164	Influenza A	3	1.31e-4	1.70e-3		☒
hsa03420	Nucleotide excision repair	1	2.43e-2	9.22e-2		☒
hsa04622	RIG-I-like receptor signaling pathway	1	3.44e-2	9.22e-2		☒
hsa05133	Pertussis	1	4.73e-2	9.22e-2		☒
hsa04974	Protein digestion and absorption	1	4.84e-2	9.22e-2		☒

Supplementary table 3.9. Summary of LPS challenge experiments performed in teleost fish. The LPS challenges vary in source, concentration, time of exposure, species, and analysis.

Fish species	Mode of administration	LPS source	LPS concentration	Stage	Time of exposition	Treatment groups	Approach	Principal effects	Authors
SERUM ASSAYS									
Oncorhynchus mykiss	ip	*E. coli O55:B5*	1 mg kg-1	Adult	24 hours	Sham vs LPS	Candidate genes	Induces hypoferraemic responses	Congleton and Wagner, 1991
Salmo salar	*in vitro*	*V. anguillarum O1*	74 MBq kg-1	Adult (Macrophage cells)	2 days	Control vs LPS	Serum assays	Enhances phagocysis, pinocytic activity, production of superoxide anion	Dalmo and Seljelid, 1995
Salmo salar	ip	*E. coli B5:55*	1 mg kg-1	Adult	1-19 days	Sham vs LPS	Serum assays	Induces hypoferraemic responses	Langston et al., 2000
Perca flavescens	ip	*E. coli O55:B5*	3 mg kg-1	Juvenile	1.5-6 hours and, 3-14 days	Sham vs LPS	Cortisol assay	Increased cortisol levels at shor-term (hours) and no effect at long-term (days)	Haukenes and Barton, 2004
Sparus aurata	immersion	*E.coli LPS*	50 µg ml-1	Larvae	30 days	Control vs LPS	Serum assays	Differences in anti-proteases activities	Hanif et al., 2005
Salvelinus fontinalis	*in vitro*	*E.coli LPS*	mg kg-1 and 0.1 g l	Adult (Macrophage cells)	24 hours	Sham vs LPS	Serum assays	Increase plasma cortisol, potentiate effects of LH and induces apoptosis	MacKenzie et al., 2006
Oreochromis mossamb	food diet	*A. hydrophila*	0.01, 0.1 and 1%/2% body weight	Adult	1-3 weeks	Control vs LPS	Serum assays	Increased innate immune responses	Christybapita et al., 2007
Lobeo rohita	ip	*E. coli O55:B5*	0.5-20 EU kg -1	Adult	7-15 days	unmanipulated control vs LPS	Serum assays	Differences in total globulin, lysozyme, myeloperoxidase and respiratory burst	Nayak et al., 2008
CANDIDATE GENES									
Danio rerio	immersion	*E. coli O111:B4, O55:B5, O127:B8*	0.1-10 ng ml-1	Eggs/embryos	4h post-fertilization	Control vs LPS	Candidate genes	Increases TNF-α and IL-1β	Watzke et al., 2007
Danio rerio	immersion	*E.coli*	1ug ml-1	Larvae	3-12 hours	Control vs LPS	Candidate genes	Complement and MBL	Wang and Han, 2013
Danio rerio	immersion	LPS	10 µg ml-1	Embryos	1-2 hours	Control vs LPS	Candidate genes and serum assays	Increased NO and ROS production	Ko et al., 2017
Notothenia coriiceps	immersion	*heat-killed E. coli O11:B4*	10 µg ml-1	Adult	6 and 12 hours	Control vs LPS	Candidate genes	Increases Toll-like receptors expression	Ahn et al, 2014
Notothenia coriiceps and N. rossii	ip	*E. coli O111:B4*	3mg kg-1	Adult	7 days	Sham vs LPS	Candidate genes and serum assays	Induces hypoferraemic responses	Martinez et al., 2020
Oncorhynchus tshawyts	*in vitro*	*E. coli O111:B4, O55:B5*	10 µg ml-1	Adult (PBMC cells)	0.5-24 hours	Control vs LPS	Candidate genes and serum assays	Increases ROS production, PBMCs, IFNγ, TNF-α, IL-10 and phagocytic activity	Lulijwa et al., 2019
Plecoglossus altivelis	*in vitro*	*E. coli O111:B4, O55:B5*	1 mg ml-1	Adult (Macrophage cells)	48-96 hours	Control vs LPS	Candidate genes	Increases TNF-α and IL-1β	Lu et al., 2018
Miichthys miiuy	ip	*E. coli O55:B5*	1 mg ml-1	Adult	12-48 hours	Sham vs LPS	Candidate genes	Increases NOD1	Chu et al., 2020
Ctenophcuyngodon ide	ip	LPS	5 µg g-1	Adult	3-48 hours	Control vs LPS	Candidate genes	Increased AdipoRs in liver	Qin et al., 2020
Trachinotus ovatus	ip	*E.coli O26:B6*	10 mg kg-1	Adult	24-72 hours	Sham vs LPS	Candidate genes	Higher expression of p65	Xie et al., 2020

METABOLIC ASSAY									
Gambusia holbrooki	ip	*E. coli O55:B5*	10 µg g-1	Adult	24-48 hours and 7 days	Sham vs LPS	Metabolic rate assays	Increase metabolic scope	Bonneaud et al., 2016
Mugil cephalus	ip	LPS	, 10 and 100 µg kg-	Juvenile	6-48 hours and 1 week	Sham vs LPS	Oxidative stress assays	Alteration of antioxidant responses	Abdel-Mageid et al., 2019
GLOBAL GENE ANALYSIS									
Eptatretus burgeri	*in vitro*	*E. coli SOLR*	1x10^6 independent plaque-forming units	Adult	unknown	Control vs LPS	Transcriptomic by EST	Innate immune related genes	Suzuki et al., 2004
Oncorhynchus mykiss	ip	*E.coli O26:B6*	6mg kg-1	Adult	24-72 hours	unmanipulated control vs LPS	DNA microarray	Metalloproteinases, collagen, extracellular matrix, MHC and Igs	MacKenzie et al., 2008
Pelteobagrus fulvidrac	ip	*E.coli O26:B6*	50 mg kg-1	Adult	6h	Sham vs LPS	Supression substractive hybridization	Complement, lysozyme, Igs, MHC, Tlrs, chemokines	Liu et al., 2016
Pelteobagrus fulvidrac	ip	LPS	unknown	Adult	12 hours	Sham vs LPS	Transcriptomic by NGS	Enhanced immune response namely CXCL2-like chemokine, goose-type lysozyme and cathepsin K	Liu et al., 2018
Lates calcarifer	ip	*E. coli O111:B4*	10 µg ml-1	Juvenile	6-72 hours and 7 days	Sham vs LPS	Transcriptomic by NGS	Increased expression of C-type lectin receptors	Zoccola et al., 2017
Salmo salar	ip	*E.coli*	6 mg kg-1	Juvenile	68-70 hours	Sham vs LPS	Transcriptomic by NGS	MHC I and II	Palstra et al., 2018
Epinephelus fuscogutta	ip	*V. harveyi GDH11385*	3.5 × 10^5 CFU/mL	Adult	7-14 days	Sham vs LPS	Transcriptomic by NGS	DEGs related to infectious and immune diseases and immune system	Cai et al., 2018
Ictalurus punctatus	immersion	*E. coli O127:B8*	3 and 10 mg ml-1	Adult	12-24 hours	Control vs LPS	Transcriptomic by NGS	Increased expression of complement and cascade coagulation pathways	Jiang et al., 2020
Schizothorax prenanti	ip	*A. hydrophila LPS and E. coli O111:B4*	2x10^7 EU kg -1	Adult	12 hours	Sham vs LPS	Transcriptomic by NGS	Increased expression of TLR5, TLR25, PTX3 and C1q	Li et al., 2020c
Larimichthys crocea	*in vitro*	*E. coli O55:B5*	unknown	Adult (Macrophage cells)	2 hours	Control vs LPS	Transcriptomic by NGS	Increases pathogen recognition receptors, chemokines, cytokines and their receptors	Li et al., 2020b
Oreochromis niloticus	ip	*Fno AOD104086*	3.3x10^5 cfu	Adult	1-2 days	Sham vs LPS	Transcriptomic by NGS	DEGs related to immune response namely complement and coagulation cascades, cytokines, lysozyme and phagosome	Maekawa et al., 2021

3.7.2 Supplementary figures

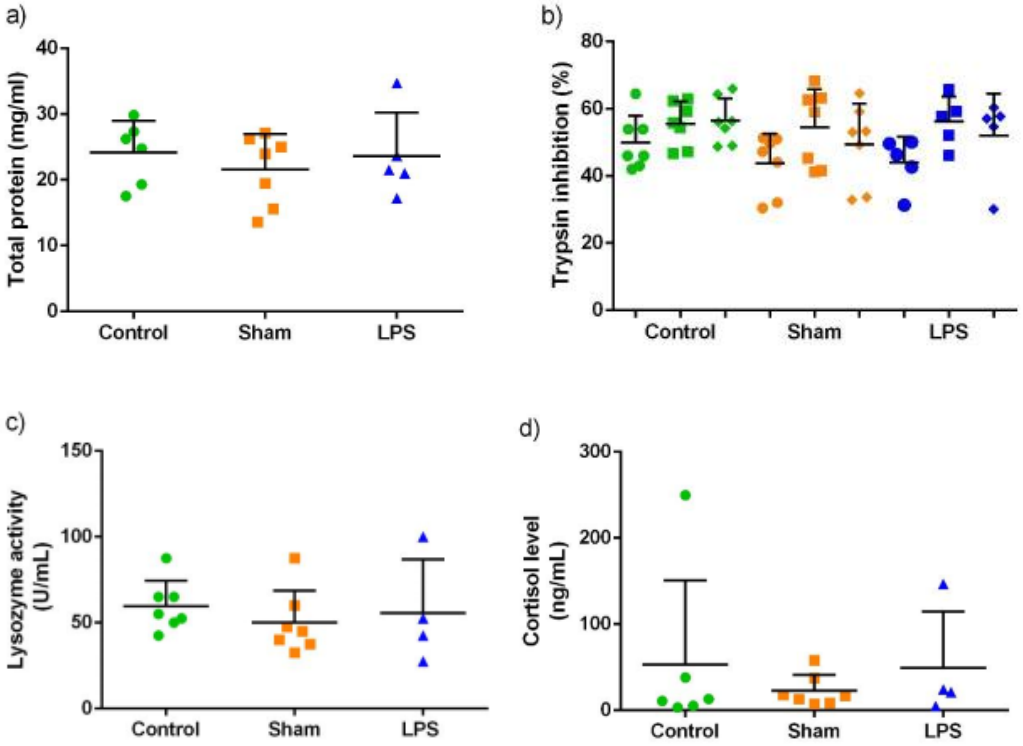

Supplementary figure 3.1. Biochemical analysis of blood plasma. Measurements of (A) total protein (mg/ml), (B) trypsin inhibition (%), (C) lysozyme (U/ml) and (D) cortisol (ng/ml) between the three treatment groups. Control-non injected in green (control), sham in orange (sham) and LPS-injected (LPS) in blue. The symbols for trypsin inhibition (B) represent different incubation temperatures during the assay, circles -37ºC, squares- 21ºC and diamonds- 4ºC. No statistically significant differences (one-way ANOVA, $p>0.05$).

CHAPTER 4

Global transcriptomic response of immune related tissues to LPS and Poly I:C immersion in *Notothenia rossii*

Global transcriptomic response of immune related tissues to LPS and Poly I:C immersion in *Notothenia rossii*

Manuscript in preparation

Acknowledgements

The authors would like to acknowledge Elsa Couto for carrying out the steroid assays and the 2019 crew of the Great Wall Chinese Antarctic Station for their hospitability and logistical support. This study was carried out with logistic and financial support of the Portuguese Polar Programme (FACC PROPOLAR 2016-2017) and funded by Portuguese Foundation for Science and Technology (FCT) through projects FCT-NSFC/0002/2016, PTDC/BIAANM/3484/2014 and CCMAR/Multi/04326/2019, and a PhD fellowship SFRH/BD/120040/2016 to CS.

Global transcriptomic response of immune related tissues to LPS and Poly I:C immersion in *Notothenia rossii*

Cármen Sousa[1], Maoxiao Peng[1,2], Pedro M Guerreiro[1], João CR Cardoso[1], Liangbiao Chen[2], Adelino VM Canário[1,2], Deborah M Power[1,2]

1 Centro de Ciências do Mar (CCMAR), Universidade do Algarve, Campus de Gambelas, 8005-139 Faro, Portugal.

2 International Research Center for Marine Biosciences, Ministry of Science and Technology, Shanghai Ocean University (SHOU), 201306 Shanghai, China.

4.1. Abstract

The notothenioid isolated evolution in the stable cold environment of the Antarctica question whether their immune system has developed unique features compared to other teleosts. To test this question, challenges with bacterial lipopolysaccharide (LPS) synthetic viral polyinosinic: polycytidylic acid (poly I:C) immersion were carried out and the transcriptomes of skin, duodenum, spleen, and liver were analysed 8h later in *Notothenia rossii*. LPS and poly I:C immersion in *N. rossii* significantly decreased plasma antiprotease activity and hematocrit levels in poly I:C treated fish. No changes were observed in liver and spleen relative sizes, lysozyme activity, plasma protein and cortisol. The transcriptomes of the two barrier tissues, skin and duodenum, were the most changed under both challenges. The skin (1825 DEGs) was most responsive to LPS and duodenum (1580 DEGs) to poly I:C. LPS changed glucose and lipid homeostasis and immune system processes while poly I:C changed glucose homeostasis, energy and ions metabolism and immune system. The main immune components that were modified in both types of challenge were those linked to pathogen-recognition receptors, toxins, iron and selenium. Our data analysis suggests that NOD-like and C-type lectin receptors may have a key role in both pathogen recognition and that other antimicrobial compounds such as the toxins, iron and selenium ions-related genes are important defence mechanisms specially against viruses in *N. rossii*.

Keywords: Marble rockcod, immune defence, pathogens, cold environment, transcriptome analysis

4.2. Introduction

The Southern Ocean has been isolated from other oceans by a circumpolar current for the last 40 million years creating a stable cold environment where notothenioid fishes evolved from a common temperate benthic ancestor (Barker et al., 2007)(Chen et al., 2019b; Matschiner et al., 2015; Wells and Eastman, 1994). Specific adaptations of the notothenioids to the low temperature include, antifreeze glycoproteins (Chen et al., 1997b), loss of the swim-bladder (Klingenberg and Ekau, 1996), loss of the heat-shock response (Hofmann et al., 2000), loss of haemoglobin in some species (Wells and Eastman, 1994), higher cellular mitochondrial density (O'Brien, 2011), constitutive levels of antioxidant enzymes (Abele and Puntarulo, 2004; Regoli et al., 2005) and increased lipid content of biological membranes (Eastman, 2000; PÖrtner et al., 2005). The marbled rockcod, *Notothenia rossii*, is a cosmopolitan species that has a widespread distribution in Antarctica particularly at low latitudes and belongs to the most diverse Nototheniidae family (Calì et al., 2017; Johnsson et al., 1993 Merrett et al., 1992). After hatching, after more than three months incubation, the *N. rossii* the fingerlings are pelagic for around 6-8 months. Then they become demersal and colonize shallow coastal areas for 6-9 years and move offshore when they reach sexual maturity (Calì et al., 2017). Overfishing in the 1970s led to near extinction of *N. rossii* and the associated population collapse caused modifications in the population structure and characteristics, including slower growth and lower resilience (Barrera-Oro and Marschoff, 2007; Hutchings and Baum, 2005). The *N. rossii* stocks are now slowly recovering although it is unclear how overfishing has affected the genetic structure including the immune system, a subject that has received little attention.

The notothenioids, in common with other vertebrates are protected from pathogens by both an innate and acquired immune system. Unlike mammals, the innate immune response in fish is proposed to be better developed than the acquired response due to the constant contact with microbiota including potential pathogens in a marine environment (Gomez et al., 2013; Kindt et al., 2007; Rauta et al., 2012). Contact with pathogen-related molecules such as lipopolysaccharide (LPS) in several teleost fish is associated with changes in gene transcripts

including pathogen-recognition receptors (PRRs), antimicrobial peptides and complement proteins (Jiang et al., 2020; Liu et al., 2018; Maekawa et al., 2021; Palstra et al., 2018). In addition, there are physiological changes which include plasma cortisol and luteinizing hormone in *Salvelinus fontinalis* (MacKenzie et al., 2006), mitochondrial metabolism in *Oncorhynchus mykiss* (MacKenzie et al., 2008) metabolic scope in *Gambusia holbrooki* (Bonneaud et al., 2016), respiratory burst in *Labeo rohita* (Nayak et al., 2008) and reactive oxygen species in *Oncorhynchus tshawytscha* (Lulijwa et al., 2019). A recent study in the marbled rockcod (*Notothenia rossii* Richardson. 1884) and the black rockcod (*N. coriiceps*) exposed to LPS revealed iron metabolism genes were modified (Martínez et al., 2020). Furthermore, in *N. coriiceps*, toll-like receptors (which are PRRs) and major histocompatibility complex I and II were modified by short exposure (6 and 12 hours) to heat-killed *Escherichia coli O11:B4* (*E. coli*) and poly I:C (Ahn et al., 2014, 2016). However, on the whole the relevant pathogens and the immune response of Antarctic fish remains poorly studied.

The present study aimed at evaluating the multi-tissue (skin, duodenum, spleen, and liver) characteristics of the immune response to proxies for bacterial (LPS) and viral (poly I:C) exposure in the marbled rockcod. The response is considered from a comparative perspective to assess if the immune repertoire and response in the marbled rockcod, diverges from other non-Antarctic teleost fish. Furthermore, the comparison of *N. rossii* with the black rockcod (*N. coriiceps*), a phylogenetically close species, that inhabits the same region and has a similar diet will provide insight into unique adaptive characteristics of the immune system in the notothenioids.

4.3. Methods

4.3.1. Experimental conditions and sample collection

Notothenia rossii (30.3 ± 0.35 cm total length and 312 ± 21.51 g weight, mean ± sem) were captured using a hook-and-line from a boat at depths 5-20 m in the waters of the bay off the Great Wall Station (62° 12' 35.40" S; 58° 57' 26.39" W) located at King George Island. The fish were captured in summer of 2019 (January and February) and maintained in a flow-through circuit, with ocean pumped seawater, in 200 L plastic tanks (n = 5 per tank) for at least 5 days before the pathogen challenges. Fish were fed daily with defrosted fish muscle, but food was withheld 24 hours prior to the experiments. The water temperature (2.1 ± 0.5°C), salinity (29 ±

0.5 ppt) and oxygen levels (1 0.7 ± 0.4 ppm) were monitored three times a day (7 am, 2 pm and 9 pm). No mortality occurred during acclimation or during the experiments.

For the simulated pathogen challenges, fish were divided into three treatment groups (n = 5) and exposed to seawater containing, 1) only seawater, in the control group, 2) *Escherichia coli* O111:B4 (2.5 µg/mL in 1.1% NaCl, L2630, Sigma-Aldrich) in the LPS group and 3) synthetic poly I:C (2.5 µg/mL water in 1.1% NaCl, P1530, Sigma-Aldrich) in the poly I:C group (**Supplementary figure 4.1**). The doses of LPS and poly I:C were chosen based on a literature review of previous immune challenge studies in fish (Ahn et al., 2014, 2016; Chen et al., 2016; Guzmán-Villanueva et al., 2014; Liu et al., 2016; Nayak et al., 2011; Seppola et al., 2015). Briefly, the flow-through system was stopped, and a concentrated solution of each treatment was added to each tank to obtain the final concentrations indicated above. Fish remained immersed in these conditions for 1 h. Aeration was increased, and oxygen levels and water temperature were closely monitored and kept constant throughout. After 1h in the treatment water the flow-through circuit was re-opened. The water flow was calculated to completely renew the tank water within 3 hours. The animals were sacrificed by overdosing with 2-phenoxyethanol (1 mL/L, Sigma-Aldrich) 8 h after the immune challenge. Fish were weighed, and blood was collected from the caudal vasculature using a heparinised 1-ml syringe fitted with a 21-gauge needle. After blood collection, the fish were decapitated, the brain destroyed, and the anterior intestine (duodenum region), skin, liver, and spleen were dissected out, weighed and placed in RNA later (Sigma-Aldrich) for 24 h at 4 ºC before storage at 20ºC. A blood fraction was used to determine the haematocrit and the remaining centrifuged at 10,000 g (4ºC) for 4 minutes (min) for blood plasma collection. The plasma was frozen at -80ºC until analysis of total protein, cortisol, lysozyme, and antitrypsin activities.

4.3.2. Hepatosomatic and Spleensomatic indices

The liver (hepatosomatic, HSI) and spleen (spleensomatic, SSI) relative weight indices were calculated for each of the treatment groups (n = 5 per group) using the following formulae: HSI = liver weight (g) x 100 / body weight (g) and SSI = fresh weight spleen (g) x 100 / fresh body weight (g).

4.3.3. Biochemical parameters

4.3.3.1. Total Plasma Protein

Total plasma protein (n = 5 per group) was measured using a Quick Start™ Bradford Protein Assay kit (Bio-Rad, Portugal) adapted for a 96-well plate (Bradford, 1976). Measurements were performed at 590 nm at 25°C in a spectrophotometer (Microplate reader Benchmark, Bio-Rad, USA).

4.3.3.2. Lysozyme activity

The lysozyme activity in blood plasma was measured using a turbidimetric method (Ellis, 1990). In brief, 130 µl of lyophilized *Micrococcus luteus* cells (0.6 mg/mL in 0.05 M sodium phosphate buffer, pH 6.2, Sigma-Aldrich) was mixed with 20 µl of plasma in a flat bottomed 96 well-plate. For the standard curve, hen egg white lysozyme (Sigma-Aldrich) and a blank (150 µl of sodium phosphate buffer, Sigma-Aldrich) were used. The reaction was incubated for 10 min at 25 °C and the absorbance measured at 450 nm in a spectrophotometer (Microplate reader Benchmark, Bio-Rad).

4.3.3.3. Antiprotease activity

The antitrypsin assay measures total antiprotease activity and was based on the method of (Ellis, 2001). The assay was performed in replicate reactions at 4°C, a temperature near to what Antarctic fish experience. In the optimized protocol 20 µl of trypsin from porcine pancreas (5 mg/mL water, Sigma-Aldrich) was mixed with 10 µL of *N. rossii* plasma for 10 min and 200 µL of 0.1 M phosphate buffer pH 7.0 and 250 µL of 2% azocasein (A-2765, Sigma-Aldrich) was added. The reaction was incubated for 1 hour at the indicated temperatures and 500 µL of 10% trichloroacetic acid (Sigma-Aldrich) was added. The reaction was incubated for 30 min at room temperature (21°C) and centrifuged at 10,000 rpm for 10 min. The supernatant (100 µL) was collected and added in duplicate to a 96-well plate followed by 100 µL sodium hydroxide (1N, NaOH, VWR, Spain).A blank reaction was prepared with NaOH (100 µl) and phosphate

buffer (100 µl, VWR). Reaction products were measured at 450 nm in a spectrophotometer (Microplate reader Benchmark, Bio-Rad).

4.3.3.4. Plasma Cortisol

Plasma cortisol was measured using a well-validated in-house radioimmunoassay (RIA) as previously described (Guerreiro et al., 2006; Rotllant et al., 2005). Briefly, *N. rossii* plasma samples were diluted in phosphate buffer with 0.5g/L gelatin (VWR), pH 7.6 and heat denatured (70°C) for 30 min, centrifuged (10,000 g, 10 min at 4ºC) and the supernatant used for the assays. The antisera used for the RIA was rabbit anti-cortisol-20 CR50 (Fitzgerald, USA). The diluted samples (1:20 in 500 µl gelatin buffer) were incubated overnight with the cortisol antisera and tritiated cortisol marker ([1,2,6,7-3H(N)]Cortisol, -), PerkinElmer, USA) in a final volume of 100 µl. Measurements were carried out in duplicate and a standard curve (0.5 pg/µl – 500 µg/µl) constructed from cortisol (Sigma-Aldrich) was used in all assays.

4.3.3.5. Hematocrit

For determination of the hematocrit, freshly obtained *N. rossii* blood was collected into heparinized microhematocrit capillary tubes (VWR). The hematocrit tubes were centrifuged at 10,000g for 5 min at 4ºC in a haematocrit rotor/centrifuge (Heraeus Biofuge) and the percentage (%) of the packed cell volume was measured.

4.3.3.6. Statistical analysis

Data is shown as mean ± SEM. Differences in plasma biochemical parameters between the control, LPS and poly I:C-treated groups and hepatosomatic and spleensomatic indices were tested using tone-way analysis of variance (ANOVA) and a post hoc Tukey´s test (Shapiro-Wilk normality test) was used for statistical tests with a threshold for significance of $p < 0.05$. For the analysis and graphs GraphPrism v6.01 was used.

4.3.4. RNA extraction and sequencing

Total RNA was extracted from *N. rossii* tissues (~25 mg, n = 3/tissue) using an E.Z.N.A. Total RNA Kit I (Omega Bio-Tek, USA) and following the manufacturer's instructions. A DNase I digestion protocol was performed directly on the columns used for RNA extraction to eliminate contaminating genomic DNA. An RNase-free DNase I kit was used following the manufacturer's instructions (Omega Bio-Tek). RNA integrity was evaluated by 1% agarose gel electrophoresis and the quantity and quality parameters of the RNA was assessed by absorbance using a NanoDrop One (Thermofisher, Spain). For the transcriptome sequencing, poly A^+ messenger RNA (mRNA) was purified using a DynaBeads mRNA Purification Kit (Life Technologies, Carlsbad, CA). A total of 36 paired-end complementary DNA (cDNA) libraries (for the control, poly I:C and LPS challenged fish) were constructed with an insert size of 250 base pairs (bp) using a VAHTS stranded mRNA-*seq* Library Prep Kit from Illumina following the manufacturer´s protocol (Vazyme Biotech Co., Ltd, China). Quality control analysis of the library was performed using an Agilent Bioanalyzer DNA 1000 Kit (Agilent, #5067-1504) and all libraries were sequenced using an Illumina 1.9 Next-Generation Sequencing (NGS) system.

4.3.5. Transcriptome assembly and gene expression quantification

The quality control and editing of raw reads to trim adapter sequences and low quality bases was performed using Trimgalore wrapper script v0.6.5 (Krueger, 2015) and output FastQC and FastP (Andrews, 2015) quality reports obtained from Galaxy software v21.01 (Afgan et al., 2018). *De novo* assembly of all reads was performed in Trinity v2.11.0 with the default conditions for the "-normalize reads" parameter (Haas et al., 2013), and the reference transcriptome obtained was used to map reads from each of the tissue sequencing libraries prepared and to run the differential expression analysis.

Clean reads were mapped using the RSEM package v1.3.3 (Li and Dewey, 2011) and differentially expressed genes (DEG; FDR < 0.05)) were identified using the DESEq2 package v1.30.0 in RStudio v1.4.1103 (Love et al., 2014) . Pairwise comparisons were made using the replicates between each of the treatment groups (Control, poly I:C and LPS) and each of the immune tissues (liver, spleen, skin and duodenum). A total of 7,865,495,667 million paired-

end (PE) raw transcriptome reads were generated from the RNA-seq analysis of the 36 sequenced libraries of the liver (Lv_1 to Lv_3), duodenum (Du_1 to Du_3), spleen (Sp_1 to Sp_3), and skin (Sk_1 to Sk_3) from the control (C1-C3, n = 3 libraries/ tissue), poly I:C (P1-P3, n = 3 libraries/ tissues) and LPS-treatment groups (L1-L3, n = 3 libraries/tissue). Index and adapter sequences were trimmed using Trimmomatic version 4.4.10 (Bolger et al., 2014) and low-quality trimmed sequences were eliminated using cutadapt when the FPKM was < 1 and/or the length was < 300 base pairs (bp). TransRate v 1.0.3 was used for quality filtering and optimization of the assembly since no reference genome was available (Smith-Unna et al., 2016).

4.3.6. Gene and Functional annotations

The annotation of genes was performed with DIAMOND v0.9.14.115 against the Nr NCBI and UniProtKB/Swiss-Prot databases using BlastX and BlastP v2.9.0 (e-value cut-off of 1e−5) for all assembled contigs (Bateman et al., 2017). In addition, functional annotation was obtained using the best deduced open reading frame (ORF) given by Transdecoder v5.5.0 (Smith-Unna et al., 2016). GO annotation was obtained directly from the UniProt/Swiss-Prot database and KEGG pathways from KAAS software (Moriya et al., 2007). GO enriched terms were summarized by REVIGO (Supek et al., 2011) which removed redundant GO terms based on semantic similarity and the graphics were represented in RStudio software 1.4.1103 with a threshold of FDR < 0.05 for tissues with < 700 DEGs and an FDR < 0.001 for tissues with > 700 DEGs. In parallel, KEGG pathway analysis of a subset of DEGs ($p < 0.001$) was conducted using clusterProfiler software in RStudio v1.4.1103 with the default parameters, and the top 10 enriched terms was plotted by ggplot2 software v3.3.0 in RStudio v1.4.1103.

4.3.7. Heatmap and Multivariate analyses in DEGs

Heatmaps were generated for DEGs using the heatmap package v1.14.0 from RStudio v1.4.1103. Analysis was performed between treatment groups (Control, poly I:C and LPS) for each of the tissues to show the magnitude of the response to the pathogen challenges. Multivariate (PCA) analysis was performed using DEGs in Factoextra R package v1.0.7 and

plot by ggplot2 software v3.3.0 in RStudio software v1.4.1103 with confidence ellipses set at > 95%. The significance threshold was set at FDR < 0.05 for tissues with < 700 DEGs and an FDR < 0.001 for tissues with > 700 DEGs in both heatmap and multivariate analyses.

4.4. Results

4.4.1. Hepatosomatic and Spleensomatic indices

No significant differences were detected in the hepatosomatic and spleensomatic index between any of the experimental groups (control or immune challenged, $p > 0.05$) (data not shown).

4.4.2. Biochemical parameters

4.4.2.1. Plasma protein

The plasma protein was not significantly modified between any of the experimental groups (control or immune challenged, $p > 0.05$) (**Figure 4.1A**).

4.4.2.2. Lysozyme and antiprotease activity

The activity of plasma lysozyme was not significantly different between any of the experimental groups (control or immune challenged, $p > 0.05$) (**Figure 4.1B**). The antiprotease inhibition (in percentage, %) was significantly decreased in the poly I:C-treated fish (approximately 14%, $p = 0.012$), indicating higher plasma protease activity in this group (**Figure 4.1C**).

4.4.2.3. Cortisol

The plasma cortisol concentration (ng/ml) was not significantly different between any of the experimental groups (control or immune challenged, p >0.05) (**Figure 4.1D**).

4.4.2.4. Hematocrit

The haematocrit significantly decreased from 39% to 35% in the poly I:C challenged fish compared to control (p = 0.0344) (**Figure 4.1E**).

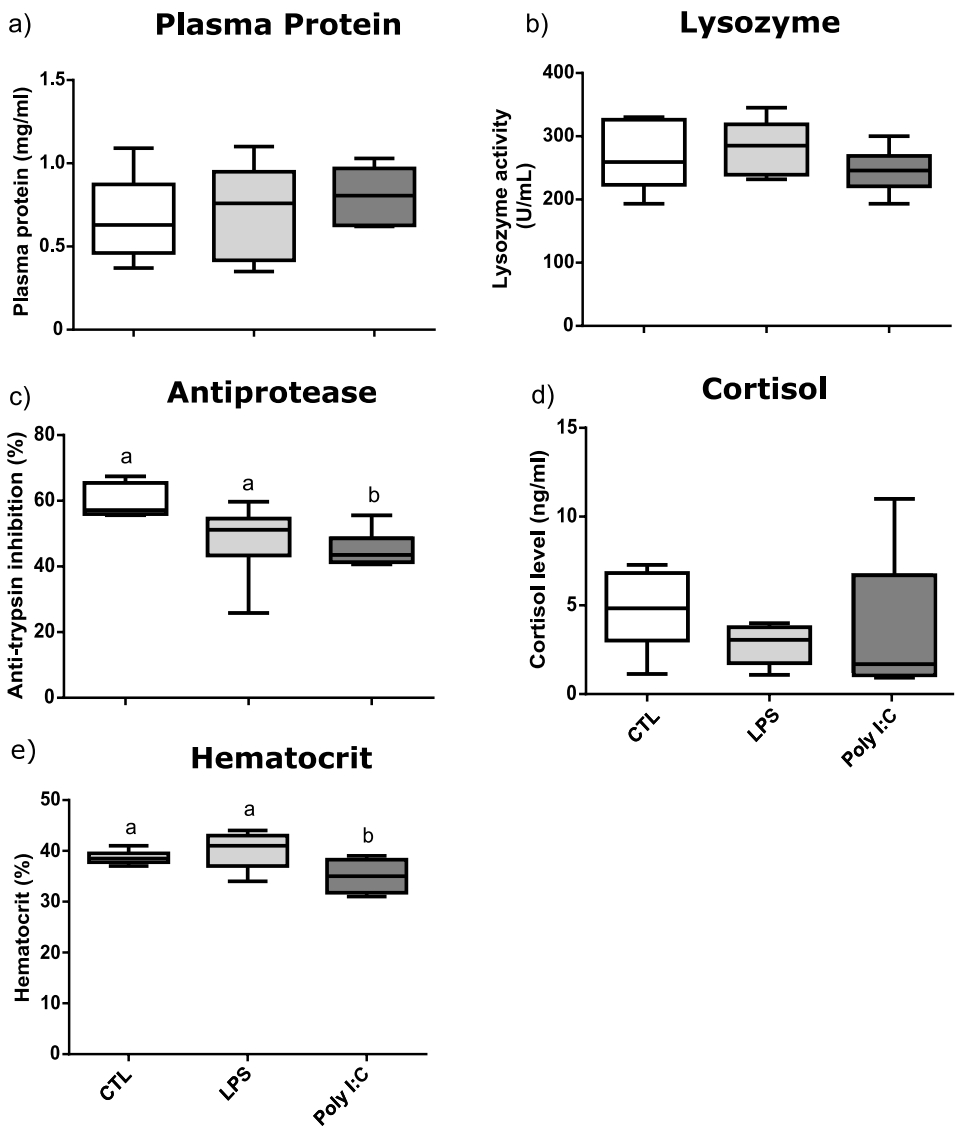

Figure 4.1. Biochemical indicators a) plasma protein, b) cortisol, c) lysozyme, d) antitrypsin, e) hematocrit in *N. rossii* blood plasma. Measurements of (a) total protein (mg/ml), (b) cortisol (ng/ml), (c) lysozyme (U/ml), (d) trypsin inhibition (%), and (e) hematocrit (%) in the control (white), LPS (light grey) and Poly I:C (dark grey).

4.4.3. Immune-tissue reference transcriptomes and assembly

The total number of reads generated by RNAseq of the cDNA libraries of the marbled rockcod was: 162,256,308 million (M) for the liver, 126,518,018 M for the spleen, 137,646,068 M for the duodenum and 139,895,294 M for the skin (Supplementary Table 1A). After filtering the total number of reads obtained was 161,460,490 M for the liver, 125,200,116 M for the spleen, 124,065,164 M for the duodenum and 129,237,478 M for the skin. After assembly, the average alignment ratio for the sequence reads against the marbled rockcod reference transcriptome was approximately 90% for the liver, 83% for the spleen, 85% for the intestine and 86% for the skin (**Supplementary table 1 B**). The number of assembled contigs were: 82,913 for liver, 130,331 for spleen, 95,423 for duodenum and 48,188 for skin (Supplementary Table 1A). The average contig length after assembly (N50) was 1836 and the GC content across the dataset was 45 % (**Supplementary table 4.1 A**). Transcript annotation with DIAMOND and using Nr NCBI and UniProtKB/Swiss-Prot databases gave 86% (71,686 contigs), 65% (84,083 contigs), 59% (56,063 contigs) and 54% (26,137 contigs) annotation for the liver, spleen, duodenum, and skin, respectively (**Table 4.1**).

Table 4.1. Annotation statistics of A) duodenum, B) skin, C) spleen and D) liver samples. The number and percentage of genes transcripts not annotated and annotated, predicted, and hypothetical or uncharacterized proteins are indicated.

	Number		Percentage (%)	
Annotated	237,969		67	
Annotation to different databases:				
Genes with BlastX and BlastP hit to NCBI	172,541		73	
Genes with BlastX and BlastP hit to SwissProt	172,782		73	
Genes with KEGG database	80,381		34	
Genes with GO database	172,921		73	
Non-annotated	118,886		33	
Treatment groups	**CTL versus LPS**		**CTL versus Poly I:C**	
	Number	**~ %**	**Number**	**~ %**
Total number of DE transcripts				
Liver	49	0,06	131	0,15
Spleen	11	0,01	23	0,02
Duodenum	220	0,23	1582	2
Skin	1827	4	195	0,42
Summary of annotation of DE transcripts:				
Annotation to known or predicted proteins				
Liver	49	100	131	100
Spleen	11	100	23	100
Duodenum	216	98	1517	96
Skin	1782	98	190	97
Annotation to hypothetical/uncharacterized proteins				
Liver	0	0	0	0
Spleen	0	0	0	0
Duodenum	4	2	65	4
Skin	45	2	5	3

4.4.4. Differentially expressed genes (DEGs) in the liver, spleen, duodenum, and skin

Comparisons of the number of DEGs identified in the two pathogen challenges (LPS and poly I:C) compared to the control and between the four tissue transcriptomes (duodenum, skin, liver, and spleen) revealed a high variation in the number of DEGs identified for each pathogen challenge and between the tissues. The comparison of the duodenum gene transcripts between the control and LPS generated 216 DEGs (195 up- and 21 down-regulated) and between control and poly I:C challenge 1582 DEGs (1531 up- and 51-down regulated) (**Supplementary table 4.2, Annex II**). In skin 1827 DEGs (698 up- and 1129-down regulated) were identified between the control and LPS and 195 DEGs (62 up- and 133-down regulated) between control and poly I:C (**Supplementary table 4.3**). A low number of DEGs were identified in the spleen, 11 in the control vs LPS challenge (9 up- and 2 down-regulated) and 23 in the control vs poly I:C challenge (11 up- and 12-down-regulated) (**Supplementary table**

4.4). The control vs LPS and control vs poly I:C challenges resulted, respectively in 49 DEGs (46 up- and 3 down-regulated) and 131 DEGs (75 up- and 56 down-regulated), respectively in liver (**Supplementary table 4.5**).

A few numbers of DEGs, less than 27, were common between the different tissues for LPS (**Figure 4.2 A**) and less than 41 for poly I:C challenges (**Figure 4.2 B**).

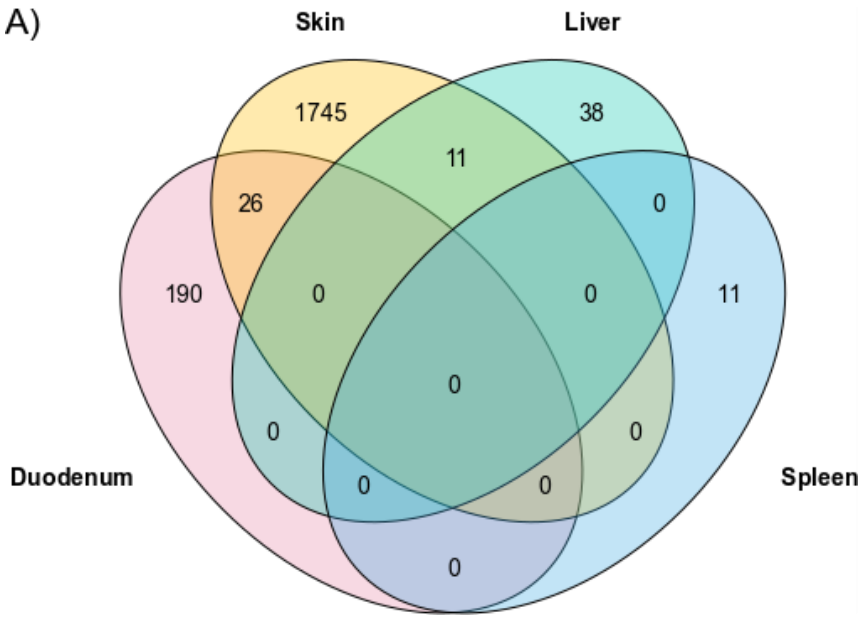

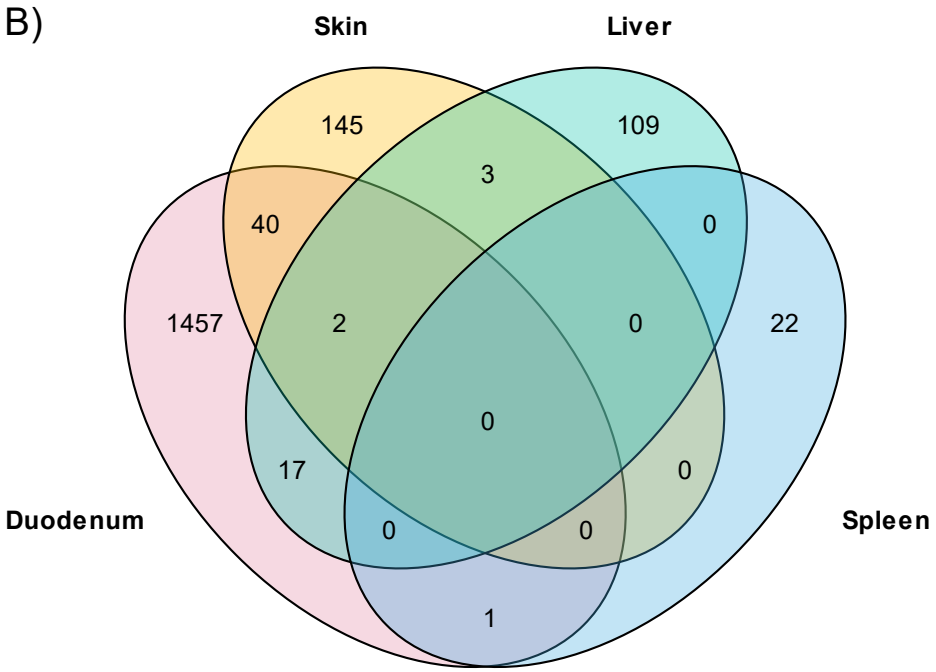

Figure 4.2. Venn diagram of the number of DEGs in the four tissue transcriptomes of A) Control versus LPS and B) Control versus Poly I:C in *N. rossii*. The numbers indicate annotated DEGs that are specific or common between tissues.

4.4.5. Heatmap and PCA analyses of DEGs

A heatmap (*log2* counts) of the DEGs for each comparison was generated using FDR < 0.01 for the duodenum and skin, which had a high number of DEGs and an FDR < 0.05 for the spleen and liver that had relatively few DEGs. The heatmap showed good clustering of the individuals by experimental group and the response varied by tissues and treatment (Control, LPS and poly I:C) (**Figure 4.3 A-D**).

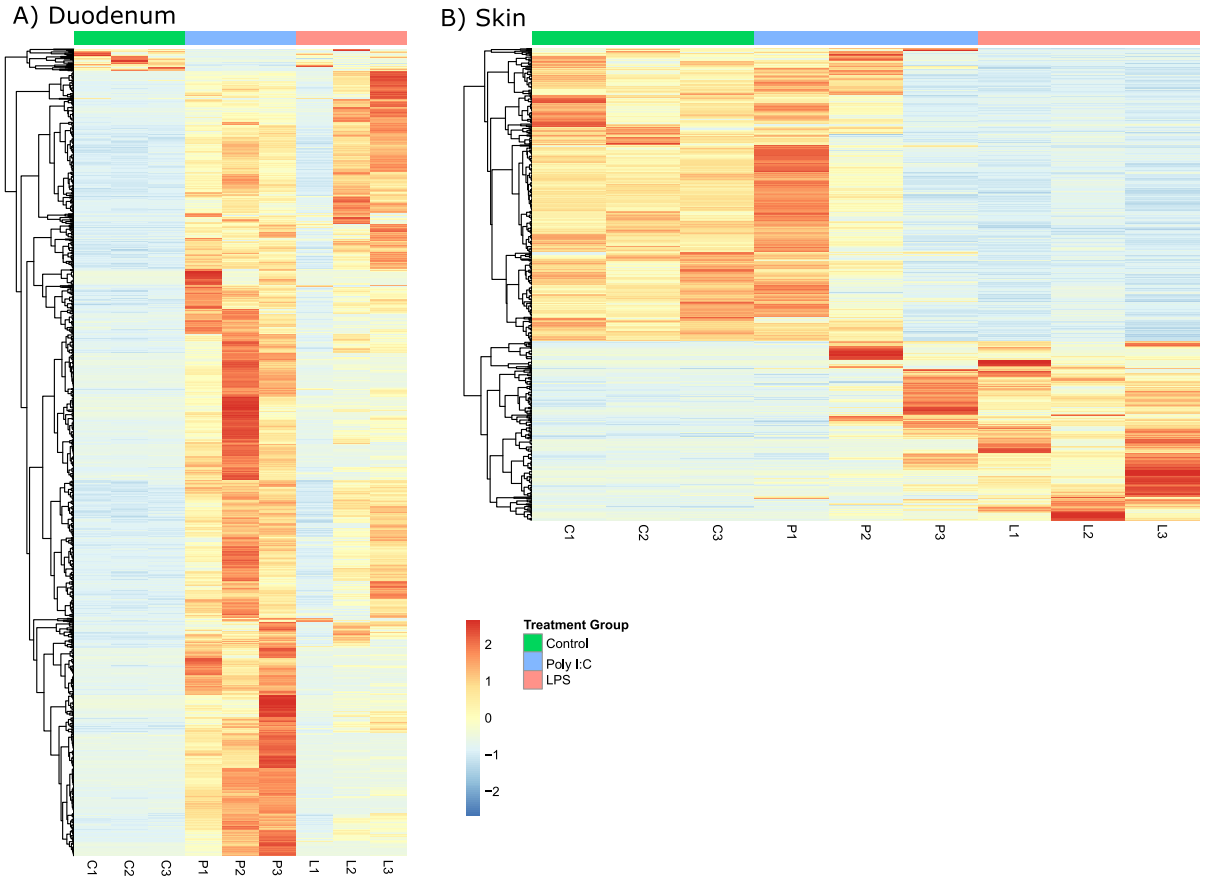
A) Duodenum
B) Skin
C1
C2
C3
P1
P2
P3
L1
L2
L3
Treatment Group
Control
Poly I:C
LPS
2
1
0
−1
−2

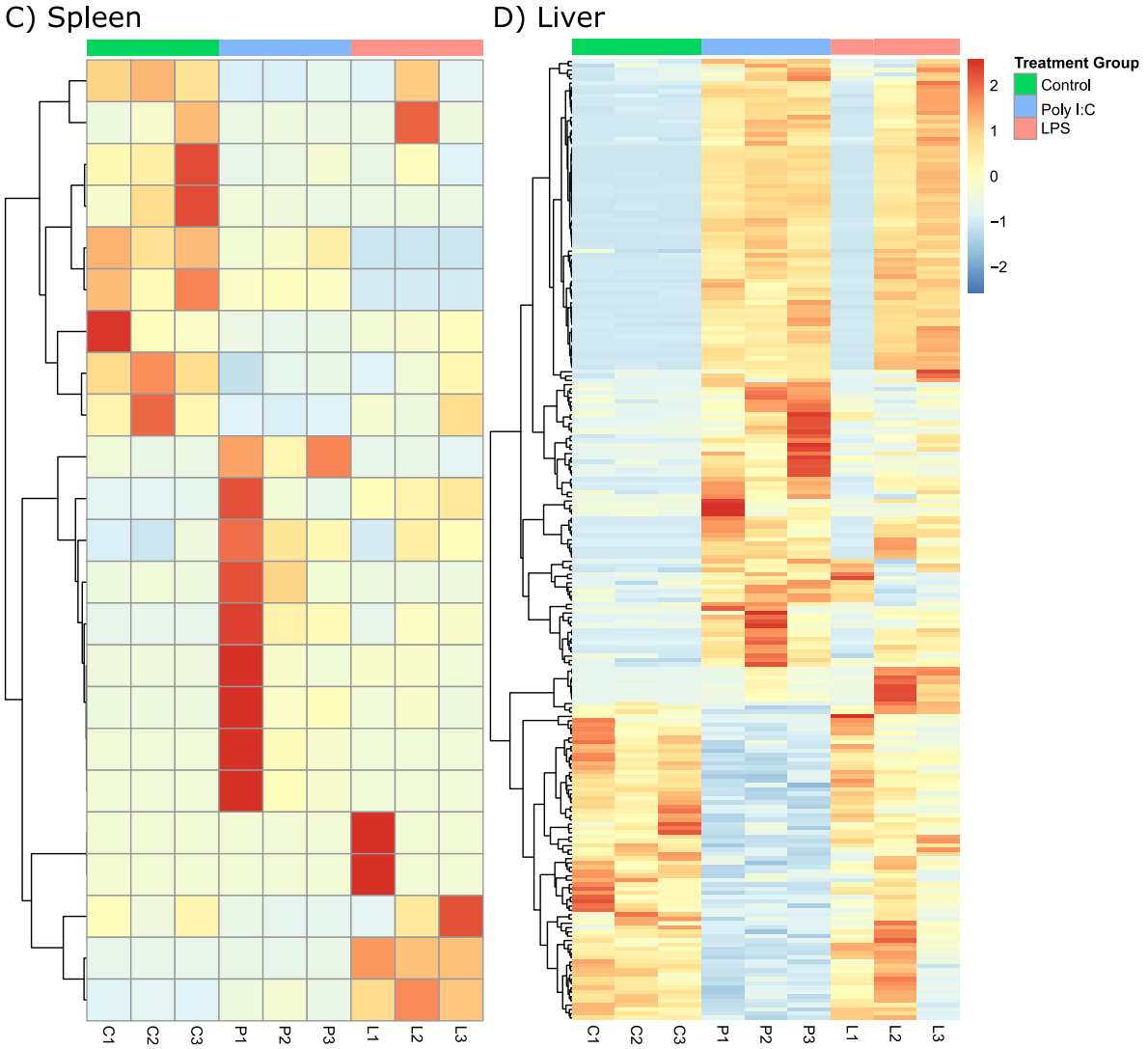

Figure 4.3. Heatmap (log2 expression) **generated from DEGs from the A) duodenum** (FDR < 0.001)**, B) skin** (FDR < 0.001)**, C) spleen** (FDR < 0.05) **and C) liver** (FDR < 0.05) **transcriptomes of control, LPS and Poly I:C treated fish.** Control (C1-C3), LPS (L1-L3) and Poly I:C (P1-P3). The intensity of red colour gradient indicates up-regulation and of the blue colour gradient indicates down-regulation.

A PCA was performed on the DEGs identified by the pairwise comparisons of the different experimental groups in 36 individuals of each tissue, The first two principal components (Dim1 and Dim2) explained 79.7% of the total variation (62.7% for Dim1 and 17% for Dim2, **Figure 4. 4 A**). The first two principal components explained 74.9% of the variance in skin (66.5% for Dim1 and 8.4% for Dim2, Figure **4.4 B**), 67.7% of the variance in spleen (42.8% for Dim1 and 24.9% for Dim2, **Figure 4.4 C**) and 79.7% of the variance in liver (63.1% for Dim1 and 16.3% for Dim2, **Figure 4.4 D**). The DEGs of the duodenum and skin had the highest individual variability for LPS and the poly I:C treatment, respectively.

A) Duodenum

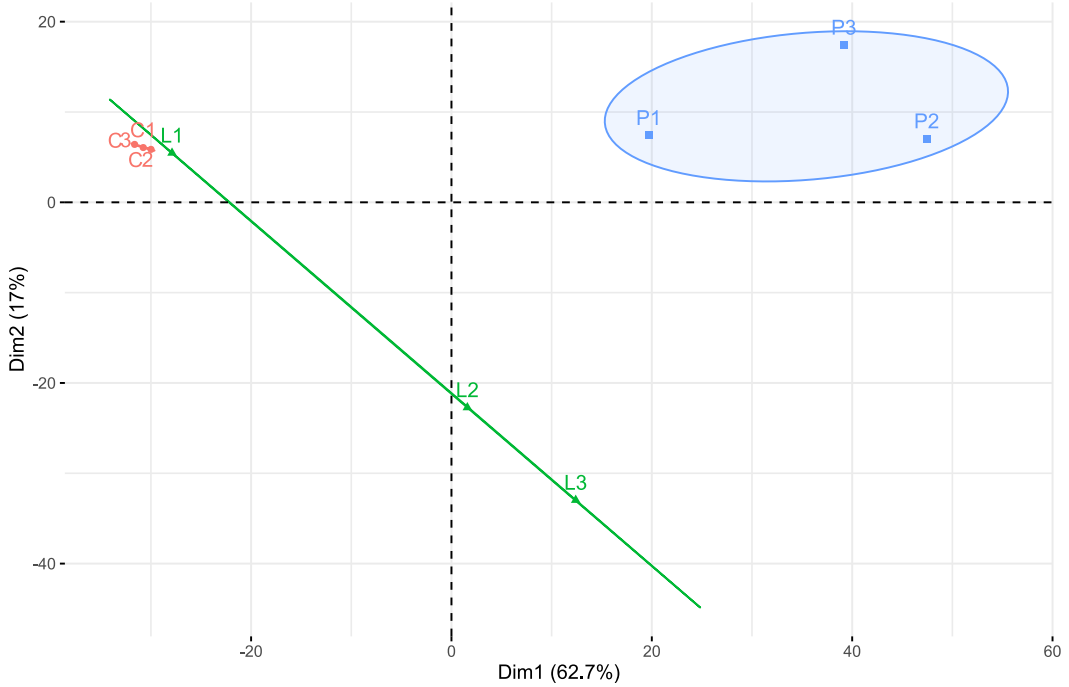

B) Skin

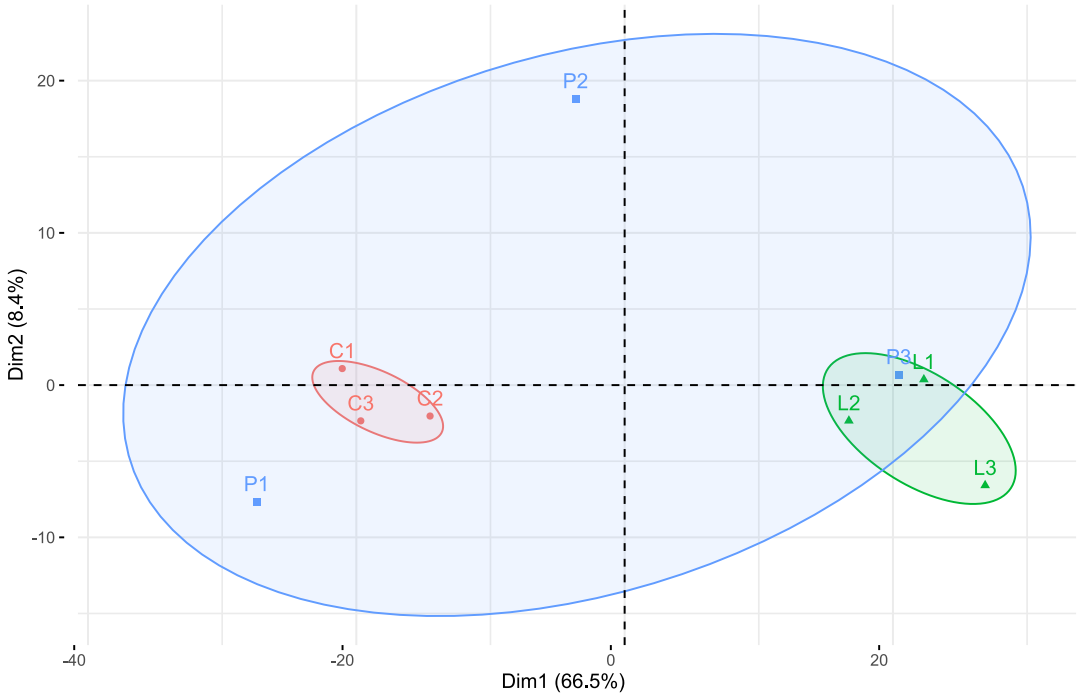

C) Spleen

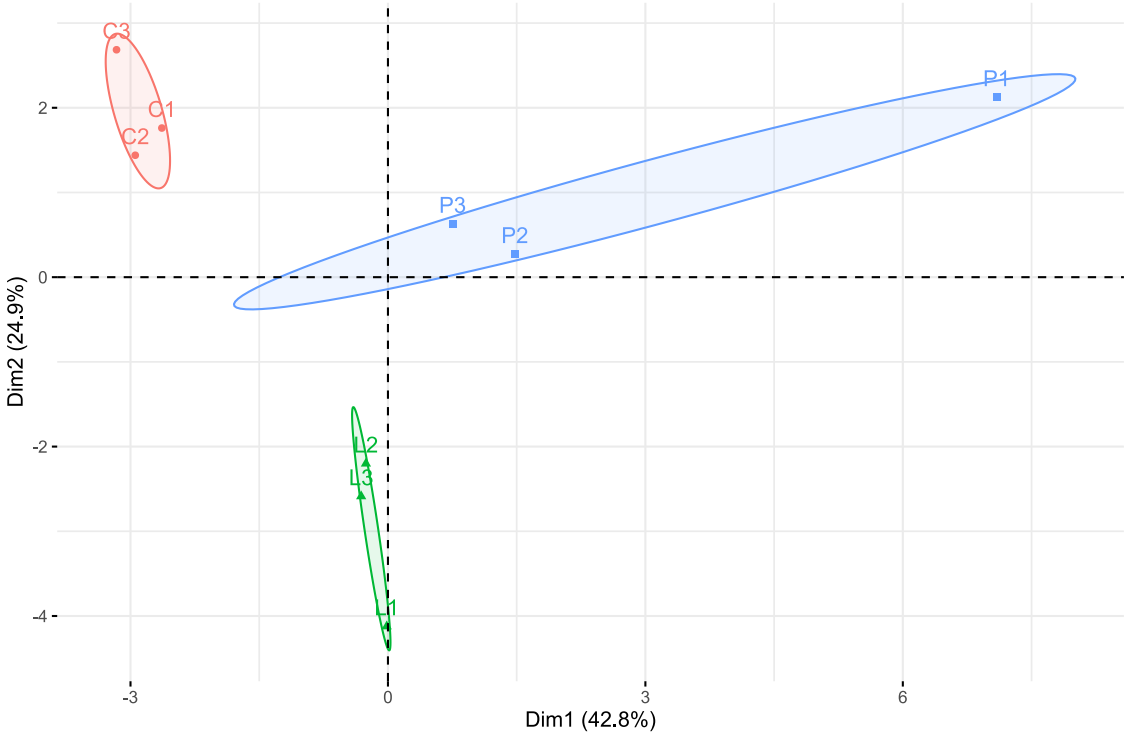

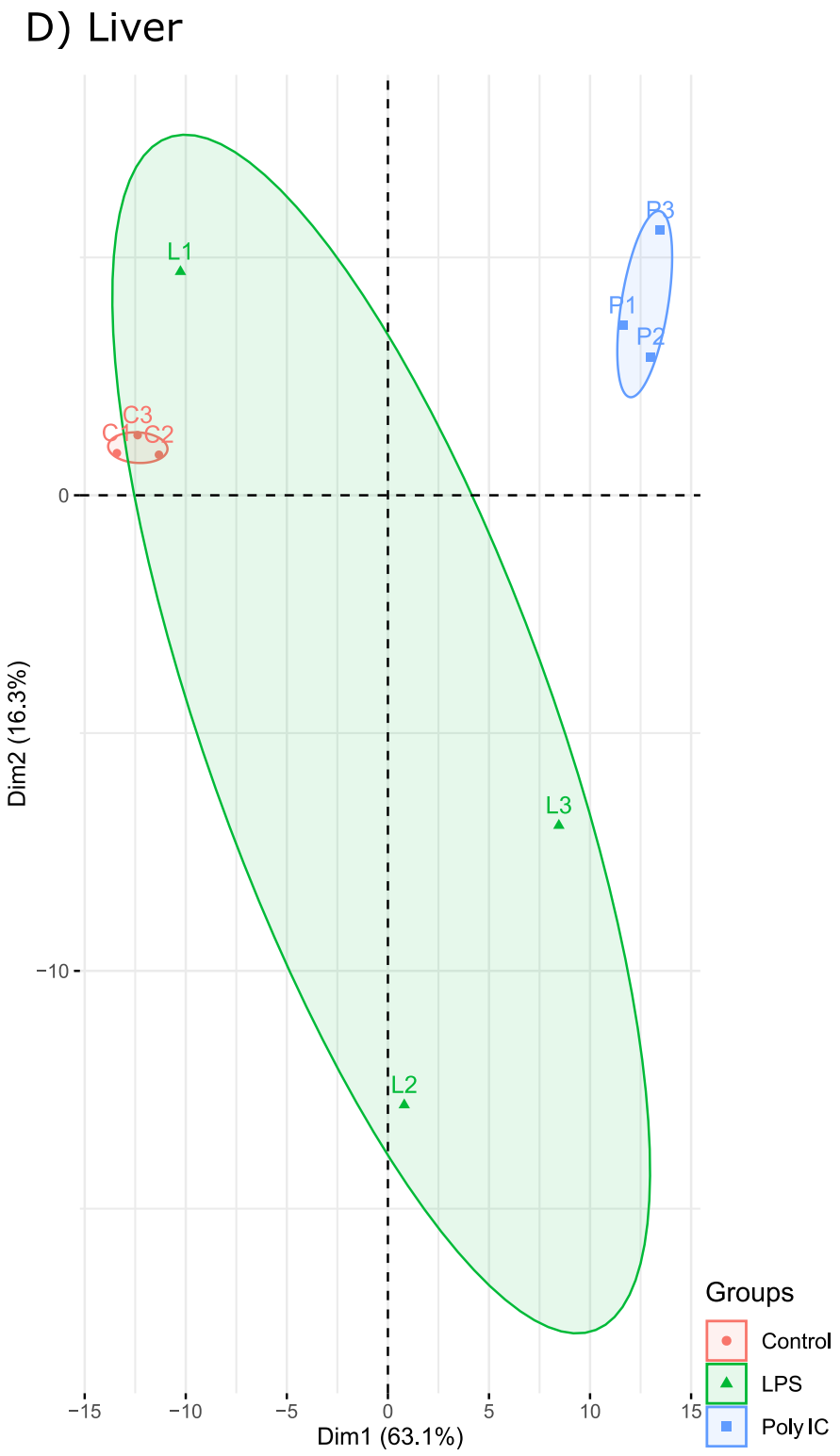

Figure 4.4. Principal components analysis (PCA) of DEGs (log2 expression, FDR < 0.05) from A) duodenum, B) skin, C) spleen and C) liver of control, LPS and Poly I:C treated fish. The control is indicated as orange circle (C1-C3), LPS as green triangle (L1-L3) and Poly I:C as blue square (P1-P3).

4.4.6. DEGs in the four tissues under different pathogen challenges

4.4.6.1. DEGs in control versus LPS

The C versus LPS DEGs with the highest fold-change in the duodenum were linked to the regulation of glucose and lipid homeostasis (up-regulated) and neutrophil degranulation (down-regulated) (**Supplementary table 4.2 A-B**); in the skin they were linked to antiviral innate immune response (up-regulated) and neutrophil degranulation (down-regulated) (**Supplementary table 4.3 A-B**); in the spleen they were linked to viral process (up-regulated) and vascular associated smooth muscle cell (down-regulated) (**Supplementary table 4.4 A-B);** in the liver they were linked to antioxidant defence (up-regulated) and metabolism of polyunsaturated fatty acids (PUFAs) (down-regulated) (**Supplementary table 4.5 A-B**). A comparative analysis of the DEGs related to immunity (up- and down-regulated) across the four immune tissues revealed common and divergent responsiveness of the tissue when exposed to the same bacterial challenge (**Table 4.2, Annex II**). For example, iron metabolism pathways were highly modified in the skin but not in the duodenum and several toxins, like stonustoxin, neoverrucotoxin and sagatoxin, were highly modified in skin but mainly absent from the duodenum.

Overall, the 26 DEGs shared between the duodenum and skin included immune response (regulation of activation-induced cell death of T cells, T cell differentiation, neutrophil degranulation, wound healing, defense response to virus, interleukin-1 beta production, programmed cell death), ion and protein transport, signal transduction, cell differentiation, cell-matrix adhesion, energy metabolism, carbohydrate binding and regulation of growth. In contrast, the 11 DEGs shared between skin and liver, belonged to apoptotic process, oxygen transport, regulation of translation, ribosome, ion binding and signal transduction.

4.4.6.2. DEGs in control versus poly I:C

The most highly modified DEGs of poly I:C challenged fish in the duodenum were ion transport (up-regulated) and innate chemokines (down-regulated) (**Supplementary table 4.2 C-D**); in the skin were protein folding (up-regulated) and citric acid cycle (down-regulated) (**Supplementary table 4.3 C-D**); in the spleen were innate chemokines (up-regulated) and vascular associated smooth muscle cell (down-regulated) (**Supplementary table 4.4 C-D**); and in the liver were ATP production (up-regulated) and protein ubiquitination (down-regulated)

(**Supplementary table 4.5 C-D**). Evaluation of immune related genes in the DEGs (**Table 4.2, Annex II**) of the four-tissues of the poly I:C challenged fish revealed some common and tissue specific DEGs. For example, pathogen recognition receptors were highly upregulated in the duodenum but absent from the skin, spleen, and liver. Several genes of the iron metabolism pathway were highly upregulated in the duodenum, but only a few genes were upregulated in the liver and none in the skin or spleen. Similarly numerous genes of innate humoral immunity were strongly upregulated in the duodenum, but not at all in the spleen and a small number were modified in the skin and liver (**Table 4.2, Annex II**).

Overall, 40 DEGs were common between the duodenum and skin related to several processes namely mitochondrial electron transport, mitochondrial damage, ion binding, ATP production, the inflammatory response, platelet degranulation, protein folding, ribosome, regulation of translation, GTPase binding, glycolysis, and DNA replication. The duodenum and liver shared 17 common genes associated with actin binding, the mitochondrial inner membrane, transcription factors, DNA binding, glucokinase regulation, the innate immune response (such as NLRs), ATP binding, endocytosis, and the citric acid cycle. The comparison between liver and skin showed they had 3 DEGs in common that were linked to ATP production and oxygen transport, while between the duodenum, skin, and liver 2 DEG related to the innate immune response was shared.

Table 4.2 (next page). Summary of differentially expressed immune genes in the four tissues between control versus LPS and control versus Poly I:C. The green colour indicates the DEGs that are up-regulated and the down-regulated at red according to the highest to the lowest log fold-change (logFC) (FDR < 0.05).

Gene name	Gene symbol	Transcript ID	Skin					
			logFC	Pvalue	Pathogen challenges		Response intensity	
					LPS	Poly I:C	LPS	Poly I:C
Pathogen recognition receptors								
Scavenger receptor class B member 1	*scarb1*							
NACHT, LRR and PYD domains-containing protein 3-like	*nlrp3*							
Macrophage mannose receptor 1	*mrc1*							
C-type lectin domain family 4 member E	*clec4e*							
Scavenger receptor cysteine-rich domain-containing group B protein	*ssc4d*	TRINITY_DN50881_c0_g1_i1	6,29E+14	1,33E-03	**x**		High	
TLR adapter interacting with SLC15A4 on the lysosome	*cxorf21*							
Toll-like receptor 3 isoform X2	*tlr3*							
Protein NLRC3	*nlrc3*	TRINITY_DN2951_c0_g1_i1	-2,42E+14	2,44E-03	**x**		High	
NACHT, LRR and PYD domains-containing protein 1	*nlrp1*							
C-type lectin domain family 11 member A	*clec11a*	TRINITY_DN16300_c0_g2_i2	-2,90E+14	3,31E-03	**x**		High	
C-type mannose receptor 2	*mrc2*	TRINITY_DN24519_c0_g1_i1	-5,34E+14	3,38E-03	**x**		High	
Iron metabolism pathway								
Transferrin receptor protein 1	*tfrc*							
Fermitin family homolog 3	*fermt3*							
Ferrochelatase, mitochondrial	*fech*							
Iron-sulfur cluster assembly enzyme ISCU, mitochondrial	*iscu*							
Cytolic Fe-S cluster assembly factor nubp2	*nubp2*	TRINITY_DN62063_c0_g1_i1	3,51E+14	1,62E-03	**x**		High	
Serotransferrin-1	*tf*	TRINITY_DN57579_c0_g1_i1	3,24E+14	8,77E-04	**x**		High	
2-oxoglutarate and iron-dependent oxygenase JMJD4	*jmjd4*	TRINITY_DN5176_c0_g1_i2	2,32E+14	4,15E-03	**x**		High	
Iron-responsive element-binding protein 2	*ireb2*	TRINITY_DN302_c0_g1_i11	1,98E+14	3,06E-03	**x**		High	
Adrenodoxin, mitochondrial	*fdx1*							
NADH dehydrogenase [ubiquinone] iron-sulfur protein 4, mitochondrial	*ndufs4*	TRINITY_DN56593_c0_g1_i1	1,14E+14	2,26E-03	**x**		High	
Ferritin, middle subunit	*fm*							
Ferritin, heavy subunit	*fth1*	TRINITY_DN58412_c0_g1_i1	-5,82E+14	1,17E-06		**x**		Medium
Selenium metabolism pathway								
Selenoprotein J	*selenoj*							
Methanethiol oxidase	*selenbp1*							
Thioredoxin reductase-like selenoprotein T1a	*selenot1a*							
Selenoprotein Pa	*sepp1a*							
Selenocysteine insertion sequence-binding protein 2	*secisbp2*	TRINITY_DN10529_c0_g1_i1	-2,72E+13	4,07E-03	**x**		High	
Selenocysteine insertion sequence-binding protein 2-like	*secisbp2l*	TRINITY_DN3745_c0_g1_i1	-1,97E+14	5,50E-04	**x**		High	
Type I iodothyronine deiodinase	*dio1*							
Toxins								
Stonustoxin subunit alpha	*stxa*	TRINITY_DN7648_c0_g1_i1	7,02E+14	1,02E-05	**x**		High	
Neoverrucotoxin subunit alpha	*ntxa*							
Anthrax toxin receptor 2	*antxr2*							
DELTA-sagatoxin-Srs1a-like	*srs1al*	TRINITY_DN8540_c0_g1_i1	4,04E+14	6,86E-05	**x**		High	
Neoverrucotoxin subunit beta	*nvtx*							
Cytolytic toxin-alpha	*clya*							
Anthrax toxin receptor 1	*antxr1*	TRINITY_DN3970_c0_g1_i3	-4,52E+14	1,84E-04	**x**		High	
Stonustoxin subunit beta	*stnxb*	TRINITY_DN2411_c0_g1_i1	-7,33E+14	2,54E-03	**x**		High	

Innate humoral immunity								
BCL2/adenovirus E1B 19 kDa protein-interacting protein 3	*bnip3*							
Mucin-5AC-like	*muc5ac*							
C-reactive protein	*crp*	TRINITY_DN73_c0_g1_i1	8,47E+14	2,00E-04	**x**		High	
Complement C1q-like protein 2	*c1ql2*	TRINITY_DN10228_c0_g2_i1	8,42E+14	2,74E-04	**x**		High	
Serpin peptidase inhibitor, clade A (alpha-1 antiproteinase, antitrypsin), member 7 isoform X1	*serpina1*							
Lysosomal alpha-mannosidase	*man2b1*							
NF-kappa-B inhibitor alpha	*nfkbia*							
Serine/threonine-protein kinase RIO3	*riok3*							
Interleukin-17 receptor A	*il17ra*							
Cytokine-inducible SH2-containing protein	*cish*							
Tumor susceptibility gene 101 protein	*tsg101*	TRINITY_DN3029_c0_g1_i1	7,54E+14	2,21E-03	**x**		High	
Interferon-related developmental regulator 2	*ifrd2*							
Plasma protease C1 inhibitor	*serping1*							
Mucin 13b, cell surface associated isoform X1	*muc13b*							
Serine/threonine-protein kinase MARK2	*mark2*							
Macrophage-stimulating protein receptor	*mst1r*							
Receptor-type tyrosine-protein phosphatase eta	*ptprj*							
Lysosomal alpha-glucosidase	*gaa*	TRINITY_DN2473_c0_g1_i1	7,03E+14	7,89E-05		**x**		Medium
Interferon regulatory factor 8	*irf8*							
Lysine-specific demethylase 5B-B	*kdm5bb*							
C-X-C chemokine receptor type 4	*cxcr4*							
Complement factor B	*cfb*							
Tumor necrosis factor receptor superfamily member 1A precursor	*tnfrsf1a*							
Lysosomal protective protein	*ctsa*							
Interleukin-1 receptor accessory protein-like 1-A isoform X1	*il1rapl1*							
Interleukin-6 receptor subunit alpha	*il6r*							
Complement C1q subcomponent subunit C	*c1qc*							
Interferon regulatory factor 2	*irf2*							
Complement C4-B	*c4b*							
Tumor necrosis factor alpha-induced protein 2 isoform X1	*tnaifp2*							
Cationic trypsin-like	*prss1*	TRINITY_DN181_c0_g4_i1	6,01E+14	1,11E-06	**x**		High	
Tumor necrosis factor receptor superfamily member 11A isoform X1	*tnfrsf11a*							
Mucin-2-like	*muc2l*	TRINITY_DN50086_c0_g1_i1	5,84E+14	3,25E-03	**x**		High	
Tumor necrosis factor, alpha-induced protein 8-like protein 2 A	*tnfaip8l2*							
Chemokine-like receptor 1	*cmklr1*	TRINITY_DN4393_c0_g1_i2	5,67E+14	3,05E-06	**x**		High	
Interleukin-1 receptor-associated kinase 3	*irak3*							
Complement C3	*c3*							
C-X-C motif chemokine 20	*cxcl20*							
Complement component C7	*c7*							
Serine/threonine-protein kinase N1	*pkn1*							
Complement C4	*c4*							
Interleukin-13 receptor subunit alpha-2	*il13ra2*							
Tumor necrosis factor alpha-induced protein 8-like protein 3	*tnfaip8l3*							
Beta-2-microglobulin	*b2m*	TRINITY_DN17923_c0_g1_i1	-6,28E+13	1,31E-04		**x**		Medium
Mucin-2	*muc2*							
C1qB	*c1qb*							
Hemoglobin subunit beta-1	*hbb1*							

Interferon-induced GTP-binding protein MxA	*mx1*							
Interferon-induced protein with tetratricopeptide repeats 1-like	*ifit1l*	TRINITY_DN3039_c0_g2_i1	4,24E+14	8,93E-07	x		High	
Hemoglobin subunit alpha-1	*hba1*	TRINITY_DN174_c0_g2_i1	4,01E+14	3,25E-05	x		High	
Serine/threonine-protein kinase TBK1	*tbk1*	TRINITY_DN14328_c0_g1_i1	4,61E+14	4,00E-04	x		High	
Complement factor D	*cfd*							
Beta-galactoside-binding lectin	*lec-1*							
Protein S100-A1	*s100a1*							
Serine/threonine-protein kinase STK11	*stk11*	TRINITY_DN11508_c0_g1_i4	3,66E+14	3,93E-04	x		High	
Hemoglobin subunit alpha-2	*hba2*	TRINITY_DN174_c0_g1_i1	3,44E+14	7,43E-04	x		High	
Leukotriene A-4 hydrolase	*lta4h*							
Sialomucin core protein 24	*cd164*							
Leucine-rich repeats and immunoglobulin-like domains protein 2	*lrig2*	TRINITY_DN2107_c0_g1_i1	3,08E+14	2,79E-03	x		High	
Protein kinase C delta type	*prkcd*							
Bactericidal permeability-increasing protein	*bpi*	TRINITY_DN4096_c0_g4_i1	2,38E+13	1,75E-04	x		High	
Protein kinase C and casein kinase II substrate protein 3	*pacsin3*	TRINITY_DN7304_c1_g1_i1	2,34E+14	2,81E-03	x		High	
Serine/threonine-protein phosphatase 6 catalytic subunit	*ppp6c*							
Nuclear factor NF-kappa-B p105 subunit	*sh2d7*	TRINITY_DN62383_c0_g1_i1	2,18E+14	3,43E-03	x		High	
Tumor suppressor candidate 2	*tusc2*	TRINITY_DN12156_c0_g1_i1	2,03E+14	1,63E-03	x		High	
Mucosa-associated lymphoid tissue lymphoma translocation protein 1 homolog	*malt1*	TRINITY_DN11915_c0_g1_i1	1,89E+14	1,31E-03	x		High	
C-C motif chemokine 20	*ccl20*							
Lysozyme g	*lyzg*	TRINITY_DN20059_c0_g1_i1	1,75E+14	4,06E-03	x		High	
Tumor necrosis factor ligand superfamily member 12	*tnfsf12*	TRINITY_DN6055_c0_g2_i1	1,69E+14	8,15E-04	x		High	
Cytokine-inducible SH2-containing protein	*cish*							
Lysomal protective protein	*ctsal*	TRINITY_DN11344_c0_g1_i1	-1,04E+14	9,69E-04	x		High	
Cbp/p300-interacting transactivator 1	*cited1*							
Influenza virus NS1A-binding protein homolog A	*ivns1abpa*							
Tumor necris factor receptor superfamily member 16	*tnr16*	TRINITY_DN772_c0_g1_i1	-1,47E+14	2,35E-04	x		High	
TGF-beta-activated kinase 1 and MAP3K7-binding protein 2	*tab2*	TRINITY_DN13332_c0_g2_i2	-1,63E+14	1,14E-03	x		High	
H-2 class I histocompatibility antigen, K-D alpha chain	*h2-q9l*	TRINITY_DN46_c0_g1_i11	-2,03E+14	1,85E-04	x		High	
Protein kinase C beta type	*prkcb*	TRINITY_DN1884_c0_g1_i10	-2,09E+14	3,08E-03	x		High	
Human immunodeficiency virus type I enhancer-binding protein 2 homolog	*hivep2*	TRINITY_DN3273_c3_g1_i2	-2,17E+14	5,23E-04	x		High	
Complement C1q tumor necrosis factor-related protein 2	*c1qtnf2*	TRINITY_DN45619_c0_g1_i1	-2,31E+14	8,83E-04	x		High	
Lysome-associated membrane glycoprotein 2	*lamp2*	TRINITY_DN22_c0_g2_i1	-2,44E+14	7,10E-04	x		High	
Serine/threonine-protein kinase D2	*prkd2*	TRINITY_DN17465_c0_g2_i1	-2,62E+14	3,01E-03	x		High	
C-X-C chemokine receptor type 3-2	*cxr32*	TRINITY_DN65203_c0_g1_i1	-2,66E+14	7,34E-05	x		High	
Inhibitor of nuclear factor kappa-B kinase subunit beta	*ikbkb*	TRINITY_DN5257_c0_g2_i1	-2,70E+14	2,10E-03	x		High	
Tumor necris factor receptor superfamily member 1A	*tnfrsf1a*	TRINITY_DN11762_c0_g1_i1	-2,83E+14	3,46E-05	x		High	
IST1 homolog	*ist1*	TRINITY_DN27175_c0_g1_i1	-2,85E+14	8,47E-07	x		High	
Serine/threonine-protein kinase 17B	*stk17b*	TRINITY_DN8006_c0_g1_i1	-3,07E+14	2,36E-06	x		High	
Transforming growth factor beta receptor type 3	*tgfbr3*	TRINITY_DN46756_c0_g1_i1	-3,10E+14	3,45E-03	x		High	
Interleukin-11 receptor subunit alpha-1	*il11ral*	TRINITY_DN1616_c3_g1_i1	-3,14E+14	1,36E-03	x		High	
Delta-like protein C	*dlc*							
Complement C1q tumor necris factor-related protein 1	*c1qtnf6*	TRINITY_DN18339_c0_g1_i1	-3,14E+14	3,89E-03	x		High	
Complement component C7	*c7*							
Chemokine (C-X-C motif) ligand 12a (stromal cell-derived factor 1) precursor	*cxcl12a*							
Thioredoxin	*txn*							

Hemoglobin subunit alpha	*hba*	TRINITY_DN5583_c0_g1_i1	-3,26E+14	1,80E-04	x	x	High	Medium
TGF-beta receptor type-1	*tgfbr1*	TRINITY_DN54036_c0_g1_i1	-4,01E+14	2,62E-03	x		High	
Leukemia inhibitory factor receptor	*lifr*	TRINITY_DN34522_c0_g1_i1	-4,46E+14	2,39E-04	x		High	
Protein kinase C iota type	*prkci*	TRINITY_DN40194_c0_g1_i1	-4,81E+14	1,20E-03	x		High	
Inter-alpha-trypsin inhibitor heavy chain H3	*itih3*	TRINITY_DN5978_c0_g1_i1	-4,86E+14	1,72E-06	x		High	
hemoglobin cathodic subunit beta	*hbb*	TRINITY_DN20221_c0_g1_i1	-6,93E+14	8,60E-05		x		Medium
Interleukin-1 receptor-associated kinase 4	*irak4*							
Interferon regulatory factor 2-binding protein 1	*irf2bp1*							
Interferon alpha/beta receptor 2	*ifnar2*							
Innate cellular immunity								
CD226 antigen	*cd226*	TRINITY_DN1527_c0_g1_i11	7,62E+14	1,99E-04	x		High	
Leukocyte elastase inhibitor	*serpinb1*	TRINITY_DN18308_c0_g1_i1	6,65E+14	1,19E-04	x		High	
Leukocyte antigen CD37	*cd37*							
Macrophage colony-stimulating factor 1 receptor 2	*csf1r*							
Platelet-derived growth factor receptor alpha	*pdgfra*	TRINITY_DN47674_c0_g1_i1	5,43E+14	1,90E-03	x		High	
Leukocyte surface antigen CD53	*cd53*							
Macrophage colony-stimulating factor 1 receptor 1	*csf1r*							
CD63 antigen	*cd63*							
CD302 antigen	*cd302*							
Macrophage-capping protein	*capg*							
CD59 glycoprotein-like	*cd59*	TRINITY_DN46287_c0_g1_i1	3,16E+14	1,45E-04	x		High	
CD151 antigen-like isoform X1	*cd151l*	TRINITY_DN1687_c0_g1_i1	2,94E+14	2,98E-05		x		Medium
CD9 antigen	*cd9*							
CD209 antigen-like protein A	*cd209a*	TRINITY_DN7897_c0_g1_i1	1,96E+13	3,31E-04	x		High	
Platelet-derived growth factor receptor beta	*pdgfrb*	TRINITY_DN4280_c0_g1_i1	1,84E+14	3,34E-04	x		High	
Macrophage-expressed gene 1 protein	*mpeg1*	TRINITY_DN15553_c0_g1_i1	-9,34E-01	3,04E-03	x		High	
Platelet-activating factor acetylhydrolase IB subunit alpha2	*pafah1b2*	TRINITY_DN56787_c0_g1_i1	-1,83E+13	3,99E-04	x		High	
Platelet-activating factor acetylhydrolase IB subunit alpha1	*pafah1b3*							
Platelet-derived growth factor subunit B	*grinal*	TRINITY_DN4201_c0_g1_i4	-4,30E+13	4,48E-05	x		High	
Mast cell tryptase	*tpsab1*	TRINITY_DN4398_c0_g1_i11	-6,16E+14	8,08E-05	x		High	
Acquired immunity								
H-2 class I histocompatibility antigen, Q10 alpha chain	*h2-q10*							
T-cell receptor alpha chain V region CTL-F3	*trav29dv5*							
Butyrophilin subfamily 2 member A2	*btn3a1*	TRINITY_DN2180_c0_g1_i10	6,83E+14	8,56E-05		x		Medium
B-cell lymphoma/leukemia 11A	*bcl11b*	TRINITY_DN3768_c0_g2_i1	6,70E+14	3,54E-06	x		High	
B-cell receptor CD22-like	*cd22l*							
Immunoglobulin kappa light chain	*igk*							
Ig mu chain C region membrane-bound form	*ighm*							
Pre-B-cell leukemia transcription factor-interacting protein 1	*pbxip1*	TRINITY_DN1020_c1_g2_i1	6,13E+14	4,38E-04	x		High	
BOLA class I histocompatibility antigen, alpha chain BL3-7	*hla-b*							
T-cell activation inhibitor, mitochondrial	*tcaim*	TRINITY_DN2427_c2_g1_i1	5,96E+14	4,60E-04	x		High	
Ig gamma chain C region	*ighd*							
Immunoglobulin kappa variable 1-12	*igkv1-12*							
H-2 class II histocompatibility antigen, E-Q beta chain	*hb24*							
HLA class II histocompatibility antigen, DP alpha 1 chain	*hla-dpa1*							
CD166 antigen homolog A	*alcamb*							

H-2 class II histocompatibility antigen gamma chain	*hg2a*							
Immunoglobulin-like domain-containing receptor 2	*ildr2*							
Cytotoxic and regulatory T-cell molecule	*crtam*	TRINITY_DN4415_c0_g1_i1	2,25E+14	9,60E-04	**x**		High	
T cell receptor beta variable 18	*trbv18*	TRINITY_DN5200_c1_g1_i1	1,71E+14	1,57E-04	**x**		High	
Class I histocompatibility antigen, F10 alpha chain	*mhc1ufa*							
Immunoglobulin superfamily containing leucine-rich repeat protein 2	*islr2*	TRINITY_DN61486_c0_g1_i1	-2,70E+14	5,54E-04	**x**		High	
Nuclear factor of activated T-cells, cytoplasmic 3	*nfatc3*	TRINITY_DN22032_c0_g1_i2	-2,83E+14	1,42E-06	**x**		High	
Lymphocyte antigen 75	*ly75*	TRINITY_DN32710_c1_g3_i1	-3,74E+14	4,90E-05	**x**		High	
Nuclear factor of activated T-cells 5	*nfat5*	TRINITY_DN20498_c0_g2_i1	-7,27E+14	3,22E-06	**x**		High	

Gene name	Gene symbol	Transcript ID	Duodenum					
			logFC	Pvalue	Pathogen challenges		Response intensity	
					LPS	Poly I:C	LPS	Poly I:C
Pathogen recognition receptors								
Scavenger receptor class B member 1	*scarb1*	TRINITY_DN7578_c0_g1_i1	7,91E+14	3,34E-04		x		High
NACHT, LRR and PYD domains-containing protein 3-like	*nlrp3*	TRINITY_DN13640_c0_g1_i1	7,80E+13	1,07E-04	x		Medium	
Macrophage mannose receptor 1	*mrc1*	TRINITY_DN49274_c0_g1_i1	7,27E+14	8,08E-06		x		High
C-type lectin domain family 4 member E	*clec4e*	TRINITY_DN10729_c0_g1_i1	7,20E+14	2,12E-05		x		High
Scavenger receptor cysteine-rich domain-containing group B protein	*ssc4d*							
TLR adapter interacting with SLC15A4 on the lysosome	*cxorf21*	TRINITY_DN18574_c0_g1_i1	5,41E+14	1,07E-03		x		High
Toll-like receptor 3 isoform X2	*tlr3*							
Protein NLRC3	*nlrc3*	TRINITY_DN88358_c0_g1_i1	5,37E+14	2,87E-03		x		High
NACHT, LRR and PYD domains-containing protein 1	*nlrp1*	TRINITY_DN15911_c0_g1_i1	5,57E+13	2,81E-03		x		High
C-type lectin domain family 11 member A	*clec11a*							
C-type mannose receptor 2	*mrc2*							
Iron metabolism pathway								
Transferrin receptor protein 1	*tfrc*	TRINITY_DN1653_c1_g3_i1	7,79E+14	1,45E-06		x		High
Fermitin family homolog 3	*fermt3*	TRINITY_DN42042_c0_g1_i1	6,74E+14	3,27E-05		x		High
Ferrochelatase, mitochondrial	*fech*	TRINITY_DN111269_c0_g1_i1	6,37E+14	9,31E-04		x		High
Iron-sulfur cluster assembly enzyme ISCU, mitochondrial	*iscu*	TRINITY_DN10976_c0_g1_i1	4,40E+14	1,04E-03		x		High
Cytolic Fe-S cluster assembly factor nubp2	*nubp2*							
Serotransferrin-1	*tf*							
2-oxoglutarate and iron-dependent oxygenase JMJD4	*jmjd4*							
Iron-responsive element-binding protein 2	*ireb2*							
Adrenodoxin, mitochondrial	*fdx1*							
NADH dehydrogenase [ubiquinone] iron-sulfur protein 4, mitochondrial	*ndufs4*							
Ferritin, middle subunit	*fm*							
Ferritin, heavy subunit	*fth1*	TRINITY_DN363_c0_g5_i1	7,83E+14	1,46E-06		x		High
Selenium metabolism pathway								
Selenoprotein J	*selenoj*	TRINITY_DN36385_c0_g1_i1	3,67E+14	3,65E-04		x		High
Methanethiol oxidase	*selenbp1*	TRINITY_DN12128_c0_g1_i1	3,06E+13	1,64E-03		x		High
Thioredoxin reductase-like selenoprotein T1a	*selenot1a*	TRINITY_DN1622_c0_g1_i1	2,70E+14	3,62E-04		x		High
Selenoprotein Pa	*sepp1a*							
Selenocysteine insertion sequence-binding protein 2	*secisbp2*							
Selenocysteine insertion sequence-binding protein 2-like	*secisbp2l*							
Type I iodothyronine deiodinase	*dio1*							
Toxins								
Stonustoxin subunit alpha	*stxa*							
Neoverrucotoxin subunit alpha	*ntxa*	TRINITY_DN13640_c0_g1_i1	7,15E+14	4,85E-06		x		High
Anthrax toxin receptor 2	*antxr2*	TRINITY_DN26261_c0_g3_i1	6,10E+14	8,92E-04		x		High
DELTA-sagatoxin-Srs1a-like	*srs1al*							
Neoverrucotoxin subunit beta	*nvtx*	TRINITY_DN73_c3_g1_i1	3,43E+14	3,84E-04	x		Medium	
Cytolytic toxin-alpha	*clya*							
Anthrax toxin receptor 1	*antxr1*							
Stonustoxin subunit beta	*stnxb*							

Innate humoral immunity								
BCL2/adenovirus E1B 19 kDa protein-interacting protein 3	*bnip3*	TRINITY_DN1380_c0_g1_i1	9,18E+14	1,28E-04		x		High
Mucin-5AC-like	*muc5ac*	TRINITY_DN8118_c0_g1_i2	8,47E+14	2,82E-04		x		High
C-reactive protein	*crp*							
Complement C1q-like protein 2	*c1ql2*							
Serpin peptidase inhibitor, clade A (alpha-1 antiproteinase, antitrypsin), member 7 isoform X1	*serpina1*	TRINITY_DN9245_c0_g1_i1	8,38E+14	3,18E-06		x		High
Lysosomal alpha-mannosidase	*man2b1*	TRINITY_DN14979_c0_g3_i2	7,78E+14	2,45E-04	x		Medium	
NF-kappa-B inhibitor alpha	*nfkbia*	TRINITY_DN1208_c0_g1_i1	7,74E+14	2,63E-04	x	x	Medium	High
Serine/threonine-protein kinase RIO3	*riok3*	TRINITY_DN26579_c0_g1_i1	7,57E+14	1,12E-03		x		High
Interleukin-17 receptor A	*il17ra*							
Cytokine-inducible SH2-containing protein	*cish*	TRINITY_DN13379_c1_g5_i1	7,54E+14	2,08E-04	x		Medium	
Tumor susceptibility gene 101 protein	*tsg101*							
Interferon-related developmental regulator 2	*ifrd2*	TRINITY_DN4775_c0_g1_i2	7,49E+14	4,63E-04	x		Medium	
Plasma protease C1 inhibitor	*serping1*	TRINITY_DN34598_c0_g1_i1	7,36E+14	1,55E-03		x		High
Mucin 13b, cell surface associated isoform X1	*muc13b*	TRINITY_DN2953_c0_g2_i1	7,32E+14	1,08E-06		x		High
Serine/threonine-protein kinase MARK2	*mark2*	TRINITY_DN29985_c0_g1_i3	7,20E+14	1,45E-06		x		High
Macrophage-stimulating protein receptor	*mst1r*	TRINITY_DN111277_c0_g1_i1	7,20E+14	2,97E-06		x		High
Receptor-type tyrosine-protein phosphatase eta	*ptprj*	TRINITY_DN913_c0_g2_i1	7,18E+14	1,42E-06		x		High
Lysosomal alpha-glucosidase	*gaa*							
Interferon regulatory factor 8	*irf8*	TRINITY_DN23619_c0_g2_i1	7,02E+14	2,41E-05		x		High
Lysine-specific demethylase 5B-B	*kdm5bb*	TRINITY_DN2659_c0_g2_i1	4,00E+14	1,57E-04		x		High
C-X-C chemokine receptor type 4	*cxcr4*	TRINITY_DN2531_c0_g1_i1	6,90E+14	3,00E-04	x		Medium	
Complement factor B	*cfb*	TRINITY_DN8991_c0_g1_i1	6,97E+14	1,86E-05		x		High
Tumor necrosis factor receptor superfamily member 1A precursor	*tnfrsf1a*	TRINITY_DN2302_c1_g3_i1	6,79E+14	1,86E-06		x		High
Lysosomal protective protein	*ctsa*	TRINITY_DN10272_c0_g1_i1	6,75E+14	2,33E-04	x		Medium	
Interleukin-1 receptor accessory protein-like 1-A isoform X1	*il1rapl1*	TRINITY_DN24413_c1_g1_i2	6,73E+14	1,19E-05		x		High
Interleukin-6 receptor subunit alpha	*il6r*	TRINITY_DN28409_c0_g1_i1	6,73E+14	4,26E-06		x		High
Complement C1q subcomponent subunit C	*c1qc*	TRINITY_DN84704_c0_g1_i1	6,60E+14	1,52E-05		x		High
Interferon regulatory factor 2	*irf2*	TRINITY_DN19171_c0_g1_i1	6,57E+14	3,21E-05		x		High
Complement C4-B	*c4b*	TRINITY_DN120530_c0_g1_i1	6,21E+14	1,08E-04		x		High
Tumor necrosis factor alpha-induced protein 2 isoform X1	*tnaifp2*	TRINITY_DN17698_c0_g1_i1	6,07E+14	1,13E-06		x		High
Cationic trypsin-like	*prss1*	TRINITY_DN4090_c0_g3_i1	5,95E+14	1,06E-03		x		High
Tumor necrosis factor receptor superfamily member 11A isoform X1	*tnfrsf11a*	TRINITY_DN26052_c0_g2_i1	5,87E+14	1,50E-03		x		High
Mucin-2-like	*muc2l*							
Tumor necrosis factor, alpha-induced protein 8-like protein 2 A	*tnfaip8l2*	TRINITY_DN17485_c1_g1_i1	5,83E+14	1,03E-03		x		High
Chemokine-like receptor 1	*cmklr1*							
Interleukin-1 receptor-associated kinase 3	*irak3*	TRINITY_DN14045_c0_g2_i1	5,66E+14	2,63E-03		x		High
Complement C3	*c3*	TRINITY_DN25542_c0_g1_i1	5,65E+14	2,29E-03		x		High
C-X-C motif chemokine 20	*cxcl20*	TRINITY_DN52692_c0_g1_i1	5,46E+14	2,83E-03		x		High
Complement component C7	*c7*	TRINITY_DN71033_c0_g1_i1	5,41E+14	5,05E-04		x		High
Serine/threonine-protein kinase N1	*pkn1*	TRINITY_DN77130_c0_g1_i1	5,23E+14	6,21E-04		x		High
Complement C4	*c4*	TRINITY_DN22680_c0_g1_i1	5,14E+14	8,65E-05		x		High
Interleukin-13 receptor subunit alpha-2	*il13ra2*	TRINITY_DN21531_c0_g1_i1	5,14E+14	1,43E-03		x		High
Tumor necrosis factor alpha-induced protein 8-like protein 3	*tnfaip8l3*	TRINITY_DN15630_c0_g1_i1	5,05E+14	1,28E-06		x		High
Beta-2-microglobulin	*b2m*	TRINITY_DN2346_c0_g1_i1	4,99E+14	2,39E-05	x	x	Medium	High
Mucin-2	*muc2*	TRINITY_DN54850_c0_g1_i1	4,91E+14	1,74E-03		x		High
C1qB	*c1qb*	TRINITY_DN37398_c0_g1_i1	4,76E+14	6,70E-04		x		High

Hemoglobin subunit beta-1	*hbb1*	TRINITY_DN27171_c0_g1_i3	4,71E+14	1,33E-04	**x**		Medium	
Interferon-induced GTP-binding protein MxA	*mx1*	TRINITY_DN6427_c0_g1_i1	4,61E+14	1,14E-03		**x**		High
Interferon-induced protein with tetratricopeptide repeats 1-like	*ifit1l*							
Hemoglobin subunit alpha-1	*hba1*	TRINITY_DN18918_c0_g1_i1	6,94E+13	5,59E-05		**x**		High
Serine/threonine-protein kinase TBK1	*tbk1*							
Complement factor D	*cfd*	TRINITY_DN3130_c0_g1_i1	3,99E+14	2,04E-06		**x**		High
Beta-galactoside-binding lectin	*lec-1*	TRINITY_DN94557_c0_g1_i1	3,96E+14	6,92E-04		**x**		High
Protein S100-A1	*s100a1*	TRINITY_DN96969_c0_g1_i1	3,88E+14	8,23E-06		**x**		High
Serine/threonine-protein kinase STK11	*stk11*							
Hemoglobin subunit alpha-2	*hba2*							
Leukotriene A-4 hydrolase	*lta4h*	TRINITY_DN62940_c0_g1_i1	3,16E+14	6,87E-04		**x**		High
Sialomucin core protein 24	*cd164*	TRINITY_DN398_c1_g2_i1	3,11E+14	1,54E-04		**x**		High
Leucine-rich repeats and immunoglobulin-like domains protein 2	*lrig2*							
Protein kinase C delta type	*prkcd*	TRINITY_DN4286_c0_g1_i1	2,80E+14	3,10E-04		**x**		High
Bactericidal permeability-increasing protein	*bpi*							
Protein kinase C and casein kinase II substrate protein 3	*pacsin3*	TRINITY_DN3167_c0_g1_i1	5,61E+14	2,53E-03		**x**		High
Serine/threonine-protein phosphatase 6 catalytic subunit	*ppp6c*	TRINITY_DN1696_c0_g3_i1	2,20E+14	2,89E-03		**x**		High
Nuclear factor NF-kappa-B p105 subunit	*sh2d7*	TRINITY_DN10879_c0_g2_i1	5,86E+14	5,32E-04		**x**		High
Tumor suppressor candidate 2	*tusc2*							
Mucosa-associated lymphoid tissue lymphoma translocation protein 1 homolog	*malt1*							
C-C motif chemokine 20	*ccl20*							
Lysozyme g	*lyzg*							
Tumor necrosis factor ligand superfamily member 12	*tnfsf12*							
Cytokine-inducible SH2-containing protein	*cish*							
Lysomal protective protein	*ctsal*							
Cbp/p300-interacting transactivator 1	*cited1*							
Influenza virus NS1A-binding protein homolog A	*ivns1abpa*	TRINITY_DN699_c0_g1_i1	5,19E+14	1,46E-04		**x**		High
Tumor necris factor receptor superfamily member 16	*tnr16*							
TGF-beta-activated kinase 1 and MAP3K7-binding protein 2	*tab2*							
H-2 class I histocompatibility antigen, K-D alpha chain	*h2-q9l*							
Protein kinase C beta type	*prkcb*							
Human immunodeficiency virus type I enhancer-binding protein 2 homolog	*hivep2*							
Complement C1q tumor necrosis factor-related protein 2	*c1qtnf2*							
Lysome-associated membrane glycoprotein 2	*lamp2*							
Serine/threonine-protein kinase D2	*prkd2*							
C-X-C chemokine receptor type 3-2	*cxr32*							
Inhibitor of nuclear factor kappa-B kinase subunit beta	*ikbkb*							
Tumor necris factor receptor superfamily member 1A	*tnfrsf1a*							
IST1 homolog	*ist1*							
Serine/threonine-protein kinase 17B	*stk17b*							
Transforming growth factor beta receptor type 3	*tgfbr3*							
Interleukin-11 receptor subunit alpha-1	*il11ral*	TRINITY_DN104972_c0_g1_i1	6,48E+14	4,62E-05		**x**		High
Delta-like protein C	*dlc*	TRINITY_DN3091_c0_g1_i1	7,29E+13	1,21E-06		**x**		High
Complement C1q tumor necris factor-related protein 1	*c1qtnf6*							
Complement component C7	*c7*	TRINITY_DN63079_c0_g1_i1	5,73E+13	1,53E-04		**x**		High
Chemokine (C-X-C motif) ligand 12a (stromal cell-derived factor 1) precursor	*cxcl12a*	TRINITY_DN483_c0_g1_i1	5,67E+13	4,37E-04		**x**		High
Thioredoxin	*txn*	TRINITY_DN788_c0_g1_i1	3,21E+13	2,07E-06		**x**		High

Hemoglobin subunit alpha	*hba*							
TGF-beta receptor type-1	*tgfbr1*							
Leukemia inhibitory factor receptor	*lifr*							
Protein kinase C iota type	*prkci*							
Inter-alpha-trypsin inhibitor heavy chain H3	*itih3*							
hemoglobin cathodic subunit beta	*hbb*							
Interleukin-1 receptor-associated kinase 4	*irak4*	TRINITY_DN22833_c0_g1_i1	-6,28E+13	7,24E-06		**x**		High
Interferon regulatory factor 2-binding protein 1	*irf2bp1*	TRINITY_DN2348_c1_g5_i1	-7,93E+13	5,83E-06	**x**		Medium	
Interferon alpha/beta receptor 2	*ifnar2*	TRINITY_DN22122_c0_g1_i1	-9,27E+14	3,00E-06		**x**		High
Innate cellular immunity								
CD226 antigen	*cd226*							
Leukocyte elastase inhibitor	*serpinb1*							
Leukocyte antigen CD37	*cd37*	TRINITY_DN21239_c0_g1_i1	6,54E+14	3,92E-04		**x**		High
Macrophage colony-stimulating factor 1 receptor 2	*csf1r*	TRINITY_DN106506_c0_g1_i1	5,98E+14	1,82E-03		**x**		High
Platelet-derived growth factor receptor alpha	*pdgfra*							
Leukocyte surface antigen CD53	*cd53*	TRINITY_DN5285_c6_g1_i1	5,36E+14	4,16E-05		**x**		High
Macrophage colony-stimulating factor 1 receptor 1	*csf1r*	TRINITY_DN29350_c0_g2_i1	4,96E+14	1,60E-03		**x**		High
CD63 antigen	*cd63*	TRINITY_DN1582_c0_g1_i1	3,92E+14	1,92E-05		**x**		High
CD302 antigen	*cd302*	TRINITY_DN30184_c0_g3_i1	3,64E+14	1,41E-06		**x**		High
Macrophage-capping protein	*capg*	TRINITY_DN2592_c0_g1_i1	3,33E+14	2,62E-05		**x**		High
CD59 glycoprotein-like	*cd59*							
CD151 antigen-like isoform X1	*cd151l*							
CD9 antigen	*cd9*							
CD209 antigen-like protein A	*cd209a*							
Platelet-derived growth factor receptor beta	*pdgfrb*							
Macrophage-expressed gene 1 protein	*mpeg1*	TRINITY_DN9586_c0_g2_i1	5,29E+14	3,80E-04	**x**	**x**	Medium	High
Platelet-activating factor acetylhydrolase IB subunit alpha2	*pafah1b2*	TRINITY_DN13666_c0_g1_i1	3,99E+14	4,34E-04		**x**		High
Platelet-activating factor acetylhydrolase IB subunit alpha1	*pafah1b3*							
Platelet-derived growth factor subunit B	*grinal*							
Mast cell tryptase	*tpsab1*							
Acquired immunity								
H-2 class I histocompatibility antigen, Q10 alpha chain	*h2-q10*	TRINITY_DN4030_c0_g1_i11	7,30134E+14	2,07E-05		**x**		High
T-cell receptor alpha chain V region CTL-F3	*trav29dv5*	TRINITY_DN6420_c0_g1_i1	6,97017E+14	3,45E-05		**x**		High
Butyrophilin subfamily 2 member A2	*btn3a1*							
B-cell lymphoma/leukemia 11A	*bcl11b*							
B-cell receptor CD22-like	*cd22l*	TRINITY_DN1151_c0_g1_i1	6,61E+14	4,78E-04		**x**		High
Immunoglobulin kappa light chain	*igk*	TRINITY_DN906_c5_g1_i1	6,31E+14	1,76E-04		**x**		High
Ig mu chain C region membrane-bound form	*ighm*	TRINITY_DN4927_c0_g1_i1	6,21E+14	3,89E-04		**x**		High
Pre-B-cell leukemia transcription factor-interacting protein 1	*pbxip1*							
BOLA class I histocompatibility antigen, alpha chain BL3-7	*hla-b*	TRINITY_DN160_c0_g2_i1	6,06E+14	4,43E-04		**x**		High
T-cell activation inhibitor, mitochondrial	*tcaim*	TRINITY_DN50319_c0_g1_i1	5,81E+14	6,59E-04		**x**		High
Ig gamma chain C region	*ighd*	TRINITY_DN53784_c0_g2_i1	5,84E+14	1,59E-03		**x**		High
Immunoglobulin kappa variable 1-12	*igkv1-12*	TRINITY_DN16331_c0_g1_i1	5,74E+14	2,23E-03		**x**		High
H-2 class II histocompatibility antigen, E-Q beta chain	*hb24*	TRINITY_DN150_c0_g2_i2	5,53E+14	3,64E-04	**x**		Medium	
HLA class II histocompatibility antigen, DP alpha 1 chain	*hla-dpa1*	TRINITY_DN45_c0_g2_i1	5,09E+14	2,00E-04	**x**		Medium	
CD166 antigen homolog A	*alcamb*	TRINITY_DN28396_c0_g1_i1	5,00E+14	4,36E-04		**x**		High

H-2 class II histocompatibility antigen gamma chain	*hg2a*	TRINITY_DN6173_c0_g3_i1	4,86E+14	9,15E-05	**x**	**x**	Medium	High
Immunoglobulin-like domain-containing receptor 2	*ildr2*	TRINITY_DN16571_c0_g1_i4	4,35E+14	2,84E-03		**x**		High
Cytotoxic and regulatory T-cell molecule	*crtam*							
T cell receptor beta variable 18	*trbv18*							
Class I histocompatibility antigen, F10 alpha chain	*mhc1ufa*	TRINITY_DN21172_c0_g1_i1	5,11E+13	4,88E-05	**x**		Medium	
Immunoglobulin superfamily containing leucine-rich repeat protein 2	*islr2*							
Nuclear factor of activated T-cells, cytoplasmic 3	*nfatc3*							
Lymphocyte antigen 75	*ly75*	TRINITY_DN23453_c0_g1_i1	4,87E+14	2,30E-03		**x**		High
Nuclear factor of activated T-cells 5	*nfat5*							

Gene name	Gene symbol	Transcript ID	Spleen					
			logFC	Pvalue	Pathogen challenges		Response intensity	
					LPS	Poly I:C	LPS	Poly I:C
Pathogen recognition receptors								
Scavenger receptor class B member 1	*scarb1*							
NACHT, LRR and PYD domains-containing protein 3-like	*nlrp3*							
Macrophage mannose receptor 1	*mrc1*							
C-type lectin domain family 4 member E	*clec4e*							
Scavenger receptor cysteine-rich domain-containing group B protein	*ssc4d*							
TLR adapter interacting with SLC15A4 on the lysosome	*cxorf21*							
Toll-like receptor 3 isoform X2	*tlr3*							
Protein NLRC3	*nlrc3*							
NACHT, LRR and PYD domains-containing protein 1	*nlrp1*							
C-type lectin domain family 11 member A	*clec11a*							
C-type mannose receptor 2	*mrc2*							
Iron metabolism pathway								
Transferrin receptor protein 1	*tfrc*							
Fermitin family homolog 3	*fermt3*							
Ferrochelatase, mitochondrial	*fech*							
Iron-sulfur cluster assembly enzyme ISCU, mitochondrial	*iscu*							
Cytolic Fe-S cluster assembly factor nubp2	*nubp2*							
Serotransferrin-1	*tf*							
2-oxoglutarate and iron-dependent oxygenase JMJD4	*jmjd4*							
Iron-responsive element-binding protein 2	*ireb2*							
Adrenodoxin, mitochondrial	*fdx1*							
NADH dehydrogenase [ubiquinone] iron-sulfur protein 4, mitochondrial	*ndufs4*							
Ferritin, middle subunit	*fm*							
Ferritin, heavy subunit	*fth1*							
Selenium metabolism pathway								
Selenoprotein J	*selenoj*							
Methanethiol oxidase	*selenbp1*							
Thioredoxin reductase-like selenoprotein T1a	*selenot1a*							
Selenoprotein Pa	*sepp1a*							
Selenocysteine insertion sequence-binding protein 2	*secisbp2*							
Selenocysteine insertion sequence-binding protein 2-like	*secisbp2l*							
Type I iodothyronine deiodinase	*dio1*							
Toxins								
Stonustoxin subunit alpha	*stxa*							
Neoverrucotoxin subunit alpha	*ntxa*							
Anthrax toxin receptor 2	*antxr2*							
DELTA-sagatoxin-Srs1a-like	*srs1al*							
Neoverrucotoxin subunit beta	*nvtx*							
Cytolytic toxin-alpha	*clya*							
Anthrax toxin receptor 1	*antxr1*							
Stonustoxin subunit beta	*stnxb*							

Innate humoral immunity								
BCL2/adenovirus E1B 19 kDa protein-interacting protein 3	*bnip3*							
Mucin-5AC-like	*muc5ac*							
C-reactive protein	*crp*							
Complement C1q-like protein 2	*c1ql2*							
Serpin peptidase inhibitor, clade A (alpha-1 antiproteinase, antitrypsin), member 7 isoform X1	*serpina1*							
Lysosomal alpha-mannosidase	*man2b1*							
NF-kappa-B inhibitor alpha	*nfkbia*							
Serine/threonine-protein kinase RIO3	*riok3*							
Interleukin-17 receptor A	*il17ra*	TRINITY_DN8545_c0_g1_i1	7,72E+14	5,37E-07		**x**		Very low
Cytokine-inducible SH2-containing protein	*cish*							
Tumor susceptibility gene 101 protein	*tsg101*							
Interferon-related developmental regulator 2	*ifrd2*							
Plasma protease C1 inhibitor	*serping1*							
Mucin 13b, cell surface associated isoform X1	*muc13b*							
Serine/threonine-protein kinase MARK2	*mark2*							
Macrophage-stimulating protein receptor	*mst1r*							
Receptor-type tyrosine-protein phosphatase eta	*ptprj*							
Lysosomal alpha-glucosidase	*gaa*							
Interferon regulatory factor 8	*irf8*							
Lysine-specific demethylase 5B-B	*kdm5bb*							
C-X-C chemokine receptor type 4	*cxcr4*							
Complement factor B	*cfb*							
Tumor necrosis factor receptor superfamily member 1A precursor	*tnfrsf1a*							
Lysosomal protective protein	*ctsa*							
Interleukin-1 receptor accessory protein-like 1-A isoform X1	*il1rapl1*							
Interleukin-6 receptor subunit alpha	*il6r*							
Complement C1q subcomponent subunit C	*c1qc*							
Interferon regulatory factor 2	*irf2*							
Complement C4-B	*c4b*							
Tumor necrosis factor alpha-induced protein 2 isoform X1	*tnaifp2*							
Cationic trypsin-like	*prss1*							
Tumor necrosis factor receptor superfamily member 11A isoform X1	*tnfrsf11a*							
Mucin-2-like	*muc2l*							
Tumor necrosis factor, alpha-induced protein 8-like protein 2 A	*tnfaip8l2*							
Chemokine-like receptor 1	*cmklr1*							
Interleukin-1 receptor-associated kinase 3	*irak3*							
Complement C3	*c3*							
C-X-C motif chemokine 20	*cxcl20*							
Complement component C7	*c7*							
Serine/threonine-protein kinase N1	*pkn1*							
Complement C4	*c4*							
Interleukin-13 receptor subunit alpha-2	*il13ra2*							
Tumor necrosis factor alpha-induced protein 8-like protein 3	*tnfaip8l3*							
Beta-2-microglobulin	*b2m*							
Mucin-2	*muc2*							
C1qB	*c1qb*							

Hemoglobin subunit beta-1	*hbb1*							
Interferon-induced GTP-binding protein MxA	*mx1*							
Interferon-induced protein with tetratricopeptide repeats 1-like	*ifit1l*							
Hemoglobin subunit alpha-1	*hba1*							
Serine/threonine-protein kinase TBK1	*tbk1*							
Complement factor D	*cfd*							
Beta-galactoside-binding lectin	*lec-1*							
Protein S100-A1	*s100a1*							
Serine/threonine-protein kinase STK11	*stk11*							
Hemoglobin subunit alpha-2	*hba2*							
Leukotriene A-4 hydrolase	*lta4h*							
Sialomucin core protein 24	*cd164*							
Leucine-rich repeats and immunoglobulin-like domains protein 2	*lrig2*							
Protein kinase C delta type	*prkcd*							
Bactericidal permeability-increasing protein	*bpi*							
Protein kinase C and casein kinase II substrate protein 3	*pacsin3*							
Serine/threonine-protein phosphatase 6 catalytic subunit	*ppp6c*							
Nuclear factor NF-kappa-B p105 subunit	*sh2d7*							
Tumor suppressor candidate 2	*tusc2*							
Mucosa-associated lymphoid tissue lymphoma translocation protein 1 homolog	*malt1*							
C-C motif chemokine 20	*ccl20*							
Lysozyme g	*lyzg*							
Tumor necrosis factor ligand superfamily member 12	*tnfsf12*							
Cytokine-inducible SH2-containing protein	*cish*							
Lysomal protective protein	*ctsal*							
Cbp/p300-interacting transactivator 1	*cited1*							
Influenza virus NS1A-binding protein homolog A	*ivns1abpa*	TRINITY_DN1519_c3_g1_i1	-1,43E+14	4,37E-05		**x**		Very low
Tumor necris factor receptor superfamily member 16	*tnr16*							
TGF-beta-activated kinase 1 and MAP3K7-binding protein 2	*tab2*							
H-2 class I histocompatibility antigen, K-D alpha chain	*h2-q9l*							
Protein kinase C beta type	*prkcb*							
Human immunodeficiency virus type I enhancer-binding protein 2 homolog	*hivep2*							
Complement C1q tumor necrosis factor-related protein 2	*c1qtnf2*							
Lysome-associated membrane glycoprotein 2	*lamp2*							
Serine/threonine-protein kinase D2	*prkd2*							
C-X-C chemokine receptor type 3-2	*cxr32*							
Inhibitor of nuclear factor kappa-B kinase subunit beta	*ikbkb*							
Tumor necris factor receptor superfamily member 1A	*tnfrsf1a*							
IST1 homolog	*ist1*							
Serine/threonine-protein kinase 17B	*stk17b*							
Transforming growth factor beta receptor type 3	*tgfbr3*							
Interleukin-11 receptor subunit alpha-1	*il11ral*							
Delta-like protein C	*dlc*							
Complement C1q tumor necris factor-related protein 1	*c1qtnf6*							
Complement component C7	*c7*							
Chemokine (C-X-C motif) ligand 12a (stromal cell-derived factor 1) precursor	*cxcl12a*							
Thioredoxin	*txn*							

Hemoglobin subunit alpha	*hba*							
TGF-beta receptor type-1	*tgfbr1*							
Leukemia inhibitory factor receptor	*lifr*							
Protein kinase C iota type	*prkci*							
Inter-alpha-trypsin inhibitor heavy chain H3	*itih3*							
hemoglobin cathodic subunit beta	*hbb*							
Interleukin-1 receptor-associated kinase 4	*irak4*							
Interferon regulatory factor 2-binding protein 1	*irf2bp1*							
Interferon alpha/beta receptor 2	*ifnar2*							
Innate cellular immunity								
CD226 antigen	*cd226*							
Leukocyte elastase inhibitor	*serpinb1*							
Leukocyte antigen CD37	*cd37*							
Macrophage colony-stimulating factor 1 receptor 2	*csf1r*							
Platelet-derived growth factor receptor alpha	*pdgfra*							
Leukocyte surface antigen CD53	*cd53*							
Macrophage colony-stimulating factor 1 receptor 1	*csf1r*							
CD63 antigen	*cd63*							
CD302 antigen	*cd302*							
Macrophage-capping protein	*capg*							
CD59 glycoprotein-like	*cd59*							
CD151 antigen-like isoform X1	*cd151l*							
CD9 antigen	*cd9*							
CD209 antigen-like protein A	*cd209a*							
Platelet-derived growth factor receptor beta	*pdgfrb*							
Macrophage-expressed gene 1 protein	*mpeg1*							
Platelet-activating factor acetylhydrolase IB subunit alpha2	*pafah1b2*							
Platelet-activating factor acetylhydrolase IB subunit alpha1	*pafah1b3*	TRINITY_DN702_c3_g2_i1	-2,26E+13	1,99E-07		**x**		Very low
Platelet-derived growth factor subunit B	*grinal*							
Mast cell tryptase	*tpsab1*							
Acquired immunity								
H-2 class I histocompatibility antigen, Q10 alpha chain	*h2-q10*							
T-cell receptor alpha chain V region CTL-F3	*trav29dv5*							
Butyrophilin subfamily 2 member A2	*btn3a1*							
B-cell lymphoma/leukemia 11A	*bcl11b*							
B-cell receptor CD22-like	*cd22l*							
Immunoglobulin kappa light chain	*igk*							
Ig mu chain C region membrane-bound form	*ighm*							
Pre-B-cell leukemia transcription factor-interacting protein 1	*pbxip1*							
BOLA class I histocompatibility antigen, alpha chain BL3-7	*hla-b*							
T-cell activation inhibitor, mitochondrial	*tcaim*							
Ig gamma chain C region	*ighd*							
Immunoglobulin kappa variable 1-12	*igkv1-12*							
H-2 class II histocompatibility antigen, E-Q beta chain	*hb24*							
HLA class II histocompatibility antigen, DP alpha 1 chain	*hla-dpa1*							
CD166 antigen homolog A	*alcamb*							

H-2 class II histocompatibility antigen gamma chain	*hg2a*							
Immunoglobulin-like domain-containing receptor 2	*ildr2*							
Cytotoxic and regulatory T-cell molecule	*crtam*							
T cell receptor beta variable 18	*trbv18*							
Class I histocompatibility antigen, F10 alpha chain	*mhc1ufa*							
Immunoglobulin superfamily containing leucine-rich repeat protein 2	*islr2*							
Nuclear factor of activated T-cells, cytoplasmic 3	*nfatc3*							
Lymphocyte antigen 75	*ly75*							
Nuclear factor of activated T-cells 5	*nfat5*							

Gene name	Gene symbol	Transcript ID	Liver					
			logFC	Pvalue	Pathogen challenges		Response intensity	
					LPS	Poly I:C	LPS	Poly I:C
Pathogen recognition receptors								
Scavenger receptor class B member 1	*scarb1*							
NACHT, LRR and PYD domains-containing protein 3-like	*nlrp3*							
Macrophage mannose receptor 1	*mrc1*							
C-type lectin domain family 4 member E	*clec4e*							
Scavenger receptor cysteine-rich domain-containing group B protein	*ssc4d*							
TLR adapter interacting with SLC15A4 on the lysosome	*cxorf21*							
Toll-like receptor 3 isoform X2	*tlr3*	TRINITY_DN9523_c0_g1_i5	-1,15E+14	5,30E-05		**x**		Low
Protein NLRC3	*nlrc3*							
NACHT, LRR and PYD domains-containing protein 1	*nlrp1*							
C-type lectin domain family 11 member A	*clec11a*							
C-type mannose receptor 2	*mrc2*							
Iron metabolism pathway								
Transferrin receptor protein 1	*tfrc*							
Fermitin family homolog 3	*fermt3*							
Ferrochelatase, mitochondrial	*fech*							
Iron-sulfur cluster assembly enzyme ISCU, mitochondrial	*iscu*							
Cytolic Fe-S cluster assembly factor nubp2	*nubp2*							
Serotransferrin-1	*tf*	TRINITY_DN2643_c0_g1_i6	6,22E+13	3,63E-05		**x**		Low
2-oxoglutarate and iron-dependent oxygenase JMJD4	*jmjd4*							
Iron-responsive element-binding protein 2	*ireb2*							
Adrenodoxin, mitochondrial	*fdx1*	TRINITY_DN2286_c0_g1_i4	1,18E+14	4,67E-05		**x**		Low
NADH dehydrogenase [ubiquinone] iron-sulfur protein 4, mitochondrial	*ndufs4*							
Ferritin, middle subunit	*fm*	TRINITY_DN358_c0_g1_i1	-1,14E+14	4,26E-05	**x**		Low	
Ferritin, heavy subunit	*fth1*							
Selenium metabolism pathway								
Selenoprotein J	*selenoj*							
Methanethiol oxidase	*selenbp1*							
Thioredoxin reductase-like selenoprotein T1a	*selenot1a*							
Selenoprotein Pa	*sepp1a*	TRINITY_DN1221_c0_g1_i2	3,09E+14	7,44E-08	**x**		Low	
Selenocysteine insertion sequence-binding protein 2	*secisbp2*							
Selenocysteine insertion sequence-binding protein 2-like	*secisbp2l*							
Type I iodothyronine deiodinase	*dio1*	TRINITY_DN1971_c0_g1_i1	-1,33E+14	8,56E-05	**x**	**x**	Low	Low
Toxins								
Stonustoxin subunit alpha	*stxa*							
Neoverrucotoxin subunit alpha	*ntxa*							
Anthrax toxin receptor 2	*antxr2*							
DELTA-sagatoxin-Srs1a-like	*srs1al*							
Neoverrucotoxin subunit beta	*nvtx*							
Cytolytic toxin-alpha	*clya*	TRINITY_DN4006_c0_g1_i13	2,45E+14	3,35E-04		**x**		Low
Anthrax toxin receptor 1	*antxr1*							
Stonustoxin subunit beta	*stnxb*							

Innate humoral immunity								
BCL2/adenovirus E1B 19 kDa protein-interacting protein 3	*bnip3*							
Mucin-5AC-like	*muc5ac*							
C-reactive protein	*crp*							
Complement C1q-like protein 2	*c1ql2*							
Serpin peptidase inhibitor, clade A (alpha-1 antiproteinase, antitrypsin), member 7 isoform X1	*serpina1*							
Lysosomal alpha-mannosidase	*man2b1*							
NF-kappa-B inhibitor alpha	*nfkbia*							
Serine/threonine-protein kinase RIO3	*riok3*							
Interleukin-17 receptor A	*il17ra*							
Cytokine-inducible SH2-containing protein	*cish*							
Tumor susceptibility gene 101 protein	*tsg101*							
Interferon-related developmental regulator 2	*ifrd2*							
Plasma protease C1 inhibitor	*serping1*							
Mucin 13b, cell surface associated isoform X1	*muc13b*							
Serine/threonine-protein kinase MARK2	*mark2*							
Macrophage-stimulating protein receptor	*mst1r*							
Receptor-type tyrosine-protein phosphatase eta	*ptprj*							
Lysosomal alpha-glucosidase	*gaa*							
Interferon regulatory factor 8	*irf8*							
Lysine-specific demethylase 5B-B	*kdm5bb*	TRINITY_DN52638_c0_g1_i1	6,98E+14	8,60E-07		**x**		Low
C-X-C chemokine receptor type 4	*cxcr4*							
Complement factor B	*cfb*							
Tumor necrosis factor receptor superfamily member 1A precursor	*tnfrsf1a*							
Lysosomal protective protein	*ctsa*							
Interleukin-1 receptor accessory protein-like 1-A isoform X1	*il1rapl1*							
Interleukin-6 receptor subunit alpha	*il6r*							
Complement C1q subcomponent subunit C	*c1qc*							
Interferon regulatory factor 2	*irf2*							
Complement C4-B	*c4b*							
Tumor necrosis factor alpha-induced protein 2 isoform X1	*tnaifp2*							
Cationic trypsin-like	*prss1*	TRINITY_DN4090_c0_g1_i1	6,46E+14	3,35E-05		**x**		Low
Tumor necrosis factor receptor superfamily member 11A isoform X1	*tnfrsf11a*							
Mucin-2-like	*muc2l*							
Tumor necrosis factor, alpha-induced protein 8-like protein 2 A	*tnfaip8l2*							
Chemokine-like receptor 1	*cmklr1*							
Interleukin-1 receptor-associated kinase 3	*irak3*							
Complement C3	*c3*							
C-X-C motif chemokine 20	*cxcl20*							
Complement component C7	*c7*							
Serine/threonine-protein kinase N1	*pkn1*							
Complement C4	*c4*							
Interleukin-13 receptor subunit alpha-2	*il13ra2*							
Tumor necrosis factor alpha-induced protein 8-like protein 3	*tnfaip8l3*							
Beta-2-microglobulin	*b2m*							
Mucin-2	*muc2*							
C1qB	*c1qb*							
Hemoglobin subunit beta-1	*hbb1*	TRINITY_DN5602_c0_g2_i1	4,25E+14	9,30E-05	**x**	**x**	Low	Low

Interferon-induced GTP-binding protein MxA	*mx1*							
Interferon-induced protein with tetratricopeptide repeats 1-like	*ifit1l*							
Hemoglobin subunit alpha-1	*hba1*	TRINITY_DN2526_c0_g1_i1	3,95E+14	8,06E-06	**x**		Low	
Serine/threonine-protein kinase TBK1	*tbk1*							
Complement factor D	*cfd*							
Beta-galactoside-binding lectin	*lec-1*							
Protein S100-A1	*s100a1*							
Serine/threonine-protein kinase STK11	*stk11*							
Hemoglobin subunit alpha-2	*hba2*							
Leukotriene A-4 hydrolase	*lta4h*							
Sialomucin core protein 24	*cd164*							
Leucine-rich repeats and immunoglobulin-like domains protein 2	*lrig2*							
Protein kinase C delta type	*prkcd*							
Bactericidal permeability-increasing protein	*bpi*							
Protein kinase C and casein kinase II substrate protein 3	*pacsin3*							
Serine/threonine-protein phosphatase 6 catalytic subunit	*ppp6c*							
Nuclear factor NF-kappa-B p105 subunit	*sh2d7*							
Tumor suppressor candidate 2	*tusc2*							
Mucosa-associated lymphoid tissue lymphoma translocation protein 1 homolog	*malt1*							
C-C motif chemokine 20	*ccl20*	TRINITY_DN2604_c0_g1_i1	1,78E+14	2,20E-05		**x**		Low
Lysozyme g	*lyzg*							
Tumor necrosis factor ligand superfamily member 12	*tnfsf12*							
Cytokine-inducible SH2-containing protein	*cish*	TRINITY_DN3768_c0_g1_i2	1,97E+14	8,05E-06		**x**		Low
Lysomal protective protein	*ctsal*							
Cbp/p300-interacting transactivator 1	*cited1*	TRINITY_DN3444_c0_g2_i7	-1,34E+13	1,78E-04		**x**		Low
Influenza virus NS1A-binding protein homolog A	*ivns1abpa*							
Tumor necris factor receptor superfamily member 16	*tnr16*							
TGF-beta-activated kinase 1 and MAP3K7-binding protein 2	*tab2*							
H-2 class I histocompatibility antigen, K-D alpha chain	*h2-q9l*							
Protein kinase C beta type	*prkcb*							
Human immunodeficiency virus type I enhancer-binding protein 2 homolog	*hivep2*							
Complement C1q tumor necrosis factor-related protein 2	*c1qtnf2*							
Lysome-associated membrane glycoprotein 2	*lamp2*							
Serine/threonine-protein kinase D2	*prkd2*							
C-X-C chemokine receptor type 3-2	*cxr32*							
Inhibitor of nuclear factor kappa-B kinase subunit beta	*ikbkb*							
Tumor necris factor receptor superfamily member 1A	*tnfrsf1a*							
IST1 homolog	*ist1*							
Serine/threonine-protein kinase 17B	*stk17b*							
Transforming growth factor beta receptor type 3	*tgfbr3*							
Interleukin-11 receptor subunit alpha-1	*il11ral*							
Delta-like protein C	*dlc*							
Complement C1q tumor necris factor-related protein 1	*c1qtnf6*							
Complement component C7	*c7*							
Chemokine (C-X-C motif) ligand 12a (stromal cell-derived factor 1) precursor	*cxcl12a*							
Thioredoxin	*txn*							

Hemoglobin subunit alpha	*hba*	TRINITY_DN455_c0_g1_i1	4,40E+14	3,18E-05	**x**	**x**	Low	Low
TGF-beta receptor type-1	*tgfbr1*							
Leukemia inhibitory factor receptor	*lifr*							
Protein kinase C iota type	*prkci*							
Inter-alpha-trypsin inhibitor heavy chain H3	*itih3*							
hemoglobin cathodic subunit beta	*hbb*							
Interleukin-1 receptor-associated kinase 4	*irak4*							
Interferon regulatory factor 2-binding protein 1	*irf2bp1*							
Interferon alpha/beta receptor 2	*ifnar2*							
Innate cellular immunity								
CD226 antigen	*cd226*							
Leukocyte elastase inhibitor	*serpinb1*							
Leukocyte antigen CD37	*cd37*							
Macrophage colony-stimulating factor 1 receptor 2	*csf1r*							
Platelet-derived growth factor receptor alpha	*pdgfra*							
Leukocyte surface antigen CD53	*cd53*							
Macrophage colony-stimulating factor 1 receptor 1	*csf1r*							
CD63 antigen	*cd63*							
CD302 antigen	*cd302*							
Macrophage-capping protein	*capg*							
CD59 glycoprotein-like	*cd59*							
CD151 antigen-like isoform X1	*cd151l*							
CD9 antigen	*cd9*	TRINITY_DN1478_c0_g1_i8	2,12E+14	4,86E-05		**x**		Low
CD209 antigen-like protein A	*cd209a*							
Platelet-derived growth factor receptor beta	*pdgfrb*							
Macrophage-expressed gene 1 protein	*mpeg1*							
Platelet-activating factor acetylhydrolase IB subunit alpha2	*pafah1b2*							
Platelet-activating factor acetylhydrolase IB subunit alpha1	*pafah1b3*							
Platelet-derived growth factor subunit B	*grinal*							
Mast cell tryptase	*tpsab1*							
Acquired immunity								
H-2 class I histocompatibility antigen, Q10 alpha chain	*h2-q10*							
T-cell receptor alpha chain V region CTL-F3	*trav29dv5*							
Butyrophilin subfamily 2 member A2	*btn3a1*							
B-cell lymphoma/leukemia 11A	*bcl11b*							
B-cell receptor CD22-like	*cd22l*							
Immunoglobulin kappa light chain	*igk*							
Ig mu chain C region membrane-bound form	*ighm*							
Pre-B-cell leukemia transcription factor-interacting protein 1	*pbxip1*							
BOLA class I histocompatibility antigen, alpha chain BL3-7	*hla-b*							
T-cell activation inhibitor, mitochondrial	*tcaim*							
Ig gamma chain C region	*ighd*							
Immunoglobulin kappa variable 1-12	*igkv1-12*							
H-2 class II histocompatibility antigen, E-Q beta chain	*hb24*							
HLA class II histocompatibility antigen, DP alpha 1 chain	*hla-dpa1*							
CD166 antigen homolog A	*alcamb*							

H-2 class II histocompatibility antigen gamma chain	*hg2a*							
Immunoglobulin-like domain-containing receptor 2	*ildr2*							
Cytotoxic and regulatory T-cell molecule	*crtam*							
T cell receptor beta variable 18	*trbv18*							
Class I histocompatibility antigen, F10 alpha chain	*mhc1ufa*							
Immunoglobulin superfamily containing leucine-rich repeat protein 2	*islr2*							
Nuclear factor of activated T-cells, cytoplasmic 3	*nfatc3*							
Lymphocyte antigen 75	*ly75*							
Nuclear factor of activated T-cells 5	*nfat5*							

4.4.7. DEGs Gene Ontology

4.4.7.1. DEGs Gene Ontology of control versus LPS

GO enrichment of the control vs LPS DEGs identified in the skin, duodenum, liver, and spleen transcriptomes. A summary of only the most enriched GO terms is outlined and a full description is presented **in Supplementary table 4. 6-9** and **Supplementary figure 4.2-5**.

The duodenum had 70 enriched GO terms in BP, 40 in CC and 28 in MF (FDR < 0.05) and most were not linked to immune processes (**Supplementary table 4.6 A**). The biological processes most affected were linked to the immune system, proteolysis and protein ubiquitination (**Supplementary figure 4.2 A**). The CC terms most affected were related to cell surface, cell membrane and cell nucleus, cytoplasm and cytosol (**Supplementary figure 4.2 B**) and the MF terms were linked to exodeoxyribonuclease activity, endopeptidase activity, metal ion binding, collagen binding, chromatin binding and major histocompatibility complex (MHC) class II receptor activity (**Supplementary figure 4.2 C**). The skin possessed numerous enriched GO terms linked to the immune response (FDR < 0.001) and included 52 GO terms for BP, 9 terms for CC and 21 for MF (**Supplementary table 4.3 A**). The enriched BP terms were principally related to the immune system (**Supplementary figure 4.3 A**), while the CC GO terms of skin bore resemblance to the terms identified for the duodenum (**Supplementary figure 4.3 B**). For MF, the terms most enriched were signalling receptor activity, protein binding, DNA and nucleic acid binding, ribosome binding and zinc ion binding (**Supplementary figure 4.3 C**).

The enriched GO terms for the spleen were not related to the immune response (FDR < 0.05). 94 GO terms belonged to BP, 35 to CC and 36 to MF (**Supplementary table 4.4 A**). The BP terms identified for spleen were also represented for the skin and duodenum (**Supplementary Figure 4.4 A**). The CC terms for spleen differed from the skin and duodenum and were associated with mitochondrion, replication fork, neuronal cell body and the guanyl-nucleotide exchange factor complex (**Supplementary Figure 4B**). The MF terms for spleen were linked to chromatin binding, ATP binding, methyl-CpG binding, chromatin binding and metal and zinc ions binding (**Supplementary figure 4.4 C**). The liver DEGs were enriched in 34 GO terms for BP, 28 for CC and 21 for MF, none related to the immune response (FDR < 0.001) (**Supplementary table 4.5 A**). The BP terms identified for the liver were shared with

the skin and duodenum (**Supplementary figure 4.5 A**). The CC terms mapped in the liver differed from the skin and duodenum and included mitochondria, membrane and plasma membrane, cytoplasm, extracellular space, cellular surface and protein-complex (**Supplementary figure 4.5 B**). The MF terms included selenium binding, metal ion binding, ribosome binding and ubiquitin binding (**Supplementary figure 4.5 C**).

4.4.7.2. DEGs Gene Ontology of control versus poly I:C

GO enrichment of the control vs poly I:C DEGs identified in the skin, duodenum, liver, and spleen transcriptomes. A summary of only the most enriched GO terms is outlined and a full description is presented **in Supplementary table 4. 6-9** and **Supplementary figure 4.2-5**.

The duodenum DEGs were enriched with 20 BP terms (Supplementary Figure 2D), 11 CC terms and 9 MF terms and most were linked to the immune response (FDR < 0.001) (**Supplementary table 4.6 B**). The BP enriched terms were related to the immune system, defence to gram-positive bacteria and signal transduction (**Supplementary figure 4.2 D**). The DEGs enriched CC terms in the duodenum were associated with the extracellular region, cytoplasm, nucleus, plasma membrane, protein complex and cell (and cell junction) (**Supplementary figure 4.2 E**). The DEGs enriched MF terms were RNA binding and activity, magnesium ion binding, ATP binding, lipid binding and interleukin-1 binding (**Supplementary figure 4.2 F**). Skin DEGs were enriched with107 BP terms (**Supplementary figure 4.3 D**), 56 CC terms and 62 MF terms and most were not immune-related (**Supplementary table 4.7 B**). The skin BP terms mostly enriched were associated to metabolic processes, ions transport and immune defence (**Supplementary figure 4.3 D**). The skin CC terms included ribosome, mitochondrial matrix, cytoplasm, extracellular space, nucleus and perikaryon (**Supplementary figure 4.3 E**). The skin MF terms included ribosome, protein binding, heme binding, nucleic acid binding and calcium and metal ions binding (**Supplementary figure 4.3 F**).

Spleen DEGs were enriched with 181 BP terms, 52 CC terms and 63 MF terms (**Supplementary table 4.8 B**). The enriched BP terms were lipid metabolism, gene expression, cell proliferation and DNA methylation (**Supplementary figure 4.4 D**). The enriched CC terms were replication fork, membrane and plasma membrane, cell junction, projection, and surface, protein-complex (**Supplementary figure 4.4 E**). Enriched MF terms were chromatin

binding, metal and zinc ion binding, ATP binding, RNA and DNA binding, poly(A) binding and interleukin-17 regulator activity (**Supplementary figure 4.4 F**). The liver DEGs were represented in 72 enriched BP terms, 36 CC terms and 62 MF terms (**Supplementary table 4.9 D**). BP terms were associated to the ribosome, fatty acid metabolism, protein ubiquitination and signal transduction (**Supplementary figure 4.5 D**). CC terms included cytoplasm, membrane, respirasome, extracellular space, cell body and retrotransposon nucleocapsid (**Supplementary figure 4.5 E).** MF terms included iron ion binding, heme binding, mRNA binding, protein-C binding, and ubiquitin transferase activity (**Supplementary figure 4.5 F**).

4.4.8. Enriched KEGG pathways in LPS and Poly I:C tissue transcriptomes

4.4.8.1. DEGs KEGG in control versus LPS

The KEGG pathways of DEGs from control vs LPS comparison were evaluated in the duodenum (Supplementary Table 10A-B), skin (**Supplementary table 4.11 A-B**), spleen (**Supplementary table 4.12 A-B**) and liver (**Supplementary table 4.13 A-B**) (FDR < 0.05). In the duodenum, among the 10 most enriched KEGG pathways were related to cellular and humoral immune responses from innate and acquired immunity, cell-cell adhesion, and apoptosis (**Figure 4.5 A**). The most enriched KEGG pathways in the skin were cellular and humoral responses from both innate and acquired immunity, cell-cell adhesion, endocytosis, actin cytoskeleton and several signal transduction pathways (**Figure 4.5 C**). The most enriched KEGG pathways in the spleen were lipid and metabolic pathways, peroxisome receptors and p53 pathways were enriched (**Figure 4.5 E**) and in the liver were calcium, bicarbonate and sodium and mineral reabsorption, intracellular cyclic GMP concentration and G-protein coupled receptors signalling pathways (**Figure 4.5 G**).

4.4.8.2. DEGs KEGG in control versus Poly I:C

The KEGG pathways of DEGs from control vs poly I:C comparison were evaluated in the duodenum (**Supplementary table 4.10 C-D**), skin (**Supplementary table 4.11 C-D**),

spleen (**Supplementary table 4.12 C-D**) and liver (**Supplementary table 4.13 C-D**) 8h post-poly I:C immersion (FDR < 0.05). Among the 10 most enriched KEGG pathways) in the duodenum were carbon and lipid metabolism, mineral absorption, oxidative phosphorylation and stress, and cell and humoral immune compounds (**Figure 4.5 B**). In the skin they were metabolism related to glucose, peroxisome, ribosome, and oxidative phosphorylation (**Figure 4.5 D**) and in spleen pathogen-recognition receptors and ribosome (**Figure 4.5 F**). In the liver, the most enriched pathways were lipid and glucose metabolism, and innate humoral and acquired cellular compounds (**Figure 4.5 H**).

Figure 5 (next page). KEGG pathways from the A-B) duodenum, C-D) skin, E-F) spleen and G-H) liver of control, LPS and Poly I:C treated ***N. rossii*****.** The DEGs, between control, LPS and control and Poly I:C, enriched KEGG orthologs were identified as up- (A) and down-regulated (B) in duodenum, (C) and (D) in skin, (E) and (F) in spleen, (G) and (H) in liver, respectively) (FDR < 0.05). IgAh indicates immunoglobulin A homologue, Th (T helper), TGF (tumour growth factor), HIF-I (hypoxia- inducible factor 1), PPAR (peroxisome proliferator-activated receptor), TNF (tumor necrosis factor).

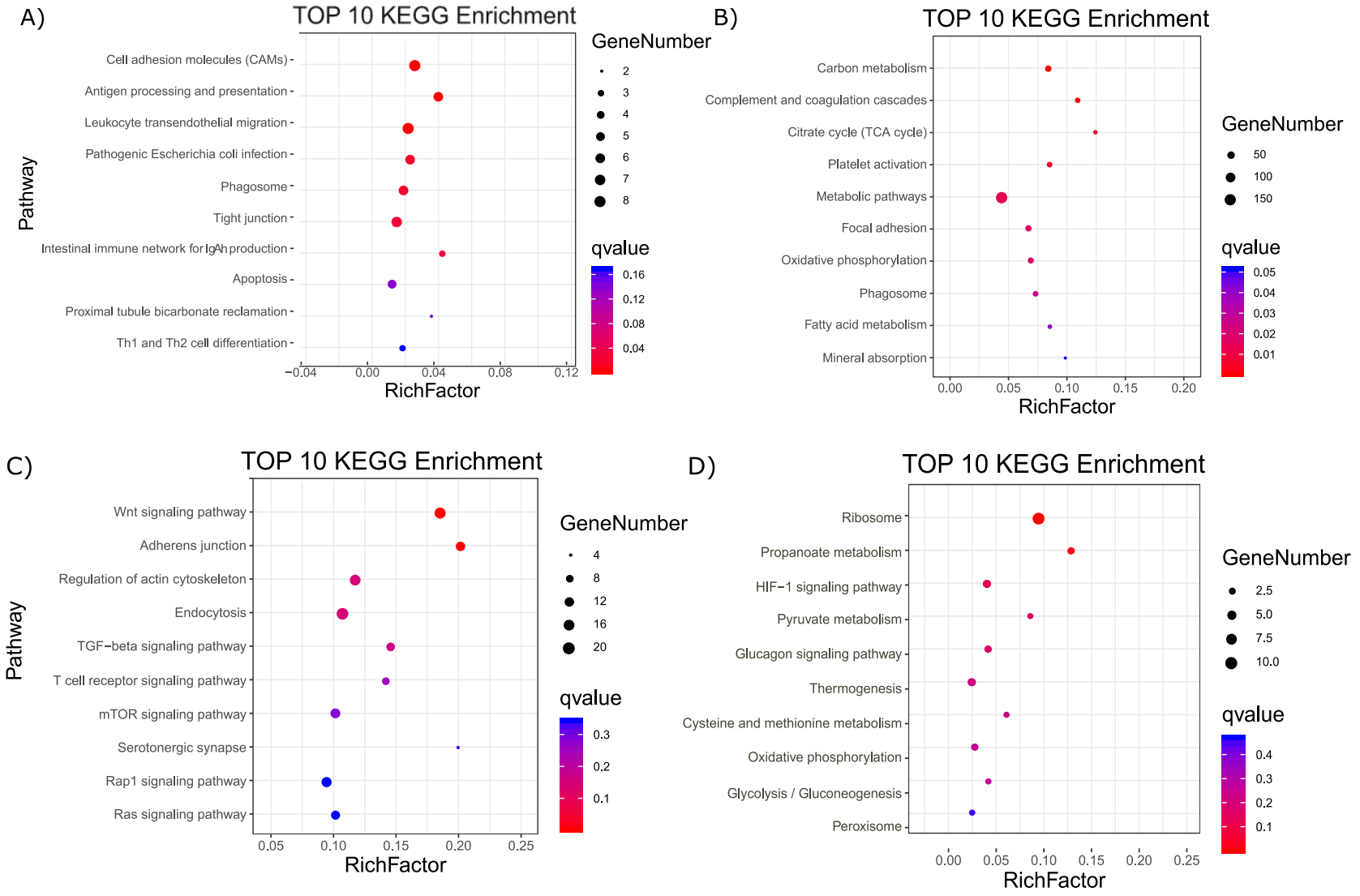
A)
TOP 10 KEGG Enrichment
Pathway
Cell adhesion molecules (CAMs)
Antigen processing and presentation
Leukocyte transendothelial migration
Pathogenic Escherichia coli infection
Phagosome
Tight junction
Intestinal immune network for IgA production
Apoptosis
Proximal tubule bicarbonate reclamation
Th1 and Th2 cell differentiation
−0.04 0.00 0.04 0.08 0.12
RichFactor
GeneNumber
2 3 4 5 6 7 8
qvalue
0.16 0.12 0.08 0.04
B)
TOP 10 KEGG Enrichment
Carbon metabolism
Complement and coagulation cascades
Citrate cycle (TCA cycle)
Platelet activation
Metabolic pathways
Focal adhesion
Oxidative phosphorylation
Phagosome
Fatty acid metabolism
Mineral absorption
0.00 0.05 0.10 0.15 0.20
RichFactor
GeneNumber
50 100 150
qvalue
0.05 0.04 0.03 0.02 0.01
C)
TOP 10 KEGG Enrichment
Pathway
Wnt signaling pathway
Adherens junction
Regulation of actin cytoskeleton
Endocytosis
TGF−beta signaling pathway
T cell receptor signaling pathway
mTOR signaling pathway
Serotonergic synapse
Rap1 signaling pathway
Ras signaling pathway
0.05 0.10 0.15 0.20 0.25
RichFactor
GeneNumber
4 8 12 16 20
qvalue
0.3 0.2 0.1
D)
TOP 10 KEGG Enrichment
Ribosome
Propanoate metabolism
HIF−1 signaling pathway
Pyruvate metabolism
Glucagon signaling pathway
Thermogenesis
Cysteine and methionine metabolism
Oxidative phosphorylation
Glycolysis / Gluconeogenesis
Peroxisome
0.00 0.05 0.10 0.15 0.20 0.25
RichFactor
GeneNumber
2.5 5.0 7.5 10.0
qvalue
0.4 0.3 0.2 0.1

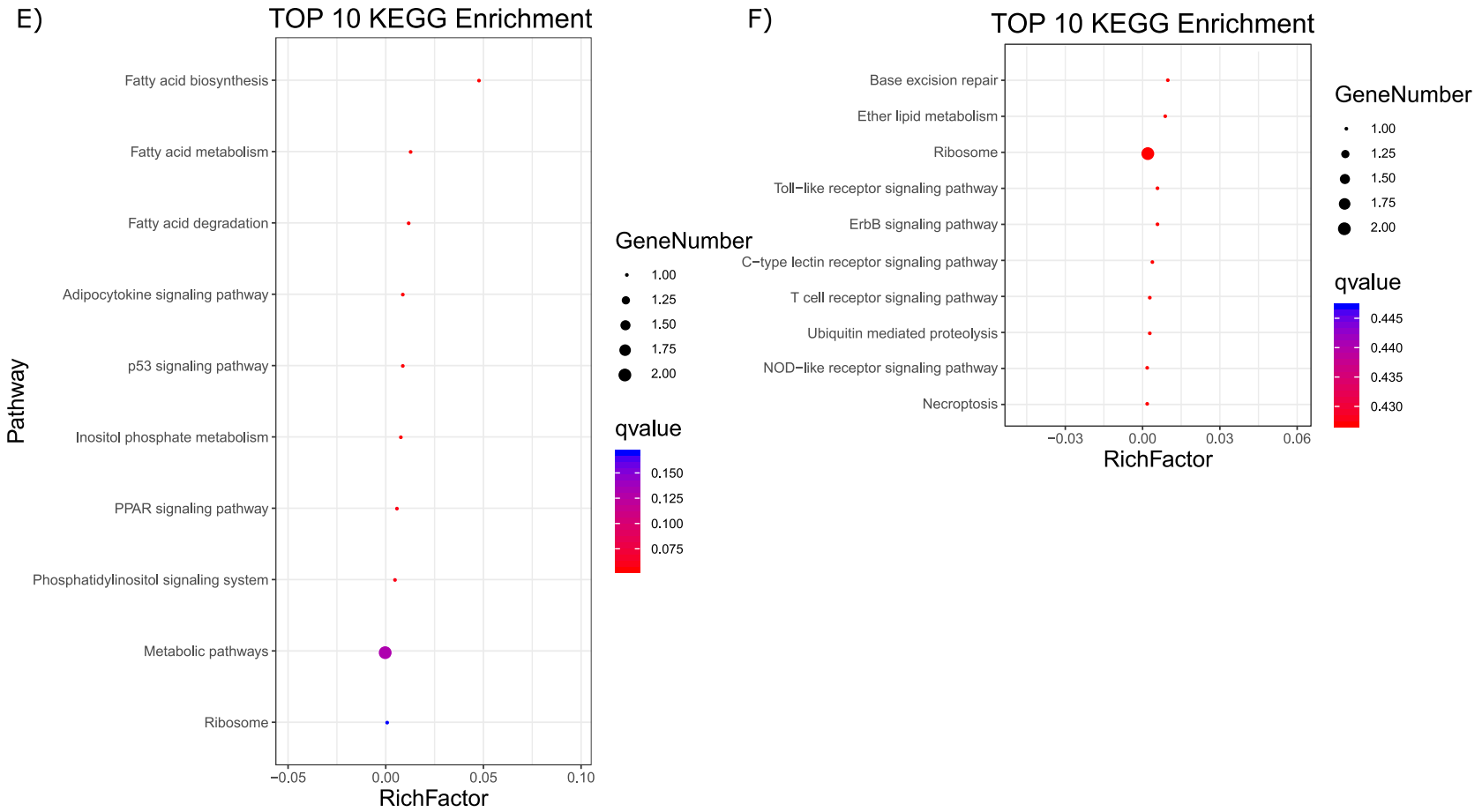
E)
TOP 10 KEGG Enrichment
Fatty acid biosynthesis
Fatty acid metabolism
Fatty acid degradation
Adipocytokine signaling pathway
p53 signaling pathway
Inositol phosphate metabolism
PPAR signaling pathway
Phosphatidylinositol signaling system
Metabolic pathways
Ribosome
Pathway
−0.05
0.00
0.05
0.10
RichFactor
GeneNumber
1.00
1.25
1.50
1.75
2.00
qvalue
0.150
0.125
0.100
0.075
F)
TOP 10 KEGG Enrichment
Base excision repair
Ether lipid metabolism
Ribosome
Toll−like receptor signaling pathway
ErbB signaling pathway
C−type lectin receptor signaling pathway
T cell receptor signaling pathway
Ubiquitin mediated proteolysis
NOD−like receptor signaling pathway
Necroptosis
−0.03
0.00
0.03
0.06
RichFactor
GeneNumber
1.00
1.25
1.50
1.75
2.00
qvalue
0.445
0.440
0.435
0.430

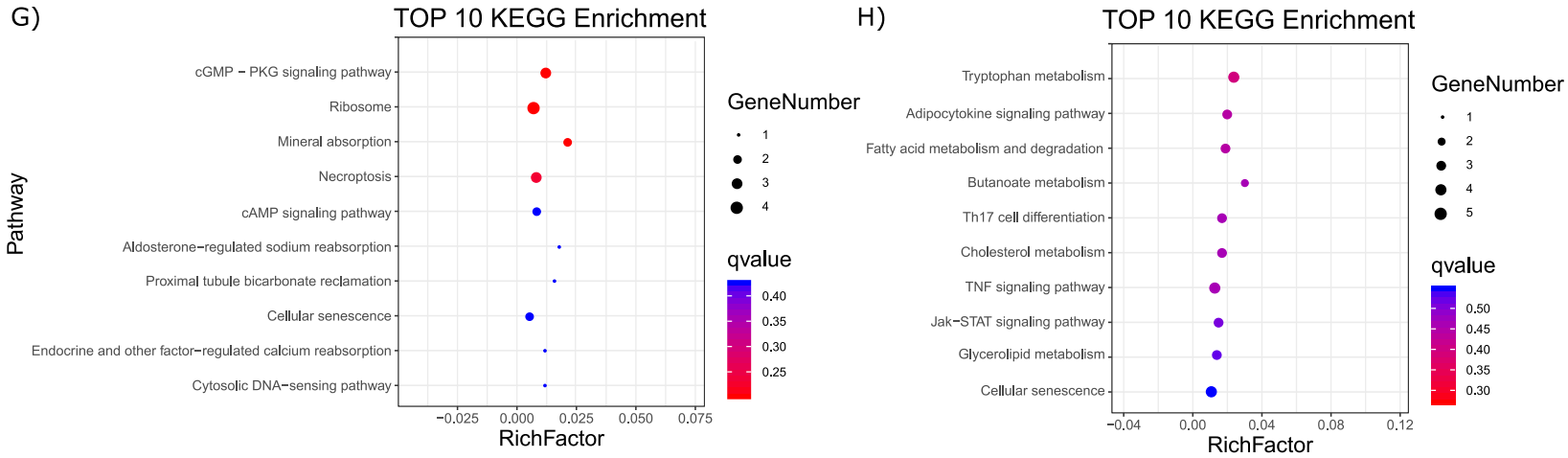
G)
TOP 10 KEGG Enrichment
cGMP − PKG signaling pathway
Ribosome
Mineral absorption
Necroptosis
cAMP signaling pathway
Aldosterone−regulated sodium reabsorption
Proximal tubule bicarbonate reclamation
Cellular senescence
Endocrine and other factor−regulated calcium reabsorption
Cytosolic DNA−sensing pathway
Pathway
−0.025
0.000
0.025
0.050
0.075
RichFactor
GeneNumber
1
2
3
4
qvalue
0.40
0.35
0.30
0.25
H)
TOP 10 KEGG Enrichment
Tryptophan metabolism
Adipocytokine signaling pathway
Fatty acid metabolism and degradation
Butanoate metabolism
Th17 cell differentiation
Cholesterol metabolism
TNF signaling pathway
Jak−STAT signaling pathway
Glycerolipid metabolism
Cellular senescence
−0.04
0.00
0.04
0.08
0.12
RichFactor
GeneNumber
1
2
3
4
5
qvalue
0.50
0.45
0.40
0.35
0.30

4.5. Discussion

Exposure of *N. rossii* to a bacterial (LPS) or viral (poly I:C) challenge by immersion provoked a different response at the level of gene expression in the duodenum, skin, spleen, and liver. Overall, the barrier tissues, such as the skin and duodenum were the most modified by administration of the immune challenge by immersion and the spleen was the least responsive. In the LPS challenge, 1827 genes were modified in the skin, 220 in duodenum, 49 in liver and 11 in spleen while in the poly I:C challenge, 195 genes were modified in the skin, 1582 in the duodenum, 131 in liver and 23 in the spleen. There was an interesting divergence in tissue responsiveness to the immersion challenge with the duodenum more responsive to a viral proxy and the skin more responsive to a bacterial proxy. In general, the most affected processes under both challenges were metabolic (e.g. glucose, lipid and energy metabolisms) and the immune system. In relation to the immune response the main transcriptional modifications were related to pathogen-recognition receptors (PRRs) namely C-type lectin receptors (CLRs), RIG-I like receptors (RLRs) and NOD-like receptors (NLRs) and other humoral and cellular immune-related genes (Figure 6). Significant modifications in gene transcripts related to iron and selenium ion metabolism is presumably linked to their involvement in innate immunity against microbial pathogens including bacteria and viruses. A conserved tissue specific response occurred across *N. rossii* individuals for both of the challenges and was linked to transcription factors, ribosome, and metabolic energy production pathways.

Biochemical indicators and pathogen challenges

In the LPS challenge there was no change in the analysed biochemical parameters. TLR4 a well-known mediator of the response to bacterial LPS in mammals is absent in fish and it remains unclear in fish the main PRRs for bacterial pathogens are detected (Beutler, 2002; Iliev et al., 2005; Sepulcre et al., 2009; Zhang et al., 2014). Furthermore, as discussed in chapter 3, the source of LPS (*E. coli O111:B4*) and environmental conditions could be determinant for LPS detection and the whole animal response, since the recognition of LPS by the immune system of fish may be influenced by its composition in O-antigen polysaccharide, sugar, and

lipids, which varies according to the gram-negative bacteria species (Garate and Oostenbrink, 2013; Raetz, 1990). Furthermore, the structure of LPS may be modified by environmental factors such as the temperature (Wu et al., 2013) and this may interfere with fish-bacteria recognition. However, taking into consideration the route of administration of LPS in the present study, immersion, which is more like a natural stimulation and the high response of the skin, the lack of a response in biochemical parameters may be indicative of a highly efficient barrier response to LPS.

In the case of the poly I:C challenge although studies of the molecular response are available for a number of different fish, Japanese flounder (*Paralichthys olivaceus*), Atlantic salmon (*Salmo salar*), Chinook salmon (*Oncorhynchus tshawytscha*) (Jensen et al., 2002; Lulijwa et al., 2020; Zhou et al., 2014), blood biochemical parameters are less common. In a study of the chinook salmon intraperitoneal (i.p.) injection of poly I:C provoked an increase in the haematocrit (Lulijwa et al., 2020), which contrasts with the results of our study where the haematocrit was depressed. The reason for the different response may be linked to the mode of exposure (we used immersion) and a species-specific response. Further studies into the mechanism underpinning the shift in haematocrit during viral infections in fish will contribute to understanding the causes of the effect. Nonetheless, a modified haematocrit has previously been observed in humans during viral infections and according to the disease either an increase or decrease in the red blood cell number may occur (Han et al., 2020).

Transcriptional response to LPS challenge

The LPS immersion treatment provoked changes that were similar across the liver, duodenum, skin, and spleen, but tissue-specific responses were also observed. The tissue-specific transcriptional responses were presumably linked to the unique function of each tissue and modification to maintain homeostasis as well as direct responses to the immune challenge. This makes identifying changes that result from a modification in tissue physiology to maintain homeostasis and the tissue-specific immune response challenging. This is exemplified by the highly modified transcriptional response, for example, in signalling pathways linked to cell junctions in the skin and is in keeping with its importance as an osmoregulatory tissue but also as a core multi-functional immune barrier (Ghosh et al., 2020; Jara et al., 1995; Wang et al., 2019). The specific gene modifications associated with cell junctions in the skin transcriptome

are in synteny with studies of changes at the level of the gut of immune challenged *Danio rerio* (Philip et al., 2017) and *Ictalurus punctatus* (Santander et al., 2014). Modifications in cell junctions have been associated with the inflammatory effect of LPS and enhanced leukocyte extravasation and migration into tissues (Ghosh et al., 2020; Kobielak and Boddupally, 2014; Rakers et al., 2010).

Recent studies of the tissue transcriptomes of the brown marbled grouper (*Epinephelus fuscoguttatus*), goldfish (*Carassius auratus*), yellowhead catfish (*Pelteobagrus fulvidraco*), carp (*Schizothorax prenanti*), Nile tilapia (*Oreochromis niloticus*) and Atlantic salmon showed differences in the humoral and cellular components of the immune system in response to a challenge using intra-peritoneal injections (Cai et al., 2018; Li et al., 2020c, 2021a; Liu et al., 2018; Maekawa et al., 2021; Palstra et al., 2018) or immersion (Jiang et al., 2020). Studies in Atlantic salmon and carp revealed a highly modified transcriptional response of toll-like receptors, complement proteins and major histocompatibility complex (MHC) I and II generally in a single tissue (Li et al., 2020c; Palstra et al., 2018). In the present study, where the challenge was administered by immersion, the barrier tissues, the duodenum and skin, were highly responsive but the responsiveness differed with the challenge. Common changes identified irrespective of the challenge (bacterial or viral) were associated with antigen processing and presentation, leukocyte migration, *E. coli* infection, phagosome, IgA homologue production, while specific transcripts in the duodenum were linked to Th1 and Th2 cell differentiation and in the skin were transforming growth factor beta (TGF-β) and the T cell receptor signalling pathway.

In the case of the spleen the most notable changes in transcripts were linked to fatty acid metabolism and signalling (e.g. PPAR and long-chain-fatty-acid-CoA ligase), which have previously been reported to have an immunomodulatory function in the sturgeon (*Acipenser dabryanus*) (Chen et al., 2019a). A metabolic response at the level of lipids in the spleen has been reported in fish fed different diets but not for LPS-challenged fish (Robinson et al., 1993; Stejskal et al., 2016). This may be a common response to a bacterial challenge, since differences in lipid metabolism have been found in the liver of *N. coriiceps* (chapter 3), the gilthead seabream (*Sparus aurata*) as well as in the liver of mammals like the pig (*Sus scrofa*) (Liu et al., 2015) and in the head-kidney cells of the yellow croaker (*Larimichthys crocea*) challenged with a bacterial endotoxin LPS (Antonopoulou et al., 2017; Li et al., 2020b). However, other studies namely in *Ctenopharyngodon Idella*, *Paralychthys olivaceus* and *Oncorhynchus mykiss* found mostly differences in coagulation and complement cascade pathways of spleen

transcriptomes challenged with similar bacterial infections, which do not corroborate our findings (Castro et al., 2019; Dang et al., 2016; Sun et al., 2020).

In the case of the liver challenged with LPS, the transcripts most modified were linked to ribosome, mineral reabsorption particularly sodium (Na^+) and calcium (Ca^{2+}) and cGMP-PKG signalling. Other studies, performed in *N. coriiceps* using heat-killed bacteria (HKEB O11:B4) as the challenge, also observed that ribosomes were most modified in GO enrichment analysis of the liver transcriptome and up-regulation of antigen processing and presentation pathway and MHC processes was also found (Ahn et al., 2016). A recent study in *N. rossii* showed up-regulation of iron-related genes in liver after LPS (*E. coli* 0111:B4) challenge similar to what was observed in our liver transcriptome results (Martínez et al., 2020). In a study performed in *Miichthys miiuy*, the spleen transcriptome showed modifications in the expression of several immune genes such as tumor necrosis factor alpha (TNF-α), interleukin 1-beta (IL-1β) and interferon (IFN)-β(Bi et al., 2018). However, these innate humoral components were not identified in our liver transcriptome.

Transcriptional response to Poly I:C challenge

The change in gene transcription induced by immersion exposure to poly I:C were distinct from the response to LPS in all four tissue transcriptomes generated for *N. rossii*. The duodenum was the most highly responsive tissue (1582 DEGs) but even in the less responsive skin, liver, and spleen the transcriptional response was similar to the response to a virus in mammals (Arrode-Brusés and Brusés, 2012; Field et al., 2010; Wu et al., 2014). The multi-tissue transcriptional response to a virus proxy was characterized by an enhanced immune response in all tissues although the specific gene transcripts modified varied. In the duodenum complement and phagosomes were highly stimulated, in the spleen PRRs were modified (TLRs, CLRs and NLRs) and in the liver TNF and Th17 were modified. In other studies of teleost fish in which exposure to poly I:C was by i.p injection and only a single tissue was analysed, an enhanced immune response was noted in the grass carp (*Ctenopharyngodon Idella*), chinook salmon, Japanese flounder and several other teleosts (Du et al., 2012; Lulijwa et al., 2020; Reyes-Cerpa et al., 2012; Zhou et al., 2014). Associated with immune activation in poly I:C treated fish was the activation of metabolic pathways involved in energy and lipid metabolism and oxidative phosphorylation in the duodenum and liver. Similar observations have also been

reported in mammals exposed to viruses (Fritsch and Weichhart, 2016; Sumbria et al., 2021). The metabolic changes in host cells were proposed to be consequence of the biosynthesis of new copies of the virus since they are metabolically inert. For example, in human cells infected by Herpes simplex virus (HSV), the tricarboxylic acid cycle (TCA) was up-regulated and this was linked to the need for TCA to produce the bases necessary for viral genome construction (Vastag et al., 2011).

Immune gene specific response to LPS

The results of the current study of the response of *N. rossii* to short-term LPS immersion revealed that immune-related genes were mainly affected in the physical barriers, the duodenum and skin. Furthermore, the skin responded more strongly to the bacterial challenge than the duodenum. This raises interesting questions in relation to partitioning function since the elevated drinking rates in marine species means exposure to LPS via the gut would occur (Aas et al., 2017; Egerton et al., 2018; Le et al., 2019). The immune related components in the duodenum were indicative of a response to LPS as elements of the major histocompatibility (MCH) system were modified [(e.g., beta(β)-2-microglobulin, MHC II (gamma chain, DP alpha 1 chain, E-Q beta chain)] along with cytokine-related factors and receptors. In the case of the skin, which was the most responsive to LPS a broad repertoire of immune-related transcripts was found including lymphocyte related transcripts, cytokines, cytokine-related and receptor transcripts as well as complement system related transcripts and for innate humoral-related proteins (e.g. antitrypsin inhibitor, lysozyme g). A similar response to LPS was identified in the liver of the phylogenetically related *N. coriiceps* after an immersion challenge (Ahn et al., 2016) as well as in other teleosts exposed to LPS by i.p. injection. For example, in the head-kidney and liver of the grass carp (Liu et al., 2016, 2018), head-kidney of the Atlantic salmon (Palstra et al., 2018), liver of the channel catfish (*Ictalurus punctatus*) (Jiang et al., 2020), spleen of the carp (Li et al., 2020c) and head-kidney and spleen of the Nile tilapia (Maekawa et al., 2021). In the liver and spleen of *N. rossii* exposed to LPS by immersion few immune genes were activated although in the liver selenium-related genes were enriched and have previously been linked to the immune system in chicken thymus and in liver of transgenic mice expressing human Sepp1 (Khoso et al., 2015; Renko et al., 2009).

Toll-like receptors (TLRs), pathogen-recognition receptors (PRRs) have generally been targeted for analysis in LPS challenge studies in both mammals and fish including *N. coriiceps* (Ahn et al., 2014). In the mammals TLR4 has been directly demonstrated to respond to LPS (Beutler, 2002), but this receptor is missing from most teleost fish (Palti, 2011), the exception is the zebrafish, and identification of the TLR in teleost that mediates the response to LPS is lacking (Zhang et al., 2014). In chapter 2 of this thesis, TLRs were identified and characterized in Antarctic fish and in chapter 3 and the present study transcriptome analysis failed to identify strong up-regulation of TLR by LPS either i.p. or by immersion. Instead, NOD receptors, that mediate the recognition of "non-self" components and have a key role in innate immune defence (Buchmann, 2014) were significantly modified in the skin and duodenum transcriptomes of *N. rossii* 7 days after LPS exposure (chapter 3). Another differentially expressed PRR in the head-kidney transcriptome of *N. coriiceps* was macrophage mannose receptor, that recognizes foreign microorganisms (Apostolopoulos et al., 2001) (chapter 3). The results of the skin transcriptome of *N. rossii*, which was highly responsive to immersion exposure to the bacterial endotoxin LPS, suggests that other PRRs may have an important role in LPS recognition. Examples of modified PRRs in the *N. rossii* skin transcriptome included membrane-bound C-type like receptors (galactase-specific lectin nattectin and c-type lectin domain family 11 member A), RIG-I-like receptors (adiponectin receptor protein 2) and, NACHT, LRR and PYD domains-containing protein 3 (NLRP3) and NLRP14). The notion that PRRs other than TLRs may have a primary role in pathogen recognition and activation of the immune response of teleosts is supported by studies in Atlantic salmon and the barramundi (*Lates calcarifer*) where C-type lectin genes were mostly stimulated, and in the Japanese flounder and Mi-iuy croaker (*Miichthys miiuy*) where NLRC3 genes and NOD1 genes, respectively were up-regulated (Chu et al., 2021; Li et al., 2016; Soanes et al., 2004; Zoccola et al., 2017).

The results from the present chapter corroborated the candidate gene study in chapter 2 of the responsiveness of genes of iron metabolism in the head-kidney and liver of *N. rossii* to LPS (Martínez et al., 2020). Iron depletion from the circulation is a defense mechanism against bacterial pathogens that require iron for their survival and replication (Collins, 2008; Johnson and Wessling-Resnick, 2012; Martínez et al., 2020). The metabolic response under immune challenge included a change in expression of gene transcripts of iron metabolism in several tissues in the present study. For example, in the skin DEGs of the iron and selenium metabolism pathways were identified, (iron-responsive element-binding protein 2 and 2-oxoglutarate and iron-dependent oxygenase, selenocysteine 2 and selenotransferrin) and in the liver ferritin was

one of the DEGs. Genes related to iron uptake and metabolism have previously been linked to bacterial infections in *N. coriiceps* and *N. rossii* (Costa et al., 2011; Lange et al., 2001; Martínez et al., 2017a; Neves et al., 2015, 2017). The confirmation by the tissue transcriptomes of the results of candidate gene studies of iron metabolism supports the pertinence of understanding the immune response and substantially expands insights into the overall changes in the iron-related system under a bacterial or viral challenge.

The representation of selenium-related gene transcripts within the DEGs in the present study were in line with the observations of a recent study with the Mozambique tilapia (*Oreochromis mossambicus*) in which selenium in the diet enhances the anti-bacterial response against *Streptococcus iniae* infection (Neamat-Allah et al., 2019). The representation within the DEGs of LPS challenged *N. rossii* of gene transcripts related to selenium shows similarities to the protective effects identified for this metal in mammals (Avery and Hoffmann, 2018; Hoffmann and Berry, 2008; Huang et al., 2012). In fish the beneficial effects of selenium for growth, antioxidant defence and the immune system means this micronutrient is frequently added to feeds as an immunopotentiator similar to Vitamin E (Dixon et al., 1988; Mansour et al., 2017; Pacitti et al., 2016).

Immune genes specific response to Poly I:C

The results of poly I:C immersion revealed a higher impact on tissue transcriptomes than LPS because the number of DEG transcripts was higher except for the skin. However, the duodenum and skin were the tissues with higher modification as observed against LPS stimuli. In duodenum both humoral and cellular components were modified, among them, interleukin-1 receptor accessory protein-like 1-A, mucins (*5 AC-like*, *13b*), nuclear factor beta (*NF-β*) inhibitor alpha, tumor necrosis factor (*TNF*), alpha-induced protein 2, alpha-induced protein 3, alpha-induced protein 8-like, complement (*C4*, *C1q*, *C7*, *C9*, *factor B*, *factor D*) proteins, *interferon* (*IFN*) *regulatory factor 8* and T cell receptors (*alpha chain V*, *alpha chain 2*), *immunoglobulin kappa light chain* while in skin was identified specifically *β-2 microglobulin* from MHC I. These immune markers were also reported in other studies in teleost fish including in *N. coriiceps* under similar stimuli (Ahn et al., 2016; Lulijwa et al., 2020; Zhou et al., 2014). Interestingly, the duodenum (another physical barrier) was the most modified tissue with more than 1500 DEG transcripts under the poly I:C challenge. Similarly, to the results observed in

skin against the LPS challenge, CLRs (*c-type lectin domain family 13 member A, c-type lectin family 4 member E*) and NLRs (*NLRP1*, *NLRC3*) seems to have a key role in poly I:C recognition and were also identified in other teleost fish in response to similar viral stimuli (Álvarez et al., 2017; Ao et al., 2015; Chang et al., 2021; Ojeda et al., 2020; Paria et al., 2016). A larger number of DEGs related to selenium (*methanethiol oxidase, selenoprotein J, selenoprotein T1a, serotransferrin*) and iron (*iron-sulfur protein 4, iron-sulfur protein 2, ferritin heavy subunit, ferrochelatase, ferroxidase, transferrin receptor, iron-sulfur cluster assembly enzyme, cytosolic iron-sulfur assembly component 2B*) metabolic pathways were identified against poly I:C than against LPS suggesting an important role of these ions in immune defence against viruses in *N. rossii*. Unlike with LPS challenge, studies related to iron -metabolism genes under viral challenge in fish are few but studies linked to the selenium-related genes had a better knowledge which indicated antiviral properties in fish (Alkie et al., 2019; Pacitti et al., 2016). The liver is a site of synthesis of complement proteins but they were not identified in the present study although they had previously been shown to be present in duodenum (Najafpour et al., 2020). However, humoral trypsin-1 component and the PRRs NLRC3 and TLR3 were identified as DEGs. A liver TLR3 DEG in *N. coriiceps* and other species has been reported as specific to poly I:C recognition (Ahn et al., 2014; Andresen et al., 2020; Zhou et al., 2014). A DEG that caught our attention was the low spleen interleukin (IL)-17, a major cytokine signalling family widely studied in mammals but little studied in fish. However, a recent study in *Ctenopharyngodon idella* indicate antiviral activity against reovirus infection in head-kidney (Zhang et al., 2020b). The poly I:C challenge also promoted several DEG of toxins in duodenum *Neoverrucotoxin* and *Anthrax toxin receptor 2* indicative of a possible role in immune defence against viruses, although knowledge about these toxins in fish is absent.

4.6. Conclusion

The present study was the first to compare four tissue transcriptomes under bacterial LPS and viral poly I:C challenges by immersion in the Antarctic Notothenioid *N. rossii*. The results indicated that exposure to bacterial LPS by immersion, a route that simulates better an infection than other forms of application, provoked the highest transcriptional response in the skin. In contrast, poly I:C exposure by immersion caused the highest transcriptional response

in the duodenum, suggesting there has been specialization in the response to pathogens by these immune barriers.

The transcriptional responses in the skin and duodenum were challenge specific although some overlap was also observed. For both pathogen challenges, the transcripts that were modified were related to cell-junctions, humoral immune and cellular immune factors, and also included iron related metabolism and selenium related metabolism transcripts. In the case of the viral challenge a shift in metabolic pathways was also observed such as in glucose metabolism.

The absence of a strong transcriptional response at the level of the liver and spleen in both the LPS and poly I:C challenge by immersion, could indicated the efficacy of the response at the level of the two innate immune barriers, skin, and the duodenum. Although further experiments with live pathogen organisms will be required to confirm the efficacy of the barrier in a real-life infection.

Of note was the PRR response, which was dominated by NOD-like receptors (NLRs) and C-type lectin receptors (CLRs), suggesting that in fish these may be important for pathogen recognition instead of TLRs, which although present in the skin and duodenum were not significantly modified by any of the challenges (with exception of TLR3). The activation of PRRs together with DEGs for iron, selenium and toxins indicates their importance in the response of *N. rossii* to bacteria and, it seems, particularly viruses. The transcripts linked to metal metabolism and toxins differed between the skin and duodenum and with the pathogen challenge and suggests that there may be tissue-specific production and release of toxins in *N. rossii*.

We created a *N. rossii* model that include the most notable changes that occurred in the four tissue transcriptomes. In duodenum, the PRRs and interferon-regulatory receptor seems to have a key role against both pathogen challenges while in skin the immune system components are being essential for defence to LPS and antioxidant and energy processes to poly I:C. The changes in spleen are mostly related to lipid metabolism in LPS and ribosome in poly I:C groups, however the DNA methylation is shared against both pathogens. Lastly, the selenium metabolism is mostly modified after LPS and protein ubiquitination after poly I:C stimulus, while in both the ATP energy production is important (**Figure 4.6**).

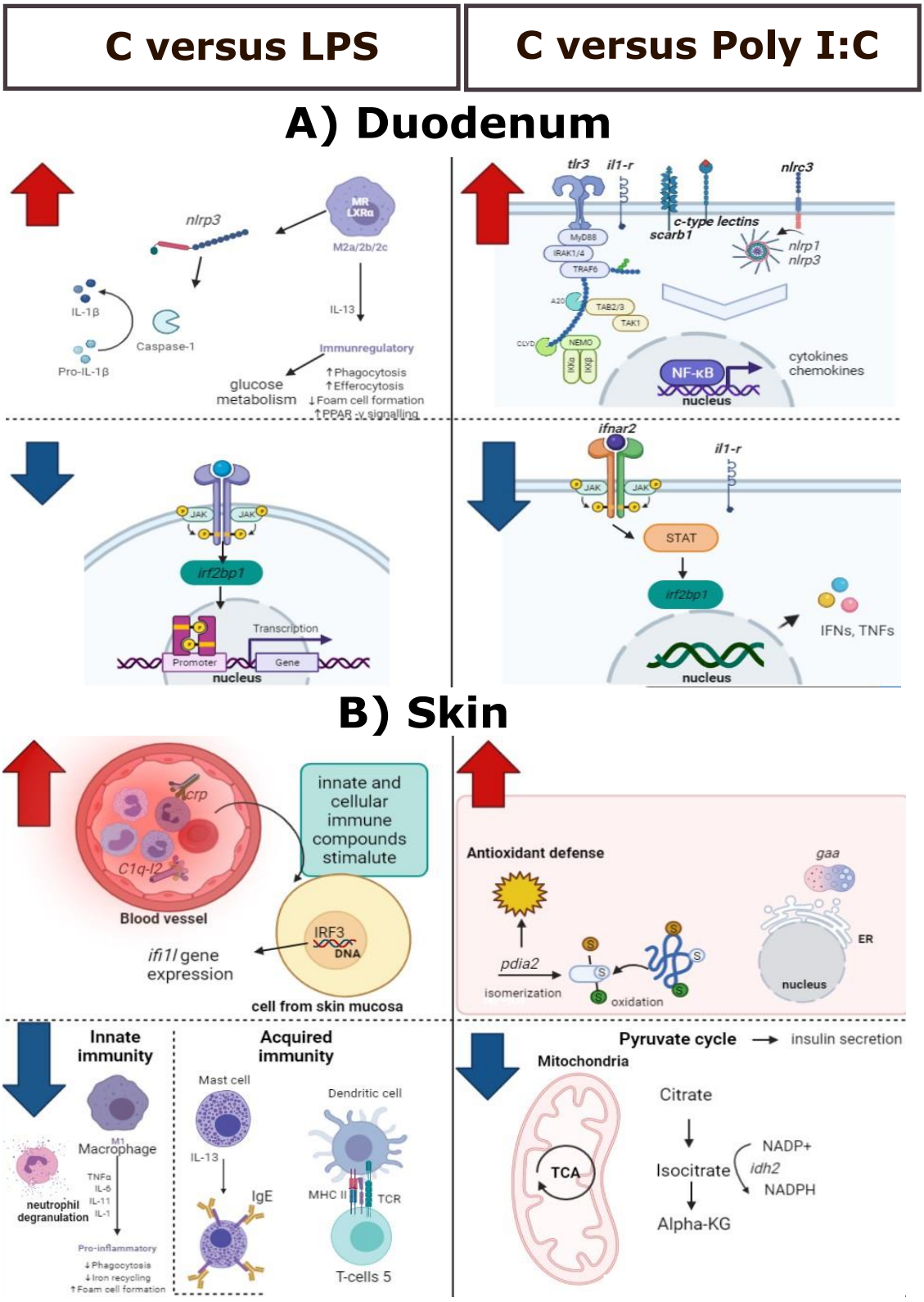
C versus LPS
C versus Poly I:C
A) Duodenum
nlrp3
MR LXRα
M2a/2b/2c
IL-1β
Caspase-1
Pro-IL-1β
IL-13
Immunregulatory
glucose metabolism
↑Phagocytosis
↑Efferocytosis
↓Foam cell formation
↑PPAR-γ signalling
tlr3
il1-r
nlrc3
c-type lectins
scarb1
nlrp1
nlrp3
MyD88
IRAK1/4
TRAF6
A20
TAB2/3
TAK1
CLYD
NEMO
IKKα
IKKβ
NF-κB
nucleus
cytokines
chemokines
JAK
irf2bp1
Transcription
Promoter
Gene
ifnar2
STAT
IFNs, TNFs
B) Skin
crp
C1q-l2
Blood vessel
innate and cellular immune compounds stimalute
IRF3
DNA
ifi1l gene expression
cell from skin mucosa
Antioxidant defense
gaa
pdia2
isomerization
oxidation
ER
Innate immunity
Acquired immunity
Mast cell
Dendritic cell
M1 Macrophage
TNFα
IL-6
IL-11
IL-1
neutrophil degranulation
IL-13
IgE
MHC II
TCR
T-cells 5
Pro-inflammatory
↓Phagocytosis
↓Iron recycling
↑Foam cell formation
Pyruvate cycle
insulin secretion
Mitochondria
TCA
Citrate
Isocitrate
NADP+
idh2
NADPH
Alpha-KG

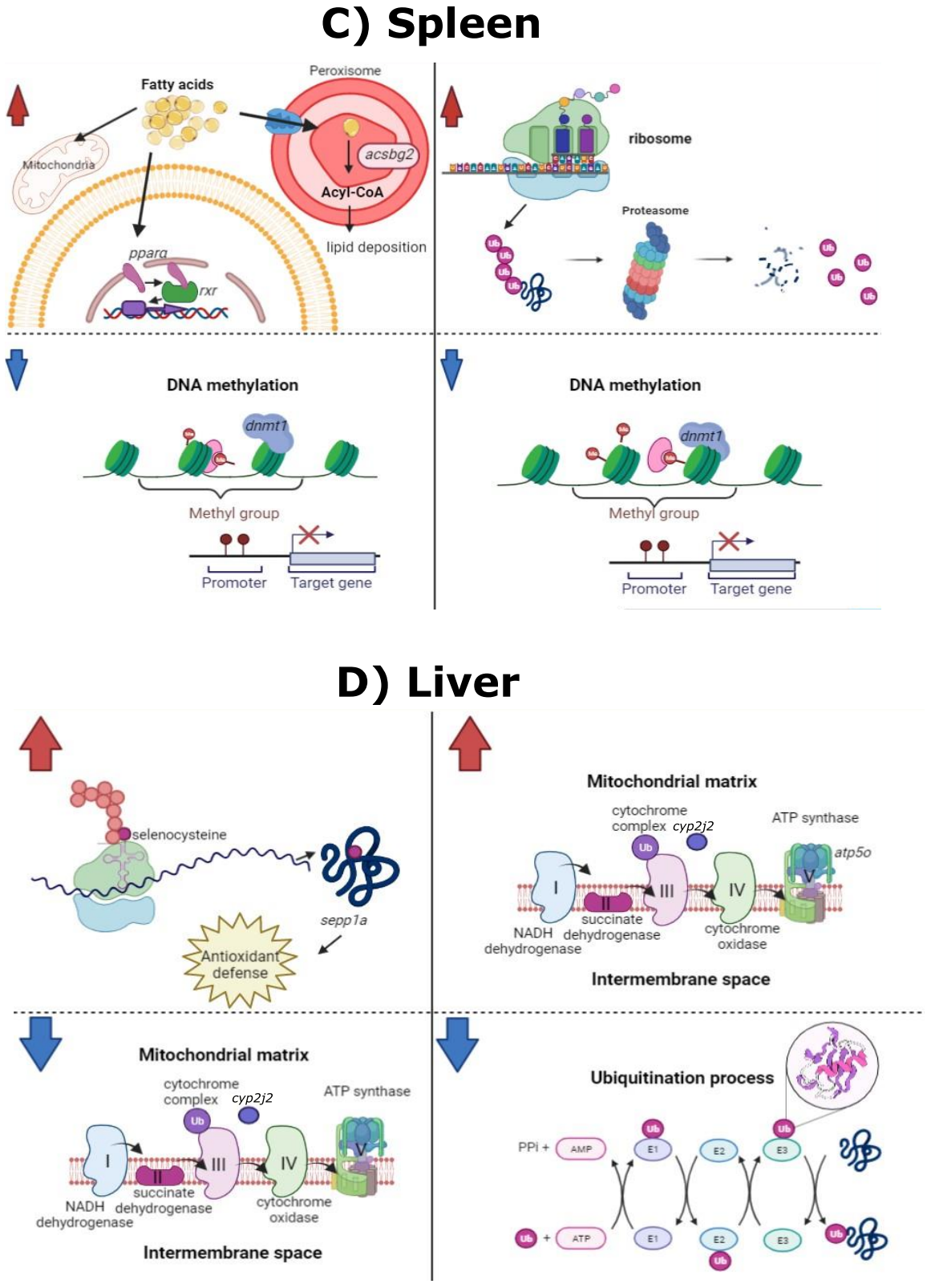

Figure 4.6. *N. rossii* interactive model of A) duodenum, B) skin, C) spleen and D) liver based on DEGs between Control versus LPS and Control versus Poly I:C. The up-regulated DEGs are represented by a red arrow and the down-regulated by a blue arrow, and the size of arrows is related to the magnitude of response. Interleukin (*il*), peroxisome proliferator-activated receptor alpha (*pparα*), C-reactive protein (*crp*), complement C1q-like 2 (c1ql2), macrophage (M or MR), Liver X receptor alpha (LXRα), toll-like receptor 3 (*tlr3*), receptor (*r*), nucleotide-binding oligomerization domain, NLR Family CARD Domain Containing 3 (*nlrc3*), leucine rich repeat and pyrin domain containing (*nlrp*),

nuclear factor (NF), interferons (IFNs), tumour necrosis factors (TNFs), interferon alpha/beta receptor 2 (*ifnra2*), interferon-induced protein with tetratricopeptide repeats 1-like (*ifit1l*), immunoglobulin (Ig), major histocompatibility complex (MHC), T-cell receptor (TCR), isocitrate dehydrogenase [NADP], mitochondrial (*idh2*), tricarboxylic acid cycle (TCA), coenzyme (Co), long-Chain-Fatty-Acid--CoA Ligase (*acsbg2*), retinoid X receptor (rxr), DNA (cytosine-5)-methyltransferase 1 (*dnmt1*), selenoprotein Pa (*sepp1a*), cytochrome P450 2J2 (*cyp2j2*), ATP synthase subunit O, mitochondrial (*atp5o*), E3 ubiquitin-protein ligase CHFR (E3).

4.7. Supplementary materials

4.7.1. Supplementary tables

Supplementary table 4.1. A) Raw data quality and B) alignment quality of individual samples in liver, spleen, duodenum, and skin. The samples, raw reads, post QC reads, bases, post QC bases (assembly input) and total sequences, length, percentage (%) GC, N50, median contig length, average contig, total assembled bases, total trinity genes and total trinity transcripts (assembly output) were evaluated for sequencing quality and representativity.

A)

Sample ID	Tissue	Treatment group	Total sequences	Before filtering	After filtering and assembly						
				Total reads (M)	Total reads (M)	Q20 (%)	Q30 (%)	GC (%)	N50	Median contig length	Average contig
Lv_C1	Liver	Control	12795792	25.591584	25480382	98.16	94.29	45.63	1865	521	1003.99
Lv_C2			10647793	21.295586	21190430	98.01	94.00				
Lv_C3			11256248	22.512496	22413154	97.87	93.63				
Lv_L1		LPS	9483284	18.966568	18851040	97.16	91.99				
Lv_L2			7539990	15.079980	15012036	97.95	93.77				
Lv_L3			7658561	15.317122	15235728	97.99	93.88				
Lv_P1		Poly I:C	8318561	16.637122	16556472	97.85	93.53				
Lv_P2			6853356	13.706712	13636292	97.98	93.84				
Lv_P3			6574569	13.149138	13084956	97.91	93.68				
Sp_C1	Spleen	Control	6785769	13.571538	13308806	97.70	93.34	45.68	2036	497	1040.39
Sp_C2			6810468	13.620936	13459164	97.83	93.58				
Sp_C3			6778110	13.556220	13271022	97.94	93.83				
Sp_L1		LPS	8946160	17.892320	17815624	98.06	94.11				
Sp_L2			6556862	13.113724	12911568	97.70	93.27				
Sp_L3			7312955	14.625910	14542766	99.43	93.38				
Sp_P1		Poly I:C	7621861	15.243722	15165208	97.95	93.86				
Sp_P2			6468579	12.937158	12854770	96.91	91.30				
Sp_P3			5978245	11.956490	11871188	97.70	93.28				
Du_C1	Duodenum	Control	7582524	15.165048	15098926	97.95	93.83	45.16	1665	461	904.31
Du_C2			6134510	12.269020	12207098	97.81	93.53				
Du_C3			6465593	12.931186	12872148	97.76	93.39				
Du_L1		LPS	6079943	12.159886	12099394	97.82	93.54				
Du_L2			6848938	13.697876	13592776	97.63	93.08				
Du_L3			10338156	20.676312	20562880	97.82	93.52				
Du_P1		Poly I:C	7725222	15.450444	15374560	97.84	93.58				
Du_P2			8643257	17.286514	17202708	97.71	93.27				
Du_P3			9004891	18.009782	17926822	97.88	93.65				
Sk_C1	Skin	Control	7978045	15.956090	15845548	98.21	94.70	44.69	1778	539	985.58
Sk_C2			7898348	15.796696	15704268	98.19	94.62				
Sk_C3			8901579	17.803158	17671224	98.10	94.46				
Sk_L1		LPS	8059046	16.118092	16000620	98.14	94.55				
Sk_L2			4783722	9.567444	9486314	98.09	94.42				
Sk_L3			5605772	11.211544	11064482	97.99	94.23				
Sk_P1		Poly I:C	8068915	16.137830	16044874	98.12	94.52				
Sk_P2			11503876	23.007752	22745920	98.22	94.68				
Sk_P3			7148344	14.296688	14160542	98.01	94.29				

B)

Sample ID	Tissue	Treatment group	Total reads	Paired reads		Aligned concordantly 0 times		Aligned concordantly 1 time		Aligned concordantly > 1 times		Total alignment ratio
				Nr_reads	Percentage	Nr_reads	Percentage	Nr_reads	Percentage	Nr_reads	Percentage	
Lv_C1	Liver	Control	12795792	12795792	100%	1271199	9.93%	2248277	17.57%	9276316	72.50%	90.07%
Lv_C2			10647793	10647793	100%	1165188	10.94%	2091045	19.64%	7391560	69.42%	89.06%
Lv_C3			11256248	11256248	100%	1201724	10.68%	2304056	20.47%	7750468	68.85%	89.32%
Lv_L1		LPS	9483284	9483284	100%	1059877	11.18%	1874613	19.77%	6548794	69.06%	88.82%
Lv_L2			7539990	7539990	100%	673943	8.94%	1574357	20.88%	5291690	70.18%	91.06%
Lv_L3			7658561	7658561	100%	843942	11.02%	1424723	18.60%	5389896	70.38%	88.98%
Lv_P1		Poly I:C	8318561	8318561	100%	731708	8.80%	1740673	20.93%	5846180	70.28%	91.2%
Lv_P2			6853356	6853356	100%	753549	11%	1350571	19.71%	4749236	69.30%	89%
Lv_P3			6574569	6574569	100%	710313	10.80%	1303382	19.82%	4560874	69.37%	89.2%
Sp_C1	Spleen	Control	6785769	6785769	100%	1178134	17.36%	1594648	23.50%	4012987	59.14%	82.64%
Sp_C2			6810468	6810468	100%	1102877	16.19%	1880943	27.62%	3826648	56.19%	83.81%
Sp_C3			6778110	6778110	100%	1057936	15.61%	1559025	23%	4161149	61.39%	84.39%
Sp_L1		LPS	8946160	8946160	100%	2722838	30.44%	2121740	23.72%	4101582	45.85%	69.56%
Sp_L2			6556862	6556862	100%	867224	13.23%	1749759	26.69%	3939879	60.09%	86.77%
Sp_L3			7312955	7312955	100%	1183422	16.18%	1766887	24.16%	4362646	59.66%	83.82%
Sp_P1		Poly I:C	7621861	7621861	100%	948167	12.44%	2087289	27.39%	4586405	60.17%	87.56%
Sp_P2			6468579	6468579	100%	1108316	17.13%	1832275	28.33%	3527988	54.54%	82.87%
Sp_P3			5978245	5978245	100%	1011222	16.92%	1620799	27.11%	3346224	55.97%	83.08%
Du_C1	Duodenum	Control	7582524	7582524	100%	958608	12.64%	2688301	35.45%	3935615	51.90%	87.36%
Du_C2			6134510	6134510	100%	874495	14.26%	2093800	34.13%	3166215	51.61%	85.74%
Du_C3			6465593	6465593	100%	991069	15.33%	2216092	34.28%	3258432	50.40%	84.67%
Du_L1		LPS	6079943	6079943	100%	898429	14.78%	2093449	34.43%	3088065	50.79%	85.22%
Du_L2			6848938	6848938	100%	1231440	17.98%	2437853	35.59%	3179645	46.43%	82.02%
Du_L3			10338156	10338156	100%	1276120	12.34%	4041754	39.10%	5020282	48.56%	87.66%
Du_P1		Poly I:C	7725222	7725222	100%	1337139	17.31%	2773991	35.91%	3614092	46.78%	82.69%
Du_P2			8643257	8643257	100%	1254933	14.52%	3030024	35.06%	4358300	50.42%	85.48%
Du_P3			9004891	9004891	100%	962034	10.68%	3406057	37.82%	4636800	51.49%	89.32%
Sk_C1	Skin	Control	7978045	7978045	100%	1446100	18.13%	3179723	39.86%	3352222	42.02%	81.87%
Sk_C2			7898348	7898348	100%	1260763	15.96%	3196347	40.47%	3441238	43.57%	84.04%
Sk_C3			8901579	8901579	100%	1474909	15.57%	3537251	39.74%	3889419	43.69%	83.43%
Sk_P1		LPS	8059046	8059046	100%	978566	12.14%	3077051	38.18%	4003429	49.68%	87.86%
Sk_P2			4783722	4783722	100%	772789	16.15%	1947808	40.72%	2063125	43.13%	83.85%
Sk_P3			5605772	5605772	100%	874943	15.61%	2214122	39.50%	2516707	44.89%	84.39%
Sk_L1		Poly I:C	8068915	8068915	100%	1402099	17.38%	3222481	39.94%	3444335	42.69%	82.62%
Sk_L2			11503876	11503876	100%	1040861	9.05%	5024421	43.68%	5438594	47.28%	90.95%
Sk_L3			7148344	7148344	100%	998757	13.97%	2934295	41.05%	3215292	44.98%	86.03%

Supplementary table 4.2. DEGs (FDR < 0.05) from duodenum A) up-regulated and B) down-regulated in the LPS group, and C) up-regulated and D) down-regulated in the poly I:C group. The DEGs common with skin are indicated with a "●" symbol in LPS and "■" in Poly I:C-treated fish. For the Poly I:C group, the DEGs common with liver are indicated with a "✹" and the DEGs common with skin and liver are indicated with a "❖". Only available on digital format in Annex II because the table is very extensive.

Supplementary table 4.3. DEGs (FDR < 0.05) from skin A) up-regulated and B) down-regulated in the LPS group, and C) up-regulated and D) down-regulated in poly I:C group. The DEGs common with duodenum are indicated with a "●" symbol and with liver with a "◆" in the LPS-treated fish. For the Poly I:C group, the DEGs common to duodenum are indicated with a "■", to liver with a "◎" and to duodenum and liver with a "❖".Only available on digital format in Annex II because the table is very extensive.

Supplementary table 4.4. DEGs (FDR < 0.05) from spleen A) up-regulated and B) down-regulated in the LPS group, and C) up-regulated and D) down-regulated in poly I:C group.

a)

TRINITY contig code	log2FC	P value	FDR	UniProt KB / NCBI ID	Gene definition	Gene symbol	Organism
TRINITY_DN13998_c1_g1_i1	7,31E+14	7,26E-07	2,55E-03	A7E3W5	Synaptogyrin-2	*syngr2*	*Bos taurus*
TRINITY_DN15055_c0_g1_i1	4,47E+14	1,12E-06	3,26E-03	Q9ESX4	Nucleolar protein of 40 kDa	*zcchc17*	*Mus musculus*
TRINITY_DN10313_c0_g1_i4	2,70E+13	1,72E-06	4,30E-03	Q5ZJU4	Ubiquitin-related modifier 1	*urm1*	*Gallus gallus*
TRINITY_DN12287_c0_g1_i1	1,80E+14	7,39E-06	1,62E-02	Q9WVQ1	Membrane-associated guanylate kinase, WW and PDZ domain-containing protein 2	*magi2*	*Mus musculus*
TRINITY_DN1774_c1_g1_i1	6,61E+14	1,06E-05	2,07E-02	Q92556	Engulfment and cell motility protein 1	*elmo1*	*Homo sapiens*
TRINITY_DN6208_c2_g4_i1	1,70E+14	1,63E-05	2,60E-02	O60291	E3 ubiquitin-protein ligase MGRN1	*mgrn1*	*Homo sapiens*
TRINITY_DN21994_c0_g1_i1	6,03E+14	2,61E-05	3,81E-02	O14681	Etoposide-induced protein 2.4 homolog	*ei24*	*Homo sapiens*
TRINITY_DN27364_c0_g1_i1	1,12E+14	3,68E-05	4,61E-02	Q7ZYC4	Long-chain-fatty-acid--CoA ligase ACSBG2	*acsbg2*	*Xenopus laevis*
TRINITY_DN33177_c0_g1_i1	6,57E+14	3,63E-05	4,61E-02	Q6PHG4	Lipoyl synthase, mitochondrial	*lias*	*Danio rerio*

b)

TRINITY contig code	log2FC	P value	FDR	UniProt KB / NCBI ID	Gene definition	Gene symbol	Organism
TRINITY_DN7243_c0_g3_i1	-3,77E+14	6,74E-07	2,55E-03	Q9Z330	DNA (cytosine-5)-methyltransferase 1	*dnmt1*	*Rattus norvegicus*
TRINITY_DN9532_c0_g1_i1	-6,73E+14	1,60E-05	2,60E-02	O14578	Citron Rho-interacting kinase	*cit*	*Homo sapiens*

c)

TRINITY contig code	log2FC	P value	FDR	UniProt KB / NCBI ID	Gene definition	Gene symbol	Organism
TRINITY_DN8545_c0_g1_i1	7,72E+14	5,37E-07	1,48E-03	Q60943	Interleukin-17 receptor A	*il17ra*	*Mus musculus*
TRINITY_DN2629_c0_g1_i1	8,03E+13	6,21E-06	1,01E-02	O35828	Coronin-7	*coro7*	*Rattus norvegicus*
TRINITY_DN53605_c0_g1_i1	7,03E+14	5,90E-06	1,01E-02	Q5HYW2	NHS-like protein 2	*nhsl2*	*Homo sapiens*
TRINITY_DN30488_c0_g1_i1	1,37E+14	9,04E-06	1,27E-02	F1REV3	Krev interaction trapped protein 1	*krit1*	*Danio rerio*
TRINITY_DN16904_c0_g1_i1	2,06E+14	1,16E-05	1,52E-02	Q4TVV3	Probable ATP-dependent RNA helicase DDX46	*ddx46*	*Danio rerio*
TRINITY_DN13998_c1_g1_i1	8,27E+13	1,27E-05	1,56E-02	A7E3W5	Synaptogyrin-2	*syngr2*	*Bos taurus*
TRINITY_DN11454_c1_g1_i1	4,61E+14	2,26E-05	2,46E-02	Q9CS84	Neurexin-1	*nrx1a*	*Mus musculus*
TRINITY_DN36415_c0_g1_i1	6,48E+14	2,16E-05	2,46E-02	Q96PQ0	VPS10 domain-containing receptor SorCS2	*sorc2*	*Homo sapiens*
TRINITY_DN9030_c2_g1_i1	6,47E+14	4,84E-05	4,13E-02	Q8C2E4	Pentatricopeptide repeat-containing protein 1, mitochondrial	*ptcd1*	*Mus musculus*
TRINITY_DN8371_c0_g1_i1	3,13E+14	5,11E-05	4,18E-02	Q04637	Eukaryotic translation initiation factor 4 gamma 1	*eif4g1*	*Homo sapiens*
TRINITY_DN54446_c0_g1_i1	5,49E+14	5,39E-05	4,23E-02	Q9NU22	Midasin	*mdn1*	*Homo sapiens*

d)

TRINITY contig codes	log2FC	P value	FDR	UniProt KB / NCBI ID	Gene definition	Gene symbol	Organism
TRINITY_DN7243_c0_g3_i1	-4,26E+14	6,32E-08	3,10E-04	Q9Z330	DNA (cytosine-5)-methyltransferase 1	*dnmt1*	*Rattus norvegicus*
TRINITY_DN702_c3_g2_i1	-2,26E+13	1,99E-07	7,80E-04	Q61205	Platelet-activating factor acetylhydrolase IB subunit alpha1	*pafah1b3*	*Mus musculus*
TRINITY_DN28598_c0_g1_i1	-1,96E+13	6,04E-07	1,48E-03	A0JNW5	UHRF1-binding protein 1-like	*uhrf1bp1l*	*Homo sapiens*
TRINITY_DN33319_c0_g1_i1	-3,38E+14	6,00E-07	1,48E-03	P47804	RPE-retinal G protein-coupled receptor	*rgr*	*Homo sapiens*
TRINITY_DN30932_c0_g1_i1	-5,09E+14	1,54E-06	3,35E-03	Q9UHF7	Zinc finger transcription factor Trps1	*trps1*	*Homo sapiens*
TRINITY_DN2334_c1_g1_i1	-4,40E+14	2,65E-06	5,20E-03	Q16829	Dual specificity protein phosphatase 7	*dusp7*	*Homo sapiens*
TRINITY_DN15215_c0_g2_i1	-1,33E+14	7,58E-06	1,14E-02	O14776	Transcription elongation regulator 1	*tcerg1*	*Homo sapiens*
TRINITY_DN8851_c0_g1_i1	-1,17E+14	2,85E-05	2,94E-02	A2AF47	Dedicator of cytokinesis protein 11	*dock11*	*Mus musculus*
TRINITY_DN75337_c0_g1_i1	-2,77E+14	3,26E-05	3,20E-02	Q9WVJ5	Beta-crystallin B1	*crybb1*	*Mus musculus*
TRINITY_DN8392_c0_g2_i1	-1,05E+12	4,09E-05	3,82E-02	Q5R723	Peptidyl-prolyl cis-trans isomerase E	*ppie*	*Pongo abelii*
TRINITY_DN1519_c3_g1_i1	-1,43E+14	4,37E-05	3,89E-02	Q5RG82	Influenza virus NS1A-binding protein homolog A	*ivns1abpa*	*Danio rerio*
TRINITY_DN36789_c0_g1_i1	-4,23E+14	5,65E-05	4,26E-02	Q9ESF4	Protein lifeguard 1	*grina*	*Mus musculus*

Supplementary table 4.5. DEGs (FDR < 0.05) from liver A) up-regulated and B) down-regulated in the LPS group, and C) up-regulated and D) down-regulated in the poly I:C group. The DEGs common with skin with a "◆" in LPS-treated fish. For Poly I:C group, the DEGs common with duodenum are indicated with a "✹", with skin are indicated with a "◎", and with duodenum and skin with a "❖". Only available on digital format in Annex II because the table is very extensive.

Supplementary table 4.6. Enriched GO terms of DEGs from *N. rossii* duodenum: A) Control versus LPS and B) Control versus poly I:C groups. FDR < 0.05 for LPS challenge and FDR < 0.001 for Poly I:C challenge). Only available on digital format in Annex II because the table is very extensive.

Supplementary table 4.7. Enriched GO terms of DEGs from *N. rossii* skin: A) Control versus LPS and B) Control versus poly I:C groups. FDR < 0.001. Only available on digital format in Annex II because the table is very extensive.

Supplementary table 4.8. Enriched GO terms of DEGs from *N. rossii* spleen: A) Control versus LPS and B) Control versus poly I:C groups. FDR < 0.05. Only available on digital format in Annex II because the table is very extensive.

Supplementary table 4.9. Enriched GO terms of DEGs from *N. rossii* liver: A) Control versus LPS and B) Control versus poly I:C groups. FDR < 0.001. Only available on digital format in Annex II because the table is very extensive.

Supplementary table 4.10. KEGG enriched pathways in duodenum after a) LPS (FDR < 0.05) and poly I:C (FDR < 0.001) challenges. Only available on digital format in Annex II because the table is very extensive.

Supplementary table 4.11. KEGG enriched pathways in skin after a) LPS (FDR < 0.05) and poly I:C (FDR < 0.001) challenges. This is only available on digital format in Annex II because the table is very extensive.

Supplementary table 4.12. KEGG enriched pathways in spleen after a) LPS (FDR < 0.05) and poly I:C (FDR < 0.001) challenges. Only available on digital format in Annex II because the table is very extensive.

Supplementary table 4.13. KEGG enriched pathways in liver after a) LPS (FDR < 0.05) and poly I:C (FDR < 0.001) challenges. Only available on digital format in Annex II because the table is very extensive.

4.7.2. Supplementary figures

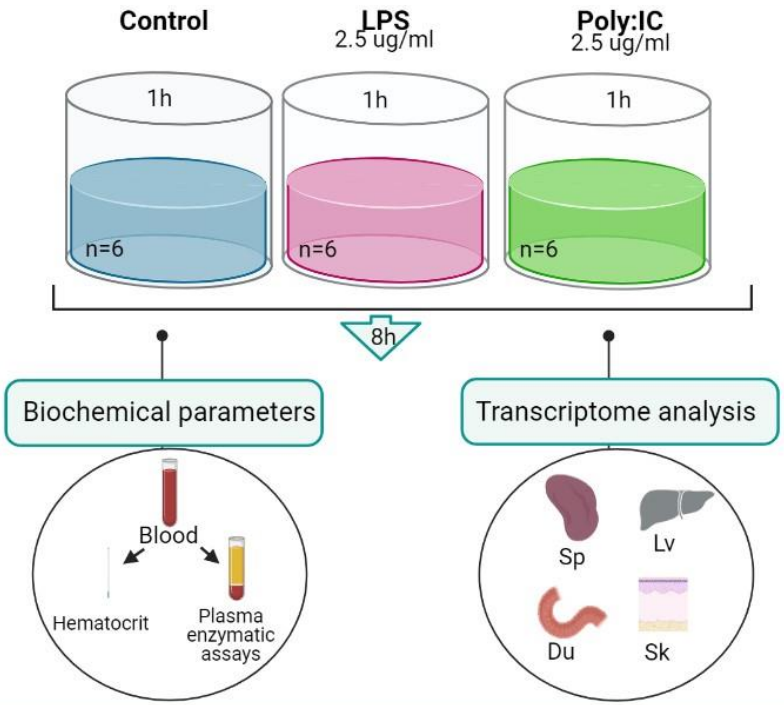

Supplementary figure 4.1. Experimental design and samples collected for analysis. Spleen (Sp), Liver (Lv), Duodenum (Du) and Skin (Sk).

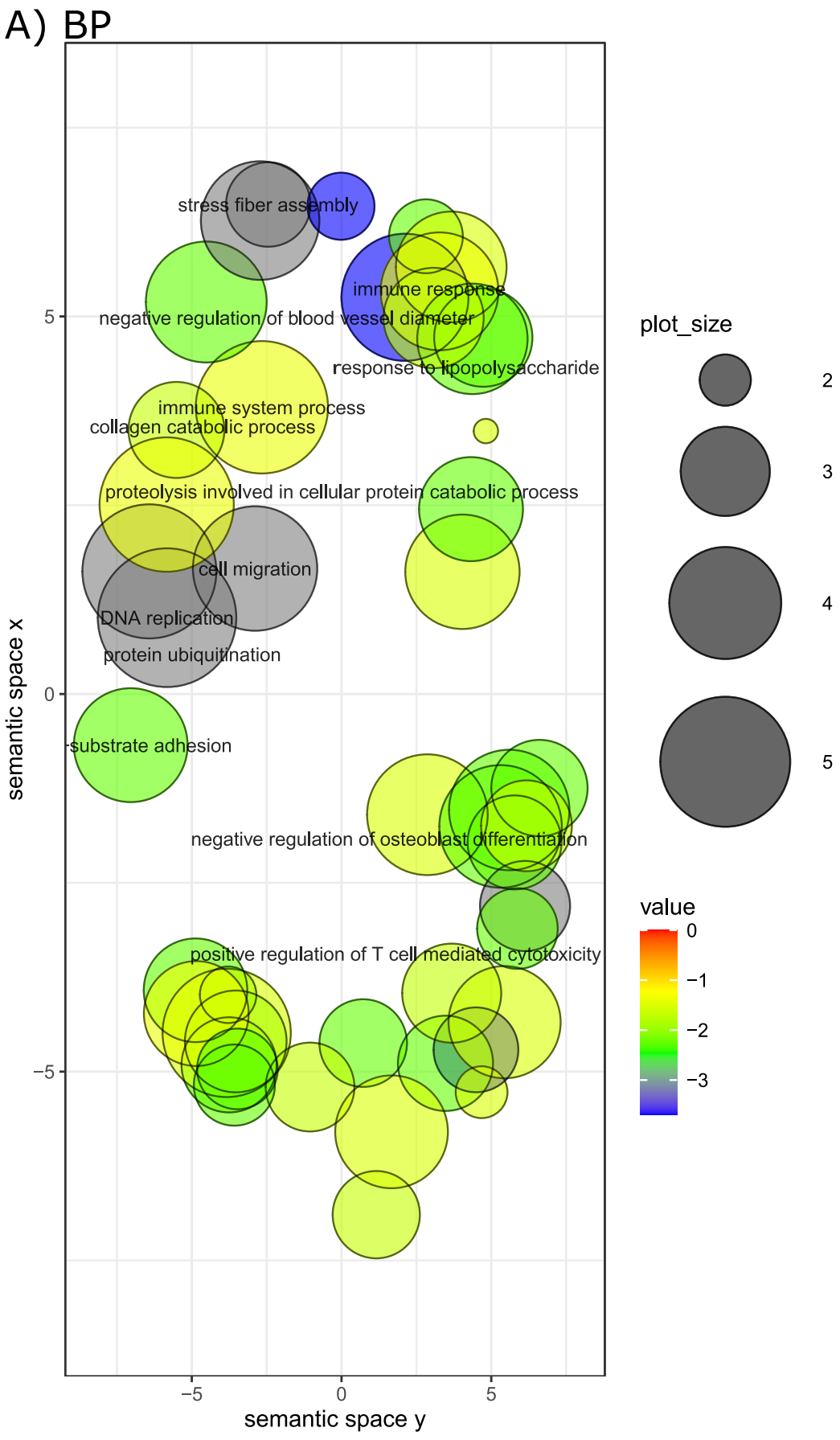
A) BP
stress fiber assembly
immune response
negative regulation of blood vessel diameter
response to lipopolysaccharide
immune system process
collagen catabolic process
proteolysis involved in cellular protein catabolic process
cell migration
DNA replication
protein ubiquitination
substrate adhesion
negative regulation of osteoblast differentiation
positive regulation of T cell mediated cytotoxicity
semantic space x
semantic space y
5
0
−5
−5
0
5
plot_size
2
3
4
5
value
0
−1
−2
−3

B) CC

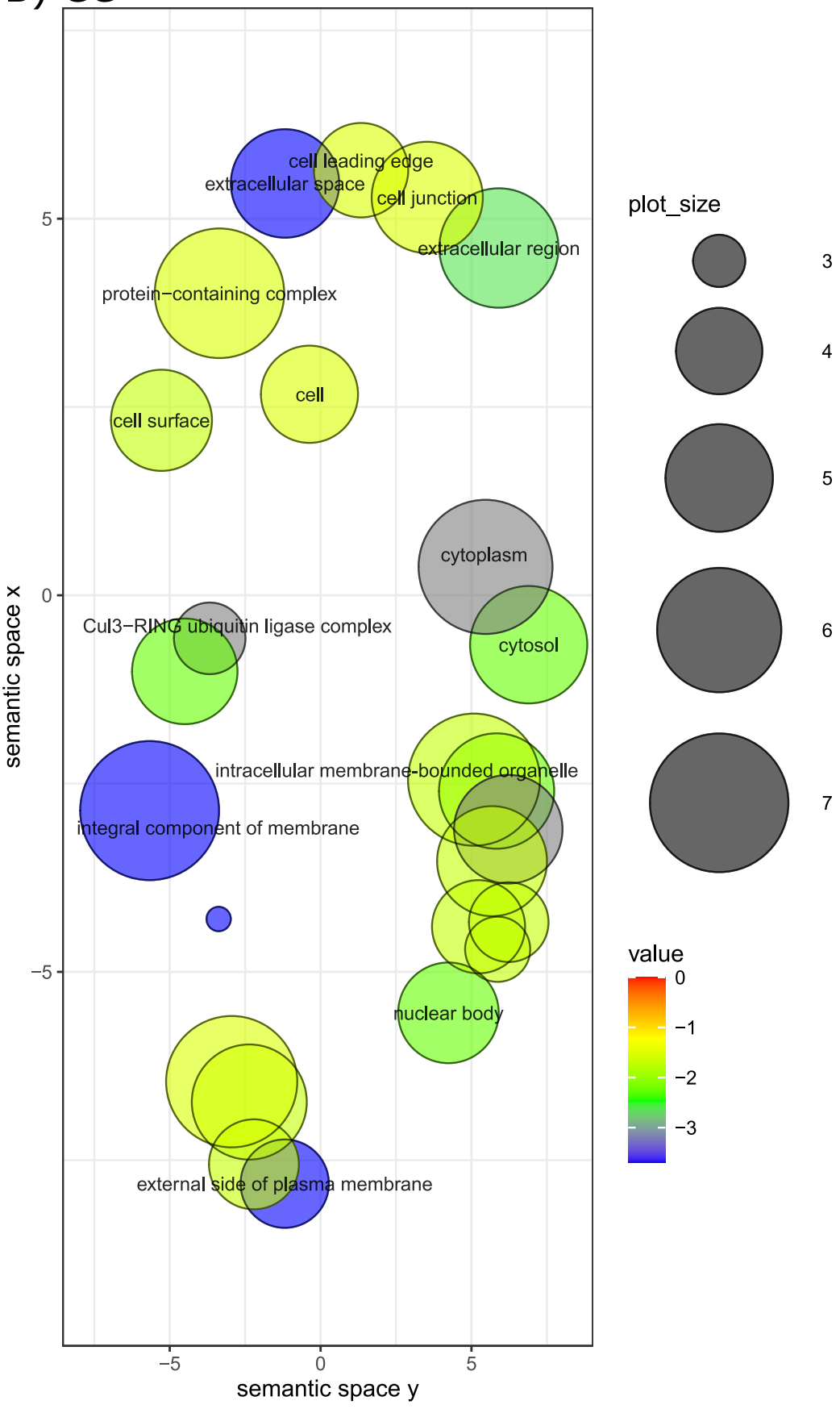
cell leading edge
extracellular space
cell junction
extracellular region
protein−containing complex
cell
cell surface
cytoplasm
Cul3−RING ubiquitin ligase complex
cytosol
intracellular membrane-bounded organelle
integral component of membrane
nuclear body
external side of plasma membrane
semantic space x
semantic space y
5
0
−5
−5
0
5
plot_size
3
4
5
6
7
value
0
−1
−2
−3

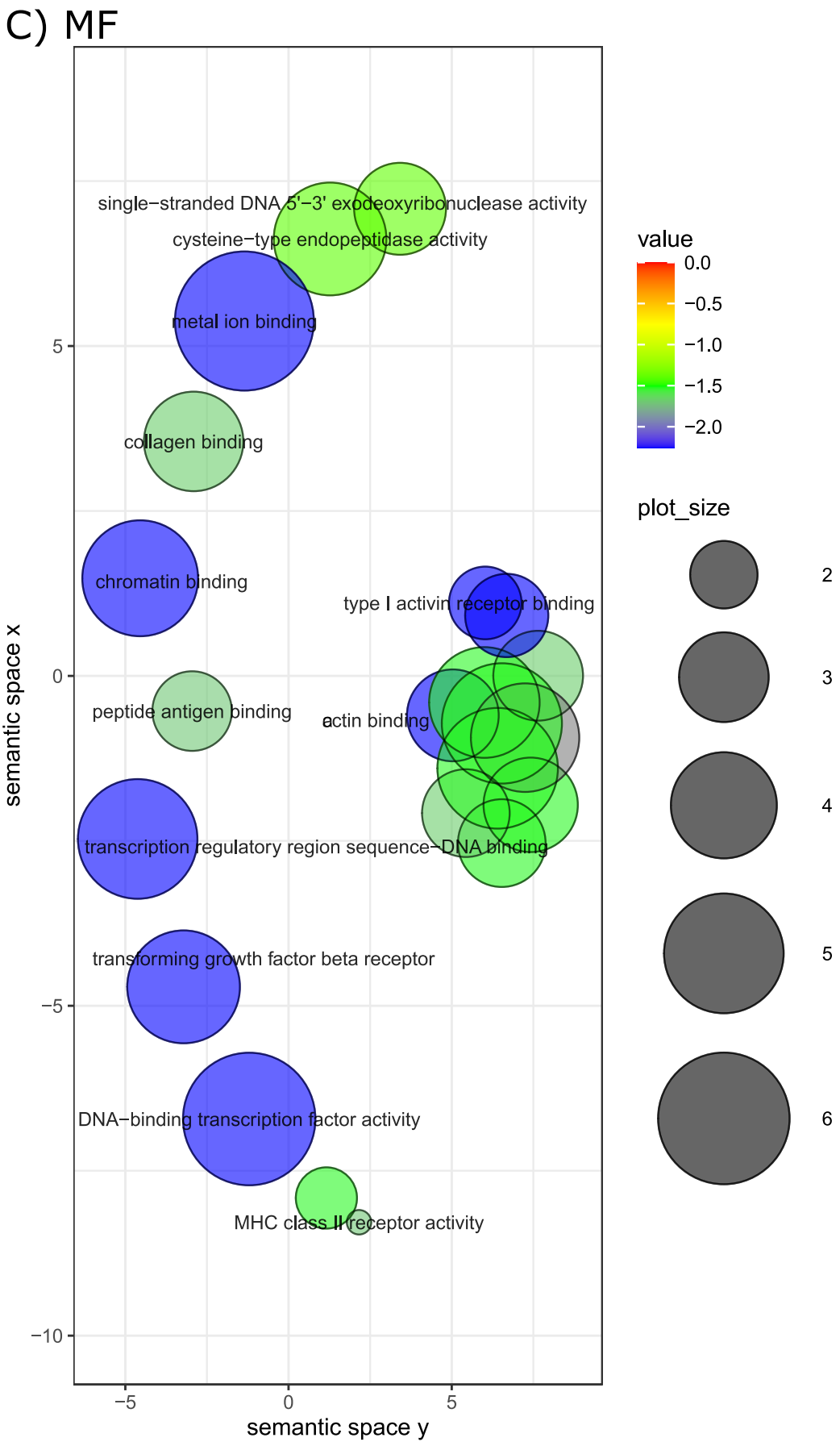
C) MF
single−stranded DNA 5'−3' exodeoxyribonuclease activity
cysteine−type endopeptidase activity
metal ion binding
collagen binding
chromatin binding
type I activin receptor binding
peptide antigen binding
actin binding
transcription regulatory region sequence−DNA binding
transforming growth factor beta receptor
DNA−binding transcription factor activity
MHC class II receptor activity
semantic space x
semantic space y
5
0
−5
−10
−5
0
5
value
0.0
−0.5
−1.0
−1.5
−2.0
plot_size
2
3
4
5
6

D) BP

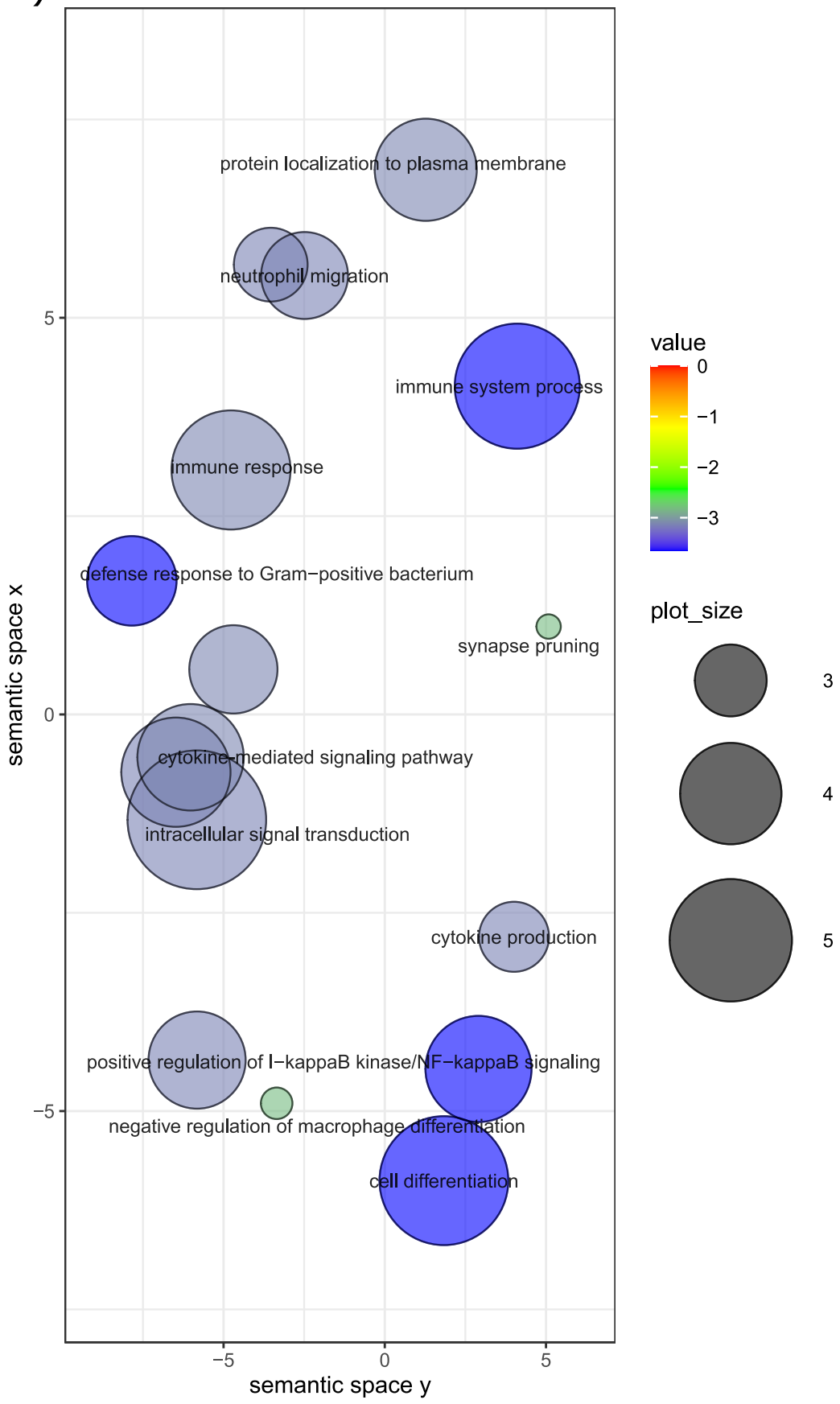
protein localization to plasma membrane
neutrophil migration
immune system process
immune response
defense response to Gram−positive bacterium
synapse pruning
cytokine-mediated signaling pathway
intracellular signal transduction
cytokine production
positive regulation of I−kappaB kinase/NF−kappaB signaling
negative regulation of macrophage differentiation
cell differentiation
semantic space x
semantic space y
5
0
−5
−5
0
5
value
0
−1
−2
−3
plot_size
3
4
5

E) CC

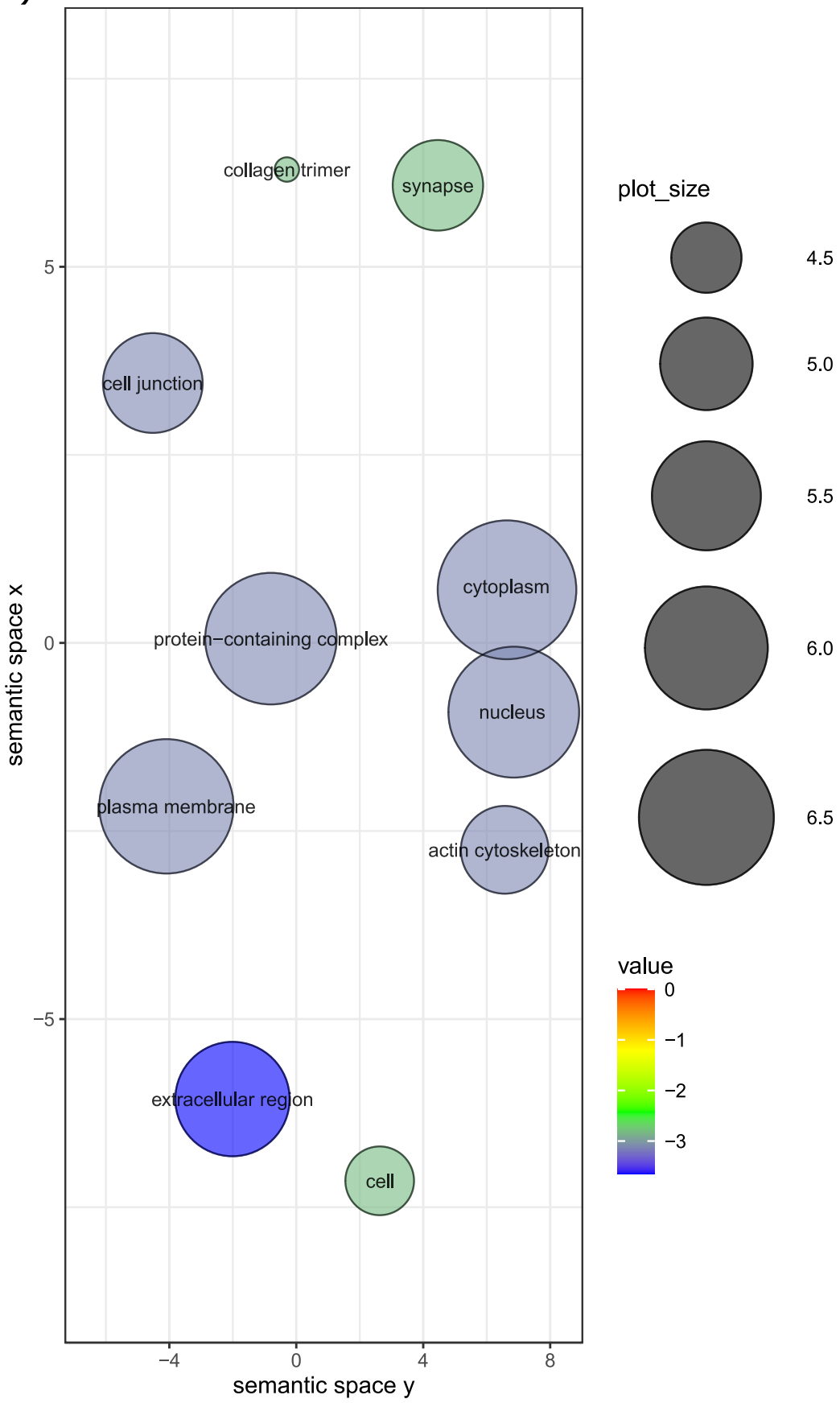
collagen trimer
synapse
cell junction
cytoplasm
protein−containing complex
nucleus
plasma membrane
actin cytoskeleton
extracellular region
cell
semantic space x
semantic space y
5
0
−5
−4
0
4
8
plot_size
4.5
5.0
5.5
6.0
6.5
value
0
−1
−2
−3

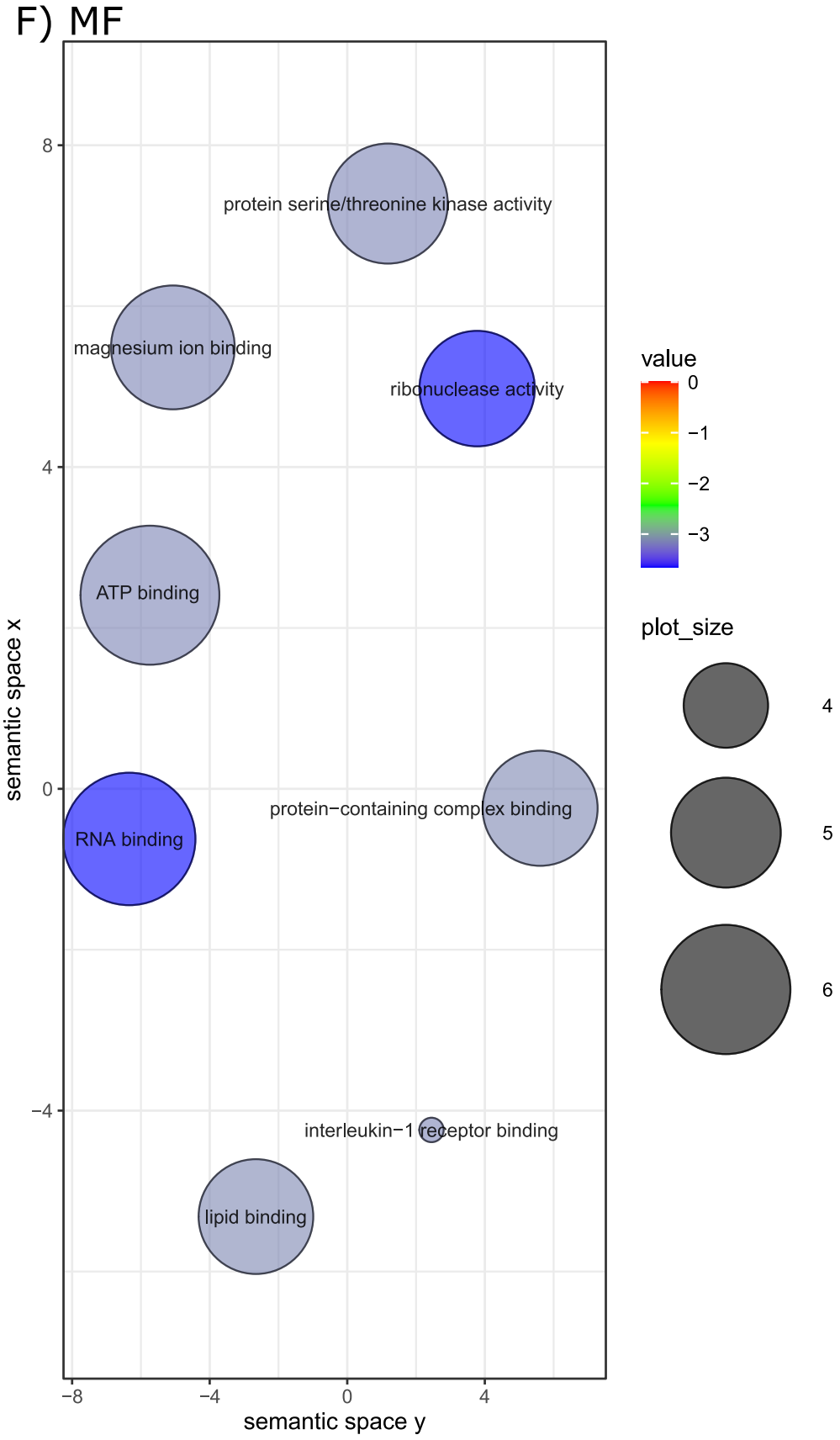

Supplementary figure 4.2. Scatterplots of enriched GO terms in duodenum. DEGs generated between Control and LPS - (A) BP, B) MF and C) CC) (FDR < 0.05) - and between Control and Poly

I:C - D) BP, E) MF and F) CC) (FDR < 0.001). The size of plots represents relative abundance (as a percentage of all DEGs from each category) and the colour gradient represents values of log10 (p-value)

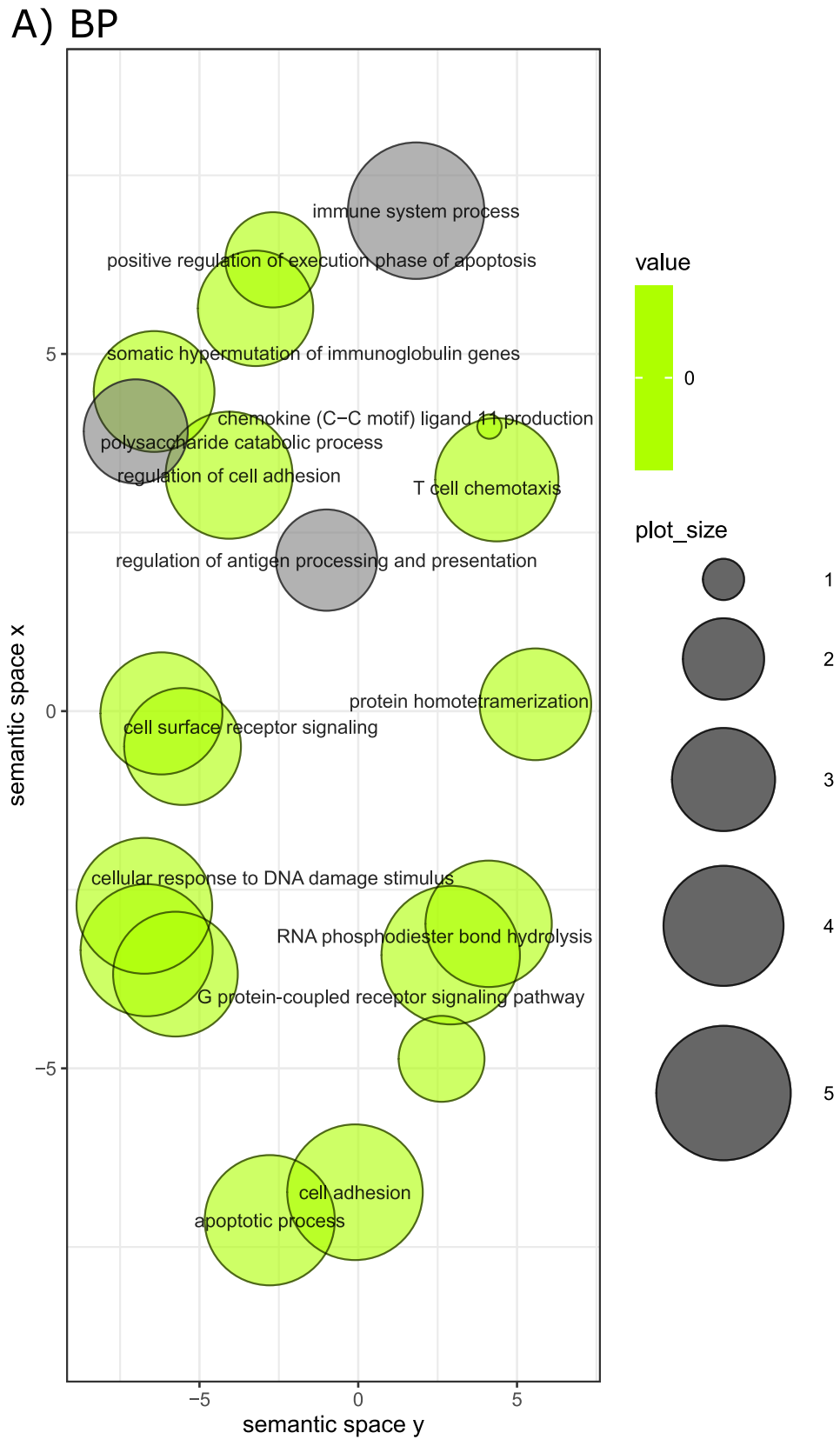

B) CC

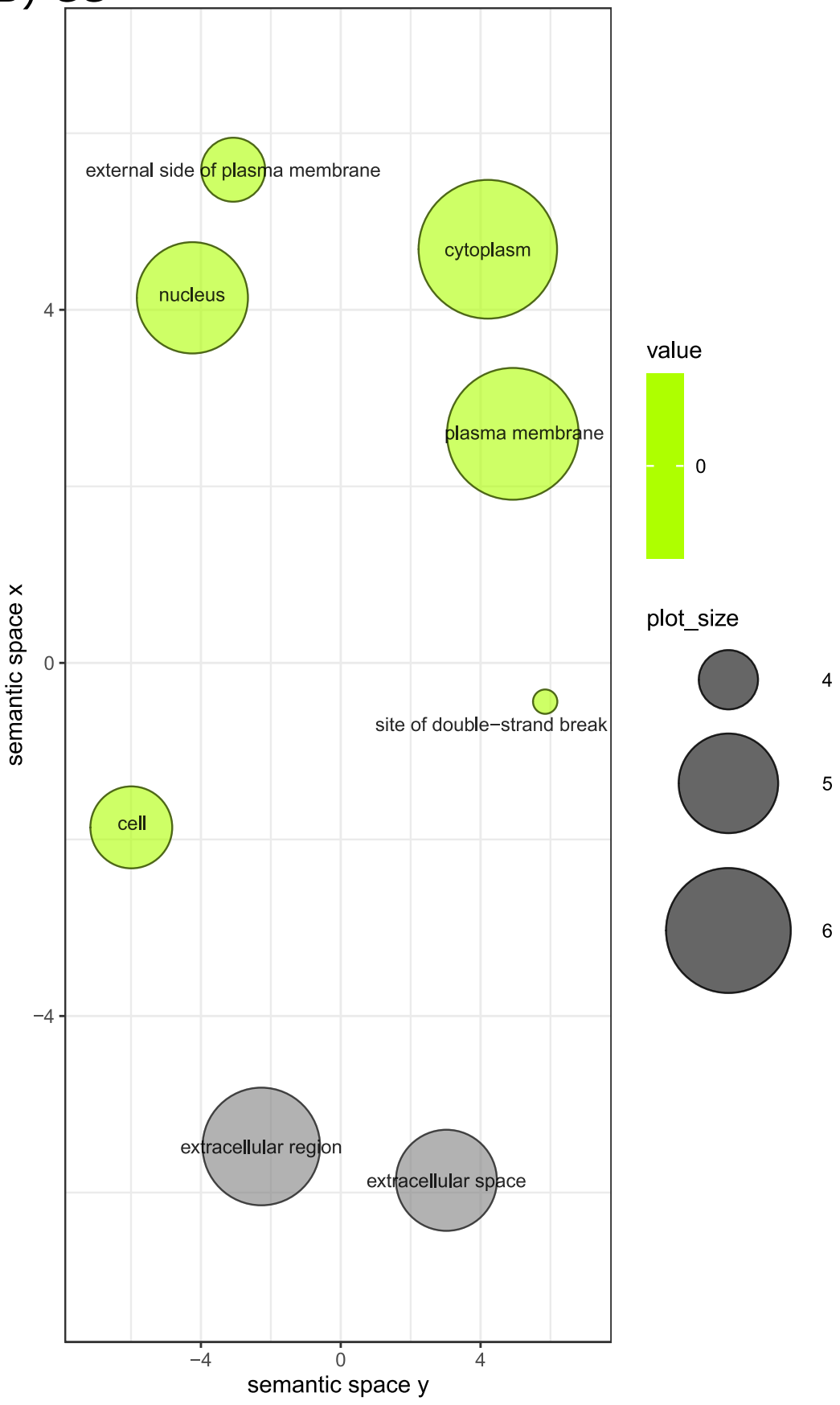
external side of plasma membrane
cytoplasm
nucleus
plasma membrane
site of double−strand break
cell
extracellular region
extracellular space
4
0
−4
semantic space x
−4
0
4
semantic space y
value
0
plot_size
4
5
6

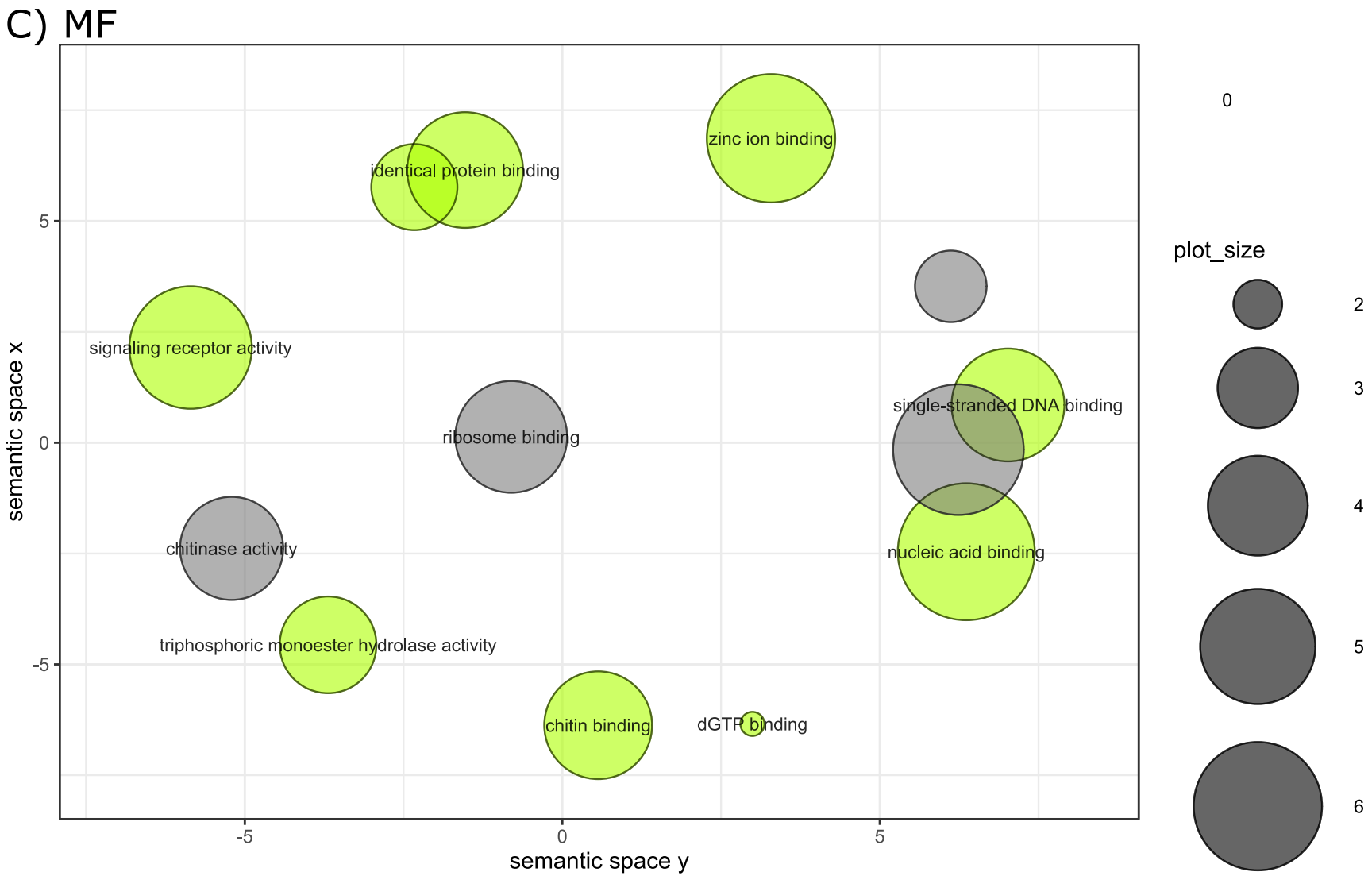
C) MF
zinc ion binding
identical protein binding
signaling receptor activity
ribosome binding
single-stranded DNA binding
chitinase activity
nucleic acid binding
triphosphoric monoester hydrolase activity
chitin binding
dGTP binding
semantic space x
semantic space y
5
0
-5
-5
0
5
plot_size
0
2
3
4
5
6

D) BP

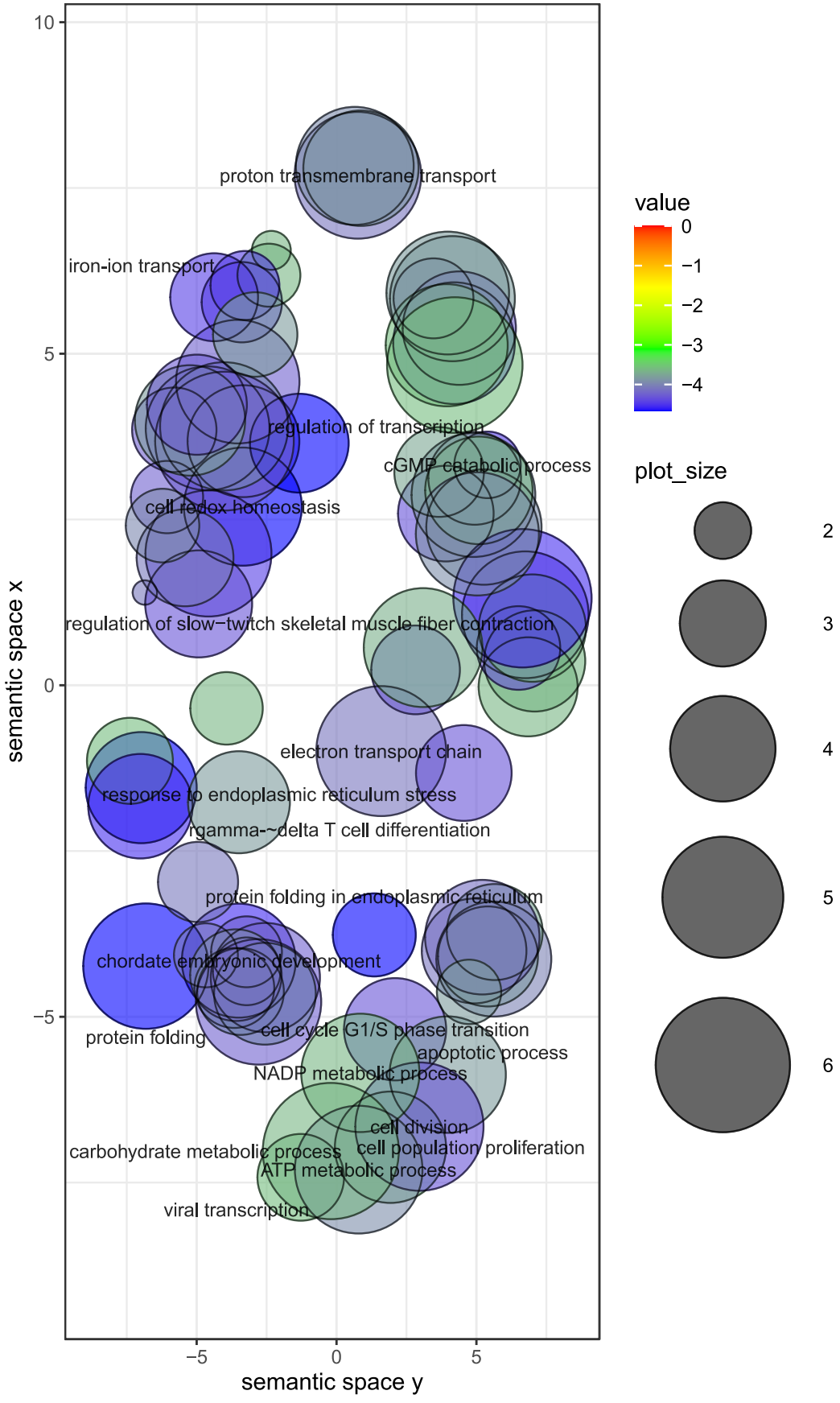
proton transmembrane transport
iron-ion transport
regulation of transcription
cGMP catabolic process
cell redox homeostasis
regulation of slow−twitch skeletal muscle fiber contraction
electron transport chain
response to endoplasmic reticulum stress
gamma-~delta T cell differentiation
protein folding in endoplasmic reticulum
chordate embryonic development
protein folding
cell cycle G1/S phase transition
apoptotic process
NADP metabolic process
cell division
cell population proliferation
carbohydrate metabolic process
ATP metabolic process
viral transcription
semantic space x
semantic space y
10
5
0
−5
−5
0
5
value
0
−1
−2
−3
−4
plot_size
2
3
4
5
6

E) CC

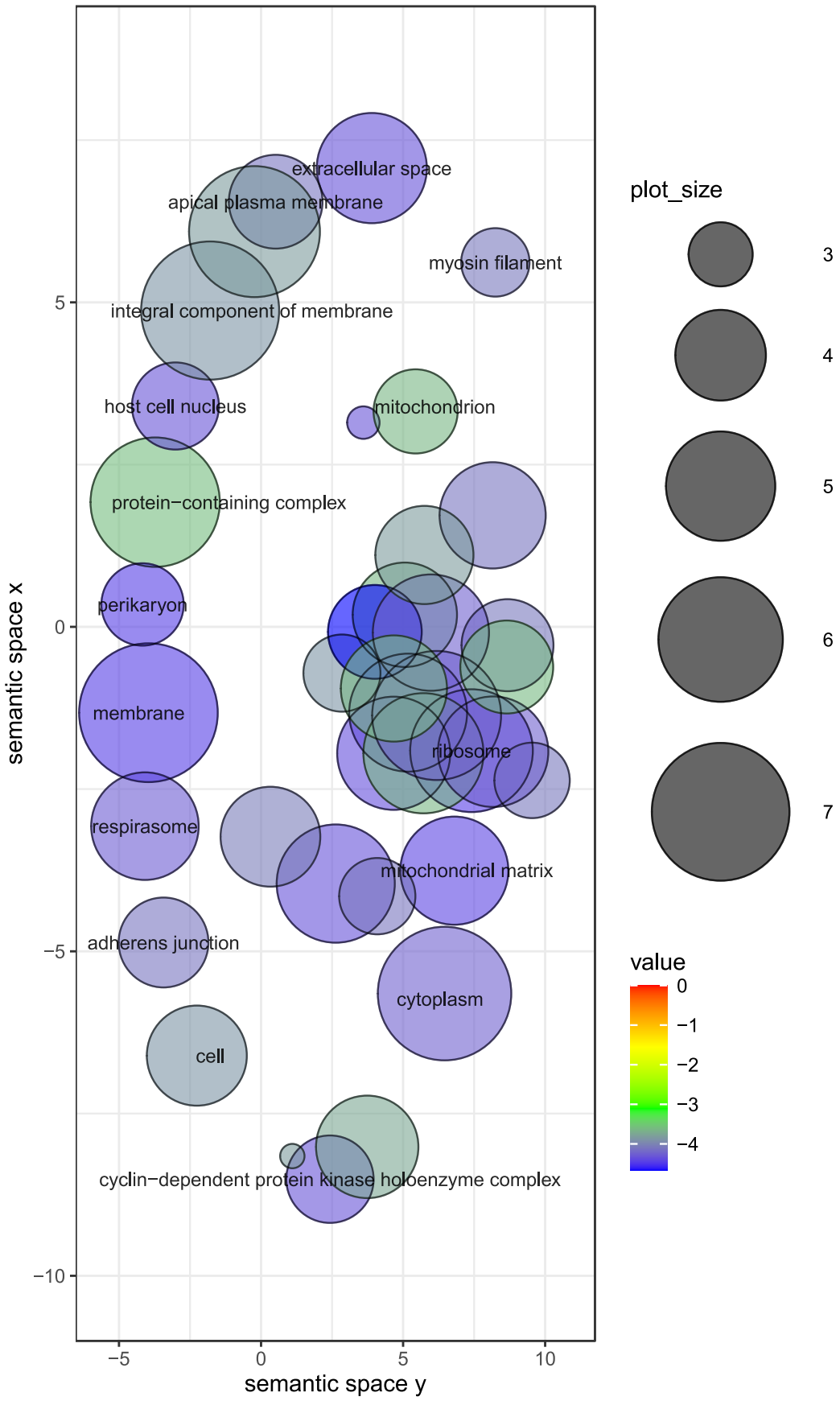
extracellular space
apical plasma membrane
myosin filament
integral component of membrane
host cell nucleus
mitochondrion
protein−containing complex
perikaryon
membrane
ribosome
respirasome
mitochondrial matrix
adherens junction
cytoplasm
cell
cyclin−dependent protein kinase holoenzyme complex
semantic space x
semantic space y
5
0
−5
−10
−5
0
5
10
plot_size
3
4
5
6
7
value
0
−1
−2
−3
−4

F) MF

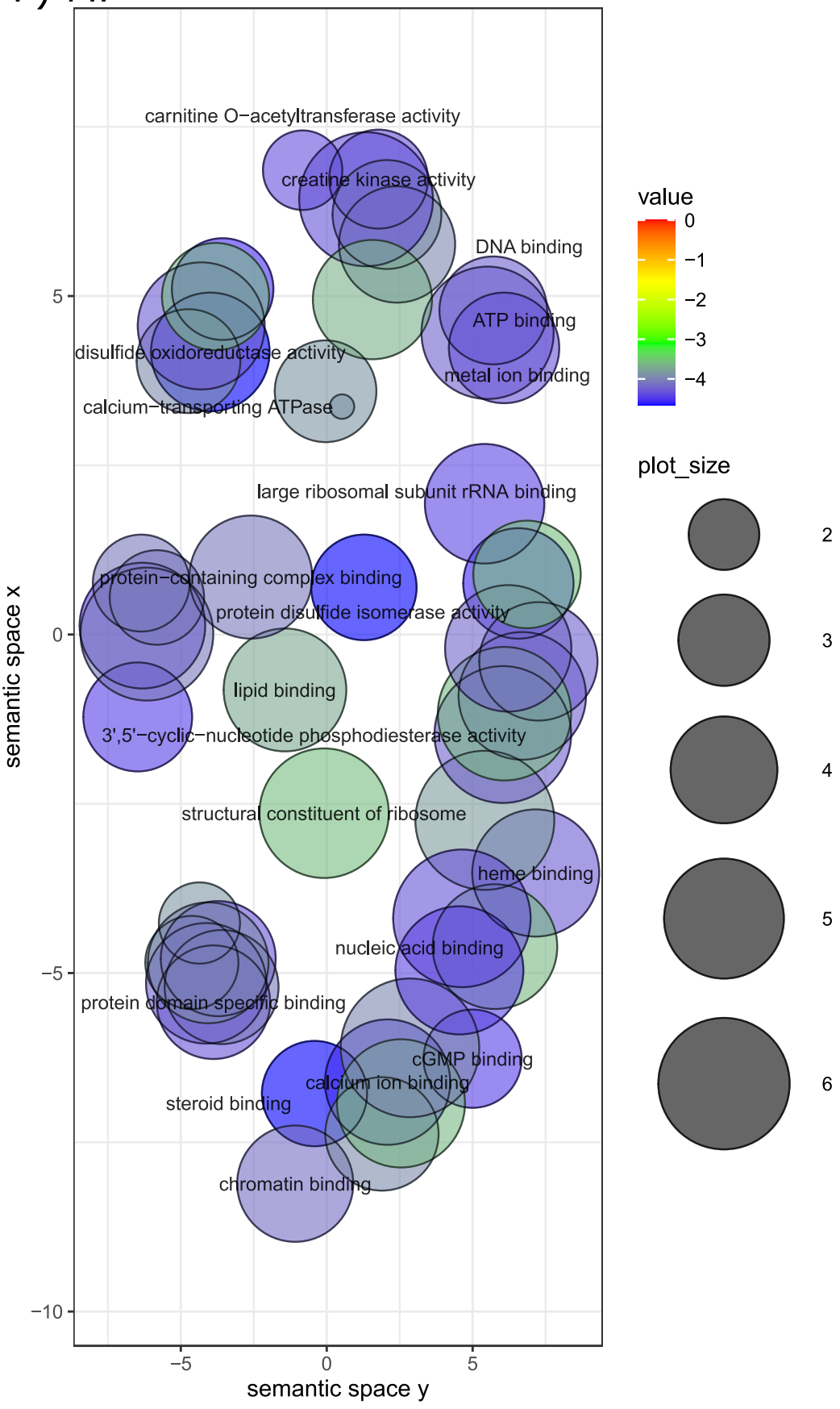
carnitine O−acetyltransferase activity
creatine kinase activity
DNA binding
ATP binding
metal ion binding
disulfide oxidoreductase activity
calcium−transporting ATPase
large ribosomal subunit rRNA binding
protein−containing complex binding
protein disulfide isomerase activity
lipid binding
3',5'−cyclic−nucleotide phosphodiesterase activity
structural constituent of ribosome
heme binding
nucleic acid binding
protein domain specific binding
cGMP binding
calcium ion binding
steroid binding
chromatin binding
semantic space x
semantic space y
5
0
−5
−10
−5
0
5
value
0
−1
−2
−3
−4
plot_size
2
3
4
5
6

Supplementary figure 4.3. Scatterplots of enriched GO terms in skin. DEGs generated between Control and LPS - (A) BP, B) MF and C) CC) (FDR < 0.05) - and between Control and Poly I:C - D) BP, E) MF and F) CC) (FDR < 0.001). The size of plots represents relative abundance (as a percentage of all DEGs from each category) and the colour gradient represents values of log10 (p-value).

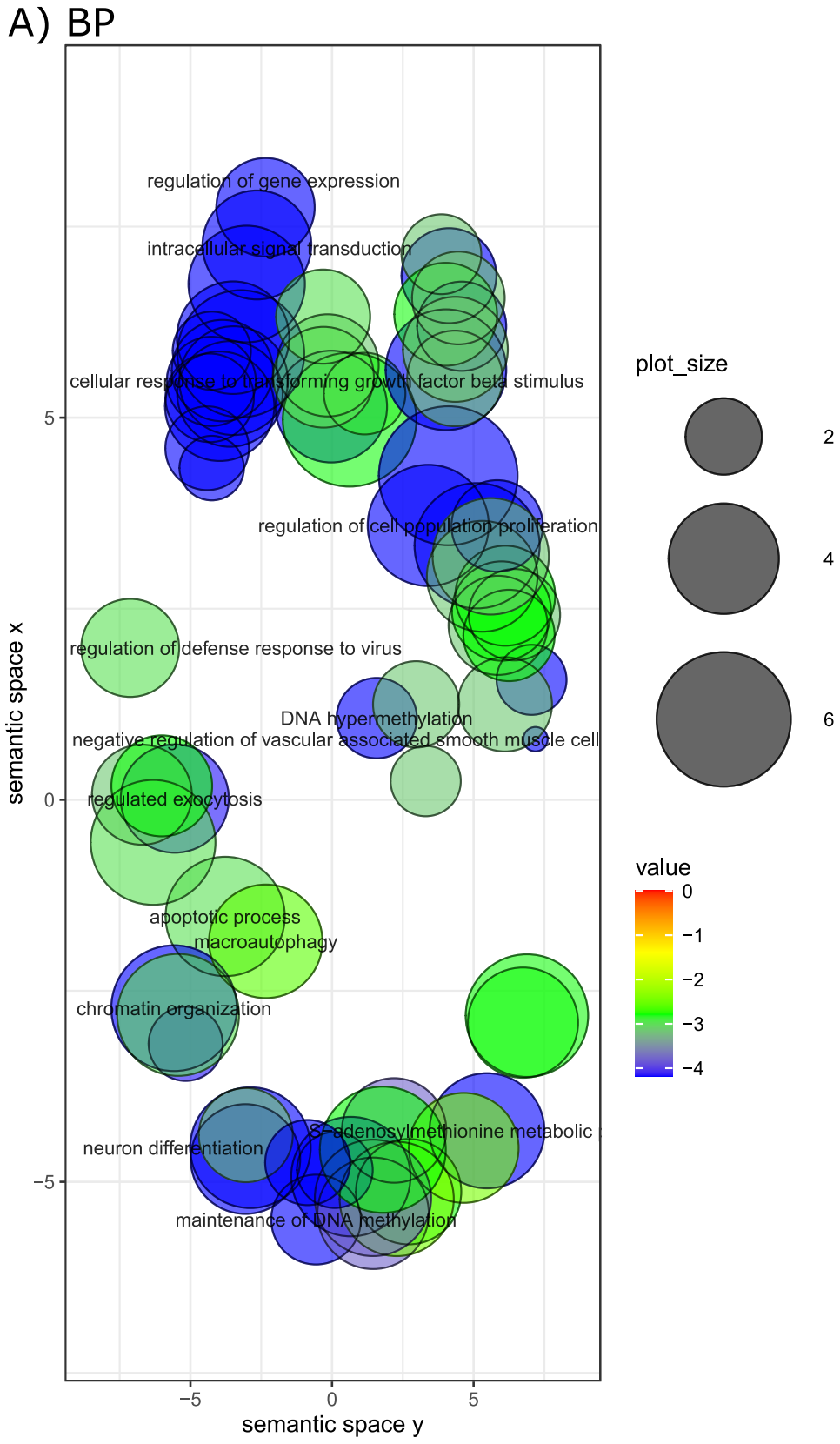

B) CC

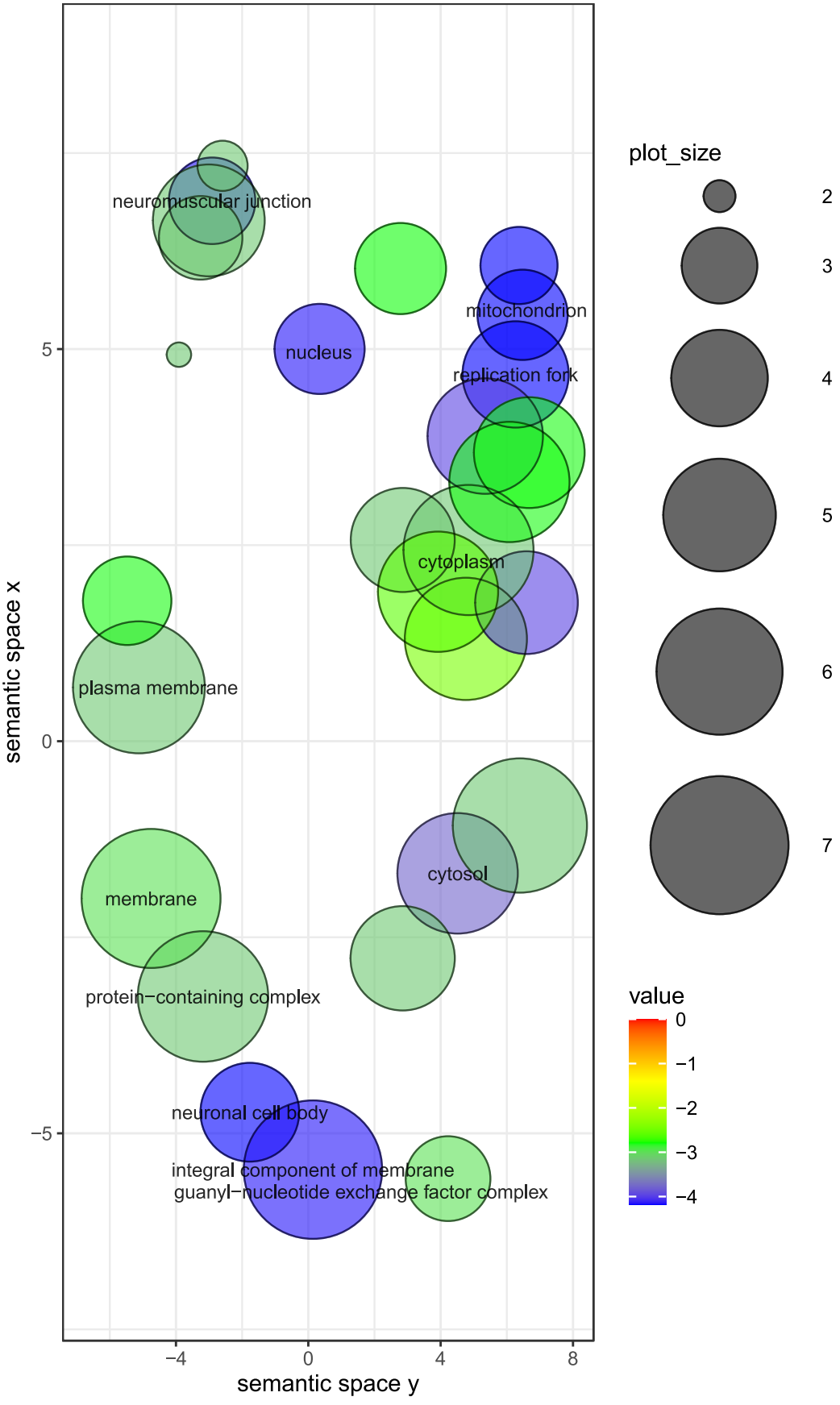
neuromuscular junction
mitochondrion
nucleus
replication fork
cytoplasm
plasma membrane
cytosol
membrane
protein−containing complex
neuronal cell body
integral component of membrane
guanyl−nucleotide exchange factor complex
semantic space x
semantic space y
5
0
−5
−4
0
4
8
plot_size
2
3
4
5
6
7
value
0
−1
−2
−3
−4

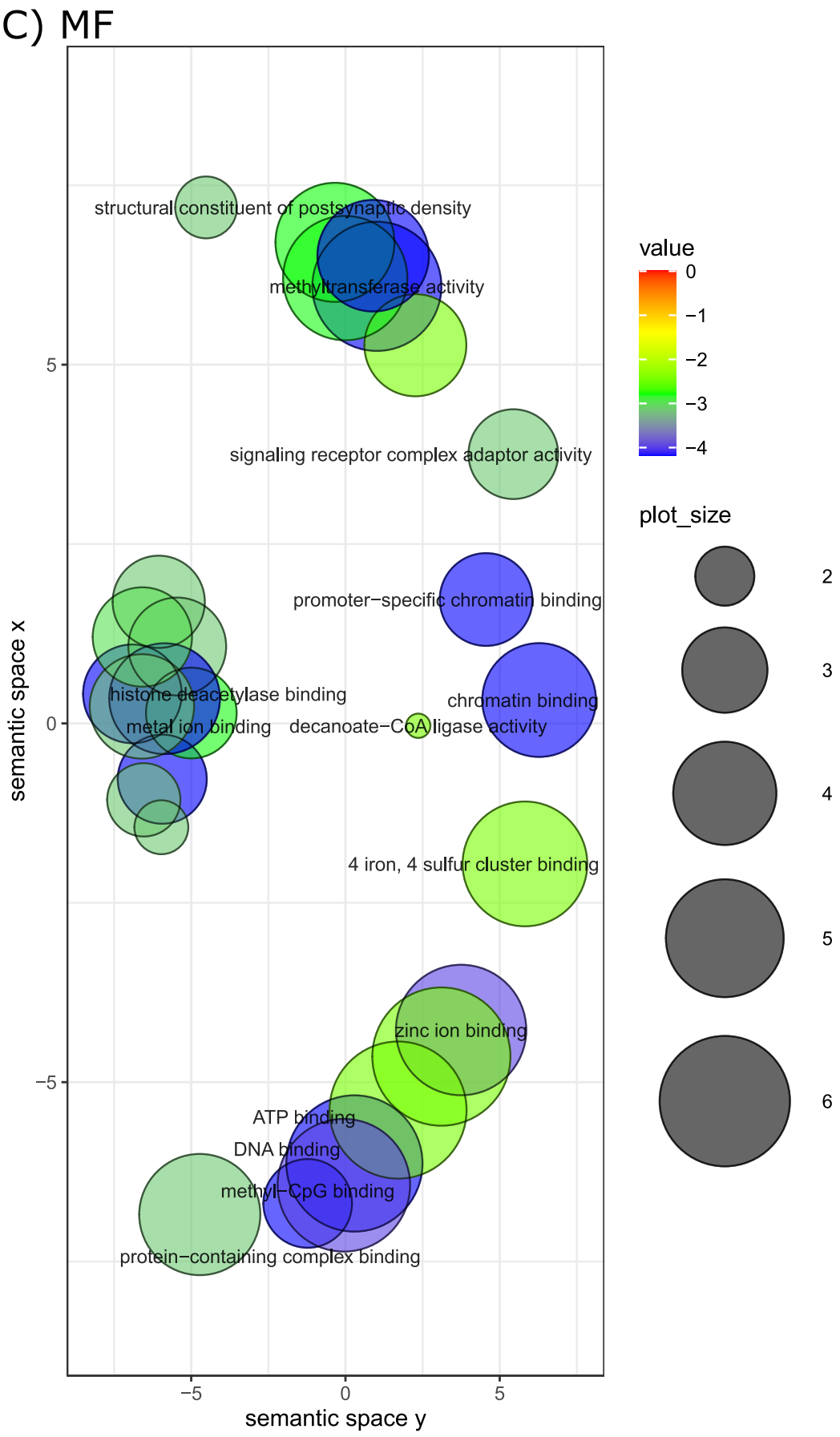
C) MF
structural constituent of postsynaptic density
methyltransferase activity
signaling receptor complex adaptor activity
promoter−specific chromatin binding
histone deacetylase binding
metal ion binding
decanoate−CoA ligase activity
chromatin binding
4 iron, 4 sulfur cluster binding
zinc ion binding
ATP binding
DNA binding
methyl−CpG binding
protein−containing complex binding
semantic space x
semantic space y
5
0
−5
−5
0
5
value
0
−1
−2
−3
−4
plot_size
2
3
4
5
6

D) BP

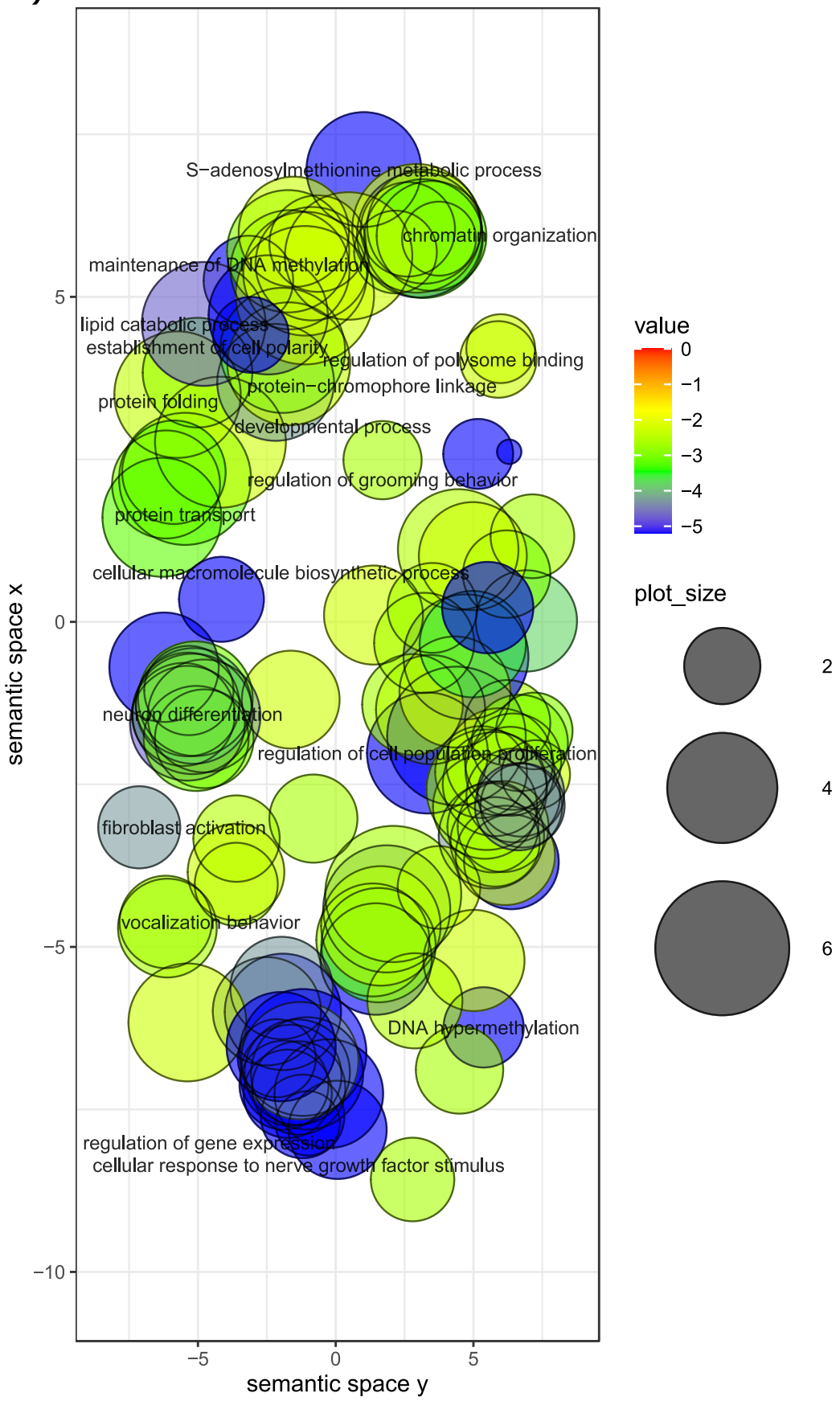
S−adenosylmethionine metabolic process
chromatin organization
maintenance of DNA methylation
lipid catabolic process
establishment of cell polarity
regulation of polysome binding
protein−chromophore linkage
protein folding
developmental process
regulation of grooming behavior
protein transport
cellular macromolecule biosynthetic process
neuron differentiation
regulation of cell population proliferation
fibroblast activation
vocalization behavior
DNA hypermethylation
regulation of gene expression
cellular response to nerve growth factor stimulus
semantic space x
semantic space y
5
0
−5
−10
−5
0
5
value
0
−1
−2
−3
−4
−5
plot_size
2
4
6

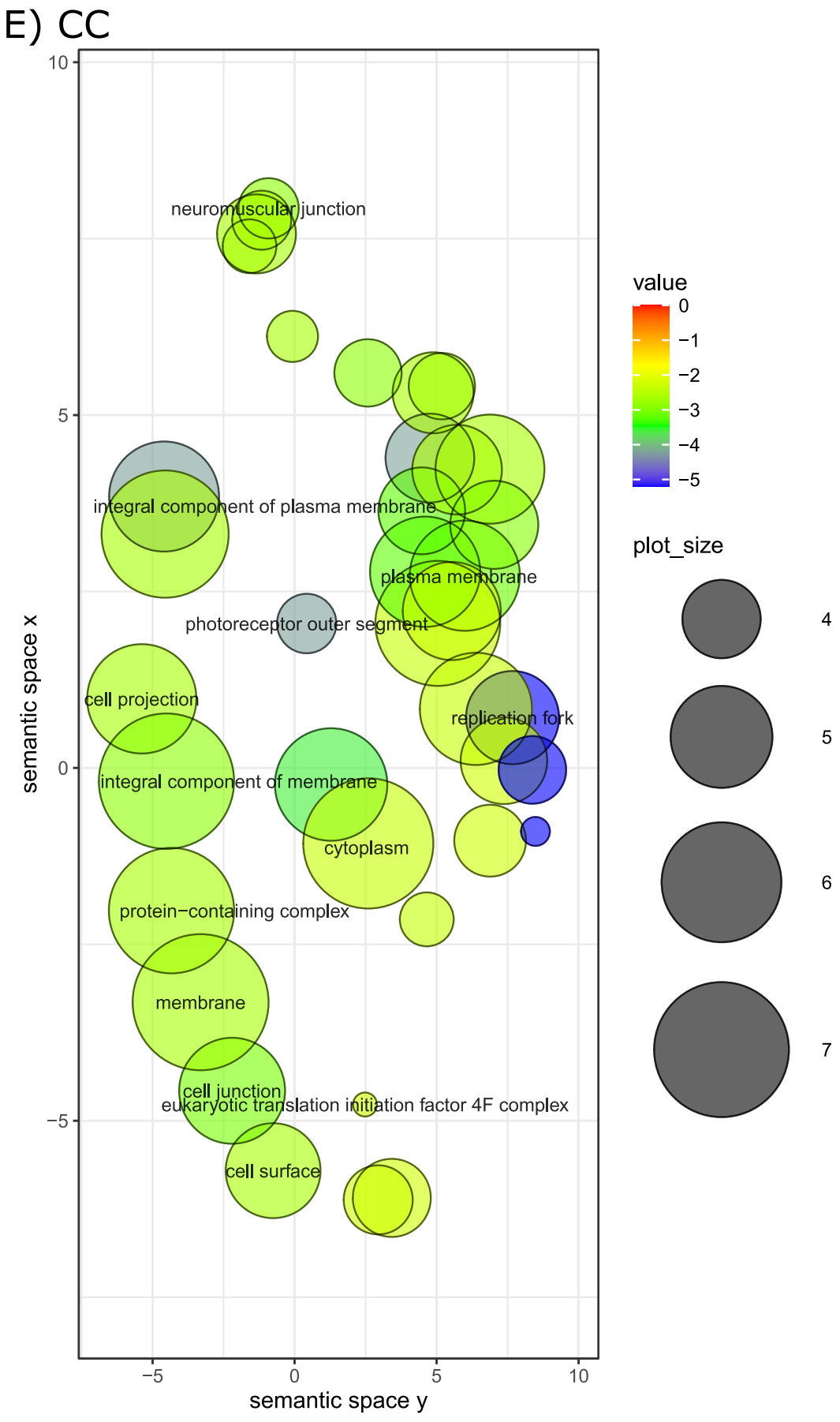
E) CC
neuromuscular junction
integral component of plasma membrane
plasma membrane
photoreceptor outer segment
cell projection
replication fork
integral component of membrane
cytoplasm
protein−containing complex
membrane
cell junction
eukaryotic translation initiation factor 4F complex
cell surface
semantic space x
semantic space y
10
5
0
−5
−5
0
5
10
value
0
−1
−2
−3
−4
−5
plot_size
4
5
6
7

F) MF

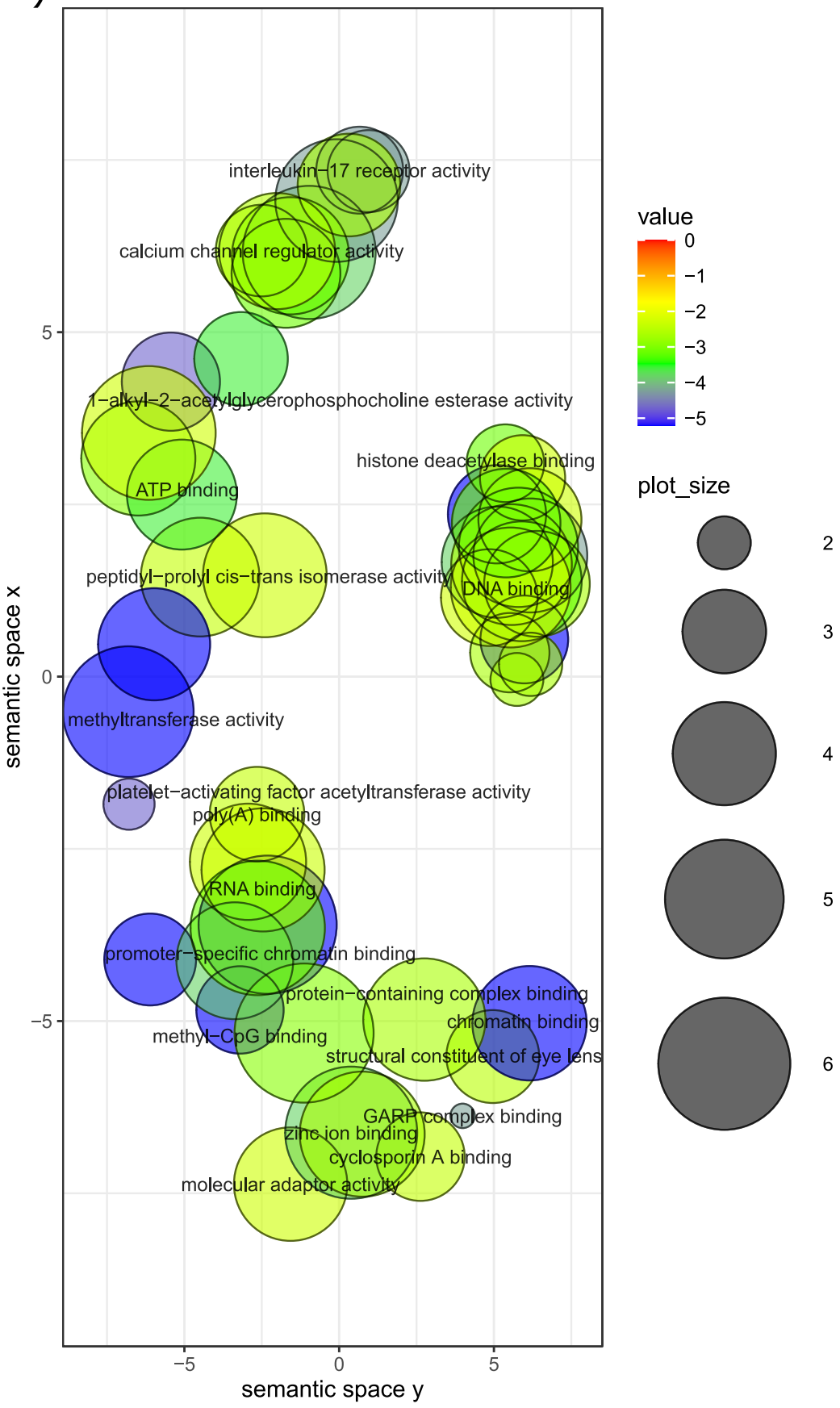
interleukin−17 receptor activity
calcium channel regulator activity
1−alkyl−2−acetylglycerophosphocholine esterase activity
histone deacetylase binding
ATP binding
peptidyl−prolyl cis−trans isomerase activity
DNA binding
methyltransferase activity
platelet−activating factor acetyltransferase activity
poly(A) binding
RNA binding
promoter−specific chromatin binding
protein−containing complex binding
chromatin binding
methyl−CpG binding
structural constituent of eye lens
GARP complex binding
zinc ion binding
cyclosporin A binding
molecular adaptor activity
semantic space x
semantic space y
5
0
−5
−5
0
5
value
0
−1
−2
−3
−4
−5
plot_size
2
3
4
5
6

Supplementary figure 4.4. Scatterplots of enriched GO terms in spleen. DEGs generated between Control and LPS - (A) BP, B) MF and C) CC) (FDR < 0.05) - and between Control and Poly I:C - D) BP, E) MF and F) CC) (FDR < 0.001). The size of plots represents relative abundance (as a percentage of all DEGs from each category) and the colour gradient represents values of log10 (p-value).

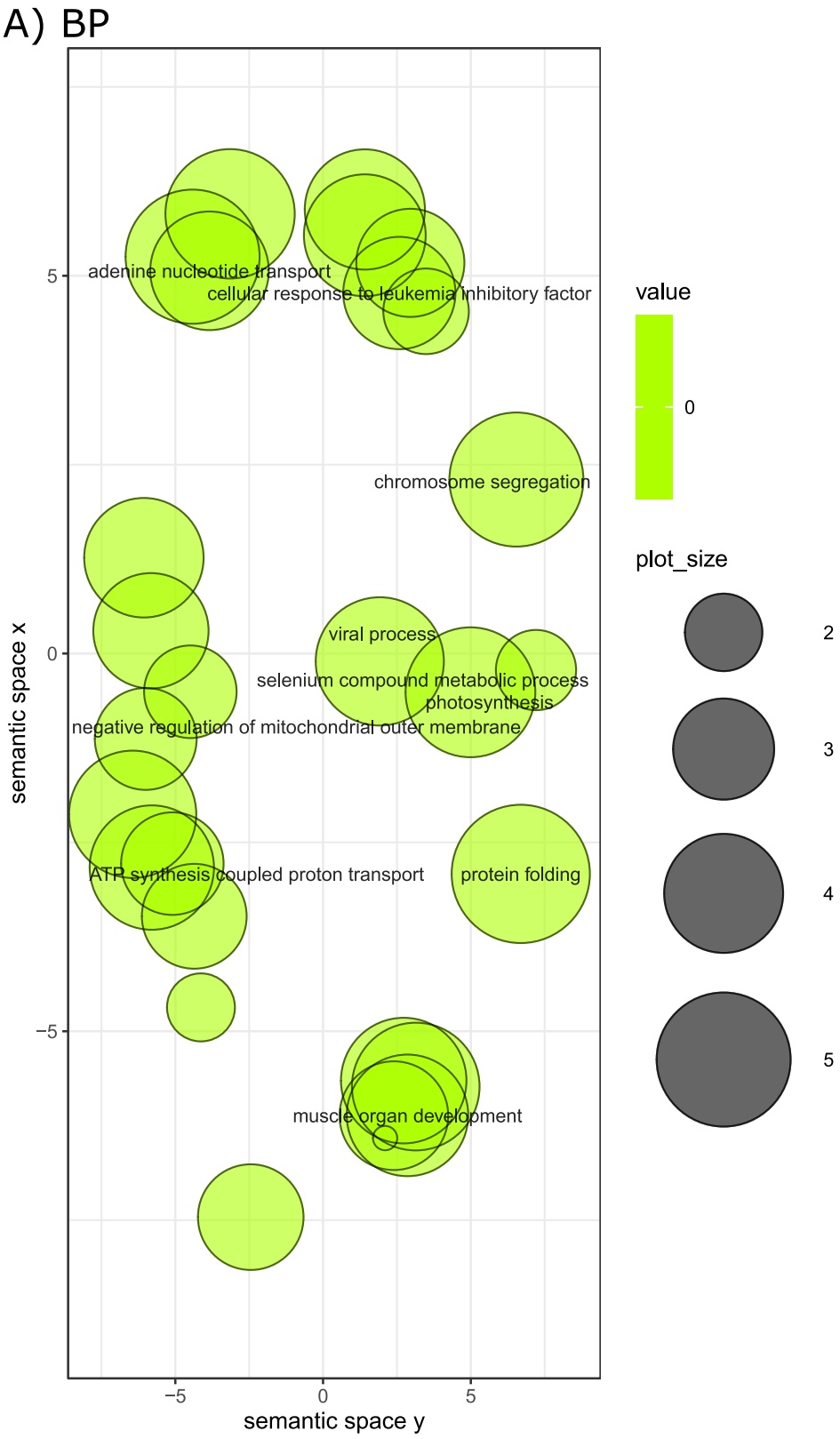

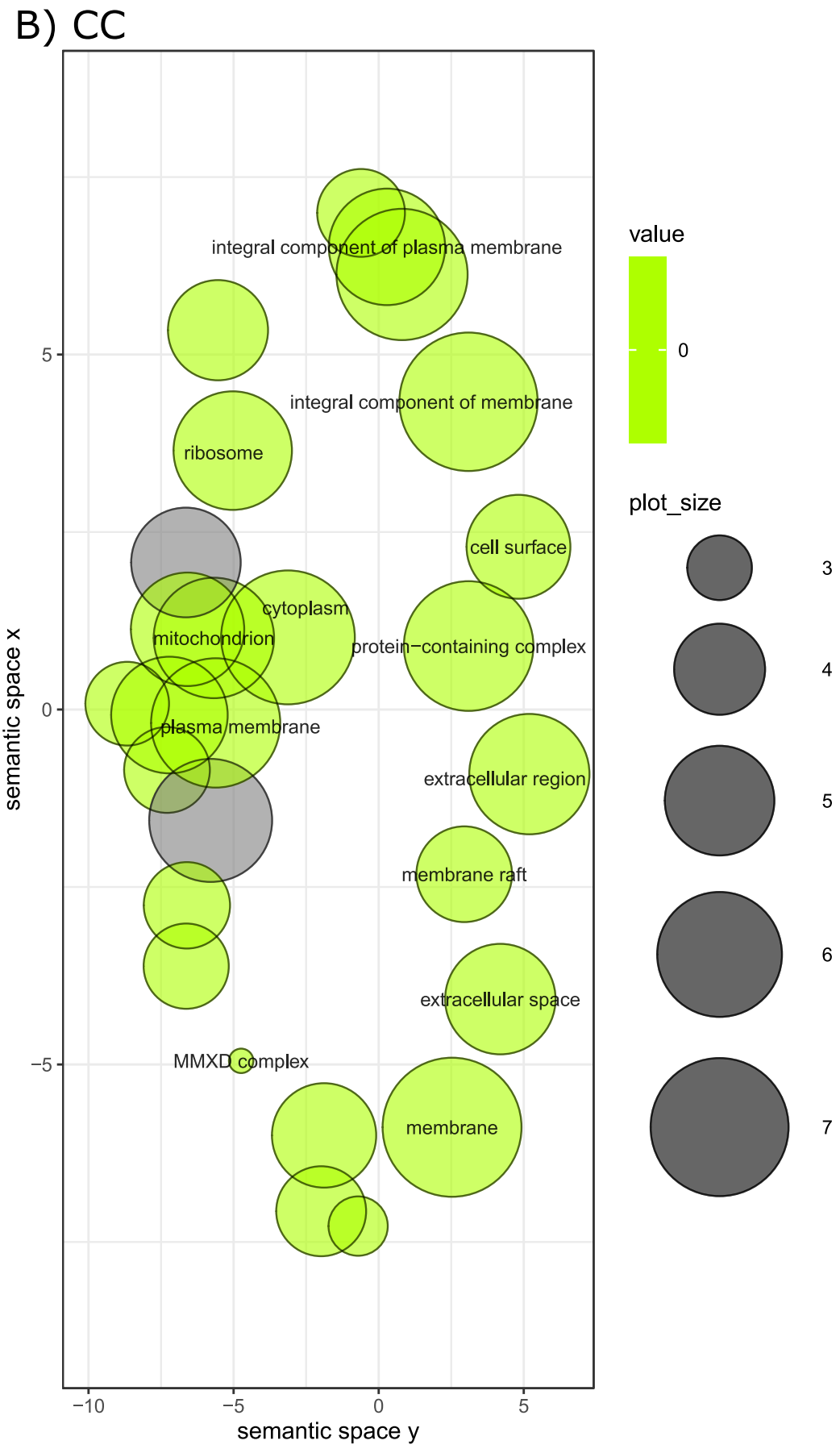
B) CC
integral component of plasma membrane
integral component of membrane
ribosome
cell surface
cytoplasm
mitochondrion
protein−containing complex
plasma membrane
extracellular region
membrane raft
extracellular space
MMXD complex
membrane
semantic space x
semantic space y
5
0
−5
−10
−5
0
5
value
0
plot_size
3
4
5
6
7

C) MF

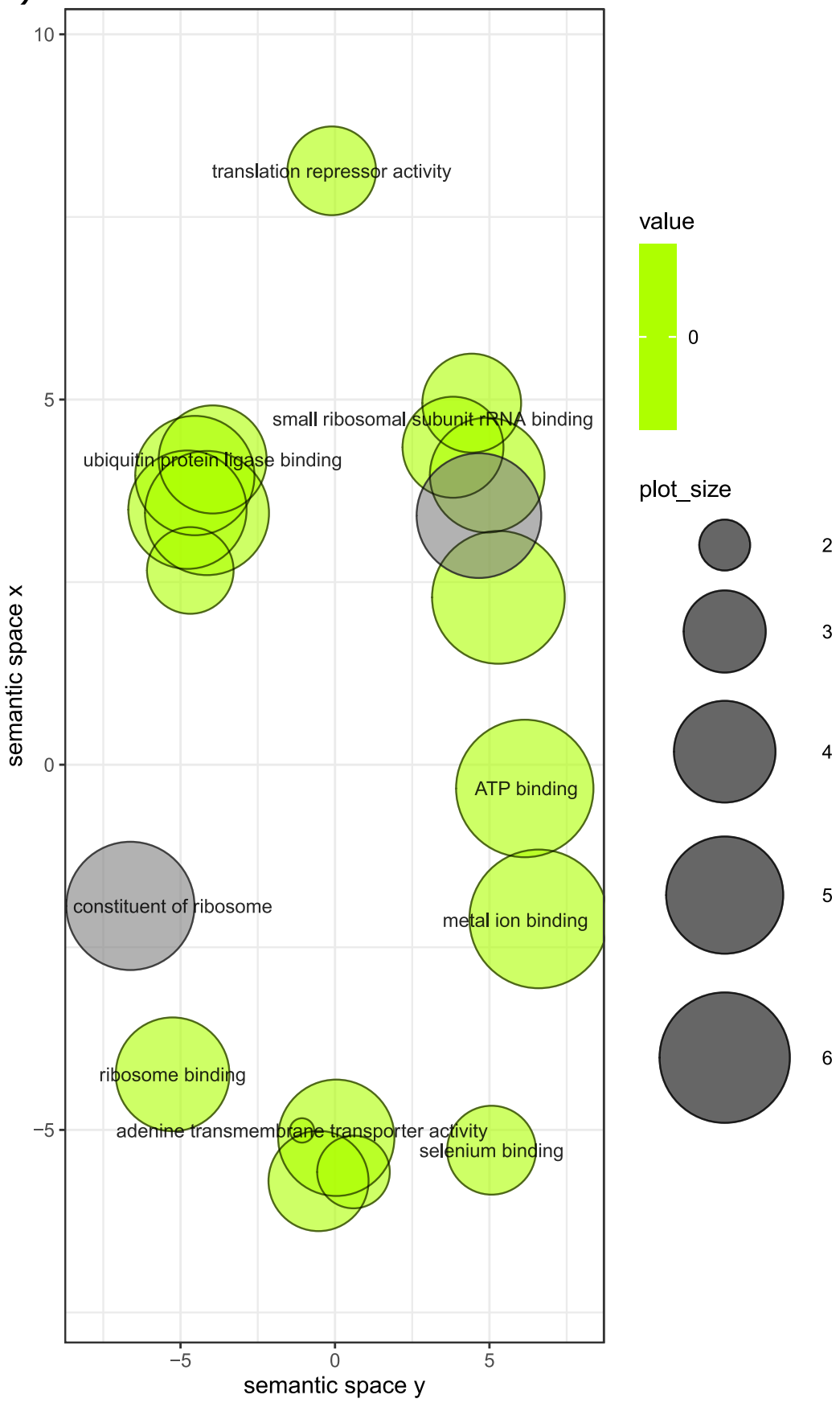
translation repressor activity
small ribosomal subunit rRNA binding
ubiquitin protein ligase binding
ATP binding
constituent of ribosome
metal ion binding
ribosome binding
adenine transmembrane transporter activity
selenium binding
semantic space x
semantic space y
10
5
0
−5
−5
0
5
value
0
plot_size
2
3
4
5
6

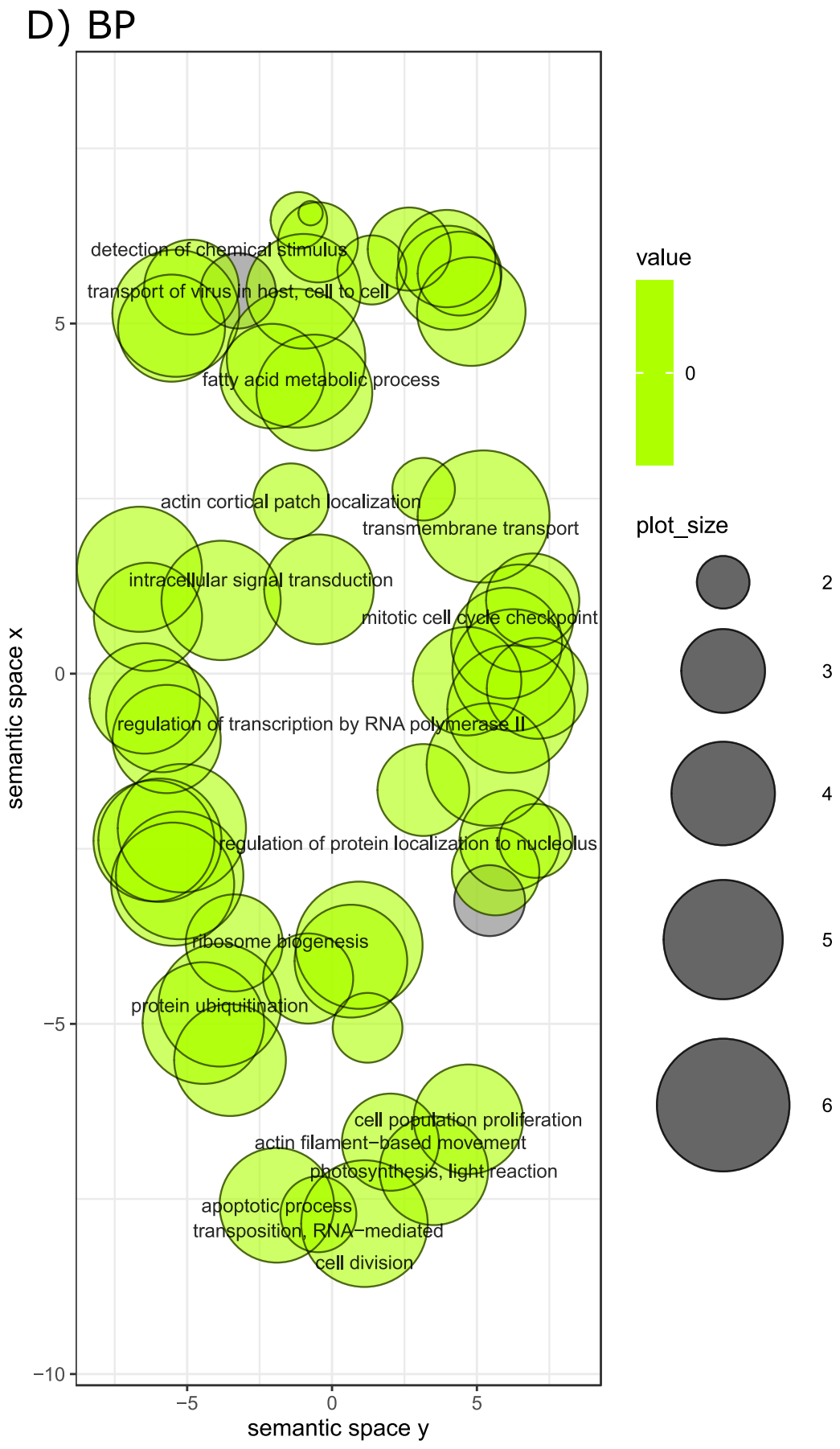
D) BP
detection of chemical stimulus
transport of virus in host, cell to cell
fatty acid metabolic process
actin cortical patch localization
transmembrane transport
intracellular signal transduction
mitotic cell cycle checkpoint
regulation of transcription by RNA polymerase II
regulation of protein localization to nucleolus
ribosome biogenesis
protein ubiquitination
cell population proliferation
actin filament−based movement
photosynthesis, light reaction
apoptotic process
transposition, RNA−mediated
cell division
semantic space x
semantic space y
5
0
−5
−10
−5
0
5
value
0
plot_size
2
3
4
5
6

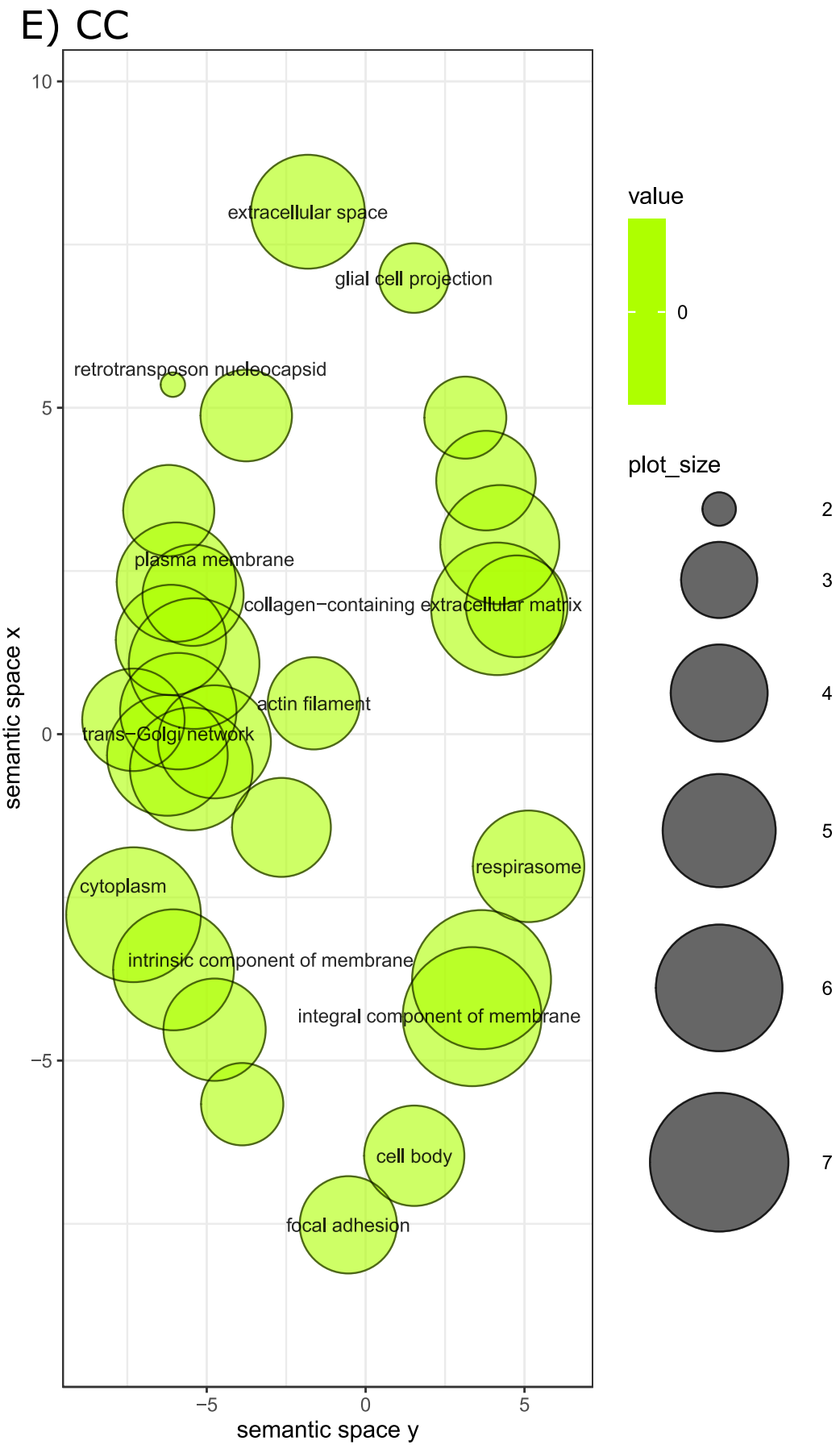
E) CC
extracellular space
glial cell projection
retrotransposon nucleocapsid
plasma membrane
collagen−containing extracellular matrix
actin filament
trans−Golgi network
respirasome
cytoplasm
intrinsic component of membrane
integral component of membrane
cell body
focal adhesion
semantic space x
semantic space y
10
5
0
−5
−5
0
5
value
0
plot_size
2
3
4
5
6
7

F) MF

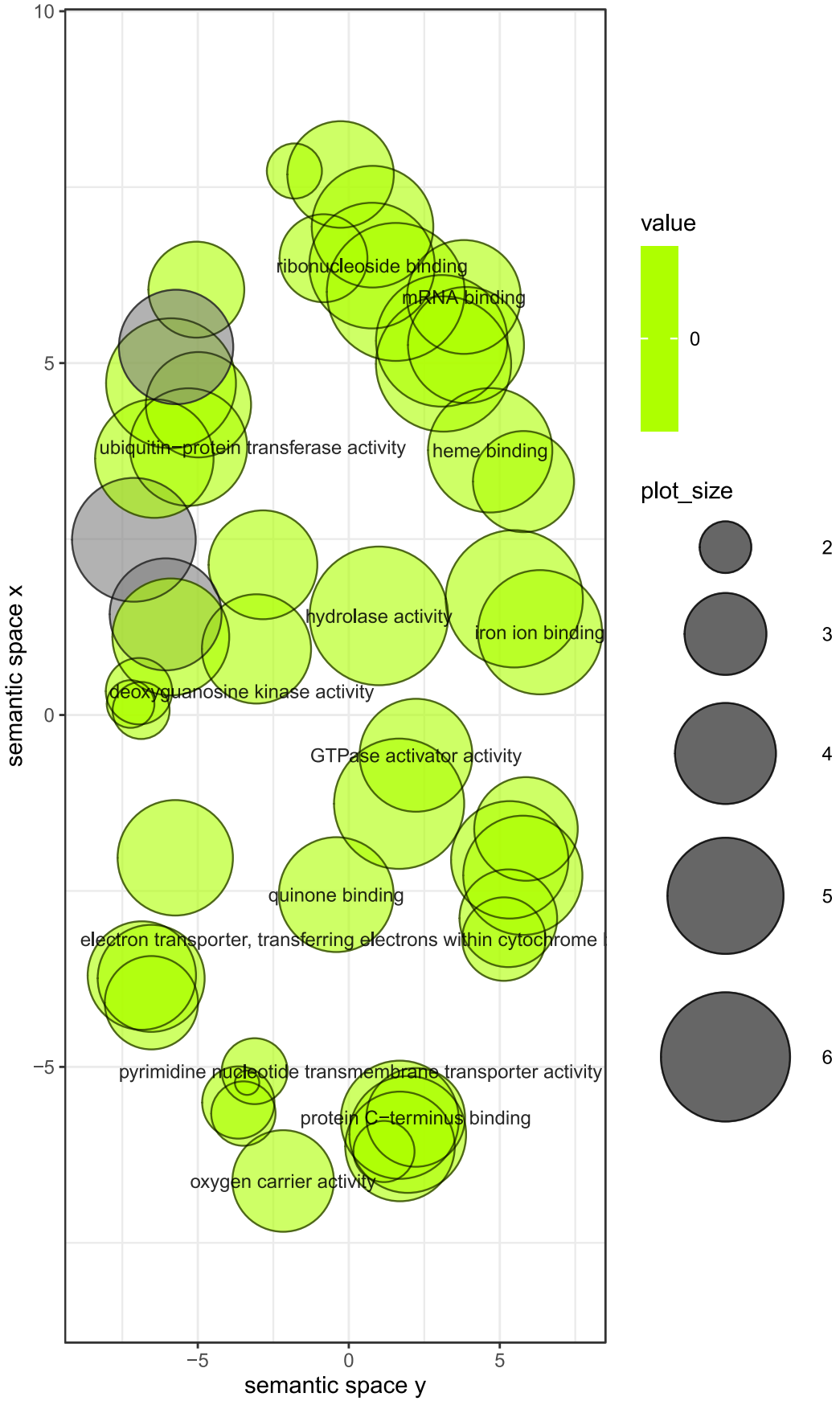
ribonucleoside binding
mRNA binding
ubiquitin−protein transferase activity
heme binding
hydrolase activity
iron ion binding
deoxyguanosine kinase activity
GTPase activator activity
quinone binding
electron transporter, transferring electrons within cytochrome
pyrimidine nucleotide transmembrane transporter activity
protein C−terminus binding
oxygen carrier activity
semantic space x
semantic space y
10
5
0
−5
−5
0
5
value
0
plot_size
2
3
4
5
6

Supplementary figure 4.5. Scatterplots of enriched GO terms in liver. DEGs generated between Control and LPS - (A) BP, B) MF and C) CC) (FDR < 0.05) - and between Control and Poly I:C - D) BP, E) MF and F) CC) (FDR < 0.001). The size of plots represents relative abundance (as a percentage of all DEGs from each category) and the colour gradient represents values of log10 (p-value).

CHAPTER 5

Microbiome diversity and response to a bacterial endotoxin in two Antarctic Notothenioids

Microbiome diversity and response to a bacterial endotoxin in two Antarctic Notothenioids

Manuscript in preparation

Acknowledgements

The authors would like to acknowledge the 2019 crew of the Great Wall Chinese Antarctic Station for their hospitability and logistical support. This study was carried out with logistic and financial support of the Portuguese Polar Programme (FACC PROPOLAR 2016-2017) and funded by Portuguese Foundation for Science and Technology (FCT) through projects FCT-NSFC/0002/2016, PTDC/BIAANM/3484/2014 and CCMAR/Multi/04326/2019, and a PhD fellowship SFRH/BD/120040/2016 to CS.

Microbiome diversity and response to a bacterial endotoxin in two Antarctic Notothenioids

Cármen Sousa[1], Wanying Zhai[2], Pedro Guerreiro[1], Liangbiao Chen[2], Deborah Power[1,2] and Adelino Canário[1,2]

[1]Centro de Ciências do Mar (CCMAR), Universidade do Algarve, Campus de Gambelas, 8005-139 Faro, Portugal.

[2]International Research Center for Marine Biosciences, Ministry of Science and Technology and Key Laboratory of Exploration and Utilization of Aquatic Genetic Resources, Ministry of Education, Shanghai Ocean University, Shanghai, China

5.1. Abstract

The perciform suborder Notothenioidei dominates the fish fauna in the Southern Ocean constituting 90% of biomass and has developed specific physiological characteristics adapted to the stable and cold-extreme environment of Antarctica. The gut microbiome protects and defends against potential pathogens but can also have digestive and nutritional functions, but it has been little studied among Notothenioids. In the present study, the microbial community of the skin and gut of the Notothenioids *N. coriiceps* and *N. rossii* was established and the impact of the bacterial endotoxin LPS and temperature on microbial richness was determined using 16S rRNA gene sequencing. As a result, 136,422 sequences were obtained from seawater, 772,334 from 16 fish soon after capture and 2,252,395 from 48 fish maintained in tanks at least for 3 days. Proteobacteria, Cyanobacteria, Firmicutes, Fusobacteria and Bacteroidetes were identified as the dominant phyla irrespective of condition, genera such as *Allivibrio*, *Mycoplasma*, *Photobacterium* and *Cetobacerium* were responsive to LPS and temperature. The number of common operational taxonomic units (OTUs) varied from 1 to 1935 in recently caught fish samples and 1 to 145 in captive fish samples, while the unique OTUs varied from 23 to 998 and 31 to 130, respectively. Overall, our findings indicate that captivity, bacterial LPS and increased temperature, impact the bacterial community composition in the two tissues of the two species studied. This study highlights the importance of the environment and physiology on bacterial microbiota diversity.

Keywords: microbiome, Antarctic fish, environmental factors, cold-water, mucosa-associated lymphoid tissues

5.2. Introduction

Microbes have a vital function in all ecosystems. They regulate global biogeochemical cycles and are crucial for ecosystem stability (Logares et al., 2020). The diversity and abundance of microbial communities in the aquatic environment depends on abiotic factors such as temperature, pH, salinity and oxygen (Bierlich et al., 2018; Butt and Volkoff, 2019; Mayer et al., 2015; Merrifield and Rodiles, 2015) and biotic factors such as food and pollutants (Kokou et al., 2018; Walburn et al., 2019; Xia et al., 2014). In mammals it is clear that both innate and acquired immunity are directly linked to commensal bacteria which are important for host fitness and survival and perturbations in meta-community structure can lead to pathologies (Logares et al., 2020; Sunagawa et al., 2015). However, meta-analysis of immune function and microbiome composition, diversity, function, and ecological determinants in different ecosystems remain a challenge, especially in polar regions.

The teleost fishes possess a complex microbial community (bacteria, viruses, fungi, and other eukaryotes) originated from the aquatic environment, and immunity is highly associated to mucosal surfaces (mucosa-associated lymphoid tissues, MALT) where microbes thrive (Gomez et al., 2013; Rauta et al., 2012). The mucosal surfaces include the skin, gut, and gills and represent important physical and chemical barriers covered by a mucus layer that contains cellular and humoral components (Gomez et al., 2013; Rauta et al., 2012). However, in teleosts, including those important for aquaculture, the microbiome is poorly understood (Llewellyn et al., 2014; Sunagawa et al., 2015) despite its likely importance in the maintenance of healthy host physiology and immune processes (Belkaid and Hand, 2014; Llewellyn et al., 2014).

The Southern Ocean is dominated by the perciforms from the suborder Notothenioidei. These fishes evolved from a common benthic ancestor and radiated in eight different families over approximately the past 10 million years (Eastman, 2000, 2005). Several morphological and physiological features that resulted from their adaptation to the Antarctic environment are shared between the different Notothenioidei family members, such as antifreeze glycoproteins, the absence of a swim-bladder, the lack of the heat-shock protein response, low bone density

and higher mitochondrial density. Other family specific adaptations include the lack of haemoglobin, increased capillary number and increased heart volume in the Channichthyidae (Auvinet et al., 2020; Matschiner et al., 2015). In contrast, relatively little is known about their microbial richness and diversity and how this has been modulated by the Southern Ocean conditions. A recent study identified a common core of bacterial communities dominated by Actinobacteria, Proteobacteria, Firmicutes, Thermi and Bacteroidetes shared between the gut microbiomes of different Notothenioidei (*C. hamatus*, *T. bernacchii*, *G. acuticeps* and *P. borchgrevinki*) (Song et al., 2016). In the same study, differences in microbial populations between the gut of Notothenioids that inhabit the surface (between 1-2 m of depth) and deeper waters (more than 100 m of depth) was found (Song et al., 2016).

The main objective of this study was to understand microbial diversity and abundance in two Notothenioid species, *Notothenia coriiceps* which is more sedentary and *Notothenia rossii*. Overfishing of *N. rossii* in the 1970's led to a population collapse which is now recovering. Although both species are classified as semipelagic, *N. coriiceps* prefers coastal waters while *N. rossii* is fairly cosmopolitan and moves offshore (Barrera-Oro et al., 2019). We characterized the microbiome of the skin-associated lymphoid tissue (SALT), and the gut-associated lymphoid tissue (GALT using 16S rRNA and next-generation sequencing. The impact of immunostimulation with bacterial lipopolysaccharide (LPS) and temperature challenge on SALT and GALT microbiota was evaluated in *N. rossii* only.

5.3. Methods

5.3.1. Fish capture and experiments

N. coriiceps (30.4 ± 0.53 cm of length and 384.4 ± 20.38 g of weight) and *N. rossii* (30 ± 4.2 cm of length and 312 ± 124.7 g of weight) were captured by hook-and-line near the Chinese Great Wall Station in King George Island (GPS coordinates: 62°13′S, 58°58′W), in the Antarctic Peninsula, during January and February of 2017. Seawater (10 L) for microbiome analysis was simultaneously collected just below the surface from the same location and taken to the laboratory where it was filtered (0.2 µm pore size, VWR, Portugal) using a vacuum pump.

Fish were maintained in 200 L plastic containers for a maximum of two hours after capture with regular water renewal to maintain natural high oxygen and low temperature until they arrived at the laboratory. At the laboratory 4 individuals (n=4) from each species were anesthetized with phenoxyethanol (0.02 ml/L, Sigma-Aldrich) measured, weighed, and sacrificed by cervical section. These fish were designated "wild" and their mucus of SALT and GALT was collected aseptically and preserved in RNAlater at 4ºC for 24 h followed by storage at -20ºC until extraction for microbiome studies.

The remaining *N. rossii* were placed in 200 L plastic tanks to acclimate for 3-5 days in a flow-through system fed with continuously pumped ocean seawater at 2ºC and were fed daily with limpets and/or fish muscle. The experiment was setup to test the effect of the immunostimulant LPS (from *E. coli* O111:B4, Sigma-Aldrich, Portugal) on the microbiome and the interactive effect of increased seawater temperature. Two days before the experiment, fish were measured, weighed, tagged with opercular self-piercing clamp tags and divided into four groups of fish of similar sizes (n=4 per group). The immune challenge consisted of two intraperitoneal (i.p.) injections at day 0 and day 2 with either 1) 0.2% (v/w) of 1.1% NaCl (control group) or 2) 0.2% (v/w) of LPS (1.5mg/ml) dissolved in 1.1% NaCl, to an effective dose of 3 mg/kg. Both groups were maintained at 2.1 ± 0.5 ºC. In parallel, two other groups of control and LPS-challenged fish, previously acclimated to increased temperature (at 1ºC/day), were maintained at 6.0 ± 0.8ºC. The tanks were monitored three times a day (7 am, 2 pm and 9 pm). Salinity was 29 ± 0.5 ppt and oxygen levels were 10.7 ± 0.4 mg/L and 9.3 ± 0.9 mg/L in the 2 ºC and 6ºC groups, respectively. At day 7, fish were anesthetized, sacrificed by cervical section and disruption of the CNS, and mucus from the SALT and GALT collected aseptically for microbiome studies. All samples were preserved in RNA later for 24 h at 4ºC and stored at -20ºC.

5.3.2. DNA Extraction

Total DNA was extracted from 50 mg of the filtered seawater and mucous collected from the SALT or GALT using a DNeasy Blood & Tissue kit (Qiagen, Germany), following the manufacturer's instructions. Enzyme lysis buffer (20mM Tris-HCl pH 8; 2mM sodium EDTA, Sigma-Aldrich, Portugal) and lysozyme (40 mg/ml, Biochemica, Spain) was added to the lysis buffer solution before mechanical lysis of the samples with silica beads (0.1mm,

Werfen, Spain) in a TissueLyser II (Qiagen) for 2 x 5 min, 30 Hz frequency. The DNA pellets were dissolved in Tris-HCl, pH 8 (Sigma-Aldrich) and stored at -20℃. DNA was quantified at 260 nm and 280 nm using a NanoDrop (ThermoFisher, USA) and the quality was assessed by electrophoresis on 1% agarose/TAE gel and using Picrogreen QC (ThermoFisher) and a spectrofluorometer (GeneQuant, TermoFisher).

5.3.3. PCR Amplification and Sequencing

A KAPA HiFi PCR kit (Roche, Switzerland) was used to prepare 48 paired-ended libraries of the SALT and GALT mucous samples and 1 library of bacterial V3-V4 regions of the seawater sample. The SALT and GALT mucous samples were sequenced using an Illumina Miseq v3 platform and the amplicon 16S rRNA and generated paired end reads of 300 base pairs (bp) in length (Laragen, USA). The water sample was sequenced using an Illumina Miseq v2 and 16S rRNA Floracheck with paired end reads of 250 bp (Admera, USA). The pass-filter PE reads per sample was around 50k.

5.3.4. Data Analysis and Statistics

The raw FASTQ files were checked for quality using Trimmomatic (Bolger et al., 2014) and merged by FLASH (Magoč and Salzberg, 2011) with the following criteria: (i) the reads were truncated at any site receiving an average quality score <20 over a 50 bp sliding window, (ii) overlap sequences > 10 bp with mismatch < 2 bp were merged, (iii) the raw data from each sample were separated according to their barcodes (exactly matching) and primers (allowing 2 nucleotide mismatches) and (iv) reads containing ambiguous bases were removed. The operational taxonomic units (OTUs) were classified and clustered with a cut-off of 97% similarity using UPARSE v. 7.0.1090 that filtered chimeras and simultaneously clustered OTU's (Edgar, 2013). The taxonomic affiliation of each 16S rRNA sequence was assigned using the Ribosomal Database Project (RDP) classifier algorithm v. 2.11 (Wang et al., 2007) against the SILVA ribosomal RNA database (16S_bacteria) (Quast et al., 2013) with a confidence threshold of 70%. OTU abundance between the two tissues and two species was compared using a Pearson chi-squared test. A nonparametric Kruskal-Wallis test was used to

compare the variance of bacterial community samples at the genus level between the two tissues, different treatments and the two species with a stress threshold value < 0.2 using the unweighted UniFrac algorithm (Lozupone and Knight, 2005) on the Majorbio Cloud Platform (www.i-sanger.com). The significance level was set at 5%.

Subsequent analyses of alpha and beta microbial diversity were performed on the normalized data output and using the Shannon diversity index (Lemos et al., 2011; Magurran, 2004) and the Simpson´s index (Lemos et al., 2011; Simpson, 1949) to estimate diversity, and the abundance-based coverage estimator (ACE) (Chao and Lee, 1992; Chao and Yang, 1993) and the Chao1 abundance estimator (Chao, 1984) to estimate community richness using Mothur v1.43.0 (Schloss, 2020; Schloss et al., 2009) hosted on the Majorbio Cloud Platform (www.i-sanger.com). A Venn Diagram was used to determine the bacterial community groups that are common and differ between the two fish species and in the different experimental treatments. A Heatmap was generated to represent the magnitude of the response in bacterial abundance at a community genus level (OTUs top < 50) using the Majorbio Cloud Platform. Non-metric multidimensional scaling (NMDS) was performed to represent the original position of different microbial communities in a multidimensional space and to show the diversity between the different tissues, species and treatments (LPS and temperature). A stress level < 0.2 indicates a good representation of samples diversity in reduced dimensions and a stress level > 0.3 indicates poor representation.

5.4. Results

5.4.1. General features of sample sequences

After quality filtering, a total of 136,442 reads containing 61.3 Mb with an average contig length of 449 bp were obtained from the seawater sample. For the 16 SALT and GALT samples of "wild" *N. coriiceps* and *N. rossii*, a total of 772,339 reads containing 286.4 Mb with an average length of 371 bp were obtained. For the 48 SALT and GALT samples of LPS and temperature treated *N. rossii* a total of 2,252,395 reads containing 1.037Gb with an average length of 461 bp were obtained. Overall, the alpha and beta diversity analysis indicated a good

representation of the richness and bacterial community diversity using a 97% similarity threshold.

5.4.2. Evaluation of the microbial complexity and microbial composition in two Notothenioids

5.4.2.1. Seawater and "Wild" SALT and GALT

Annotation of the seawater samples revealed a microbiome belonging to one kingdom with 4 phyla, 5 classes, 14 orders, 18 families, 29 genus, 37 species and 43 OTU. The microbial complexity of the "wild" SALT and GALT samples was also contained in one kingdom, but the diversity was higher than seawater, covering 21 phyla, 38 classes, 84 orders, 132 families, 200 genus, 244 species and 5886 OTU (**Figure 5.1 A**). The seawater sample rarefaction curves showed a saturation plateau at 100k reads and in the "wild" SALT and GALT samples the plateau was reached between 15k and 72k reads (**Figure 5.1 B**). The OTU classification ($p < 0.01$) revealed that the most represented annotated phyla in seawater were Bacteroidetes (44%), Proteobacteria, (35%) and Cyanobacteria (20%). In addition, the most abundant annotated genera were related to *Polaribacter_1* (~1%) and *Sulfitobacter* (1%).

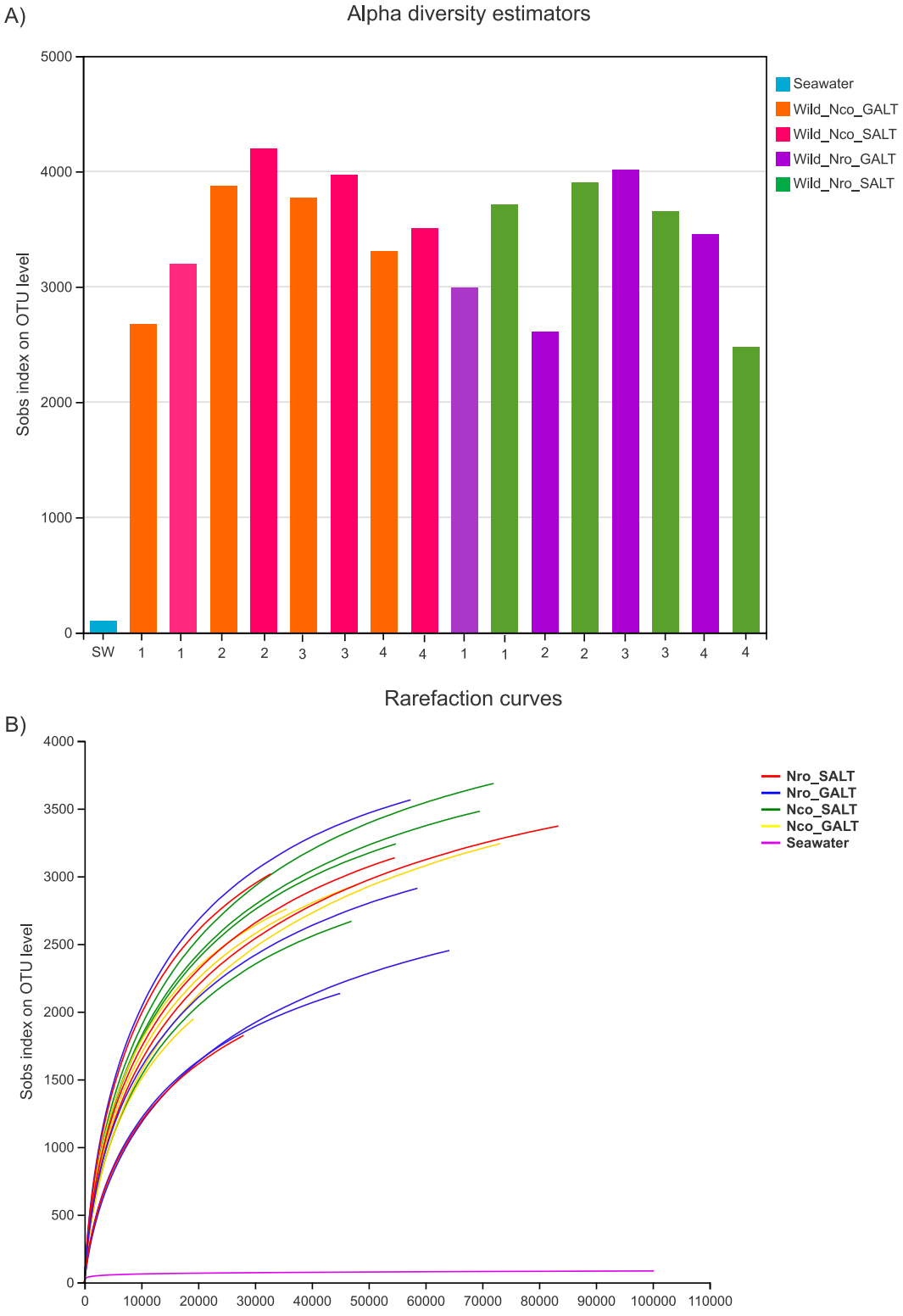

Figure 5.1. Bacterial community A) Alpha diversity and B) rarefaction curves. Bacteria were collected from seawater, and from gut-associated lymphoid tissue (GALT) and skin-associated lymphoid tissue (SALT) of recently captured *N. coriiceps* (Nco) and *N. rossii* (Nro).

In *N. coriiceps*, the most abundant phyla in the skin (SALT) and duodenum (GALT) were Proteobacteria (~1%), Firmicutes (~0.8%) and Cyanobacteria (~0.3%) (**Figure 5.2 A**).

Allivibrio (~0.6%) and *Mycoplasma* (~0.5%) were the most abundant genera with *Mycoplasma* mostly present in the SALT (**Figure 5.2 B**). In *N. rossii* SALT and GALT, the most represented phyla were Proteobacteria (~18%), Fusobacteriota (~12%) and Firmicutes (~6%) (**Figure 5.2 A**) and the genera were *Photobacterium* (~14%), *Cetobacterium* (~12%), and *Allivibrio* (~7%), with *Cetobacterium* particularly abundant in GALT (**Figure 5.2 B**).

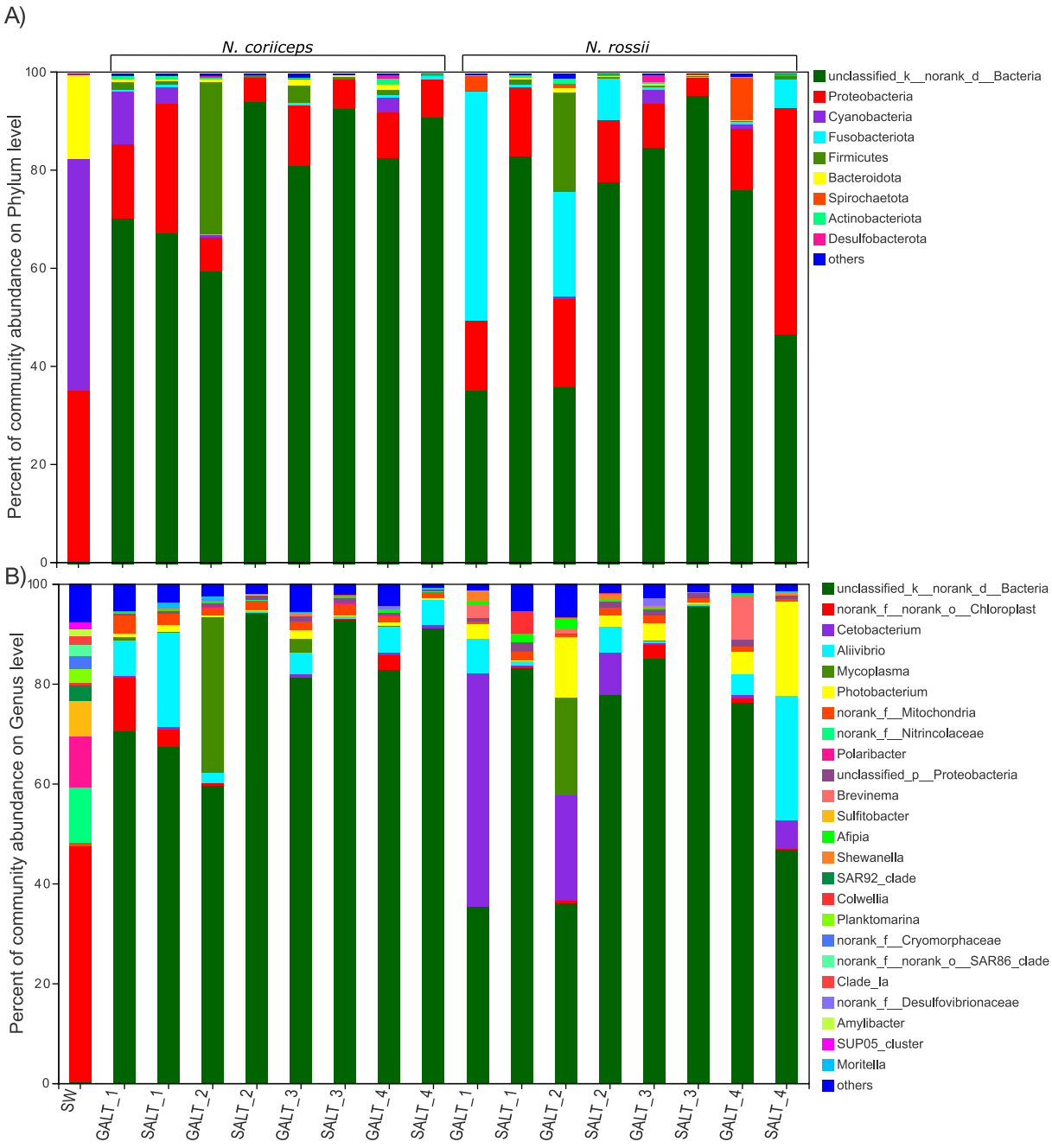

Figure 5.2. Bacterial community diversity - A) phyla and **B)** genus. Bacteria were collected from seawater (SW), and from gut-associated lymphoid tissue (GALT) and skin-associated lymphoid tissue (SALT) of wild *N. coriiceps* (Nco) and *N. rossii* (Nro).

The minimum number of shared bacterial communities between SALT and GALT of the two fishes and seawater sample is 1 (between seawater and GALT of *N. coriiceps*) and a maximum of 1935 (between SALT and GALT of both Notothenioids), and 17 shared bacterial communities between all (**Figure 5.3 A**). The SALT and GALT of *N. coriiceps* and *N. rossii*, shared 1275 OTU and 1428 out, respectively (**Figure 5.3 A**). The microbial composition between seawater and SALT and GALT from both Notothenioids differed (Pearson´s chi square test $p < 0.001$, **Table 5.1 A**). However, similar results were observed between GALT and SALT in the two fish species, except for *Colwellia* genus that was significantly increased in SALT of *N. rossii* based on Kruskal-Wallis test ($p < 0.05$, **Figure 5.3 B**). Overall, there were 23 unique bacterial communities in seawater, 686 in GALT and 990 in SALT of *N. coriiceps* while 998 and 868 were observed in GALT and SALT of *N. rossii* (**Figure 5.3 A**).

The heatmap clustering analysis confirmed the NMDS grouping and placed the seawater clearly separately from the fish samples (**Figure 5.4 A-B**). The GALT and SALT also clustered together which indicates similar overall bacterial composition with small differences between the fish individuals (**Figure 5.4 A-B**).

A)

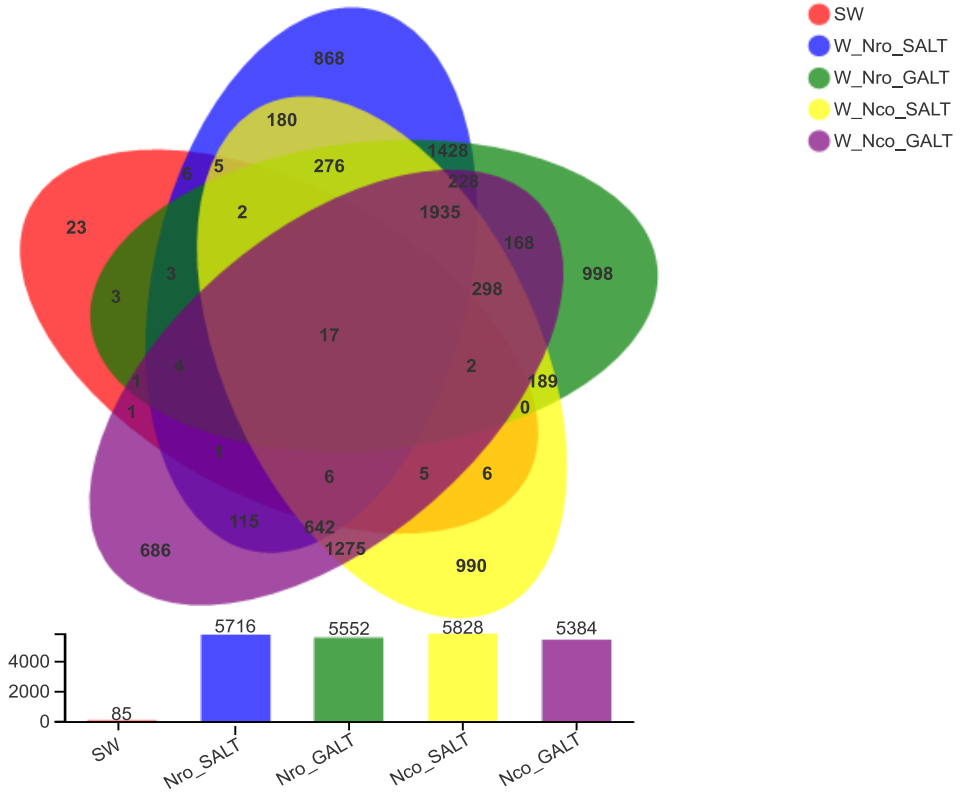

B)

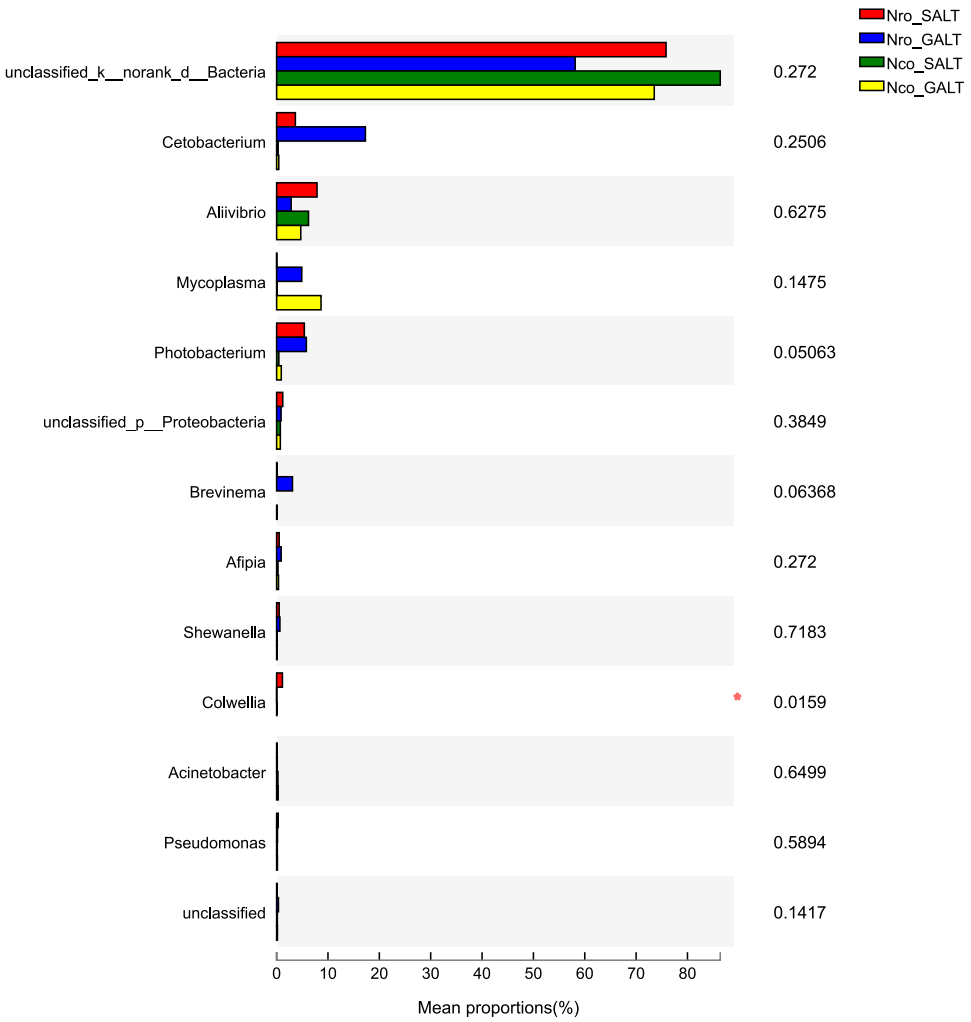

Figure 5.3. A) Venn diagram of bacterial community at OTU level and 2) relative abundance of genera. Bacteria were collected from seawater (SW), gut-associated lymphoid tissue (GALT) and skin-associated lymphoid tissue (SALT) of *N. coriiceps* (Nco) and *N. rossii* (Nro). Numbers on the right-hand side are probabilities following the Kruskal-Wallis H test and post hoc Dunn.

A) Community heatmap analysis on Genus level

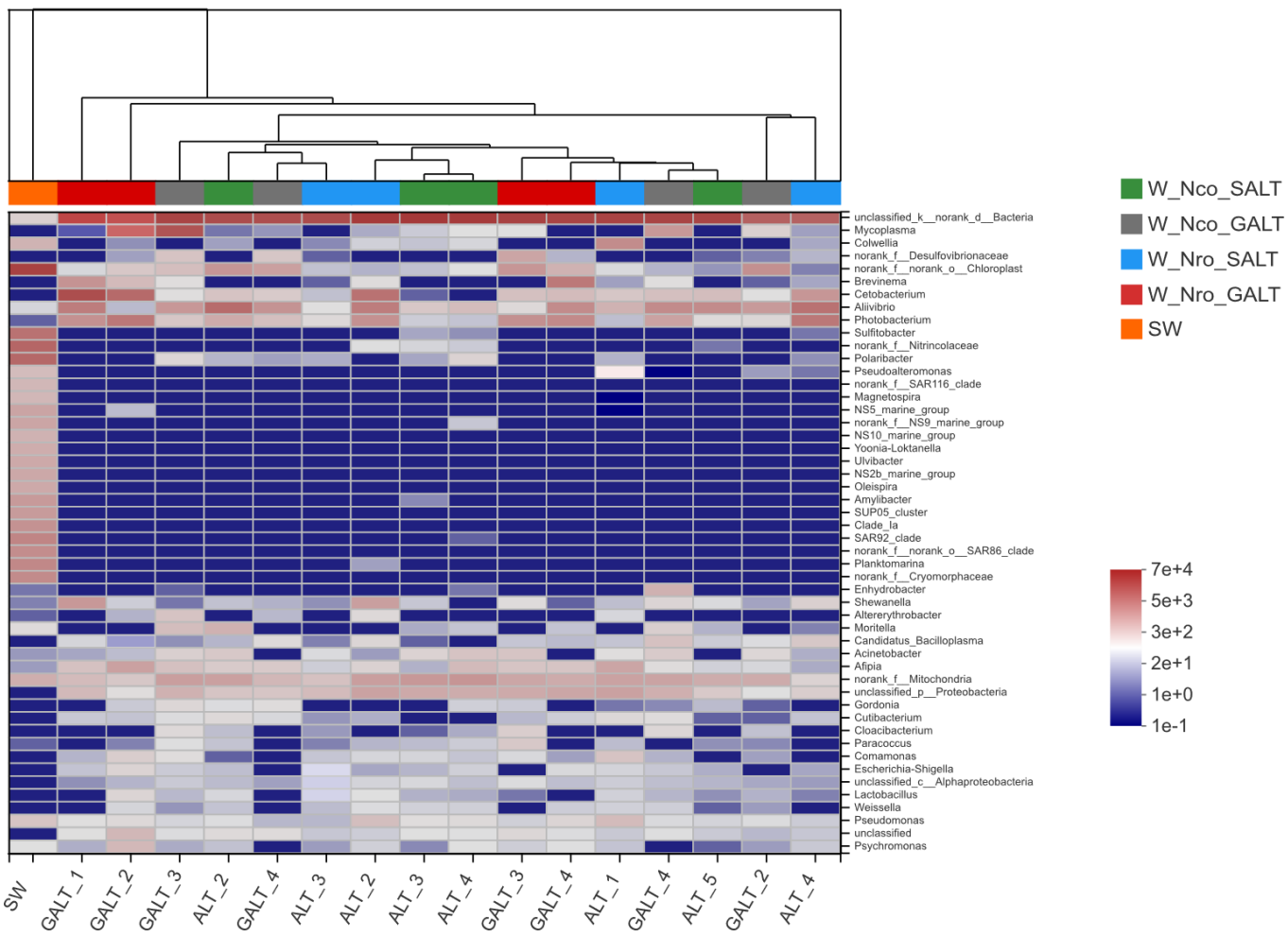

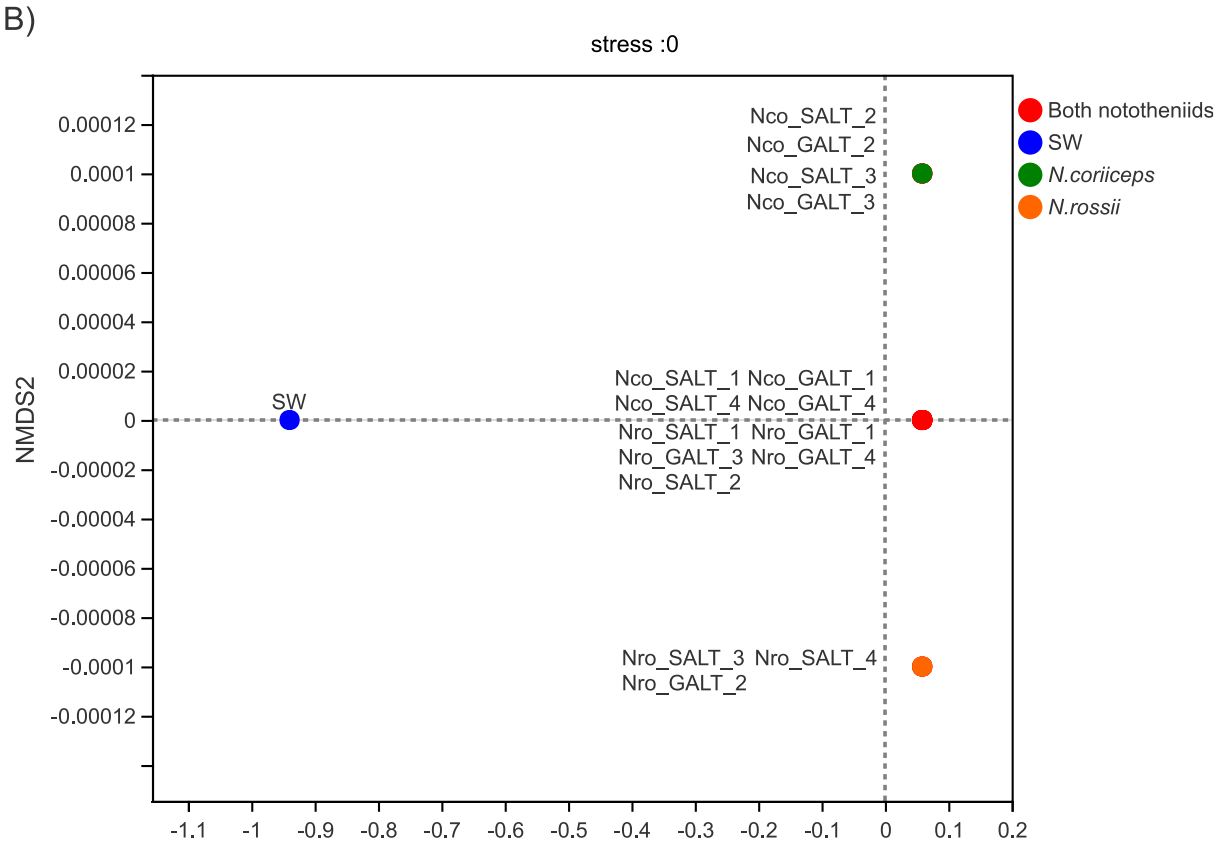

Figure 5.4. A) Heatmap and B) NMDS of bacterial community OTUs. Bacterial communities were collected from seawater (SW), in gut-associated lymphoid tissue (GALT) and skin-associated lymphoid tissue (SALT) of wild *N. coriiceps* (Nco) and *N. rossii* (Nro).

5.4.2.2. Immune and temperature challenged SALT and GALT

The bacterial complexity of the SALT and GALT in fish stimulated with LPS at 2ºC and 6ºC belonged to 2 kingdoms and was distributed between 20 phyla, 290 classes, 96 orders, 198 families, 402 genus, 543 species and 896 OTU. The alpha-diversity index at OTU level of GALT and SALT varied between 20 and 240 in *N. coriiceps* (**Figure 5.5 A**) and between 10 and 225 in *N. rossii* (**Figure 5.5 B**) indicating species richness of the same order of magnitude between the two species. The rarefaction curves for SALT and GALT in the Control, LPS and temperature experiment reached saturation at 12k reads (**Figure 5.5 C and 5.5 D**).

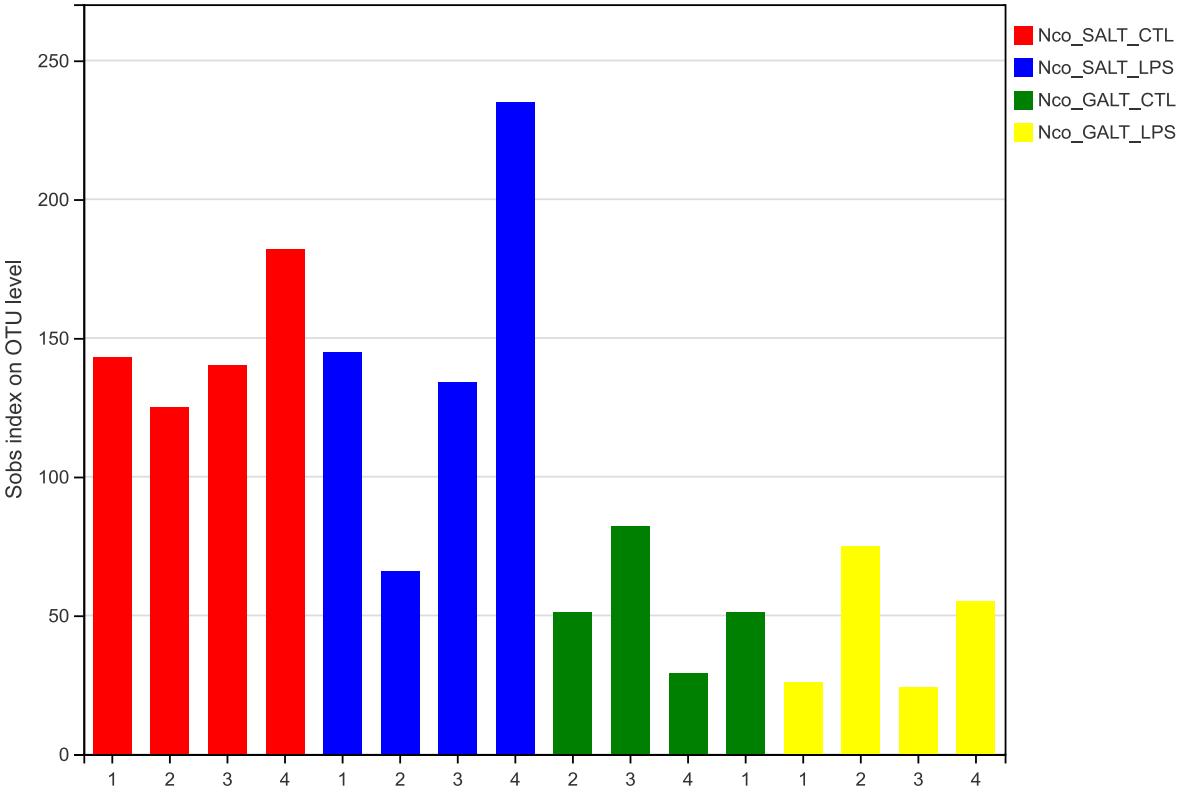
Sobs index on OTU level
0
50
100
150
200
250
1 2 3 4 1 2 3 4 2 3 4 1 1 2 3 4
Nco_SALT_CTL
Nco_SALT_LPS
Nco_GALT_CTL
Nco_GALT_LPS

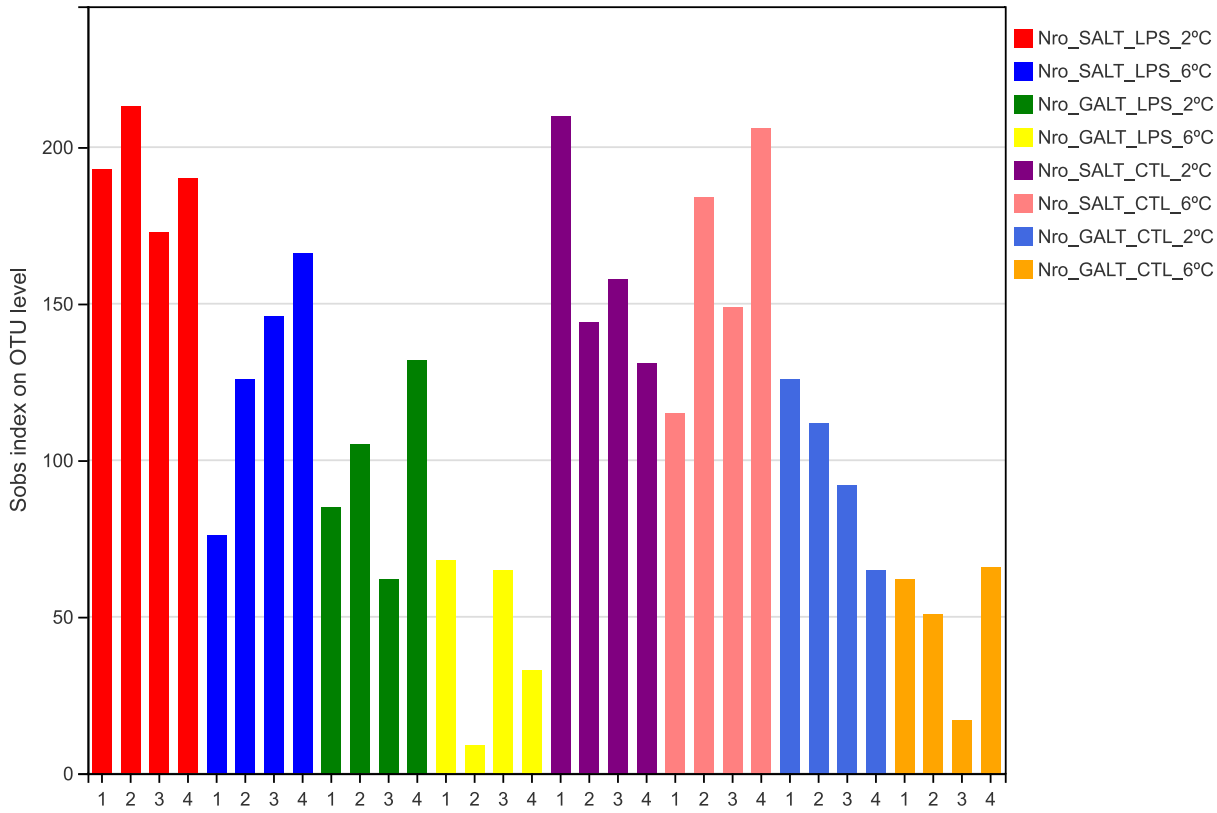
Sobs index on OTU level
0
50
100
150
200
1 2 3 4 1 2 3 4 1 2 3 4 1 2 3 4 1 2 3 4 1 2 3 4 1 2 3 4 1 2 3 4 1 2 3 4
Nro_SALT_LPS_2ºC
Nro_SALT_LPS_6ºC
Nro_GALT_LPS_2ºC
Nro_GALT_LPS_6ºC
Nro_SALT_CTL_2ºC
Nro_SALT_CTL_6ºC
Nro_GALT_CTL_2ºC
Nro_GALT_CTL_6ºC

C)

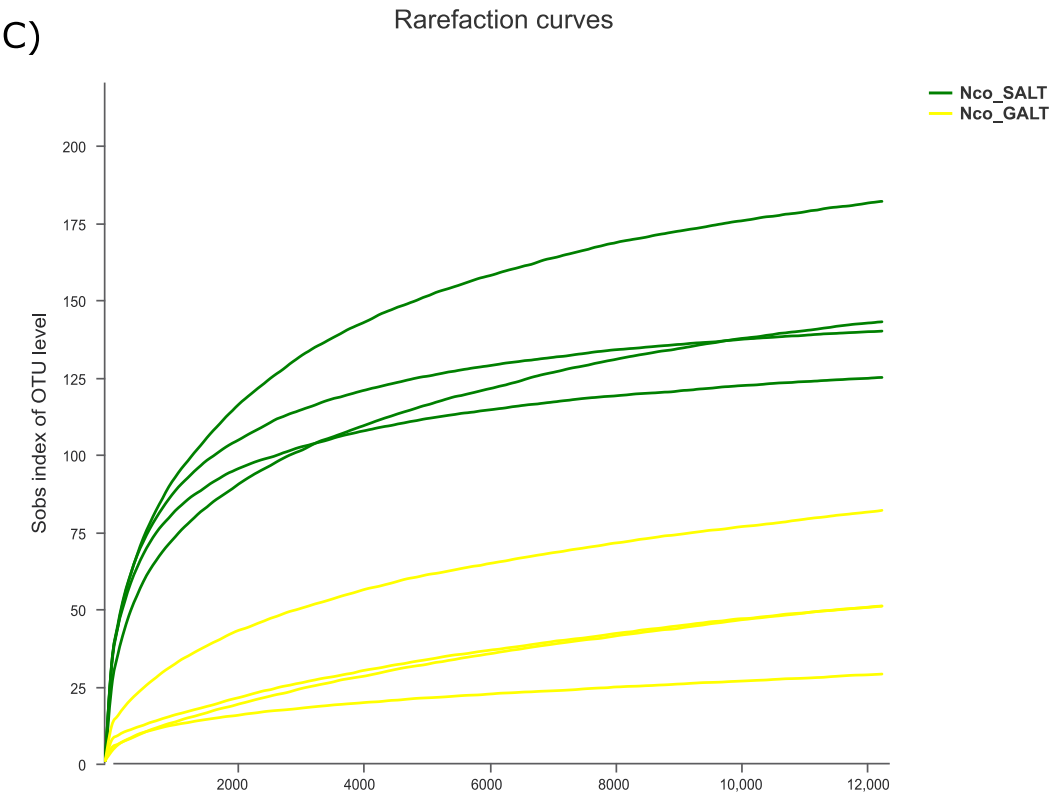
Rarefaction curves
Nco_SALT
Nco_GALT
Sobs index of OTU level
0
25
50
75
100
125
150
175
200
2000
4000
6000
8000
10,000
12,000

D)

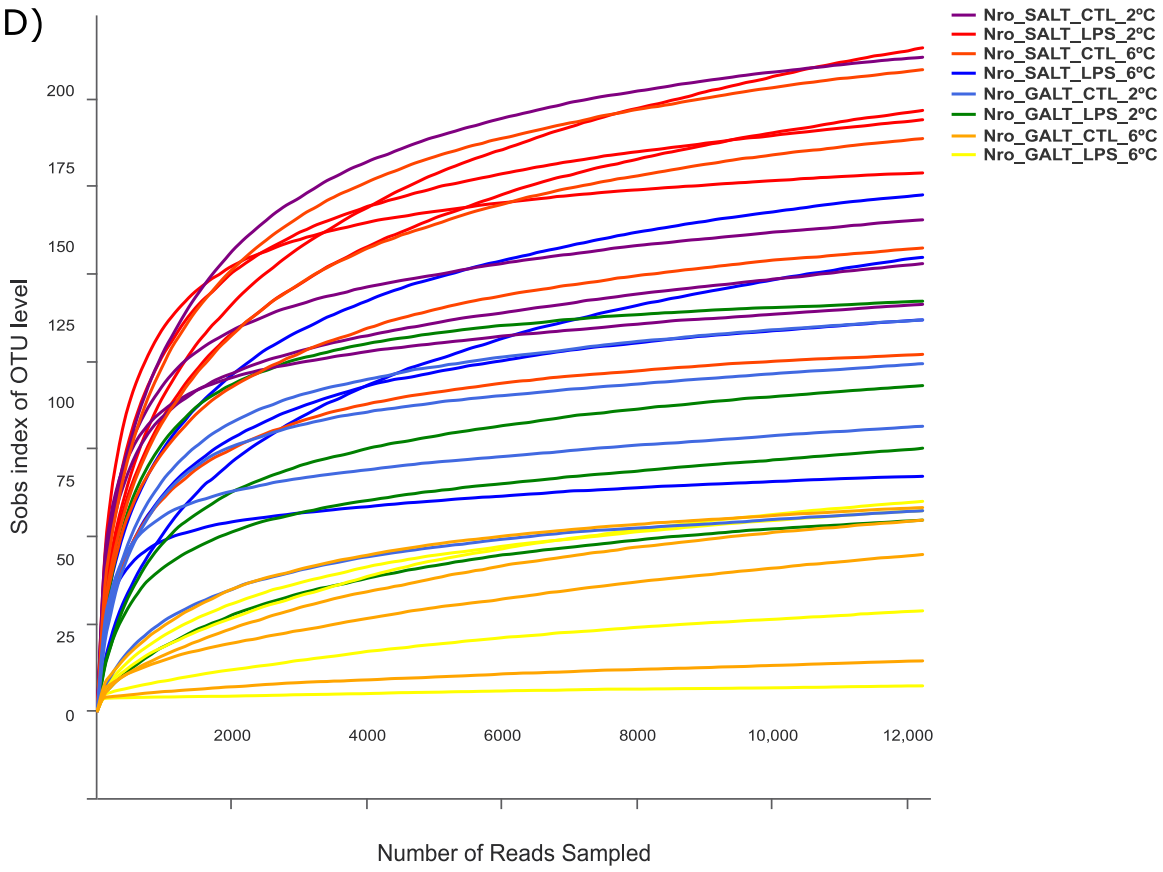
Nro_SALT_CTL_2ºC
Nro_SALT_LPS_2ºC
Nro_SALT_CTL_6ºC
Nro_SALT_LPS_6ºC
Nro_GALT_CTL_2ºC
Nro_GALT_LPS_2ºC
Nro_GALT_CTL_6ºC
Nro_GALT_LPS_6ºC
Sobs index of OTU level
0
25
50
75
100
125
150
175
200
2000
4000
6000
8000
10,000
12,000
Number of Reads Sampled

Figure 5.5. Bacterial community alpha diversity (A, B) and rarefaction curves (C,D). A-C) GALT and SALT of control and LPS-treated *N. coriiceps*; **B-D)** GALT and SALT of control and LPS-treated *N. rossii* at 2ºC and 6ºC.

5.4.2.3. The N. coriiceps microbiome response to LPS and temperature

For *N. coriiceps*, in control and LPS-treated GALT at 2ºC the most abundant phyla were Proteobacteria (~68%) and Fusobacteria (~15%) (Figure 6A). The most abundant genera were *Allivibrio* (~48%), *Photobacterium* (~19%) and *Cetobacterium* (~16%) (**Figure 5.6 B**). In SALT of both control and LPS-treated fish, the predominant phyla were Proteobacteria (~77%), Bacteroidetes (~13%) and Epsilonbacterareota (~4%) (**Figure 5.6 A**) and the most abundant genera were *Colwellia* (~65%), *Pseudoalteromonas* (~13%) and *Moritella* (~12%) (**Figure 5.6 B**). The number of OTU in SALT (608) was higher than GALT (268) and increased in the LPS-immune challenged SALT (from 280 to 328) and decreased in GALT (from 146 to 122) (Pearson´s chi square test $p < 0.05$, **Table 5.1 B**, **Figure 5.7 A**). There were statistically significant differences in genera abundance between SALT and GALT: *Allivibrio*, *Colwellia*, *Psychromonas*, *Pseudoalteromonas*, *Moritella*, unclassified Flavobacteriaceae, *Arcobacter*, *Tenacibaculum* and *Vibrio* (Kruskal-Wallis H test $p < 0.05$). The genera *Allivibrio* and *Vibrio* were more abundant in GALT and the others in SALT (**Figure 5.7 B**). Overall, there were 99 and 10 shared bacterial communities between control and LPS-treated fish in SALT and GALT of *N. coriiceps*, respectively. LPS treatment seems to modify microbial composition particularly in SALT of *N. coriiceps* (**Figure 5.7 A-B**).

The heatmap clustering showed distinct microbial compositions between the two different tissues and grouped more closely GALT control and LPS-treated than SALT in *N. coriiceps* (**Figure 5.8 A**) which is in agreement with the NMDS plot (**Figure 5.8 B**). These results indicate that both tissues had specific bacterial communities that clustered separately and the LPS challenge modified the microbial community of SALT (**Figure 5.8 A-B**).

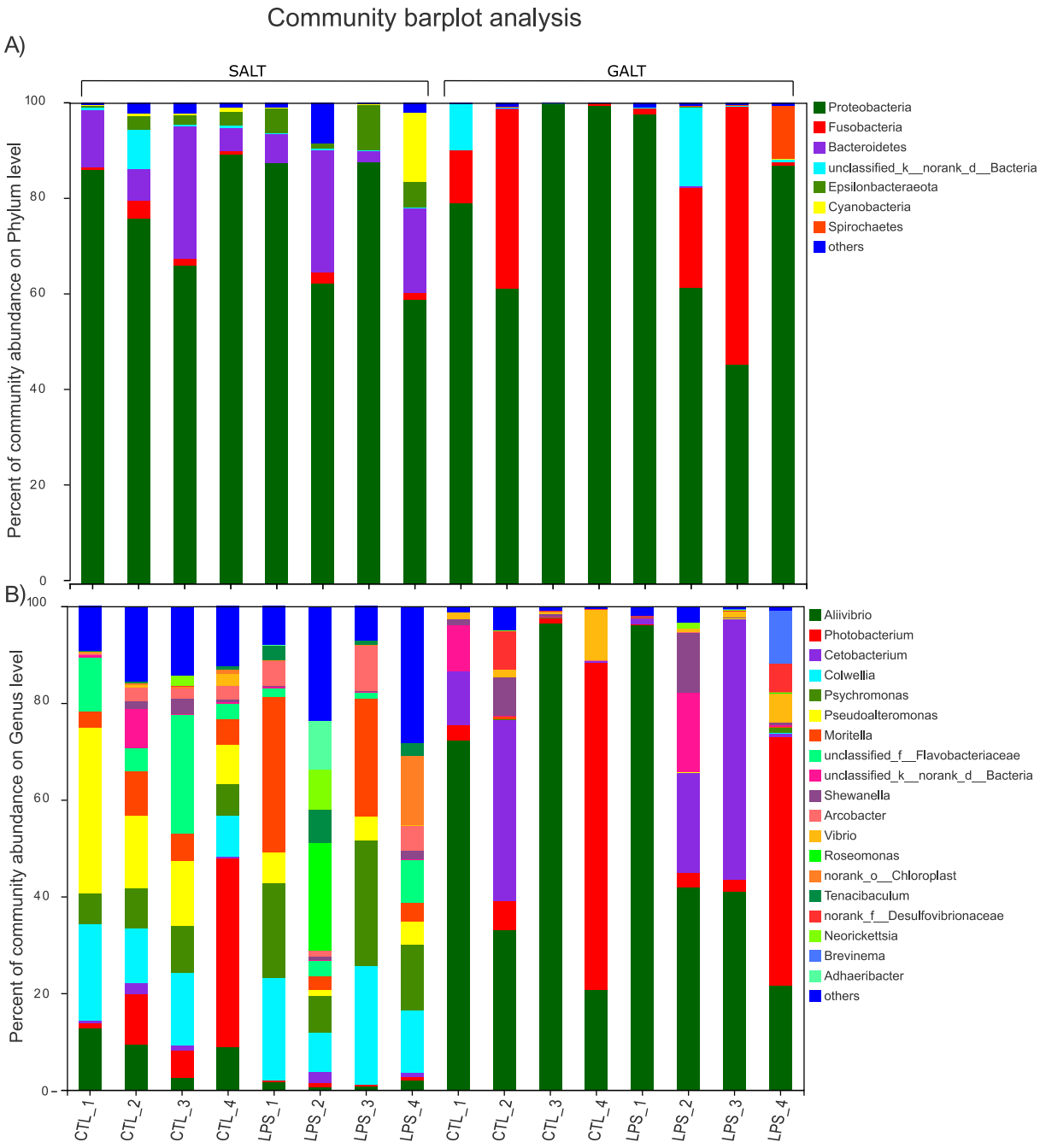

Figure 5.6. Bacterial community relative abundance. A) phyla and **B)** genus in GALT and SALT of control and LPS-treated *N. coriiceps*.

Table 5.1. Contingency table of bacterial community abundance. A) seawater, gut-associated lymphoid tissue (GALT) and skin-associated lymphoid tissue (SALT) of wild *N. coriiceps* (Nco) and *N. rossii* (Nro); **B)** GALT and SALT of control and LPS-treated *N. coriiceps*; **C)** SALT of control and LPS-treated *N. rossii* at 2ºC and 6ºC of seawater temperatures; **D)** GALT of control and LPS-treated *N. rossii* at 2ºC and 6ºC.

a)

	Count

	Nro	Nro	SW	Total
SALT	5716	5828	0	11544
GALT	5552	5384	0	10936
SW	0	0	85	85
Total	11268	11212	85	22565
	Expected count			
SALT	5764,582	5735,933	43,48504	11544
GALT	5460,973	5433,833	41,19477	10936
SW	42,44538	42,23443	0,320186	85
Total	11268	11212	85	22565
Person Chi Square test				
Pvalue	0			

b)

Count

	CTL	LPS	Total
SALT	280	328	608
GALT	146	122	268
Total	426	450	876
	Expected count		
SALT	295,6712	312,3288	608
GALT	130,3288	137,6712	268
Total	426	450	876
Person Chi Square test			
Pvalue	0,021508		

c)

Count

	CTL	LPS	Total
2ºC	262	247	509
6ºC	138	135	273
Total	400	382	782
	Expected count		
2ºC	371,6992	355,3008	509
6ºC	308,3008	294,6992	273
Total	400	382	782
Person Chi Square test			
Pvalue	0,016801		

d)

Count

	CTL	LPS	Total
2ºC	350	377	727
6ºC	330	273	603
Total	680	650	1330
	Expected count		
2ºC			727
6ºC			603
Total	680	650	1330
Person Chi Square test			
Pvalue	0,805361		

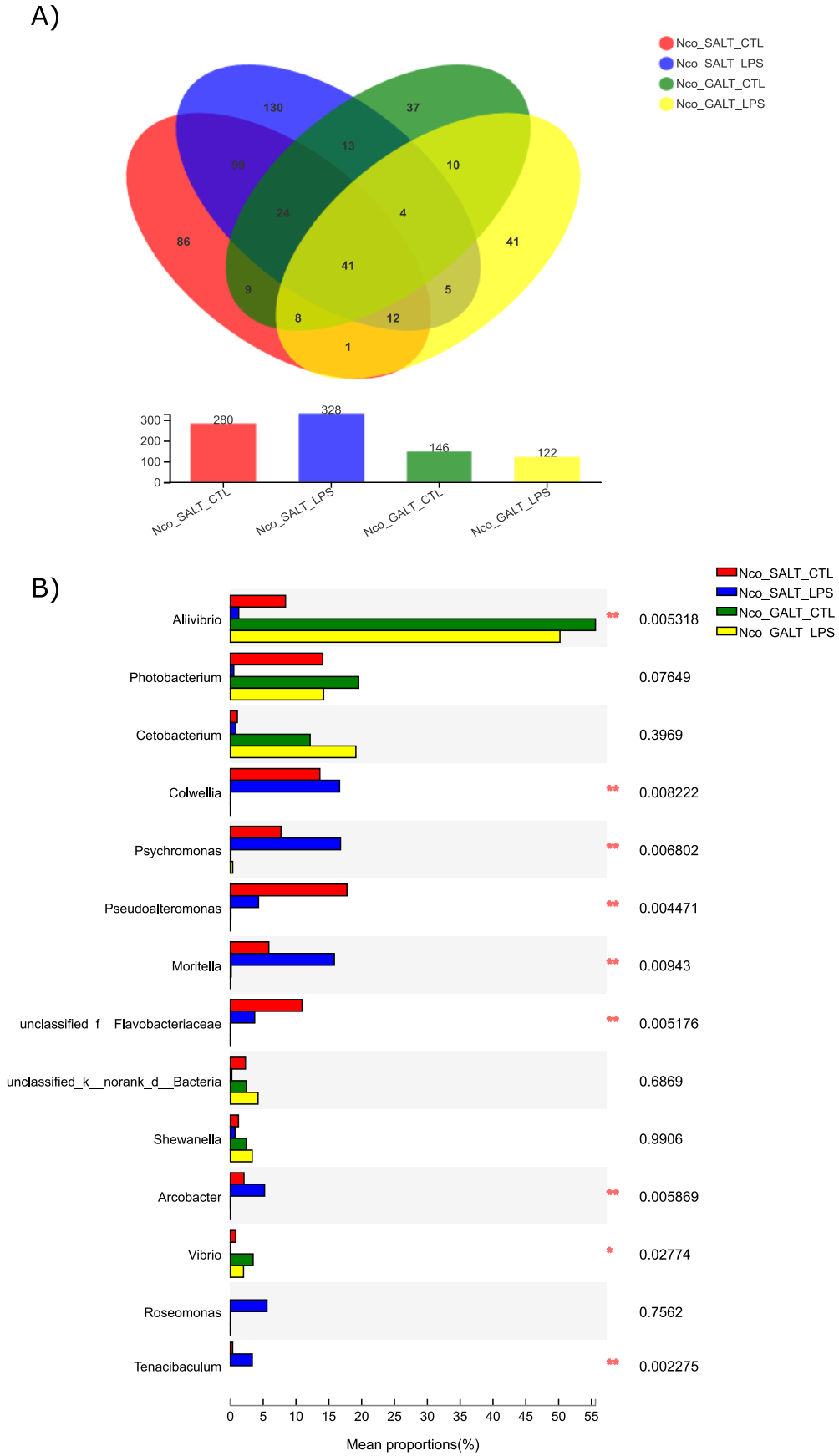

Figure 5.7. A) Venn diagram of bacterial community OUT abundance and B) relative genus abundance in GALT and SALT of control and LPS-treated *N. coriiceps*. The * indicates $p \leq 0.05$; ** $p \leq 0.01$; *** $p \leq 0.001$, Kruskal-Wallis H test.

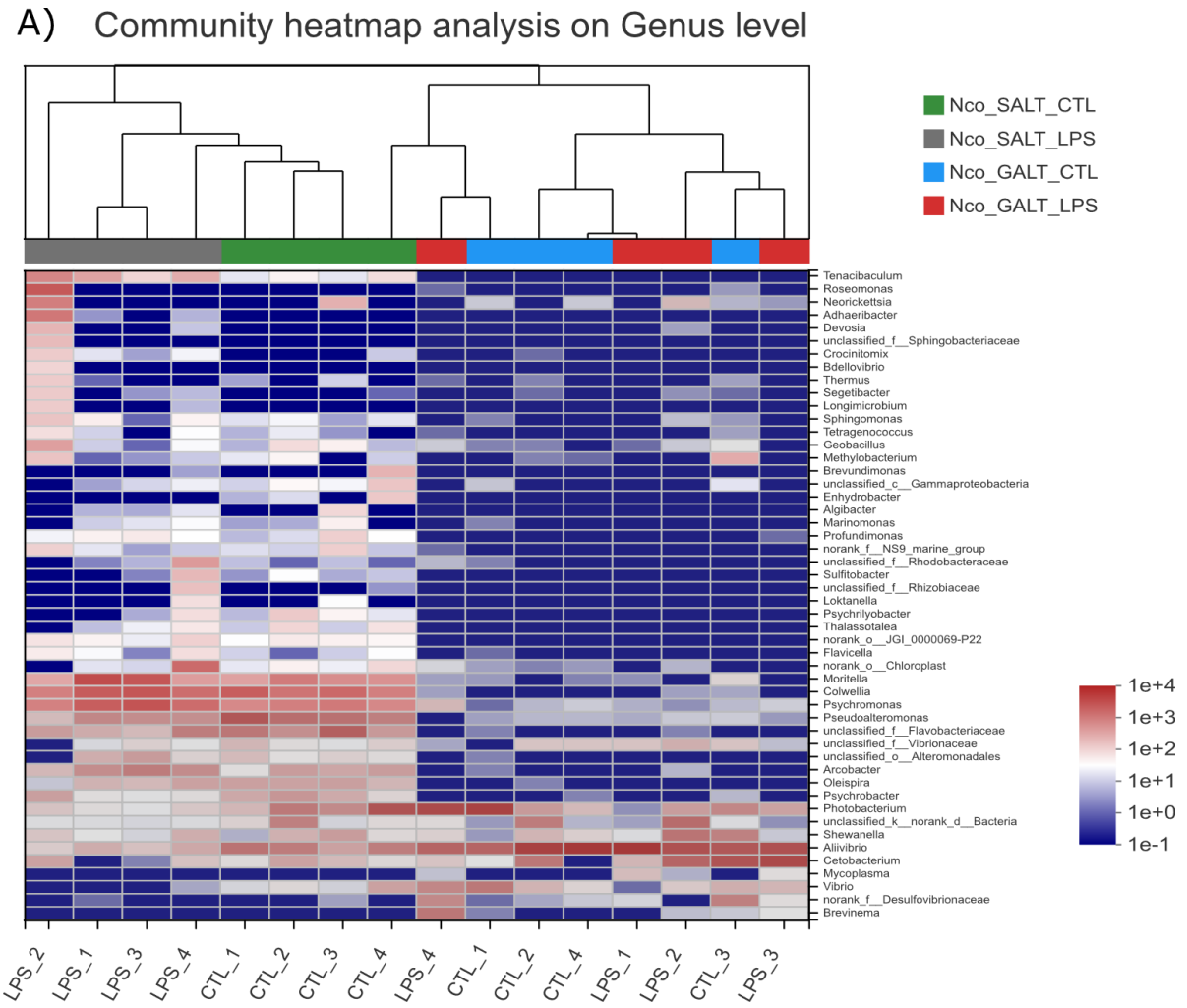
A) Community heatmap analysis on Genus level
Nco_SALT_CTL
Nco_SALT_LPS
Nco_GALT_CTL
Nco_GALT_LPS
Tenacibaculum
Roseomonas
Neorickettsia
Adhaeribacter
Devosia
unclassified_f__Sphingobacteriaceae
Crocinitomix
Bdellovibrio
Thermus
Segetibacter
Longimicrobium
Sphingomonas
Tetragenococcus
Geobacillus
Methylobacterium
Brevundimonas
unclassified_c__Gammaproteobacteria
Enhydrobacter
Algibacter
Marinomonas
Profundimonas
norank_f__NS9_marine_group
unclassified_f__Rhodobacteraceae
Sulfitobacter
unclassified_f__Rhizobiaceae
Loktanella
Psychrilyobacter
Thalassotalea
norank_o__JGI_0000069-P22
Flavicella
norank_o__Chloroplast
Moritella
Colwellia
Psychromonas
Pseudoalteromonas
unclassified_f__Flavobacteriaceae
unclassified_f__Vibrionaceae
unclassified_o__Alteromonadales
Arcobacter
Oleispira
Psychrobacter
Photobacterium
unclassified_k__norank_d__Bacteria
Shewanella
Aliivibrio
Cetobacterium
Mycoplasma
Vibrio
norank_f__Desulfovibrionaceae
Brevinema
1e+4
1e+3
1e+2
1e+1
1e+0
1e-1
LPS_2
LPS_1
LPS_3
LPS_4
CTL_1
CTL_2
CTL_3
CTL_4
LPS_4
CTL_1
CTL_2
CTL_4
LPS_1
LPS_2
CTL_3
LPS_3

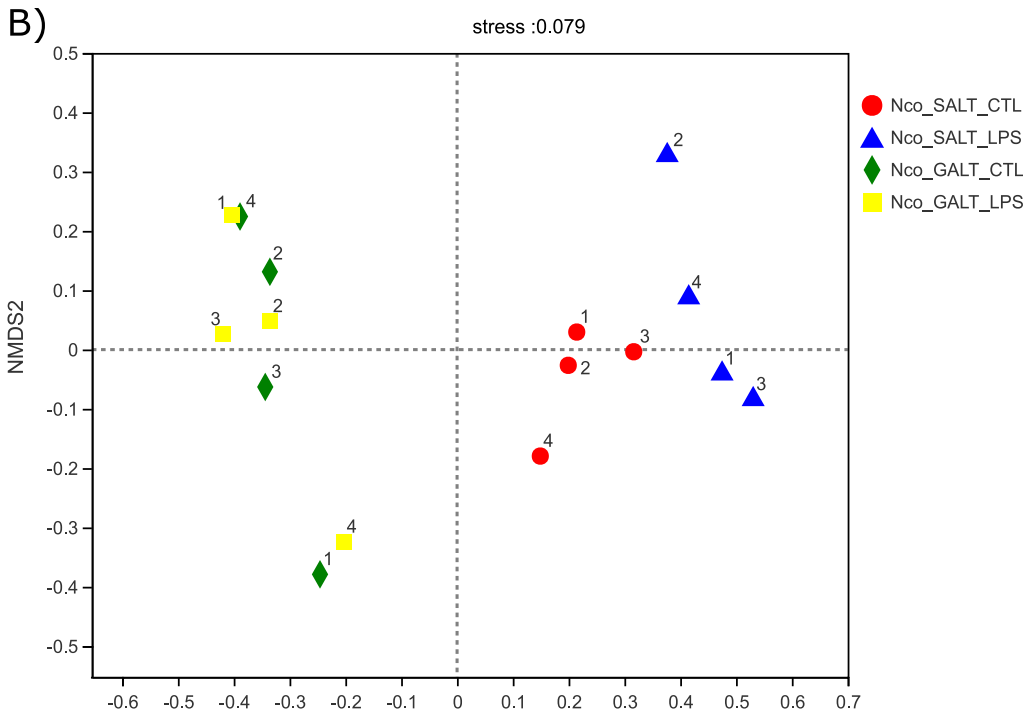
B)
stress :0.079
NMDS2
Nco_SALT_CTL
Nco_SALT_LPS
Nco_GALT_CTL
Nco_GALT_LPS
0.5
0.4
0.3
0.2
0.1
0
-0.1
-0.2
-0.3
-0.4
-0.5
-0.6
-0.5
-0.4
-0.3
-0.2
-0.1
0
0.1
0.2
0.3
0.4
0.5
0.6
0.7

Figure 5.8 (previous page). A) Heatmap and B) NMDS of bacterial community OTUs in GALT and SALT of control and LPS-treated *N. coriiceps*.

5.4.2.4. The N. rossii microbiome response to lps and temperature

For *N. rossii*, the Proteobacteria (~71%), Fusobacteria (~16 %) and Bacteroidetes (~11%) were the dominant phyla of both GALT and SALT (**Figure 5.9 A**). Moreover, *Allivibrio* (~44%), *Cetobacterium* (~24%) and *Photobacterium* (~16%) were the most abundant genera in GALT and *Allivibrio* (~16%), *Colwellia* (~13%) and *Psychromonas* (~1%) the most abundant in SALT (**Figure 5.9 B**).

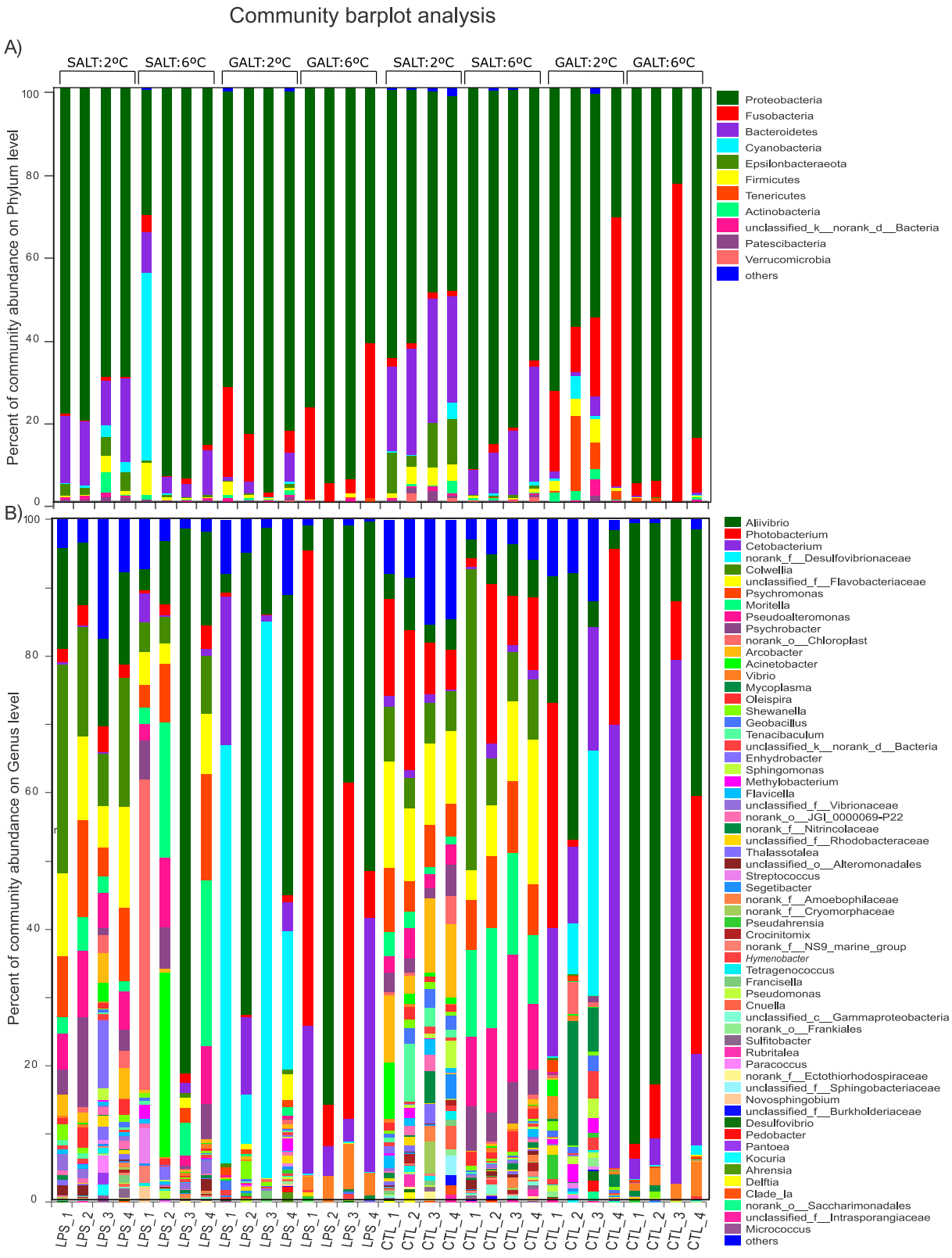

Figure 5.9. Bacterial community relative abundance of A) phyla and of B) genus in GALT and SALT of control and LPS-treated *N. rossii* at 2ºC and 6ºC.

The OTU abundance at 2ºC in GALT was lower in the LPS-treated fish (135) than in the control (247) and the increase in temperature to 6ºC reduced the microbial composition both in control (138) and LPS- treated fish (135) (**Figure 5.10 A-B**). The genera comparison, between the two tissues (SALT and GALT) and all treatment groups (control and LPS at both temperatures), indicate that *Colwellia*, unclassified Flavobacteriaceae, *Psychromonas*, *Moritella*, *Pseudoalteromonas* and *Psychrobacter* were predominantly in SALT irrespective of the experimental group and *Acinetobacter* appeared in SALT LPS-treated fish at 6ºC (Kruskal-Wallis H test, $p<0.05$, **Figure 5.10 C**). *Cetobacterium* was abundant in GALT of control fish at both 2ºC and 6ºC ($p \leq 0.01$); norank_ Desulfovibrionaceae was more abundant in GALT of LPS-treated fish at 2ºC ($p \leq 0.01$); *Photobacterium* ($p \leq 0.05$) and *Vibrio* ($p \leq 0.01$) were more abundant in GALT of LPS-treated fish at 6ºC and *Mycoplasma* was more abundant in GALT of control fish at 2ºC ($p \leq 0.001$) (**Figure 5.10 C**).

To evaluate the effect of LPS and temperature on the composition of the bacterial communities in the two tissues in *N. rossii*, a Pearson´s chi square test was performed and showed that only the GALT microbial composition was significantly different between the two treatment groups and the two temperatures ($p < 0.05$, **Table 5.1 C-D**). Overall, unique OTU's were also observed in each experimental group at both temperatures. The LPS-treated SALT at 6ºC had the lowest OTU number (38) and the LPS-treated SALT at 2ºC had the highest number of OTUs (95). The shared microbial communities varied from 8, between control SALT at both temperatures and LPS-treated SALT at 6ºC, to 145 OTUs between the four experimental groups, which was indicative of a core microbiome that was stable irrespective of the experimental challenges (**Figure 5.10 A-B**). In the GALT, 5 was the lowest number of shared bacterial communities and corresponded to the control and LPS treatment at 6ºC and 56 was the highest shared number of OTUs between the control and LPS at 2ºC, which indicates that LPS treatment and increased temperature provoked a reduction in the GALT microbial communities (**Figure 5.10 A-B**). In the heatmap, two distinct clusters from the different tissues were observed, which indicates tissue-specificity, although the individual variability in the microbiomes of different experimental groups meant clustering was not totally driven by treatment. The SALT microbiome was more divergent between experimental groups than the GALT (**Figure 5.11 A**). The NMDS plot showed similar clustering results and so the relative contribution of LPS and temperature to changes in the microbiome could not be clearly established for both tissues in *N. rossii* (**Figure 5.11 B**).

Figure 5.10 (next page). A) Venn diagram of bacterial community OTUs and B) relative genus abundance in GALT and SALT of control and LPS-treated *N. rossii* at 2ºC and 6ºC. The * indicates $p \leq 0.05$; ** $p \leq 0.01$; *** $p \leq 0.001$, **Kruskal-Wallis H test** and **post hoc Dunn**.

A)

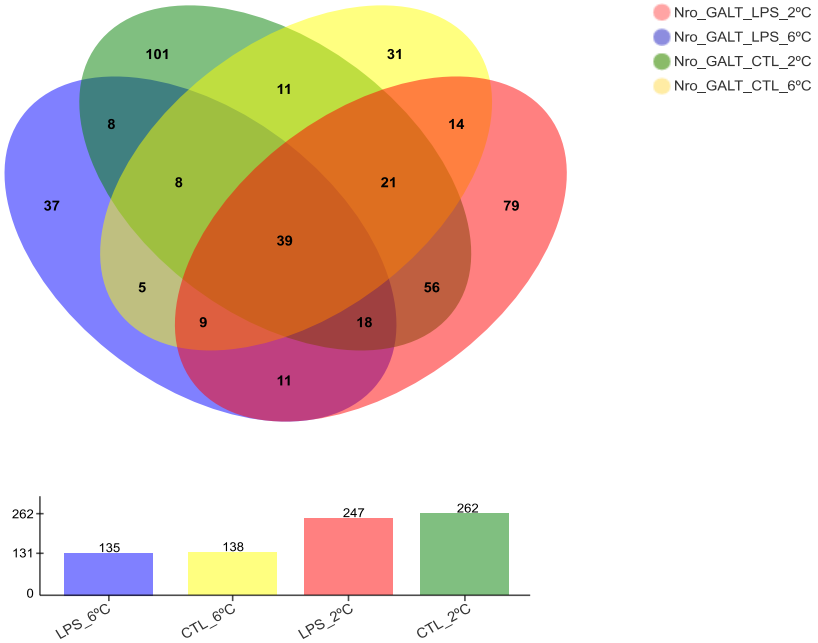
Nro_GALT_LPS_2ºC
Nro_GALT_LPS_6ºC
Nro_GALT_CTL_2ºC
Nro_GALT_CTL_6ºC
101
31
11
8
14
8
21
37
79
39
5
56
9
18
11
262
131
0
135
138
247
262
LPS_6ºC
CTL_6ºC
LPS_2ºC
CTL_2ºC

B)

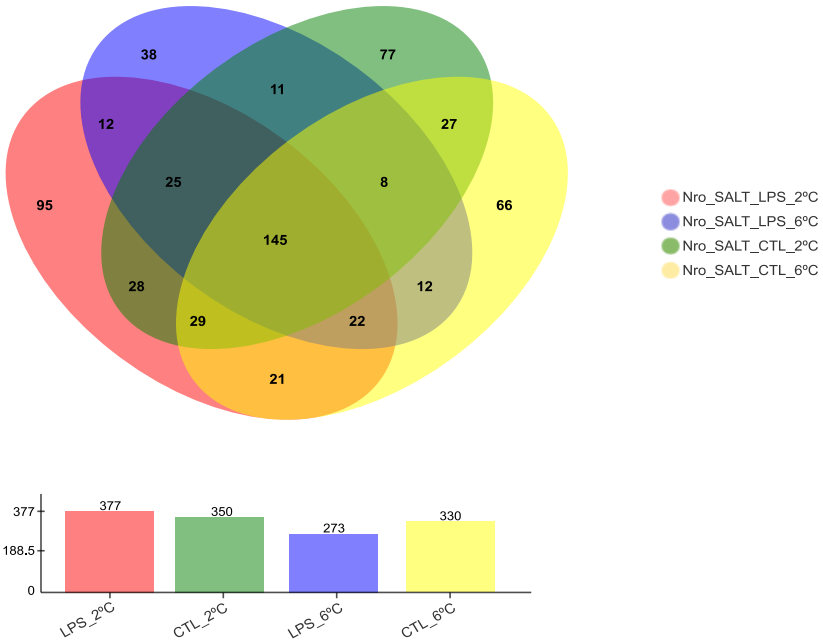
Nro_SALT_LPS_2ºC
Nro_SALT_LPS_6ºC
Nro_SALT_CTL_2ºC
Nro_SALT_CTL_6ºC
38
77
11
12
27
25
8
95
66
145
28
12
29
22
21
377
188.5
0
377
350
273
330
LPS_2ºC
CTL_2ºC
LPS_6ºC
CTL_6ºC

C)

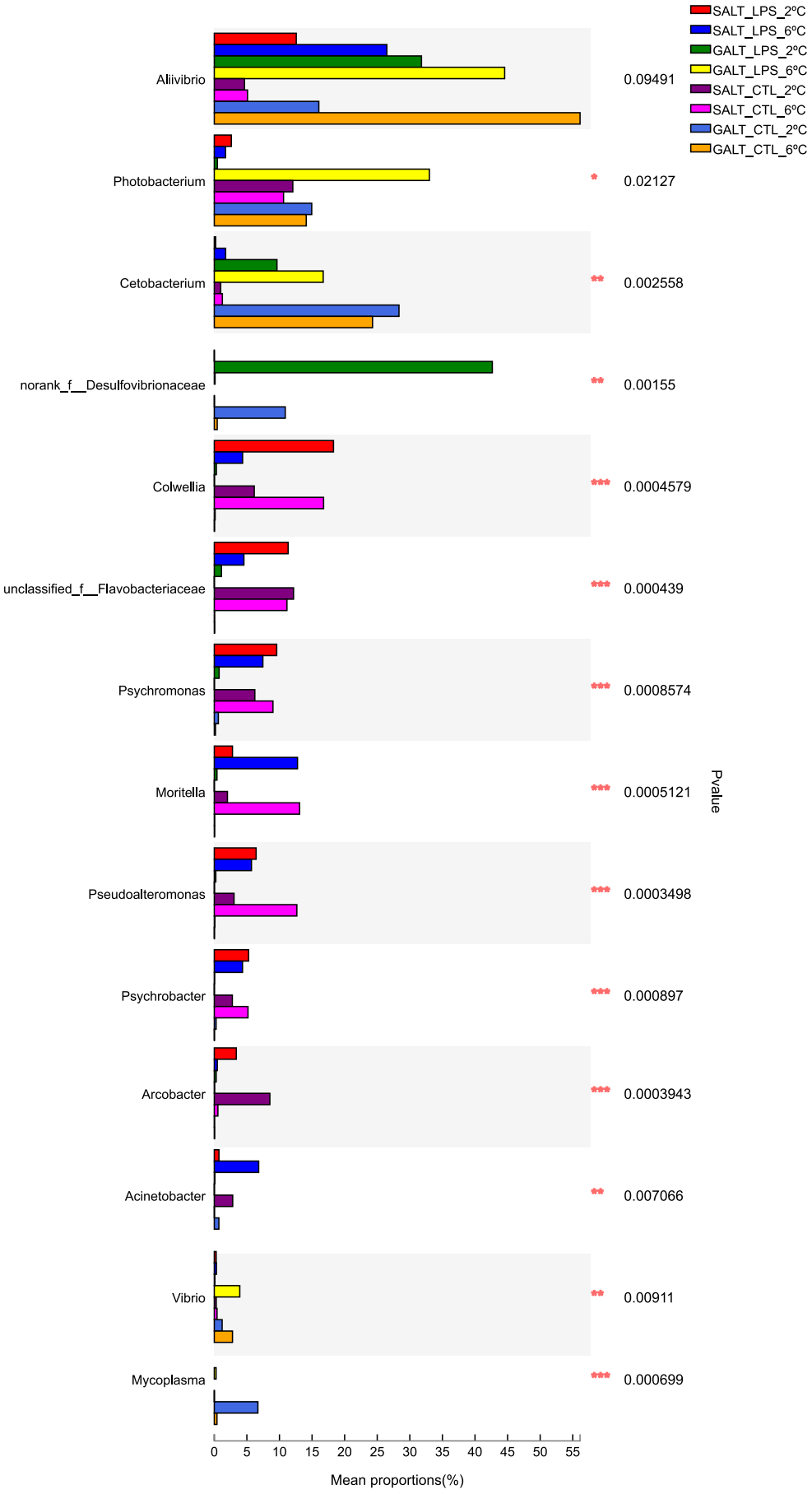
SALT_LPS_2ºC
SALT_LPS_6ºC
GALT_LPS_2ºC
GALT_LPS_6ºC
SALT_CTL_2ºC
SALT_CTL_6ºC
GALT_CTL_2ºC
GALT_CTL_6ºC
Aliivibrio
Photobacterium
Cetobacterium
norank_f__Desulfovibrionaceae
Colwellia
unclassified_f__Flavobacteriaceae
Psychromonas
Moritella
Pseudoalteromonas
Psychrobacter
Arcobacter
Acinetobacter
Vibrio
Mycoplasma
0.09491
*
0.02127
**
0.002558
**
0.00155
***
0.0004579
***
0.000439
***
0.0008574
***
0.0005121
***
0.0003498
***
0.000897
***
0.0003943
**
0.007066
**
0.00911
***
0.000699
Pvalue
0
5
10
15
20
25
30
35
40
45
50
55
Mean proportions(%)

A)

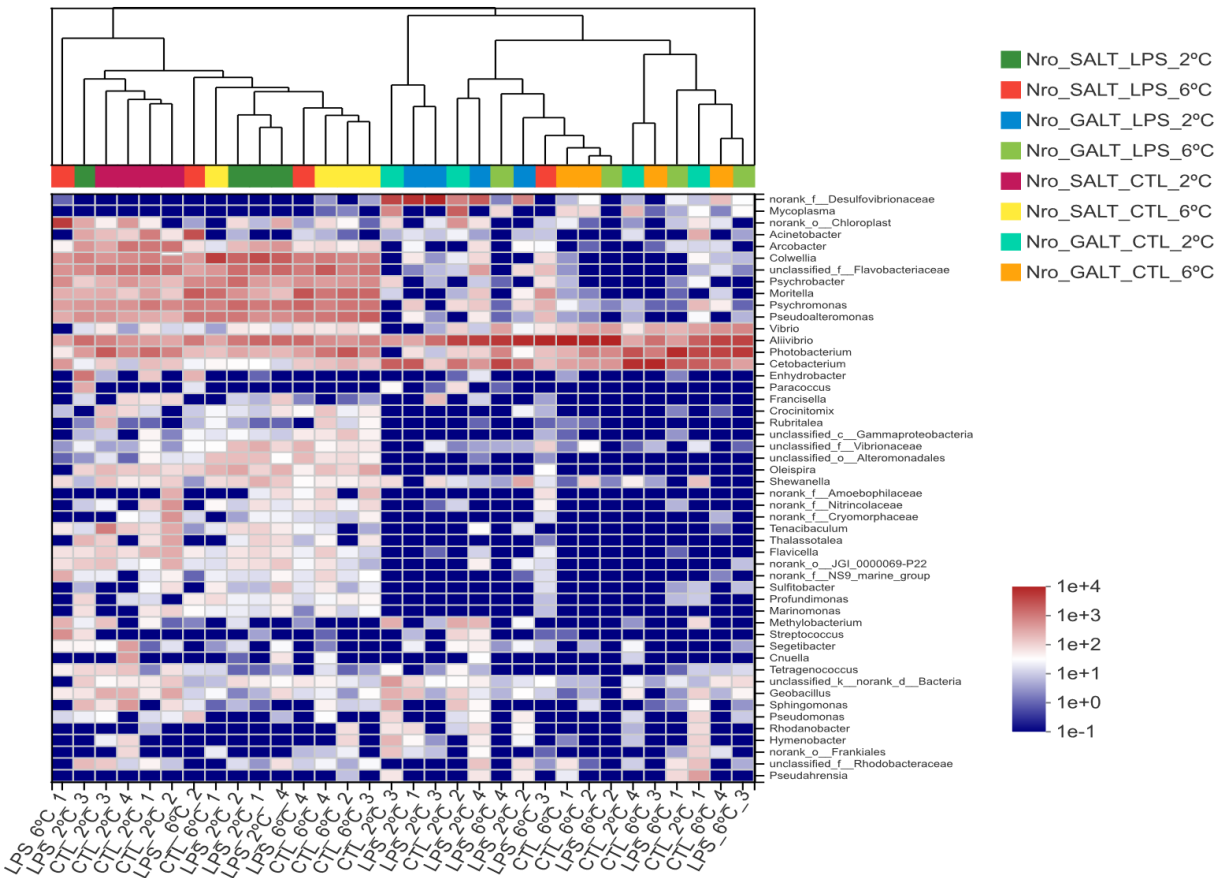
Community heatmap analysis on Genus level
Nro_SALT_LPS_2ºC
Nro_SALT_LPS_6ºC
Nro_GALT_LPS_2ºC
Nro_GALT_LPS_6ºC
Nro_SALT_CTL_2ºC
Nro_SALT_CTL_6ºC
Nro_GALT_CTL_2ºC
Nro_GALT_CTL_6ºC
norank_f__Desulfovibrionaceae
Mycoplasma
norank_o__Chloroplast
Acinetobacter
Arcobacter
Colwellia
unclassified_f__Flavobacteriaceae
Psychrobacter
Moritella
Psychromonas
Pseudoalteromonas
Vibrio
Aliivibrio
Photobacterium
Cetobacterium
Enhydrobacter
Paracoccus
Francisella
Crocinitomix
Rubritalea
unclassified_c__Gammaproteobacteria
unclassified_f__Vibrionaceae
unclassified_o__Alteromonadales
Oleispira
Shewanella
norank_f__Amoebophilaceae
norank_f__Nitrincolaceae
norank_f__Cryomorphaceae
Tenacibaculum
Thalassotalea
Flavicella
norank_o__JGI_0000069-P22
norank_f__NS9_marine_group
Sulfitobacter
Profundimonas
Marinomonas
Methylobacterium
Streptococcus
Segetibacter
Cnuella
Tetragenococcus
unclassified_k__norank_d__Bacteria
Geobacillus
Sphingomonas
Pseudomonas
Rhodanobacter
Hymenobacter
norank_o__Frankiales
unclassified_f__Rhodobacteraceae
Pseudahrensia
1e+4
1e+3
1e+2
1e+1
1e+0
1e-1

B)

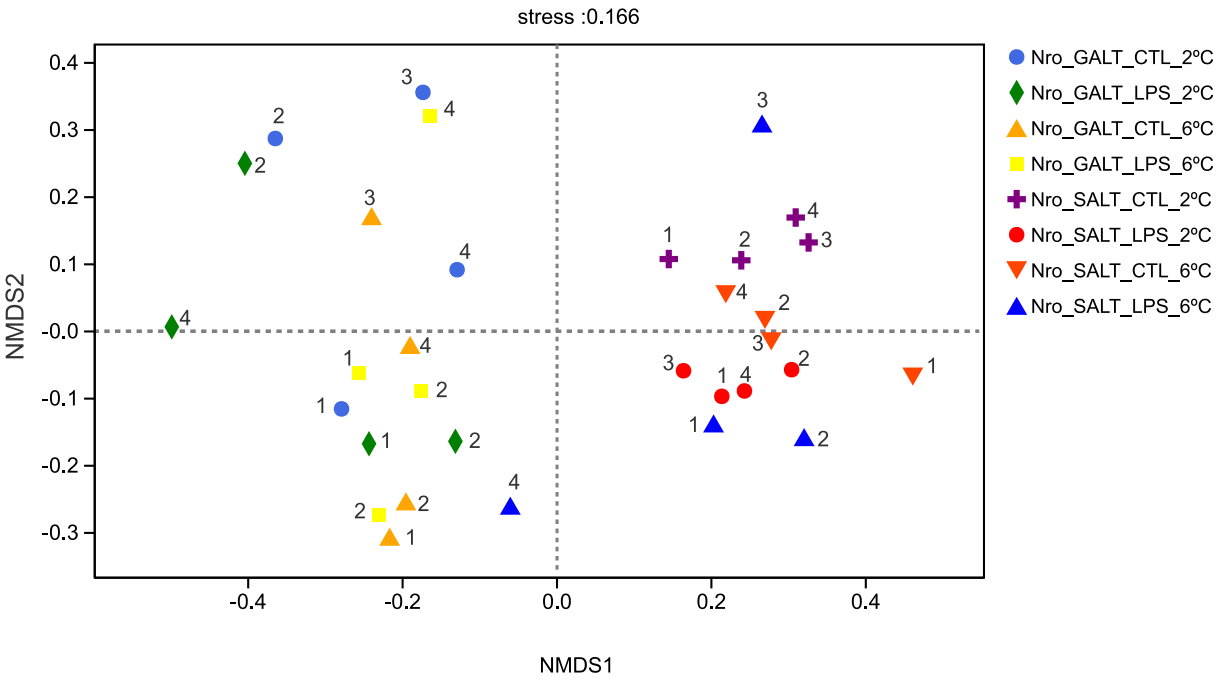
stress :0.166
NMDS1
NMDS2
Nro_GALT_CTL_2ºC
Nro_GALT_LPS_2ºC
Nro_GALT_CTL_6ºC
Nro_GALT_LPS_6ºC
Nro_SALT_CTL_2ºC
Nro_SALT_LPS_2ºC
Nro_SALT_CTL_6ºC
Nro_SALT_LPS_6ºC

Figure 5.11 (previous page). A) Heatmap and B) NMDS of bacterial community at OTU level in GALT and SALT of control and LPS-treated *N. rossii* at 2ºC and 6ºC.

5.5. Discussion

Our study provides the first description and comparisons of the bacterial communities of two Antarctic Notothenioids species and their modulation by immune challenge and temperature. The results, which were based on 16S rRNA gene sequencing, revealed reduced microbial abundance in seawater relative to fish tissues which suggested that other factors, such as diet and habitat may contribute substantially to the bacterial composition (Parata et al., 2021; Song et al., 2016; Zhang et al., 2020a). In seawater the predominant bacterial phyla were Proteobacteria, Cyanobacteria and Bacteroidota (Kim et al., 2019b; Zhang et al., 2020a). At a genus level, *Polaribacter* and *Sulfitobacter* were found but several other unclassified genera were also present (Grzymski et al., 2012). The Proteobacteria and Bacteroidota are gram-negative bacteria and include several genera such as *Escherichia* and *Vibrio* and *Bacillus subtilis* that have a role in nitrogen fixation (Byrd et al., 2020; Liba et al., 2006). In the Antarctica seawater, most genera of Bacteroidota have not been identified and represent a taxon with many unidentified strains. Recent studies indicated that 78% of the OTU microbiota in the Southern Ocean is unique, and some cold-adapted strains identified as prevalent in polar regions are almost undetectable in temperate seawaters. Moreover, metabolic pathway reconstruction of these microbial communities suggests high versatility for carbon dioxide (CO_2) fixation, nitrate and sulphate reduction, saccharide and lipid biosynthesis, and the presence of bioactive molecules with new antimicrobial properties (Núñez-Montero and Barrientos, 2018; Zhang et al., 2020a).

The abundance of bacterial communities in the SALT and GALT of wild *N. rossii* and *N. coriiceps* appeared higher than in seawater. The most abundant phylum in both Notothenioids have not yet been classified and failed to retrieve a hit from public databases, but the second most abundant phyla belonged to the Proteobacteria that have previously been identified in the GALT of Antarctic fish (Song et al., 2016) and in Antarctic seawater (Kim et al., 2019b; Zhang et al., 2020a). In addition, the Fusobacteriota were also abundant in both tissues of *N. rossii* and were previously reported in the gut of *N. coriiceps* and *Chaenocephalus aceratus* (Ward et al., 2009). Similar bacterial groups have been identified in the freshwater cyprinid *Cyprinus carpio* GALT with Proteobacteria, Bacteroidetes, Firmicutes, Fusobacteria

and Actinobacteria as the dominant phyla (Eichmiller et al., 2016). At the genus level, most bacteria were unclassified, however there were evidences that *Allivibrio* was highly abundant in both tissues of *N. coriiceps* and *N. rossii*, which corroborates observations from previous studies of the gut in these species (Ward et al., 2009) and suggests conservation of the core microbiota despite changing environmental conditions and increased incursions of humans into Antarctica. *Cetobacterium* were identified for the first time in *N. rossii* and were abundant in both the SALT and GALT, although they are generally more common in the gut in other marine fish (Egerton et al., 2018). Additionally, *Colwellia* was more abundant in the SALT than GALT of *N. rossii*. Several *Colwellia* strains have been used by the biotechnology industry exploiting their cold-adapted features and using them as additives in low-temperature food processing, the detergent industry and the textiles industry (Bruno et al., 2019). The differences between SALT and GALT from the same species may be explained by the physiology of the tissue, although physiology studies related to the microbiome are more common with human (Arumugam et al., 2011; Yatsunenko et al., 2012), while in fish they are scarce specially for skin tissue (Ross et al., 2019; Sehnal et al., 2021). Physiologically, both SALT and GALT constitute the primary physical barrier to the external environment, with immune components important to host defence against foreign microorganisms (Gomez et al., 2013; Salinas, 2015). In fish, the SALT is more exposed to unusual environmental conditions providing a barrier to ice propagation (in freezing waters) and to inward oxygen diffusion (Eastman and Hikida, 1991). Also, fish skin mucus is nutrient-rich facilitating bacterial growth and the adhesion of higher number of bacteria (Larsen et al., 2013). GALT plays an important role in feeding, digestion and absorption of nutrients and acid-base homeostasis (Zhang et al., 2016). A comparison between fresh and saltwater fish indicated that the gut microbiome reflect the host ecology and environment (Wong and Rawls, 2012). Studies in *Gadus morhua* and *Pangasius hypophthalmus* suggest that the SALT microbiome composition is strongly influenced by host species which corroborates our findings in SALT and in GALT (Larsen et al., 2013; Le Nguyen et al., 2008; Wilson et al., 2008). Overall, these studies indicate that the skin microbiome is more dependent on the environment and the gut microbiome is more conserved and both are species-specific which suggest that physiology can be an important factor to microbial communities diversity although this needs to be clarified (Sylvain et al., 2020).

Comparisons of the bacterial composition between the mucous from *N. coriiceps* sampled immediately after capture and the control fish from the experimental challenge revealed that captivity for only 7 days drastically reduced OTU abundance (from 5000 in wild

to 300 in captive fish), irrespective of the tissue, and despite the constant supply of fresh sea water. Similar observations about how captivity affects microbiota diversity and abundance exist for the Atlantic cod (Lavoie et al., 2018), but also for several terrestrial vertebrates such as black rhinos (Gibson et al., 2019), and glass lizard (Zhou et al., 2020). Nonetheless, when the GALT and SALT are compared the former has a higher OTU abundance than the latter in both the control and LPS-stimulated fish and the genus most abundant was *Allivibrio* that has been previously been associated with this species (Ward et al., 2009). The SALT bacterial community composition was more variable than GALT 7 days after LPS exposure with the most abundant genera, *Colwellia*, *Psychromonas*, *Moritella*, *Arcobacter*, *Roseomonas* and *Tenacibaculum*. This could indicate that these genera may also develop pathogenic infections to the fish causing diseases and mortality as previously reported in other animals (Nowlan et al., 2020; Ramees et al., 2017; Tunsjø et al., 2007)

For *N. rossii* at 6ºC there was no significant difference in bacterial community composition of the GALT compared to 2ºC. However, exposure to LPS at ambient temperature (2ºC) led to an increase in OTU abundance of one of the unidentified genus related to the *Desulfovibrionaceae*. In contrast, the SALT in *N. coriiceps* responded differently to temperature and LPS and seemed to be more susceptible to both factors with a decrease in *Arcobacter* and *Tenacibaculum*. These two genera have not previously been identified in Antarctic fish, although *Arcobacter* were reported in the microbiota associated with Antarctic krill (Clarke et al., 2019). Furthermore, in the microbiota of *N. rossii* SALT *Photobacterium* was more susceptible to LPS treatment and its abundance was significantly reduced, while *Pseudoalteromonas* in control fish and *Moritella* in both control and LPS-treated fish increased in abundance with temperature. These three genera were previously reported in the microbiota of the GALT of wild Antarctic fish (Gallet et al., 2019; Giordano et al., 2012; Xu et al., 2003), but the role in immune defence and their function remains to be clarified.

In summary, using metagenomics approaches this study uncovered unique bacterial communities in Antarctic seawater, and in the GALT and SALT of two Notothenioids, *N. coriiceps* and *N. rossii*. The results indicated that the cold and temperature stable Antarctic environment has shaped the microbiota of the two Notothenioids. Furthermore, the bacterial community compositions between the two species diverged despite living in similar habitat but with lifestyle specificities of the adult populations.

5.6. Conclusion

Overall, the present study revealed modulation of the microbiota in the GALT and SALT by stressors like confinement, exposure to LPS endotoxin and increased seawater temperatures. Furthermore, the response of the GALT and SALT to the stressors was tissue specific and varied by species indicating that caution is needed when generalizing about the effects of stressors on fish microbiota. The two Notothenioids studied inhabit similar Antarctic regions at depths lower than 200 m with similar dietary habits but different food preferences at the adult stage although is essentially based on krill, especially *Euphasia superba*, amphipods and small fish (namely *Pleuragramma Antarcticum*) in both Notothenioids (La Mesa et al., 2004; McBride et al., 2014). Divergence in the microbiota and its response to stressors in the two Notothenioids may be evidence supporting the importance of host-microbiota cross-talk and our results suggest that this may vary by species. The significant effect of confinement on the microbiota of *N. coriiceps* and *N. rossii* despite a continuous supply of seawater from the environment hints at the importance of the diet, fish physiology and possibly other as yet unidentified factors on the SALT and GALT microbiome. Further studies will be required to better comprehend the factors shaping the microbiota of fish and also the role of bacterial communities of the SALT and GALT in shaping fish immunity.

CHAPTER 6

General discussion and future perspectives

6.1 General discussion

In fish the innate immune system is the main defence mechanism against pathogens and is of fundamental importance since they are permanently exposed to aquatic pathogens as well as other harmful agents in the environment. Innate immunity was the first defence system to evolve and provides a rapid and non-specific response to protect animals against pathogens and consists of physical barriers, together with humoral and cellular defence mechanisms (Smith et al., 2019; Uribe et al., 2011). Teleost fish are the most specious and successful group of vertebrates with species living and adapted to a wide range of aquatic environments and to diverse water microbiomes which are likely to have played a modulatory role in the development of their immune defence. Available studies of immunity in teleost fish have mostly used molecules extracted from pathogens (e.g. *E. coli* LPS, to mimic bacteria), heat killed bacteria or synthetic compounds (e.g. Poly I:C, agonist of a viral challenge) to stimulate the immune system and characterize the humoral and cellular response (Alkie et al., 2019; Jiang et al., 2020; Li et al., 2020a; Lulijwa et al., 2020; MacKenzie et al., 2006, 2008; Watzke et al., 2007; Zhou et al., 2014; Zoccola et al., 2017).

The Notothenioids are a class of teleost fish that inhabit the cold and freezing waters of the Antarctic region. To survive under such extreme environmental conditions during their radiation these fish underwent extreme morphological and physiological adaptations, but the impact of this on the immune system is currently poorly understood. This thesis aimed to understand if ***unique innovations occurred in the immune system of the Antarctic Notothenioids*** when they radiated (over 10 – 20 million years ago) and adapted to the Antarctic. In the experimental analysis I focussed on two phylogenetically proximate species, the black rockcod (*N. coriiceps*) and the marbled rockcod (*N. rossii*) and transcriptomes and microbiomes of innate immune barriers were analysed and compared with non-Antarctic teleosts under control and immune challenged conditions. The specific systems studied were candidate genes linked to iron metabolism (chapter 2.1), a gene family of the innate immune system, important for pathogen recognition, the toll-like receptor (TLR) family (chapter 2.2) and the multi-immune tissue response in *N. coriiceps* and *N. rossii* exposed to multiple stressors including a pathogen challenge (chapter 3 and chapter 4) as well as the environmental microbiome and its involvement in innate immune defence in Notothenioids (chapter 5).

The following sections discusses the main outcomes of this PhD thesis.

6.1.1. Iron deprivation defence mechanism in Notothenioids

Iron is an important metal for growth and survival of bacteria. In the rockcods several iron-related genes were studied that are involved in the defence response. In non-Antarctic fish exposed to LPS, changes in iron-related gene expression have been linked to iron deficiency, which directly impacts bacterial growth and metabolism (Martínez et al., 2017b; Neves et al., 2009, 2015, 2017). Since in Antarctic seawater, iron is frequently a limiting metal in the environment (Wu et al., 2019), I wanted to test if an adaptive change in iron metabolism occurred and influenced the evolution of the iron-based immune response in Antarctic fish. In this thesis I showed that both Notothenioids responded to LPS in a way similar to non-Antarctic fish and the modifications in the expression of iron-related genes was indicative of modified cellular iron homeostasis in the liver and head-kidney (chapter 2.1).

The response to LPS of *N. coriiceps* was of higher magnitude than *N. rossii* in head-kidney and liver when genes that contribute to intracellular accumulation of iron and inhibition of extracellular export (*Fm, Fp, Tf, TfRC1, Hamp2*) were evaluated (chapter 2.1). Physiological differences between *N. coriiceps* and *N. rossii* may explain the divergence in their responsiveness to LPS and a similar trend was also observed for other genes studied in this thesis. The differences in gene responsiveness may be linked to evolutionary pressures caused by habitat and dietary preferences of *N. coriiceps* and *N. rossii* (Calì et al., 2017; Ferreira et al., 2017; Klein et al., 2017a). As far as I am aware this is the first evidence of a conserved transcriptional response of iron-related genes to LPS exposure in Notothenioids. However, the factors explaining the differing magnitude of the response between *N. coriiceps* and *N. rossii* remains to be established as does a more detailed consideration of the consequence for the homeostasis of metals in blood and other systems of the duration and route of exposure to the immune challenge.

6.1.2. Peculiarities of the immune system in adaptation to cold

The Tlr genes are conserved and phylogenetically ancient PRRs across vertebrates and have previously been described in some Notothenioids, including *N. coriiceps*, as innate immune receptors that recognize and are stimulated by heat killed *E. coli* (Ahn et al., 2014, 2016). In chapter 2.2 the Tlr repertoire was comprehensively explored in *N. coriiceps*, *N. rossii* as well as five other Notothenioid species. Tlr number across teleost fishes including the Notothenioids was variable and in *N. coriiceps* and *N. rossii* 15 and 12 Tlr, respectively were identified while in the other Notothenioids 10 to 15 Tlr were found. Tlrs in all the Notothenoids analysed had representatives in each of the Tlr superfamilies 1, 3, 5, 7 and 11. The difference in the total number of Tlrs detected in the Notothenioid species analysed was due to gene duplication or gene loss. In our extended comparison, Tlrs were identified for the first time in *N. rossii* and homologues of the teleost *tlr2b*, *tlr13* and *tlr25*, were identified in *N. coriiceps* and the *tlr* family repertoire was revised.

Comparative genomics of Tlr in Notothenioids and other teleost and non-teleost fish revealed that gene number was similar. This indicated that the recent radiation of the Notothenioids in a cold-stable environment did not significantly affect *tlr* gene number or representation in the main gene families, which is similar to what has been observed for other gene families such as antifreeze glycoproteins and zona pellucida proteins (Chen et al., 1997b, 2008; Kim et al., 2019a). However, it was demonstrated for the first time that some Tlrs in teleosts were under positive selection and in the Notothenoids Tlr5, Tlr8, Tlr13, Tlr22 and Tlr23 underwent positive selection. The region most affected was the pathogen recognition domain suggesting that pressure from the unique microbiota of the Antarctic may have driven this change (chapter 2.2).

The Notothenioid species in which the Tlr repertoire was most different were *D. mawsoni* where gene deletions occurred and *G. acuticeps* in which Tlr21 was duplicated. A reduction in Tlr gene number was also identified in flatfish that had fewer Tlrs than other teleosts (Shi et al., 2018; Takano et al., 2011). Our results contrast with those reported for other cold-water fish such as the cod (*Gadus morhua*) from Arctic waters where extreme cold was proposed to have fuelled a large *tlr* gene family expansion (Solbakken et al., 2016). Gene family expansion was not observed in Notothenioid species and instead gene number was generally conserved, although positive selection and codon usage bias led to modifications in the LRR motifs of Tlr5, Tlr8, Tlr13, Tlr22 and Tlr23 suggesting modifications in pathogen recognition. In the future it will be of interest to determine if this is an adaptation to the unique Antarctic marine microbiota.

Through the transcriptome analysis in chapter 3, candidate Tlr receptors (Tlr5, Tlr21 and Tlr22) present in the head-kidney and intestine were analysed by qPCR after LPS exposure for 8h and 24h of *N. rossii* in ambient (2ºC) and increased (6ºC) seawater temperatures. No significant modifications of the candidate Tlrs were observed, although in other non-Antarctic teleosts under LPS stimulation modifications in Tlr expression have been reported (Li et al., 2017; Meijer et al., 2004; Palti, 2011; Qiu et al., 2019; Tsujita et al., 2004). The absence of a response to LPS by *N. rossii* was unexpected but may be explained by a diversity of factors including the source of LPS (from human dwelling bacteria), changes in LPS structure under extreme cold, the route of administration (I.P.) or concentration or duration of exposure. In a previous study on *N. coriiceps* exposed to LPS a transcriptional response of several *tlrs* was observed and presumably differences in experimental procedures explain the conflicting observations in the present study (Ahn et al., 2014). Nonetheless, the increase in plasma lysozyme in *N. rossii* in seawater at 2ºC after LPS exposure in the present study is indicative of a PRR triggered response as was previously reported in Atlantic salmon (*S. salar*) (Nya and Austin, 2010).

In summary, the stable-cold environmental conditions in Antarctica and the recent radiation of the Notothenioids did not significantly influence Tlr gene number. However, positive selection in the PRR domain, which is important for pathogen recognition in the Notothenioids is indicative of an adaptation to the unique Antarctic microbiota and of species-specific adaptations to their ecological niches.

In chapter 3, we used NGS to determine for the first time the transcriptome of the main hematopoietic tissues, the head-kidney and two mucosa-associated lymphoid tissues, the skin and intestine (duodenum region) in *N. coriiceps*. The transcriptome response of the head-kidney, skin and duodenum after 7 days of LPS (*E. coli* O111:B4, I.P.) administered i.p. was also determined. Tissue specific molecular signatures linked to the LPS challenge were established for the first time in the three tissues. The large datasets generated will be made publicly available and contribute significantly to improve molecular tools and knowledge about this species. The analysis of five individual transcriptomes per treatment group gave a robust analytical outcome (FDR < 0.05) and was complemented with plasma biochemical parameters.

A relatively low number of DEGs (< 300) were identified after the LPS challenge and were poorly enriched in immune genes. Instead, genes related to energy metabolism, energy production and mitochondria were most evident. Furthermore, very few DEGs were identified

in skin, which was poorly responsive to LPS the DEGs were mainly associated with mitochondrial function and ROS. The poor response to LPS conflicts with the outcome of a similar previous study also in *N. coriiceps* (Ahn et al., 2016) which analysed the liver after 12 h i.p. LPS and of studies in non-Antarctic teleosts that showed increased expression of immune related genes namely *tlrs, c-type lectin receptors, complement, MHC I and II, coagulation cascade, lysozyme* and other *cytokines* and *chemokines* (Cai et al., 2018; Li et al., 2020b; Liu et al., 2018; Maekawa et al., 2021; Palstra et al., 2018; Zoccola et al., 2017) (chapter 3). The reason for this discrepancy was unclear but may be explained by the type of LPS used (as discussed later).

A shift in transcripts related to energy metabolism has previously been reported in the head kidney of rainbow trout (*O. mykiss*) after LPS (i.p..) exposure (*E. coli* O26:B6) (MacKenzie et al., 2008). The modification of mitochondrial-related gene transcripts among the DEGs was more specific to *N. coriiceps* and it remains to be established if this is a specific adaptive response linked to the higher mitochondrial density that exists in Antarctic fish (O'Brien and Sidell, 2000). The DEGs related to the immune system, included *nlrc3*, which has previously been associated with antibacterial defence in teleosts such as in *Miichthys miiuy*, *Paralichthys olivaceus* and *Cirrhinus mrigala* (Chu et al., 2021; Li et al., 2015; Park et al., 2012; Swain et al., 2013). The chemokines such as interleukins and PRRs (*nlrp3*) down-regulated in the duodenum of *N. coriiceps* were shown to be linked to cytokine processing and secretion in *Danio rerio* (Li et al., 2020a). The immune-related processes enriched in the skin in the present study were interleukins and antigen processing and presentation and have previously been reported in the liver of *N. coriiceps* exposed for 12h to heat-killed *E. coli* bacteria (HKEB O11:B4) (Ahn et al., 2016).

Overall, LPS induced a relatively small response in *N. coriiceps* in our study, which was also reflected by the absence of a response in plasma lysozyme and antiproteases. The general absence of a systemic response was consistent with the results of chapter 2.1 and chapter 2.2. Interestingly, the Tlr transcripts although present in the transcriptome were not represented among the DEGs identified, consistent with the results of chapter 2.2 where LPS did not significantly modify *tlr* expression. Possible factors that may explain the low immune response in *N. coriiceps* may be linked to the origin of the LPS (it was obtained from bacteria adapted to humans), a change in its structure caused by the low temperature and possibly route, dose, and duration of administration. Temperature is known to modify LPS structure (Chattopadhyay, 2006; Kumar et al., 2002; Wu et al., 2013) and the low water temperatures used in the study

may have interfered with the recognition by PRRs (including Tlrs) and consequently immune system activation (Akira et al., 2006).

In chapter 4, a NGS sequencing approach was also used to generate for the first-time transcriptomes of duodenum, skin, spleen, and liver in *N. rossii* 8h after a challenge using a proxy for bacteria (LPS) and virus (poly I:C) at 2ºC. Since, the sequenced genome of *N. rossii* is not publicly available an annotation strategy based on mapping of the transcripts to the genomes of other Antarctic Nototheniids was followed and resulted in approximately 70% annotated transcripts. Although 4 samples per treatment and tissue were collected, quality control issues meant that only three individuals per treatment group were considered in the analysis. Plasma biochemical parameters (n = 6 fish, lysozyme, antitrypsin, cortisol, plasma protein and haematocrit) were analysed to obtain an insight into the physiological status of the fish. The LPS and the poly I:C treatments provoked a tissue-specific response, and the skin and duodenum were the most responsive (more than 1500 DEGs/tissue). An unexpected observation was the strong gene transcript response of the skin to LPS and of the duodenum to poly I:C suggesting specialization in the protective role of these two immune barriers.

In both pathogen challenges GO and KEGG enrichment analysis identified changes in the core tissue transcriptome linked to energy metabolism and tissue specific changes linked to metabolic pathways namely lipid and glucose metabolism. Immune system processes were well represented among the DEGs and were predominantly up-regulated and involved humoral and cellular components many of which were of innate immunity. In the LPS challenge DEGs of the immune system included *lysozyme g*, *MHC I* and *II*, *antitrypsin*, *chemokines type 1* and *4*, *IL-11*, *macrophages*, *B* and *T* cells and a similar response was reported in an *N. coriiceps* liver transcriptome (Ahn et al., 2016) as well as in yellowhead catfish (Liu et al., 2016, 2018), Atlantic salmon (Palstra et al., 2018), channel catfish (Jiang et al., 2020), carp (*S. prenanti*, (Li et al., 2020c) and Nile tilapia (Maekawa et al., 2021). The immune related genes identified with poly I:C challenge included, *IFN*, *IL-1*, *MHC I*, several proteins of the complement system (*C4*, *C1q*, *C7*, *C9*, *factor B*, *factor D*) and immunoglobulins and this response was similar to that reported in other teleosts and in *N. coriiceps* under similar stimuli (Ahn et al., 2016; Lulijwa et al., 2020; Zhou et al., 2014).

Interestingly, a clear separation of response between the skin and duodenum revealed tissue-specificity and the recruitment of a different suite of immune genes was observed depending on the challenge, bacterial or viral. The skin was most responsive to a bacterial LPS

challenge and the duodenum to viral poly: IC. However, both tissues responded by increasing cell junction adherence and reinforcing the barrier and make it more impermeable to the perceived pathogens. This presumably explains the lower response of the liver and spleen to both challenges and suggests the immune barrier function of skin and duodenum was highly effective.

The search for PRR among the DEGs of the duodenum and skin revealed that Tlrs were absent. These results contrast with previous findings in *N. coriiceps* and other teleosts (Ahn et al., 2014; Li et al., 2020c; Liu et al., 2016) and suggest that TLRs may be less important for LPS recognition than other factors. The results of chapters 3 and 4 suggest that in *N. coriiceps* (chapter 3) and *N. rossii* (chapter 4) PRRs such as NLRs, CLRs and RLRs, that have so far been poorly studied in fish, may have an important role, since they unlike Tlrs, they were upregulated in response to treatments . The role of these PRRs in pathogen recognition is unlikely to be a specialization of Antarctic fish, since they also responded to LPS stimulation in other teleosts - , C-type lectin genes in the Atlantic salmon and barramundi, NLRC3 genes in the olive flounder and NOD1 genes in Miiuy croaker (Chu et al., 2021; Li et al., 2016; Soanes et al., 2004; Zoccola et al., 2017). The absence of Tlrs represented in the DEGs in *N. rossii* stimulated with LPS is consistent with the results of chapter 2.2 and chapter 3 where tlr genes were also unresponsive to LPS exposure. Similar PRRs were identified in the duodenum in poly I:C treated fish. However, a response of TLRs was elicited by poly I:C exposure and *tlr3* was modified in liver of *N. rossii*, which is coherent with the results of previous studies in which poly I:C modified *tlr3* in *N. coriiceps* liver and in several other teleosts (Ahn et al., 2014; Andresen et al., 2020; Zhou et al., 2014).

Poly I:C challenge also stimulated iron-related genes and this is an aspect that merits further study, since this response has been associated with LPS challenge in other teleosts (Costa et al., 2011; Lange et al., 2001; Martínez et al., 2017a; Neves et al., 2015, 2017).

LPS exposure did not cause a change in plasma biochemical parameters but poly I:C decreased antiproteases and the haematocrit revealing it caused a systemic response. The plasma biochemical changes in *N. rossii* exposed to poly I:C do not corroborate those previously reported in Chinook salmon (Lulijwa et al., 2020).

Overall, the transcriptome results brought new insights into the responsiveness of *N. rossii* to LPS and the robustness of the results was supported by their consistency with the results of chapter 2.1 (iron-related genes) and chapter 2.2 (absence of *tlr* response) as well as

work published by other authors. Similarities were found with the transcriptome generated for the skin, duodenum, and head-kidney of *N. coriiceps*, namely related to energy metabolism and energy production (Chapter 3) under LPS challenge. Furthermore, a novel observation resulting from this work was the likely importance of the less known PRRs (NLRs, CLRs and RLRs) and the selenium ion genes in LPS and poly I:C recognition in *N. rossii*.

The partitioning of genes that responded to LPS or poly I:C was unexpected, and a clear division of the immune defence components identified in skin and duodenum was observed. In the skin, which was most modified by LPS challenge, several humoral factors were identified including *C-reactive protein, lysozyme g, C1q, trypsin, mucin 2-like, bactericidal permeability-increasing protein, interleukin 11 receptor, chemokines like receptor 1* and *type 3-2, TNF, TGF-β,* and cellular components such as leukocytes, *CD9, CD59, CD151, CD209, platelet-activating factors* and *mast cells*. A number of gene transcripts associated with acquired immunity and more specifically B and T cells, were identified. The transcriptional response to a viral poly I:C challenge included genes of the complement proteins, *cytokine inducing SH2*, interferons, *mucin 2, sialomucin, protein kinase C, chemokines 12A, 20 and receptor type 4, MHC I* and *II,* leukocytes, macrophages, *CD63* and *CD302*. Several immunoglobulin (Ig) genes were identified particularly in the duodenum in response to a poly I:C challenge, which was surprising since extracellular antigens are normally considered to activate B lymphocytes and stimulate secretion of Igs. Further investigation of the acquired immune response in the future should provide new insights into the teleost acquired response.

6.1.3. Microbiota adaptation to the cold

The present thesis provides the first comparison between bacterial communities of two mucosa-associated lymphoid tissues, SALT and GALT, from recently captured *N. coriiceps* and *N. rossii*, and in *N. rossii* after a short period of captivity, under stimulation by bacterial endotoxin and under a thermal challenge (chapter 5). The 16s rRNA sequencing approach (V3-V4 region) was applied to identify bacterial communities in surface seawater and tissues samples from the two Notothenioids and revealed unique and shared bacterial communities between the tissues, species, and seawater. The failure to specifically identity several bacterial communities was indicative of the uniqueness of the, yet little studied, Antarctic microbiota. The predominant phylum identified in seawater and fish was Proteobacteria, but the bacterial

richness fish tissues was higher (more than 5000 OTU) than seawater (approximately 85 OTU), which suggests the physiology of the fish and environmental factors may have a strong contribution in shaping the microbiome (Bottos et al., 2020). The Proteobacteria is a major phylum of gram-negative bacteria and have frequently been found in Antarctic environments (Di Lorenzo et al., 2020). It is known that the gram-negative Antarctic bacteria have developed strategies to flourish under extreme cold (Tribelli and López, 2018). Also, it had been described that these bacteria modify the structure of their LPS especially lipid A to improve fluidity and allow protein flexibility, which is important for function (Di Lorenzo et al., 2020). Consistent with previous studies, members of the *Allivibrio* genus were abundant in both skin and gut of the two Notothenioids studied (Ward et al., 2009). However, two novel observations in *N. rossii*, were i) the abundance of *Cetobacterium* in the skin and gut, which had not previously been reported in Antarctic fish but it is common in the gut of marine teleosts (Egerton et al., 2018) and ii) the higher abundance of *Colwellia* in the skin than in the gut. This genus has been well studied in the context of the enzymes they produce with high thermal tolerance and makes them of considerable interest for industry (used in detergent, textile, paper, and food industries). However, the genus is not well studied due to their limited representation in microbiota so far (Bruno et al., 2019). The contribution of this bacteria to skin function will be an interesting future avenue of research.

Significant changes in bacterial richness were observed in fish kept in tanks with a flow through system, compared to "wild" (i.e., immediately after capture) although Proteobacteria remained predominant. In captivity the diet was restricted compared to the fish in the wild, which could be a reason for a change in the microbiome, particularly in the GALT because of its role in digestion.

After LPS stimulation of the GALT and SALT, bacterial richness was only found to vary in the SALT. This response was particularly intriguing considering that this was a tissue that had a high transcriptional response to LPS by immersion in *N. rossii* (chapter 4). It is therefore possible that the change in bacterial richness in SALT is linked to the significant modifications in the immune activity of the tissue.

In contrast, a rise in seawater temperature from 2 ºC to 6ºC caused an increase in bacterial richness in both the SALT and GALT of *N. rossii*. The study revealed a hitherto unidentified richness in the bacterial communities of Antarctic fish with *Psychromonas*, *Moritella*, *Arcobacter*, *Roseomonas* and *Tenacibaculum* represented, while previously only

Psychromonas and *Moritella* had been reported (Song et al., 2016; Ward et al., 2009). Overall, the results indicate that increases in temperature in the context of climate change is likely to cause a significant modification in the microbiota of the GALT and SALT of *N. rossii* with as yet unknown consequences.

6.2 Conclusion and future perspectives

Our initial hypothesis was to assess if the evolution of the immune system was shaped by the unique environmental conditions of Antarctica, and we showed specific evolution of the Tlr gene family in the Antarctic fishes. Also, the transcriptional response of *N. coriiceps* and *N. rossii* provide new insights that have an immunological significance with broad functions in the two Notothenioids, indicating that NLR, CLR and RLR PRRs, toxins and selenium-related genes may have a key role in bacterial and viral recognition and antimicrobial properties defence. In addition, there was a clear evidence of skin and duodenum function as immune barriers with specific immune responses to bacterial and viral challenges. In addition, it was possible to show common immune defence mechanisms to other teleosts, namely the iron deprivation after bacterial endotoxin exposure. Divergence was observed in the immune responses of the two Notothenioids, and this will form the basis of future studies to further dissect out immune system evolution and defence mechanisms.

Overall, our findings indicate species and tissues-specificity of microbiota as well as susceptibilities to LPS and increased seawater temperature as summarized in **Table 6.1**.

Table 6.1. Comparative analysis of the immune response of *N. coriiceps* and *N. rossii*. The arrows indicate the genes or groups of genes linked to specific processes. Some of the DEGs are identified and their expression (up- or down-regulated) is indicated. Fe indicates iron and Se indicates selenium genes.

Comparative immune response results	*N. coriiceps* 	*N. rossii* 	Other teleosts
Iron-immune related genes in head-kidney (Hk) and liver (Lv) after LPS i.p. (7 days)	↑ *fth1* (Lv, Hk) ↑ *ftl* (Hk) ↑ *hp4* (Lv, Hk) ↑ *fp* (Lv, Hk) ↑ *tf* (Lv, Hk) ↑ *tfr* (Hk)	↑ *fth1* (Hk) ↑ *ftl* (Hk) ↑ *cp* (Lv, Hk) ↑ *tf* (Hk) ↑ *tfr* (Lv) ↑ *hp4* (Lv)	**Induce** hypoferraemic responses
Toll-like receptors genes family evolution and LPS i.p. stimuli (8 and 24 hours)	●TLR1 SF: *tlr1, tlr2, tlr14/18* ●TLR3 SF: *tlr3* ●TLR5 SF: *tlr5, tlr5S* ●TLR7 SF: *tlr7, tlr8, tlr9* ●TLR11 SF: *tlr13, tlr21, tlr22, tlr23* **LPS i.p. not performed**	●TLR1 SF: *tlr1, tlr2, tlr14/18* ●TLR3 SF: *tlr3* ●TLR5 SF: *tlr5* ●TLR7 SF: *tlr7, tlr8, tlr9* ●TLR11 SF: *tlr21, tlr22, tlr23* ↑ lysozyme (24h) = effects on gene expression	**Induce** several TLRs gene expression from the 5 families (TLR1, TLR3, TLR5, TLR7 and TLR11) Increase the lysozyme and the antiprotease activities
Head-kidney, skin (Sk) and duodenum (Du) transcriptomes after LPS i.p. (7 days)	↓ *PRRs (NLR, MCR)* ↑ *energy metabolism* ↑ *mitochondrial polarization* ↑ *protein ubiquitination* = effects on plasma enzymes	**Not analyzed**	**Increase gene expression:** C-type lectin receptors, ILs, TGFs, MHC I and II, globulin, respiratory burst, metabolic scope, cortisol and antioxidant responses
Skin, duodenum, spleen (Sp) and liver transcriptomes after LPS and Poly I:C immersion (8 and 24 hours)	**Not performed**	↑ Fe genes (LPS, Poly I:C) ↑ Se genes (LPS, Poly I:C) ↑ *NLR, CLR, RLR* (LPS, Poly I:C) ↑ toxins (LPS, Poly I:C) ↑ *tlr3* (Poly I:C)	**Increase gene expression:** TLR3 and other TLRs, ILs, TGFs, IFNs, complement, MHC I and II, coagulation cascade, Igs, B and T cells, innate cells, iron-related metabolism
SALT and GALT microbiomes in "wild" and after LPS i.p. and increased (6ºC) temperature (7 days)	**"Wild":** predominance of unidentified phyla **Identified phyla:** Proteobacteria and Cyanobacteria *Allivibrio* genus (SALT, GALT) ↑ LPS: *Psychromonas, Moritella, Arobacter, Roseomonas, Tenacibaculum* (SALT) ↑ LPS: *Allivibrio* (GALT)	**"Wild":** predominance of unidentified phyla **Identified phyla:** Proteobacteria and Cyanobacteria *Allivibrio, Colwellia, Cetobacterium* (SALT, GALT) ↑ CTL: *Pseudoalteromonas, Arcobacter (SALT 2/6ºC)* ↑ LPS: *Photobacterium, Cetobacterium, Vibrio* (GALT 6ºC)	"Wild": predominance of Proteobacteria, Firmicutes and Actinobacteria from seawater fish. The genera are too variable across species. Poorly explored under LPS and increased temperature

This study also draws attention to the importance of LPS source. Despite commonly used in experiments with teleosts and mammals, the LPS sold commercially may not be adequate to use in fish living at low temperature in Antarctica. Further investigations are needed to clarify this issue.

The lack of a genome for *N. rossii* and the incomplete genome for *N. coriiceps* (rough draft genome released in 2014) limited the depth of analysis. This is compounded by the very limited conditions to do experiments in Antarctica.

It will be important to carry out pathogenicity studies in Antarctic fish and relate to global warming conditions. Better knowledge of the Southern Ocean microbiota (bacteria, viruses, parasites) is needed, covering different geographical scales and organisms to better comprehend their interaction and potential functions in host immune defence. In addition, several scientific questions remain open: Are toxins, selenium and PRRs instead of well-

described Tlrs as highly expressed against LPS, unique immune system innovations of these Notothenioids compared to other teleosts? Which other immune genes beyond the TLRs were modified under selective pressure of cold temperatures? Which are the common and species-specific bacterial microbiota, if at all, important for Notothenioid immune system defence and their specific role? Are the Notothenioids capable to adapt and survive in longer exposure (months and/or years) to increased seawater temperatures?

Bibliography

Aas, T. S., Sixten, H. J., Hillestad, M., Sveier, H., Ytrestøyl, T., Hatlen, B., et al. (2017). Measurement of gastrointestinal passage rate in Atlantic salmon (*Salmo salar*) fed dry or soaked feed. *Aquac. Reports* 8, 49–57. doi:10.1016/j.aqrep.2017.10.001.

Abdel-Mageid, A. D., Zaki, A. G., El Senosi, Y. A., El Asely, A. M., Fahmy, H. A., El-Kassas, S., et al. (2020). The extent to which lipopolysaccharide modulates oxidative stress response in *Mugil cephalus* juveniles. *Aquac. Res.* 51, 426–431. doi:10.1111/are.14309.

Abdel-Tawwab, M., Monier, M. N., Hoseinifar, S. H., and Faggio, C. (2019). Fish response to hypoxia stress: growth, physiological, and immunological biomarkers. *Fish Physiol. Biochem.* 45, 997–1013. doi:10.1007/s10695-019-00614-9.

Abele, D., and Puntarulo, S. (2004). Formation of reactive species and induction of antioxidant defence systems in polar and temperate marine invertebrates and fish. *Comp. Biochem. Physiol. - A Mol. Integr. Physiol.* 138, 405-415. doi:10.1016/j.cbpb.2004.05.013.

Abram, Q. H., Dixon, B., and Katzenback, B. A. (2017). Impacts of low temperature on the teleost immune system. *Biology.* 6, 39. doi:10.3390/biology6040039.

Acerete, L., Balasch, J. C., Castellana, B., Redruello, B., Roher, N., Canario, A. V., et al. (2007). Cloning of the glucocorticoid receptor (GR) in gilthead seabream (*Sparus aurata*). Differential expression of GR and immune genes in gilthead seabream after an immune challenge. *Comp. Biochem. Physiol. - B Biochem. Mol. Biol.* 148, 32-43. doi:10.1016/j.cbpb.2007.04.015.

Afgan, E., Baker, D., Batut, B., van den Beek, M., Bouvier, D., Čech, M., et al. (2018). The Galaxy platform for accessible, reproducible and collaborative biomedical analyses: 2018 update. *Nucleic Acids Res.* 46, W537–W544. doi:10.1093/nar/gky379.

Ahn, D. H., Kang, S., and Park, H. (2016). Transcriptome analysis of immune response genes induced by pathogen agonists in the Antarctic bullhead notothen *Notothenia coriiceps*. *Fish Shellfish Immunol.* 55, 315–322. doi:10.1016/j.fsi.2016.06.004.

Ahn, D. H., Shin, S. C., and Park, H. (2014). Characterization of Toll-like receptor gene expression and the pathogen agonist response in the antarctic bullhead notothen *Notothenia coriiceps*. *Immunogenetics.* 66, 563–573. doi:10.1007/s00251-014-0792-3.

Ahn, I.-Y., Lee, S. H., Kim, K. T., Shim, J. H., and Kim, D.-Y. (1996). Baseline heavy metal concentrations in the Antarctic clam, *Laternula elliptica* in Maxwell Bay, King George Island, Antarctica. *Mar. Pollut. Bull.* 32, 592–598. doi:10.1016/0025-326X(95)00247-K.

Ahola, A. J., Lassenius, M. I., Forsblom, C., Harjutsalo, V., Lehto, M., and Groop, P. H. (2017). Dietary patterns reflecting healthy food choices are associated with lower serum LPS activity. *Sci. Rep.* 7, 6511. doi:10.1038/s41598-017-06885-7.

Ainsworth, A. J. (1992). Fish granulocytes: Morphology, distribution, and function. *Annu. Rev. Fish Dis.* 2, 123-148. doi:10.1016/0959-8030(92)90060-B.

Ainsworth, A. J., Dexiang, C., Waterstrat, P. R., and Greenway, T. (1991). Effect of temperature on the immune system of channel catfish (*Ictalurus punctatus*)-I. Leucocyte distribution and phagocyte function in the anterior kidney at 10°C. *Comp. Biochem. Physiol. - Part A Physiol.* 100, 907-12. doi:10.1016/0300-9629(91)90313-2.

Akira, S., Uematsu, S., and Takeuchi, O. (2006). Pathogen recognition and innate immunity. *Cell*. 124, 783–801. doi:10.1016/j.cell.2006.02.015.

Albertson, R. C., Yan, Y. L., Titus, T. A., Pisano, E., Vacchi, M., Yelick, P. C., et al. (2010). Molecular pedomorphism underlies craniofacial skeletal evolution in Antarctic notothenioid fishes. *BMC*

Evol. Biol. 10, 4. doi:10.1186/1471-2148-10-4.

Alcaide, M., Edwards, S. V., Negro, J. J., Serrano, D., and Tella, J. L. (2008). Extensive polymorphism and geographical variation at a positively selected MHC class II B gene of the lesser kestrel (*Falco naumanni*). *Mol. Ecol.* 17, 2652–65. doi:10.1111/j.1365-294X.2008.03791.x.

Ali, M., Chernova, T. A., Newnam, G. P., Yin, L., Shanks, J., Karpova, T. S., et al. (2014). Stress-dependent proteolytic processing of the actin assembly protein LSB1 modulates a yeast prion. *J. Biol. Chem.* 289, 27625-39. doi:10.1074/jbc.M114.582429.

Alkie, T. N., de Jong, J., Jenik, K., Klinger, K. M., and DeWitte-Orr, S. J. (2019). Enhancing innate antiviral immune responses in rainbow trout by double stranded RNA delivered with cationic phytoglycogen nanoparticles. *Sci. Rep.* 9, 13619. doi:10.1038/s41598-019-49931-2.

Altschul, S. F., Gish, W., Miller, W., Myers, E. W., and Lipman, D. J. (1990). Basic local alignment search tool. *J. Mol. Biol.* 215, 403-10. doi:10.1016/S0022-2836(05)80360-2.

Álvarez, C. A., Ramírez-Cepeda, F., Santana, P., Torres, E., Cortés, J., Guzmán, F., et al. (2017). Insights into the diversity of NOD-like receptors: Identification and expression analysis of NLRC3, NLRC5 and NLRX1 in rainbow trout. *Mol. Immunol.* 87, 102–113. doi:10.1016/j.molimm.2017.03.010.

Alves, R. N., Sundell, K. S., Anjos, L., Sundh, H., Harboe, T., Norberg, B., et al. (2018). Structural and functional maturation of skin during metamorphosis in the Atlantic halibut (*Hippoglossus hippoglossus*). *Cell Tissue Res.* 372, 469–492. doi:10.1007/s00441-018-2794-1.

Amparyup, P., Charoensapsri, W., Samaluka, N., Chumtong, P., Yocawibun, P., and Imjongjirak, C. (2020). Transcriptome analysis identifies immune-related genes and antimicrobial peptides in Siamese fighting fish (*Betta splendens*). *Fish Shellfish Immunol.* 99, 403–413. doi:10.1016/j.fsi.2020.02.030.

Andresen, A. M. S., Boudinot, P., and Gjøen, T. (2020). Kinetics of transcriptional response against poly (I:C) and infectious salmon anemia virus (ISAV) in Atlantic salmon kidney (ASK) cell line. *Dev. Comp. Immunol.* 110, 103716. doi:10.1016/j.dci.2020.103716.

Andrews, N. C. (1999). The iron transporter DMT1. *Int. J. Biochem. Cell Biol.* 31, 991–994. doi:10.1016/S1357-2725(99)00065-5.

Andrews, S. (2015). FASTQC A Quality Control tool for High Throughput Sequence Data. [online]

Ángeles Esteban, M. (2012). An Overview of the Immunological Defenses in Fish Skin. *ISRN Immunol.* 2012, 853470. doi:10.5402/2012/853470.

Angosto, D., López-Castejón, G., López-Muñoz, A., Sepulcre, M. P., Arizcun, M., Meseguer, J., et al. (2012). Evolution of inflammasome functions in vertebrates: Inflammasome and caspase-1 trigger fish macrophage cell death but are dispensable for the processing of IL-1β. *Innate Immun.* 18, 815-24. doi:10.1177/1753425912441956.

Angosto, D., and Mulero, V. (2014). The zebrafish as a model to study the inflammasome. *Inflammasome.* 1, 27–29. doi:10.2478/infl-2014-0002.

Antonopoulou, E., Kaitetzidou, E., Castellana, B., Panteli, N., Kyriakis, D., Vraskou, Y., et al. (2017). In vivo effects of lipopolysaccharide on peroxisome proliferator-activated receptor expression in juvenile gilthead seabream (*Sparus aurata*). *Biology.* 6, 36. doi:10.3390/biology6040036.

Ao, J., Ding, Y., Chen, Y., Mu, Y., and Chen, X. (2015). Molecular Characterization and Biological Effects of a C-Type Lectin-Like Receptor in Large Yellow Croaker (*Larimichthys crocea*). *Int. J. Mol. Sci.* 16, 29631–29642. doi:10.3390/ijms161226175.

Apostolopoulos, V. and MacKenzie, I. F. C. (2001). Role of the Mannose Receptor in the Immune Response. Curr. Mol. Med. 1, 469–474. doi:10.2174/1566524013363645.

Araya, M. A., Valenzuela, T., Inostroza, N. G., Maruyama, F., Jorquera, M. A., and Acuña, J. J. (2020). Isolation and characterization of cold-tolerant hyper-ACC-degrading bacteria from the rhizosphere, endosphere, and phyllosphere of antarctic vascular plants. *Microorganisms*. 8, 1788. doi:10.3390/microorganisms8111788.

Armstrong, P. B. (2015). Comparative Biology of the Pentraxin Protein Family: Evolutionarily Conserved Component of Innate Immune System. *Int. Rev. Cell Mol. Biol.* 316, 1-47. doi:10.1016/bs.ircmb.2015.01.002.

Arrode-Brusés, G., and Brusés, J. L. (2012). Maternal immune activation by poly I:C induces expression of cytokines IL-1β and IL-13, chemokine MCP-1 and colony stimulating factor VEGF in fetal mouse brain. *J. Neuroinflammation* 9, 83. doi:10.1186/1742-2094-9-83.

Artimo, P., Jonnalagedda, M., Arnold, K., Baratin, D., Csardi, G., De Castro, E., et al. (2012). ExPASy: SIB bioinformatics resource portal. *Nucleic Acids Res.* 40, W597-603. doi:10.1093/nar/gks400.

Arumugam, M., Raes, J., Pelletier, E., Le Paslier, D., Yamada, T., Mende, D. R., et al. (2011). Enterotypes of the human gut microbiome. *Nature*. 473, 174–180. doi:10.1038/nature09944.

Ashfaq, H., Soliman, H., Saleh, M., and El-Matbouli, M. (2019). CD4: A vital player in the teleost fish immune system. *Vet. Res.* 50, 1-11. doi:10.1186/s13567-018-0620-0.

Assmy, P., Lochte, K., and Smetacek, V. (2009). Plankton productivity and the role of iron in the Southern Ocean. Biological Studies in Polar Oceans: Exploration of Life in Icy Waters. *Wirtschaftsvlg*. Ed. Gotthilf and Hempel, I. 227–235.

Auvinet, J., Graça, P., Dettai, A., Amores, A., Postlethwait, J. H., Detrich, H. W., et al. (2020). Multiple independent chromosomal fusions accompanied the radiation of the Antarctic teleost genus *Trematomus* (Notothenioidei:Nototheniidae). *BMC Evol. Biol.* 20, 39. doi:10.1186/s12862-020-1600-3.

Avery, J. C., and Hoffmann, P. R. (2018). Selenium, selenoproteins, and immunity. *Nutrients.* 10, 1203. doi:10.3390/nu10091203.

Azam, S., Jakaria, M., Kim, I. S., Kim, J., Ezazul Haque, M., and Choi, D. K. (2019). Regulation of toll-like receptor (TLR) signaling pathway by polyphenols in the treatment of age-linked neurodegenerative diseases: Focus on TLR4 signaling. *Front. Immunol.* 10, 1000. doi:10.3389/fimmu.2019.01000.

Baalsrud, H. T., Tørresen, O. K., Solbakken, M. H., Salzburger, W., Hanel, R., Jakobsen, K. S., et al. (2018). *De Novo* Gene Evolution of Antifreeze Glycoproteins in Codfishes Revealed by Whole Genome Sequence Data. *Mol. Biol. Evol.* 35, 593–606. doi:10.1093/molbev/msx311.

Bai, S. C., and Lee, S. (2010). Culture of Olive Flounder: Korean Perspective. Practical Flatfish Culture Stock Enhancement. *Blackwell*. Ed. Daniels, H. V. and Watanabe, W. O. 156–168. doi:10.1002/9780813810997.ch9.

Baird, T. T. (2013). Trypsin. Brenner's Encyclopedia of Genetics. *Academic Press*. Ed. Maloy, S. and Hughes, K. 4368, 216-219. doi:10.1016/B978-0-12-374984-0.01589-8.

Balasch, J. C., and Tort, L. (2019). Netting the stress responses in fish. *Front. Endocrinol.* 10, 1–12. doi:10.3389/fendo.2019.00062.

Balla, K. M., Lugo-Villarino, G., Spitsbergen, J. M., Stachura, D. L., Hu, Y., Bañuelos, K., et al. (2010). Eosinophils in the zebrafish: Prospective isolation, characterization, and eosinophilia induction by helminth determinants. *Blood*. 116, 3944-54. doi:10.1182/blood-2010-03-267419.

Baoprasertkul, P., Peatman, E., Somridhivej, B., and Liu, Z. (2006). Toll-like receptor 3 and TICAM genes in catfish: Species-specific expression profiles following infection with *Edwardsiella*

ictaluri. *Immunogenetics*. 58, 817-30. doi:10.1007/s00251-006-0144-z.

Barandica, L., and Tort, L. (2008). Neuroendocrinología e inmunologia de la respuesta al estres en peces. *Rev. la Acad. Colomb. Ciencias Exactas, Físicas y Nat.* 32, 267–284. http://link.gale.com/apps/doc/A188490578/IFME?u=anon~43b22271&sid=googleScholar&xid=1766c7a5.

Bargagli, R. (2008). Environmental contamination in Antarctic ecosystems. *Sci. Total Environ.* 400, 212–226. doi:10.1016/j.scitotenv.2008.06.062.

Barker, P. F., Filippelli, G. M., Florindo, F., Martin, E. E., and Scher, H. D. (2007). Onset and role of the Antarctic Circumpolar Current. *Deep. Res. Part II Top. Stud. Oceanogr.* 54, 2388-2398. doi:10.1016/j.dsr2.2007.07.028.

Barnes, D., Webb, K., and Linse, K. (2006). Slow growth of Antarctic bryozoans increases over 20 years and is anomalously high in 2003. *Mar. Ecol. Prog. Ser.* 314, 187–195. doi:10.3354/meps314187.

Barreiro, L. B., Ben-Ali, M., Quach, H., Laval, G., Patin, E., Pickrell, J. K., et al. (2009). Evolutionary dynamics of human toll-like receptors and their different contributions to host defense. *PLoS Genet.* 5, e1000562. doi:10.1371/journal.pgen.1000562.

Barrera-Oro, E., La Mesa, M., and Moreira, E. (2014). Early life history timings in marbled rockcod (*Notothenia rossii*) fingerlings from the South Shetland Islands as revealed by otolith microincrement. *Polar Biol.* 37, 1099-1109. doi:10.1007/s00300-014-1503-0.

Barrera-Oro, E., Moreira, E., Seefeldt, M. A., Valli Francione, M., and Quartino, M. L. (2019). The importance of macroalgae and associated amphipods in the selective benthic feeding of sister rockcod species *Notothenia rossii* and *N. coriiceps* (Nototheniidae) in West Antarctica. *Polar Biol.* 42, 317–334. doi:10.1007/s00300-018-2424-0.

Barrera-Oro, E. R., and Marschoff, E. R. (2007). Information on the status of fjord *Notothenia rossii*, *Gobionotothen gibberifrons* and *Notothenia coriiceps* in the lower South Shetland Islands, derived from the 2000-2006 monitoring program at Potter Cove. *CCAMLR Sci.*14, 83-87.

Bassity, E., and Clark, T. G. (2012). Functional identification of dendritic cells in the teleost model, rainbow trout (*Oncorhynchus mykiss*). *PLoS One*. 7, e33196. doi:10.1371/journal.pone.0033196.

Bateman, A., Martin, M. J., O'Donovan, C., Magrane, M., Alpi, E., Antunes, R., et al. (2017). UniProt: The universal protein knowledgebase. *Nucleic Acids Res.* 45, D158-D169. doi:10.1093/nar/gkw1099.

Bayne, C. J., and Gerwick, L. (2001). The acute phase response and innate immunity of fish. *Dev. Comp. Immunol.* 25, 725-743.doi:10.1016/S0145-305X(01)00033-7.

Beers, J. M., and Jayasundara, N. (2015). Antarctic notothenioid fish: what are the future consequences of "losses" and "gains" acquired during long-term evolution at cold and stable temperatures? *J. Exp. Biol.* 218, 1834–1845. doi:10.1242/jeb.116129.

Béland, K., Lapierre, P., Djilali-Saiah, I., and Alvarez, F. (2012). Liver Restores Immune Homeostasis after Local Inflammation despite the Presence of Autoreactive T Cells. *PLoS One*. 7, e48192. doi:10.1371/journal.pone.0048192.

Belkaid, Y., and Hand, T. W. (2014). Role of the microbiota in immunity and inflammation. *Cell*. 157, 121-141. doi:10.1016/j.cell.2014.03.011.

Ben Menachem-Zidon, O., Avital, A., Ben-Menahem, Y., Goshen, I., Kreisel, T., Shmueli, E. M., et al. (2011). Astrocytes support hippocampal-dependent memory and long-term potentiation via interleukin-1 signaling. *Brain. Behav. Immun.* 25, 1008-16. doi:10.1016/j.bbi.2010.11.007.

Berczi, I., Bertók, L., and Bereznai, T. (1966). Comparative studies on the toxicity of *Escherichia coli* lipopolysaccharide endotoxin in various animal species. *Can. J. Microbiol.* 12, 1070–1071.

doi:10.1139/m66-143.

Berczi, I., and Szentivanyi, A. (2003). The acute phase response. *NeuroImmune Biol.* 3, 463-494. doi:10.1016/S1567-7443(03)80059-5.

Bethke, J., Poblete-Morales, M., Irgang, R., Yáñez, A., and Avendaño-Herrera, R. (2016). Iron acquisition and siderophore production in the fish pathogen *Renibacterium salmoninarum*. *J. Fish Dis.* 39, 1275–1283. doi:10.1111/jfd.12456.

Bethke, J., Yáñez, A. J., and Avendaño-Herrera, R. (2018). Comparative genomic analysis of two Chilean *Renibacterium salmoninarum* isolates and the type strain ATCC 33209T. *Genome Biol. Evol.* 10, 1816–1822. doi:10.1093/gbe/evy138.

Beutler, B. (2002). TLR4 as the mammalian endotoxin sensor. *Curr. Top. Microbiol. Immunol.* 270, 109–120. doi:10.1007/978-3-642-59430-4_7.

Bi, D., Wang, Y., Gao, Y., Li, X., Chu, Q., Cui, J., et al. (2018). Recognition of Lipopolysaccharide and activation of NF-κB by cytosolic sensor NOD1 in teleost fish. *Front. Immunol.* 9, 1413. doi:10.3389/fimmu.2018.01413.

Biacchesi, S., LeBerre, M., Lamoureux, A., Louise, Y., Lauret, E., Boudinot, P., et al. (2009). Mitochondrial Antiviral Signaling Protein Plays a Major Role in Induction of the Fish Innate Immune Response against RNA and DNA Viruses. *J. Virol.* 83, 7815-26. doi:10.1128/jvi.00404-09.

Bierlich, K. C., Miller, C., DeForce, E., Friedlaender, A. S., Johnston, D. W., and Apprill, A. (2018). Temporal and regional variability in the skin microbiome of humpback whales along the Western Antarctic Peninsula. *Appl. Environ. Microbiol.* 84, e02574-17. doi:10.1128/AEM.02574-17.

Bilyk, K. T., Vargas-Chacoff, L., and Cheng, C. H. C. (2018). Evolution in chronic cold: Varied loss of cellular response to heat in Antarctic notothenioid fish. *BMC Evol. Biol.* 18, 143. doi:10.1186/s12862-018-1254-6.

Bishop, R. E. (2005). Fundamentals of endotoxin structure and function. Concepts in Bacterial Virulence. *Contrib. Microbiol.* Ed. Russell, W. and Herwald, H. 12, 1–27. doi:10.1159/000081687.

Bly, J. E., and Clem, L. W. (1992). Temperature and teleost immune functions. *Fish Shellfish Immunol.* 2, 159-171. doi:10.1016/S1050-4648(05)80056-7.

Boes, M. (2000). Role of natural and immune IgM antibodies in immune responses. *Mol. Immunol.* 37, 1141-9. doi:10.1016/S0161-5890(01)00025-6.

Bolger, A. M., Lohse, M., and Usadel, B. (2014). Trimmomatic: A flexible trimmer for Illumina sequence data. *Bioinformatics*. 30, 2140-2120. doi:10.1093/bioinformatics/btu170.

Bonneaud, C., Wilson, R. S., and Seebacher, F. (2016). Immune-challenged fish up-regulate their metabolic scope to support locomotion. *PLoS One* 11, 1–14. doi:10.1371/journal.pone.0166028.

Boshra, H., Li, J., and Sunyer, J. O. (2006). Recent advances on the complement system of teleost fish. *Fish Shellfish Immunol*. 20, 239-62. doi:10.1016/j.fsi.2005.04.004.

Botos, I., Segal, D. M., and Davies, D. R. (2011). The structural biology of Toll-like receptors. *Structure* 19, 447–459. doi:10.1016/j.str.2011.02.004.

Bottos, E. M., Laughlin, D. C., Herbold, C. W., Lee, C. K., McDonald, I. R., and Cary, S. C. (2020). Abiotic factors influence patterns of bacterial diversity and community composition in the Dry Valleys of Antarctica. *FEMS Microbiol. Ecol.* 96. doi:10.1093/femsec/fiaa042.

Bowden, T. J., Cook, P., and Rombout, J. H. W. M. (2005). Development and function of the thymus in teleosts. *Fish Shellfish Immunol.* 19, 413–427. doi:10.1016/j.fsi.2005.02.003.

Bradford, M. M. (1976). A rapid and sensitive method for the quantitation of microgram quantities of protein utilizing the principle of protein-dye binding. *Anal. Biochem.* 72, 248–254. doi:10.1016/0003-2697(76)90527-3.

Bridges, A. F., and Manning, M. J. (1991). The effects of priming immersions in various human gamma globulin (HGG) vaccines on humoral and cell-mediated immune responses after intraperitoneal HGG challenge in the carp, *Cyprinus carpio L. Fish Shellfish Immunol.* 1, 119-129. doi:10.1016/S1050-4648(06)80012-4.

Briolat, V., Jouneau, L., Carvalho, R., Palha, N., Langevin, C., Herbomel, P., et al. (2014). Contrasted Innate Responses to Two Viruses in Zebrafish: Insights into the Ancestral Repertoire of Vertebrate IFN-Stimulated Genes. *J. Immunol.* 192, 4328–4341. doi:10.4049/jimmunol.1302611.

Brocker, C., Thompson, D., Matsumoto, A., Nebert, D. W., and Vasiliou, V. (2010). Evolutionary divergence and functions of the human interleukin (IL) gene family. *Hum. Genomics*. 5, 30-55. doi:10.1186/1479-7364-5-1-30.

Bromage, E. S., Kaattari, I. M., Zwollo, P., and Kaattari, S. L. (2004). Plasmablast and Plasma Cell Production and Distribution in Trout Immune Tissues. *J. Immunol.* 173, 7317-23. doi:10.4049/jimmunol.173.12.7317.

Brubaker, S. W., Bonham, K. S., Zanoni, I., and Kagan, J. C. (2015). Innate immune pattern recognition: A cell biological perspective. *Annu. Rev. Immunol.* 33, 257–90. doi:10.1146/annurev-immunol-032414-112240.

Bruno, S., Coppola, D., Di Prisco, G., Giordano, D., and Verde, C. (2019). Enzymes from marine polar regions and their biotechnological applications. *Mar. Drug.s* 17, 1–36. doi:10.3390/md17100544.

Brussaard, C. P. D., Timmermans, K. R., Uitz, J., and Veldhuis, M. J. W. (2008). Virioplankton dynamics and virally induced phytoplankton lysis versus microzooplankton grazing southeast of the Kerguelen (Southern Ocean). *Deep Sea Res. Part II Top. Stud. Oceanogr.* 55, 752–765. doi:10.1016/j.dsr2.2007.12.034.

Bryant, D. M., Johnson, K., DiTommaso, T., Tickle, T., Couger, M. B., Payzin-Dogru, D., et al. (2017). A Tissue-Mapped Axolotl *De Novo* Transcriptome Enables Identification of Limb Regeneration Factors. *Cell Rep.* 18, 762-776. doi:10.1016/j.celrep.2016.12.063.

Bu, D., Luo, H., Huo, P., Wang, Z., Zhang, S., He, Z., et al. (2021). KOBAS-i: intelligent prioritization and exploratory visualization of biological functions for gene enrichment analysis. *Nucleic Acids Res.* 49, W317–W325. doi:10.1093/nar/gkab447.

Buchmann, K. (2014). Evolution of innate immunity: Clues from invertebrates via fish to mammals. *Front. Immunol.* 5, 1-8. doi:10.3389/fimmu.2014.00459.

Buick, D. P., and Ivany, L. C. (2004). 100 years in the dark: Extreme longevity of Eocene bivalves from Antarctica. *Geology.* 32, 921–924. doi:10.1130/G20796.1.

Bukin, Y. S., Galachyants, Y. P., Morozov, I. V., Bukin, S. V., Zakharenko, A. S., and Zemskaya, T. I. (2019). The effect of 16s rRNA region choice on bacterial community metabarcoding results. *Sci. Data*. 6, 190007. doi:10.1038/sdata.2019.7.

Buonocore, F., Bernini, C., Coscia, M. R., Giacomelli, S., de Pascale, D., Randelli, E., et al. (2016). Immune response of the Antarctic teleost *Trematomus bernacchii* to immunization with *Psychrobacter sp.* (TAD1). *Fish Shellfish Immunol.* 56, 192–198. doi:10.1016/j.fsi.2016.07.009.

Buonocore, F., Randelli, E., Paderi, F., Bird, S., Secombes, C. J., Mazzini, M., et al. (2006). The cytokine IL-1β from the crocodile icefish *Chionodraco hamatus* (Perciformes: Channichthyidae). *Polar Biol.* 29, 1018-1027. doi:10.1007/s00300-006-0145-2.

Bury, N., and Grosell, M. (2003). Iron acquisition by teleost fish. *Comp. Biochem. Physiol. C Toxicol.*

Pharmacol. 135, 97–105. doi:10.1016/s1532-0456(03)00021-8.

Butt, R. L., and Volkoff, H. (2019). Gut microbiota and energy homeostasis in fish. *Front. Endocrinol.* 10, 9. doi:10.3389/fendo.2019.00009.

Byrd, A. L., Liu, M., Fujimura, K. E., Lyalina, S., Nagarkar, D. R., Charbit, B., et al. (2020). Stability and dynamics of the human gut microbiome and its association with systemic immune traits. *bioRxiv*. 909853. doi:10.1101/2020.01.17.909853.

Cai, Y., Wang, S., Guo, W., Xie, Z., Zheng, Y., Cao, Z., et al. (2018). Transcriptome analysis provides insights into the immune responsive pathways and genes in the head kidney of tiger grouper (*Epinephelus fuscoguttatus*) fed with *Spatholobus suberectus*, *Phellodendron amurense*, or *Eclipta prostrata*. *Fish Shellfish Immunol.* 73, 100–111. doi:10.1016/j.fsi.2017.12.004.

Calì, F., Riginella, E., La Mesa, M., and Mazzoldi, C. (2017). Life history traits of *Notothenia rossii* and *N. coriiceps* along the southern Scotia Arc. *Polar Biol.* 40, 1409-1423. doi:10.1007/s00300-016-2066-z.

Callewaert, C., Ravard Helffer, K., and Lebaron, P. (2020). Skin Microbiome and its Interplay with the Environment. *Am. J. Clin. Dermatol.* 21, 4–11. doi:10.1007/s40257-020-00551-x.

Calquín, P., Ruiz, P., Oliver, C., Sánchez, P., Haro, R., Oliva, H., et al. (2018). Physiological evidence that Piscirickettsia salmonis produces siderophores and uses iron from different sources. *J. Fish Dis.* 41, 553–558. doi:10.1111/jfd.12745.

Campbell, H. A., Fraser, K. P. P., Bishop, C. M., Peck, L. S., and Egginton, S. (2011). Hibernation in an antarctic fish: On ice for winter. Research Progress in Fisheries Science. *Apple Academic Press*. Ed. III, W. H. 19. doi:10.1201/b14534-10.

Campos, C., Castanheira, M. F., Engrola, S., Valente, L. M. P., Fernandes, J. M. O., and Conceição, L. E. C. (2013). Rearing temperature affects Senegalese sole (*Solea senegalensis*) larvae protein metabolic capacity. *Fish Physiol. Biochem.* 39, 1485-1496. doi:10.1007/s10695-013-9802-x.

Canapa, A., Barucca, M., Gorbi, S., Benedetti, M., Zucchi, S., Biscotti, M. A., et al. (2007). Vitellogenin gene expression in males of the Antarctic fish *Trematomus bernacchii* from Terra Nova Bay (Ross Sea): A role for environmental cadmium? *Chemosphere.* 66, 1270–1277. doi:10.1016/j.chemosphere.2006.07.026.

Cao, L., Huang, Q., Wu, Z., Cao, D. D., Ma, Z., Xu, Q., et al. (2016). Neofunctionalization of zona pellucida proteins enhances freeze-prevention in the eggs of Antarctic notothenioids. *Nat. Commun.* 7. doi:10.1038/ncomms12987.

Casaux, R. J., Mazzotta, A. S., and Barrera-Oro, E. R. (1990). Seasonal aspects of the biology and diet of nearshore nototheniid fish at Potter Cove, South Shetland Islands, Antarctica. *Polar Biol.* 11, 63-72. doi:10.1007/BF00236523.

Castillo, J., Teles, M., Mackenzie, S., and Tort, L. (2009). Stress-related hormones modulate cytokine expression in the head kidney of gilthead seabream (*Sparus aurata*). *Fish Shellfish Immunol.* 27, 493-9. doi:10.1016/j.fsi.2009.06.021.

Castro, R., Coll, J., Blanco, M. D. M., Rodriguez-Bertos, A., Jouneau, L., Fernández-Garayzábal, J. F., et al. (2019). Spleen and head kidney differential gene expression patterns in trout infected with *Lactococcus garvieae* correlate with spleen granulomas. *Vet. Res.* 50, 32. doi:10.1186/s13567-019-0649-8.

Castro, R., Zou, J., Secombes, C. J., and Martin, S. A. M. (2011). Cortisol modulates the induction of inflammatory gene expression in a rainbow trout macrophage cell line. *Fish Shellfish Immunol.* 30, 215-23. doi:10.1016/j.fsi.2010.10.010.

Cerdà, J., and Manchado, M. (2013). Advances in genomics for flatfish aquaculture. *Genes Nutr.*, 5–17.

doi:10.1007/s12263-012-0312-8.

Cesta, M. F. (2006). Normal Structure, Function, and Histology of Mucosa-Associated Lymphoid Tissue. *Toxicol. Pathol.* 34, 599-608. doi:10.1080/01926230600865531.

Chaigneau, A., and Morrow, R. (2002). Surface temperature and salinity variations between Tasmania and Antarctica, 1993-1999. *J. Geophys. Res. Ocean.* 107, 1993–1999. doi:10.1029/2001jc000808.

Chao, A. (1984). Nonparametric Estimation of the Number of Classes in a Population. *Scand. J. Stat.* 11, 265–270. http://www.jstor.org/stable/4615964.

Chang, D. T., Jones, J. A., Meyerson, H., Colton, E., Kwon, I. K., Matsuda, T., et al. (2008). Lymphocyte/macrophage interactions: biomaterial surface-dependent cytokine, chemokine, and matrix protein production. *J. Biomed. Mater. Res. A* 87, 676–687. doi:10.1002/jbm.a.31630.

Chang, M. X., Xiong, F., Wu, X. M., and Hu, Y. W. (2021). The expanding and function of NLRC3 or NLRC3-like in teleost fish: Recent advances and novel insights. *Dev. Comp. Immunol.* 114, 103859. doi:https://doi.org/10.1016/j.dci.2020.103859.

Chantanachookhin, C., Seikai, T., and Tanaka, M. (1991). Comparative study of the ontogeny of the lymphoid organs in three species of marine fish. *Aquaculture*. 99, 143-155. doi:10.1016/0044-8486(91)90294-H.

Chao, A., and Lee, S.-M. (1992). Estimating the Number of Classes via Sample Coverage. *J. Am. Stat. Assoc.* 87, 210–217. doi:10.1080/01621459.1992.10475194.

Chao, A., and Yang, M. C. K. (1993). Stopping rules and estimation for recapture debugging with unequal failure rates. *Biometrika* 80, 193–201. doi:10.1093/biomet/80.1.193.

Chattopadhyay, M. K. (2006). Mechanism of bacterial adaptation to low temperature. *J. Biosci.* 31, 157–165. doi:10.1007/BF02705244.

Chaves-Pozo, E., Pelegrín, P., García-Castillo, J., García-Ayala, A., Mulero, V., and Meseguer, J. (2004). Acidophilic granulocytes of the marine fish gilthead seabream (*Sparus aurata L.*) produce interleukin-1β following infection with *Vibrio anguillarum*. *Cell Tissue Res.* 316, 189-195. doi:10.1007/s00441-004-0875-9.

Chen, H., Wang, B., Yu, N., Qi, J., Tang, N., Wang, S., et al. (2019a). Transcriptome analysis and the effects of polyunsaturated fatty acids on the immune responses of the critically endangered angtze sturgeon (*Acipenser dabryanus*). *Fish Shellfish Immunol.* 94, 199–210. doi:10.1016/j.fsi.2019.09.012.

Chen, L., DeVries, A. L., and Cheng, C. H. (1997a). Convergent evolution of antifreeze glycoproteins in Antarctic notothenioid fish and Arctic cod. *Proc. Natl. Acad. Sci. USA.* 94, 3817–3822. doi:10.1073/pnas.94.8.3817.

Chen, L., Devries, A. L., and Cheng, C. H. C. (1997b). Evolution of antifreeze glycoprotein gene from a trypsinogen gene in Antarctic notothenioid fish. *Proc. Natl. Acad. Sci. USA.* 94, 3811–3816. doi:10.1073/pnas.94.8.3811.

Chen, L., Lu, Y., Li, W., Ren, Y., Yu, M., Jiang, S., et al. (2019b). The genomic basis for colonizing the freezing Southern Ocean revealed by Antarctic toothfish and Patagonian robalo genomes. *Gigascience* 22, 2472–2479. doi:10.1093/gigascience/giz016.

Chen, S., Cheng, A., and Wang, M. (2013). Innate sensing of viruses by pattern recognition receptors in birds. *Vet. Res.* 82. doi:10.1186/1297-9716-44-82.

Chen, S. N., Zou, P. F., and Nie, P. (2017). Retinoic acid-inducible gene I (RIG-I)-like receptors (RLRs) in fish: current knowledge and future perspectives. 151, 16-25. *Immunology*. doi:10.1111/imm.12714.

Chen, Y., Zhou, S., Jiang, Z., Wang, X., and Liu, Y. (2016). Chemokine receptor CXCR3 in turbot (*Scophthalmus maximus*): cloning, characterization and its responses to lipopolysaccharide. *Fish Physiol. Biochem.* 42, 659–671. doi:10.1007/s10695-015-0167-1.

Chen, Z., Cheng, C. H. C., Zhang, J., Cao, L., Chen, L., Zhou, L., et al. (2008). Transcriptomic and genomic evolution under constant cold in Antarctic notothenioid fish. *Proc. Natl. Acad. Sci. USA.* 105, 12944–12949. doi:10.1073/pnas.0802432105.

Cheng, C. H. C., and Chen, L. (1999). Evolution of an antifreeze glycoprotein. *Nature*. 401, 443-444. doi:10.1038/46721.

Cheng, C. H. C., and Detrich, H. W. (2007). Molecular ecophysiology of Antarctic notothenioid fishes. *Philos. Trans. R. Soc. B Biol. Sci.* 362, 2215-2232. doi:10.1098/rstb.2006.1946.

Cheng, L. S., Liu, Y., and Jiang, W. (2015). Restoring homeostasis of CD4+ T cells in hepatitis-B-virusrelated liver fibrosis. *World J. Gastroenterol.* 21, 10721-10731. doi:10.3748/wjg.v21.i38.10721.

Cheng, Y., Zak, O., Aisen, P., Harrison, S. C., Walz, T., and York, N. (2004). Structure of the Human Transferrin Receptor-Transferrin Complex. *Cell.* 116, 565–576. doi:S0092867404001308.

Chilmonczyk, S. (1992). The thymus in fish: Development and possible function in the immune response. *Annu. Rev. Fish Dis.* 2, 181–200. doi:10.1016/0959-8030(92)90063-4.

Choi, H. J., Ji, J., Chung, K.-H., and Ahn, I.-Y. (2007). Cadmium bioaccumulation and detoxification in the gill and digestive gland of the Antarctic bivalve *Laternula elliptica*. *Comp. Biochem. Physiol. Part C Toxicol. Pharmacol.* 145, 227–235. doi:10.1016/j.cbpc.2006.12.005.

Christybapita, D., Divyagnaneswari, M., and Dinakaran Michael, R. (2007). Oral administration of Eclipta alba leaf aqueous extract enhances the non-specific immune responses and disease resistance of *Oreochromis mossambicus*. *Fish Shellfish Immunol.* 23, 840-852. doi:10.1016/j.fsi.2007.03.010.

Chu, Q., Bi, D., Zheng, W., and Xu, T. (2020). MicroRNA negatively regulates NF-κB-mediated immune responses by targeting NOD1 in the teleost fish *Miichthys miiuy*. *Sci. China Life Sci.* 64, 803-815. doi:10.1007/s11427-020-1777-y.

Čikoš, Š., Bukovská, A., and Koppel, J. (2007). Relative quantification of mRNA: Comparison of methods currently used for real-time PCR data analysis. *BMC Mol. Biol.* 8, 1–14. doi:10.1186/1471-2199-8-113.

Clarke, A., Murphy, E. J., Meredith, M. P., King, J. C., Peck, L. S., Barnes, D. K. ., et al. (2007). Climate change and the marine ecosystem of the western Antarctic Peninsula. *Philos. Trans. R. Soc. B Biol. Sci.* 362, 149-166. doi:10.1098/rstb.2006.1958.

Clarke, L. J., Suter, L., King, R., Bissett, A., and Deagle, B. E. (2019). Antarctic Krill Are Reservoirs for Distinct Southern Ocean Microbial Communities. *Front. Microbiol.* 9, 3226. doi:10.3389/fmicb.2018.03226.

Cocca, E., Ratnayake-Lecamwasam, M., Parker, S. K., Camardella, L., Ciaramella, M., di Prisco, G., et al. (1995). Genomic remnants of alpha-globin genes in the hemoglobinless antarctic icefishes. *Proc. Natl. Acad. Sci. USA.* 92, 1817–1821. doi:10.1073/pnas.92.6.1817.

Collazo, A., Fraser, S. E., and Mabee, P. M. (1994). A dual embryonic origin for vertebrate mechanoreceptors. *Science.* 264, 426-430. doi:10.1126/science.8153631.

Collins, H. L. (2008). Withholding iron as a cellular defence mechanism - Friend or foe? *Eur. J. Immunol.* 38, 1803–1806. doi:10.1002/eji.200838505.

Congleton, J. L., and Wagner, E. J. (1991). Acute-phase hypoferremic response to in rainbow trout. *Comp. Biochem. Physiol.* 98A, 195–200. doi:0300-9629191.

Cook, A. J., Fox, A. J., Vaughan, D. G., and Ferrigno, J. G. (2005). Retreating glacier fronts on the Antarctic Peninsula over the past half-century. *Science.* 308, 541-544. doi:10.1126/science.1104235.

Coppe, A., Agostini, C., Marino, I. A. M., Zane, L., Bargelloni, L., Bortoluzzi, S., et al. (2013). Genome evolution in the cold: Antarctic icefish muscle transcriptome reveals selective duplications increasing mitochondrial function. *Genome Biol. Evol.* 5, 45–60. doi:10.1093/gbe/evs108.

Corbin, E., Vicente, J., Martin-Hernando, M. P., Acevedo, P., Pérez-Rodríguez, L., and Gortazar, C. (2008). Spleen mass as a measure of immune strength in mammals. *Mamm. Rev.* 38, 108-115. doi:10.1111/j.1365-2907.2007.00112.x.

Cossa, D., Heimbürger, L.-E., Lannuzel, D., Rintoul, S. R., Butler, E. C. V, Bowie, A. R., et al. (2011). Mercury in the Southern Ocean. *Geochim. Cosmochim. Acta.* 75, 4037–4052. doi:10.1016/j.gca.2011.05.001.

Costa, M. M., Maehr, T., Diaz-Rosales, P., Secombes, C. J., and Wang, T. (2011). Bioactivity studies of rainbow trout (*Oncorhynchus mykiss*) interleukin-6: Effects on macrophage growth and antimicrobial peptide gene expression. *Mol. Immunol.* 48, 1903–1916. doi:10.1016/j.molimm.2011.05.027.

Cronin, K. E., Walker, S. E., Mann, R., Chute, A. S., Long, M. C., and Bowser, S. S. (2020). Growth and longevity of the Antarctic scallop Adamussium colbecki under annual and multiannual sea ice. *Antarct. Sci.* 32, 466–475. doi:10.1017/S0954102020000322.

Cunha Da Silva, J. R. M., Cooper, E. L., Sinhorini, I. L., Borges, J. C. S., Jensch, B. E., Porto-Neto, L. R., et al. (2005). Microscopical study of experimental wound healing in *Notothenia coriiceps* (Cabeçuda) at 0°C. *Cell Tissue Res.* 321, 401-410. doi:10.1007/s00441-005-1139-z.

Dalmo, R. A., and Seijelid, R. (1995). The immunomodulatory effect of LPS, laminaran and sulphated laminaran [β(l,3)-D-glucan] on Atlantic salmon, *Salmo salar L.*, macrophages *in vitro*. *J. Fish Dis.* 18, 175-185. doi:10.1111/j.1365-2761.1995.tb00275.x.

Dang, Y., Xu, X., Shen, Y., Hu, M., Zhang, M., Li, L., et al. (2016). Transcriptome Analysis of the Innate Immunity-Related Complement System in Spleen Tissue of *Ctenopharyngodon idella* Infected with *Aeromonas hydrophila*. *PLoS One* 11, 1–22. doi:10.1371/journal.pone.0157413.

Darfour-Oduro, K. A., Megens, H. J., Roca, A. L., Groenen, M. A. M., and Schook, L. B. (2015). Adaptive evolution of Toll-like receptors (TLRs) in the family Suidae. *PLoS One.* 10, e0124069. doi:10.1371/journal.pone.0124069.

Davis, D. J., Bryda, E. C., Gillespie, C. H., and Ericsson, A. C. (2016). Microbial modulation of behavior and stress responses in zebrafish larvae. *Behav. Brain Res.* 311, 219–227. doi: 10.1016/j.bbr.2016.05.040.

Davison, W., and Franklin, C. E. (2002). The Antarctic nemertean *Parborlasia corrugatus*: An example of an extreme oxyconformer. *Polar Biol.* 25, 238–240. doi:10.1007/s00300-001-0341-z.

de Castro, E., Sigrist, C. J. A., Gattiker, A., Bulliard, V., Langendijk-Genevaux, P. S., Gasteiger, E., et al. (2006). ScanProsite: Detection of PROSITE signature matches and ProRule-associated functional and structural residues in proteins. *Nucleic Acids Res.* 34, 362–5. doi:10.1093/nar/gkl124.

De Haas, C. J. C., Van Leeuwen, E. M. M., Van Bommel, T., Verhoef, J., Van Kessel, K. P. M., and Van Strijp, J. A. G. (2000). Serum amyloid P component bound to gram-negative bacteria prevents lipopolysaccharide-mediated classical pathway complement activation. *Infect. Immun.* 68, 1753-9. doi:10.1128/IAI.68.4.1753-1759.2000.

De Souza, W. M., Fumagalli, M. J., Martin, M. C., de Araujo, J., Orsi, M. A., Sanfilippo, L. F., et al. (2019). Pingu virus: A new picornavirus in penguins from Antarctica. *Virus Evol.* 5, vez047.

doi:10.1093/ve/vez047.

Deguine, J., and Barton, G. M. (2014). MyD88: A central player in innate immune signaling. *F1000Prime Rep.* 6, 97. doi:10.12703/P6-97.

Demers, N. E., and Bayne, C. J. (1997). The immediate effects of stress on hormones and plasma lysozyme in rainbow trout. *Dev. Comp. Immunol.* 21, 363-373. doi:10.1016/S0145-305X(97)00009-8.

Detrich, H. W., and Amemiya, C. T. (2010). Antarctic notothenioid fishes: Genomic resources and strategies for analyzing an adaptive radiation. *Integrative and Comparative Biology* 50, 1009-1017. doi:10.1093/icb/icq071.

Detrich, H. W., Johnson, K. A., and Marchese-Ragona, S. P. (1989). Polymerization of Antarctic Fish Tubulins at Low Temperatures: Energetic Aspects. *Biochemistry*. 28, 10085-10093. doi:10.1021/bi00452a031.

Detrich, H. W., Parker, S. K., Williams, R. C., Nogales, E., and Downing, K. H. (2000). Cold adaptation of microtubule assembly and dynamics. Structural interpretation of primary sequence changes present in the alpha- and beta-tubulins of Antarctic fishes. *J. Biol. Chem.* 275, 37038-37047. doi:10.1074/jbc.M005699200.

DeVries, A. L., and Cheng, C. H. C. (2005). Antifreeze Proteins and Organismal Freezing Avoidance in Polar Fishes. *Fish Physiol.* 22, 155-201. doi:10.1016/S1546-5098(04)22004-0.

DeVries, A. L., and Wohlschlag, D. E. (1969). Freezing resistance in some antarctic fishes. *Science.* 163, 1073-1075. doi:10.1126/science.163.3871.1073.

Dexiang, C., and Ainsworth, A. J. (1991). Effect of temperature on the immune system of channel catfish (*Ictalurus punctatus*)-II. Adaptation of anterior kidney phagocytes to 10°C. *Comp. Biochem. Physiol. A Comp. Physiol.* 100, 913-918. doi:10.1016/0300-9629(91)90314-3.

Dhar, D., Dey, D., and Basu, S. (2019). Insights into the evolution of extracellular leucine-rich repeats in metazoans with special reference to Toll-like receptor 4. *J. Biosci.* 44, 1-17. doi:10.1007/s12038-018-9821-y.

Di Lorenzo, F., Crisafi, F., La Cono, V., Yakimov, M. M., Molinaro, A., and Silipo, A. (2020). The Structure of the Lipid A of Gram-Negative Cold-Adapted Bacteria Isolated from Antarctic Environments. *Mar. Drugs.* 18, 1-14. doi:10.3390/md18120592.

Di Prisco, G., Pisano, E., Clarke, A., Eastman, J. T., and Clarke, A. (1998). A Comparison of Adaptive Radiations of Antarctic Fish with those of NonAntarctic Fish. *Fishes of Antarctica*. 3-26. doi:10.1007/978-88-470-2157-0_1.

Dixon, B. a, Ph, D., and Bramlett, B. (1988). The Effect of Selenium on the Growth of Bacterial Fish Pathogens. 170–172.

Donatti, L., Zaleski, T., Calil, P., and Fanta, E. (2008). Photoperiod and feeding behavior of the Antarctic fish *Notothenia rossii* (Perciformes: Nototheniidae) and functional morphology of chemical and visual sensory structures used in foraging. *Rev. Bras. Zool.* 25, 254-262. doi:10.1590/S0101-81752008000200014.

Dong, X., Li, J., He, J., Liu, W., Jiang, L., Ye, Y., et al. (2016). Anti-infective mannose receptor immune mechanism in large yellow croaker (*Larimichthys crocea*). *Fish Shellfish Immunol.* 54, 257–265. doi:10.1016/j.fsi.2016.04.006.

Donovan, a, Brownlie, a, Zhou, Y., Shepard, J., Pratt, S. J., Moynihan, J., et al. (2000). Positional cloning of zebrafish ferroportin1 identifies a conserved vertebrate iron exporter. *Nature*. 403, 776–81. doi:10.1038/35001596.

Dorrington, M. G., and Fraser, I. D. C. (2019). NF-κB signaling in macrophages: Dynamics, crosstalk,

and signal integration. *Front. Immunol.* 10, 1-12. doi:10.3389/fimmu.2019.00705.

Douxfils, J., Mathieu, C., Mandiki, S. N. M., Milla, S., Henrotte, E., Wang, N., et al. (2011). Physiological and proteomic evidences that domestication process differentially modulates the immune status of juvenile Eurasian perch (*Perca fluviatilis*) under chronic confinement stress. *Fish Shellfish Immunol.* 31, 1113-1121. doi:10.1016/j.fsi.2011.10.001.

Du, L., Yang, X., Yang, L., Wang, X., Zhang, A., and Zhou, H. (2012). Molecular evidence for the involvement of RORα and RORγ in immune response in teleost. *Fish Shellfish Immunol.* 33, 418–426. doi:10.1016/j.fsi.2012.05.033.

Eastman, J. T. (2000). Antarctic notothenioid fishes as subjects for research in evolutionary biology. *Antarct. Sci.* 12, 276-287. doi:10.1017/s0954102000000341.

Eastman, J. T. (2005). The nature of the diversity of Antarctic fishes. *Polar Biol.* 28-93-107. doi:10.1007/s00300-004-0667-4.

Eastman, J. T., Barrera-Oro, E., and Moreira, E. (2011). Adaptive radiation at a low taxonomic level: Divergence in buoyancy of the ecologically similar Antarctic fish *Notothenia coriiceps* and *N. rossii*. *Mar. Ecol. Prog. Ser.* 438, 195-206. doi:10.3354/meps09287.

Eastman, J. T., and Devries, A. L. (1986). Renal glomerular evolution in Antarctic notothenioid fishes. *J. Fish Biol.* 29, 649-662. doi:10.1111/j.1095-8649.1986.tb04981.x.

Eastman, J. T., and DeVries, A. L. (1981). Buoyancy adaptations in a swim-bladderless Antarctic fish. *J. Morphol.* 167, 91–102. doi:10.1002/jmor.1051670108.

Eastman, J. T., and Hikida, R. S. (1991). Skin structure and vascularization in the Antarctic notothenioid fish Gymnodraco acuticeps. *J. Morphol.* 208, 347–365. doi:10.1002/jmor.1052080309.

Edgar, R. C. (2013). UPARSE: Highly accurate OTU sequences from microbial amplicon reads. *Nat. Methods* 10, 996–998. doi:10.1038/nmeth.2604.

Egerton, S., Culloty, S., Whooley, J., Stanton, C., and Ross, R. P. (2018). The gut microbiota of marine fish. *Front. Microbiol.* 9, 1-17. doi:10.3389/fmicb.2018.00873.

Eichmiller, J. J., Hamilton, M. J., Staley, C., Sadowsky, M. J., and Sorensen, P. W. (2016). Environment shapes the fecal microbiome of invasive carp species. *Microbiome*. 4, 1-13. doi:10.1186/s40168-016-0190-1.

Ellis, A. E. (1977). The leucocytes of fish: A review. *J. Fish Biol.* 11, 453-491. doi:10.1111/j.1095-8649.1977.tb04140.x.

Ellis, A. E. (1990). Lysozyme assays. Techniques in Fish Immunology. *SOS Publications*. Ed. Stolen J.S., Fletcher T.C., Anderson D.P., Roberson B.S. and Van Muiswinkel, W. B. 101–103.

Ellis, A. E. (2001). Innate host defense mechanisms of fish against viruses and bacteria. *Dev. Comp. Immunol.* 25, 827–39. doi:10.1016/S0145-305X(01)00038-6.

Emanuelsson, O., Brunak, S., von Heijne, G., and Nielsen, H. (2007). Locating proteins in the cell using TargetP, SignalP and related tools. *Nat. Protoc.* 2, 953-971. doi:10.1038/nprot.2007.131.

Engelsma, M. Y., Stet, R. J. M., Schipper, H., and Verburg-Van Kemenade, B. M. L. (2001). Regulation of interleukin 1 beta RNA expression in the common carp, *Cyprinus carpio L*. *Dev. Comp. Immunol.* 25, 195-203. doi:10.1016/S0145-305X(00)00059-8.

Esteban, M. Á., and Cerezuela, R. (2015). Fish mucosal immunity: skin. Mucosal Health in Aquaculture. *Academic Press*. Ed. Benjamin H. B. and Peatman, E. 67-92. doi: 10.1016/C2013-0-06826-0.

Evans, C., and Brussaard, C. P. D. (2012). Regional variation in lytic and lysogenic viral infection in the Southern Ocean and its contribution to biogeochemical cycling. *Appl. Environ. Microbiol.* 78,

6741–6748. doi:10.1128/AEM.01388-12.

Evans, D. L., and Jaso-Friedmann, L. (1992). Nonspecific cytotoxic cells as effectors of immunity in fish. *Annu. Rev. Fish Dis.* 2, 109-121. doi:10.1016/0959-8030(92)90059-7.

Fang, J., Tian, X., and Dong, S. (2010). The influence of water temperature and ration on the growth, body composition and energy budget of tongue sole (*Cynoglossus semilaevis*). *Aquaculture*. 299, 106-114. doi:10.1016/j.aquaculture.2009.11.026.

Fanta, E., and Meyer, A. A. (1998). Behavioural strategies for feeding of six species of the Antarctic fish family Nototheniidae (Pisces, Notothenioidei) in a tank. *Antarct. Rec.* 42, 227-243.

Feng, W., Gu, Y.-F., Nie, L., Guo, D.-Y., Xiang, L., and Shao, J. (2016). Characterization of SIGIRR/IL-1R8 Homolog from Zebrafish Provides New Insights into Its Inhibitory Role in Hepatic Inflammation. *J. Immunol.* 197, 151-167. doi:10.4049/jimmunol.1502334.

Fernández, D. A., Ceballos, S. G., Malanga, G., Boy, C. C., and Vanella, F. A. (2012). Buoyancy of sub-Antarctic notothenioids including the sister lineage of all other notothenioids (Bovichtidae). *Polar Biol.* 35, 99-106. doi:10.1007/s00300-011-1037-7.

Ferreira, M. F., Varela, M. L., Lo Nostro, F., Ansaldo, M., and Genovese, G. (2017). Reproductive aspects of *Notothenia rossii* and *N. coriiceps* (Perciformes, Nototheniidae) at Potter Cove, 25 de Mayo (King George) Island during austral summer. *Polar Biol.* 40, 1–11. doi:10.1007/s00300-016-1918-x.

Field, R., Campion, S., Warren, C., Murray, C., and Cunningham, C. (2010). Systemic challenge with the TLR3 agonist poly I:C induces amplified IFNalpha/beta and IL-1beta responses in the diseased brain and exacerbates chronic neurodegeneration. *Brain. Behav. Immun.* 24, 996–1007. doi:10.1016/j.bbi.2010.04.004.

Filby, A. L., Paull, G. C., Bartlett, E. J., Van Look, K. J. W., and Tyler, C. R. (2010). Physiological and health consequences of social status in zebrafish (*Danio rerio*). *Physiol. Behav.* 101, 576-587. doi:10.1016/j.physbeh.2010.09.004.

Finn, R. D., Clements, J., and Eddy, S. R. (2011). HMMER web server: Interactive sequence similarity searching. *Nucleic Acids Res.* 39, W29-W37. doi:10.1093/nar/gkr367.

Fischer, U., Koppang, E. O., and Nakanishi, T. (2013). Teleost T and NK cell immunity. *Fish Shellfish Immunol.* 35, 197-206. doi:10.1016/j.fsi.2013.04.018.

Fitch, N. A., Johnson, I. A., and Wood, R. E. (1984). Skeletal muscle capillary supply in a fish that lacks respiratory pigments. *Respir. Physiol.* 57, 201-211. doi:10.1016/0034-5687(84)90093-8.

Fornůsková, A., Vinkler, M., Pagès, M., Galan, M., Jousselin, E., Cerqueira, F., et al. (2013). Contrasted evolutionary histories of two Toll-like receptors (Tlr4 and Tlr7) in wild rodents (MURINAE). *BMC Evol. Biol.* 13, 1-17. doi:10.1186/1471-2148-13-194.

Franchini, P., Fruciano, C., Frickey, T., Jones, J. C., and Meyer, A. (2014). Erratum: The gut microbial community of midas cichlid fish in repeatedly evolved limnetic-benthic species pairs. *PLoS One*. 9, e95027. doi:10.1371/journal.pone.0103923.

Freedman, S. J. (1991). The role of alpha 2-macroglobulin in furunculosis: A comparison of rainbow trout and brook trout. *Comp. Biochem. Physiol. - Part B Biochem.* 98, 549-553. doi:10.1016/0305-0491(91)90252-9.

Fritsch, S. D., and Weichhart, T. (2016). Effects of interferons and viruses on metabolism. *Front. Immunol.* 7, 1–13. doi:10.3389/fimmu.2016.00630.

Fritz, J. H., and Girardin, S. E. (2005). How Toll-like receptors and Nod-like receptors contribute to innate immunity in mammals. *J. Endotoxin Res.* 11, 390–394. doi:10.1177/09680519050110060301.

Fujita, T., Matsushita, M., and Endo, Y. (2004). The lectin-complement pathway - Its role in innate immunity and evolution. *Immunol. Rev.* 198, 185-202. doi:10.1111/j.0105-2896.2004.0123.x.

Furbino, L. E., Godinho, V. M., Santiago, I. F., Pellizari, F. M., Alves, T. M. A., Zani, C. L., et al. (2014). Diversity Patterns, Ecology and Biological Activities of Fungal Communities Associated with the Endemic Macroalgae Across the Antarctic Peninsula. *Microb. Ecol.* 67, 775–787. doi:10.1007/s00248-014-0374-9.

Gallet, A., Koubbi, P., Léger, N., Scheifler, M., Ruiz-Rodriguez, M., Suzuki, M. T., et al. (2019). Low-diversity bacterial microbiota in Southern Ocean representatives of lanternfish genera Electrona, Protomyctophum and Gymnoscopelus (family Myctophidae). *PLoS One*. 14, 1-17. doi:10.1371/journal.pone.0226159.

Gao, F., Chen, C., Arab, D. A., Du, Z., He, Y., and Ho, S. Y. W. (2019). EasyCodeML: A visual tool for analysis of selection using CodeML. *Ecol. Evol.* 9, 3891–3898. doi:10.1002/ece3.5015.

Garate, J. A., and Oostenbrink, C. (2013). Lipid a from lipopolysaccharide recognition: Structure, dynamics and cooperativity by molecular dynamics simulations. *Proteins Struct. Funct. Bioinforma.* 81, 658-674. doi:10.1002/prot.24223.

García-Angulo, A., Merlo, M. A., Rodríguez, M. E., Portela-Bens, S., Liehr, T., and Rebordinos, L. (2019). Genome and phylogenetic analysis of genes involved in the immune system of *Solea senegalensis* - Potential applications in aquaculture. *Front. Genet.* 10, 529. doi:10.3389/fgene.2019.00529.

Garraffoni, A. R. S., Moura, F. R., Vasconcelos, P. E., Araújo, F. F., and Passos, F. D. (2012). Levantamento de Polychaeta (Annelida) na Baía do Almirantado, Ilha Rei George (Antártica). *Avulsos Zool.* 52, 151–165. doi: 10.1590/S0031-10492012001300001.

Geven, E. J. W., and Klaren, P. H. M. (2017). The teleost head kidney: Integrating thyroid and immune signalling. *Dev. Comp. Immunol.* 66, 73-83. doi:10.1016/j.dci.2016.06.025.

Ghosh, S. S., Wang, J., Yannie, P. J., and Ghosh, S. (2020). Intestinal Barrier Dysfunction, LPS Translocation, and Disease Development. *J. Endocr. Soc.* 4, bvz039–bvz039. doi:10.1210/jendso/bvz039.

Gibson, K. M., Nguyen, B. N., Neumann, L. M., Miller, M., Buss, P., Daniels, S., et al. (2019). Gut microbiome differences between wild and captive black rhinoceros – implications for rhino health. *Sci. Rep.* 9, 7570. doi:10.1038/s41598-019-43875-3.

Giglio, D., and Johnson, G. C. (2016). Subantarctic and polar fronts of the Antarctic Circumpolar Current and Southern Ocean heat and freshwater content variability: A view from Argo. *J. Phys. Oceanogr.* 46, 749-768. doi:10.1175/JPO-D-15-0131.1.

Giordano, D., Russo, R., di Prisco, G., and Verde, C. (2012). Molecular adaptations in Antarctic fish and marine microorganisms. *Mar. Genomics* 6, 1–6. doi:10.1016/j.margen.2011.09.003.

Glass, C. K., and Olefsky, J. M. (2012). Inflammation and lipid signaling in the etiology of insulin resistance. *Cell Metab.* 15, 635–45. doi:10.1016/j.cmet.2012.04.001.

Gomez, D., Sunyer, J. O., and Salinas, I. (2013). The mucosal immune system of fish: The evolution of tolerating commensals while fighting pathogens. *Fish Shellfish Immunol.* 35, 1729-1739. doi:10.1016/j.fsi.2013.09.032.

Gong, Z., Liang, Y., Wang, M., Jiang, Y., Yang, Q., Xia, J., et al. (2018). Viral Diversity and Its Relationship With Environmental Factors at the Surface and Deep Sea of Prydz Bay, Antarctica. *Front. Microbiol.* 9, 2981. doi:10.3389/fmicb.2018.02981.

Grayfer, L., Kerimoglu, B., Yaparla, A., Hodgkinson, J. W., Xie, J., and Belosevic, M. (2018). Mechanisms of fish macrophage antimicrobial immunity. *Front. Immunol.* 9, 1105.

doi:10.3389/fimmu.2018.01105.

Groff, J. M. (2001). Cutaneous biology and diseases of fish. *Vet. Clin. North Am. - Exot. Anim. Pract.* 4, 321–411. doi:10.1016/S1094-9194(17)30037-3.

Grzymski, J. J., Riesenfeld, C. S., Williams, T. J., Dussaq, A. M., Ducklow, H., Erickson, M., et al. (2012). A metagenomic assessment of winter and summer bacterioplankton from Antarctica Peninsula coastal surface waters. *ISME J.* 6, 1901–1915. doi:10.1038/ismej.2012.31.

Guerreiro, P. M., Rotllant, J., Fuentes, J., Power, D. M., and Canario, A. V. M. (2006). Cortisol and parathyroid hormone-related peptide are reciprocally modulated by negative feedback. *Gen. Comp. Endocrinol.* 148, 227-235. doi:10.1016/j.ygcen.2006.03.004.

Gunshin, H., Mackenzie, B., Berger, U. V., Gunshin, Y., Romero, M. F., Boron, W. F., et al. (1997). Cloning and characterization of a mammalian proton-coupled metal-ion transporter. *Nature*. 388, 482–488. doi:10.1038/41343.

Gurung, P., Lukens, J. R., and Kanneganti, T.-D. (2015). Mitochondria: diversity in the regulation of the NLRP3 inflammasome. *Trends Mol. Med.* 21, 193–201. doi:10.1016/j.molmed.2014.11.008.

Guzman-Villanueva, D., El-Sherbiny, I. M., Herrera-Ruiz, D., and Smyth, H. D. C. (2013). Design and in vitro evaluation of a new nano-microparticulate system for enhanced aqueous-phase solubility of curcumin. *Biomed Res. Int.* 2013, 1-9. doi:10.1155/2013/724763.

Guzmán-Villanueva, L. T., Ascencio-Valle, F., Macías-Rodríguez, M. E., and Tovar-Ramírez, D. (2014). Effects of dietary β-1,3/1,6-glucan on the antioxidant and digestive enzyme activities of Pacific red snapper (*Lutjanus peru*) after exposure to lipopolysaccharides. *Fish Physiol. Biochem.* 40, 827–837. doi:10.1007/s10695-013-9889-0.

Haas, B. J., Papanicolaou, A., Yassour, M., Grabherr, M., Blood, P. D., Bowden, J., et al. (2013). De novo transcript sequence reconstruction from RNA-seq using the Trinity platform for reference generation and analysis. *Nat. Protoc.* 8, 1494-1512. doi:10.1038/nprot.2013.084.

Hamdani, S. H., McMillan, D. N., Pettersen, E. F., Wergeland, H., Endresen, C., Ellis, A. E., et al. (1998). Isolation of rainbow trout neutrophils with an anti-granulocyte monoclonal antibody. *Vet. Immunol. Immunopathol.* 63, 369-380. doi:10.1016/S0165-2427(98)00115-9.

Han, C., Li, Q., Zhang, Z., and Huang, J. (2017). Characterization, expression, and evolutionary analysis of new TLR3 and TLR5M genes cloned from the spiny eel *Mastacembelus armatus*. *Dev. Comp. Immunol.* 77, 174–187. doi:10.1016/j.dci.2017.08.007.

Han, Q., Wen, X., Wang, L., Han, X., Shen, Y., Cao, J., et al. (2020). Role of hematological parameters in the diagnosis of influenza virus infection in patients with respiratory tract infection symptoms. *J. Clin. Lab. Anal.* 34, e23191. doi:10.1002/jcla.23191.

Hanif, A., Bakopoulos, V., Leonardos, I., and Dimitriadis, G. J. (2005). The effect of sea bream (*Sparus aurata*) broodstock and larval vaccination on the susceptibility by *Photobacterium damsela* subsp. *piscicida* and on the humoral immune parameters. *Fish Shellfish Immunol.* 19, 345-361. doi:10.1016/j.fsi.2004.12.009.

Harris, Z. L., Durley, A. P., Man, T. K., and Gitlin, J. D. (1999). Targeted gene disruption reveals an essential role for ceruloplasmin in cellular iron efflux. *Proc. Natl. Acad. Sci. USA.* 96, 10812–7. doi:10.1073/pnas.96.19.10812.

Haukenes, A. H., and Barton, B. A. (2004). Characterization of the cortisol response following an acute challenge with lipopolysaccharide in yellow perch and the influence of rearing density. *J. Fish Biol.* 64, 851-862. doi:10.1111/j.1095-8649.2004.00354.x.

Havixbeck, J. J., and Barreda, D. R. (2015). Neutrophil development, migration, and function in teleost fish. *Biology.* 4, 715-734. doi:10.3390/biology4040715.

Hayashi, F., Smith, K. D., Ozinsky, A., Hawn, T. R., Yi, E. C., Goodlett, D. R., et al. (2001). The innate immune response to bacterial flagellin is mediated by Toll-like receptor 5. *Nature*. 410, 1099–103. doi:10.1038/35074106.

Hemmingsen, E. A., Douglas, E. L., Johansen, K., and Millard, R. W. (1972). Aortic blood flow and cardiac output in the hemoglobin-free fish *Chaenocephalus aceratus*. *Comp. Biochem. Physiol. - Part A Physiol.* 43, 1045-1051. doi:10.1016/0300-9629(72)90176-4.

Henson, S. A., Sanders, R., and Madsen, E. (2012). Global patterns in efficiency of particulate organic carbon export and transfer to the deep ocean. *Global Biogeochem. Cycles*. 26, GB1028. doi:10.1029/2011GB004099.

Hentze, M. W., Muckenthaler, M. U., and Andrews, N. C. (2004). Balancing Acts: Molecular Control of Mammalian Iron Metabolism. *Cell*. 117, 285–297. doi: 10.1016/s0092-8674(04)00343-5.

Heymann, F., and Tacke, F. (2016). Immunology in the liver-from homeostasis to disease. *Nat. Rev. Gastroenterol. Hepatol.* 13, 88-110. doi:10.1038/nrgastro.2015.200.

Hine, P. M., and Thorne, T. (1997). Replication of herpes-like viruses in haemocytes of adult flat oysters *Ostrea angasi*: An ultrastructural study. *Dis. Aquat. Org.* 29, 189-196. doi:10.3354/dao029189.

Hodgkinson, J. W., Grayfer, L., and Belosevic, M. (2015). Biology of bony fish macrophages. *Biology.* 4, 881–906. doi:10.3390/biology4040881.

Hoffmann, P. R., and Berry, M. J. (2008). The influence of selenium on immune responses. *Mol. Nutr. Food Res.* 52, 1273–1280. doi:10.1002/mnfr.200700330.

Hofmann, G. E., Buckley, B. A., Airaksinen, S., Keen, J. E., and Somero, G. N. (2000). Heat-shock protein expression is absent in the antarctic fish *Trematomus bernacchii* (family Nototheniidae). *J. Exp. Biol.* 203, 2331–9. doi:10.1242/jeb.203.15.2331.

Holland, J. W., Pottinger, T. G., and Secombes, C. J. (2002). Recombinant interleukin-1β activates the hypothalamic-pituitary-interrenal axis in rainbow trout, *Oncorhynchus mykiss*. *J. Endocrinol.* 175, 261-267. doi:10.1677/joe.0.1750261.

Hong, J., Yoon, D., Nam, Y., Seo, D., Kim, J. H., Kim, M. S., et al. (2020). Lipopolysaccharide administration for a mouse model of cerebellar ataxia with neuroinflammation. *Sci. Rep.* 10, 1–10. doi:10.1038/s41598-020-70390-7.

Hong, S., Peddie, S., Campos-Pérez, J. J., Zou, J., and Secombes, C. J. (2003). The effect of intraperitoneally administered recombinant IL-1β on immune parameters and resistance to *Aeromonas salmonicida* in the rainbow trout (*Oncorhynchus mykiss*). *Dev. Comp. Immunol.* 27, 801-812. doi:10.1016/S0145-305X(03)00056-9.

Hong, S., Zou, J., Crampe, M., Peddie, S., Scapigliati, G., Bols, N., et al. (2001). The production and bioactivity of rainbow trout (*Oncorhynchus mykiss*) recombinant IL-1β. *Vet. Immunol. Immunopathol.* 81, 1-14. doi:10.1016/S0165-2427(01)00328-2.

Hoover, G. J., El-Mowafi, A., Simko, E., Kocal, T. E., Ferguson, H. W., and Hayes, M. A. (1998). Plasma proteins of rainbow trout (*Oncorhynchus mykiss*) isolated by binding to lipopolysaccharide from *Aeromonas salmonicida*. *Comp. Biochem. Physiol. - B Biochem. Mol. Biol.* 120, 559-569. doi:10.1016/S0305-0491(98)10042-1.

Hoshino, K., Takeuchi, O., Kawai, T., Sanjo, H., Ogawa, T., Takeda, Y., et al. (1999). Cutting edge: Toll-like receptor 4 (TLR4)-deficient mice are hyporesponsive to lipopolysaccharide: evidence for TLR4 as the Lps gene product. *J. Immunol.* 162, 3749–3752. http://www.jimmunol.org/content/162/7/3749.

Hou, Z., Ye, Z., Zhang, D., Gao, C., Su, B., Song, L., et al. (2017). Characterization and expression profiling of NOD-like receptor C3 (NLRC3) in mucosal tissues of turbot (*Scophthalmus maximus*

L.) following bacterial challenge. *Fish Shellfish Immunol.* 66, 231–239. doi:10.1016/j.fsi.2017.05.014.

Hu, Y., Ghigliotti, L., Vacchi, M., Pisano, E., Detrich, H. W., and Albertson, R. C. (2016). Evolution in an extreme environment: Developmental biases and phenotypic integration in the adaptive radiation of antarctic notothenioids. *BMC Evol. Biol.* 16, 142. doi:10.1186/s12862-016-0704-2.

Huang, Z., Rose, A. H., and Hoffmann, P. R. (2012). The role of selenium in inflammation and immunity: from molecular mechanisms to therapeutic opportunities. *Antioxid. Redox Signal.* 16, 705–743. doi:10.1089/ars.2011.4145.

Huber, M., Kalis, C., Keck, S., Jiang, Z., Georgel, P., Du, X., et al. (2006). R-form LPS, the master key to the activation of TLR4/MD-2-positive cells. *Eur. J. Immunol.* 36, 701-711. doi:10.1002/eji.200535593.

Hughes, L. C., Ortí, G., Huang, Y., Sun, Y., Baldwin, C. C., Thompson, A. W., et al. (2018). Comprehensive phylogeny of ray-finned fishes (*Actinopterygii*) based on transcriptomic and genomic data. *Proc. Natl. Acad. Sci. USA.* 115, 6249 LP – 6254. doi:10.1073/pnas.1719358115.

Huh, J. W., Shibata, T., Hwang, M., Kwon, E. H., Jang, M. S., Fukui, R., et al. (2014). UNC93B1 is essential for the plasma membrane localization and signaling of Toll-like receptor 5. *Proc. Natl. Acad. Sci. USA.* 111, 7072–7077. doi:10.1073/pnas.1322838111.

Huising, M. O., Kruiswijk, C. P., and Flik, G. (2006). Phylogeny and evolution of class-I helical cytokines. *J. Endocrinol.* 189, 1-25. doi:10.1677/joe.1.06591.

Huizinga, H. W., and Nadakavukaren, M. J. (1997). Cellular responses of goldfish, *Carassius auratus* (L.), to metacercariae of *Ribeiroia marini* (Faust and Hoffman, 1934). *J. Fish Dis.* 20, 401-408. doi:10.1046/j.1365-2761.1997.00311.x.

Hureau, J.-C. (1970). Biologie cornparee de quelques Poissons antarctiques (Nototheniidae). *Bull. Inst. Océanogr. Monaco*. 68, 1-250.

Hutchings, J. A., and Baum, J. K. (2005). Measuring marine fish biodiversity: Temporal changes in abundance, life history and demography. *Philosophical Transactions of the Royal Society B: Biological Sciences*. 360, 315-338. doi:10.1098/rstb.2004.1586.

Huth, T. J., and Place, S. P. (2013). De novo assembly and characterization of tissue specific transcriptomes in the emerald notothen, *Trematomus bernacchii*. *BMC Genomics*. 14, 805. doi:10.1186/1471-2164-14-805.

Iliev, D. B., Roach, J. C., Mackenzie, S., Planas, J. V., and Goetz, F. W. (2005). Endotoxin recognition: In fish or not in fish? *FEBS Lett.* 579, 6519-6528. doi:10.1016/j.febslet.2005.10.061.

IPCC (2019). The Ocean and Cryosphere in a Changing Climate. *Intergov. Panel Clim. Chang. Special Report.* Ed. Portner, H.- O., Roberts, D. C., Masson-Delmonte, V., Zhai, P., et al. 1-765.

Jara, P. I., Boric, M. P., and Saez, J. C. (1995). Leukocytes express connexin 43 after activation with lipopolysaccharide and appear to form gap junctions with endothelial cells after ischemia-reperfusion. *Proc. Natl. Acad. Sci. USA.* 92, 7011–7015. doi:10.1073/pnas.92.15.7011.

Jaton, J. C., and Riesen, W. (1976). The relationship between hypervariable regions, antigen-binding specificity and the three-dimensional structure of antibodies. *Ann. Immunol.* 127, 273–283.

Jensen, I., Albuquerque, A., Sommer, A. I., and Robertsen, B. (2002). Effect of poly I:C on the expression of Mx proteins and resistance against infection by infectious salmon anaemia virus in Atlantic salmon. *Fish Shellfish Immunol.* 13, 311-326. doi:10.1006/fsim.2001.0406.

Jensen, L. E., Hiney, M. P., Shields, D. C., Uhlar, C. M., Lindsay, A. J., and Whitehead, A. S. (1997). Acute phase proteins in salmonids: evolutionary analyses and acute phase response. *J. Immunol.* 158, 384-92.

Ji, J., Rao, Y., Wan, Q., Liao, Z., and Su, J. (2018). Teleost-Specific TLR19 Localizes to Endosome, Recognizes dsRNA, Recruits TRIF, Triggers both IFN and NF-κB Pathways, and Protects Cells from Grass Carp Reovirus Infection. *J. Immunol.* 200, 573–585. doi:10.4049/jimmunol.1701149.

Jiang, H., Wang, M., Fu, L., Zhong, L., Liu, G., Zheng, Y., et al. (2020). Liver transcriptome analysis and cortisol immune-response modulation in lipopolysaccharide-stimulated in channel catfish (*Ictalurus punctatus*). *Fish Shellfish Immunol.* 101, 19–50. doi:10.1016/j.fsi.2020.03.024.

Jiang, S., Zhang, D., Li, J., and Liu, Z. (2008). Molecular characterization, recombinant expression and bioactivity analysis of the interleukin-1β from the yellowfin sea bream, *Acanthopagrus latus* (Houttuyn). *Fish Shellfish Immunol.* 24, 323-336. doi:10.1016/j.fsi.2007.11.020.

Jiang, Z., Georgel, P., Du, X., Shamel, L., Sovath, S., Mudd, S., et al. (2005). CD14 is required for MyD88-independent LPS signaling. *Nat. Immunol.* 6, 565-570. doi:10.1038/ni1207.

Jin, M. S., and Lee, J.-O. (2008). Structures of the Toll-like Receptor Family and Its Ligand Complexes. *Immunity* 29, 182–191. doi:10.1016/j.immuni.2008.07.007.

Johnsson, B., and Karl-Herman, K. (1993). Antarctic fish and fisheries. *J. Ani. Ecol.* 62, 596. doi:10.2307/5212.

Johansson, M. E. V., Larsson, J. M. H., and Hansson, G. C. (2011). The two mucus layers of colon are organized by the MUC2 mucin, whereas the outer layer is a legislator of host-microbial interactions. *Proc. Natl. Acad. Sci. USA.* 108, 4659-4665. doi:10.1073/pnas.1006451107.

Johnson, E. E., and Wessling-Resnick, M. (2012). Iron metabolism and the innate immune response to infection. *Microbes Infect.* 14, 207–216. doi:10.1016/j.micinf.2011.10.001.

Johnston, I. A., Calvo, J., Guderley, H., Fernandez, D., and Palmer, L. (1998). Latitudinal variation in the abundance and oxidative capacities of muscle mitochondria in perciform fishes. *J. Exp. Biol.* 201, 1-12. doi:10.1242/jeb.201.1.1

Jollès, P., and Jollès, J. (1984). What's new in lysozyme research? - Always a model system, today as yesterday. *Mol. Cell. Biochem.* 63, 165-89. doi:10.1007/BF00285225.

Jones, C., Damerau, M., Deitrich, K., Driscoll, R., Kock, K. H., Kuhn, K., et al. (2009). Demersal Finfish Survey of the South Orkney Islands. *AMLR 2008/2009 F. Seas. Rep.* 49–66.

Ka, J., and Jin, S.-W. (2021). Zebrafish as an emerging model for dyslipidemia and associated diseases. *J. Lipid Atheroscler.* 10, 42–56. doi:10.12997/jla.2021.10.1.42.

Kandalski, P. K., de Souza, M. R. D. P., Herrerias, T., Machado, C., Zaleski, T., Forgati, M., et al. (2018). Effects of short-term thermal stress on the plasma biochemical profiles of two Antarctic nototheniid species. *Rev. Fish Biol. Fish.* 28, 925–940. doi:10.1007/s11160-018-9535-0.

Kanehisa, M., Furumichi, M., Sato, Y., Ishiguro-Watanabe, M., and Tanabe, M. (2021). KEGG: integrating viruses and cellular organisms. *Nucleic Acids Res.* 49, D545–D551. doi:10.1093/nar/gkaa970.

Kanitakis, J., Narvaez, D., and Claudy, A. (2002). Differential expression of the CD10 antigen (neutral endopeptidase) in primary versus metastatic malignant melanomas of the skin. *Melanoma Res.* 12, 241-244. doi:10.1097/00008390-200206000-00007.

Katzenback, B. (2015). Antimicrobial Peptides as Mediators of Innate Immunity in Teleosts. *Biology.* 4, 607–39. doi:10.3390/biology4040607.

Kawabata, H., Yang, R., Hirama, T., Vuong, P. T., Kawano, S., Gombart, A. F., et al. (1999). Molecular Cloning of Transferrin Receptor 2:a new member of the transferrin receptor-like family. *J. Biol. Chem.* 274, 20826–20832. doi:10.1074/jbc.274.30.20826.

Kawai, T., and Akira, S. (2010). The role of pattern-recognition receptors in innate immunity: update

on Toll-like receptors. *Nat. Immunol.* 11, 373-384. doi:10.1038/ni.1863.

Khoso, P. A., Yang, Z., Liu, C., and Li, S. (2015). Selenium Deficiency Downregulates Selenoproteins and Suppresses Immune Function in Chicken Thymus. *Biol. Trace Elem. Res.* 167, 48–55. doi:10.1007/s12011-015-0282-y.

Killen, S. S., Marras, S., Nadler, L., and Domenici, P. (2017). The role of physiological traits in assortment among and within fish shoals. *Philos. Trans. R. Soc. B Biol. Sci.* 372. doi:10.1098/rstb.2016.0233.

Kim, B.-M., Amores, A., Kang, S., Ahn, D.-H., Kim, J.-H., Kim, I.-C., et al. (2019a). Antarctic blackfin icefish genome reveals adaptations to extreme environments. *Nat. Ecol. Evol.* 3, 469–478. doi:10.1038/s41559-019-0812-7.

Kim, S.-J., Kim, J.-G., Lee, S.-H., Park, S.-J., Gwak, J.-H., Jung, M.-Y., et al. (2019b). Genomic and metatranscriptomic analyses of carbon remineralization in an Antarctic polynya. *Microbiome*. 7, 29. doi:10.1186/s40168-019-0643-4.

Kindt, T. J., Goldsby, R. A., Osborne, B. A., and Kuby, J. (2007). Kuby immunology. *New York*. Ed. Freeman, W. H.

Klein, R. D., Borges, V. D., Rosa, C. E., Colares, E. P., Robaldo, R. B., Martinez, P. E., et al. (2017a). Effects of increasing temperature on antioxidant defense system and oxidative stress parameters in the Antarctic fish *Notothenia coriiceps* and *Notothenia rossii*. *J. Therm. Biol.* 68, 110–118. doi:10.1016/j.jtherbio.2017.02.016.

Klein, R. D., Rosa, C. E., Colares, E. P., Robaldo, R. B., Martinez, P. E., and Bianchini, A. (2017b). Antioxidant defense system and oxidative status in Antarctic fishes: The sluggish rockcod *Notothenia coriiceps* versus the active marbled notothen *Notothenia rossii*. *J. Therm. Biol.* 68, 119–127. doi:10.1016/j.jtherbio.2017.02.013.

Klingenberg, C. P., and Ekau, W. (1996). A combined, morphometric and phylogenetic analysis of an ecomorphological trend: Pelagization in Antarctic fishes (Perciformes: Nototheniidae). *Biol. J. Linn. Soc.* 59, 143-177. doi:10.1111/j.1095-8312.1996.tb01459.x.

Ko, E.-Y., Cho, S.-H., Kwon, S.-H., Eom, C.-Y., Jeong, M. S., Lee, W. W., et al. (2017). The roles of NF-κB and ROS in regulation of pro-inflammatory mediators of inflammation induction in LPS-stimulated zebrafish embryos. *Fish Shellfish Immunol.* 68, 525–529. doi:10.1016/j.fsi.2017.07.041.

Köberlin, M. S., Heinz, L. X., and Superti-Furga, G. (2016). Functional crosstalk between membrane lipids and TLR biology. *Curr. Opin. Cell Biol.* 39, 28–36. doi:10.1016/j.ceb.2016.01.010.

Kobielak, A., and Boddupally, K. (2014). Junctions and inflammation in the skin. *Cell Commun. Adhes.* 21, 141–147. doi:10.3109/15419061.2014.905930.

Köbsel, N., and Ramadori, G. (1994). Human hepatoma cells synthesize and secrete lysozyme: Modulation by cytokines. *Hepatology.* 19, 1182–1188. doi:10.1002/hep.1840190516.

Kock, K.-H., and Kellermann, A. (1991). Reproduction in Antarctic notothenioid fish. *Antarct. Sci.* 3, 125-150. doi:10.1017/S0954102091000172.

Kokou, F., Sasson, G., Nitzan, T., Doron-Faigenboim, A., Harpaz, S., Cnaani, A., et al. (2018). Host genetic selection for cold tolerance shapes microbiome composition and modulates its response to temperature. *Elife*. 7, e36398. doi:10.7554/eLife.36398.001.

Kopp, R., Lang, Š., Brabec, T., and Mareš, J. (2014). The influence of physicochemical properties of water on plasma indices in brook trout (*Salvelinus fontinalis* , Mitchill) reared under conditions of intensive aquaculture. *Acta Vet. Brno.* 82, 427–433. doi:10.2754/avb201382040427.

Kopp, R., Mareš, J., Lang, Š., Brabec, T., and Ziková, A. (2011). Assessment of ranges plasma indices

in rainbow trout (*Oncorhynchus mykiss*) reared under conditions of intensive aquaculture. 59, 181–188. doi:10.11118/actaun201159060181.

Krause, A., Neitz, S., Mägert, H. J., Schulz, A., Forssmann, W. G., Schulz-Knappe, P., et al. (2000). LEAP-1, a novel highly disulfide-bonded human peptide, exhibits antimicrobial activity. *FEBS Lett.* 480, 147-150. doi:10.1016/S0014-5793(00)01920-7.

Krogh, A., Larsson, B., Von Heijne, G., and Sonnhammer, E. L. L. (2001). Predicting transmembrane protein topology with a hidden Markov model: Application to complete genomes. *J. Mol. Biol.* 305, 567-580. doi:10.1006/jmbi.2000.4315.

Krueger, F. (2015). Trim Galore!: A wrapper tool around Cutadapt and FastQC to consistently apply quality and adapter trimming to FastQ files. *Babraham Inst.* 516, 517.

Kumar, G. S., Jagannadham, M. V., and Ray, M. K. (2002). Low-temperature-induced changes in composition and fluidity of lipopolysaccharides in the antarctic psychrotrophic bacterium *Pseudomonas syringae*. *J. Bacteriol.* 184, 6746-6749. doi:10.1128/JB.184.23.6746-6749.2002.

Kumar, S., Stecher, G., Li, M., Knyaz, C., and Tamura, K. (2018). MEGA X: Molecular evolutionary genetics analysis across computing platforms. *Mol. Biol. Evol.* 35, 1547–1549. doi:10.1093/molbev/msy096.

La Mesa, M., Eastman, J. T., and Vacchi, M. (2004). The role of notothenioid fish in the food web of the Ross Sea shelf waters: A review. *Polar Biol.* 27, 321-338. doi:10.1007/s00300-004-0599-z.

Laarson, A. (2014). AliView: a fast and lightweight alignment viewer and editor for large data sets. *Bioinformatics*. 30, 3276–8. 10.1093/bioinformatics/btu531.

Lages, M. A., Balado, M., and Lemos, M. L. (2019). The expression of virulence factors in *Vibrio anguillarum* is dually regulated by iron levels and temperature. *Front. Microbiol.* 10, 1-11. doi:10.3389/fmicb.2019.02335.

Laing, K. J., Purcell, M. K., Winton, J. R., and Hansen, J. D. (2008). A genomic view of the NOD-like receptor family in teleost fish: Identification of a novel NLR subfamily in zebrafish. *BMC Evol. Biol.* 8, 42. doi:10.1186/1471-2148-8-42.

Laiz-Carrión, R., Guerreiro, P. M., Fuentes, J., Canario, A. V. M., Martín Del Río, M. P., and Mancera, J. M. (2005). Branchial osmoregulatory response to salinity in the gilthead sea bream, *Sparus auratus*. *J. Exp. Zool. Part A Comp. Exp. Biol.* 303A, 563-576. doi:10.1002/jez.a.183.

Lange, S., Gudmundsdottir, B. K., and Magnadottir, B. (2001). Humoral immune parameters of cultured Atlantic halibut (*Hippoglossus hippoglossus L.*). *Fish Shellfish Immunol.* 11, 523-535. doi:10.1006/fsim.2000.0333.

Langmead, B., Trapnell, C., Pop, M., and Salzberg, S. L. (2009). Ultrafast and memory-efficient alignment of short DNA sequences to the human genome. *Genome Biol.* 10, R25. doi:10.1186/gb-2009-10-3-r25.

Langston, A. L., Johnstone, R., and Ellis, A. E. (2001). The kinetics of the hypoferraemic response and changes in levels of alternative complement activity in diploid and triploid Atlantic salmon, following injection of lipopolysaccharide. *Fish Shellfish Immunol.* 11, 333-345. doi:10.1006/fsim.2000.0319.

Larsen, A., Tao, Z., Bullard, S. A., and Arias, C. R. (2013). Diversity of the skin microbiota of fishes: evidence for host species specificity. *FEMS Microbiol. Ecol.* 85, 483–494. doi:10.1111/1574-6941.12136.

Lavoie, C., Courcelle, M., Redivo, B., and Derome, N. (2018). Structural and compositional mismatch between captive and wild Atlantic salmon (*Salmo salar*) parrs' gut microbiota highlights the relevance of integrating molecular ecology for management and conservation methods. *Evol. Appl.*

11, 1671–1685. doi:10.1111/eva.12658.

Law, R. H. P., Caradoc-Davies, T., Cowieson, N., Horvath, A. J., Quek, A. J., Encarnacao, J. A., et al. (2012). The X-ray Crystal Structure of Full-Length Human Plasminogen. *Cell Rep.* 1, 185-190. doi:10.1016/j.celrep.2012.02.012.

Le, H. T. M. D., Shao, X., Krogdahl, Å., Kortner, T. M., Lein, I., Kousoulaki, K., et al. (2019). Intestinal Function of the Stomachless Fish, Ballan Wrasse (*Labrus bergylta*). *Front. Mar. Sci.* 6, 140. doi:10.3389/fmars.2019.00140.

Le Morvan-Rocher, C., Troutaud, D., and Deschaux, P. (1995). Effects of temperature on carp leukocyte mitogen-induced proliferation and nonspecific cytotoxic activity. *Dev. Comp. Immunol.* 19, 87-95. doi:10.1016/0145-305x(94)00057-m.

Le Morvan, C., Clerton, P., Deschaux, P., and Troutaud, D. (1997). Effects of environmental temperature on macrophage activities in carp. *Fish Shellfish Immunol.* 7, 209-212. doi:10.1006/fsim.1996.0075.

Le Morvan, C., Troutaud, D., and Deschaux, P. (1998). Differential effects of temperature on specific and nonspecific immune defences in fish. *J. Exp. Biol.* 201, 165-168.

Le Nguyen, D. D., Ngoc, H. H., Dijoux, D., Loiseau, G., and Montet, D. (2008). Determination of fish origin by using 16S rDNA fingerprinting of bacterial communities by PCR-DGGE: An application on Pangasius fish from Viet Nam. *Food Control.* 19, 454–460. doi:10.1016/j.foodcont.2007.05.006.

Lemieux, H., and Blier, P. U. (2007). Trypsin Activity Measurement in Fish and Mammals. *J. Aquat. Food Prod. Technol.* 16, 13-26. doi:10.1300/j030v16n04_03.

Lemos, L. N., Fulthorpe, R. R., Triplett, E. W., and Roesch, L. F. W. (2011). Rethinking microbial diversity analysis in the high throughput sequencing era. *J. Microbiol. Methods* 86, 42–51. doi:10.1016/j.mimet.2011.03.014.

Lerouge, I., and Vanderleyden, J. (2002). O-antigen structural variation: Mechanisms and possible roles in animal/plant-microbe interactions. *FEMS Microbiol. Rev.* 26, 17-47. doi:10.1016/S0168-6445(01)00070-5.

Letunic, I., Khedkar, S., and Bork, P. (2021). SMART: Recent updates, new developments and status in 2020. *Nucleic Acids Res.* 49, D458–D460. doi:10.1093/nar/gkaa937.

Lewis, S. M., Williams, A., and Eisenbarth, S. C. (2019). Structure and function of the immune system in the spleen. *Sci. Immunol.* 4, aau6085. doi:10.1126/sciimmunol.aau6085.

Li, B., and Dewey, C. N. (2011). RSEM: Accurate transcript quantification from RNA-Seq data with or without a reference genome. *BMC Bioinformatics*. 12, 323. doi:10.1186/1471-2105-12-323.

Li, C., Jiang, J., Xie, J., Yang, W., and Wang, Y. (2021). Transcriptome profiling and differential expression analysis of the immune-related genes during the acute phase of infection with *Mycobacterium marinum* in the goldfish (*Carassius auratus L.*). *Aquaculture.* 533, 736198. doi:10.1016/j.aquaculture.2020.736198.

Li, H., Yang, G., Ma, F., Li, T., Yang, H., Rombout, J. H. W. M., et al. (2017). Molecular characterization of a fish-specific toll-like receptor 22 (TLR22) gene from common carp (*Cyprinus carpio L.*): Evolutionary relationship and induced expression upon immune stimulants. *Fish Shellfish Immunol.* 63, 74–86. doi:10.1016/j.fsi.2017.02.009.

Li, J.-Y., Wang, Y.-Y., Shao, T., Fan, D.-D., Lin, A.-F., Xiang, L.-X., et al. (2020a). The zebrafish NLRP3 inflammasome has functional roles in ASC-dependent interleukin-1β maturation and gasdermin E–mediated pyroptosis. *J. Biol. Chem.* 295, 1120–1141. 10.1074/jbc.RA119.011751.

Li, J., Kong, L., Gao, Y., Wu, C., and Xu, T. (2015). Characterization of NLR-A subfamily members in

miiuy croaker and comparative genomics revealed NLRX1 underwent duplication and lose in actinopterygii. *Fish Shellfish Immunol.* 47, 397–406. doi:10.1016/j.fsi.2015.09.024.

Li, L., Cardoso, J. C. R., Félix, R. C., Mateus, A. P., Canário, A. V. M., and Power, D. M. (2020b). Fish lysozyme gene family evolution and divergent function in early development. *Dev. Comp. Immunol.* 114, 103772. doi:10.1016/j.dci.2020.103772.

Li, Q., Cui, K., Wu, M., Xu, D., Mai, K., and Ai, Q. (2020c). Polyunsaturated Fatty Acids Influence LPS-Induced Inflammation of Fish Macrophages Through Differential Modulation of Pathogen Recognition and p38 MAPK/NF-κB Signaling. *Front. Immunol.* 11, 1–11. doi:10.3389/fimmu.2020.559332.

Li, R., Yu, C., Li, Y., Lam, T. W., Yiu, S. M., Kristiansen, K., et al. (2009). SOAP2: An improved ultrafast tool for short read alignment. *Bioinformatics*. 25, 1966-1967. doi:10.1093/bioinformatics/btp336.

Li, S., Chen, X., Hao, G., Geng, X., Zhan, W., and Sun, J. (2016). Identification and characterization of a novel NOD-like receptor family CARD domain containing 3 gene in response to extracellular ATP stimulation and its role in regulating LPS-induced innate immune response in Japanese flounder (*Paralichthys olivaceus*). *Fish Shellfish Immunol.* 50, 79–90. doi:10.1016/j.fsi.2016.01.029.

Li, T., Shan, S., Wang, L., Yang, G., and Zhu, J. (2018). Identification of a fish-specific NOD-like receptor subfamily C (NLRC) gene from common carp (*Cyprinus carpio L.*): Characterization, ontogeny and expression analysis in response to immune stimulation. *Fish Shellfish Immunol.* 82, 371–377. doi:10.1016/j.fsi.2018.08.045.

Li, W., Simmons, P., Shrader, D., Herrman, T. J., and Dai, S. Y. (2013). Talanta Microwave plasma-atomic emission spectroscopy as a tool for the determination of copper , iron , manganese and zinc in animal feed and fertilizer. *Talanta.* 112, 43–48. doi:10.1016/j.talanta.2013.03.029.

Li, X., Wang, S., Qi, J., Echtenkamp, S. F., Chatterjee, R., Wang, M., et al. (2007). Zebrafish peptidoglycan recognition proteins are bactericidal amidases essential for defense against bacterial infections. *Immunity.* 27, 518–529. doi:10.1016/j.immuni.2007.07.020.

Li, Y., Xia, P., Wu, J., Huang, A., Bu, G., Meng, F., et al. (2020d). The potential sensing molecules and signal cascades for protecting teleost fishes against lipopolysaccharide. *Fish Shellfish Immunol.* 97, 235–247. doi:10.1016/j.fsi.2019.12.050.

Liba, C. M., Ferrara, F. I. S., Manfio, G. P., Fantinatti-Garboggini, F., Albuquerque, R. C., Pavan, C., et al. (2006). Nitrogen-fixing chemo-organotrophic bacteria isolated from cyanobacteria-deprived lichens and their ability to solubilize phosphate and to release amino acids and phytohormones. *J. Appl. Microbiol.* 101, 1076–1086. doi:10.1111/j.1365-2672.2006.03010.x.

Lie, Ø., Evensen, Ø., Sørensen, A., and Frøysadal, E. (1989). Study on lysozyme activity in some fish species. *Dis. Aquat. Organ.* 6, 1–5. doi:10.3354/dao006001.

Liu, G., Zhang, H., Zhao, C., and Zhang, H. (2019). Evolutionary History of the Toll-Like Receptor Gene Family across Vertebrates. *Genome Biol. Evol.* 12, 3615–3634. doi:10.1093/gbe/evz266.

Liu, Q., and Jiang, Y. (2020). Application of microbial network analysis to discriminate environmental heterogeneity in Fildes Peninsula, Antarctica. *Mar. Pollut. Bull.* 156, 111244. doi:10.1016/j.marpolbul.2020.111244.

Liu, Q.-N., Xin, Z.-Z., Chai, X.-Y., Jiang, S.-H., Li, C.-F., Zhang, H.-B., et al. (2016). Characterization of immune-related genes in the yellow catfish *Pelteobagrus fulvidraco* in response to LPS challenge. *Fish Shellfish Immunol.* 56, 248-254. doi:10.1016/j.fsi.2016.05.019.

Liu, Q.-N., Xin, Z.-Z., Liu, Y., Zhang, D.-Z., Jiang, S.-H., Chai, X.-Y., et al. (2018). *De novo* transcriptome assembly and analysis of differential gene expression following lipopolysaccharide

challenge in *Pelteobagrus fulvidraco*. *Fish Shellfish Immunol.* 73, 84–91. doi:10.1016/j.fsi.2017.11.045.

Liu, T., Zhang, L., Joo, D., and Sun, S. C. (2017). NF-κB signaling in inflammation. *Signal Transduct. Target. Ther.* 2, 17023. doi:10.1038/sigtrans.2017.23.

Liu, Y., Yu, S., Chai, Y., and Zhu, Q. (2012). Transferrin gene expression in response to LPS challenge and heavy metal exposure in roughskin sculpin (*Trachidermus fasciatus*). *Fish Shellfish Immunol.* 32, 223–229. doi:10.1016/j.fsi.2011.10.023.

Liu, Z., Liu, W., Huang, Y., Guo, J., Zhao, R., and Yang, X. (2015). Lipopolysaccharide significantly influences the hepatic triglyceride metabolism in growing pigs. *Lipids Health Dis.* 14, 1–10. doi:10.1186/s12944-015-0064-8.

Livak, K. J., and Schmittgen, T. D. (2001). Analysis of relative gene expression data using real-time quantitative PCR and the 2^{-ddct} Method. *Methods* 25, 402–408. doi:10.1006/meth.2001.1262.

Llewellyn, M. S., Boutin, S., Hoseinifar, S. H., and Derome, N. (2014). Teleost microbiomes: The state of the art in their characterization, manipulation and importance in aquaculture and fisheries. *Front. Microbiol.* 5, 1-17. doi:10.3389/fmicb.2014.00207.

Loes, A. N., Hinman, M. N., Farnsworth, D. R., Miller, A. C., Guillemin, K., and Harms, M. J. (2019). Identification and characterization of zebrafish Tlr4 co-receptor Md-2. *J. Immunol*. 206, 1046-1057. doi:10.4049/jimmunol.1901288..

Logares, R., Deutschmann, I. M., Junger, P. C., Giner, C. R., Krabberød, A. K., Schmidt, T. S. B., et al. (2020). Disentangling the mechanisms shaping the surface ocean microbiota. *Microbiome.* 8, 55. doi:10.1186/s40168-020-00827-8.

Love, M. I., Huber, W., and Anders, S. (2014). Moderated estimation of fold change and dispersion for RNA-seq data with DESeq2. *Genome Biol.* 15, 550. doi:10.1186/s13059-014-0550-8.

Lozupone, C., and Knight, R. (2005). UniFrac: a new phylogenetic method for comparing microbial communities. *Appl. Environ. Microbiol.* 71, 8228–8235. doi:10.1128/AEM.71.12.8228-8235.2005.

Lu, X.-J., Ning, Y.-J., Liu, H., Nie, L., and Chen, J. (2018). A novel lipopolysaccharide recognition mechanism mediated by internalization in teleost macrophages. *Front. Immunol.* 9, 1-18. doi:10.3389/fimmu.2018.02758.

Lulijwa, R., Alfaro, A. C., Merien, F., Burdass, M., Meyer, J., Venter, L., et al. (2020). Metabolic and immune responses of Chinook salmon (*Oncorhynchus tshawytscha*) smolts to a short-term poly (I:C) challenge. *J. Fish Biol.* 96, 731–746. doi:10.1111/jfb.14266.

Lulijwa, R., Alfaro, A. C., Merien, F., Burdass, M., Venter, L., and Young, T. (2019). In vitro immune response of chinook salmon (*Oncorhynchus tshawytscha*) peripheral blood mononuclear cells stimulated by bacterial lipopolysaccharide. *Fish Shellfish Immunol.* 94, 190-198. doi:10.1016/j.fsi.2019.09.003.

Lund, V., and Olafsen, J. A. (1998). A comparative study of pentraxin-like proteins in different fish species. *Dev. Comp. Immunol.* 22, 185-194. doi:10.1016/S0145-305X(97)00051-7.

MacCarthy, E. M., Burns, I., Irnazarow, I., Polwart, A., Greenhough, T. J., Shrive, A. K., et al. (2008). Serum CRP-like protein profile in common carp *Cyprinus carpio* challenged with *Aeromonas hydrophila* and *Escherichia coli* lipopolysaccharide. *Dev. Comp. Immunol.* 32, 0-1289. doi:10.1016/j.dci.2008.04.004.

Machado, C., Zaleski, T., Rodrigues, E., Carvalho, C. dos S., Cadena, S. M. S. C., Gozzi, G. J., et al. (2014). Effect of temperature acclimation on the liver antioxidant defence system of the Antarctic nototheniids *Notothenia coriiceps* and *Notothenia rossii*. *Comp. Biochem. Physiol. Part - B*

Biochem. Mol. Biol. 172–173, 21–28. doi:10.1016/j.cbpb.2014.02.003.

Mackenzie, D. I. (2006). Modeling the Probability of Resource Use: The Effect of, and Dealing with, Detecting a Species Imperfectly. *J. Wildl. Manage.* 70, 367-374. doi:10.2193/0022-541x(2006)70[367:mtporu]2.0.co;2.

MacKenzie, S. A., Roher, N., Boltaña, S., and Goetz, F. W. (2010). Peptidoglycan, not endotoxin, is the key mediator of cytokine gene expression induced in rainbow trout macrophages by crude LPS. *Mol. Immunol.* 47, 1450-1457. doi:10.1016/j.molimm.2010.02.009.

MacKenzie, S., Balasch, J. C., Novoa, B., Ribas, L., Roher, N., Krasnov, A., et al. (2008). Comparative analysis of the acute response of the trout, *O. mykiss*, head kidney to *in vivo* challenge with virulent and attenuated infectious hematopoietic necrosis virus and LPS-induced inflammation. *BMC Genomics.* 9, 1–21. doi:10.1186/1471-2164-9-141.

MacKenzie, S., Montserrat, N., Mas, M., Acerete, L., Tort, L., Krasnov, A., et al. (2006). Bacterial lipopolysaccharide induces apoptosis in the trout ovary. *Reprod. Biol. Endocrinol.* 31, 46. doi:10.1186/1477-7827-4-46.

MacPherson, A. J., McCoy, K. D., Johansen, F. E., and Brandtzaeg, P. (2008). The immune geography of IgA induction and function. *Mucosal Immunol.* 1, 11-22. doi:10.1038/mi.2007.6.

Maekawa, S., Pulpipat, T., Wang, P.-C., and Chen, S.-C. (2021). Transcriptome analysis of immune- and iron-related genes after *Francisella noatunensis subsp. orientalis* infection in Nile tilapia (*Oreochromis niloticus*). *Fish Shellfish Immunol.* 111, 36–48. doi:10.1016/j.fsi.2020.11.009.

Magnadottir, B. (2010). Immunological control of fish diseases. *Mar. Biotechnol.* 12, 361-379. doi:10.1007/s10126-010-9279-x.

Magnadóttir, B. (2006). Innate immunity of fish (overview). *Fish and Shellfish Immunol*. 20, 137-151. doi:10.1016/j.fsi.2004.09.006.

Magnadóttir, B., Bambir, S. H., Gudmundsdóttir, B. K., Pilström, L., and Helgason, S. (2002). Atypical *Aeromonas salmonicida* infection in naturally and experimentally infected cod, *Gadus morhua L. J. Fish Dis.* 25, 583-597. doi:10.1046/j.1365-2761.2002.00407.x.

Magnadottir, B., Gudmundsdottir, B. K., Lange, S., Steinarsson, A., Oddgeirsson, M., Bowden, T., et al. (2006). Immunostimulation of larvae and juveniles of cod, *Gadus morhua L. J. Fish Dis.* 29, 147-155. doi:10.1111/j.1365-2761.2006.00701.x.

Magnadottir, B., Lange, S., Gudmundsdottir, S., Bøgwald, J., and Dalmo, R. A. (2005). Ontogeny of humoral immune parameters in fish. *Fish Shellfish Immunol.* 19, 429-439. doi:10.1016/j.fsi.2005.03.010.

Magnoni, L. J., Roher, N., Crespo, D., Krasnov, A., and Planas, J. V. (2015). *In vivo* molecular responses of fast and slow muscle fibers to Lipopolysaccharide in a Teleost fish, the rainbow trout (*Oncorhynchus mykiss*). *Biology.* 4, 67-87. doi:10.3390/biology4010067.

Magoč, T., and Salzberg, S. L. (2011). FLASH: fast length adjustment of short reads to improve genome assemblies. *Bioinformatics*. 27, 2957–2963. doi:10.1093/bioinformatics/btr507.

Magor, B. G., and Magor, K. E. (2001). Evolution of effectors and receptors of innate immunity. *Dev. Comp. Immunol.* 25, 651-82. doi:10.1016/S0145-305X(01)00029-5.

Magurran, A. (2004). Measuring Biologcial Diversity. *Wiley-Blackwell*. 266.

Malachowicz, M., Wenne, R., and Burzynski, A. (2017). *De novo* assembly of the sea trout (*Salmo trutta m. trutta*) skin transcriptome to identify putative genes involved in the immune response and epidermal mucus secretion. *PLoS One*. 12, e0172282. doi:10.1371/journal.pone.0172282.

Mansour, A. T.-E., Goda, A. A., Omar, E. A., Khalil, H. S., and Esteban, M. Á. (2017). Dietary

supplementation of organic selenium improves growth, survival, antioxidant and immune status of meagre, *Argyrosomus regius*, juveniles. *Fish Shellfish Immunol.* 68, 516–524. doi:10.1016/j.fsi.2017.07.060.

Margesin, R. (2017). Psychrophiles: From Biodiversity to Biotechnology. *Springer*. Ed. Margesin, R. 1–685.

Martínez, D., Oyarzún, R., Pontigo, J., Romero, A., Yáñez, A., and Vargas-Chacoff, L. (2017a). Nutritional Immunity Triggers the Modulation of Iron Metabolism Genes in the Sub-Antarctic Notothenioid *Eleginops maclovinus* in Response to *Piscirickettsia salmonis*. *Front. Immunol.* 8, 1153. doi:10.3389/fimmu.2017.01153.

Martínez, D., Oyarzún, R., Vargas-Lagos, C., Pontigo, J. P., Soto-Dávila, M., Saravia, J., et al. (2017b). Identification, characterization and modulation of ferritin-H in the sub-Antarctic Notothenioid *Eleginops maclovinus* challenged with *Piscirickettsia salmonis*. *Dev. Comp. Immunol.* 73, 88–96. doi:10.1016/j.dci.2017.03.015.

Martínez, D. P., Sousa, C., Oyarzún, R., Pontigo, J. P., Canario, A. V. M., Power, D. M., et al. (2020). LPS Modulates the Expression of Iron-Related Immune Genes in Two Antarctic Notothenoids. *Front. Physiol.* 11, 102. doi:10.3389/fphys.2020.00102.

Matschiner, M., Colombo, M., Damerau, M., Ceballos, S., Hanel, R., and Salzburger, W. (2015). The adaptive radiation of notothenioid fishes in the waters of antarctica. *Springer*. Ed. Riesch, R., Tobler, M., Plath, M. 35-97. doi:10.1007/978-3-319-13362-1_3.

Matsumoto, M., Oshiumi, H., and Seya, T. (2011). Antiviral responses induced by the TLR3 pathway. *Rev. Med. Virol.* 21, 67-77. doi:10.1002/rmv.680.

Matsuo, A., Oshiumi, H., Tsujita, T., Mitani, H., Kasai, H., Yoshimizu, M., et al. (2008). Teleost TLR22 Recognizes RNA Duplex to Induce IFN and Protect Cells from Birnaviruses. *J. Immunol.* 181, 3474–3485. doi:10.4049/jimmunol.181.5.3474.

Mayden, R. L., Page, L. M., and Burr, B. M. (1992). A Field Guide to Freshwater Fishes of North America North of Mexico. *Copeia*. 1992, 920. doi:10.2307/1446175.

Mayer, E. a, Tillisch, K., Gupta, A., Mondello, P., Mian, M., Aloisi, C., et al. (2015). Gut/brain axis and the microbiota. *J. Clin. Inv.* 125, 463–479. doi:10.1172/JCI76304.

McBride, M. M., Dalpadado, P., Drinkwater, K. F., Godø, O. R., Hobday, A. J., Hollowed, A. B., et al. (2014). Krill, climate, and contrasting future scenarios for Arctic and Antarctic fisheries. *ICES J. Mar. Sci.* 71, 1934-1955. doi:10.1093/icesjms/fsu002.

Meijer, A. H., Krens, S. F. G., Rodriguez, I. A. M., Shuning, H., Bitter, W., Snaar-Jagalska, B. E., et al. (2004). Expression analysis of the Toll-like receptor and TIR domain adaptor families of zebrafish. *Mol. Immunol.* 40, 773–783. doi:10.1016/j.molimm.2003.10.003.

Meredith, T. C., Aggarwal, P., Mamat, U., Lindner, B., and Woodard, R. W. (2006). Redefining the requisite lipopolysaccharide structure in *Escherichia coli*. *ACS Chem. Biol.* 1, 33–42. doi:10.1021/cb0500015.

Merrett, N. R., Gon, O., and Heemstra, P. C. (1992). Fishes of the Southern Ocean. *Copeia*. Ed. Merret, N. R. 1992, 260-261. doi:10.2307/1446568.

Merrifield, D. L., and Rodiles, A. (2015). The fish microbiome and its interactions with mucosal tissues. Mucosa Health in Aquacultute. *Elsevier*. Ed. Beck, B. H. and Peatman, E. 273–295. doi:10.1016/B978-0-12-417186-2.00010-8.

Migale, R., Herbert, B. R., Lee, Y. S., Sykes, L., Waddington, S. N., Peebles, D., et al. (2015). Specific Lipopolysaccharide Serotypes Induce Differential Maternal and Neonatal Inflammatory Responses in a Murine Model of Preterm Labor. *Am. J. Pathol.* 185, 2390–401.

doi:10.1016/j.ajpath.2015.05.015.

Mikami, T., Miyashita, H., Takatsuka, S., Kuroki, Y., and Matsushima, N. (2012). Molecular evolution of vertebrate Toll-like receptors: Evolutionary rate difference between their leucine-rich repeats and their TIR domains. *Gene.* 503, 235–243. doi:10.1016/j.gene.2012.04.007.

Miller, M. A., Pfeiffer, W., and Schwartz, T. (2010). Creating the CIPRES Science Gateway for inference of large phylogenetic trees. *Gateway Computing Environments Workshop (GCE)*. 2010, 1–8. doi:10.1109/GCE.2010.5676129.

Miranda, J. A., Culley, A. I., Schvarcz, C. R., and Steward, G. F. (2016). RNA viruses as major contributors to Antarctic virioplankton. *Environ. Microbiol.* 18, 3714–3727. doi:10.1111/1462-2920.13291.

Möller, A.-M., Korytář, T., Köllner, B., Schmidt-Posthaus, H., and Segner, H. (2014). The teleostean liver as an immunological organ: Intrahepatic immune cells (IHICs) in healthy and benzo[a]pyrene challenged rainbow trout (*Oncorhynchus mykiss*). *Dev. Comp. Immunol.* 46, 518-529. doi:10.1016/j.dci.2014.03.020.

Mommsen, T. P., Vijayan, M. M., and Moon, T. W. (1999). Cortisol in teleosts: dynamics, mechanisms of action, and metabolic regulation. *Rev. Fish Biol. Fish.* 9, 211-268. doi:10.1023/A:1008924418720.

Mor, A., and Avtalion, R. R. (1990). Transfer of antibody activity from immunized mother to embryo in tilapias. *J. Fish Biol.* 37, 249–255. doi:10.1111/j.1095-8649.1990.tb05856.x.

Moresco, E. M. Y., LaVine, D., and Beutler, B. (2011). Toll-like receptors. *Curr. Biol.* 21, R488–R493. doi:10.1016/j.cub.2011.05.039.

Moriya, Y., Itoh, M., Okuda, S., Yoshizawa, A. C., and Kanehisa, M. (2007). KAAS: An automatic genome annotation and pathway reconstruction server. *Nucleic Acids Res.* 35, W182-5. doi:10.1093/nar/gkm321.

Najafpour, B., Cardoso, J. C. R., Canário, A. V. M., and Power, D. M. (2020). Specific Evolution and Gene Family Expansion of Complement 3 and Regulatory Factor H in Fish. *Front. Immunol.* 11, 1-27. doi:10.3389/fimmu.2020.568631.

Nauta, A. J., Daha, M. R., Van Kooten, C., and Roos, A. (2003). Recognition and clearance of apoptotic cells: A role for complement and pentraxins. *Trends Immunol.* 24, 148-154. doi:10.1016/S1471-4906(03)00030-9.

Nayak, S. K., Swain, P., Nanda, P. K., Dash, S., Shukla, S., Meher, P. K., et al. (2008). Effect of endotoxin on the immunity of Indian major carp, *Labeo rohita*. *Fish Shellfish Immunol.* 24, 394-399. doi:10.1016/j.fsi.2007.09.005.

Nayak, S. K., Swain, P., Nanda, P. K., Mohapatra, D., and Behera, T. (2011). Immunomodulating potency of lipopolysaccharides (LPS) derived from smooth type of bacterial pathogens in Indian major carp. *Vet. Microbiol.* 151, 413–417. doi:10.1016/j.vetmic.2011.03.021.

Neamat-Allah, A. N. F., Mahmoud, E. A., and Abd El Hakim, Y. (2019). Efficacy of dietary Nano-selenium on growth, immune response, antioxidant, transcriptomic profile and resistance of Nile tilapia, *Oreochromis niloticus* against *Streptococcus iniae* infection. *Fish Shellfish Immunol.* 94, 280–287. doi:10.1016/j.fsi.2019.09.019.

Near, T. J., Dornburg, A., Harrington, R. C., Oliveira, C., Pietsch, T. W., Thacker, C. E., et al. (2015). Identification of the notothenioid sister lineage illuminates the biogeographic history of an Antarctic adaptive radiation. *BMC Evol. Biol.* 15, 109. doi:10.1186/s12862-015-0362-9.

Near, T. J., Dornburg, A., Kuhn, K. L., Eastman, J. T., Pennington, J. N., Patarnello, T., et al. (2012). Ancient climate change, antifreeze, and the evolutionary diversification of Antarctic fishes. *Proc.*

Natl. Acad. Sci. USA. 109, 3434–3439. doi:10.1073/pnas.1115169109.

Neilson, J. D., Waiwood, K. G., and Smith, S. J. (1989). Survival of Atlantic halibut (*Hippoglossus hippoglossus*) caught by longline and otter trawl gear. *Can. J. Fish. Aquat. Sci.* 46, 887-897. doi:10.1139/f89-114.

Nemeth, E., Rivera, S., Gabayan, V., Keller, C., Taudorf, S., Pedersen, B. K., et al. (2004a). IL-6 mediates hypoferremia of inflammation by inducing the synthesis of the iron regulatory hormone hepcidin. *J. Clin. Invest.* 113, 1271–1276. doi:10.1172/JCI200420945.

Nemeth, E., Tuttle, M. S., Powelson, J., Vaughn, M. B., Donovan, A., Ward, D. M., et al. (2004b). Hepcidin Regulates Cellular Iron Efflux by Binding to Ferroportin and Inducing Its Internalization. *Science.* 306, 2090–2093. doi:10.1126/science.1104742.

Neves, J., Caldas, C., Ramos, M. F., and Rodrigues, P. N. S. (2016). Hepcidin-Dependent Regulation of Erythropoiesis during Anemia in a Teleost. *PLoS One*. 11, e0153940. doi:10.1371/journal.pone.0153940.

Neves, J. V., Caldas, C., Vieira, I., Ramos, M. F., and Rodrigues, P. N. S. (2015). Multiple Hepcidins in a Teleost Fish, *Dicentrarchus labrax* : Different Hepcidins for Different Roles. *J. Immunol.* 195, 2696–2709. doi:10.4049/jimmunol.1501153.

Neves, J. V., Ramos, M. F., Moreira, A. C., Silva, T., Gomes, M. S., and Rodrigues, P. N. S. (2017). Hamp1 but not Hamp2 regulates ferroportin in fish with two functionally distinct hepcidin types. *Sci. Rep.* 7, 14793. doi:10.1038/s41598-017-14933-5.

Neves, V., Wilson, J. M., and Rodrigues, P. N. S. (2009). Transferrin and ferritin response to bacterial infection : The role of the liver and brain in fish. 33, 848–857. doi:10.1016/j.dci.2009.02.001.

Nie, L., Cai, S.-Y., Shao, J.-Z., and Chen, J. (2018). Toll-Like Receptors, Associated Biological Roles, and Signaling Networks in Non-Mammals. *Front. Immunol.* 9, 1523. doi:10.3389/fimmu.2018.01523.

Nielsen, H. (2017). Predicting secretory proteins with signaIP. Protein Fuction Prediction: Methods and Protocols, Methods in Molecular Biology. *Springer*. Ed. Kihara, D. 611, 59–73. doi:10.1007/978-1-4939-7015-5_6.

Nilsson, C., Skoglund, A., Moran, A. P., Annuk, H., Engstrand, L., and Normark, S. (2008). Lipopolysaccharide diversity evolving in *Helicobacter pylori* communities through genetic modifications in fucosyltransferases. *PLoS One* 3, e3811. doi:10.1371/journal.pone.0003811.

Nowlan, J. P., Lumsden, J. S., and Russell, S. (2020). Advancements in Characterizing *Tenacibaculum* Infections in Canada. *Pathog.* 9, 1029. doi:10.3390/pathogens9121029.

Nowlin, W. D., and Klinck, J. M. (1986). The physics of the Antarctic Circumpolar Current. *Rev. Geophys.* 24, 469-491. doi:10.1029/RG024i003p00469.

Nozawa, M., Suzuki, Y., and Nei, M. (2009). Reliabilities of identifying positive selection by the branch-site and the site-prediction methods. *Proc. Natl. Acad. Sci. USA.* 106, 6700–6705. doi:10.1073/pnas.0901855106.

Núñez-Montero, K., and Barrientos, L. (2018). Advances in Antarctic Research for Antimicrobial Discovery: A Comprehensive Narrative Review of Bacteria from Antarctic Environments as Potential Sources of Novel Antibiotic Compounds Against Human Pathogens and Microorganisms of Industrial Importance. *Antibiot.* 7, 90. doi:10.3390/antibiotics7040090.

Nya, E. J., and Austin, B. (2010). Use of bacterial lipopolysaccharide (LPS) as an immunostimulant for the control of *Aeromonas hydrophila* infections in rainbow trout *Oncorhynchus mykiss* (Walbaum). *J. Appl. Microbiol.* 108, 686–694. doi:10.1111/j.1365-2672.2009.04464.x.

O'Brien, K. M. (2011). Mitochondrial biogenesis in cold-bodied fishes. *J. Exp. Biol.* 214, 275-285.

doi:10.1242/jeb.046854.

O'Brien, K. M., and Crockett, E. L. (2013). The promise and perils of Antarctic fishes: The remarkable life forms of the Southern Ocean have much to teach science about survival, but human activity is threatening their existence. *EMBO Rep.* 14, 17-24. doi:10.1038/embor.2012.203.

O'Brien, K. M., and Sidell, B. D. (2000). The interplay among cardiac ultrastructure, metabolism and the expression of oxygen-binding proteins in Antarctic fishes. *J. Exp. Biol.* 203, 1287-1297. doi:10.1242/jeb.203.8.1287.

O'Neill, J. G., White, M. G., Sims, T. A., and Barber, D. L. (1988). An inflammatory response of the Antarctic silverfish, *Pleuragramma antarcticum* Boulenger, 1902, to a plerocercoid (species unknown) infestation. *Br. Antarc. Surv. Bull.* 79, 51-63.

Obach, A., Quentel, C., and Baudin Laurencin, F. (1993). Effects of alpha-tocopherol and dietary oxidized fish oil on the immune response of sea bass *Dicentrarchus labrax*. *Dis. Aquat. Organ.* 15, 175-185.

Ohno, N., and Morrison, D. C. (1989). Lipopolysaccharide interactions with lysozyme differentially affect lipopolysaccharide immunostimulatory activity. *Eur. J. Biochem.* 186, 629–636. doi:10.1111/j.1432-1033.1989.tb15253.x.

Ojeda, N., Salazar, C., Cárdenas, C., and Marshall, S. H. (2020). Expression of DC-SIGN-like C-Type Lectin Receptors in *Salmo salar*. *Dev. Comp. Immunol.* 113, 103806. doi:10.1016/j.dci.2020.103806.

Ono, S. J., Nakamura, T., Miyazaki, D., Ohbayashi, M., Dawson, M., and Toda, M. (2003). Chemokines: Roles in leukocyte development, trafficking, and effector function. *J. Allergy Clin. Immunol.* 111, 1185-1199. doi:10.1067/mai.2003.1594.

Onywera, H., and Meiring, T. L. (2020). Comparative analyses of Ion Torrent V4 and Illumina V3-V4 16S rRNA gene metabarcoding methods for characterization of cervical microbiota: taxonomic and functional profiling. *Sci. African.* 7, e00278. doi:10.1016/j.sciaf.2020.e00278.

Pacitti, D., Lawan, M. M., Feldmann, J., Sweetman, J., Wang, T., Martin, S. A. M., et al. (2016). Impact of selenium supplementation on fish antiviral responses: a whole transcriptomic analysis in rainbow trout (*Oncorhynchus mykiss*) fed supranutritional levels of Sel-Plex®. *BMC Genomics*. 17, 116. doi:10.1186/s12864-016-2418-7.

Paiola, M., Moreira, C., Hétru, J., Duflot, A., Pinto, P. I. S., Scapigliati, G., et al. (2021). Prepubertal gonad investment modulates thymus function: evidence in a teleost fish. *J. Exp. Biol.* 224, jeb238576. doi:10.1242/jeb.238576.

Palstra, A. P., Kals, J., Garcia, A. B., Dirks, R. P., and Poelman, M. (2018). Immunomodulatory effects of dietary seaweeds in LPS challenged Atlantic Salmon *Salmo salar* as determined by deep RNA sequencing of the head kidney transcriptome. *Front. Physiol.* 9, 625. doi:10.3389/fphys.2018.00625.

Palti, Y. (2011). Toll-like receptors in bony fish: From genomics to function. *Dev. Comp. Immunol.*, 35, 1263–1272. doi:10.1016/j.dci.2011.03.006.

Papetti, C., Babbucci, M., Dettai, A., Basso, A., Lucassen, M., Harms, L., et al. (2021). Not Frozen in the Ice: Large and Dynamic Rearrangements in the Mitochondrial Genomes of the Antarctic Fish. *Genome Biol. Evol.* 13, evab017. doi:10.1093/gbe/evab017.

Parata, L., Mazumder, D., Sammut, J., and Egan, S. (2021). Correction: Diet type influences the gut microbiome and nutrient assimilation of Genetically Improved Farmed Tilapia (*Oreochromis niloticus*). *PLoS One.* 16, 1–2. doi:10.1371/journal.pone.0237775.

Paria, A., Deepika, A., Sreedharan, K., Makesh, M., Chaudhari, A., Purushothaman, C. S., et al. (2016).

Identification of Nod like receptor C3 (NLRC3) in Asian seabass, *Lates calcarifer*: Characterisation, ontogeny and expression analysis after experimental infection and ligand stimulation. *Fish Shellfish Immunol.* 55, 602–612. doi:10.1016/j.fsi.2016.06.029.

Parish, N., Wrathmell, A., Hart, S., and Harris, J. E. (1986). The leucocytes of the elasmobranch *Scyliorhinus canicula L.*—a morphological study. *J. Fish Biol.* 28, 545-561. doi:10.1111/j.1095-8649.1986.tb05192.x.

Park, B. S., and Lee, J.-O. (2013). Recognition of lipopolysaccharide pattern by TLR4 complexes. *Exp. Mol. Med.* 45, e66. doi:10.1038/emm.2013.97.

Park, S. B., Hikima, J.-I., Suzuki, Y., Ohtani, M., Nho, S. W., Cha, I. S., et al. (2012). Molecular cloning and functional analysis of nucleotide-binding oligomerization domain 1 (NOD1) in olive flounder, *Paralichthys olivaceus*. *Dev. Comp. Immunol.* 36, 680–687. doi:10.1016/j.dci.2011.11.007.

Park, C. H., Valore, E. V., Waring, A. J., and Ganz, T. (2001). Hepcidin, a Urinary Antimicrobial Peptide Synthesized in the Liver. *J. Biol. Chem.* 276, 7806-7810. doi:10.1074/jbc.M008922200.

Patarnello, T., Verde, C., di Prisco, G., Bargelloni, L., and Zane, L. (2011). How will fish that evolved at constant sub-zero temperatures cope with global warming? Notothenioids as a case study. *BioEssays*. 33, 260-268. doi:10.1002/bies.201000124.

Paulsen, S. M., Engstad, R. E., and Robertsen, B. (2001). Enhanced lysozyme production in Atlantic salmon (*Salmo salar L.*) macrophages treated with yeast β-glucan and bacterial lipopolysaccharide. *Fish Shellfish Immunol.* 11, 23–37. doi:10.1006/fsim.2000.0291.

Pelegrín, P., Chaves-Pozo, E., Mulero, V., and Meseguer, J. (2004). Production and mechanism of secretion of interleukin-1β from the marine fish gilthead seabream. *Dev. Comp. Immunol.* 28, 229-237. doi:10.1016/j.dci.2003.08.002.

Pérez-Sánchez, J., Estensoro, I., Redondo, M. J., Calduch-Giner, J. A., Kaushik, S., and Sitjà-Bobadilla, A. (2013). Mucins as diagnostic and prognostic biomarkers in a fish-parasite model: transcriptional and functional analysis. *PLoS One*. 8, e65457. doi:10.1371/journal.pone.0065457.

Perry, W. B., Lindsay, E., Payne, C. J., Brodie, C., and Kazlauskaite, R. (2020). The role of the gut microbiome in sustainable teleost aquaculture. *Proc. R. Soc. B Biol. Sci.* 287, 20200184. doi:10.1098/rspb.2020.0184.

Phelan, P. E., Mellon, M. T., and Kim, C. H. (2005). Functional characterization of full-length TLR3, IRAK-4, and TRAF6 in zebrafish (*Danio rerio*). *Mol. Immunol.* 42, 1057-1071. doi:10.1016/j.molimm.2004.11.005.

Philip, A. M., Wang, Y., Mauro, A., El-Rass, S., Marshall, J. C., Lee, W. L., et al. (2017). Development of a zebrafish sepsis model for high-throughput drug discovery. *Mol. Med.* 23, 134–148. doi:10.2119/molmed.2016.00188.

Pietretti, D., and Wiegertjes, G. F. (2014). Ligand specificities of Toll-like receptors in fish: Indications from infection studies. *Dev. Comp. Immunol.* 43, 205–22. doi:10.1016/j.dci.2013.08.010.

Pigeon, C., Ilyin, G., Courselaud, B., Leroyer, P., Turlin, B., Brissot, P., et al. (2001). A New Mouse Liver-specific Gene, Encoding a Protein Homologous to Human Antimicrobial Peptide Hepcidin, Is Overexpressed during Iron Overload. *J. Biol. Chem.* 276, 7811-7819. doi:10.1074/jbc.M008923200.

Place, S. P., and Hofmann, G. E. (2005a). Comparison of Hsc70 orthologs from polar and temperate notothenioid fishes: differences in prevention of aggregation and refolding of denatured proteins. *Am. J. Physiol. Regul. Integr. Comp. Physiol.* 288, R1195-R1202. doi:10.1152/ajpregu.00660.2004.

Place, S. P., and Hofmann, G. E. (2005b). Constitutive expression of a stress-inducible heat shock

protein gene, hsp70, in phylogenetically distant Antarctic fish. *Polar Biol.* 28, 261-267. doi:10.1007/s00300-004-0697-y.

Place, S. P., Zippay, M. L., and Hofmann, G. E. (2004). Constitutive roles for inducible genes: Evidence for the alteration in expression of the inducible hsp70 gene in Antarctic notothenioid fishes. *Am. J. Physiol. - Regul. Integr. Comp. Physiol.* 287, R429-R436. doi:10.1152/ajpregu.00223.2004.

Poltorak, A., He, X., Smirnova, I., Liu, M. Y., Van Huffel, C., Du, X., et al. (1998). Defective LPS signaling in C3H/HeJ and C57BL/10ScCr mice: mutations in Tlr4 gene. *Science*. 282, 2085–2088. doi:10.1126/science.282.5396.2085.

Pörtner, H. O. (2006). Climate-dependent evolution of Antarctic ectotherms: An integrative analysis. *Deep. Res. Part II Top. Stud. Oceanogr.* 53, 1071-1104. doi:10.1016/j.dsr2.2006.02.015.

Portner, H. O., Lucassen, M., and Storch, D. (2005). Metabolic Biochemistry: Its Role in Thermal Tolerance and in the Capacities of Physiological and Ecological Function. Fish Physiology: The Physiology of Polar Fishes. *Elsevier.* 22, 79-154. doi:10.1016/S1546-5098(04)22003-9.

Prieto-Álamo, M.-J., Abril, N., Osuna-Jiménez, I., and Pueyo, C. (2009). *Solea senegalensis* genes responding to lipopolysaccharide and copper sulphate challenges: Large-scale identification by suppression subtractive hybridization and absolute quantification of transcriptional profiles by real-time RT-PCR. *Aquat. Toxicol.* 91, 312-319. doi:10.1016/j.aquatox.2008.11.001.

Pulgar, R., Hödar, C., Travisany, D., Zuñiga, A., Domínguez, C., Maass, A., et al. (2015). Transcriptional response of Atlantic salmon families to *Piscirickettsia salmonis* infection highlights the relevance of the iron-deprivation defence system. *BMC Genomics*. 16, 495. doi:10.1186/s12864-015-1716-9.

Qi, D., Chao, Y., Zhang, C., Wang, Z., Wang, W., Chen, Q., et al. (2019). Duplication of toll-like receptor 22 in teleost fishes. *Fish Shellfish Immunol.* 94, 752–760. doi:10.1016/j.fsi.2019.09.067.

Qi, Z., Wang, S., Zhu, X., Yang, Y., Han, P., Zhang, Q., et al. (2018). Molecular characterization of three toll-like receptors (TLR21, TLR22, and TLR25) from a primitive ray-finned fish Dabry's sturgeon (*Acipenser dabryanus*). *Fish Shellfish Immunol.* 82, 200–211. doi:10.1016/j.fsi.2018.08.033.

Qin, C., Zhao, W., Deng, D., Lu, R., Yang, G., Yan, X., et al. (2020). Effects of glucose, insulin, glucagon, LPS and poly (I:C) on adiponectin receptors expression in grass carp (*Ctenophcuyngodon idellus*). *Aquaculture.* 528, 735501. doi:10.1016/j.aquaculture.2020.735501.

Qiu, H. T., Fernandes, J. M. O., Hong, W. S., Wu, H. X., Zhang, Y. T., Huang, S., et al. (2019). Paralogues From the Expanded Tlr11 Gene Family in Mudskipper (*Boleophthalmus pectinirostris*) Are Under Positive Selection and Respond Differently to LPS/Poly(I:C) Challenge. *Front. Immunol.* 10, 343. doi:10.3389/fimmu.2019.00343.

Quast, C., Pruesse, E., Yilmaz, P., Gerken, J., Schweer, T., Yarza, P., et al. (2013). The SILVA ribosomal RNA gene database project: improved data processing and web-based tools. *Nucleic Acids Res.* 41, D590-596. doi:10.1093/nar/gks1219.

Qureshi, S. T., Larivière, L., Leveque, G., Clermont, S., Moore, K. J., Gros, P., et al. (1999). Endotoxin-tolerant mice have mutations in toll-like receptor 4 (Tlr4). *J. Exp. Med.* 189, 615-625. doi:10.1084/jem.189.4.615.

Rackis, J. J. (1965). Physiological properties of soybean trypsin inhibitors and their relationship to pancreatic hypertrophy and growth inhibition of rats. *Fed. Proc.* 24, 1488-1493.

Raetz, C. R. H. (1990). Biochemistry of endotoxins. *Annu. Rev. Biochem.* 59, 129-170. doi:10.1146/annurev.bi.59.070190.001021.

Raetz, C. R. H., and Whitfield, C. (2002). Lipopolysaccharide endotoxins. *Annu. Rev. Biochem.* 71, 635-

700. doi:10.1146/annurev.biochem.71.110601.135414.

Ragland, S. A., and Criss, A. K. (2017). From bacterial killing to immune modulation: Recent insights into the functions of lysozyme. *PLoS Pathog.* 13, e1006512. doi:10.1371/journal.ppat.1006512.

Rakers, S., Gebert, M., Uppalapati, S., Meyer, W., Maderson, P., Sell, A. F., et al. (2010). Fish matters: the relevance of fish skin biology to investigative dermatology. *Exp. Dermatol.* 19, 313–324. doi:10.1111/j.1600-0625.2009.01059.x.

Rambaut, A. (2016). FigTree v1.4.3 software. *Institute of Evolutionary Biology, University of Edinburgh*. http://tree.bio.ed.ac.uk/software/figtree.

Ramees, T. P., Dhama, K., Karthik, K., Rathore, R. S., Kumar, A., Saminathan, M., et al. (2017). Arcobacter: an emerging food-borne zoonotic pathogen, its public health concerns and advances in diagnosis and control – a comprehensive review. *Vet. Q.* 37, 136–161. doi:10.1080/01652176.2017.1323355.

Rasmussen, R. (2001). Rapid Cyclee Real-time PCR, Methods and Applications. *Springer*. Ed. Meuer, S. et al. 1, 223. doi:10.1007/978-3-642-59524-0_3.

Ratledge, C., and Dover, L. G. (2000). Iron Metabolism in Pathogenic Bacteria. *Annu. Rev. Micribiology*, 881–941. doi:10.1146/annurev.micro.54.1.881.

Rauta, P. R., Nayak, B., and Das, S. (2012). Immune system and immune responses in fish and their role in comparative immunity study: A model for higher organisms. *Immunol. Lett.* 148, 23-33. doi:10.1016/j.imlet.2012.08.003.

Ray, M. K., Kumar, G. S., and Shivaji, S. (1994). Phosphorylation of lipopolysaccharides in the antarctic psychrotroph *Pseudomonas syringae*: A possible role in temperature adaptation. *J. Bacteriol.* 176, 4243–4249. doi:10.1128/jb.176.14.4243-4249.1994.

Regoli, F., Nigro, M., Benedetti, M., Fattorini, D., and Gorbi, S. (2005). Antioxidant efficiency in early life stages of the Antarctic silverfish, *Pleuragramma antarcticum*: Responsiveness to pro-oxidant conditions of platelet ice and chemical exposure. *Aquat. Toxicol.* 75, 43-52. doi:10.1016/j.aquatox.2005.07.003.

Reite, O. B., and Evensen, Ø. (2006). Inflammatory cells of teleostean fish: A review focusing on mast cells/eosinophilic granule cells and rodlet cells. *Fish Shellfish Immunol.* 20, 192–208. doi:10.1016/j.fsi.2005.01.012.

Renko, K., Hofmann, P. J., Stoedter, M., Hollenbach, B., Behrends, T., Köhrle, J., et al. (2009). Down-regulation of the hepatic selenoprotein biosynthesis machinery impairs selenium metabolism during the acute phase response in mice. *FASEB J.* 23, 1758–1765. doi:10.1096/fj.08-119370.

Reyes-Cerpa, S., Maisey, K., Reyes-Lpez, F., Toro-Ascuy, D., Mara, A., and Imarai, M. (2012). Fish Cytokines and Immune Response. New Advances and Contributions to Fish Biology. *IntechOpen*. Ed. Turker, Akan. doi:10.5772/53504.

Rintoul, S. R. (2010). Antarctic Circumpolar Current. Encyclopedia of Ocean Sciences. 178-190. doi:10.1016/B978-012374473-9.00603-2.

Robertson, S., Bradley, J. E., and Maccoll, A. D. C. (2016). Measuring the immune system of the three-spined stickleback - investigating natural variation by quantifying immune expression in the laboratory and the wild. *Mol. Ecol. Resour.* 16, 701–713. doi:10.1111/1755-0998.12497.

Robinson, D. R., Xu, L. L., Knoell, C. T., Tateno, S., and Olesiak, W. (1993). Modification of spleen phospholipid fatty acid composition by dietary fish oil and by n-3 fatty acid ethyl esters. *J. Lipid Res.* 34, 1423–1434.

Robinson, E., and Davison, W. (2008). The Antarctic notothenioid fish *Pagothenia borchgrevinki* is thermally flexible: acclimation changes oxygen consumption. *Polar Biol.* 31, 317–326.

doi:10.1007/s00300-007-0361-4.

Robinson, M. D., McCarthy, D. J., and Smyth, G. K. (2009). edgeR: A Bioconductor package for differential expression analysis of digital gene expression data. *Bioinformatics*. 26, 139-140. doi:10.1093/bioinformatics/btp616.

Rodríguez, A., Esteban, M. A., and Meseguer, J. (2003). A mannose-receptor is possibly involved in the phagocytosis of *Saccharomyces cerevisiae* by seabream (*Sparus aurata L.*) leucocytes. *Fish Shellfish Immunol.* 14, 375-388. doi:10.1006/fsim.2002.0446.

Rodriguez, M. F., Wiens, G. D., Purcell, M. K., and Palti, Y. (2005). Characterization of Toll-like receptor 3 gene in rainbow trout (*Oncorhynchus mykiss*). *Immunogenetics*. 57, 510-9. doi:10.1007/s00251-005-0013-1.

Rombout, J. H. W. M., Bot, H. E., and Taverne-Thiele, J. J. (1989). Immunological importance of the second gut segment of carp. II. Characterization of mucosal leucocytes. *J. Fish Biol.* 35, 167-178. doi:10.1111/j.1095-8649.1989.tb02966.x.

Rombout, J. H. W. M., Lamers, C. H. J., Helfrich, M. H., Dekker, A., and Taverne-Thiele, J. J. (1985). Uptake and transport of intact macromolecules in the intestinal epithelium of carp (*Cyprinus carpio L.*) and the possible immunological implications. *Cell Tissue Res.* 239, 519-530. doi:10.1007/BF00219230.

Rombout, J. H. W. M., Yang, G., and Kiron, V. (2014). Adaptive immune responses at mucosal surfaces of teleost fish. *Fish Shellfish Immunol.* 40, 634-643. doi:10.1016/j.fsi.2014.08.020.

Rombout, J. H. W. M., Abelli, L., Picchietti, S., Scapigliati, G., and Kiron, V. (2011). Teleost intestinal immunology. *Fish Shellfish Immunol.* 31, 616-626. doi:10.1016/j.fsi.2010.09.001.

Ronquist, F., Teslenko, M., Van der Mark, P., Ayres, D. L., Darling, A., Höhna, S., et al. (2012). MrBayes 3.2: efficient Bayesian phylogenetic inference and model Choice across a Large model space. *Syst. Biol.* 61, 539–542. doi:10.1093/sysbio/sys029.

Rosado, D., Pérez-Losada, M., Severino, R., Cable, J., and Xavier, R. (2019). Characterization of the skin and gill microbiomes of the farmed seabass (*Dicentrarchus labrax*) and seabream (*Sparus aurata*). *Aquaculture*. 500, 57-64. doi:10.1016/j.aquaculture.2018.09.063.

Rosenstiel, P., Philipp, E. E. R., Schreiber, S., and Bosch, T. C. G. (2009). Evolution and function of innate immune receptors - Insights from marine invertebrates. *J. Innate Immun*. 1, 291-300. doi:10.1159/000211193.

Ross, A. A., Rodrigues Hoffmann, A., and Neufeld, J. D. (2019). The skin microbiome of vertebrates. *Microbiome*. 7, 79. doi:10.1186/s40168-019-0694-6.

Rotllant, J., Guerreiro, P. M., Anjos, L., Redruello, B., Canario, A. V. M., and Power, D. M. (2005). Stimulation of cortisol release by the N terminus of teleost parathyroid hormone-related protein in interrenal cells *in vitro*. *Endocrinology*. 146, 71-76. doi:10.1210/en.2004-0644.

Rowley, P. D., Farrar, E., Carrara, P. E., Vennum, W. R., and Kellogg, K. S. (1988). Porphyry-type copper deposits and potassium-argon ages of plutonic rocks of the Orville Coast and Eastern Ellsworth Land, Antarctica. *US Geol. Surv. Prof. Pap.* 1351, 35-49.

Roy, S., Kumar, V., Kumar, V., and Behera, B. K. (2016). Acute Phase Proteins and their Potential Role as an Indicator for Fish Health and in Diagnosis of Fish Diseases. *Protein Pept. Lett.* 24, 78-89. doi:10.2174/0929866524666161121142221.

Ruud, J. T. (1954). Vertebrates without erythrocytes and blood pigment. *Nature*. 173, 848-850. doi:10.1038/173848a0.

Ruysschaert, J.-M., and Lonez, C. (2015). Role of lipid microdomains in TLR-mediated signalling. *Biochim. Biophys. Acta - Biomembr.* 1848, 1860–7. doi:10.1016/j.bbamem.2015.03.014.

Sahoo, B. R. (2020). Structure of fish Toll-like receptors (TLR) and NOD-like receptors (NLR). *Int. J. Biol. Macromol.* 161, 1602–1617. doi:10.1016/j.ijbiomac.2020.07.293.

Sahoo, B. R., Dikhit, M. R., Bhoi, G. K., Maharana, J., Lenka, S. K., Dubey, P. K., et al. (2015). Understanding the distinguishable structural and functional features in zebrafish TLR3 and TLR22, and their binding modes with fish dsRNA viruses: An exploratory structural model analysis. *Amino Acids.* 47, 381–400. doi:10.1007/s00726-014-1872-2.

Sakai, M., Hikima, J., and Kono, T. (2021). Fish cytokines: current research and applications. *Fish. Sci.* 87, 1–9. doi:10.1007/s12562-020-01476-4.

Salinas, I. (2015). The mucosal immune system of teleost fish. *Biology.* 4, 525-39. doi:10.3390/biology4030525.

Salinas, I., LaPatra, S. E., and Erhardt, E. B. (2015). Nasal vaccination of young rainbow trout (*Oncorhynchus mykiss*) against infectious hematopoietic necrosis and enteric red mouth disease. *Dev. Comp. Immunol.* 53, 105-111. doi:10.1016/j.dci.2015.05.015.

Salinas, I., Zhang, Y.-A., and Sunyer, J. O. (2011). Mucosal immunoglobulins and B cells of teleost fish. *Dev. Comp. Immunol.* 35, 1346-65. doi:10.1016/j.dci.2011.11.009.

Santander, J., Kilbourne, J., Park, J. Y., Martin, T., Loh, A., Diaz, I., et al. (2014). Inflammatory effects of Edwardsiella ictaluri lipopolysaccharide modifications in catfish gut. *Infect. Immun.* 82, 3394–3404. doi:10.1128/IAI.01697-14.

Sasaki, Y., Maita, M., and Okamoto, N. (2002). Rainbow trout neutrophils are responsible for non-specific cytotoxicity. *Fish Shellfish Immunol.* 12, 243-252. doi:10.1006/fsim.2001.0368.

Satake, H., and Sasaki, N. (2010). Comparative Overview of Toll-Like Receptors in Lower Animals. *Zoolog. Sci.* 27, 154–61. doi:10.2108/zsj.27.154.

Saurabh, S., and Sahoo, P. K. (2008). Lysozyme: An important defence molecule of fish innate immune system. *Aquac. Res.* 39, 223-239. doi:10.1111/j.1365-2109.2007.01883.x.

Säwström, C., Anesio, M. A., Granéli, W., and Laybourn-Parry, J. (2007). Seasonal Viral Loop Dynamics in Two Large Ultraoligotrophic Antarctic Freshwater Lakes. *Microb. Ecol.* 53, 1–11. doi:10.1007/s00248-006-9146-5.

Schloss, P. D. (2020). Reintroducing mothur: 10 years later. *Appl. Environ. Microbiol.* 86, 1–13. doi:10.1128/AEM.02343-19.

Schloss, P. D., Westcott, S. L., Ryabin, T., Hall, J. R., Hartmann, M., Hollister, E. B., et al. (2009). Introducing mothur: Open-source, platform-independent, community-supported software for describing and comparing microbial communities. *Appl. Environ. Microbiol.* 75, 7537–7541. doi:10.1128/AEM.01541-09.

Scudiero, R., Trinchella, F., and Parisi, E. (2009). Iron metabolism genes in Antarctic notothenioids: A review. *Mar. Genomics.* 1, 79–85. doi:10.1016/j.margen.2008.12.001.

Scudiero, R., Trinchella, F., Riggio, M., and Parisi, E. (2007). Structure and expression of genes involved in transport and storage of iron in red-blooded and hemoglobin-less antarctic notothenioids. *Gene.* 397, 1–11. doi:10.1016/j.gene.2007.03.003.

Seco, J., Xavier, J. C., Coelho, J. P., Pereira, B., Tarling, G., Pardal, M. A., et al. (2019). Spatial variability in total and organic mercury levels in Antarctic krill *Euphausia superba* across the Scotia Sea. *Environ. Pollut.* 247, 332–339. doi:10.1016/j.envpol.2019.01.031.

Sehnal, L., Brammer-Robbins, E., Wormington, A. M., Blaha, L., Bisesi, J., Larkin, I., et al. (2021). Microbiome Composition and Function in Aquatic Vertebrates: Small Organisms Making Big Impacts on Aquatic Animal Health. *Front. Microbiol.* 12, 567408. doi:10.3389/fmicb.2021.567408.

Seppola, M., Mikkelsen, H., Johansen, A., Steiro, K., Myrnes, B., and Nilsen, I. W. (2015). Ultrapure LPS induces inflammatory and antibacterial responses attenuated invitro by exogenous sera in Atlantic cod and Atlantic salmon. *Fish Shellfish Immunol.* 44, 66–78. doi:10.1016/j.fsi.2015.01.018.

Sepulcre, M. P., Alcaraz-Pérez, F., López-Muñoz, A., Roca, F. J., Meseguer, J., Cayuela, M. L., et al. (2009). Evolution of Lipopolysaccharide (LPS) Recognition and Signaling: Fish TLR4 Does Not Recognize LPS and Negatively Regulates NF-κB Activation. *J. Immunol.* 182, 1836-1845. doi:10.4049/jimmunol.0801755.

Sfacteria, A., Brines, M., and Blank, U. (2015). The mast cell plays a central role in the immune system of teleost fish. *Mol. Immunol.* 63, 3-8. doi:10.1016/j.molimm.2014.02.007.

Shan, M.-R., Zhou, S.-N., Fu, C.-N., Song, J.-W., Wang, X.-Q., Bai, W.-W., et al. (2020). Vitamin B6 inhibits macrophage activation to prevent lipopolysaccharide-induced acute pneumonia in mice. *J. Cell. Mol. Med.* 24, 3139–3148. doi:10.1111/jcmm.14983.

Shi, J., and Camus, A. C. (2006). & Comparative Hepcidins in amphibians and fishes : Antimicrobial peptides or iron-regulatory hormones ?. 30, 746–755. doi:10.1016/j.dci.2005.10.009.

Shi, W., Chen, S., Kong, X., Si, L., Gong, L., Zhang, Y., et al. (2018). Flatfish monophyly refereed by the relationship of Psettodes in Carangimorphariae. *BMC Genomics.* 19, 400. doi:10.1186/s12864-018-4788-5.

Shin, S. C. hu., Ahn, D. H. wa., Kim, S. J. i., Pyo, C. W. o., Lee, H., Kim, M. K., et al. (2014). The genome sequence of the Antarctic bullhead notothen reveals evolutionary adaptations to a cold environment. *Genome Biol.* 15, 468. doi:10.1186/s13059-014-0468-1.

Shin, S. C., Kim, S. J., Lee, J. K., Ahn, D. H., Kim, M. G., Lee, H., et al. (2012). Transcriptomics and comparative analysis of three Antarctic Notothenioid fishes. *PLoS One.* 7, e43762. doi:10.1371/journal.pone.0043762.

Shishido, C. M., Woods, H. A., Lane, S. J., Toh, M. W. A., Tobalske, B. W., and Moran, A. L. (2019). Polar gigantism and the oxygen–temperature hypothesis: a test of upper thermal limits to body size in Antarctic pycnogonids. *Proc. R. Soc. B Biol. Sci.* 286, 20190124. doi:10.1098/rspb.2019.0124.

Signorino, G., Mohammadi, N., Patanè, F., Buscetta, M., Venza, M., Venza, I., et al. (2014). Role of toll-like receptor 13 in innate immune recognition of group B *streptococci*. *Infect. Immun.* 82, 5013–22. doi:10.1128/IAI.02282-14.

Silva, F. C. de P., Nicoli, J. R., Zambonino-Infante, J. L., Kaushik, S., and Gatesoupe, F. J. (2011). Influence of the diet on the microbial diversity of faecal and gastrointestinal contents in gilthead sea bream (*Sparus aurata*) and intestinal contents in goldfish (*Carassius auratus*). *FEMS Microbiol. Ecol.* 78, 285-296. doi:10.1111/j.1574-6941.2011.01155.x.

Silva, J. R. M. C., Hernadez-Blazquez, F. J., and Barbieri, R. L. (1998). Induced inflammatory process in the Antarctic fish *Notothenia neglecta*. *Polar Biol.* 20, 206-212. doi:10.1007/s003000050297.

Silva, J. R. M. C., Staines, N. A., Hernandez-Blazquez, F. J., Porto-Neto, L. R., and Borges, J. C. S. (2002). Phagocytosis and giant cell formation at 0°C by macrophage (MØ) of *Notothenia coriiceps*. *J. Fish Biol.* 60, 466-478. doi:10.1006/jfbi.2001.1858.

Silva, J. R. M. C., Staines, N. A., Parra, O. M., and Hernandez-Blazquez, F. J. (1999). Experimental studies on the response of the fish (*Notothenia coriiceps* Richardson, 1844) to parasite (*Pseudoterranova decipiens* Krabbe, 1878) and other irritant stimuli at Antarctic temperatures. *Polar Biol.* 22, 417-424. doi:10.1007/s003000050436.

Simide, R., Richard, S., Prévot-D'Alvise, N., Miard, T., and Gaillard, S. (2016). Assessment of the accuracy of physiological blood indicators for the evaluation of stress, health status and welfare in Siberian sturgeon (*Acipenser baerii*) subject to chronic heat stress and dietary supplementation.

Int. Aquat. Res. 8, 121–135. doi:10.1007/s40071-016-0128-z.

Simpson, E. H. (1949). Measurement of Diversity. *Nature.* 163, 688. doi:10.1038/163688a0.

Sipka, S., and Bruckner, G. (2014). The immunomodulatory role of bile acids. *Int. Arch. Allergy Immunol.* 165, 1-8. doi:10.1159/000366100.

Skaar, E. P. (2010). The battle for iron between bacterial pathogens and their vertebrate hosts. *PLoS Pathog.* 6, 1–2. doi:10.1371/journal.ppat.1000949.

Slack, J. L., Schooley, K., Bonnert, T. P., Mitcham, J. L., Qwarnstrom, E. E., Sims, J. E., et al. (2000). Identification of two major sites in the type I interleukin-1 receptor cytoplasmic region responsible for coupling to pro-inflammatory signaling pathways. *J. Biol. Chem.* 275, 4670–4678. doi:10.1074/jbc.275.7.4670.

Smith-Unna, R., Boursnell, C., Patro, R., Hibberd, J. M., and Kelly, S. (2016). TransRate: Reference-free quality assessment of *de novo* transcriptome assemblies. *Genome Res.* 26, 1134-1144. doi:10.1101/gr.196469.115.

Smith, N. C., Rise, M. L., and Christian, S. L. (2019). A Comparison of the Innate and Adaptive Immune Systems in Cartilaginous Fish, Ray-Finned Fish, and Lobe-Finned Fish. *Front. Immunol.* 10, 2292. doi:10.3389/fimmu.2019.02292.

Smith, W. W. (1940). Production of Anti-Bacterial Agglutinins by Carp and Trout at 10° G. *Proc. Soc. Exp. Biol. Med.* 45, 726–729. doi:10.3181/00379727-45-11814.

Soanes, K. H., Figuereido, K., Richards, R. C., Mattatall, N. R., and Ewart, K. V. (2004). Sequence and expression of C-type lectin receptors in Atlantic salmon (*Salmo salar*). *Immunogenetics.* 56, 572–584. doi:10.1007/s00251-004-0719-5.

Sodeland, M., Jorde, P. E., Lien, S., Jentoft, S., Berg, P. R., Grove, H., et al. (2016). Islands of Divergence in the atlantic cod genome represent polymorphic chromosomal rearrangements. *Genome Biol. Evol.* 8, 1012–1022. doi:10.1093/gbe/evw057.

Solbakken, M. H., Tørresen, O. K., Nederbragt, A. J., Seppola, M., Gregers, T. F., Jakobsen, K. S., et al. (2016). Evolutionary redesign of the Atlantic cod (*Gadus morhua L.*) Toll-like receptor repertoire by gene losses and expansions. *Sci. Rep.* 6, 25211. doi:10.1038/srep25211.

Solbakken, M. H., Voje, K. L., Jakobsen, K. S., and Jentoft, S. (2017). Linking species habitat and past palaeoclimatic events to evolution of the teleost innate immune system. *Proc. R. Soc. B Biol. Sci.* 284, 2016810. doi:10.1098/rspb.2016.2810.

Soleto, I., Fischer, U., Tafalla, C., and Granja, A. G. (2018). Identification of a potential common ancestor for mammalian cross-presenting dendritic cells in teleost respiratory surfaces. *Front. Immunol.* 9, 59. doi:10.3389/fimmu.2018.00059.

Sompayrac, L. (2012). How System immune works. *Willey-Blackwell.* 168.

Song, W., Li, L., Huang, H., Jiang, K., Zhang, F., Chen, X., et al. (2016). The Gut Microbial Community of Antarctic Fish Detected by 16S rRNA Gene Sequence Analysis. *Biomed Res. Int.* 2016, 3241529. doi:10.1155/2016/3241529.

Soulliere, C., and Dixon, B. (2017). Immune System Organs of Bony Fishes. *Elsevier Ltd.* 1-5. doi:10.1016/B978-0-12-809633-8.12179-X.

Souza, M. R. D. P. de, Herrerias, T., Zaleski, T., Forgati, M., Kandalski, P. K., Machado, C., et al. (2018). Heat stress in the heart and muscle of the Antarctic fishes *Notothenia rossii* and *Notothenia coriiceps*: Carbohydrate metabolism and antioxidant defence. *Biochimie.* 146, 43–55. doi:10.1016/j.biochi.2017.11.010.

Souza, P. P. C., and Lerner, U. H. (2019). Finding a toll on the route: The fate of osteoclast progenitors

after toll-like receptor activation. *Front. Immunol.* 10, 1663. doi:10.3389/fimmu.2019.01663.

Stafford, J. L., and Belosevic, M. (2003). Transferrin and the innate immune response of fish: Identification of a novel mechanism of macrophage activation. *Dev. Comp. Immunol.* 27, 539-554. doi:10.1016/S0145-305X(02)00138-6.

Stamatakis, A. (2014). RAxML version 8: A tool for phylogenetic analysis and post-analysis of large phylogenies. *Bioinformatics.* 30, 1312–1313. doi:10.1093/bioinformatics/btu033.

Stein, D. L. (2012). Snailfishes (Family *Liparidae*) of the Ross Sea, Antarctica, and Closely Adjacent Waters. *Zootaxa*. 3285, 1-20. doi:10.11646/zootaxa.3285.1.1.

Stejskal, V., Kouřil, J., Policar, T., and Svobodová, Z. (2016). Splenic lipidosis in intensively cultured perch, Perca fluviatilis L. *J. Fish Dis.* 39, 87–93. doi:10.1111/jfd.12327.

StG Howell, C. J. (1987). A chemokinetic factor in the carp *Cyprinus carpio*. *Dev. Comp. Immunol.* 11, 139–146. doi:10.1016/0145-305X(87)90015-2.

Sumbria, D., Berber, E., Mathayan, M., and Rouse, B. T. (2021). Virus Infections and Host Metabolism—Can We Manage the Interactions? *Front. Immunol.* 11, 1–14. doi:10.3389/fimmu.2020.594963.

Sun, B., Li, X., Ning, X., and Sun, L. (2020). Transcriptome analysis of *Paralichthys olivaceus* erythrocytes reveals profound immune responses induced by *Edwardsiella tarda* infection. *Int. J. Mol. Sci.* 21, 3094. doi:10.3390/ijms21093094.

Sun, M., Mu, Y., Ding, Y., Ao, J., and Chen, X. (2016). Molecular and functional characterization of Toll-like receptor 21 in large yellow croaker (*Larimichthys crocea*). *Fish Shellfish Immunol.* 59, 179–188. doi:10.1016/j.fsi.2016.10.024.

Sunagawa, S., Coelho, L. P., Chaffron, S., Kultima, J. R., Labadie, K., Salazar, G., et al. (2015). Structure and function of the global ocean microbiome. *Science.* 348, 1261359. doi:10.1126/science.1261359.

Sundaram, A. Y., Kiron, V., Dopazo, J., and Fernandes, J. M. (2012a). Diversification of the expanded teleost-specific toll-like receptor family in Atlantic cod, *Gadus morhua*. *BMC Evol. Biol.* 12, 256. doi:10.1186/1471-2148-12-256.

Sundaram, A. Y. M., Consuegra, S., Kiron, V., and Fernandes, J. M. O. (2012b). Positive selection pressure within teleost toll-like receptors *tlr21* and *tlr22* subfamilies and their response to temperature stress and microbial components in zebrafish. *Mol. Biol. Rep.* 39, 8965–8975. doi:10.1007/s11033-012-1765-y.

Sunyer, J. O. (2013). Fishing for mammalian paradigms in the teleost immune system. *Nat. Immunol.* 14, 320-326. doi:10.1038/ni.2549.

Sunyer, J. O., and Tort, L. (1995). Natural hemolytic and bactericidal activities of sea bream *Sparus aurata* serum are effected by the alternative complement pathway. *Vet. Immunol. Immunopathol.* 45, 333-345. doi:10.1016/0165-2427(94)05430-Z.

Supek, F., Bošnjak, M., Škunca, N., and Šmuc, T. (2011). REVIGO summarizes and visualizes long lists of gene ontology terms. *PLoS One*. 6, e21800. doi:10.1371/journal.pone.0021800.

Suyama, M., Torrents, D., and Bork, P. (2006). PAL2NAL: Robust conversion of protein sequence alignments into the corresponding codon alignments. *Nucleic Acids Res.* 34, W609–W612. doi:10.1093/nar/gkl315.

Suzuki, T., Shin-I, T., Kohara, Y., and Kasahara, M. (2004). Transcriptome analysis of hagfish leukocytes: A framework for understanding the immune system of jawless fishes. *Dev. Comp. Immunol.* 28, 993–1003. doi:10.1016/j.dci.2004.04.005.

Svingerud, T., Solstad, T., Sun, B., Nyrud, M. L. J., Kileng, Ø., Greiner-Tollersrud, L., et al. (2012). Atlantic Salmon Type I IFN Subtypes Show Differences in Antiviral Activity and Cell-Dependent Expression: Evidence for High IFNb/IFNc–Producing Cells in Fish Lymphoid Tissues. *J. Immunol.* 189, 5912-5923. doi:10.4049/jimmunol.1201188.

Swain, B., Basu, M., and Samanta, M. (2013). NOD1 and NOD2 receptors in mrigal (*Cirrhinus mrigala*): inductive expression and downstream signalling in ligand stimulation and bacterial infections. *J. Biosci.* 38, 533–548. doi:10.1007/s12038-013-9330-y.

Swain, P., Nayak, S. K., Nanda, P. K., and Dash, S. (2008). Biological effects of bacterial lipopolysaccharide (endotoxin) in fish: A review. *Fish Shellfish Immunol.* 25, 191-201. doi:10.1016/j.fsi.2008.04.009.

Syahputra, K., Kania, P. W., Al-Jubury, A., Marnis, H., Setyawan, A. C., and Buchmann, K. (2019). Differential immune gene response in gills, skin, and spleen of rainbow trout *Oncorhynchus mykiss* infected by *Ichthyophthirius multifiliis*. *PLoS One*. 14, 1-14. doi:10.1371/journal.pone.0218630.

Sylvain, F.-É., Holland, A., Bouslama, S., Audet-Gilbert, É., Lavoie, C., Val, A. L., et al. (2020). Fish Skin and Gut Microbiomes Show Contrasting Signatures of Host Species and Habitat. *Appl. Environ. Microbiol.* 86, e00789-20. doi:10.1128/AEM.00789-20.

Szalai, A. J., Bly, J. E., and Clem, L. W. (1994). Changes in serum concentrations of channel catfish (*Ictalurus punctatus Rafinesque*) phosphorylcholine-reactive protein (PRP) in response to inflammatory agents, low temperature-shock and infection by the fungus *Saprolegnia sp*. *Fish Shellfish Immunol.* 4, 323-336. doi:10.1006/fsim.1994.1029.

Takano, T., Kondo, H., Hirono, I., Endo, M., Saito-Taki, T., and Aoki, T. (2011). Toll-like receptors in teleosts. *Dis. Asian Aquac*. 385, 197–208.

Tang, L., Liang, Y., Jiang, Y., Liu, S., Zhang, F., He, X., et al. (2015). Identification and expression analysis on bactericidal permeability-increasing protein/lipopolysaccharide-binding protein of blunt snout bream, *Megalobrama amblycephala*. *Fish Shellfish Immunol.* 45, 630–640. doi:10.1016/j.fsi.2015.05.013.

Tapping, R. I., and Tobias, P. S. (1999). Soluble CD44-mediated cellular responses to lipopolysaccharide. *Chem. Immunol.* 74, 108-21. doi:10.1159/000058751.

Thaiss, C. A., Itav, S., Rothschild, D., Meijer, M. T., Levy, M., Moresi, C., et al. (2016a). Persistent microbiome alterations modulate the rate of post-dieting weight regain. *Nature.* 540, 544–551. doi:10.1038/nature20796.

Thaiss, C. A., Zmora, N., Levy, M., and Elinav, E. (2016b). The microbiome and innate immunity. *Nature* 535, 65–74. doi:10.1038/nature18847.

Thatje, S., and Arntz, W. E. (2004). Antarctic reptant decapods: More than a myth? *Polar Biol.* 27, 195–201. doi:10.1007/s00300-003-0583-z.

Toda, H., Saito, Y., Koike, T., Takizawa, F., Araki, K., Yabu, T., et al. (2011). Conservation of characteristics and functions of CD4 positive lymphocytes in a teleost fish. *Dev. Comp. Immunol.* 35, 650-660. doi:10.1016/j.dci.2011.01.013.

Tørresen, O. K., Star, B., Jentoft, S., Reinar, W. B., Grove, H., Miller, J. R., et al. (2017). An improved genome assembly uncovers prolific tandem repeats in Atlantic cod. *BMC Genomics.* 18, 95. doi:10.1186/s12864-016-3448-x.

Tort, L., Balasch, J. C., and Mackenzie, S. (2003). Fish immune system. A crossroads between innate and adaptive responses. *Immunologia.* 22, 277–286. doi: 10.1016/j.dci.2011.07.002.

Torti, F. M., and Torti, S. V. (2002). Regulation of ferritin genes and protein. *Blood.* 99, 3505–3516. doi:10.1182/blood.V99.10.3505.

Tribelli, P. M., and López, N. I. (2018). Reporting Key Features in Cold-Adapted Bacteria. *Life.* 8, 8. doi:10.3390/life8010008.

Tsujita, T., Tsukada, H., Nakao, M., Oshiumi, H., Matsumoto, M., and Seya, T. (2004). Sensing bacterial flagellin by membrane and soluble orthologs of toll-like receptor 5 in rainbow trout (*Onchorhynchus mikiss*). *J. Biol. Chem.* 279, 48588–97. doi:10.1074/jbc.M407634200.

Tunsjø, H. S., Paulsen, S. M., Mikkelsen, H., L'Abée-Lund, T. M., Skjerve, E., and Sørum, H. (2007). Adaptive response to environmental changes in the fish pathogen *Moritella viscosa*. *Res. Microbiol.* 158, 244–250. doi:10.1016/j.resmic.2006.11.014.

Tynan, E., Clarke, J. S., Humphreys, M. P., Ribas-Ribas, M., Esposito, M., Rérolle, V. M. C., et al. (2016). Physical and biogeochemical controls on the variability in surface pH and calcium carbonate saturation states in the Atlantic sectors of the Arctic and Southern Oceans. *Deep. Res. Part II Top. Stud. Oceanogr.* 127, 7–27. doi:10.1016/j.dsr2.2016.01.001.

Uribe, C., Folch, H., Enriquez, R., and Moran, G. (2011). Innate and adaptive immunity in teleost fish: A review. *Vet. Med.* 56, 486–503. doi:10.17221/3294-VETMED.

Van der Marel, M., Caspari, N., Neuhaus, H., Meyer, W., Enss, M. L., and Steinhagen, D. (2010). Changes in skin mucus of common carp, *Cyprinus carpio L.*, after exposure to water with a high bacterial load. *J. Fish Dis.* 33, 431-439. doi:10.1111/j.1365-2761.2010.01140.x.

Varriale, S., Ferraresso, S., Giacomelli, S., Coscia, M. R., Bargelloni, L., and Oreste, U. (2012). Evolutionary analysis of Antarctic teleost Toll-like receptor 2. *Fish Shellfish Immunol.* 33, 1076–1085. doi:10.1016/j.fsi.2012.07.010.

Vastag, L., Koyuncu, E., Grady, S. L., Shenk, T. E., and Rabinowitz, J. D. (2011). Divergent effects of human cytomegalovirus and herpes simplex virus-1 on cellular metabolism. *PLoS Pathog.* 7, e1002124. doi:10.1371/journal.ppat.1002124.

Vergara, A., Franzese, M., Merlino, A., Vitagliano, L., Verde, C., Di Prisco, G., et al. (2007). Structural characterization of ferric hemoglobins from three Antarctic fish species of the suborder notothenioidei. *Biophys. J.* 93, 2822-2829. doi:10.1529/biophysj.107.105700.

Vernerey, F. J., and Barthelat, F. (2014). Skin and scales of teleost fish: Simple structure but high performance and multiple functions. *J. Mech. Phys. Solids*. 68, 66–76. doi:10.1016/j.jmps.2014.01.005.

Verschuere, L., Heang, H., Criel, G., Sorgeloos, P., and Verstraete, W. (2000). Selected bacterial strains protect *Artemia spp.* from the Pathogenic effects of *Vibrio proteolyticus* CW8T2. *Appl. Environ. Microbiol.* 66, 1139-1146. doi:10.1128/aem.66.3.1139-1146.2000.

Vogel, S. N., Fitzgerald, K. A., and Fenton, M. J. (2003). TLRs: differential adapter utilization by toll-like receptors mediates TLR-specific patterns of gene expression. *Mol. Interv.* 3, 466-77. doi:10.1124/mi.3.8.466.

Vojtech, L. N., Scharping, N., Woodson, J. C., and Hansen, J. D. (2012). Roles of inflammatory caspases during processing of zebrafish interleukin-1β in *Francisella noatunensis* infection. *Infect. Immun.* 80, 2878-2885. doi:10.1128/IAI.00543-12.

Volff, J.-N. (2005). Genome evolution and biodiversity in teleost fish. *Heredity.* 94, 280–294. doi:10.1038/sj.hdy.6800635.

Vulpe, C. D., Kuo, Y. M., Murphy, T. L., Cowley, L., Askwith, C., Libina, N., et al. (1999). Hephaestin, a ceruloplasmin homologue implicated in intestinal iron transport, is defective in the sla mouse. *Nat. Genet.* 21, 195–199. doi:10.1038/5979.

Walburn, J. W., Wemheuer, B., Thomas, T., Copeland, E., O'Connor, W., Booth, M., et al. (2019). Diet and diet-associated bacteria shape early microbiome development in Yellowtail Kingfish (*Seriola*

lalandi). *Microb. Biotechnol.* 12, 275-288. doi:10.1111/1751-7915.13323.

Wang, J., Lei, P., Gamil, A. A. A., Lagos, L., Yue, Y., Schirmer, K., et al. (2019). Rainbow Trout (*Oncorhynchus mykiss*) Intestinal Epithelial Cells as a Model for Studying Gut Immune Function and Effects of Functional Feed Ingredients. *Front. Immunol.* 10, 152. doi:10.3389/fimmu.2019.00152.

Wang, J., Zhang, Z., Liu, J., Zhao, J., and Yin, D. (2016a). Ectodomain Architecture Affects Sequence and Functional Evolution of Vertebrate Toll-like Receptors. *Sci. Rep.* 6, 1–10. doi:10.1038/srep26705.

Wang, L., Liu, L., Zhou, Y., Zhao, X., Xi, M., Wei, S., et al. (2014). Molecular cloning and expression analysis of mannose receptor C type 1 in grass carp (*Ctenopharyngodon idella*). *Dev. Comp. Immunol.* 43, 54-58. doi:10.1016/j.dci.2013.10.006.

Wang, Q., Garrity, G. M., Tiedje, J. M., and Cole, J. R. (2007). Naive Bayesian classifier for rapid assignment of rRNA sequences into the new bacterial taxonomy. *Appl. Environ. Microbiol.* 73, 5261–5267. doi:10.1128/AEM.00062-07.

Wang, W. B., Li, A. H., Cai, T. Z., and Wang, J. G. (2005). Effects of intraperitoneal injection of cortisol on non-specific immune functions of *Ctenopharyngodon idella*. *J. Fish Biol.* 67, 779-793. doi:10.1111/j.0022-1112.2005.00779.x.

Wang, X., Zheng, Y., Zhang, Y., Li, J., Zhang, H., and Wang, H. (2016b). Effects of β-diketone antibiotic mixtures on behavior of zebrafish (*Danio rerio*). *Chemosphere* 144, 2195–2205. doi:10.1016/j.chemosphere.2015.10.120.

Wang, Y., Bi, X., Chu, Q., and Xu, T. (2016c). Discovery of toll-like receptor 13 exists in the teleost fish: *Miiuy croaker* (Perciformes, *Sciaenidae*). *Dev. Comp. Immunol.* 61, 25–33. doi:10.1016/j.dci.2016.03.005.

Wang, Z., and Han, Y. (2013). Response of gene expression to LPS challenge manifests the ontogeny and maturation of the complement system in zebrafish larvae. *J. Mar. Biol. Assoc. United Kingdom*. 93, 1965-1971. doi:10.1017/S0025315413000817.

Ward, N. L., Steven, B., Penn, K., Methé, B. A., and Detrich, W. H. III. (2009). Characterization of the intestinal microbiota of two Antarctic notothenioid fish species. *Extremophiles*. 13, 679-685. doi:10.1007/s00792-009-0252-4.

Watzke, J., Schirmer, K., and Scholz, S. (2007). Bacterial lipopolysaccharides induce genes involved in the innate immune response in embryos of the zebrafish (*Danio rerio*). *Fish Shellfish Immunol.* 23, 901-905. doi:10.1016/j.fsi.2007.03.004.

Wells, R. M. G., and Eastman, J. T. (1994). Antarctic Fish Biology: Evolution in a Unique Environment. *Copeia*. 1994, 255, doi:10.2307/1446701.

Werling, D., Jann, O. C., Offord, V., Glass, E. J., and Coffey, T. J. (2009). Variation matters: TLR structure and species-specific pathogen recognition. *Trends Immunol.* 30, 124–30. doi:10.1016/j.it.2008.12.001.

Weyts, F. A. A., Flik, G., Rombout, J. H. W. M., and Verburg-Van Kemenade, B. M. L. (1998a). Cortisol induces apoptosis in activated B cells, not in other lymphoid cells of the common carp, *Cyprinus carpio L*. *Dev. Comp. Immunol.* 22, 551-562. doi:10.1016/S0145-305X(98)00033-0.

Weyts, F. A. A., Flik, G., and Verburg-Van Kemenade, B. M. L. (1998b). Cortisol inhibits apoptosis in carp neutrophilic granulocytes. *Dev. Comp. Immunol.* 22, 563-572. doi:10.1016/S0145-305X(98)00027-5.

Whitfield, C., Williams, D. M., and Kelly, S. D. (2020). Lipopolysaccharide O-antigens-bacterial glycans made to measure. *J. Biol. Chem.* 295, 10593–10609. doi:10.1074/jbc.REV120.009402.

Whyte, S. K. (2007). The innate immune response of finfish - A review of current knowledge. *Fish Shellfish Immunol.* 23, 1127-1151. doi:10.1016/j.fsi.2007.06.005.

Wilkins, D., Yau, S., Williams, T. J., Allen, M. A., Brown, M. V., Demaere, M. Z., et al. (2013). Key microbial drivers in Antarctic aquatic environments. *FEMS Microbiol. Rev.* 37, 303-335. doi:10.1111/1574-6976.12007.

Wilson, B., Danilowicz, B. S., and Meijer, W. G. (2008). The Diversity of Bacterial Communities Associated with Atlantic Cod *Gadus morhua*. *Microb. Ecol.* 55, 425–434. doi:10.1007/s00248-007-9288-0.

Wong, S., and Rawls, J. F. (2012). Intestinal microbiota composition in fishes is influenced by host ecology and environment. *Mol. Ecol.* 21, 3100–3102. doi:10.1111/j.1365-294x.2012.05646.x.

Wong, W. S. W., Yang, Z., Goldman, N., and Nielsen, R. (2004). Accuracy and power of statistical methods for detecting adaptive evolution in protein coding sequences and for identifying positively selected sites. *Genetics*. 168, 1041–1051. doi:10.1534/genetics.104.031153.

Wright, S. D., Ramos, R. A., Tobias, P. S., Ulevitch, R. J., and Mathison, J. C. (1990). CD14, a receptor for complexes of lipopolysaccharide (LPS) and LPS binding protein. *Science.* 249, 1431-1433. doi:10.1126/science.1698311.

Wu, E. L., Engström, O., Jo, S., Stuhlsatz, D., Yeom, M. S., Klauda, J. B., et al. (2013). Molecular dynamics and NMR spectroscopy studies of *E. coli* lipopolysaccharide structure and dynamics. *Biophys. J.* 105, 1444–1455. doi:10.1016/j.bpj.2013.08.002.

Wu, J., Huang, S., Zhao, X., Chen, M., Lin, Y., Xia, Y., et al. (2014). Poly(I:C) treatment leads to interferon-dependent clearance of hepatitis B virus in a hydrodynamic injection mouse model. *J. Virol.* 88, 10421–10431. doi:10.1128/JVI.00996-14.

Wu, M., McCain, J. S. P., Rowland, E., Middag, R., Sandgren, M., Allen, A. E., et al. (2019). Manganese and iron deficiency in Southern Ocean Phaeocystis antarctica populations revealed through taxon-specific protein indicators. *Nat. Commun.* 10, 3582. doi:10.1038/s41467-019-11426-z.

Xia, J. H., Lin, G., Fu, G. H., Wan, Z. Y., Lee, M., Wang, L., et al. (2014). The intestinal microbiome of fish under starvation. *BMC Genomics*. 15, 266. doi:10.1186/1471-2164-15-266.

Xie, J. H., Nomura, N., Lu, M., Chen, S.-L., Koch, G. E., Weng, Y., et al. (2003). Antibody-mediated blockade of the CXCR3 chemokine receptor results in diminished recruitment of T helper 1 cells into sites of inflammation. *J. Leukoc. Biol.* 73, 771-780. doi:10.1189/jlb.1102573.

Xie, J., Liao, S., Wang, R., He, X., Fang, H., Zhuang, Z., et al. (2020). Molecular cloning, functional characterization and expression analysis of p65 subunit of golden pompano (*Trachinotus ovatus*) and response to high fat diet and LPS administration. *Aquaculture* 514, 734508. doi:10.1016/j.aquaculture.2019.734508.

Xu, P., Bao, B., He, Q., Peatman, E., He, C., and Liu, Z. (2005). Characterization and expression analysis of bactericidal permeability-increasing protein (BPI) antimicrobial peptide gene from channel catfish Ictalurus punctatus. *Dev. Comp. Immunol.* 29, 865–878. doi:10.1016/j.dci.2005.03.004.

Xu, Q., Cheng, C. H. C., Hu, P., Ye, H., Chen, Z., Cao, L., et al. (2008). Adaptive evolution of hepcidin genes in antarctic notothenioid fishes. *Mol. Biol. Evol.* 25, 1099-1112. doi:10.1093/molbev/msn056.

Xu, S., Tian, R., Lin, Y., Yu, Z., Zhang, Z., Niu, X., et al. (2019). Widespread positive selection on cetacean TLR extracellular domain. *Mol. Immunol.* 106, 135–142. doi:10.1016/j.molimm.2018.12.022.

Xu, Y., Feller, G., Gerday, C., and Glansdorff, N. (2003). *Moritella* cold-active dihydrofolate reductase: are there natural limits to optimization of catalytic efficiency at low temperature? *J. Bacteriol.*

185, 5519–5526. doi:10.1128/JB.185.18.5519-5526.2003.

Yada, K., Yoshida, K., Sakurai, Y., Kimura, M., Yasuhara, H., Tanaka, I., et al. (2008). Casein hydrolysate formula-induced liver dysfunction in a neonate with non-immunoglobulin E-mediated cow's milk allergy. *J. Investig. Allergol. Clin. Immunol.* 18, 67-70.

Yang, G.-J., Lu, X.-J., Chen, Q., and Chen, J. (2015). Molecular characterization and functional analysis of a novel C-type lectin receptor-like gene from a teleost fish, *Plecoglossus altivelis*. *Fish Shellfish Immunol.* 44, 603-610. doi:10.1016/j.fsi.2015.03.037.

Yang, M., Wang, K.-J., Chen, J.-H., Qu, H.-D., and Li, S.-J. (2007). Genomic organization and tissue-specific expression analysis of hepcidin-like genes from black porgy (*Acanthopagrus schlegelii B.*). *Fish Shellfish Immunol.* 23, 1060-1071. doi:10.1016/j.fsi.2007.04.011.

Yang, I. V., Wade, C. M., Kang, H. M., Alper, S., Rutledge, H., Lackford, B., et al. (2009). Identification of novel genes that mediate innate immunity using inbred mice. *Genetics*. 183, 1535–1544. doi:10.1534/genetics.109.107540.

Yang, Z. (2007). PAML 4: phylogenetic analysis by maximum likelihood. *Mol. Biol. Evol.* 24, 1586–1591. doi:10.1093/molbev/msm088.

Yang, Z., Wong, W. S. W., and Nielsen, R. (2005). Bayes empirical Bayes inference of amino acid sites under positive selection. *Mol. Biol. Evol.* 22, 1107–1118. doi:10.1093/molbev/msi097.

Yatsunenko, T., Rey, F. E., Manary, M. J., Trehan, I., Dominguez-Bello, M. G., Contreras, M., et al. (2012). Human gut microbiome viewed across age and geography. *Nature*. 486, 222–227. doi:10.1038/nature11053.

Yau, S., and Seth-Pasricha, M. (2019). Viruses of polar aquatic environments. *Viruses*. 11, 189. doi:10.3390/v11020189.

Ye, L., Amberg, J., Chapman, D., Gaikowski, M., and Liu, W. T. (2014). Fish gut microbiota analysis differentiates physiology and behavior of invasive Asian carp and indigenous American fish. *ISME J.* 8, 541-551. doi:10.1038/ismej.2013.181.

Yildiz, H. Y., and Altunay, S. (2011). Physiological stress and innate immune response in gilthead sea bream (*Sparus aurata*) and sea bass (*Dicentrarchus labrax)* exposed to combination of trimethoprim and sulfamethoxazole (TMP-SMX). *Fish Physiol. Biochem.* 37, 401–409. doi:10.1007/s10695-010-9440-5.

Yu, M., and Levine, S. J. (2011). Toll-like receptor 3, RIG-I-like receptors and the NLRP3 inflammasome: Key modulators of innate immune responses to double-stranded RNA viruses. *Cytokine Growth Factor Rev.* 22, 63-72. doi:10.1016/j.cytogfr.2011.02.001.

Zahringer, J., Baliga, B. S., and Munro, H. N. (1976). Novel mechanism for translational control in regulation of ferritin synthesis by iron. *Proc. Nat. Acad. Sci. USA.* 73, 857–861. doi:10.1073/pnas.73.3.857.

Zanoni, I., Ostuni, R., Marek, L. R., Barresi, S., Barbalat, R., Barton, G. M., et al. (2011). CD14 controls the LPS-induced endocytosis of toll-like receptor 4. *Cell*. 147, 868-880. doi:10.1016/j.cell.2011.09.051.

Zhang, F., Shan, S., Xu, X., Wang, Y., Zhang, Y., Yin, M., et al. (2019). Molecular characterization and expression analysis of two peptidoglycan recognition proteins (CcPGRP5, CcPGRP6) in larvae ontogeny of common carp *Cyprinus carpio L.* and upon immune stimulation by bacteria. *BMC Vet. Res.* 15, 10. doi:10.1186/s12917-018-1744-1.

Zhang, J., Kong, X., Zhou, C., Li, L., Nie, G., and Li, X. (2014). Toll-like receptor recognition of bacteria in fish: Ligand specificity and signal pathways. *Fish Shellfish Immunol.* 41, 380-388. doi:10.1016/j.fsi.2014.09.022.

Zhang, J., Nielsen, R., and Yang, Z. (2005). Evaluation of an improved branch-site likelihood method for detecting positive selection at the molecular level. *Mol. Biol. Evol.* 22, 2472–2479. doi:10.1093/molbev/msi237.

Zhang, W., Cao, S., Ding, W., Wang, M., Fan, S., Yang, B., et al. (2020a). Structure and function of the Arctic and Antarctic marine microbiota as revealed by metagenomics. *Microbiome*. 8, 47. doi:10.1186/s40168-020-00826-9.

Zhang, Y., Zhang, X., Liang, Z., Dai, K., Zhu, M., Zhang, M., et al. (2020b). Interleukin-17 suppresses grass carp reovirus infection in *Ctenopharyngodon idellus* kidney cells by activating NF-κB signaling. *Aquaculture.* 520, 734969. doi:10.1016/j.aquaculture.2020.734969.

Zhang, Z., Tian, X., and Li, D. (2016). Tissue pH and gut ecomorphology in six freshwater teleosts occupying different trophic levels. *Turkish J. Zool.* 40, 713–719. doi:10.3906/zoo-1511-5.

Zhou, J., Zhao, Y.-T., Dai, Y.-Y., Jiang, Y.-J., Lin, L.-H., Li, H., et al. (2020). Captivity affects diversity, abundance, and functional pathways of gut microbiota in the northern grass lizard *Takydromus septentrionalis*. *MicrobiologyOpen.* 9, e1095. doi:10.1002/mbo3.1095.

Zhou, Z.-X., Zhang, B.-C., and Sun, L. (2014). Poly(I:C) induces antiviral immune responses in Japanese flounder (*Paralichthys olivaceus*) that require TLR3 and MDA5 and is negatively regulated by Myd88. *PLoS One.* 9, e112918. doi:10.1371/journal.pone.0112918.

Zhu, L.-Y., Nie, L., Zhu, G., Xiang, L.-X., and Shao, J.-Z. (2013). Advances in research of fish immune-relevant genes: A comparative overview of innate and adaptive immunity in teleosts. *Dev. Comp. Immunol.* 39, 39-62. doi:10.1016/j.dci.2012.04.001.

Zhu, Y., Qi, C., Shan, S., Zhang, F., Li, H., An, L., et al. (2016). Characterization of common carp (*Cyprinus carpio L.*) interferon regulatory factor 5 (IRF5) and its expression in response to viral and bacterial challenges. *BMC Vet. Res.* 12, 127. doi:10.1186/s12917-016-0750-4.

Zhuang, X., Yang, C., Murphy, K. R., and Cheng, C.-H. C. (2019). Molecular mechanism and history of non-sense to sense evolution of antifreeze glycoprotein gene in northern gadids. *Proc. Natl. Acad. Sci. USA.* 116, 4400–4405. doi:10.1073/pnas.1817138116.

Zoccola, E., Kellie, S., and Barnes, A. C. (2017). Immune transcriptome reveals the mincle C-type lectin receptor acts as a partial replacement for TLR4 in lipopolysaccharide-mediated inflammatory response in barramundi (*Lates calcarifer*). *Mol. Immunol.* 83, 33–45. doi:10.1016/j.molimm.2017.01.010.

Zou, J., Grabowski, P. S., Cunningham, C., and Secombes, C. J. (1999). Molecular cloning of interleukin 1β from rainbow trout *Oncorhynchus mykiss* reveals no evidence of an ice cut site. *Cytokine*. 11, 522-560. doi:10.1006/cyto.1998.0470.

Zwollo, P. (2011). Dissecting teleost B cell differentiation using transcription factors. *Dev. Comp. Immunol.* 35, 898-905. doi:10.1016/j.dci.2011.01.009.